Studies on the Mechanism and Kinetics of Bioleaching with Special Reference to the Bioleaching of Refractory Gold-bearing Arsenopyrite/pyrite Concentrates

Ashley Wayne Breed

Department of Chemical Engineering, University of Cape Town

March 2000

Abstract

The objectives of this work were to evaluate the applicability of the multiple sub-process mechanism for the bioleaching of arsenopyrite, to provide kinetic information on the sub-processes involved and to determine the relationship between arsenic toxicity and interruptions in the aeration of continuous bioreactors. These objectives were addressed by performing batch and continuous bioleaching, chemical ferric leaching and bacterial ferrous-iron oxidation experiments. Off-gas analysis and redox potential measurement were used to determine the concentration and metabolic activity of the bacteria and the rate of mineral leaching.

Trends in the concentration of the iron and arsenic species, and their relationship to the bacterial activity, together with the identification of *Leptospirillum ferrooxidans* as the dominant ferrous-iron oxidising species confirmed that the bioleaching of arsenopyrite occurs via a multiple sub-process mechanism. The response of the system to interruptions in the aeration and the results obtained at elevated arsenic concentrations indicated that arsenic resistance may be attributed to an energy dependent efflux pump and a membrane system which influences the rate at which arsenic species enter the micro-organisms.

The chemical ferric leaching rate of arsenopyrite was found to increase with increasing redox potential and could be described using a Butler-Volmer based model. On the other hand, the rate at which ferrous-iron was utilised by the predominantly *L. ferrooxidans* culture increased with a decrease in the redox potential and could be described using a Michaelis-Menten type model modified to account for the effect of temperature and pH. An increase in the temperature resulted in an increase in the maximum specific ferrous-iron utilisation rate whereas an increase in the pH resulted in a proportional increase in the kinetic constant.

A model developed using the kinetics of the chemical and bacterial sub-processes proposes that the residence time and characteristics of the microbial species determine the redox potential of the bioleaching solution. The redox potential of the solution, the characteristics of the mineral being leached and the residence time in turn determine the mineral conversion. Comparisons between the model prediction and experimental data suggest that the model has potential for predicting the performance of continuous bioleach reactors.

Studies on the Mechanism and Kinetics of Bioleaching with Special Reference to the Bioleaching of Refractory Gold-bearing Arsenopyrite/pyrite Concentrates

by

Ashley Wayne Breed
B.Sc. Eng. (Chem.) M.Sc. Eng. (Chem.)

Thesis presented for the degree of
Doctor of Philosophy
in the Department of Chemical Engineering
University of Cape Town
March 2000

Summary

Bioleaching is now an established technology for the leaching of whole-ore copper heaps and the pre-treatment of refractory arsenical gold ores and concentrates. For the case of refractory arsenical gold concentrates, it offers an economically feasible alternative to pressure oxidation and has environmental advantages over roasting with regard to the quality of the liquid and gaseous effluent (Van Aswegen, 1993). The major disadvantage of bioleaching is the long residence time required to achieve sufficiently high oxidation levels. Other potential complications include the solubilisation of substances in the mineral, or the use of reagents, that are toxic to the micro-organisms.

In spite of the increased commercial application of bioleaching, there are currently no mechanistic models that can be used to predict the performance of bioleach reactors. This can be attributed to the complex nature of microbial interactions and difficulties encountered when attempting to measure the biomass concentration and growth rate, and the ferrous- and ferric-iron concentrations within 3-phase systems. In order for bioleaching to compete successfully with other pre-treatment processes, it needs to be optimised with regard to the parameters that affect the process. Thus, there is a growing need for knowledge of the stoichiometry of the bioleaching reactions and mechanistically based kinetic models that can then be used to derive performance equations for use in the design, optimisation and control of bioleaching operations.

Until recently, *T. ferrooxidans* was considered the micro-organism responsible for the bioleaching of sulfide ores and concentrates. For this reason most of the bioleaching research performed to date has been carried out using this micro-organism. However, recent research has shown that *L. ferrooxidans* is at least as important, if not more important than *T. ferrooxidans* (Rawlings *et al.*, 1999(a); Rawlings *et al.*, 1999(b); Dew *et al.*, 1997; Boon, 1996; Rawlings, 1995; Sand *et al.*, 1992; Hallmann *et al.*, 1993; Norris *et al.*, 1988; Helle and Onken, 1988). In addition, although most commercial bioleaching operations using mesophilic bacteria are continuous processes and operate at about 40°C and pH 1.2-1.8, most bioleaching research performed to date has been carried out in batch culture, at about 30°C and pH 1.8-2.0.

Recent work on the bioleaching of pyrite has indicated that it occurs via a multiple sub-process mechanism (Boon *et al.*, 1995). According to this mechanism, the pyrite is chemically oxidised by the ferric-iron present in the bioleaching medium; the ferrous-iron produced by this reaction is subsequently oxidised to the ferric form by the bacteria. This maintains a high redox potential in the bioreactors, thereby ensuring the continued leaching of the mineral. The existence of a multiple sub-process mechanism implies that the overall process can be reduced to a number of independent sequential and/or parallel sub-processes, that the kinetics of these sub-processes may be studied separately, and that the results can be used to predict the performance of bioleach reactors.

The objectives of this work were to determine the applicability of the multiple sub-process mechanism for the bioleaching of arsenopyrite, and to provide kinetic information on the chemical ferric leaching and ferrous-iron oxidation sub-processes for use in a model based on this mechanism. An additional objective of the work was to attempt to gain some insight into the mechanism of arsenic toxicity, and resistance, and its relationship to perturbations in the aeration and agitation of bioleach reactors.

The above objectives were addressed by:

i) performing steady-state and perturbation experiments using a 2-stage continuous bioleaching mini-plant,
ii) performing batch bioleaching experiments at elevated arsenite and arsenate concentrations,
iii) performing ferric leaching experiments using a dynamic redox method,
iv) performing continuous ferrous-iron oxidation experiments at temperatures ranging from 30 to 40°C and pH values ranging from pH 1.10 to pH 1.70., and
v) attempting to use the independently determined chemical ferric and bacterial ferrous-iron oxidation kinetics to predict the performance of a continuous bioleach reactor.

During steady-state operation of the bioleaching mini-plant, the ferrous-iron and arsenite concentrations were higher in the primary bioreactor than in the secondary bioreactor. On the other hand, the ferric-iron and arsenate concentrations in the secondary bioreactor were higher than in the primary bioreactor. During the perturbation studies, the ferrous-iron and arsenite concentrations in the bioreactors increased during the period in which the bioreactors were not aerated and decreased on resumption of aeration and agitation. Similar trends in the concentrations of ferrous-iron and arsenite were observed during the lag and exponential growth phases of the batch bioleaching experiments performed at elevated arsenite and arsenate concentrations. These trends, together with the identification of *Leptospirillum ferrooxidans* and *Thiobacillus caldus* (Rawlings *et al.*, 1999) as the dominant species present during the continuous bioleaching of this arsenopyrite/pyrite concentrate therefore suggests that the bioleaching of arsenopyrite occurs via a multiple sub-process mechanism.

The results obtained during the steady-state, perturbation and arsenic tolerance investigations also indicated that the chemical oxidation of arsenopyrite and arsenite, the precipitation of ferric arsenate, and possibly the ferric leaching of pyrite are competing reactions. In the absence of bacterial activity, high initial redox potentials and low arsenic concentrations (arsenite and arsenate) resulted in the ferric leaching of arsenopyrite being the dominant reaction. However, high initial redox potentials, elevated arsenite or arsenate concentrations and the absence of bacterial activity resulted in the oxidation of arsenite to arsenate, or the precipitation of ferric arsenate being the dominant reaction. In contrast to the above, in the presence of rapid bacterial oxidation, the oxidation of both arsenopyrite and arsenite and the precipitation of ferric arsenate was observed. The relative rates of the above reactions therefore depend on the concentrations of arsenopyrite, pyrite, arsenite and arsenate and the availability of ferric-iron in the bioleaching slurry. The availability of ferric-iron is in turn determined by the activity of the bacteria, and is indicated by the redox potential of the solution.

Two disruption tests were carried out while the mini-plant was operating at a residence time of 4 days. The first test comprised a 15-minute interruption in the aeration and agitation of the secondary bioreactor and the second test consisted of a 17-hour interruption in the agitation and aeration of the primary bioreactor. The disruption test performed using the secondary bioreactor indicated that short interruptions in the aeration and agitation of continuous bioleach reactors do not affect the long term or short term activity of the bacteria. The oxygen utilisation rate of the bacterial culture in the primary bioreactor, decreased during the period in which aeration and agitation was stopped, and increased once aeration and agitation was restored. However, the culture did not achieve the same level of activity as exhibited before the interruption. This result therefore suggests that

extended periods without aeration and agitation have a long term (detrimental) effect on the activity of the bacteria.

Although the arsenite concentration in the primary bioreactor increased slightly during the period in which the bioreactor was not aerated, the maximum level reached was only about 5 mmol As(III).ℓ^{-1}. In comparison, during the arsenic tolerance investigation, exposure to an initial concentration of 20 mmol As(III).ℓ^{-1} did not have a significant effect on the batch bioleaching performance of the bacterial culture.* Although exposure to an initial concentration of 40 mmol As(III).ℓ^{-1} reduced both the initial and maximum oxygen utilisation rates of the bacterial culture, the bacterial culture exhibited the ability to recover. Furthermore, the elevated arsenite concentrations did not result in a significant increase in the lag phase.

In contrast to the above, no significant change in the arsenate concentration was observed during the perturbation test performed using the primary bioreactor. The arsenate concentration, before, during and after the perturbation test was in the region of 100-150 mmol.ℓ^{-1}. During the arsenate tolerance investigation, exposure to an initial concentration of 107 mmol As(V).ℓ^{-1} increased the lag phase of the bacterial culture by 12 days and reduced both the initial and maximum oxygen utilisation rates of the bacterial culture.* The addition of 220 mmol As(V).ℓ^{-1} to the bacterial culture resulted in a lag phase that lasted for more than 31 days.

The above therefore suggests that the slow recovery of the mini-plant subsequent to the interruption in the aeration and agitation of the primary bioreactor can be attributed to the inhibitory effect of the arsenic concentration and speciation present during routine mini-plant operation. In other words, the mechanism of arsenic resistance in *L. ferrooxidans* and *T. caldus* may be attributed to an energy dependent efflux pump and a membrane system which influences the (relative) rates at which arsenite and arsenate are able to enter the micro-organisms. The membrane system, which may or may not be attributable to $Pst^{+}Pit^{-}$ (chromosomal) mutations, enables the bacteria to survive in solutions in which the dissolved arsenate concentration is significantly higher than the dissolved arsenite concentration. However, in the absence of an energy source, *i.e.* ferrous-iron or oxygen, or during periods of reduced bacterial activity, the bacteria are unable to protect themselves from the toxic effects of arsenic, hence the inhibitory effect thereof may manifest at concentrations to which the culture has previously been adapted.

According to the multiple sub-process mechanism, it is possible to determine the kinetics of the chemical ferric leaching and bacterial ferrous-iron oxidation sub-processes separately and then use the independently derived kinetic parameters to predict the performance of continuous bioleach reactors for a range of operating conditions. However, before this could be done it was necessary to establish the stoichiometry of the reaction by which arsenopyrite is degraded by ferric-iron. Because of difficulties encountered with regard to obtaining samples of pure arsenopyrite, this work was performed using an arsenopyrite/pyrite flotation concentrate.

Although the competitive nature of the reactions involving ferric-iron described above influenced the observed stoichiometry of the ferric leaching reaction, the results obtained were consistent with the stoichiometry postulated previously by Iglesias *et al.* (1993):

$$FeAsS + 5Fe^{3+} \rightarrow S^{0} + As^{3+} + 6Fe^{2+} \qquad (1)$$

The rate at which arsenopyrite was degraded by ferric-iron, expressed as the specific rate of ferrous-iron production, was determined using the Nernst Equation, the reaction stoichiometry shown in Equation 1 and the

* The concentrate used in the arsenite and arsenate tolerance investigations was the same as the concentrate used in the continuous bioleaching mini-plant, and the inoculii were obtained from the mini-plant (primary bioreactor).

measured variation in the redox potential of the slurry during the course of the experiment. In most of the experiments the ferric leaching rate increased with a decrease in the redox potential, passed through a maximum, and then decreased with a further decrease in the redox potential. It is suggested that this is a transient phenomenon, and can be attributed to the rearrangement of the ions on the surface and in the electrical double layer surrounding the mineral, *i.e.* it is not a result of leaching of the mineral.

In the region in which the specific rate of ferrous-iron production decreased with a decrease in the redox potential, the results could be accurately described using the Butler-Volmer based model suggested by May *et al.* (1997):

$$\upsilon_{Fe^{2+}} = \upsilon_0 \left(e^{\alpha\beta(E - E')} - e^{(1-\alpha)\beta(E - E')} \right) \qquad (2)$$

High concentrations of ferric iron and protons, and a reduction in the solids concentration were found to impede the leach rate. The "rest potential", *i.e.* the redox potential at which the dissolution of arsenopyrite stops, of the arsenopyrite was found to be higher under these conditions. However, no occluding sulphur layer could be detected on the surface of leached mineral particles, nor did mineral that had been leached previously appear "unreactive" when placed in fresh leaching solution. The results therefore suggest that the reactivity of the mineral decreases with an increase in the effective concentration of the ferric iron and proton species. This is regarded as highly unusual as most reaction mechanisms are favoured by an increase in the reactant concentration. Therefore, although the results suggest the likelihood of an electrochemical mechanism being operative, it is necessary to modify the Butler-Volmer based model to account for the above observations in order to obtain a model capable of predicting the ferric leaching rate of arsenopyrite across a broad range of operating conditions.

The ferrous-iron oxidising micro-organism in the mixed culture used in the continuous bioleaching mini-plant was isolated by growing an inoculum from the mini-plant in continuous culture with ferrous sulfate as the feed. Restriction enzyme analysis of PCR amplified 16S rDNA extraccted from the micro-organisms isolated in this manner was only able to detect the presence of *L. ferrooxidans*. This showed that *L. ferrooxidans*, and not *T. ferrooxidans*, is the dominant ferrous-iron oxidising species during the continuous bioleaching of this arsenopyrite/pyrite flotation concentrate.

The ferrous-iron oxidation kinetics of the predominantly *L. ferrooxidans* culture were studied in continuous-flow bioreactors. The bacterial culture was fed with a salts solution containing 12 g.ℓ^{-1} ferrous-iron, at dilution rates ranging from 0.01 to 0.10 h^{-1}, temperatures ranging from 30 to 40°C and pH values ranging from pH 1.10 to pH 1.70. The growth rate and the oxygen and ferrous-iron utilisation rates of the bacteria were monitored by means of off-gas analysis and redox potential measurement. The degree-of-reduction balance was used to compare the theoretical and experimental values of r_X, $-r_{O_2}$ and $-r_{Fe^{+2}}$, and the correlation found to be good.

The biomass concentration in the bioreactors increased with increasing temperature; the greatest biomass concentrations were achieved at intermediate residence times irrespective of the temperature and/or pH in the bioreactor. Although the biomass concentration in the bioreactors appeared to be independent of the pH, the bacterial culture maintained at 40°C and pH 1.30 "washed out" at the highest dilution rate. However, the highest calculated maximum specific growth rate, $\mu^{max} = 0.1238\ h^{-1}$, was calculated from the data obtained at 40°C and pH 1.50.

Statistical analysis suggested that the values of the maximum bacterial yields on ferrous-iron and oxygen and their respective maintenance coefficients were functions of both temperature and pH. However, the statistical

techniques employed did not take into account the poor correlation coefficients obtained during the regression analysis. For this reason, average values of the maximum bacterial yields and their respective maintenance coefficients were also determined assuming that neither temperature, nor pH, has an effect. The values of $Y^{max}_{Fe^{2+}X}$, $Y^{max}_{O_2X}$, $m_{Fe^{2+}}$ and m_{O_2}, calculated in this manner were similar to those reported previously for both *L. ferrooxidans* and *T. ferrooxidans*.

During the ferrous-iron oxidation experiments the rate at which ferrous-iron was utilised by the bacteria increased with a decrease in the redox potential of the solution and could be described using the modified Michaelis-Menten type model suggested by Boon (1996). The maximum bacterial specific ferrous-iron and oxygen utilisation rates, $q^{max}_{Fe^{2+}}$ and $q^{max}_{O_2}$, and their respective kinetic constants, $K_{Fe^{2+}}$ and K_{O_2}, increased with increasing temperature. The temperature dependence of the maximum bacterial specific ferrous-iron and oxygen utilisation rates could be described using the Arrhenius Equation whereas the relationship between temperature and the kinetic constants appeared to be linear. The kinetic constants also increased linearly with increasing pH. Although both the maximum bacterial specific ferrous-iron and oxygen utilisation rates appeared to achieve maximum values at pH 1.50, no simple relationship between these parameters and pH was evident. The effect of pH on the maximum bacterial specific ferrous-iron and oxygen utilisation rates was far less pronounced than the effect of temperature. Therefore, in an attempt to simplify the modelling, it was assumed that pH had no effect on the either $q^{max}_{Fe^{2+}}$ or $q^{max}_{O_2}$.

The above trends and assumptions were incorporated into the Michaelis-Menten based model proposed by Boon (1996). This resulted in a model capable of predicting the bacterial specific ferrous-iron utilisation rate as a function of the ferric/ferrous-iron ratio, for temperatures ranging from 30 to 40°C and pH values ranging from pH 1.10 to pH 1.70:

$$q_{Fe^{2+}} = \frac{1.204 \times 10^{7}\, e^{-\frac{35.33}{RT}}}{1 + \left(7.530 \times 10^{-7}\, T + 0.0043\, pH - 0.0040\right)\frac{[Fe^{3+}]}{[Fe^{2+}]}} \qquad (3)$$

In addition it was assumed that the stoichiometry of the overall ferrous-iron oxidation equation was independent of the dilution rate, *i.e.* $Y_{O_2X} : Y_{Fe^{2+}X}$ = constant. This allowed the value of the frequency factor for the oxygen based kinetic equation to be calculated from the stoichiometry of the overall ferrous-iron oxidation equation. In addition, the degree of reduction balance, written in terms of $q^{max}_{Fe^{2+}}$, $q^{max}_{O_2}$ and μ^{max}, can be used to show that $K_{Fe^{2+}} = K_{O_2} = K_{\mu}$, hence:

$$q_{O_2} = \frac{2.915 \times 10^{6}\, e^{-\frac{35.33}{RT}}}{1 + \left(7.530 \times 10^{-7}\, T + 0.0043\, pH - 0.0040\right)\frac{[Fe^{3+}]}{[Fe^{2+}]}} \qquad (4)$$

Comparison of the variation in the specific ferrous-iron and oxygen utilisation rates with changes in the ferric/ferrous-iron ratio predicted by the resulting models with the experimentally obtained data showed adequate agreement. The results also indicated that the effect of temperature and pH on the ferrous-iron oxidation kinetics of the predominantly *L. ferrooxidans* culture can be summarised as follows:

i) an increase in temperature results in an increase in the maximum specific ferrous-iron and oxygen utilisation rates respectively, and

ii) an increase in the pH results in a proportional increase in the kinetic constant, K.†

If, during the steady-state bioleaching of sulfide minerals, the bacteria follow Monod growth kinetics, the maximum yield and maintenance coefficient on ferrous-iron can be related via the Pirt equation (Pirt, 1982) and the bacterial specific ferrous-iron utilisation rate can be described as a function of the ferric/ferrous-iron ratio, then it can be shown that the resulting ferric/ferrous-iron ratio of the bioleaching solution is only a function of the residence time and the characteristics of the bacterial species. Furthermore, if the rate at which the mineral is leached by ferric-iron can be described as a function of the ferric/ferrous-iron ratio, then the mineral conversion during steady-state leaching in a continuous bioreactor is only a function of the residence time, the characteristics of the bacterial species and the characteristics of the mineral. Although this may not be an intuitive result, it is expected from the assumption of Monod or Michaelis-Menten type kinetics.

The model developed therefore proposes that the residence time and characteristics of the microbial species determine the redox potential of the bioleaching solution. The redox potential of the solution, the characteristics of the mineral being leached and the residence time in turn determine the degree of sulphide mineral leaching, *i.e.* the mineral conversion. A change in the residence time will result in a change in the solution redox potential, and hence in the overall leaching rate of the mineral. In addition, it may also influence the bacterial speciation.

A comparison of the model prediction with the pyrite conversion measured during a previous investigation showed good agreement if it was assumed that the bacterial species present was *L. ferrooxidans*. However, although the agreement between the redox potential measured in the first stage of a continuous BIOX® mini-plant oxidising a range of arsenopyrite/pyrite concentrates and the redox potential predicted by the model was good, the agreement between the predicted conversion and the experimental data was poor. This was anticipated and can be attributed to the fact that the " relatively low" concentrations of arsenopyrite in the mineral resulted in a large proportion of it being occluded by pyrite and/or gangue. This results in some of the arsenopyrite being inaccessible to the leaching solution and manifests as a reduced rate of "arsenopyrite" leaching, relative to the rate of leaching observed during studies performed using pure arsenopyrite.

The over-prediction of the model therefore suggests that the rate of mineral leaching needs to based on the exposed surface area of the mineral being leached, and needs to incorporate changes in the exposed surface area with time. Furthermore, the model does not consider the fate of the sulphur moiety of the mineral; this may be important in the bioleaching of base metal sulfides as sulphur products may result in passivation of the mineral surface. Although sulphur oxidising bacteria should assist in the solubilisation of this passivating layer, sulfur oxidation may be rate limiting during the bioleaching of these minerals. Therefore, refinement of the model to include the kinetics of bacterial sulfur oxidation is also necessary.

It is however apparent that the methodology employed can be extended to incorporate these effects. Therefore, although the above hypothesis has yet to be extensively tested, the results obtained to date suggest that the model has potential for predicting the performance of continuous bioleach reactors, and hence finding use in engineering and industrial applications.

† Although an increase in the temperature also resulted in a proportional increase in the kinetic constant, K, the effect of temperature was far less pronounced than the effect of pH, for the temperature and pH ranges used.

The world
is your exercise-book, the pages
on which you do your sums.
It is not reality,
although you can express reality
there if you wish.

You are also
free to write nonsense,
or lies, or to tear
the pages.

ILLUSIONS – Richard Bach

Acknowledgements

One of the many advantages of having taken a while to complete this body of work lies in the opportunity that it has afforded me to learn from, socialise with, or merely interact with very many wonderful people. I would therefore like to begin by thanking everyone that I have come into contact over the last 6 years for their contribution to my educational and/or recreational pursuits.

However, I would like to attempt to acknowledge those persons with whom I have been fortunate enough to work, those persons who have contributed to how much I have enjoyed being at work, and those who have contributed to how much I have at times enjoyed being away from work, personally:

My supervisor, Professor Geoff Hansford for his assistance and guidance throughout the project, for encouraging me to generate ideas and solutions, and for allowing me the opportunity to make, and hopefully learn, from my mistakes.

My co-supervisor, Associate Professor Sue Harrison, for her interest throughout the project, and her assistance and supervision during Professor Hansford's sabbatical.

Anlyn Breed for providing the moral, financial and physical support without which this thesis would never have seen the light of day.

Sue Jobson for her encouragement, support and warm friendship throughout my time spent within the department.

Jim Petrie for his friendship, sense of humour and profound advice, and for suffering conversations while jogging.

Dee Bradshaw for her encouragement and friendship, and providing a shoulder to lean on in times of need.

Nick Dempers for his assistance in much of the experimental work, and for lightening my load in the laboratory.

Alexandra Glatz, Renate Ruitenberg, Giles Searby and Susan Karcher for their contributions to the experimental work presented in this thesis.

Professor Doug Rawlings and Murray Gardner for their assistance with all things microbiological.

Professor Tim Dunne for his assistance with some of the statistical analyses.

Bill Randal for his sense of humor and assistance with all things electronic.

Pamela Lockey and Andrea MacDonald for making solutions, calibrating pH probes and cheerful disposition in the laboratory.

Meg Winter, Pauline Bettison, Zedré Hartman, Jill Stevenson and Helen Divey for friendship, smiles and assistance whenever requested.

Granville de la Cruz, James Daniels and Martin Williams for always finding the time to help fix things, make things or clean things.

Peter Tobias and Jochen Macke for their help in making, modifying and maintaining anything that I required.

Craig Balfour for assistance with problems originating in cyberspace.

Robin Nash, Dorothee van Scherpenzeel, Rein Weber, James Vaughan, Frank Heese, Andrew Dustan, Dave Deglon, Martin Harris, Heiko Manstein, Uwe Wilkenhöner, Peter Schwan, Linda Edlund, Silvie Bonavia and all beer club members past and present for being sources of advice, laughter and companionship, and most of all for their help in keeping everything in perspective.

Terry-Anne Fowler, Suzi Illing, Sashnee Raja, Shehnaaz Moosa, Clive Erasmus, Jo-anne Moon, Andrew Robinson, Greg and Tracy Dickason, Ashraf Jaffer, Tendai Furamera, Neil Ristow, Sigrun Jahren and other members of the BIOMIN and BIOS Groups, past and present, for their encouragement and assistance whenever requested.

Postgraduate students and staff members of the Department of Chemical Engineering, past and present for their interest and companionship.

Billiton Process Research, the Foundation for Research Development (South Africa) and the Gold Field's Foundation (South Africa) for financial and material support of the work presented.

Beth Jaholkowski for always being around.

Julian and Vernice Young, Michael and Angela Smith, Gerrie, Anne, Abigail and James van Niekerk and Jenny Algie for providing me with beds, meals, hugs, conversations, and companionship whenever needed, and for believing in me more than I did at times.

Mandy Schreiber for smiles, chats, hugs, encouragement and for letting me use my mug.

Annya Piskunova for providing the incentive to end it all.

My family, without whom nothing would matter.

Publication Declaration

In terms of Rule GP 8 for PhD theses, I give my permission for the inclusion in this thesis of material that has been published in the following publications;

Journal Publications:

Breed, A.W., Glatz, A., Hansford, G.S. and Harrison, S.T.L. 1996. The effect of As(III) and As(V) on the batch bioleaching of a pyrite-arsenopyrite concentrate. Minerals Engineering **9**(12): 1235-1252.

Breed, A.W., Harrison, S.T.L. and Hansford, G.S. 1997. Technical note: A preliminary investigation of the ferric leaching of a pyrite/arsenopyrite flotation concentrate. Minerals Engineering **10**(9): 1023-1030.

Breed, A.W. and Hansford, G.S. 1999. Studies on the mechanism and kinetics of bioleaching. Minerals Engineering **12**(4): 383-392.

Ruitenberg, R., Hansford, G.S., Reuter, M.A. and Breed, A.W. 1999. The ferric leaching kinetics of arsenopyrite. Hydrometallurgy **52**(1): 37-55

Breed, A.W. and Hansford, G.S. 1999. Effect of pH on ferrous-iron oxidation kinetics of *Leptospirillum ferrooxidans* in continuous culture. Biochemical Engineering Journal **3**(3): 193-201.

Breed, A.W., Dempers, C.J.N., Searby, G.E., Gardner, M.N, Rawlings, D.E. and Hansford, G.S. 1999. The effect of temperature on the continuous ferrous-iron oxidation kinetics of a predominantly *Leptospirillum ferrooxidans* culture. Biotechnology and Bioengineering **65**: 44-53.

Breed, A.W. and Hansford, G.S. 1999. Modelling continuous bioleach reactors. Biotechnology and Bioengineering **64**(6): 671-677.

Conference Publications (Refereed):

Breed, A.W., Harrison, S.T.L. and Hansford, G.S. 1997. The bioleaching of a pyrite-arsenopyrite flotation concentrate in a continuous bioleaching mini-plant. Steady-state operation and behaviour during periods without aeration and agitation. In: Biotechnology comes of age, Proceedings of IBS-BIOMINE 97, pp. M.8.3.1-M8.3.10. AMF, Glenside, Australia.

Breed, A.W., Dempers, C.J.N and Hansford, G.S. 1999. Studies on the bioleaching of refractory gold concentrates. In: Metallurgy Africa '99, Symposium Series S22, pp. 23-34. SAIMM, Johannesburg, South Africa.

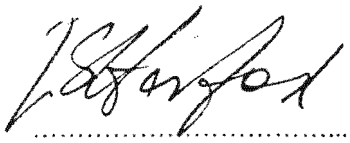

.....

Professor G.S. Hansford (Ph.D. Supervisor)

Table of Contents

List of Tables

List of Figures

For Josh

Live
never to be
ashamed if anything you do
or say is published
around the world -
even if
what is published
is not true.

ILLUSIONS – Richard Bach

Chapter One

Introduction

Bioleaching can be defined as the process in which the bacterial oxidation of minerals results in the release of valuable metals (*e.g.* copper) into the resulting acid solution Brierley (1997(a)). Bioleaching for the extraction of copper has been practised since the 16th century (Wadsworth, 1987). However, it was not until 1947, when the bacterium *Thiobacillus ferrooxidans* was isolated from acidic mine water, that the process was understood to be bacterially catalysed (Colmer and Hinkle, 1947). Although copper extraction was the first commercial application of bioleaching, it was research initiated during the 1950's and aimed at recovering uranium from Witwatersrand gold ores (Livessey-Goldblatt *et al.*, 1977) that led to research, performed during the late 1970's, into the use of bioleaching for the recovery of gold from refractory sulfide ores (Van Aswegen *et al.*, 1991).

In many cases, bioleaching offers economic, environmental and technical advantages over pressure oxidation and roasting (Van Aswegen, 1993; Poulin and Lawrence, 1996). It is now an established technology for the leaching of whole-ore copper heaps and the pre-treatment of refractory arsenical gold ores and concentrates, and has significant potential for the extraction of nickel, cobalt and other base metals. It also has potential for the generation of acidic ferric sulfate for use as a leaching medium in extractive hydrometallurgical processes. Although the spontaneous bioleaching of wastes containing sulfide minerals contributes to acid mine drainage, it has the potential to be used in such a way as to benefit the environment. It has been considered for the desulfurisation of coal and in the decontamination of soils and sludges containing heavy metals.

In the case of refractory arsenical gold concentrates, bioleaching using mixed mesophilic cultures offers an economically feasible alternative to pressure oxidation (or may be used to increase the capacity of pressure oxidation plants) and has environmental advantages over roasting with regard to the quality of gaseous and liquid effluent (Van Aswegen, 1993). Other advantages of bioleaching are the mild conditions employed compared to those used in pressure oxidation, *viz.* mild acidity and slightly elevated temperatures as opposed to high pressures, temperatures and acidity (Haines and Van Aswegen, 1990). At present there are plants in South Africa, Australia, Brazil and Ghana which treat flotation concentrates (Dew *et al.*, 1997), and heap leaching operations in the USA (Brierley, 1997(b)).

The major disadvantage of bioleaching is the long residence time required to achieve sufficiently high oxidation levels. This results in large leaching vessels being required, which in turn results in difficulties with regard to temperature control, aeration and solids suspension. In addition long residence times result in long recovery periods subsequent to system upsets.* Further potential complications include:

i) the solubilisation of substances (metals) present in the mineral to concentrations toxic to the micro-organisms (Lindström and Sehlin, 1989; Norris and Kelly, 1978; Pol'kin *et al.*, 1975),
ii) the inhibitory effect of flotation (Lan *et al.*, 1991) and other reagents on the bacteria, and
iii) the fact that adaptation, or resistance to one metal does not necessarily imply adaptation or resistance to another.

Furthermore, in spite of the increased commercial application of bioleaching, there are currently no mechanistic models that can be used to predict the performance of bioleach reactors. This can be primarily attributed to the fact that the modelling of bioleach reactors is complicated by the complex nature of microbial interactions and by difficulties encountered when attempting to measure the biomass concentration and growth rate, and the ferric and ferrous-iron concentrations. These analyses are further complicated by the presence of solids within the system. However, in order for bioleaching to compete successfully with other pre-treatment processes such as pressure oxidation and roasting it needs to be optimised with regard to the parameters that affect the bioleaching reactions, and the growth of the micro-organisms involved. Thus, there is a growing need for knowledge of the stoichiometry of the bioleaching reactions and mechanistically based kinetic models that can then be used to derive performance equations for use in the design, optimisation and control of bioleaching operations.

1.1 Mechanism and Kinetics of Bioleaching

Recent work on the bioleaching of pyrite has provided strong evidence that it occurs via a multiple sub-process mechanism (Boon *et al.*, 1995). According to this mechanism, the pyrite is chemically oxidised by the ferric-iron present in the bioleaching medium according to;

$$FeS_2 + 14Fe^{3+} + 8H_2O \rightarrow 15Fe^{2+} + 2SO_4^{2-} + 16H^+ \quad (1\text{-}1)$$

The ferrous-iron produced by this reaction is subsequently oxidised to the ferric form by the bacteria according to;

$$4Fe^{2+} + O_2 + 4H^+ \rightarrow 4Fe^{3+} + 2H_2O \quad (1\text{-}2)$$

The oxidation of ferrous-iron to ferric-iron ensures that a high redox potential is maintained in the bioreactors, thereby ensuring the continued leaching of the mineral.

Although the results presented by Boon *et al.* (1995) cannot be considered proof that the bioleaching of all sulfides occurs via an "indirect" mechanism, the isolation and identification of *Leptospirillum ferrooxidans* and *Thiobacillus caldus* as the dominant species in continuous bioleaching plants oxidising a range of sulfide concentrates (Rawlings *et al.*, 1999(a)), suggests that they do. This statement can be explained as follows:

* A related (advantageous) phenomenon is the relative stability that arises from the time taken for upsets to be transmitted through the bioreactor cascade.

Although *L. ferrooxidans* is able to oxidise ferrous-iron, it is unable to oxidise reduced sulfur compounds or elemental sulfur. Furthermore, during the bioleaching of pyrite, the role of the microorganisms (*T. ferrooxidans* and *L. ferrooxidans*) was found to be the oxidation of the ferrous-iron back to the ferric form, *i.e.* the bacteria did not oxidise the pyrite mineral directly (Boon, 1996). On the other hand, *T. caldus* is able to oxidise elemental sulfur and reduced sulfur compounds, but cannot oxidise sulfidic sulfur, *i.e.* sulfides. Therefore, the identification of *L. ferrooxidans* and *T. caldus* in bioleach reactors oxidising a range of sulfide concentrates containing chalcopyrite and arsenopyrite (Rawlings *et al.*, 1999(a)) indicates the presence of ferrous-iron and either elemental sulfur or reduced sulfur compounds.

The above together with the fact that the ferric-iron leaching of chalcopyrite and arsenopyrite has been shown to result in the formation of ferrous-iron and elemental sulfur (Kametani and Aoki, 1985; Iglesias *et al.*, 1993), therefore suggests that the bioleaching of these minerals occurs via an "indirect", or multiple sub-process mechanism. Furthermore, if the bioleaching of pyrite, arsenopyrite and chalcopyrite occurs via an "indirect", or multiple sub-process mechanism, then it is likely that the bioleaching all sulfides occurs an "indirect", or multiple sub-process mechanism.

According to the "indirect", or multiple sub-process mechanism the mineral is chemically leached by the ferric-iron in the bioleaching solution and the role of the bacteria is to oxidise the ferrous-iron and sulfur to ferric-iron and sulfate, respectively.

A multiple sub-process mechanism has a number of important implications for the modelling of bioleaching, *viz.*:

i) the overall process can be reduced to a number of independent sequential and/or parallel sub-processes,
ii) the kinetics of these respective sub-processes may be studied separately, and
iii) the results used to predict the performance of bioleach reactors for a variety of different minerals, micro-organisms and operating conditions (*e.g.* pH, T, inhibitory ion concentration).

Of course, in order to carry out the ferrous-iron and sulfur oxidation reactions, the micro-organisms require a source of oxygen, carbon dioxide and other nutrients. Therefore, in order to optimise the process it is necessary to consider the mass transfer requirements and the inherent limitations of the systems employed. These factors are however, beyond the scope of the work presented in this thesis.

1.1.1 Effect of Toxic Species

As stated previously, a potential complication encountered during bioleaching is the solubilisation of substances (metals) present in the mineral which may be toxic to the micro-organisms. Fortunately, in comparison to other bacterial species, acidophilic chemolithoautotrophic bacteria are characterised by their high degree of resistance to the toxic effect of metal ions. This resistance can be attributed to the inherent resistance of the bacteria used, specific resistance mechanisms and chemical factors attributed to their growth conditions (Barrett *et al.*, 1993).

The inherent resistance of wild-type bacterial strains may vary depending on their respective habitat; strains more resistant to the toxic effects of specific metals may be isolated from regions associated with leaching of these metals. In addition, the resistance of these bacteria will be influenced by their physiological state. Specific

resistance mechanisms include detoxification of the ionic species by oxidation or reduction. This may be linked to, or independent of, the active excretion of the toxic species, *e.g.* plasmid encoded resistance. Chemical factors attributed to the conditions in which the micro-organisms grow, such as T and pH, may also influence the oxidation state and chemical form of the metal ion; this may alleviate the toxicity of the metal with respect to the micro-organisms (Norris and Kelly, 1978).

Because of the high concentrations of arsenic encountered during the leaching of refractory arsenical sulfides, the toxicity of arsenic to bacteria and the mechanisms of bacterial resistance to arsenic are especially important. Furthermore, as arsenite, As(III), is alleged to be more toxic than arsenate, As(V), the conditions affecting the speciation of arsenic, such as ore mineralogy, pH, redox potential and galvanic interactions, will also affect the process.

The mechanism of resistance to arsenite, antimony and arsenate in *T. caldus* has been shown to be a result of reduced cellular accumulation of these ions and an energy dependent efflux of the accumulated species (Hallberg, 1995). Resistance to these ions is induced by growth in the presence of non-toxic concentrations of any one of these species (Hallberg, 1995). Although it has been claimed that arsenic resistance in *T. ferrooxidans* is plasmid borne (Nicolau and Raimond, 1993), the mechanism of arsenic resistance in acidophilic chemoautotrophs other than *T. caldus* has not been determined (Lindström *et al.*, 1992). However, the fact that arsenite is more toxic to the micro-organisms used in bioleaching than arsenate suggests that arsenate resistance may be attributed to chromosomal mutations, *i.e.* natural selection (Lawson, 1993).

1.1.2 Bacterial Ferrous-iron Oxidation Kinetics

A number of kinetic models for bacterial ferrous-iron oxidation have been proposed (Nemati *et al.*, 1998; Boon, 1996). These models can be broadly classified as being either empirical, or based on Monod or Michaelis-Menten kinetics. Empirical models use tools such as the logistic equation to model the ferrous-iron oxidation kinetics. Models based on the Monod equation assume that bacterial growth on ferrous-iron can be described by means of the Monod equation. Michaelis-Menten based models assume that the rate limiting reactions involve the formation of an enzyme-substrate complex, and can therefore be described using traditional enzyme kinetics.

A major limitation of the logistic equation is that it is not mechanistically based, *i.e.* it does not contain terms that reflect the characteristics of the bacteria, *e.g.* growth rate, or the bioreactor conditions, *e.g.* T, pH. This means that it is not possible to use the logistic equation to predict the performance of the micro-organisms across a range of operating conditions. In spite of this limitation it has however proved useful, especially in the modelling of bioleaching. In contrast to the logistic equation, kinetic models based on Monod or Michaelis-Menten kinetics can be easily modified to include terms to account for changes in the conditions under which the micro-organisms are grown, *e.g.* temperature, pH, or the presence of inhibitory substances.

Most of the kinetic studies performed to date have been carried out using *T. ferrooxidans*, at temperatures in the region of 30°C and pH values in the region of pH 2.0. Under these conditions, most researchers have found *T. ferrooxidans* to be competitively inhibited by ferric-iron (Harvey and Crundwell, 1997; Huberts 1994; Nikolov and Karamev, 1992; Lizama and Suzuki, 1989; Liu *et al.*, 1988; Jones and Kelly, 1983; Kelly and Jones, 1978). Under certain conditions *T. ferrooxidans* has been found to be subject to inhibition by ferrous-iron (substrate) (Nemati and Webb, 1997; Nikolov and Karamev, 1992), cells (Nemati and Webb, 1997; Suzuki and Lizama, 1989; Lizama and Suzuki, 1989) and arsenite (Harvey and Crundwell, 1997). Apart from the work

performed by Nemati and Webb (1997), however, the effect of temperature has not been studied extensively, and there is very little data on the effect of pH on the ferrous-iron oxidation kinetics.

In general, however, the growth and substrate (CO_2, O_2, Fe^{2+}) utilisation kinetics have been found to follow a reverse sigmoidal curve with increasing ferric/ferrous-iron ratio, which is consistent with chemiosmotic potential theory (Ingledew, 1986). The above resulted in Boon (1996) suggesting that the ferrous-iron kinetics could be described in terms of a maximum ferrous-iron utilisation rate and the ferric/ferrous-iron ratio, *i.e.* redox potential. The model proposed by Boon (1996) has subsequently been used to describe the ferrous-iron kinetics of both *T. ferrooxidans* (Boon, 1996) and *L. ferrooxidans* (Van Scherpenzeel, 1996). Therefore, although, most kinetic studies performed to date have been carried out at 30°C and pH 2.0,† and although it has been shown that *T. ferrooxidans* is unlikely to predominate in commercial bioleach reactors (Rawlings *et al.*, 1999(a); Rawlings *et al.*, 1999(b); Dew *et al.*, 1997; Boon, 1996; Rawlings, 1995; Hallmann *et al.*, 1993; Helle and Onken, 1988; Norris *et al.*, 1988), the work carried out by Van Scherpenzeel (1996) suggests that the ferrous-iron oxidation kinetics of *L. ferrooxidans* and *T. ferrooxidans* may be described using the same kinetic models.

1.1.3 Chemical Ferric Leaching Kinetics

The kinetic models used to describe the ferric leaching kinetics of sulfide minerals can be classified as being either chemical or electrochemical in nature. Chemical models assume that the reaction rate at the surface is limiting, whereas electrochemical models assume that the difference between the rest potential of the mineral and the leaching medium is the driving force and that the electron transfer from the surface to the surrounding medium is limiting. Both models can be modified to account for diffusion limitations.

If sulfide minerals undergo dissolution by electrochemical means as suggested by Shuey (1975), then, as iron is the electron donor, the ferric leaching kinetics may depend on the ferric/ferrous-iron ratio (*i.e.* redox potential) rather than the total or ferric-iron concentrations (May *et al.*, 1997; Boon, 1996). However, although many researchers have identified the ferric/ferrous-iron ratio as being an important parameter during the chemical ferric leaching of sulfide minerals, apart from the model proposed by May *et al.* (1997), few workers have attempted to use a model based on electrochemical/corrosion theory. In general, however, the rate at which both pyrite and arsenopyrite are leached by ferric-iron has been found to increase with an increase in the ferric/ferrous-iron ratio, or redox potential (Malatt, 1998; May *et al.*, 1997). In addition, comparison between the rates of chemical ferric leaching achieved by May *et al.* (1997) and previously reported rates for the bioleaching of pyrite suggest that it is possible to achieve high rates in sterile medium provided that the redox potential is kept sufficiently high.

However, in spite of the fact that considerable work on the leaching of pyrite using ferric-iron has been performed, to date very little work on the ferric leaching kinetics of arsenopyrite has been reported. For this reason, there is still considerable controversy with regard to the stoichiometry of the ferric leaching reaction.

† In contrast to the conditions at which most bioleaching research has been performed, most commercial bioleaching operations using mesophiles use mixed cultures, and operate at temperatures in the region of 40°C and pH values in the region of pH 1.2-1.8.

1.1.4 Modelling Bioleaching Operations

As stated previously, difficulties with regard to the measurement of the biomass concentration and growth rate and the ferric- and ferrous-iron concentrations have resulted in the logistic equation being the rate expression which has found the most widespread application to date. Because the logistic equation is not mechanistically based it does not require knowledge of the bacterial concentration, or their activity. However, the lack of a mechanistic basis means that it cannot be used to predict the performance of bioleaching operations for different micro-organism/mineral combinations or across a range of operating conditions. In spite of this limitation, it has proved useful in modelling batch and continuous laboratory, pilot and full-scale plant data for several pyrite and arsenopyrite/pyrite flotation concentrates (Crundwell, 1994; Dew *et al.*, 1993; Hansford and Miller, 1993; Hansford and Bailey, 1992; Hansford and Chapman, 1992; Miller and Hansford, 1992(a); Miller and Hansford, 1992(b); Pinches *et al.*, 1988).

Konishi and co-workers (Konishi *et al.*, 1994; Konishi and Asai, 1993; Asai *et al.*, 1992; Konishi *et al.*, 1992; Konishi *et al.*, 1990) developed a model based on the number of micro-organisms which adsorb to the surface of the mineral. This model fitted data obtained during the batch bioleaching of pyrite.
In contrast to most workers, Nagpal *et al.* (1994) assumed that the dissolution of arsenopyrite occurred via an "indirect" mechanism, *i.e.* mineral degradation occurred solely as a result of chemical ferric leaching, and the role of the bacteria was to regenerate the ferric-iron and oxidise the sulfur moiety. This model is clearly consistent with the multiple sub-process mechanism of bioleaching. However, Nagpal *et al.* (1994) determined the kinetic parameters of the chemical and bacterial sub-processes during the bioleaching of a pyrite/arsenopyrite concentrate. As stated previously, the existence of a multiple sub-process mechanism for the bioleaching of sulfide minerals implies that the kinetics of the chemical and bacterial sub-processes may be studied separately, and the results of the individual studies used to predict the performance of bioleach reactors. Furthermore, no attempt was made to use the kinetic data in order to compare the model prediction with data obtained by other workers.

1.2 Objectives of the Study

The objectives of the work presented were to attempt to test the applicability of the multiple sub-process mechanism for the bioleaching of arsenopyrite. A further objective was to attempt to gain some insight into the mechanism of arsenic toxicity, and resistance, and its relationship to perturbations in aeration and agitation of bioleach reactors. The above overall objective was therefore reduced to the following specific objectives.

i) To determine the ferric leaching kinetics of arsenopyrite. In view of the disparity with regard to the stoichiometry proposed by other workers, an initial objective of the work was to attempt to determine the stoichiometry of the reaction. Further objectives included the determination of the effect of various parameters (*viz.* $E_{initial}$, $[Fe]_{tot}$, ρ_{pulp}, pH) on the leaching kinetics.

ii) To identify the dominant ferrous-iron oxidising species in the mixed culture used for the bioleaching of an arsenopyrite/pyrite concentrate obtained from the BIOX® plant at the Fairview Gold Mine in Barberton, South Africa, and to determine the effect of temperature and pH on the ferrous-iron oxidation kinetics of this micro-organism.

iii) To determine the relationship between perturbations in the aeration and agitation of the mixed culture from the Fairview BIOX® plant while oxidising a sample of arsenopyrite/pyrite flotation concentrate from the Fairview Gold Mine, and arsenic toxicity.

iv) To determine whether the independently determined chemical ferric-iron (mineral) leaching and bacterial ferrous-iron oxidation kinetics could be used to develop a model for predicting the performance of continuous bioleach reactors.

Although the rate at which the oxidation of ferrous-iron occurs has been alleged to be the rate controlling step during the bioleaching of sulfides (Boon *et al.*, 1998), the slow kinetics of chalcopyrite bioleaching using mesophiles suggests that this is not the case for all sulfides. However, the fate of the sulfur moiety during the leaching of arsenopyrite is beyond the scope of the work presented in this thesis.

1.3 Thesis Layout

The thesis is therefore divided into the following chapters.

i) **Chapter Two, Literature Review**: a review of the literature relevant to the bioleaching of arsenopyrite, *viz.* the mechanism by which it has been alleged to occur, the micro-organisms involved and the effect of arsenic on these micro-organisms and the models used previously to describe the kinetics of bioleaching, bacterial ferrous-iron oxidation and the ferric leaching of sulfide minerals.

ii) **Chapter Three, The Ferric Leaching of Arsenopyrite**: the results of an investigation into the stoichiometry and kinetics of the ferric leaching of arsenopyrite using a dynamic redox method.

iii) **Chapter Four, The Effect of Temperature and pH on the Continuous Ferrous-iron Oxidation Kinetics of a Predominantly *Leptospirillum ferrooxidans* Culture**: presentation of the results of investigations into the continuous ferrous–iron oxidation kinetics of a predominantly *L. ferrooxidans* culture isolated from a continuous bioleaching mini-plant oxidising a sample of arsenopyrite/pyrite flotation concentrate.

iv) **Chapter Five, The Effect of As(III) and As(V) on the Batch Bioleaching of an Arsenopyrite/pyrite Concentrate**: the results of an investigation into the effect of arsenite and arsenate on the batch bioleaching of an arsenopyrite/pyrite flotation concentrate in batch culture.

v) **Chapter Six, Steady-state Operation and Aeration Perturbations of a Continuous Bioleaching Mini-plant Treating an Arsenopyrite/pyrite Flotation Concentrate**: reports the results of steady-state and perturbation studies performed using a continuous bioleaching mini-plant oxidising a sample of arsenopyrite/pyrite flotation concentrate.

vi) **Chapter Seven, Modelling Continuous Bioleach Reactors**: develops and tests a model, based on the multiple sub-process mechanism, that predicts the mineral conversion in a continuous bioleach reactor.

vii) **Chapter Eight, Conclusions**.

1.4 Nomenclature

$E_{initial}$	initial redox potential of the solution	mV
$[Fe]_{tot}$	concentration of iron	mmol Fe.ℓ^{-1}
T	temperature	°C
ρ_{pulp}	concentration of solids	% (m.v^{-1})

1.5 References

Asai, S., Konishi, Y. and Yoshida, K. 1992. Kinetic model for batch bacterial dissolution of pyrite particles by *Thiobacillus ferrooxidans*. Chemical Engineering Science **47**(1): 133-139.

Barrett, J., Hughes, M.N., Karavaiko, G.I. and Spencer, P.A. 1993. Metal extraction by bacterial oxidation of minerals. Ellis Horwood, New York.

Boon, M. 1996. Theoretical and experimental methods in the modelling of bio-oxidation kinetics of sulphide minerals. Ph.D. Thesis. Delft University of Technology, Delft.

Boon, M., Hansford, G.S. and Heijnen, J.J. 1995. The role of bacterial ferrous-iron oxidation in the bio-oxidation of pyrite, pp. 153-163. In: T. Vargas, C.A. Jerez, J.V. Wiertz and H. Toledo (eds.), Biohydrometallurgical Processing **1**. University of Chile, Santiago.

Boon, M., Hansford, G.S. and Heijnen, J.J. 1998. The mechanism and kinetics of bioleaching sulphide minerals. Min. Pro. Ext. Met. Rev. **19**: 107-115.

Brierley, C.L. 1997(a). Application of biotechnology to the economic recovery of metals from ores and concentrates. Australian Mineral Foundation Course No 100D/97, 7-8 August 1997. Sydney, Australia.

Brierley, C.L. 1997(b). Mining biotechnology: research to commercial development and beyond, pp. 3-17. In D.E. Rawlings (ed.), Biomining: theory, microbes and industrial processes. Springer-Verlag and Landes Bioscience, Berlin.

Colmer, A.R. and Hinkle, M.E. 1947. The role of micro-organisms in acid mine-drainage. Science **106**: 253-256.

Crundwell, F.K. 1994. Mathematical modelling of batch and continuous bacterial leaching. Chem. Eng. J. **54**: 207-220.

Dew, D.W., Lawson, E.N. and Broadhurst, J.L. 1997. The BIOX® process for biooxidation of gold-bearing ores or concentrates, pp. 45-80. In D.E. Rawlings (ed.), Biomining: theory, microbes and industrial processes. Springer-Verlag and Landes Bioscience, Berlin.

Dew, D.W., Miller, D.M. and Van Aswegen, P.C. 1993. GENMIN's commercialisation of the bacterial oxidation process for the treatment of refractory gold concentrates, pp. 229-237. In: Randol Gold Forum, Randol International.

Haines, A.K. and Van Aswegen, P.C. 1990. Process and engineering challenges in the treatment of refractory gold ores, pp. 103-110. In: Innovations in Metallurgical Plant, Proc. International Deep Mining Conference. SAIMM, Johannesburg.

Hallberg, K.B. 1995. Role of arsenic toxicity to and resistance of thermophilic bioleaching micro-organisms. Ph.D. Thesis, Umeå University, Umeå.

Hallmann, R., Friedrich, A., Koops, H.P., Pommering-Röser, A., Zenneck, C. and Sand, W. 1993. Physicological characteristics of *Thiobacillus ferrooxidans* and *Leptospirillum ferrooxidans* and physicochemical factors influence microbial metal leaching. Geomicrobiology Journal **10**: 193-205.

Hansford, G.S. and Bailey, A.D. 1992. The logistic equation for modelling bacterial oxidation kinetics. Minerals Engineering **5**: 1355-1364.

Hansford, G.S. and Chapman, J.T. 1992. Batch and continuous bio-oxidation kinetics of a refractory gold-bearing pyrite/arsenopyrite concentrate. Minerals Engineering **5**(6): 597-612.

Hansford, G.S. and Miller, D.M. 1993. Biooxidation of a gold-bearing pyrite-arsenopyrite concentrate. FEMS Microbiology Reviews **11**: 175-182.

Harvey, P.I. and Crundwell, F.K. 1997. Growth of *Thiobacillus ferrooxidans*: a novel experimental design for batch growth and bacterial leaching studies. Applied and Environmental Microbiology **63**(7): 2586-2592.

Helle, U. and Onken, U. 1988. Continuous bacterial leaching of pyritic flotation concentrate by mixed cultures, pp. 61-75. In: P.R. Norris and D.P. Kelly (eds.), Biohydrometallurgy. Science and Technology Letters, Kew, Surrey.

Huberts, R. 1994. Modelling of ferrous sulphate oxidation by iron oxidizing bacteria – a chemiosmotic and electrochemical approach. Ph.D. Thesis. University of the Witwatersrand, Johannesburg.

Iglesias, N., Palencia, I. and Carranza, F. 1993. Removal of the refractoriness of a gold bearing pyrite-arsenopyrite ore by ferric sulphate leaching at low concentration, pp. 99-115. In: J.P. Hager (ed.), EPD Congress 1993, The Minerals, Metals and Materials Society, Warrendale, Co..

Ingledew, W.J. 1986. Ferrous iron oxidation by *Thiobacillus ferrooxidans*. Biotechnology and Bioengineering Symposium Series **16**: 23-33.

Jones, C.A. and Kelly, D.P. 1983. Growth of *Thiobacillus ferrooxidans* on ferrous iron in chemostat culture: influence of product and substrate inhibition. Journal of Chemical Technology and Biotechnology **33B**(4): 241-261.

Kametani, H. and Aoki, A. 1985. Effect of suspension potential on the oxidation rate of copper concentrate in a sulphuric acid solution. Metallurgical Transactions B **16B**(December): 695-705.

Kelly, D.P. and Jones, C.A. 1978. Factors affecting metabolism and ferrous iron oxidation in suspensions and batch cultures of *Thiobacillus ferrooxidans*: relevance to ferric iron leach solution generation, pp. 19-44. In: L.E. Murr, A.E. Torma and J.A. Brierley (eds.), Metallurgical Applications of Bacterial Leaching and Related Microbiological Phenomena. Academic Press, New York.

Konishi, Y. and Asai, S. 1993. A biochemical engineering approach to the bioleaching of pyrite in batch continuous tank reactors. In: A.E. Torma, J.E. Wey, V.I. Lakshmanan (eds.), Biohydrometallurgical Technologies **I**. The Minerals, Metals and Materials Society, Warrendale, Pa..

Konishi, Y., Asai, S. and Katoh, H. 1990. Bacterial dissolution of pyrite by *Thiobacillus ferrooxidans*. Bioprocess Engineering **5**: 231-237

Konishi, Y., Kubo, H. and Asai, S. 1992. Bioleaching of zinc sulfide concentrate by *Thiobacillus ferrooxidans*. Biotechnology and Bioengineering **39**(1): 66-74.

Konishi, Y., Takasaka, Y. and Asai, S. 1994. Kinetics of growth and elemental sulfur oxidation in batch culture of *Thiobacillus ferrooxidans*. Biotechnology and Bioengineering **44**(6): 667-673.

Lan X., Jia-jun, K. and Rong-qing, Q. 1991. Effect of flotation reagents on the growth of bacteria and the bioleaching of arsenic-bearing gold concentrate, pp. 59-67. In: D.R. Gaskell (ed.), Proc. EPD Congress '91, The Minerals Metals and Materials Society, Warrendale, Pa..

Lawson, E.N. 1993. Arsenic toxicity, bacterial resistance and bacterial oxidation/reductions. Phase 1: literature review. Report No. PR 93/109C of Project No. PR 93/132. GENMIN Process Research, Johannesburg.

Lindström, E.B. and Sehlin, H.M. 1989. Toxicity of arsenic compounds to the sulphur-dependent archaebacterium *Sulfolobus*, pp. 59-70. In: J. Salley, R.G.L. McCready and P.L. Wichlacz (eds.), Proc. Biohydrometallurgy-89. Jackson Hole, July 1989.

Lindström, E.B., Gunneriusson, E. and Tuovinen, O.H. 1992. Bacterial oxidation of refractory sulfide ores for gold recovery. Critical Reviews in Biotechnology **12**(1/2): 133-155.

Liu, M.S., Branion, R.M.R. and Duncan, D.W. 1988. The effects of ferrous iron, dissolved oxygen, and inert solids concentration on the growth of *Thiobacillus ferrooxidans*. The Canadian Journal of Chemical Engineering **66** (June): 445-451.

Livessey-Goldblatt, E., Tunley, T.H. and Nagy, I.F. 1977. Pilot-plant bacterial film oxidation (bacfox process) of recycled acidified uranium plant ferrous sulphate leach solution, pp. 175-190. In: W. Schwartz (ed.), Conference Bacterial Leaching. Verlag-Chemie, Weinheim, New York.

Lizama, H.M. and Suzuki, I. 1989. Synergistic competitive inhibition of ferrous iron oxidation by *Thiobacillus ferrooxidans* by increasing concentrations of ferric iron and cells. Applied and Environmental Microbiology **55**(10): 2588-2591.

Malatt, K. 1998. The bacterial oxidation of gold-bearing pyrite/arsenopyrite concentrates. Ph.D. Thesis, Curtin University of Technology, Perth, WA.

May, N., Ralph, D.E. and Hansford, G.S. 1997. Dynamic redox potential measurement for determining the ferric leach kinetics of pyrite. Minerals Engineering **10**(11): 1279-1290.

Miller, D.M. and Hansford, G.S. 1992(a). Batch biooxidation of a gold-bearing pyrite-arsenopyrite concentrate. Minerals Engineering **5**(6): 613-629.

Miller, D.M. and Hansford, G.S. 1992(b). The use of the logistic equation for modelling the performance of a biooxidation pilot plant treating a gold-bearing arsenopyrite-pyrite concentrate. Minerals Engineering **5**(7): 737-749.

Nagpal, S., Dahlstrom, D. and Oolman, T. 1994. A mathematical model for the bacterial oxidation of a sulfide ore concentrate. Biotechnology and Bioengineering **43**(5): 357-364.

Nemati, M. and Webb, C. 1997. A kinetic model for biological oxidation of ferrous-iron by *Thiobacillus ferrooxidans*. Biotechnology and Bioengineering **53**(5): 478-486.

Nemati, M., Harrison, S.T.L., Webb, C. and Hansford, G.S. 1998. Biological oxidation of ferrous sulphate by *Thiobacillus ferrooxidans*: a review on the kinetic aspects. Biochemical Engineering Journal **1**: 171-190.

Nicolau, C. and Raimond, J. 1983. As cited by Lawson, E.N. 1993. Arsenic toxicity, bacterial resistance and bacterial oxidation/reductions. Phase 1: literature review. Report No. PR 93/109C of Project No. PR 93/132. GENMIN Process Research, Johannesburg.

Nikolov, L.N. and Karamanev, D.G. 1992. Kinetics of the ferrous-iron oxidation by resuspended cells of *Thiobacillus ferrooxidans*. Biotechnology Progress **8**(3): 252-255.

Norris, P.R. and Kelly, D.P. 1978. Toxic metals in leaching systems, pp. 83-102. In: L.E. Murr, A.E. Torma, J.A. Brierley (eds.), Metallurgical applications of bacterial leaching and related microbiological phenomena. Academic Press, New York.

Norris, P.R., Barr, D.W. and Hinson, D. 1988. Iron and mineral oxidation by acidophilic bacteria: affinities for iron and attachment to pyrite, pp. 43-59. In: P.R. Norris and D.P. Kelly (eds.), Biohydrometallurgy. Science and Technology Letters, Kew, Surrey.

Pinches, A., Chapman, J.T., Te Riele, W.A.M. and Van Staden, M. 1988. The performance of bacterial leach reactors for the pre-oxidation of refractory gold-bearing sulphide concentrates, pp. 329-344. In: P.R. Norris and D.P. Kelly (eds.), Biohydrometallurgy. Science and Technology Letters, Kew, Surrey.

Pol'kin, S.I., Panin, V.V., Adamov, E.V., Karavaiko, G.I. and Chernyak, A.S. 1975. Theory and practice of utilizing micro-organisms in difficult-to-dress ores and concentrates, pp. 901-923. In: Proc. 11th International Mineral Processing Congress. Cagliari, 20-26 April 1975.

Poulin, R. and Lawrence, R.W. 1996. Economic and environmental niches of biohydrometallurgy. Minerals Engineering **9**(8): 799-810.

Rawlings, D.E. 1995. Restriction enzyme analysis of 16S rDNA genes for the rapid identification of *Thiobacillus ferrooxidans, Thiobacillus thiooxidans* and *Leptospirillum ferrooxidans* strains in leaching environments, pp. 9-17. In: T. Vargas, C.A. Jerez., J.V. Wiertz and H. Toledo (eds.), Biohydrometallurgical Processing **1**. University of Chile, Santiago.

Rawlings, D.E., Coram, N.J., Gardner, M.N. and Deane, M.N. 1999(a). *Thiobacillus caldus* and *Leptospirillum ferrooxidans* are widely distributed in continuous flow biooxidation tanks used to treat a variety of metal containing ores and concentrates, pp. 777-786. In: R. Amils, A. Ballester (eds.), Biohydrometallurgy and the environment toward the mining of the 21st century **A**. Elsevier, Amsterdam.

Rawlings, D.E., Tributsch, H. and Hansford, G.S. 1999(b). Reasons why *Thiobacillus ferrooxidans* is not the dominant iron-oxidising bacterium in many commercial processes for the biooxidation of pyrite and related ores. Microbiology **145**(1): 5-13.

Shuey, T.T. 1975. Semiconducting Ore Minerals. Elsevier Scientific Publishing Company, Amsterdam.

Suzuki, I. and Lizama, H.M. 1989. Synergistic inhibition of ferrous iron oxidation by *Thiobacillus ferrooxidans* by increasing concentrations of cells. Applied and Environmental Microbiology **55**(5): 1117-1121.

Van Aswegen, P.C., Godfrey, M.W., Miller, D.M. and Haines, A.K. 1991. Developments and innovations in bacterial oxidation of refractory ores. Minerals and Metallurgical Processing **November**: 188-191.

Van Aswegen, P.C. 1993. Bio-oxidation of refractory gold ores. the GENMIN experience, pp. 15.1-15.14. In: Biomine '93. Australian Mineral Foundation, Glenside, SA.

Van Scherpenzeel, D.A. 1996. The kinetics of ferrous-iron oxidation by *Leptospirillum*-like bacteria in absence and in presence of pyrite and pyrite/arsenopyrite mixtures in continuous and batch cultures. M.Sc. Dissertation, University of Cape Town, Cape Town.

Wadsworth, M.E. 1987. Leaching – metals applications, pp. 500-539. In: R.W. Rosseau (ed.), Handbook of Separation Process Technology. John Wiley and Sons, New York.

For my mother, Shirley Breed

Here is
a test to find
whether your mission on earth
is finished:

If you're alive,
it isn't.

ILLUSIONS – Richard Bach

Chapter Two

Literature Review

As stated previously, the objectives of the work were to test the applicability of the multiple sub-process mechanism for the bioleaching of arsenopyrite and to provide kinetic information on the chemical (mineral) ferric leaching and the (bacterial) ferrous-iron oxidation sub-processes for use in a model based on this mechanism. An additional objective of the work was to attempt to gain some insight into the mechanism of arsenic toxicity, and resistance, and its relationship to perturbations in the aeration and agitation of bioleach reactors.

To date most of the work presented in the literature has treated bioleaching as occurring as a single step rather than a series of parallel and/or sequential sub-processes. However, the existence of a multiple sub-process mechanism implies that the bacterial and chemical sub-processes may be studied separately and then combined to yield a model of the overall process. For this reason, the literature review presented below is not intended as a comprehensive review of bioleaching in general, nor of the bioleaching of arsenopyrite.* It has instead been limited to those sub-processes which are directly related to the investigations undertaken, and the models used to describe them. The material covered in the literature review has therefore been limited to the following topics, *viz.*:

i) a brief description of why sulfide ores and concentrates are refractory, the alternative pre-treatment methods available, and the factors which influence bioleaching,
ii) a description of the micro-organisms encountered during bioleaching,
iii) a discussion of the mechanisms by which the bioleaching of arsenopyrite has been alleged to occur,
iv) a review of the toxicity of iron and arsenic, with the emphasis on the mechanism by which arsenic inhibits the metabolic activity of micro-organisms,
v) a review of the models used to describe bioleaching when treated as occurring in a single step,
vi) a discussion of the multiple sub-process mechanism for the bioleaching of sulfide minerals,

---

* Additional information on bioleaching in general and its current and potential applications may be obtained from Rossi (1990), Barrett *et al.* (1993(a)) and Rawlings (1997(a)).

vii) a review of the mechanism and kinetics by which the electrochemical oxidation and ferric leaching of arsenopyrite, and the ferric leaching of pyrite are alleged to occur, and

viii) a review of the models used to describe the oxidation of ferrous-iron by the micro-organisms encountered during the bioleaching of sulfide minerals.

2.1 The Recovery of Gold from Refractory Ores and Concentrates

If gold particles are less than 50 μm in diameter, they may be rendered refractory by encapsulation in minerals such as pyrite, arsenopyrite, pyrrhotite and chalcopyrite. This occurs when the gold and sulfides present in the mineralising fluids precipitate at the same time. Encapsulation renders cyanidation ineffective, even after milling of the ore and concentration of the valuable minerals by flotation. This is because the mineral forms an impervious barrier between most of the gold and the sodium cyanide. Therefore, destruction of the crystalline structure of the sulfide mineral is necessary in order to make the gold amenable to recovery via cyanidation. This can be achieved in a number of ways, the most important of which are roasting, pressure oxidation and bioleaching.*

2.1.1 Roasting

The conventional treatment of gold-bearing refractory ores and concentrates is to roast them in the presence of atmospheric oxygen. Roasting is performed at 600-800°C, and oxidises the sulfur, arsenic and iron in the mineral to sulfur dioxide, SO_2, arsenic trioxide, As_2O_3, and ferric oxide, Fe_2O_3, respectively; the containment of sulfur dioxide and arsenic trioxide contributes to the cost of the process. In addition the gold may be re-encapsulated in dense fused structures resulting from the coexistence of the arsenopyrite oxidation products, troilite and iron arsenate (Zhukov and Smagunov, 1971).

2.1.2 Pressure Oxidation

Pressure oxidation makes use of oxygen, at pressures in the region of 20 atmospheres and temperatures in the region of 200°C, to oxidise the mineral and has been proven by full-scale plant operation. Pressure oxidation of arsenopyrite oxidises the sulfur, arsenic and iron to sulfate, SO_4^{2-}, arsenate, As(V), and ferric-iron, Fe^{+3}, respectively. Like bioleaching, pressure oxidation does not suffer from the production of atmospheric pollutants. However, the severe operating conditions demand a high standard of plant design and choice of materials of construction.

* Although other chemical methods of oxidising sulfide minerals, *viz.* using chlorine, nitric acid and/or sulfuric acid, are possible, they suffer from plant complexity and/or non-competitive economics.

2.1.3 Bioleaching

Bacterial oxidation, or bioleaching, makes use of bacteria to catalyse the oxidation reactions using atmospheric oxygen as the oxidising agent. It may be carried out *in-situ*, using heaps or dumps, or using aerated bioreactors, *i.e.* the slurry process. *In-situ* and heap and dump leaching have the advantage of being cheap and simple to operate. This has resulted in these methods being the most widespread bacterial leaching processes; although the slurry process enables better control of the process, the relatively slow kinetics and the aeration and agitation costs result in it only being feasible for the extraction of high value products, such as gold, from relatively high grade concentrates. Therefore, improvements in the rate of oxidation per unit of reactor volume are important when considering the feasibility of the slurry process; these can be achieved by optimising process conditions such as pH, temperature, solids concentration, particle size, ferric-iron concentration and the bacterial species and concentration.

During the bioleaching of arsenopyrite the sulfur, arsenic and iron in the mineral are oxidised to sulfate, arsenate and ferric-iron, respectively (Van Aswegen, 1993). Therefore, like pressure oxidation, bioleaching does not suffer from the production of atmospheric pollutants. Furthermore, at throughputs of less than 1200 $t.day^{-1}$, bioleaching using aerated bioreactors has an economic advantage over pressure oxidation (Haines and Van Aswegen, 1990).

The first commercial plant to use biooxidation for the liberation of gold from refractory ores was commissioned in 1986 at Fairview Gold Mine in Barberton, South Africa. At present there are stirred tank processes in operation in South Africa, Brazil, Australia and Ghana (Dew *et al.*, 1997), and bioheap operations in the USA (Brierley, 1997). The stirred tank operations in operation at present make use of either the BIOX®* or BACOX† processes; the major difference between these processes is the operating temperature and hence the bacterial species employed. The BIOX® process operates best at a temperature of 40°C and makes use of a mixed mesophilic culture. The BIOX® culture was initially thought to consist of *Leptospirillum ferrooxidans*, *Thiobacillus ferrooxidans* and *Thiobacillus thiooxidans* (Dew *et al.*, 1997). However recent work has shown that it consists primarily of *L. ferrooxidans* and *Thiobacillus caldus* (Rawlings *et al.*, 1999(a)). In contrast to the BIOX® process, the BACOX process uses a moderately thermophilic culture which grows optimally at temperatures between 45 and 55°C (Miller, 1997). The historical background to, and descriptions of, the BIOX® and BACOX processes are presented in Dew *et al.* (1997) and Miller (1997), respectively.

As stated above, heap leaching operations are cheap and simple to operate. For this reason, they have found application in the recovery of copper and of gold from relatively low grade ores. However, in order to facilitate percolation of the liquor through the heap, larger particle sizes are used in heap leaching operations than in slurry processes. This, in turn, results in the overall metal recoveries of heap leaching operations being lower than those obtained in slurry processes (Brierley, 1997). In an attempt to overcome the lower recoveries obtained during conventional heap leaching operations, without incurring the expense associated with slurry processes, Geobiotics Inc. has developed a process whereby refractory gold concentrates are coated onto a support material, with subsequent bioleaching occurring in a stacked heap (Whitlock, 1997). Details on the recovery of gold from refractory gold ores using both conventional heaps and the Geobiotics Process are described in detail in Brierley (1997) and Whitlock (1997), respectively.

* Developed by Gencor S.A. Ltd., Johannesburg, South Africa.
† Developed by BacTech (Australia) Limited, Perth, Australia.

2.1.3.1 Factors affecting bioleaching

The rate and efficiency at which bioleaching proceeds is affected by a number of parameters, many of which are inter-related. Therefore, changes in one parameter may lead to changes in several others within the bioreactor cascade. These interactions increase the complexity of the process and require that a holistic approach be followed when considering a change in the operating conditions of the process.

Concentrate/ore composition and particle size

The relative ease with which a mineral may be degraded depends on its rest potential. The mineral rest potential in turn depends on the nature of the mineral and the type of semi-conduction exhibited, *viz.* p-or n-type (Barrett, 1991). A typical list depicting the ease with which a number of minerals are oxidised is shown in Table 2-1. However, because the rest potential is affected by weaknesses in the crystal lattice, caused by inclusions and impurities, and on variables such as temperature, pH *etc.*, Table 2-1, and similar tables, should only be considered guides. In general however, in such tables pyrite has a higher rest potential than arsenopyrite, which suggests that where pyrite and arsenopyrite are in contact, galvanic interactions will result in arsenopyrite being preferentially leached (Beattie and Poling, 1987).* This phenomenon has been reported for both the chemical (Beattie and Poling, 1987) and bioleaching (Miller and Hansford, 1992(a); Morin *et al.*, 1991) of arsenopyrite/pyrite ores and concentrates. In addition to temperature, galvanic interactions between the minerals will be affected by a number of factors including the relative surface areas of the anodic and cathodic minerals, the efficiency of contact between the minerals and the reaction conditions (pH, conductivity, $[O_2]$, presence of other redox species, *etc.*) (Natarajan and Iwasaki, 1985).

Table 2-1: Galvanic series of sulfide minerals (after Brierley (1993))

Level of difficulty of bacterial oxidation	Mineral	Formula
least difficult	Pyrrhotite	FeS_{1-x}
	Chalcocite	Cu_2S
	Covellite	CuS
↓	Tetrahedrite	$Cu_3(As, Sb)S_{3.25}$
	Bornite	Cu_5FeS_4
	Galena	PbS
	Arsenopyrite	FeAsS
	Sphalerite	ZnS
	Pyrite	FeS_2
	Enargite	$Cu_3(As, Sb)S_4$
	Marcasite	FeS
	Chalcopyrite	$CuFeS_2$
most difficult	Molybdenite	MoS_2

As stated previously, in addition to arsenopyrite, refractory arsenical gold ores generally contain varying amounts of other minerals such as pyrrhotite, pyrite and chalcopyrite. The relative abundance in which these minerals are present will therefore have an effect on the process. Furthermore, other metals such as Pb, Se, Sb

* However, it has been suggested that this effect will decrease with increasing temperature (Beattie and Poling, 1987; Rimstidt *et al.*, 1994).

and Zn may be present in the feed to the process; these may be toxic to the bacterial culture, even in low concentrations.

During bioleaching, pyrrhotite is acid consuming whereas both pyrite and arsenopyrite are acid producing. Therefore, during normal operation of continuous bioleaching plants, a degree of pH correction will be necessary. In addition, the dissolution of pyrrhotite leads to elevated concentrations of ferrous-iron and elemental sulfur in solution (relative to those encountered during the bioleaching of pyrite). Under normal conditions, these species are oxidised to ferric-iron and sulfate. However, if ferrous-iron is present in excess, the reduced redox potential of the bioleaching solution may result in elevated levels of arsenite, As(III), due to conditions being unfavourable for its conversion to arsenate (see Section 2.3). This may in turn have an adverse effect on the bacteria. Furthermore, if arsenite is present in the waste liquor it will precipitate as calcium arsenate, which is unsuitable for long term waste disposal. However, as the Fe:As ratio of the waste liquor should be at least 3:1 in order to produce a stable ferric arsenate residue (Broadhurst, 1994), it is desirable that the feed contain some pyrite or pyrrhotite.

In addition to the presence of some pyrite and/or pyrrhotite in the feed, the presence of carbonate in the mineral is desirable as it increases the carbon dioxide concentration in the bioleaching solution. However, if too much is present it may result in the pH increasing to values that do not favour bioleaching.

The rate of bioleaching has been shown to depend on the surface area of the mineral (Hansford and Chapman, 1992; Miller and Hansford, 1992(a); Hansford and Drossou, 1988), hence a change in the feed size distribution to the process will affect the heat duty, and may require adjustments in the aeration rate. Increasing the solids concentration will have a similar effect to a reduction in the particle size. However, at high pulp densities, the rate and extent of leaching may be affected by oxygen transfer limitations caused by the increased viscosity of the slurry (Bailey and Hansford, 1993; Bailey and Hansford, 1994).

Temperature, T

The exothermic nature of bioleaching reactions, convective heat losses from the bioreactor surfaces and the detrimental effect of temperature variations on the bacteria used in bioleaching make temperature control critical. Furthermore, as each species has its own optimum temperature, if the inoculum is a mixed culture, the operating temperature will determine which species predominates. Therefore, the heat transfer requirement at any particular stage will be affected by the bacterial culture used, its activity and the ambient temperature and relative humidity. However, some degree of temperature tolerance may also be obtained by the micro-organisms. For example, the BIOX® process is generally operated at 40°C. However the primary and secondary bioreactors have been maintained at 45°C and 50°C, respectively, for extended periods without any significant decrease in the performance of the culture (Miller, 1991).*

In addition, variations in temperature have an effect on the rest potential of the mineral and the solubility and mass transfer rates of both oxygen and carbon dioxide.

---

* The increased temperature tolerance in the secondary bioreactors was thought to be related to the fact that the proportion of *T. thiooxidans* increased while the proportion of attached *L. ferrooxidans* decreased down the bioreactor cascade (Dew *et al.*, 1997). However, subsequent work has indicated that the species thought to be *T. thiooxidans* was actually *T. caldus* (Rawlings *et al.*, 1999(a)). *T. caldus* is a moderate thermophile and is capable of growth at temperatures up to 55°C whereas *T. thiooxidans* is a mesophilic micro-organism.

pH

Each species also has its own optimum pH (see Section 2.2), hence pH will also have an effect on which species will predominate. Furthermore, the pH will have an effect on the degree and rate of jarosite and ferric arsenate precipitation and on the rest potential of the mineral (Fernandez *et al.*, 1996), and hence on the leaching rate. However, variations in the pH of the bioleaching slurry may occur as a result of variations in the mineralogical composition of the ore being treated and the activity of the bacterial population.

Redox potential, E_h

The driving force in bioleaching is determined by the difference in the rest potentials of the minerals present, and the redox potential of the bioleaching solution. In addition, the redox potential provides a good indication of the ferric/ferrous-iron ratio, hence providing a quick and easy method for the early detection of a reduction in the bacterial activity, *viz.* an increase in the ferrous-iron concentration.

Toxic effect of metals

In comparison to other bacterial species, acidophilic chemolithoautotrophic bacteria are characterised by their high degree of inherent resistance to the toxic effect of metal ions. The principles which govern the resistance of these bacteria to metal ions depends on their physiological state and the oxidation state and chemical form of the metal ion (Norris and Kelly, 1978). Furthermore, the resistance of wild-type bacterial strains will vary depending on their respective habitat; strains more resistant to the toxic effects of specific metals may be isolated from regions associated with leaching of minerals containing these metals.

The high tolerance of chemolithoautotrophic bacteria to metals can be attributed to bacterial resistance mechanisms, *e.g.* plasmid mediated resistance, and chemical factors attributed to their growth conditions (Barrett *et al.*, 1993(a)), *viz.*:

i) the protonation of the anionic sites on the cell walls, as a result of the low pH of the medium, reduces the availability of binding sites for the metal cations,
ii) the presence of ions which facilitate the precipitation of the metal ions, or their conversion into complexes which have a reduced bio-availability, and
iii) the presence of substances that compete with the toxic species for sites on the cell wall of the bacteria, *e.g.* K^+ and Th^+.

Furthermore, bacteria may acquire resistance through a process of natural selection.

Because of the high concentrations of arsenic encountered during the bioleaching of arsenopyrite, the toxicity of arsenic to bacteria and the mechanisms of bacterial resistance to arsenic are described in greater detail below (see Section 2.4). Furthermore, as arsenite is alleged to be more toxic than arsenate, the conditions affecting the oxidation of arsenite to arsenate will also affect the process, *e.g.* ore mineralogy, pH, redox potential, galvanic interactions *etc.* (see Section 2.3).

Bacterial species and concentration

The bacterial species, and their respective concentrations in each of the bioreactors in the bioreactor cascade will be determined to a large degree by the conditions (T, pH, E_h, substrate concentration, toxic species concentration, *etc.*) in each of the bioreactors, and the inoculum used.

Dissolved oxygen, $[O_2]$, and carbon dioxide, $[CO_2]$, concentrations

Oxygen and carbon dioxide are generally supplied to the process in the form of compressed air. In most instances oxygen supply is the rate-limiting step, even though the oxygen utilisation rate is only in the region of 30 % (Miller, 1997; Van Aswegen, 1993). Dissolved oxygen concentrations in the region of 0.063 mmol $O_2.\ell^{-1}$ are generally maintained (Miller, 1997; Van Aswegen, 1993).* It has been shown that, in the absence of carbon dioxide supplementation, it will become mass transfer limiting before oxygen (Nagpal *et al.*, 1991; Liu *et al.*, 1988). However, the presence of carbonate in the feed to the process generally serves to eliminate this limitation. In addition, carbonate may be used to control the pH in the primary bioreactor, further ensuring that the dissolved carbon dioxide concentration does not become limiting.

The solids concentration and the operating temperature will also have an effect on the mass transfer rate and the solubility of both oxygen and carbon dioxide.

The oxygen utilisation rate, $-r_{O_2}$, is the most important parameter in the assessment of bacterial culture activity. During stable operation the dissolved oxygen concentration of the bioleaching slurry should remain constant and can be related to the extent of sulfide oxidation. A decrease in the dissolved oxygen concentration indicates an increase in the oxygen demand because of an increase in the bacterial activity. Conversely, an increase in the dissolved oxygen concentration indicates a decrease in the oxygen demand because of a reduction in the bacterial activity. High oxygen utilisation rates therefore indicate good plant performance while low oxygen utilisation rates indicate poor plant performance.

Chloride concentration, $[Cl^-]$

The bacterial strains used in the bioleaching of sulfide minerals are generally not tolerant to saline process water; this has been found to be a result of intolerance to chloride, Cl^-, and not to sodium ions, Na^+, (Lawson *et al.*, 1995). Lawson *et al.* (1995) found *T. ferrooxidans* to be affected detrimentally at $[Cl^-] \approx 14$ mmol.ℓ^{-1} and Dew *et al.* (1997) reported that the BIOX® culture was inhibited at $[Cl^-] \approx$ 0-140 mmol.ℓ^{-1}. In contrast to the above, Madgewick (1989) observed competitive inhibition of iron oxidation at [NaCl] > 151 mmol.ℓ^{-1} and reported that a tolerance to chloride can be obtained, especially in the case of heap leaching operations. However, this phenomenon may be a result of natural selection with regard to the species present rather than to a particular species becoming tolerant to chloride.

Chloride also contributes to the formation of jarosite precipitates which may reduce the efficiency of bioleaching by coating the mineral surfaces and/or lead to a reduction in the efficiency of cyanidation (Dew, 1995).

* It has been reported that *T. ferrooxidans* will not grow at dissolved oxygen concentrations below 0.0063 mmol.ℓ^{-1}, and that dissolved oxygen concentrations in excess of 0.091-0.022 mmol.ℓ^{-1} are required to ensure that oxygen is not the limiting substrate (Liu *et al.*, 1988).

Nutrients

Inorganic nutrient salts need to be added to the bioleaching medium; these provide a source of nitrogen, potassium and phosphorous,* and are generally added as $(NH_4)_2SO_4$, $(NH_4)_2HPO_4$ and K_2SO_4, respectively.* The nutrient levels in the medium need to be monitored, as they may precipitate in the form of jarosite.

Trace elements such as zinc and manganese are usually available in the required quantities from the dissolution of the mineral itself.

2.2 Bioleaching Micro-organisms

Bioleaching is generally carried out using acidophilic bacteria, *i.e.* bacteria that grow at pH values below pH 4.0. Several acidophilic bacteria have been reported to be capable of growth at pH values below pH 1.0 (Hallberg, 1995). The use of acidophilic bacteria in bioleaching is important due to the low solubility of many metals liberated during the leaching process at higher pH values, *e.g.* ferric-iron precipitates as jarosite at pH values greater than pH 2.0. In addition to the above pH classification, the micro-organisms used in bioleaching may be classified according to the temperature at which they grow optimally; the three classes proposed on this basis are: mesophiles, moderate thermophiles and extreme thermophiles. The most important and commonly encountered (autotrophic) bioleaching micro-organisms are listed in Table 2-2.

At present most commercial bioleaching operations make use of mesophilic cultures and are operated at temperatures in the region of 40°C. Although no commercial plants using thermophiles are currently in operation, the accelerated biological and chemical reaction rates possible at higher temperatures have led to considerable research into the use of these micro-organisms.

2.2.1 Mesophiles

The mesophilic bacteria most commonly isolated from inorganic mining environments are *T. ferrooxidans*, *L. ferrooxidans* and *T. thiooxidans*. Until recently, *T. ferrooxidans* was considered the micro-organism primarily responsible for the bioleaching of sulfide ores and concentrates. For this reason most of the research relating to the mechanism, kinetics and other factors affecting bioleaching has focussed on *T. ferrooxidans*. However, recent research has shown that *L. ferrooxidans* is at least as important, if not more important than *T. ferrooxidans* (Rawlings *et al.*, 1999(a); Rawlings *et al.*, 1999(b); Dew *et al.*, 1997; Boon, 1996; Rawlings, 1995; Sand *et al.*, 1992; Hallmann *et al.*, 1993; Norris *et al.*, 1988; Helle and Onken, 1988). Furthermore, the results of recent research has indicated that, in many cases, the organism thought to have been *T. thiooxidans* may have in fact been *T. caldus* (Rawlings *et al.*, 1999(a)).

Helle and Onken (1988) found that the batch bioleaching rates observed using mixed cultures of *T. ferrooxidans* and a *Leptospirillum*-like bacterium did not differ significantly from those observed using *T. ferrooxidans* alone. However, the presence of *Leptospirillum*-like bacteria in continuous bioleaching systems resulted in a leaching

* Arsenate is an analog of phosphate, hence phosphate plays an important role in bacterial resistance to arsenate.

rate that was 3.9 times greater than the rate achieved in their absence. Sand *et al.* (1992) confirmed that for indirect leaching *L. ferrooxidans* is as important as *T. ferrooxidans*. Norris *et al.* (1988) reported *L. ferrooxidans* to have a higher affinity for ferrous-iron than *T. ferrooxidans* and suggested that this characteristic was responsible for their different oxidation capacities.

Table 2-2: Temperature range and substrate utilised by the most important and commonly encountered (autotrophic) bioleaching micro-organisms (after Hallberg (1995), unless otherwise stated)

Optimal temperature range	Substrate utilised	Micro-organism
Mesophiles 20-45°C	Reduced inorganic sulfur compounds	*Thiobacillus acidophilus* *T. thiooxidans* *T. ferrooxidans*
	Ferrous-iron	*T. ferrooxidans* *L. ferrooxidans*
	Sulfide minerals	*T. ferrooxidans* *L. ferrooxidans*
Moderate thermophiles 45-55°C	Reduced inorganic sulfur compounds	*T. caldus* *Sulfobacillus thermosulfidooxidans*
	Ferrous-iron	*S. thermosulfidooxidans*
	Sulfide minerals	*S. thermosulfidooxidans*
Extreme thermophiles > 55°C	Reduced inorganic sulfur compounds	*Sulfolobus acidocaldarius* *Acidianus brierleyi* *Sulfolobus metallicus*†
	Ferrous-iron	*S. acidocaldarius* *A. brierleyi* *S. metallicus*‡
	Sulfide minerals	*S. acidocaldarius* *A. brierleyi* *S. metallicus**

T. ferrooxidans, *T. thiooxidans* and *L. ferrooxidans* are all Gram-negative, obligately autotrophic bacteria. *T. ferrooxidans* and *T. thiooxidans* are rod shaped, ranging from 0.3 to 0.8 μm in diameter and from 0.9 to 2 μm in length (Barrett *et al.*, 1993(a)), whereas *L. ferrooxidans* is generally spiral shaped and 0.5 to 3 μm in size (Van Scherpenzeel, 1996). However, if the concentration of ferric-iron in the bioleaching liquor is high *L. ferrooxidans* may take on a coccoid appearance as a result of ferric-iron being incorporated into the EPS (Barrett *et al.*, 1993(a)).

T. ferrooxidans is able to obtain energy by using either ferrous-iron or reduced sulfur compounds as an electron donor. However, *L. ferrooxidans* and *T. thiooxidans* are only able to use ferrous-iron and reduced sulfur compounds as an electron donor, respectively. This enables *T. ferrooxidans* to produce more energy per mole of pyrite oxidised than either *L. ferrooxidans* or *T. thiooxidans*. A difficulty in using the ability to oxidise both iron

* Although *L. ferrooxidans*, *T. ferrooxidans* and *T. thiooxidans* have the genes required to fix atmospheric nitrogen, to date only *L. ferrooxidans* and *T. ferrooxidans* have been shown capable of doing so (Dew *et al.*, 1997).
† Norris (1997).
‡ Searby and Hansford, unpublished data.

and sulfur to differentiate between *T. ferrooxidans* and *T. thiooxidans* is that many *T. ferrooxidans* strains exhibit a delay when switching from sulfur to iron substrates and/or vice versa.

For many years, *T. ferrooxidans* and *T. thiooxidans* were considered to be obligate aerobes. However, both can reduce ferric-iron to ferrous-iron anaerobically provided reduced sulfur compounds are available to serve as an electron donor (Brock and Gustafson, 1976). In the case of *T. ferrooxidans* this has been shown to provide energy for growth (Pronk, 1992).

The temperature and pH ranges across which *T. ferrooxidans*, *T. thiooxidans* and *L. ferrooxidans* are able to grow, and their respective optimal conditions for growth are listed in Table 2-3.

Table 2-3: Temperature and pH ranges across which *T. ferrooxidans*, *T. thiooxidans* and *L. ferrooxidans* are able to grow, and their reported optimal values (*T. ferrooxidans*, *T. thiooxidans* data was obtained from Barrett *et al.* (1993(a)); *L. ferrooxidans* data was obtained from Van Scherpenzeel (1996))

Property	*T. ferrooxidans*	*T. thiooxidans*	*L. ferrooxidans*
pH range	1.0-6.0	0.5-6.0	0.5-4
pH_{opt}	2.0-2.5	2.0-2.5	1.5-2.0
Temperature range (°C)	2-40	2-40	15-45
T_{opt} (°C)	28-35	28-30	35

T. ferrooxidans has a mean generation time, t_g, of between 5 and 12 hours whereas *L. ferrooxidans* has a mean generation time of between 10 and 15 hours. However, as *L. ferrooxidans* has a greater affinity for ferrous-iron, *i.e.* it is less sensitive to ferric-iron inhibition, it will continue to thrive at higher redox potentials than *T. ferrooxidans* (Norris *et al.*, 1988; Sand *et al.*, 1992). The above characteristics result in *T. ferrooxidans* dominating in batch culture while *L. ferrooxidans* dominates in continuous culture, and contributed to *T. ferrooxidans* being (incorrectly) regarded as the micro-organism primarily responsible for the bioleaching of sulfide ores and concentrates.

In addition to the species listed in Table 2-3, a thermotolerant strain of *L. ferrooxidans*, with a proposed name of *Leptospirillum thermoferrooxidans*, has been described by Golovacheva *et al.* (1992). It is alleged to have temperature and pH optima of 45-50°C and pH 1.65-1.90, respectively (Golovacheva *et al.*, 1992). However, its detailed characteristics and phylogenetic relationship to *L. ferrooxidans* have not yet been completely determined.

2.2.2 Moderate Thermophiles

Moderately thermophilic bacteria may be isolated from sulfide ore dumps, volcanic regions and thermal springs. It is possible that the use of moderate thermophiles in bioleaching operations will constitute an economically viable compromise between the advantages and disadvantages of extreme thermophiles, *viz.*:

i) accelerated rates of biological and chemical reactions in comparison with mesophiles, and
ii) increased solubility of oxygen and carbon dioxide in comparison with thermophiles.

The moderately thermophilic bacteria most commonly encountered within the context of bioleaching are *T. caldus* and *S. thermosulfidooxidans*.

T. caldus may be readily isolated from bioleaching processes operating at temperatures between 30 and 40°C which has led to the suggestion that their role in commercial bioleaching operations may have been under-estimated to date (Rawlings *et al.*, 1999(a); Rawlings, 1997(b)). The cells are short, motile, Gram-negative rods. They are capable of chemolithoautotrophic growth on reduced sulfur substrates such as thiosulfate, tetrathionate, sulfide, sulfur and molecular hydrogen, and have been described as the moderately thermophilic equivalent of *T. thiooxidans* (Hallberg, 1995).

S. thermosulfidooxidans are commonly isolated from the heating region in dumps, which suggests that they play an important role in the leaching of metals in these environments. The cells are Gram-positive and although the morphology of the different subspecies may vary to a degree, they generally occur as straight rods 0.5-1 µm by 1-6 µm (Karavaiko *et al.*, 1988). Although none of the subspecies has flagella, they do have pili (Karavaiko *et al.*, 1988).

All the subspecies of *S. thermosulfidooxidans* are facultatively autotrophic, aerobic eubacteria. They are unable to assimilate sulfate into proteins, hence they cannot grow on pyrite or ferrous-iron unless a source of reduced sulfur is present (Norris and Barr, 1985). However, they are capable of growth under heterotrophic conditions without losing their ability to catalyse mineral oxidation. The temperature and pH ranges across which *T. caldus* and the different subspecies of *S. thermosulfidooxidans* are able to grow are listed in Table 2-4, together with the optimal conditions for each.

Table 2-4: Temperature and pH ranges across which *T. caldus* and *S. thermosulfidooxidans* are able to grow, and their reported optimal values (*T. caldus* data was obtained from Hallberg (1995); *S. thermosulfidooxidans* data was obtained from Karavaiko *et al.* (1988))

	pH range	pH_{opt}	Temperature range (°C)	T_{opt} (°C)
T. caldus	1.0-3.5	2.0-2.5	32-52	45
S. thermosulfidooxidans				
type strain VKM B-1269	1.5-5.5	1.9-2.4	$T_{max} \approx 58$	50
subsp. *asporogenes*	1.2-4.2	2.5-2.7	$T_{max} \approx 50$-58	37-42
subsp. *thermotolerans* *	2.0-4.5	2.3-2.5	$T_{max} \approx 58$-60	50

2.2.3 Extreme Thermophiles

As stated previously, bioleaching using extreme thermophiles has the potential of accelerated rates of biological and chemical reactions in comparison with those possible at lower temperatures. A further advantage of operating at elevated temperatures would be the reduction in the cooling duty. Miller (1991) calculated the cooling duty to be a minimum for a 150 $t.day^{-1}$ BIOX® plant operating at about 65°C. Although the optimum

* The pH ranges listed for subsp. *thermotolerans* in Table 2-4 are for growth on sulfur. For growth on ferrous-iron, the pH range for growth is pH 1.5 to 3.9 with $1.6 < pH_{opt} < 1.8$.

operating temperature will depend on the local climatic conditions, the above example does however illustrate a potential advantage of bioleaching using extreme thermophiles.

In addition to advantages, operating at elevated temperatures does have a number of disadvantages, *viz.*:

i) the reduced solubility of both oxygen and carbon dioxide,
ii) increased evaporative losses (or a condensation requirement), and
iii) the aggressive nature of highly oxidising acidic slurries at temperatures in excess of 50°C requires the choice of appropriate materials of construction.

The only acidophilic extreme thermophiles described to date are archae. Archae represent an independent branch in the evolution of micro-organisms and have been isolated from geothermal hot springs and burning coal tips. In addition, temperatures in the region 50-80°C have been measured in heap leaching operations which suggests that extreme thermophiles may occur naturally in such environments.

The only archae genera of importance in biohydrometallurgy are alleged to be *Sulfolobus* and *Acidianus* (Barrett *et al.*, 1993(a)). Although they have a negative response to the gram-staining test, they cannot be described as being Gram-negative. Both *Sulfolobus* and *Acidianus* are coccoid shaped, with diameters in the region of 1 μm, and immotile. Neither have flagella. However the *Sulfolobus* species have pili-like structures; it is suspected that they are involved in the mechanism of attachment to surfaces.

S. acidocaldarius and *A. brierleyi* are facultative chemolithoautotrophs and grow under autotrophic, mixotrophic or heterotrophic conditions (Barrett *et al.*, 1993(a)), whereas *S. metallicus*, is strictly chemolithoautotrophic (Huber and Stetter, 1991). *S. acidocaldarius* can oxidise elemental sulfur under anaerobic conditions, utilising ferric-iron as the terminal electron acceptor (Brock and Gustafson, 1976). Although both *S. acidocaldarius* and *A. brierleyi* have been shown to be capable of using Mo^{6+} as a terminal electron acceptor (Brierley and Brierley, 1982), this has not been shown to be an energy conserving process for *S. acidocaldarius* (Hallberg, 1995). For this reason *S. acidocaldarius* (Hallberg, 1995) and *S. metallicus* (Huber and Stetter, 1991) are considered to be strict aerobes. In contrast to the above, *A. brierleyi* is capable of anaerobic growth on sulfur; this energetic pathway produces H_2S. The temperature and pH ranges across which *S. acidocaldarius*, *S. metallicus* and *A. brierleyi* are able to grow, and their respective optimal conditions for growth are listed in Table 2-5.

Table 2-5: Temperature and pH ranges across which *S. acidocaldarius*, *S. metallicus* and *A. brierleyi* are active, and their reported optimal values (*S. acidocaldarius* and *A. brierleyi* data was obtained from Barrett *et al.* (1993(a)); *S. metallicus* data was obtained from Huber and Stetter (1991))

Property	*S. acidocaldarius*	*A. brierleyi*	*S. metallicus*
pH range	1.0-5.9	1.0-5.9	1.0-4.5
pH_{opt}	2.0-3.0	1.5-2.0	
Temperature range (°C)	55-80	55-80	50-75
T_{opt} (°C)	70	70	65

2.3 The Bioleaching of Arsenopyrite

Arsenopyrite, FeAsS, is the most commonly occurring arsenic containing sulfide mineral. It is chiefly associated with other metallic sulfides such as galena (PbS), sphalerite (ZnS), chalcopyrite ($CuFeS_2$) and pyrite (FeS_2).

The bioleaching of arsenical sulfides solubilises iron, arsenic and sulfur and is thought to take place in a number of parallel and/or sequential stages, the overall reaction of which is (Barrett *et al.*, 1993(a)):

$$2\,FeAsS + 7O_2 + 2H_2O \rightarrow 2Fe^{3+} + 2H_3AsO_4 + 2HSO_4^- \quad (2\text{-}1)$$

It is accepted that the first stage of the process results in the solubilisation of the iron and the arsenic in the mineral, as ferrous-iron, Fe^{2+}, and arsenite, As(III), respectively (Barrett *et al.*, 1993(b); Barrett *et al.*, 1989; Shrestha, 1988; Pol'kin *et al.*, 1975). However, there is still some controversy with regard to the fate of the sulfur moiety. Barrett *et al.* (1993(b)), Barrett and Hughes (1993) and Shrestha (1988) alleged that the sulfur is solubilised as sulfate, SO_4^{2-}, whereas Fernandez *et al.* (1995), Morin *et al.* (1991) and Pol'kin *et al.* (1975) claimed that the sulfur is solubilised as elemental sulfur, S^0. The solubilisation of arsenopyrite to produce sulfate and elemental sulfur is shown in Equations 2-2 and 2-3, respectively:*

$$4\,FeAsS + 11O_2 + 6H_2O \rightarrow 4FeSO_4 + 4H_3AsO_3 \quad (2\text{-}2)$$

$$4\,FeAsS + 3O_2 + 2H_2O \rightarrow 2Fe^{2+} + 4HAsO_2 + 4S^0 \quad (2\text{-}3)$$

The ferrous-iron is subsequently oxidised to the ferric form by the ferrous-iron-oxidising bacteria in the bioleaching slurry according to;

$$2Fe^{2+} + \tfrac{1}{2}O_2 + 2H^+ \leftrightarrow 2Fe^{3+} + H_2O \quad (2\text{-}4)$$

At 35°C, $\Delta G_f^0 = -42.381$ kJ.(mol FeAsS)$^{-1}$ (Malatt, 1998) for the above reaction.

In the case of elemental sulfur formation, the suspended elemental sulfur is allegedly oxidised to sulfate by sulfur oxidising bacteria in the bioleaching solution (Pol'kin *et al.*, 1975) according to;

$$2S + 3O_2 + 2H_2O \rightarrow 2H_2SO_4 \quad (2\text{-}5)$$

Depending on the conditions employed, the dissolution of arsenopyrite may be followed by the oxidation of arsenite, As(III), to arsenate, As(V), followed by the precipitation of ferric-iron and arsenate as ferric arsenate (Dew *et al.*, 1997):

$$2H_3AsO_4 + Fe_2(SO_4) \rightarrow 2FeAsO_4 + 3H_2SO_4 \quad (2\text{-}6)$$

* According to the bioleaching mechanism proposed by Sand *et al.* (1999), the sulfur moiety of sulfide minerals is oxidised, via either thiosulfate or polysulfides, to sulfate; this step may occur either chemically or bacterially. However, Sand *et al.* (1999) do not specify which sulfur pathway is followed during the bioleaching of arsenopyrite. This mechanism is discussed in greater detail in Section 2.6.

Arsenite is alleged to be the most toxic form of arsenic (Coddington, 1986), hence the oxidation of arsenite to arsenate is a very important reaction during the bioleaching of ores containing arsenic. However, at present there is a lack of consensus in the literature with regard to the mechanism by which this reaction occurs. It has been suggested that the arsenite is oxidised to arsenate by either oxygen (Panin *et al.*, 1985):

$$H_3AsO_3 + \tfrac{1}{2}O_2 \rightarrow H_3AsO_4 \qquad (2\text{-}7)$$

or by ferric-iron (Shrestha, 1988):

$$H_3AsO_3 + 2Fe^{3+} + H_2O \rightarrow H_3AsO_4 + 2Fe^{2+} + 2H^+ \qquad (2\text{-}8)$$

At 35°C, ΔG^0_f of the reactions shown in Equations 2-7 and 2-8, is –125.41 and 33.687 kJ.(mol H_3AsO_4)$^{-1}$, respectively (Malatt, 1998).

Although the oxidation of arsenite to arsenate by oxygen (Equation 2-7) is thermodynamically possible, it has been shown to be extremely slow (Eary and Schramke, 1990). Therefore, as the positive free energy value for the reaction shown in Equation 2-8 indicates that it is not thermodynamically possible, the arsenic in solution after the leaching of arsenopyrite would be expected to be in the form of arsenite. The above was confirmed by Morin *et al.* (1991), who found that the conversion of arsenite to arsenate proceeded at a low rate during the bioleaching of a concentrate which consisted primarily of arsenopyrite. More than 87 % of the arsenic in solution was present as arsenite.

However, during the bioleaching of ores and concentrates that contain both pyrite and arsenopyrite, most of the arsenic in solution is found to exist as arsenate. This suggests that the oxidation of arsenite to arsenate is more rapid than the leaching of arsenopyrite (Barrett *et al.*, 1993(a)). However, neither the mixed culture used by Barrett *et al.* (1993(b); 1989), nor *T. ferrooxidans* (Mandl *et al.*, 1992; Wakao *et al.*, 1988; Braddock *et al.*, 1984), nor *T. thiooxidans* (Wakao *et al.*, 1988) have been found capable of oxidising arsenite to arsenate.

In spite of the above, the results obtained by Barrett *et al.* (1993(b)) led these workers to conclude that the oxidation of arsenite to arsenate by ferric-iron requires the presence of both active bacteria and a pyrite (Barrett *et al.*, 1993(b); Barrett *et al.*, 1989) or chalcopyrite (Barrett *et al.*, 1993(b)) surface.* Barrett *et al.* (1993(a)) offered two possible explanations for the above:

i) the bacteria "condition" the surface of the mineral thereby catalysing the oxidation reaction, or
ii) some of the ferrous-iron released at the surface does not enter the bulk solution, but is oxidised to ferric-iron by the bacteria attached to the pyrite surface. The ferric-iron formed in this way may be in the form of a sulfato-complex and if an arsenite ion entered the system, it would be oxidised to arsenate. The arsenate would then reach the bulk solution as a ligand to a ferric-iron species.

A review of the literature available on the oxidation of arsenite to arsenate led Welham (1994) to conclude that the oxidation reaction was only possible by a 2é step and not a 1é step, *e.g.* As(III) is rapidly oxidised to As(V) by iodine, bromate, cerium(IV) or manganate(IV) in the presence of iodate catalyst. However ferric-iron alone is unable to oxidise arsenite to arsenate.

* In contrast to the above, Mandl *et al.* (1992) found that the bioleaching of a chalcopyrite contaminated with arsenopyrite resulted in a constant arsenite concentration, with about 70 % of the arsenic present as arsenite. In other words, the chalcopyrite was unable to catalyse the oxidation of arsenite to arsenate.

The results obtained by Barrett *et al.* (1989) and the conclusions drawn by Welham (1994) suggest that sulfide minerals higher in the galvanic series than arsenopyrite may catalyse the oxidation of arsenite by acting as conduits of charge. In other words, they facilitate the transfer of electrons from one arsenite ion to two ferric-iron ions. According to the proposed mechanism the ability of, and degree to which, a mineral is able to act as catalyst depends on its relative position in the galvanic series. In the case of minerals that leach more easily than arsenopyrite, the kinetic preference would be the dissolution of the mineral rather than the catalysis of the arsenite to arsenate reaction. In addition, the catalytic ability of a mineral may be affected by the stoichiometry of its ferric leaching reaction; if the stoichiometric coefficient of ferric-iron is one, leaching of the catalysing mineral may be significant. A schematic representation of the proposed mechanism is shown in Figure 2.1.

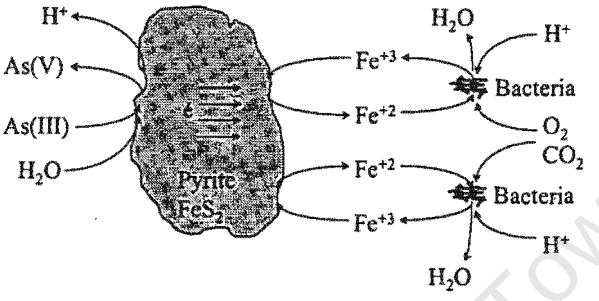

Figure 2.1: Diagrammatic representation of the proposed mechanism of arsenite oxidation.

According to the above mechanism, the differences between the catalytic activity of chalcopyrite observed by Barrett *et al.* (1993(b)) and Mandl *et al.* (1992) can be attributed to differences in the rest potential of the mineral used during the respective investigations. These differences could be attributed to the presence of different impurities being present in the respective samples, to differences in the experimental conditions employed, or to differences between the chalcopyrite itself.*

2.4 The Toxicity of Iron and Arsenic to Bioleaching Micro-organisms

High concentrations of iron and arsenic in solution have been found to inhibit bacterial activity (Barrett *et al.*, 1989; Shrestha, 1988; Trevors *et al.*, 1985; Braddock *et al.*, 1984; Norris and Kelly, 1978; Pol'kin *et al.*, 1975).

2.4.1 The Inhibitory Effect of Iron

Ferrous-iron, Fe^{2+}, concentrations in excess of 700 mmol.ℓ^{-1} have been reported to inhibit carbon dioxide fixation in *T. ferrooxidans*. In addition, ferrous-iron has been reported to be more toxic to *T. ferrooxidans* than *T. thiooxidans* (Collinet and Morin, 1990).

* Natarajan (1988) reported pyrite to be nobler than chalcopyrite, whereas Brierley (1993) reported chalcopyrite to be nobler than pyrite.

On the other hand, ferric-iron, Fe^{3+}, has been found to inhibit ferrous-iron oxidation by *T. ferrooxidans* competitively. Therefore, the rate at which ferrous-iron is oxidised by *T. ferrooxidans* is dependent on the redox potential of the solution (Kelly and Jones, 1978). In addition, although ferric-iron has been found to have a similar effect on *T. thiooxidans* and *T. ferrooxidans* at low ferric-iron concentrations, at high concentrations it has been found to be less toxic to *T. thiooxidans* than *T. ferrooxidans*. Although it has been reported that the ferric-iron inhibition of *T. ferrooxidans* can be partially relieved by increased concentrations of potassium (Kelly and Jones, 1978), this may simply be attributable to an increase in the degree of jarosite formation.

2.4.2 The Inhibitory Effect of Arsenic

Arsenite, As(III), is alleged to be the most toxic form of arsenic (Coddington, 1986). It inactivates enzymes with thiol (HS) groups at the active centre by binding to two different groups on the enzyme (Coddington, 1986). This results in carbohydrate depletion and diminished glutathione (GSH) (Aposhian and Aposhian, 1989). The latter protects cells against radiation effects, oxidative damage and certain toxic compounds (Aposhian and Aposhian, 1989). On the other hand, the toxicity of arsenate to micro-organisms is related to its similarity to phosphate.* It enters the cell via the phosphate transport system and may replace the phosphate in ATP to form an unstable ADP-arsenate complex (Coddington, 1986).

Arsenite is allegedly present in the bioleaching medium as either $HAsO_2$ (Barrett *et al.*, 1989; Shrestha, 1988) or H_3AsO_3 (Pol'kin *et al.*, 1975) (arsenious acid). It has been reported to inhibit a wide range of micro-organisms (Barrett *et al.*, 1993(b); Barrett and Hughes, 1993; Huysmans and Frankenberger, 1992; Lindström and Sehlin, 1989; Barrett *et al.*, 1989; Dabbs and Sole, 1988; Silver *et al.*, 1981), including *T. ferrooxidans* (Cassity and Pesic, 1995; Collinet and Morin, 1990; Pol'kin *et al.*, 1975), *T. thiooxidans* (Collinet and Morin, 1990), *T. caldus* (Hallberg, 1995) and the mixed culture used in commercial BIOX ® operations (Lawson, 1993) to a greater degree than arsenate.† Furthermore, arsenite has been reported to have a more pronounced effect on *T. thiooxidans* than on *T. ferrooxidans*, whereas arsenate has been reported to have a similar effect on both *T. thiooxidans* and *T. ferrooxidans* (Collinet and Morin, 1990).

The addition of non-lethal concentrations of arsenite to thiobacilli has been reported to result in an increase in the lag time prior to bioleaching of the mineral (Cassity and Pesic, 1995; Collinet and Morin, 1990; Barrett *et al.*, 1989; Pol'kin *et al.*, 1975). The above has been attributed to the fact that the required membrane-associated enzyme protecting systems develop, or the selection of tolerant cells occurs, during the lag period (Tuovinen *et al.*, 1971). However, as the arsenite is usually oxidised to arsenate‡ during this lag period, it may simply be a result of the fact that arsenate is less toxic to the species present than arsenite. This phenomenon may also be related to the fact that the extent of arsenic toxicity is less pronounced if the substrate is a sulfide mineral *cf.* ferrous-iron as substrate (Norris and Kelly, 1978; Tuovinen *et al.*, 1971).

The addition of 10 mmol.ℓ^{-1} arsenite to a culture of *T. caldus*, unconditioned to arsenite, had a bactericidal effect on the culture (Hallberg, 1995). However, bacteria that had been grown in the presence of sub-toxic concentrations of arsenite for a few generations were capable of growth, without experiencing a lag phase, when inoculated into medium containing 10 mmol.ℓ^{-1} arsenite (Hallberg, 1995). Furthermore, growth in media

* Arsenate is an analog to phosphate (Huysmans and Frankenberger, 1992; Coddington, 1986), *e.g.* phosphate fertilisers mobilise arsenate because of competition for adsorption sites (Hindmarsh and McCurdy, 1986).

† The mixed culture used in the BIOX® process was initially resistant to 13.3 mmol As.ℓ^{-1}. However, this resistance has subsequently increased to 293.3 mmol As.ℓ^{-1} (Lawson, 1993).

‡ The arsenate has been reported to occur as either H_3AsO_4 (Barrett *et al.*, 1989; Shrestha, 1988) or $H_2AsO_4^-$ (Pol'kin *et al.*, 1975) (arsenic acid).

containing sub-toxic amounts of arsenite, arsenate or antimony conferred similar resistance to all three of these ionic species; this suggests that the resistance to these ions is due to the same genetic locus (Hallberg, 1995). No detoxification of the ions was observed during these experiments; the spent arsenical media was still toxic to uninduced *T. caldus* (Hallberg, 1995).* Instead the resistance appeared to be due to a reduction in the bio-accumulation of the ions; induced strains took up approximately 10-fold less arsenate than uninduced strains (Hallberg, 1995). Furthermore, induced strains also exhibited an energy dependent efflux of accumulated arsenate (Hallberg, 1995). An increase in the phosphate concentration in the nutrient media also resulted in a reduction in the bio-accumulation of arsenate. This suggests that the arsenate enters via the phosphate uptake system; this is the mechanism by which arsenate has been shown to enter *Escherichia coli* (see Section 2.4.3).

During an investigation into the effect of arsenite and arsenate on a mixed culture of thiobacilli, not conditioned to high arsenic levels and growing on pyrite ($\rho_{pulp} \approx 1$ %, T≈42°C), arsenite concentrations in the region of 30 mmol.ℓ^{-1} were found toxic to the micro-organisms; arsenite concentrations in the region of 90 mmol.ℓ^{-1} were found in dead cultures (Barrett *et al.*, 1989).† The results obtained by Barrett *et al.* (1989) led these workers to conclude that the toxicity of arsenite to the bacteria encountered during bioleaching operations is in the region of three times that of arsenate. The results obtained by Barrett *et al.* (1989) are shown in Figure 2.2.

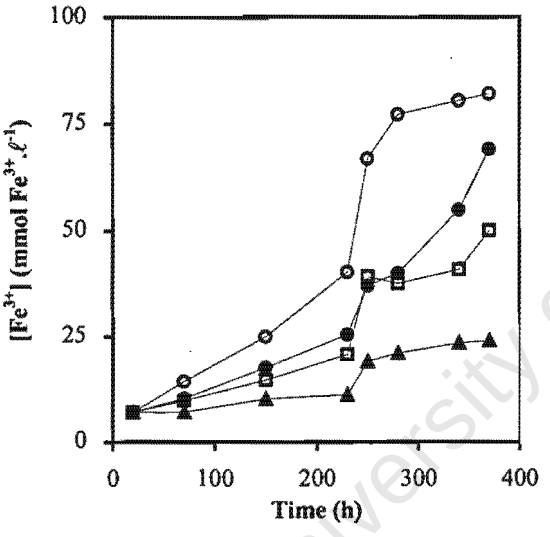

Figure 2.2(a): Effect of arsenite on the solubilisation of ferric-iron during the bioleaching of pyrite (after Barrett *et al.* (1989)).
[o] 0 mmol As(III).ℓ^{-1}; [•] 2 mmol As(III).ℓ^{-1};
[□] 19 mmol As(III).ℓ^{-1}; [▲] 46 mmol As(III).ℓ^{-1}.

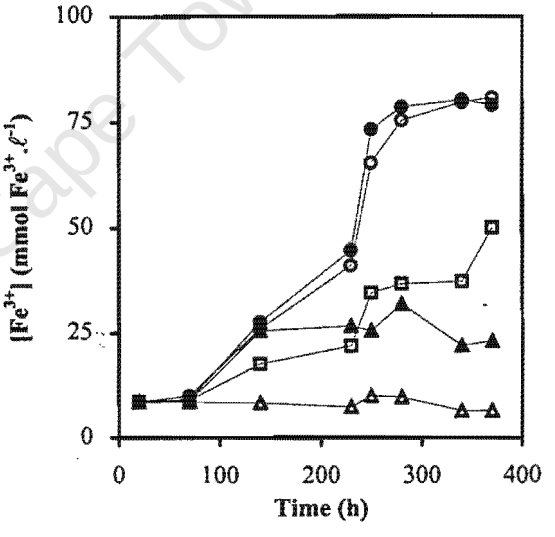

Figure 2.2(b): Effect of arsenate on the solubilisation of ferric-iron during the bioleaching of pyrite (after Barrett *et al.* (1989)).
[o] 0 mmol As(V).ℓ^{-1}; [•] 23 mmol As(V).ℓ^{-1};
[□] 56 mmol As(V).ℓ^{-1}; [▲] 112 mmol As(V).ℓ^{-1};
[Δ] 220 mmol As(V).ℓ^{-1}.

* The conferred resistance was not attributable to the selection of resistant strains as growth in the absence of these toxic species resulted in the bacteria losing their resistance.

† In contrast to the results reported by Barrett *et al.* (1989), Morin *et al.* (1991) reported arsenite concentrations of up to 145 mmol.ℓ^{-1} in actively growing cultures accustomed to high arsenite concentrations (Morin *et al.*, 1991).

2.4.3 The Mechanism of Arsenic Resistance in Micro-organisms

There are two main forms of arsenic resistance in bacteria; plasmid determined arsenic resistance and chromosomal arsenate resistance (Cullen and Reimer, 1989; Coddington, 1986; Silver and Nakahara, 1983; Novick and Roth, 1968).

2.4.3.1 Chromosomal arsenate resistance

Chromosomal arsenate resistance reduces the amount of arsenate entering the cell via the phosphate transport system (Cullen and Reimer, 1989; Coddington, 1986; Silver and Nakahara, 1983; Silver, 1978). *E. coli* has two active phosphate uptake systems (Silver *et al.*, 1981; Willsky and Malamy, 1980; Silver, 1978). The Pst phosphate transport system is specific to phosphate, while the Pit system will transport either phosphate or arsenate (Coddington, 1986; Willsky and Malamy, 1980; Silver, 1978). Chromosomal arsenate resistance occurs with the $Pst^{+}Pit^{-}$ mutation (Coddington, 1986; Silver and Nakahara, 1983; Silver *et al.*, 1981; Willsky and Malamy, 1980). At present, however, chromosomal arsenite resistance is poorly understood (Cullen and Reimer, 1989; Silver and Nakahara, 1983).

2.4.3.2 Plasmid-encoded resistance

Plasmid-encoded resistance protects bacteria by pumping arsenic from the cells via an energy dependent membrane pump (Huysmans and Frankenberger, 1992; Cullen and Reimer, 1989; Coddington, 1986; Silver and Nakahara, 1983; Mobley and Rosen, 1982; Silver and Keach, 1982). In addition to an *arsR* regulatory gene, the *ars* operon in plasmid R773 of *E. coli* contains three reading frames, *viz. arsA*, *arsB* and *arsC* (Silver and Misra, 1988). These encode an ATP-binding protein (ArsA), an inner membrane protein (ArsB) and a smaller polypeptide (ArsC), respectively (Silver and Misra, 1988). ArsA appears in solution as a monomeric protein and is loosely associated with the cell membrane (Silver and Misra, 1988). ArsB is postulated to be both the anion-conducting unit and the membrane anchor for the ArsA protein. Therefore, ArsA and ArsB form a membrane-bound complex, localised in the inner membrane (Rosen *et al.*, 1990), and interact to form an arsenite pump. ArsC reduces arsenate to arsenite and is stimulated by the reduced thiol compound, dithioreitol (Ji and Silver, 1992). A diagrammatic representation of the phosphate (arsenate) transport system and the arsenate efflux system of *E. coli* is shown in Figure 2.3.

Certain micro-organisms express only ArsA and ArsB. These organisms are therefore only able to extrude arsenite; this suggests that resistance to arsenate and arsenite is genetically separable (Rosen *et al.*, 1990).

The arsenic resistance plasmids of *Staphylococcus aureus* (plasmid pI258) (Ji and Silver, 1992) and *Staphylococcus xylosus* (plasmid pSx267) (Rosenstein *et al.*, 1992) do not have the *arsA* gene. However, it has been suggested that ArsB alone is sufficient for anion (arsenite) conduction in these species (Lawson, 1993).
In an attempt to increase the arsenic tolerance of a bioleaching culture which contained *Acidiphilium*, *T. ferrooxidans* and *L. ferrooxidans*, arsenic resistance plasmids were transferred into a strain of the acidophilic heterotroph, *Acidiphilium*. Although these plasmids were expressed in subsequent subcultures, they had no effect on the leaching performance of the culture (Bruhn and Roberto, 1993).

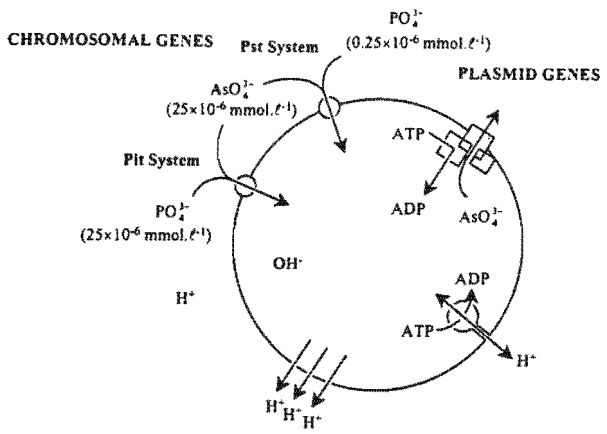

Figure 2.3: Diagrammatic representation of the phosphate (arsenate) transport system and the arsenate efflux system of *E. coli*. 0.25×10^{-6} mmol.ℓ^{-1} and 25×10^{-6} mmol.ℓ^{-1} are the values of K_m for PO_4^{3-} and AsO_4^{3-} as competitors for the Pit and Pst chromosomal transport systems. The three boxes for the plasmid arsenic ATPase represent the ArsA, ArsB and ArsC polypeptides (modified from Silver and Misra (1988) and Silver and Nakahara (1983)).

2.4.3.3 The oxidation of arsenite to arsenate

The oxidation of arsenite to arsenate has also been suggested to be a resistance mechanism towards arsenite (Lindström and Sehlin, 1989; Cullen and Reimer, 1989; Williams and Silver, 1984; Silver and Nakahara, 1983; Abdrashitova *et al.*, 1982). This reaction has been reported to occur in many micro-organisms (Sehlin and Lindström, 1992; Lindström and Sehlin, 1989; Cullen and Reimer, 1989; Wakao *et al.*, 1988; Osborne and Ehrlich, 1976; Phillips and Taylor, 1976) but there is no evidence that the energy of oxidation is used for growth (Cullen and Reimer, 1989; Wakao *et al.*, 1988; Pol'kin *et al.*, 1975). *T. ferrooxidans* (Mandl *et al.*, 1992; Wakao *et al.*, 1988; Braddock *et al.*, 1984), *T. thiooxidans* (Wakao *et al.*, 1988), and a mixed culture of thiobacilli (Barrett *et al.*, 1993(b); Barrett et *al.*, 1989) have however, been shown to be incapable of oxidising arsenite to arsenate.*

S. acidocaldarius strain BC is able to oxidise arsenite to arsenate in the late exponential phase (Lindström and Sehlin, 1989). This reaction also occurred in a cell-free extract if the cells were grown in the presence of arsenite and occurred to a larger degree in the presence of cell debris. This led Lindström and Sehlin (1989) to conclude that the oxidation is enzymatic and that the enzymes responsible for the oxidation reaction are membrane bound and located near the outside of the membrane.

An enzyme capable of oxidising arsenite to arsenate has also been isolated and purified from *Alcaligenes faecalis* (Rinderle *et al.*, 1984).

* In contrast to most researchers, Torma and Oolman (1992) reported that *T. ferrooxidans* was capable of oxidising arsenite to arsenate.

2.4.3.4 The reduction of arsenate to arsenite

Under certain conditions bacteria have also been observed to reduce arsenate to arsenite (Sehlin and Lindström, 1992; Cullen and Reimer, 1989; Wakao *et al.*, 1988), or release arsine from arsenite (Wakao *et al.*, 1988). Among methanogens the resistance mechanism proceeds via the reduction of arsenate to arsenite, followed by the methylation in the presence of coenzyme M (Huysmans and Frankenberger, 1992).

2.4.3.5 The mechanism of arsenic resistance in bioleaching bacteria

Resistance to arsenite, antimony and arsenate may be induced by growing *T. caldus* in the presence of non lethal concentrations of any one of these ions, hence resistance to these ions is due to the same genetic locus (Hallberg, 1995). The resistance mechanism to these ions is attributable to reduced cellular accumulation of these ions and an energy dependent efflux of the accumulated species similar to the mechanism found in *E. coli*. It is not, however, a result of to the $Pst^+ Pit^-$ mutation (Hallberg, 1995).

Although it has been claimed that arsenic resistance in *T. ferrooxidans* is plasmid borne (Nicolau and Raimond, 1993), the mechanism of arsenic resistance in acidophilic chemoautotrophs other than *T. caldus* has not been determined. However, the fact that arsenite is more toxic to *T. ferrooxidans* and *T. thiooxidans* than arsenate, and because increased tolerance to arsenic can be achieved by culture adaptation, it is suggested that arsenic resistance in these species may be attributed to $Pst^+ Pit^-$ mutations.

2.5 Modelling Bioleaching Operations

2.5.1 The Logistic Equation

Although bacterial growth is most simply described by a first order model, this only applies to the exponential growth phase. On the other hand, the logistic growth curve takes into account the lag phase, exponential growth, declining growth and stationary phases (La Motta, 1976):

$$C_X = \frac{C_X^{max}}{1 + m e^{-n t}} \qquad (2\text{-}9)$$

Although the logistic equation was originally intended to describe the growth of cells, it has been successfully used to describe the rate and degree of oxidation of sulfide minerals. It has been suggested that its applicability is based on the assumption that the oxidation rate is proportional to the bacterial concentration in the bioleaching medium (Crundwell, 1995(a)). The form of the logistic equation applicable to bacterial sulfide oxidation is (Pinches *et al.*, 1988):

$$\frac{dX}{dt} = k_M X\left[1 - \frac{X}{X_M}\right] \qquad (2\text{-}10)$$

The phases in the sigmoidal oxidation curve are analogous to the various stages of bacterial growth, *viz.*:

i) an initial lag phase with slow oxidation (bacterial lag phase),
ii) a faster (linear) oxidation phase (exponential growth), and
iii) a decrease in the oxidation rate (stationary phase and cell death due to substrate exhaustion).

Integration and re-arrangement of Equation 2.10 yields (Pinches *et al.*, 1988):

$$X = \frac{X_0 e^{k_M t}}{1 - \frac{X_0}{X_M}\left[1 - e^{k_M t}\right]} \qquad (2\text{-}11)$$

The values of X_M, k_M and X_0 can be determined by linear regression using a trial and error technique or by minimising the sum of the errors between the predicted and experimental values of X.

Initial modelling work suggested that the values for the rate constant, k_M, determined in batch culture were lower than those determined in continuous culture (Dew *et al.*, 1993; Hansford and Chapman, 1992; Pinches *et al.*, 1988). This was initially attributed to a larger inoculum being present in the case of continuous bioleaching.

However, subsequent work showed that the rate of bioleaching is proportional to the surface area of the mineral (Hansford and Chapman, 1992; Miller and Hansford, 1992(a)). This led to the use of a population balance model which incorporated changes in the size distribution of the mineral into the logistic equation (Crundwell, 1994).* Crundwell (1994) used the batch data of Hansford and Chapman (1992) and Miller and Hansford (1992(a)) to calculate the kinetic parameters for the population balance model and found that the parameters calculated in this manner also fitted the continuous data. In addition, the model proposed by Crundwell (1994) included terms that accounted for the flow rates into, and out of, the bioreactor, and a bacterial cell balance.

A major limitation of the logistic equation is that it is not mechanistically based, *i.e.* it does not contain terms which reflect the characteristics of the mineral being leached, *e.g.* particle size, the characteristics of the bacteria, *e.g.* growth rate, or the bioreactor conditions, *e.g.* slurry density.† It is therefore not possible to use the logistic equation to predict the performance of bioleaching operations for different micro-organism and mineral combinations or across a range of operating conditions. In spite of this limitation, it has however, proved useful in modelling batch and continuous laboratory, pilot and full-scale plant data for several pyrite and pyrite-arsenopyrite flotation concentrates (Crundwell, 1994; Hansford and Miller, 1993; Hansford and Bailey, 1992; Hansford and Chapman, 1992; Miller and Hansford, 1992(a); Miller and Hansford, 1992(b); Pinches *et al.*, 1988), and to predict the optimal reactor configuration and retention time for a particular ore, rate of bacterial growth and degree of sulfide oxidation (Dew *et al.*, 1993).

2.5.2 Modelling Bioleaching According to the *Direct* Mechanism‡

Konishi *et al.* (1990) reported that the adsorption of *T. ferrooxidans* onto pyrite was rapid, relative to the rate of dissolution of the mineral, and followed a Langmuir isotherm. Although the maximum adsorption was affected by the particle size distribution, the adsorption equilibrium was not affected (Konishi *et al.* (1990). In

* The population model approach has proved to be successful in spite of the fact that it assumes a shrinking core model and the bioleaching of pyrite has been shown to occur via a propagating pore model (Hansford and Drossou, 1988).

† An associated advantage is that modelling the oxidation rate in this way requires no knowledge of the bacterial concentration, or their activity. As stated previously these parameters are difficult to measure in bioleaching systems.

‡ Differences between the **direct** and **indirect** mechanism of bioleaching are described in detail in Section 2.6.

subsequent work by Konishi *et al.* (1992), an increase in the initial pyrite concentration was observed to result in a decrease in the rate of dissolution. This was attributed to a decrease in the number of vacant active sites. The above assumptions were incorporated into a model in which it was assumed that the micro-organisms attach to the mineral, and oxidise it directly (Konishi *et al.*, 1994; Konishi and Asai, 1993; Asai *et al.*, 1992; Konishi *et al.*, 1992; Konishi *et al.*, 1990). In the model proposed by Konishi and co-workers, the growth rate of bacteria was assumed to be proportional to the product of the number of adsorbed cells and the fraction of the surface not occupied by the bacteria. This model has been shown to fit data obtained during the batch bioleaching of pyrite (Konishi and Asai, 1993; Asai *et al.*, 1992; Konishi *et al.*, 1990) and zinc sulfide (Konishi *et al.*, 1994; Konishi *et al.*, 1992) concentrates.

2.5.3 Modelling Bioleaching According to the *Indirect* Mechanism

Nagpal *et al.* (1994) studied the bioleaching of a pyrite-arsenopyrite concentrate in a continuous bioreactor. They assumed that the dissolution of the minerals occurred solely because of chemical ferric leaching and that the leaching rates depended on the redox potential of the solution and the rest potential of the minerals. The model proposed by Nagpal *et al.* (1994) is based upon inhibited Monod kinetics and the assumption that the specific growth rate is directly proportional to the specific rate of ferrous-iron oxidation. Rearrangement of the model proposed by Nagpal *et al.* (1994) yields:

$$q_{Fe^{2+}} = \frac{q_{Fe^{2+}}^{max}}{1 + \frac{K_s}{[Fe^{2+}]} + \frac{K_s}{K_{As(V)}} \frac{[As(V)]^2}{[Fe^{2+}]}} \qquad (2\text{-}12)$$

The model proposed by Nagpal *et al.* (1994) showed that arsenic inhibition completely overshadowed ferric-iron inhibition. Although the model did not give good predictions of the dissolved iron concentration, it did give good predictions of the dissolved arsenic concentration and the trends in the dissolved iron and arsenic concentrations with changes in the dilution rate. It also gave good predictions of the transient data resulting from the removal of carbon dioxide supplementation and from pulsed additions of arsenic and ferrous sulfate. A limitation of the model developed by Nagpal *et al.* (1994) is that the kinetic parameters for the bacterial and chemical sub-processes were determined during the bioleaching of an arsenopyrite/pyrite concentrate.

2.6 The Multiple Sub-process Mechanism of Bioleaching

The mechanism by which thiobacilli leach or decompose sulfide minerals has been debated in the literature for many years. According to the **direct mechanism** the bacteria attach to the mineral surface and oxidise the sulfide component of the mineral to sulfate, simultaneously dissolving the metal component. The enzymes involved in sulfide oxidation were alleged to be contained within the cell envelope, hence attachment was considered a prerequisite of the direct mechanism (Konishi *et al.*, 1992; Lundgren and Tano, 1978). The iron in the mineral is solubilised as ferrous-iron and oxidised to ferric-iron by the bacteria before diffusing, together with the sulfate ion, away from the surface and into the bulk solution. The stoichiometry for the bioleaching of pyrite via the direct mechanism is:

$$FeS_2 + \tfrac{15}{4}O_2 + \tfrac{1}{2}H_2O \rightarrow Fe^{3+} + 2SO_4^{2-} + 2H^+ \quad (2\text{-}13)$$

According to the **indirect mechanism,** the mineral is chemically leached by the ferric-iron in the bioleaching solution. The ferrous-iron and in some cases sulfur produced by the ferric leaching reaction are oxidised by the bacteria to ferric-iron and sulfate, respectively. These species diffuse away from the mineral surface/bacteria microenvironment, and into the bulk solution. Thus in the indirect mechanism the role of the bacteria is to regenerate the ferric-iron, thereby ensuring the continued leaching of the sulfide mineral. For the bioleaching of pyrite the reactions involved are:

Chemical: $$FeS_2 + 14Fe^{3+} + 8H_2O \rightarrow 15Fe^{2+} + 2SO_4^{2-} + 16H^+ \quad (2\text{-}14)$$

Bacterial: $$4Fe^{2+} + O_2 + 4H^+ \rightarrow 4Fe^{3+} + 2H_2O \quad (2\text{-}15)$$

Overall: $$4FeS_2 + 15O_2 + 2H_2O \rightarrow 4Fe^{3+} + 8SO_4^{2-} + 4H^+ \quad (2\text{-}16)$$

It is clear that the overall reaction for the indirect mechanism is the same as the reaction for the direct mechanism. It is also clear from the equations listed that the direct and indirect mechanisms are more appropriately described as being one- and two-step mechanisms, respectively.

Although bioleaching according to the indirect mechanism does not require that the bacteria attach to the mineral, close association of the mineral and bacteria ensures a favourable microenvironment for leaching. For this reason, investigations in which the bacteria and mineral were separated, and the poor leaching rates observed considered to be "evidence" that bioleaching occurs via a direct mechanism, are misleading. Other investigations in which the mineral leaching rate was found to be directly proportional to both the sulfide and biomass concentrations were also considered "evidence" that bioleaching occurs via a direct mechanism. However, this result is also consistent with the hypothesis that bioleaching occurs via an indirect mechanism.

After a review of the literature Boon (1996) concluded that there was little agreement on whether or not bioleaching according to a direct mechanism was possible in principle, nor whether it was a rate determining process in the overall bioleaching of sulfide minerals. Subsequent work by Boon *et al.* (1995) has however provided strong evidence that the bioleaching of pyrite occurs via a two-step, or indirect, mechanism. According to this mechanism, the role of the bacteria is to regenerate ferric-iron, thereby maintaining a high redox potential within the system.

By staged additions of pyrite at four hourly intervals to a batch bioreactor, Boon *et al.* (1995) were able to measure the bacterial specific oxygen utilisation rate, q_{O_2}, as a function of the ferric/ferrous-iron ratio, $[Fe^{3+}]/[Fe^{2+}]$, or redox potential. The oxygen utilisation rate was also related to the pyrite concentration via the pyrite specific oxygen utilisation rate, v_{O_2}. The results of a typical experiment are shown in Figure 2.4 where it can be seen that q_{O_2} decreases with increasing ferric/ferrous-iron ratio while v_{O_2} increases with increasing ferric/ferrous-iron ratio.

In addition, samples were taken from the batch bioreactor, the pyrite removed by centrifugation, and the bacterial specific oxygen utilisation rate of the bacteria measured in an off-line respirometer, or BOM, using ferrous-iron medium. This enabled the specific oxygen utilisation rate to be measured over a wider range of ferric/ferrous-iron ratios than in the pyrite batch bioreactor. However, in the region where the ranges overlapped, the data for the pyrite- and ferrous-iron-grown bacteria coincided, as shown in Figure 2.5.

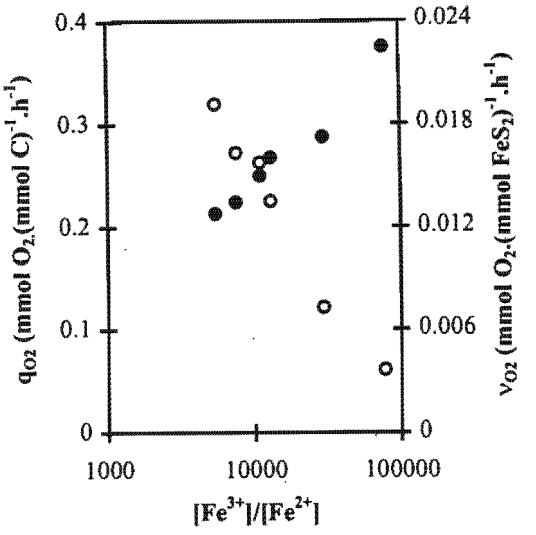

Figure 2.4: Variation in the [o] bacterial and [•] pyrite specific oxygen utilisation rates with changing ferric/ferrous-iron ratio during the bioleaching of pyrite by a *Leptospirillum*-like bacterium. Data was obtained from Boon *et al.* (1995).

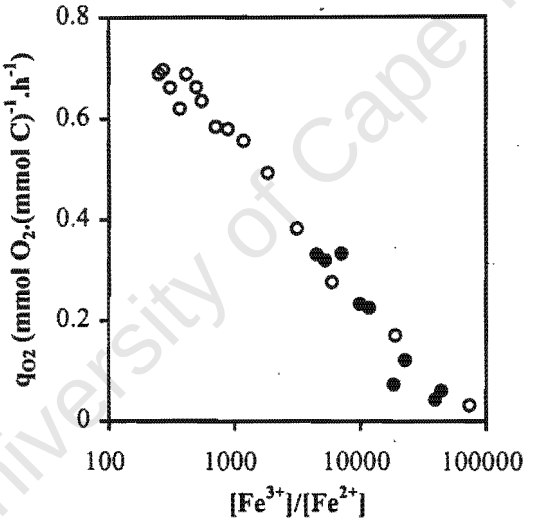

Figure 2.5: Variation in the bacterial specific oxygen utilisation rates of [o] ferrous-iron and [•] pyrite grown *Leptospirillum*-like bacteria with changing ferric/ferrous-iron ratio. Data was obtained from Boon *et al.* (1995).

From Figure 2.5 it can be seen that the agreement between the values obtained during the staged-addition experiments and the pyrite free ferrous-iron oxidation experiments performed in the respirometer is excellent. Similar results were obtained for a series of batch runs performed at initial bacterial concentrations ranging from 15 to 150 mg C.ℓ^{-1} and iron concentrations ranging from 2 to 20 g.ℓ^{-1} (Boon, 1996). These results led Boon *et al.* (1995) to conclude that in both cases ferrous-iron was the primary substrate and that the bioleaching of pyrite occurs according to an **indirect** or two-step mechanism.

Recent work by Schippers and Sand (1999) has shown that the bioleaching of metal sulfides occurs via one of two indirect mechanisms; the mechanism followed is determined by the structure of the mineral being oxidised. According to Schippers and Sand (1999), the disulfides, pyrite (FeS_2), molybdenite (MoS_2) and tungstenite (WS_2) are chemically attacked by iron(III) hexahydrate; this reaction produces M^{2+} (where M depends on the mineral being oxidised), ferrous-iron and thiosulfate. The thiosulfate is degraded in a cyclic process to sulfate,

with elemental sulfur as a side product (Schippers and Sand, 1999). The oxidation of thiosulfate may occur chemically or as a result of bacterial oxidation. However, the fact that ferrous-iron oxidising species alone are capable of degrading these minerals suggests that the chemical oxidation of thiosulfate is the dominant reaction (Schippers and Sand, 1999).

Galena (PbS), sphalerite (ZnS), chalcopyrite ($CuFeS_2$), hauerite (MnS_2), orpiment (As_2S_3) and realgar (As_4S_4) are degraded by iron(III) ion and proton attack (Schippers and Sand, 1999). The dissolution of these minerals is via a H_2S^{*+}-radical and polysulfides to elemental sulfur (Schippers and Sand, 1999). The elemental sulfur is in turn oxidised to sulfate by sulfur oxidising bacterial species present in the bioleaching solution (Schippers and Sand, 1999). Although the polysulfide mechanism has not been proven for the bioleaching of arsenopyrite, the presence of both *L. ferrooxidans* and *T. caldus* in continuous-flow bioreactors treating flotation concentrates containing arsenopyrite (Rawlings *et al.*, 1999(a)) suggests that the bioleaching of arsenopyrite proceeds via this mechanism.

It is also apparent from the above discussion that the term "multiple sub-process mechanism" describes the process by which the bioleaching of sulfide minerals occurs better than the terms "direct mechanism", "indirect mechanism", "two-step mechanism" or "two sub-process mechanism". Diagrammatic representations of pyrite and arsenopyrite bioleaching via the multiple sub-process mechanism are shown in Figure 2.6.

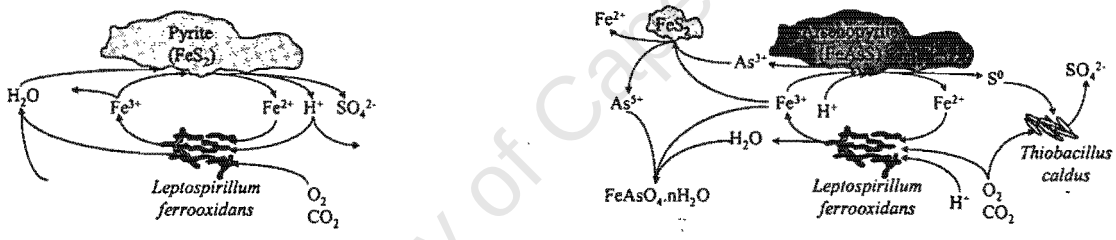

Figure 2.6: Diagrammatic representation of the bioleaching of pyrite and arsenopyrite via the multiple sub-process mechanism. The bacteria shown are planktonic (*i.e.* unattached) for reasons of clarity. However, the mechanism is the same for both attached and unattached micro-organisms.

The existence of a multiple sub-process mechanism for the bioleaching of sulfide minerals has a number of important implications for the modelling of the process, *viz.*:

i) the overall process can be reduced to a number of independent sequential and/or parallel sub-processes,
ii) the kinetics of each of these sub-processes can be studied independently, and
iii) the kinetic constants derived during the separate studies can be used to predict both the steady-state and dynamic performance of bioleach systems for a variety of different minerals, bacteria and operating conditions.

2.7 The Chemical Oxidation of Arsenopyrite

As stated previously arsenopyrite is the most common arsenic containing sulfide mineral and is chiefly associated with other metallic sulfides such as galena (PbS), sphalerite (ZnS), chalcopyrite ($CuFeS_2$) and pyrite (FeS_2). Its association with galena, sphalerite and chalcopyrite result in it being an unwanted mineral in the

extraction of base metal sulfides, whereas its association with pyrite generally results in it being a valuable constituent of gold bearing sulfides.

The above has resulted in most of the research on the oxidation of arsenopyrite having been aimed at developing a means of controlling its hydrophobicity in order to either enhance or suppress its flotation response relative to the other minerals present. Therefore, as most of the research performed to date has attempted to determine the chemical composition of the mineral surface under flotation conditions, it has been carried out at ambient temperatures and alkaline pH values rather than the conditions encountered during bioleaching operations. Furthermore, difficulties encountered with regard to obtaining pure mineral samples have resulted in most of the work having been performed with samples containing significant quantities of other sulfides. This has in turn led to considerable controversy with regard to the nature and stoichiometry of the reactions that occur under oxidising conditions.

2.7.1 The Electrochemical Oxidation of Arsenopyrite

Studies using cyclic voltametry have shown that the oxidation of arsenopyrite in both alkaline (Beattie and Poling, 1987) and acidic media (Lázaro *et al.*, 1997) is irreversible.* The irreversible nature of the dissolution can be attributed to the formation of arsenate and sulfate. In addition the oxidation of arsenopyrite has been reported to occur more readily in equimolar alkaline (sodium hydroxide) than equimolar acidic (sulfuric and hydrochloric acid) solutions (Kostina and Chernyak, 1976). In contrast to the above the electrochemical oxidation of pyrite (FeS_2), pyrrhotite (FeS_{1-x}), galena (PbS) and chalcopyrite ($CuFeS_2$) (Lázaro, 1995) and the oxidation of sphalerite (ZnS) (Jin *et al.*, 1984) have been shown to be reversible.†

In alkaline media the rest potential of arsenopyrite decreases with an increase in the pH (Sanchez and Hiskey, 1991; Kostina and Chernyak, 1976) and temperature (Kostina and Chernyak, 1976), hence an increase in either the pH or temperature results in an increased rate of mineral dissolution. The effect of temperature is similar in acidic solutions, however, the effect is less marked. Furthermore, in acidic solutions, the effect of temperature is more marked for pyrite than arsenopyrite.

2.7.1.1 Electrochemical oxidation in alkaline media

Sanchez and Hiskey (1991) reported that the electrochemical oxidation of arsenopyrite in alkaline media occurs according to a two-step mechanism, the first of which produces ferric hydroxide, arsenite and elemental sulfur:

$$FeAsS + 6H_2O \rightarrow Fe(OH)_3 + H_2AsO_3^- + S^0 + 13H^+ + 6\acute{e} \qquad (2\text{-}17)$$

The second step involves the oxidation of the arsenite and elemental sulfur formed during the first step, to arsenate and sulfate, respectively:

$$H_2AsO_3^- + H_2O \rightarrow HAsO_4^{2-} + 3H^+ + 2\acute{e} \qquad (2\text{-}18)$$

* During investigations in which the electrochemical oxidation of minerals is investigated using cyclic voltametry the process is considered to be reversible if the anodic and cathodic sweeps produce equal but opposite waves.

† It has been suggested that the wave linked to the cathodic sweep observed during the electrochemical oxidation of chalcopyrite is linked to reduction on chalcopyrite rather than the formation of chalcopyrite from S^0, Fe^{2+} and Cu^{2+} (Vargas, 2000), thus the electrochemical oxidation of chalcopyrite may in fact be an irreversible process.

$$S^0 + 4H_2O \rightarrow SO_4^{2-} + 3H^+ + 6e \quad (2\text{-}19)$$

The arsenate formed during the second step was incorporated into the ferric hydroxide deposits on the mineral surface whereas the sulfate was found to diffuse into the bulk solution (Beattie and Poling, 1987).

The morphology of the ferric hydroxide deposit was found to be dependent on both the redox potential and the pH; its porosity decreased with an increase in pH from pH 10 to pH 12, and with an decrease in the redox potential (Sanchez and Hiskey, 1991). Temperatures from 30 to 45°C had no effect on the quantity of hydroxide formed. However, at temperatures in excess of 45°C, thick, porous films were formed (Beattie and Poling, 1987).

An E_h-pH diagram for the Fe-As-S system, at a dissolved species concentration of 1 mmol.ℓ^{-1}, is shown in Figure 2.7 (Beattie and Poling, 1987); the stoichiometries of reactions 2-17 to 2-19 are clearly consistent with Figure 2-7.

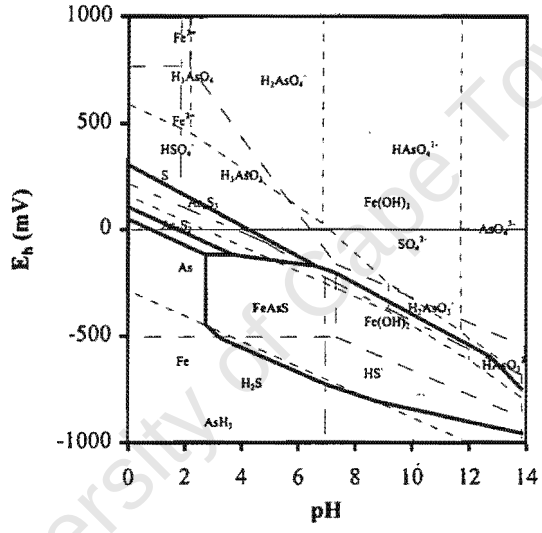

Figure 2.7: E_h-pH diagram for the Fe-As-S system at a dissolved species concentration of 1 mmol.ℓ^{-1} (after Beattie and Poling (1987)).

Buckley and Walker (1988) carried out a series of experiments in which the species formed when arsenopyrite fracture surfaces were produced under different conditions were determined by means of X-ray photoelectron spectroscopy, XPS. These workers found that iron and arsenic oxides were produced in both air and air saturated alkaline solutions. The arsenic was observed to oxidise faster than the iron, and sulfur was not involved in the initial reaction. Furthermore, in alkaline solutions, the oxidised iron was retained at the mineral surface and most of the arsenic was present as arsenite.

Immersion of these fracture surfaces in an air-saturated acid solution removed the iron and arsenic from the mineral surface and resulted in the mineral surface becoming increasingly enriched in sulfur. However, the sulfur was not present as elemental sulfur as reported by Beattie and Poling (1987) but in the form of a metal deficient sulfide (Buckley and Walker, 1988). The above led Buckley and Walker (1988) to suggest that the initial oxidation of arsenopyrite occurs according to;

$$FeAsS + (\tfrac{3}{4}x + \tfrac{1}{2}by)O_2 \rightarrow \tfrac{1}{2}x\,Fe_2O_3 + y\,AsO_b + Fe_{1-x}As_{1-y}S \quad (2\text{-}20)$$

In Equation 2-20, $y > x$, $b \leq 1.5$ and both x and 1-y are small. The disagreement between the stoichiometry of Equation 2-20 and the speciation predicted by Figure 2-7 can be attributed to Equation 2-20 only being applicable during the initial stages of the oxidation.

2.7.1.2 Electrochemical oxidation in acidic media

The oxidation of arsenopyrite in acidic solutions has also been reported to occur in 2 steps (Lázaro *et al.*, 1997). The first step, at $E_h < 550$ mV, produces realgar, As_2S_2,* and dissolved ferrous-iron, Fe^{2+}. During the second step, at $E_h > 550$ mV, these interfacial products are oxidised to produce arsenate, H_3AsO_4, and ferric-iron, Fe^{3+}, in solution. Although Lázaro *et al.* (1997) detected no elemental sulfur on the surface of the mineral, previous researchers have identified a non-passivating surface phase consisting of α-sulfur (Dunn *et al.*, 1989).

In addition to identifying the existence of a non-passivating surface phase consisting of α-sulfur, Dunn *et al.* (1989) proposed that the electrochemical oxidation rate of arsenopyrite could be determined using:

$$R_{FeAsS} = \frac{24 \times 3600 \times 10^4 \, iM}{zF\rho A} \qquad (2\text{-}21)$$

Equation 2-21 suggests that 30 micron particles can be completely dissolved in 2 days and led Dunn *et al.* (1989) to conclude that the dissolution rates possible during the electrochemical oxidation of arsenopyrite were comparable with those achieved during bioleaching and pressure leaching. However, based on different experimental data, Linge and Jones (1993) suggested that the electricity cost† prevented the process from being economically feasible, unless the cost of the process could be reduced by a factor of 5.

Linge and Jones (1993) performed oxidation experiments in an electrochemical cell using arsenopyrite particles suspended in acidic media. Using an inert anode yielded variable results and lower rates than using mineral electrodes. However, if a potential difference of 1.5 V was maintained across the cell dissolution rates of 17-58 $\times 10^{-9}$ mmol FeAsS.s^{-1}.cm^{-2} were obtained at 49 and 81°C, respectively. On average, 14 electrons were transferred per mole of FeAsS oxidised. The process resulted in the formation of ferric- and ferrous-iron, arsenite and arsenate, and sulfate and elemental sulfur, with about 70 % of the sulfur present as elemental sulfur. The rate of arsenopyrite dissolution at 25 and 81°C increased to 50-70 $\times 10^{-9}$ mmol FeAsS.s^{-1}.cm^{-2} if NaCl was added to mimic the salinity effect encountered when using plant water. As in the absence of NaCl, the oxidation resulted in the formation of both sulfate and elemental sulfur, with about 60 % of the sulfur present as elemental sulfur.

Although the economic assessments presented by Linge and Jones (1993) and Buckley and Walker (1988) disagree, the reaction schemes observed by these researchers are similar. Furthermore, both reaction schemes are consistent with the E_h-pH diagram for the Fe-As-S system (Figure 2-7) and the suggestion that the leaching of arsenopyrite occurs via the polysulfide mechanism proposed by Sand and co-workers (Sand *et al.*, 1999; Schippers and Sand, 1999).

* As realgar has been found to be degraded via the polysulfide mechanism, this result suggests that the oxidation of arsenopyrite also occurs via the polysulfide mechanism proposed by Sand and co-workers (Sand *et al.*, 1999; Schippers and Sand, 1999).

† The calculations performed by Dunn *et al.* (1989) were based on the prevailing Perth domestic grid charge of 12 cents per kWh.

2.7.2 Ferric Leaching Studies

Although considerable work on the leaching of pyrite using ferric-iron has been reported in the literature (May *et al.*, 1997; McKibben and Barnes, 1986; Mathews and Robins, 1972; Garrels and Thompson, 1960), to date very little work on the leaching of arsenopyrite, using ferric-iron at concentrations and conditions similar to those used in bioleaching, has been reported. For this reason, some controversy still exists in the literature with regard to the stoichiometry of the leaching reaction.

2.7.2.1 Reaction stoichiometry

The oxidation of arsenopyrite using ferric-iron complexes,* and forming ferrous-iron, Fe^{2+}, arsenite, As(III), and sulfate, SO_4^{2-}, is thermodynamically possible (ΔG_f^0 at 35°C = -526.967 kJ.(mol FeAsS)$^{-1}$) (Malatt, 1998). Although the available data is limited, it suggests that the dissolution is stoichiometric; one of the causes of apparent non-stoichiometric dissolution is the precipitation of residues (Malatt, 1998).

Barrett *et al.* (1990) reported that the ratio of ferrous-iron, Fe^{2+}, to arsenite, As(III), produced during the ferric leaching of arsenopyrite was 12, and that the ferric leaching of arsenopyrite occurs according to;

$$FeAsS + 11\,Fe^{3+} + 7\,H_2O \rightarrow 12\,Fe^{2+} + H_3AsO_3 + SO_4^{-} + 11\,H^{+} \quad (2\text{-}22)$$

On the other hand, Iglesias *et al.* (1993) found that the ferric leaching of arsenopyrite solubilised the arsenic and sulfur as arsenite, As^{3+}, and elemental sulfur, S^0, respectively:

$$FeAsS + 5\,Fe^{3+} \rightarrow S^0 + As^{3+} + 6\,Fe^{2+} \quad (2\text{-}23)$$

In contrast to the above, Nagpal (1994) reported that the oxidation of arsenopyrite using ferric-iron complexes formed ferrous-iron, Fe^{2+}, arsenate, As(III), sulfate, SO_4^{2-}, and elemental sulfur, S^0:

$$FeAsS + 13\,Fe^{3+} + 8\,H_2O \rightarrow 14\,Fe^{2+} + H_3AsO_4 + SO_4^{2-} + 13\,H^{+} \quad (2\text{-}24)$$

$$FeAsS + 7\,Fe^{3+} + 4\,H_2O \rightarrow 8\,Fe^{2+} + H_3AsO_4 + S^0 + 5\,H^{+} \quad (2\text{-}25)$$

From the above it seems as though the arsenic and sulfur moieties may be oxidised to varying oxidation states during the ferric leaching of arsenopyrite. Presumably, the final oxidation states of the arsenic and sulfur will depend on the conditions employed, *viz.* T, E_h, mineralogy *etc.*, as these parameters have previously been found to affect the oxidation states of the surface species formed during the electrochemical oxidation of arsenopyrite. A more general equation, which makes provision for the arsenic and sulfur moieties being oxidised to varying oxidation states has been proposed by Welham and Linge (1994):†

* During the leaching of pyrite, ferric-iron has been reported to be the dominant oxidant, even in the presence of oxygen saturated solutions (Moses *et al.*, 1987). As a first approximation, it can therefore be assumed that the same holds for the ferric leaching of arsenopyrite.

† If kinetic considerations are taken into account, Equation 2-26 is in agreement with the results obtained by Linge and Jones (1993), and the E_h-pH diagram shown in Figure 2.7 (Beattie and Poling, 1987).

$$FeAsS + (8x - 4y)H_2O \rightarrow w\,Fe^{2+} + (1-w)Fe^{3+} + x\,H_3AsO_3 + (1-x)H_3AsO_4 + y\,S^0 + (1-y)SO_4^{2-} + (12-2x-7y)H^+ + (14-w-2x-6y)\acute{e} \quad (2\text{-}26)$$

From Equation 2-26 it is clear that the final oxidation states of arsenic and sulfur affect the observed consumption of ferric-iron by electrons and hence the stoichiometry of the equation. If only arsenite, As(III), and elemental sulfur, S^0, are formed, Equation 2-26 reduces to the equation obtained by Iglesias *et al.* (1993) (Equation 2-23). On the other hand, if only arsenate, As(V), and sulfate, SO_4^{2-}, are formed, Equation 2-26 reduces to the equation obtained by Nagpal *et al.* (1994) (Equation 2-24).

The formation of elemental sulfur during the bioleaching of refractory arsenical ores and concentrates has a number of implications for the process:

i) it requires less oxygen than complete oxidation of the mineral, which, in turn, reduces the aeration requirement,
ii) it reacts with cyanide to form thiocyanate which increases cyanide consumption, and
iii) it may result in the process becoming acid consuming instead of acid generating.

2.7.2.2 Ferric leaching kinetics

The kinetic models used to describe the ferric leaching kinetics of sulfide minerals can be broadly classified as being either chemical or electrochemical in nature. Chemical models assume that the reaction rate at the surface is limiting, whereas electrochemical models assume that the difference between the rest potential of the mineral and the leaching medium is the driving force, *i.e.* that electron transfer from the surface to the surrounding medium is limiting.

As very little work on the ferric leaching of arsenopyrite has been reported to date, and because both pyrite and arsenopyrite have been reported to undergo dissolution by electrochemical means (Shuey, 1975), some of the models used to describe the ferric leaching kinetics of pyrite are described below. It is not however intended to be a comprehensive review of the ferric leaching kinetics of pyrite. A more comprehensive review of this material may be obtained from May (1997).

The ferric leaching of pyrite

During the oxidation of pyrite by ferric chloride, Wiersma and Rimstidt (1984) observed a high initial rate of leaching. This phenomenon was attributed to surface effects rather than dissolution of the bulk mineral, hence it was not considered during the determination of the kinetics. These authors suggested that the rate at which pyrite is leached by ferric-iron is first order with respect to the ferric-iron concentration and controlled by a surface (chemical) reaction.

In contrast to the above, Boogerd *et al.* (1991) found that the initial rate at which pyrite was leached by ferric chloride was a function of the temperature and the ferric-iron and pyrite concentrations. These workers also observed an apparent saturation with respect to the ferric-iron and pyrite concentrations at each temperature:

$$-r_{FeS_2} = k\left(\frac{[FeS_2]}{30+[FeS_2]}\right)\left(\frac{[Fe^{3+}]}{95+[Fe^{3+}]}\right) \quad (2\text{-}27)$$

Mathews and Robins (1972) postulated that the rate at which pyrite is leached by ferric-iron is dependent on the ratio of the ferric-iron to total iron concentration. However, Williamson and Rimstidt (1994) and McKibben and Barnes (1984) reported the rate to be proportional to the square root of the ferric-iron concentration. The half-order dependence of the rate on the ferric-iron concentration is consistent with the hypothesis that an electrochemical mechanism exists (Pletcher, 1984).

Tal (1986) and Garrels and Thompson (1960) postulated that the rate of leaching was dependent on the ratio of the ferric to ferrous-iron concentration, *i.e.* the solution redox potential. Tal (1986) postulated that the rate at which pyrite is oxidised by ferric-iron could be described using:

$$-r_{FeS_2} = k\left(\frac{[Fe^{3+}]}{[Fe^{2+}]}\right)^{0.682} \quad (2\text{-}28)$$

On the other hand, Zheng *et al.* (1986) reported the rate at which pyrite is oxidised by ferric-iron to be proportional to both the ferric/ferrous-iron ratio and the ferric-iron concentration. In addition, Zheng *et al.* (1986) found that the leaching rate became constant at high potentials and total iron concentrations:

$$-r_{FeS_2} = k\frac{k_1 - k_2\left(\frac{[Fe^{3+}]}{[Fe^{2+}]}\right)^{\frac{1}{2}}}{\frac{1}{[Fe^{3+}]^{\frac{1}{2}}} + k_3 + k_4\left(\frac{[Fe^{3+}]}{[Fe^{2+}]}\right)^{\frac{1}{2}}} \quad (2\text{-}29)$$

Williamson and Rimstidt (1994) also reanalysed the results presented by previous workers. Two different rate expressions, depending on whether or not oxygen was present, were postulated.* Equation 2-30 is for the ferric leaching of pyrite in the absence of oxygen whereas Equation 2-31 is for the ferric leaching of pyrite in the presence of oxygen:

$$-r_{FeS_2} = k\frac{[Fe^{3+}]^{0.93}}{[Fe^{2+}]^{0.40}} \quad (2\text{-}30)$$

$$-r_{FeS_2} = k\frac{[Fe^{3+}]^{0.30}}{[Fe^{2+}]^{0.47}[H^+]^{0.32}} \quad (2\text{-}31)$$

However, both laws express the ferric leaching rate as a function of the ferric/ferrous-iron ratio, which is also consistent with the hypothesis that the ferric leaching of pyrite occurs via an electrochemical model, *i.e.* that the electron transfer from the mineral surface to the surrounding medium is limiting.

In contrast to previous workers, Boon (1996) chose to describe the rate at which pyrite is degraded by ferric-iron by means of a Monod-type equation. In this model the rate at which pyrite is leached by ferric-iron is considered to be a function of a maximum rate of leaching and the ferric/ferrous -iron ratio:

* In the presence of oxygen, the reaction rate was found to be higher at high redox potentials. However, the dissolved oxygen concentration had no effect on the reaction rate.

$$\upsilon_{FeS_2} = \frac{\upsilon_{FeS_2}^{max}}{1 + B\dfrac{[Fe^{2+}]}{[Fe^{3+}]}} \qquad (2\text{-}32)$$

May (1997) re-analysed previously published data on the rate at which pyrite is chemically leached by ferric-iron in an attempt to determine whether or not the rate equations reported in the literature could be expressed as a function of the ferric/ferrous-iron ratio or redox potential. Because most authors had attributed the high initial leach rates to the existence of reactive sites on the mineral surface or to a rearrangement of the electrical double layer, and not to dissolution of the mineral itself, this data was also ignored during the reanalysis performed by May (1997). Furthermore, because different researchers had made different assumptions, May (1997) chose to use the raw data and not the published rates or rate laws. In addition to reanalysing the data of previous research, May *et al.* (1997) performed dynamic redox experiments in an attempt to relate the rate of chemical ferric leaching to the ferric/ferrous-iron ratio or redox potential. The results of the reanalysis are shown in Figure 2.8, together with the results of the dynamic redox experiments performed by May *et al.* (1997).

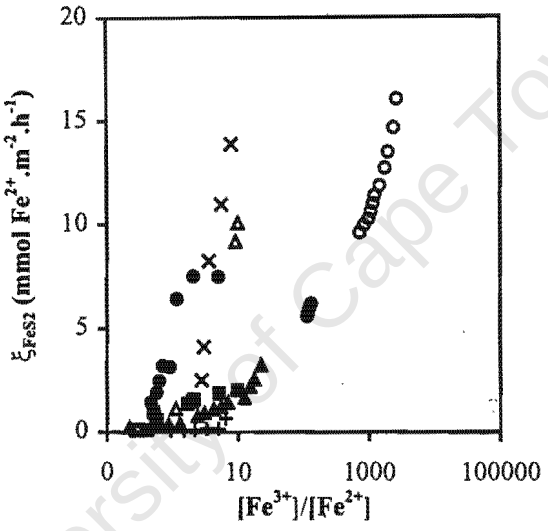

Figure 2.8: Comparison between the reported rates of chemical ferric leaching of pyrite (after May (1997). [o] May *et al.* (1997); [•] Boogerd *et al.* (1991); [□] Kawakami *et al.* (1988); [▲] Tal (1986); [Δ] Zheng *et al.* (1986); [■] McKibben and Barnes (1984); [+] Wiersma and Rimstidt (1984); [×] Mathews and Robins (1972).

In general, the results shown in Figure 2.8 indicate an increase in the leaching rate with an increase in the ferric/ferrous-iron ratio, or redox potential. Furthermore, although the rate laws published by a number of authors suggest that a maximum rate is reached (Boon, 1996; Boogerd *et al.*, 1991; McKibben and Barnes, 1986; Zheng *et al.*, 1986), those of others can be considered to suggest no upper limit (May *et al.*, 1997; Tal, 1991).

Although it was possible to fit the models proposed by Williamson and Rimstidt (1994), Boogerd *et al.* (1991) and Zheng *et al.* (1986) to the data generated by May *et al.* (1997), the lack of a fundamental basis for these models resulted in a model based on electrochemical (corrosion) theory being used instead (May, 1997). The equation chosen is similar in form to the Butler-Volmer equation, and can be written as:

$$\upsilon_{Fe^{2+}} = \upsilon_0 \left(e^{\alpha\beta(E-E')} - e^{(1-\alpha)\beta(E-E')} \right) \qquad (2\text{-}33)$$

It is interesting to note that, according to the Butler-Volmer based model, the dependence of the ferric leaching kinetics on the overpotential is linear at low overpotentials (0-20 mV). However, most bioleaching plants operate at higher overpotentials, which results in non-linear kinetics.

The ferric leaching of arsenopyrite

To date the most comprehensive studies on the chemical ferric leaching of arsenopyrite have been performed by Iglesias and co-workers (Iglesias *et al.*, 1996; Iglesias and Carranza, 1994; Iglesias *et al.*, 1993), and Malatt (1998). Iglesias and co-workers performed batch ferric leaching experiments in stirred tanks whereas Malatt (1998) performed batch leaching experiments in shake flasks and stirred tanks and ferric leaching studies using a rotating disk.*

In the shake flask experiments performed by Malatt (1998), the ferric leaching rate of arsenopyrite, measured as the rate at which arsenic was solubilised, was found to decrease with increasing temperature across the range 35 to 50°C. A decrease in the leaching rate with an increase in temperature was also observed during the ferric chloride leaching of arsenopyrite (Rimstidt *et al.*, 1994). Rimstidt *et al.* (1994) reported the optimum temperature to be 25°C; increasing the temperature above this resulted in a reduced rate of mineral dissolution.†

For slurry experiments performed in shake flasks, Malatt (1998) found the rate of leaching increased with increasing pH and followed an expression of the form:

$$-r_{FeAsS} = k'[H^+]^a \qquad (2\text{-}34)$$

The values of "k′" and "a" were however dependent on the temperature at which the experiment was performed. Furthermore, no simple relationship between temperature and either "k′" or "a" was apparent.

Malatt (1998) also found that the slurry experiments performed in batch reactors could be adequately described using both the logistic equation, *viz.* Equation 2-11, and a shrinking particle model:

$$1 - \sqrt[3]{1-\alpha} = \frac{k'}{R_0 \rho} t \qquad (2\text{-}35)$$

In addition to the trends mentioned above, during the rotating disk experiments the rate of reaction was observed to increase with an increase in the redox potential (Malatt, 1998). The change in the reaction rate with changes in the redox potential followed the form of the Tafel equation, and could be described using:

$$-r_{FeAsS} = e^{k' E_h} \qquad (2\text{-}36)$$

The exponential dependence of the leaching rate on the solution redox potential depicted in Equation 2-36 is also evident in the Butler-Volmer based model, Equation 2-33. Furthermore, both models are consistent with the hypothesis that the ferric leaching of arsenopyrite occurs via an electrochemical mechanism.

* A limitation of the work performed by Iglesias and co-workers, however, is that most of their work was performed using silver, Ag^+, to catalyse the ferric leaching reaction.

† In contrast to the results reported by Malatt (1998) and Rimstidt *et al.* (1994), Iglesias and Carranza (1996) found that the silver catalysed ferric leaching of arsenopyrite increased with an increase in temperature.

Comparison between bioleaching and chemical ferric leaching rates

As stated in Section 2.6, the low leaching rates measured during the ferric leaching of pyrite and arsenopyrite, relative to those measured during the bioleaching of these minerals, were considered "proof" that bioleaching occurred via a direct mechanism. For example, Barrett *et al.* (1990) reported that the rate at which arsenopyrite was leached by ferric-iron was in the region of six times lower than the rates achieved during bioleaching.*

However, a comparison between the rates of chemical ferric leaching achieved by May *et al.* (1997) and previously reported rates for the bioleaching of pyrite shown in Figure 2.9, suggests that it is possible to achieve high rates in sterile medium, provided the redox potential is kept sufficiently high. Furthermore, if one takes into consideration differences in experimental techniques and conditions; *viz.* pyrite mineralogy, particle size, ρ_{pulp}, micro-organisms used *etc.*, the agreement between the chemical and bioleaching rates shown in Figure 2.9 is remarkable.

The results shown in Figure 2.9 therefore suggest that the low rates reported previously for the ferric leaching of pyrite can be attributed to the stoichiometry of the leaching reaction. From Equation 2-14 it is apparent that each mole of pyrite leached consumes 14 moles of ferric-iron and produces 15 moles of ferrous-iron. This results in a rapid decrease in the redox potential of the leaching medium, which in turn results in a reduction in the pyrite leaching rate. Thus, the major difficulty encountered during chemical (ferric) leaching studies using pyrite is the maintenance of a high redox potential within the leaching liquor.

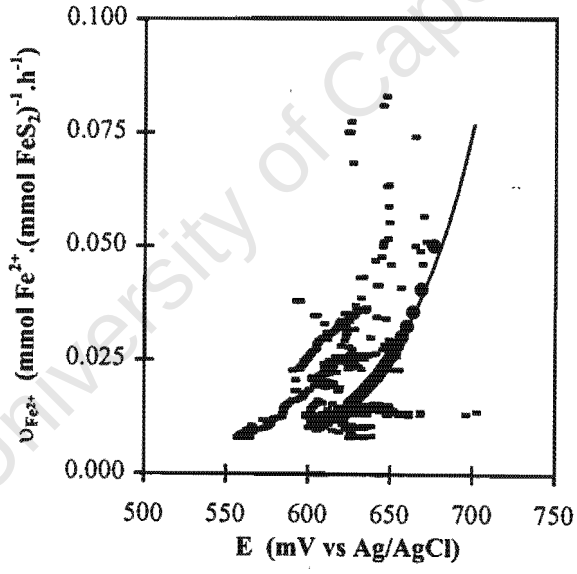

Figure 2.9: Comparison between the reported rates of [▬] bioleaching and [•] chemical ferric leaching of pyrite and the [——] prediction by the Butler-Volmer based model (after May *et al.* (1997)).

A comparison between the ferric and bioleaching rates of arsenopyrite, based on the surface area of the mineral, is listed in Table 2-6. From Table 2-6 it is apparent that the surface area based rates of chemical ferric leaching listed are at least an order of magnitude greater than those reported for bioleaching. Although the results listed in Table 2-6 should not be considered evidence that higher rates will be achieved in sterile systems, they do suggest that rates similar to those achieved in bioleaching systems are possible in sterile systems, provided that the redox potential is kept sufficiently high.

* This led these authors to conclude that the use of processes which use bacterially generated solutions for the chemical leaching of arsenopyrite could not be as efficient as bioleaching.

Table 2-6: Comparison between reported rates of bioleaching and chemical ferric leaching of arsenopyrite.

Type of Leaching	Rate (g FeAsS.m^{-2}.h^{-1})	Reference
Chemical	0.20 to 10 (rotating disk)	Malatt (1998)
	3.30 to 29 (slurry)	Malatt (1998)
	1.92	Rimstidt *et al.* (1994)
	0.41	Linge and Jones (1993)
	2.96	Barrett *et al.* (1990)
Bacterial	0.02	Malatt (1998)
	0.06	Hansford and Chapman (1992)
	0.02	Miller and Hansford (1992(a))

In addition to difficulties encountered when attempting to maintain a sufficiently high redox potential whilst performing ferric leaching experiments, changes in the surface area of the mineral particles may influence the leaching kinetics, even over relatively short periods of time, *i.e.* t < 5 h (Malatt, 1998). This may also result in differences between the rates of leaching measured during different investigations.

2.8 Bacterial Ferrous-iron Oxidation Kinetics

According to the multiple sub-process mechanism, during the bioleaching of sulfide minerals, the role of the micro-organisms is the oxidation of the ferrous-iron to the ferric form, and, in certain cases, the oxidation of the sulfur moiety to sulfate. It has been alleged that the ferrous-iron oxidation sub-process is the rate controlling step during the bioleaching of sulfides (Boon *et al.*, 1998). However, the incomplete oxidation, and slow kinetics of copper extraction during the bioleaching of chalcopyrite, using mesophiles, has been attributed to diffusional resistance caused by the build-up of sulfur layers on the mineral surface (Schnell, 1997). This suggests that the biooxidation of the sulfur moiety is the rate controlling sub-process during the bioleaching of chalcopyrite. Nonetheless, bacterial oxidation of ferrous-iron to the ferric form is an important sub-process during the bioleaching of sulfide minerals.

To date a number of kinetic models for bacterial ferrous-iron oxidation have been proposed (Nemati *et al.*, 1998; Boon, 1996). These models can be broadly classified as being either empirical, or based on Monod or Michaelis-Menten kinetics. Empirical models use tools such as the logistic equation to model the ferrous-iron oxidation kinetics (see Section 2.5.1).

Models based on the Monod equation assume that bacterial growth on ferrous-iron can be described by means of the Monod equation.* The Monod equation for uninhibited growth on ferrous-iron is:

$$\mu = \frac{\mu_{max}}{1 + \frac{K_s}{[Fe^{2+}]}} \qquad (2\text{-}37)$$

* The Monod equation was originally derived from Michaelis-Menten kinetics for the case in which the growth limiting substrate is incorporated as cellular material. This is not the case for the bacteria used in the bioleaching of sulfide minerals. Furthermore,

Different terms may be added to Equation 2-37 to account for changes in the conditions under which the micro-organisms are grown, *e.g.* temperature, pH, or the presence of inhibitory substances.

Michaelis-Menten based models assume that the rate limiting reactions involve the formation of an enzyme-substrate complex. According to this model the enzyme, E, and substrate, S, combine to form an enzyme-substrate complex, ES, which in a subsequent step decomposes to form product, P, and free enzyme:

$$E + S \leftrightarrow ES \rightarrow E + P \tag{2-38}$$

The rate equation for uninhibited growth with ferrous-iron as the rate limiting substrate is:

$$V = \frac{V_{max}}{1 + \frac{K_m}{[Fe^{2+}]}} \tag{2-39}$$

As in the case of the Monod equation, different terms may be added to Equation 2-39 to account for the effect of changes in the reaction conditions, or to account for changes in the reaction scheme of Equation 2-38 resulting from inhibitory effects.

Schnaitman *et al.* (1969) used Michaelis-Menten kinetics to describe the initial rate of bacterial ferrous-iron oxidation by bacteria harvested after 48 hours of growth in batch culture. The rate of reaction was found to be directly proportional to the concentration of cells added and followed zero order kinetics. K_m remained constant over the pH range pH 2.4 to pH 3.6. However, the change in V_{max} over the same pH range was significant. Schnaitman *et al.* (1969) also reported that neither sulfate, nor chloride inhibited iron oxidation and that the bacteria required sulfate for both growth and iron oxidation. The inability of BO_3^-, MoO_4^{2-}, Cl^- or NO_3^{2-} to promote ferrous-iron oxidation in the same way as sulfate and the ability of HPO_4^{2-} and $HAsO_4^{2-}$ to partially replace sulfate led to the importance of sulfate being attributed to the divalent ion. It was suggested that sulfate might expose more enzymatic sites, thereby increasing V_{max} without affecting K_m. In addition to the above Schnaitman *et al.* (1969) found formate and molybdate to be good inhibitors of iron oxidation.

Lacy and Lawson (1970) measured the ferrous-iron oxidation kinetics of *T. ferrooxidans* in batch culture. By neglecting maintenance and assuming that the substrate utilisation rate could be directly related to the growth rate via a yield constant, Lacey and Lawson (1970) were able to derive a model based on the Monod equation to describe the rate of ferrous-iron oxidation by the bacteria:

$$q_{Fe^{2+}} = \frac{\mu_{max}}{Y_{Fe^{2+}X}\left(1 + \frac{K_s}{[Fe^{2+}]}\right)} \tag{2-40}$$

The resulting equation was found to accurately describe the rate of ferrous-iron oxidation by the bacteria. In addition, the highest specific growth rate was measured at a temperature of 31°C and was observed to decrease with increasing iron concentration.

Macdonald and Clark (1970) performed both batch and continuous ferrous-iron oxidation experiments and used the Monod equation to determine the optimum growth conditions for *T. ferrooxidans*. Cultures grown in

although the Monod model may be easily modified to account for an increase in yield with increasing growth rate (*i.e.* maintenance), it is less readily adaptable to account for a decrease in yield with increasing growth rate (Pirt, 1975).

continuous bioreactors were found to be more active than those grown in batch vessels, *i.e.* K_s was higher in batch culture whereas μ_{max} was higher in continuous culture. This phenomenon was attributed to wall growth. The optimum growth conditions for *T. ferrooxidans* were found to be 33°C and an initial pH in the range pH 2.5 to pH 3.5. The specific growth rate was found to be independent of the carbon dioxide concentration at carbon dioxide concentrations greater than 0.01 %. However, carbon dioxide concentrations below 2 % resulted in a reduced yield on ferrous-iron.

Guay *et al.* (1977) also performed ferrous-iron oxidation experiments in both batch and continuous culture. Like previous workers they neglected maintenance and did not consider ferric-iron inhibition. Guay *et al.* (1977) reported that the maximum rate of ferrous-iron oxidation, V_{max}, increased with an increase in the concentration of ferrous-iron in the feed. This increase in V_{max} was however accompanied by a decrease in the dilution rate at which washout occurred, *i.e.* the dilution rate at which washout occurred decreased with an increase in the concentration of ferric-iron in the bioreactor.

Kelly and Jones (1978) investigated the ferrous-iron oxidation kinetics of *T. ferrooxidans* in batch and continuous culture and using off-line respirometric measurements. They found the ferrous-iron oxidation kinetics to be subject to competitive inhibition by ferric-iron and non-competitive inhibition by uranyl ions and increased proton concentrations, *i.e.* decreased pH. Ferric-iron was not however observed to influence carbon dioxide fixation. However, ferrous-iron, at concentrations in excess of 500 mmol.ℓ^{-1}, were found to inhibit both ferrous-iron oxidation and carbon dioxide fixation. Furthermore, the high rates of ferrous-iron oxidation observed in the absence of carbon dioxide led Kelly and Jones (1978) to suggest that growth and the oxidation of ferrous-iron can be uncoupled.

Further work on the ferrous-iron oxidation kinetics of *T. ferrooxidans* in continuous flow bioreactors indicated that both iron oxidation and growth were subject to product inhibition by ferric-iron, and under certain conditions, substrate inhibition by ferrous-iron (Jones and Kelly, 1983). Most of the data obtained suggested that the ferrous-iron oxidation kinetics of *T. ferrooxidans* were subject to competitive product inhibition. However, anomalous results led to these authors suggesting that the ferric (product) inhibition could be either predominantly competitive or non-competitive and that the mode observed depended on the previous steady-state conditions employed (Jones and Kelly, 1983):

Competitive:
$$\mu = \frac{\mu_{max}}{1 + \frac{K_s}{[Fe^{2+}]} + \frac{K_s}{K_p}\frac{[Fe^{3+}]}{[Fe^{2+}]}} \qquad (2\text{-}41)$$

Non-competitive:
$$\mu = \frac{\mu_{max}}{1 + \frac{K_s}{[Fe^{2+}]} + \frac{K_s}{K_p}\frac{[Fe^{3+}]}{[Fe^{2+}]} + \frac{[Fe^{3+}]}{K_p}} \qquad (2\text{-}42)$$

Braddock *et al.* (1984) examined the iron-limited growth of an arsenic tolerant strain of *T. ferrooxidans*, in both batch and continuous culture, and reported no evidence of ferric-iron inhibition for ferrous-iron concentrations of 9.0 to 23.3 mmol $Fe^{2+}.\ell^{-1}$. The addition of 2.67 mmol.ℓ^{-1} sodium arsenite had no effect on the steady-state biomass concentration or growth kinetics observed in continuous culture. The growth kinetics of the culture could be described using a modified Monod model, in which a threshold concentration of ferrous-iron, $[Fe^{2+}]_t = 0.25$ mmol $Fe^{2+}.\ell^{-1}$, was included:

$$\mu = \frac{\mu_{max}}{1 + \frac{K_s}{[Fe^{2+}] - [Fe^{2+}]_t}} \quad (2\text{-}43)$$

The threshold concentration of ferrous-iron represents a concentration of ferrous-iron below which there was insufficient energy available for cell growth. In addition, Braddock *et al.* (1984) calculated the threshold concentration of ferrous-iron to be the same for both growth and iron oxidation; this led them to conclude that growth and iron oxidation are tightly coupled, which is in contrast to the results obtained by Kelly and Jones (1978).

Liu *et al.* (1988) investigated the effect of inert solids, ferrous-iron and dissolved oxygen concentrations on the ferrous-iron oxidation kinetics of *T. ferrooxidans*. In addition to reporting that the ferrous-iron oxidation kinetics were inhibited by ferric-iron, Liu *et al.* (1988) found that a Monod-based model, analogous to the model proposed by Braddock *et al.* (1984), could be used to describe the growth kinetics of *T. ferrooxidans* under conditions in which the dissolved oxygen concentration was limiting:

$$\mu = \frac{\mu_{max}}{1 + \frac{K'_s}{[O_2] - [O_2]_t}} \quad (2\text{-}44)$$

The ferrous-iron oxidation rate measured in shake flask experiments decreased when the volume of inert solids was increased from 0.5 to 1 % and was effectively zero at volumes in excess of 1 %. However, in stirred tanks, solids concentrations up to 15 % had little effect on the rate of ferrous-iron oxidation. This led Liu *et al.* (1988) to suggest that attrition resulting from the gyratory motion of the shaker was responsible for the inhibitory effects observed in shake flasks.

Nikolov and Karamev (1992) reported that *T. ferrooxidans* cells obtained by re-suspension from biofilms were able to oxidise ferrous-iron at rates of up to 39.39 mmol $Fe^{2+}.\ell^{-1}.h^{-1}$. This was more than 5 times the highest value, *viz.* 7.16 mmol $Fe^{2+}.\ell^{-1}.h^{-1}$, previously reported in the literature. Nikolov and Karamev (1992) suggested that the bacteria change their activity owing to alterations during fixation in a biofilm. The observed change was found to be irreversible; the behaviour of the micro-organisms was unchanged 12 months after re-suspension. The ferrous-iron kinetics of the re-suspended cells could be accurately described using a Monod model modified to account for both substrate (ferrous-iron) and product (ferric-iron) inhibition:

$$\mu = \frac{\mu_{max}}{1 + \frac{K_s}{[Fe^{2+}]} + \frac{K_s}{K_p}\frac{[Fe^{3+}]}{[Fe^{2+}]} + \frac{[Fe^{2+}]}{K_{si}}} \quad (2\text{-}45)$$

Harvey and Crundwell (1997) investigated the ferrous–iron oxidation kinetics of *T. ferrooxidans* in the presence and absence of arsenite, As(III), using a redox-controlled reactor. In the apparatus used by these workers, the ferric/ferrous-iron ratio was controlled by electrolysis and the current passed used as a continuous and instantaneous measurement of the rate of bacterial ferrous-iron oxidation. The experimental results obtained by Harvey and Crundwell (1997) could be accurately described by the Monod growth equation modified to account for product (ferric-iron) inhibition and inhibition by arsenite:

$$\mu = \frac{\mu_{max}}{1 + \frac{K_s}{[Fe^{2+}]} + \frac{K_s}{K_p}\frac{[Fe^{3+}]}{[Fe^{2+}]} + \frac{[As(III)]}{K_{As(III)}[Fe^{2+}]}} \quad (2\text{-}46)$$

Harvey and Crundwell (1997) showed that the model parameters determined using the redox-controlled reactor were the same as those obtained during conventional batch oxidation experiments; this confirmed that the applied current did not influence the experimental results obtained.

Ingledew (1986) attempted to explain the mechanism by which ferrous-iron oxidation occurs at the level of individual reactions. He proposed a mechanism of electron transport from the ferric/ferrous-iron oxidation half reaction to the oxygen, hydrogen/water half reaction following ATP formation. Ingledew (1986) claimed that the rate of leaching by rusticyanin, as required by the direct mechanism, was too slow for it to be the primary oxidant. He therefore postulated that ferric-iron ions bound to the cell wall are the primary oxidant. According to Ingledew (1986) the ferrous-iron ions are oxidised to ferric-iron ions outside the cell wall. This creates a potential difference between the inside and outside of the cell; the electrons pass through the periplasm and the cell membrane and are relieved of their high energy in the formation of ATP, before being used in the second half reaction to form water. Thus the ferric/ferrous-iron ratio controls the rate of oxidation and consequently the rate of electron production, the rate of ATP formation and finally the rate of cell growth.

Huberts (1994) used the electron transport pathway proposed by Ingledew (1986) to develop an electrical circuit that accounted for the flow of electrons and protons through the cytoplasm. This included a six-step ATP formation process (energy storage) and a ten-step process for NADPH formation (CO_2 fixation). He also determined the free energy requirements of the system. Huberts (1994) used the above sub-processes and electrochemical theory to formulate rate equations for each of the steps which occur during the bacterial oxidation of ferrous-iron; each was taken in turn to be rate limiting. This enabled Huberts (1994) to model the kinetics using redox potential as a measure of the ferric- and ferrous-iron concentrations. The rate equations obtained in this manner were however rather complex.

Huberts also used Michaelis-Menten kinetics to describe the ferrous-iron oxidation kinetics; the proposed rate equation incorporated the effects of both the ferric/ferrous-iron ratio and the dissolved oxygen concentration. This model can be written in the following form:

$$q_{Fe^{2+}} = \frac{q^{max}_{Fe^{2+}}}{\left(1 + \frac{K_S}{[Fe^{2+}]} + \frac{K_S}{K_p}\frac{[Fe^{3+}]}{[Fe^{2+}]}\right)\left(1 + \frac{K_{O_2}}{[O_2]}\right)} \quad (2\text{-}47)$$

Suzuki and co-workers determined the ferrous-iron oxidation kinetics of *T. ferrooxidans* by monitoring the rate at which cells grown in batch culture, and then re-suspended in ferrous-iron media, utilised oxygen (Suzuki and Lizama, 1989; Lizama and Suzuki, 1989). Suzuki and Lizama (1989) found that although the rate at which ferrous-iron was oxidised increased with an increase in the ferrous-iron concentration of the media in which the cells were re-suspended, the specific rate of ferrous-iron oxidation by certain strains decreased with an increase in the concentration of cells. The above led Suzuki and Lizama (1989) to suggest that the ferrous-iron oxidising ability of a cell may be competitively inhibited by other cells, *i.e.* the ferrous-iron binding sites of the cells compete for the available ferrous-iron. The experimental results obtained for the strains found to be subject to this form of inhibition could be described using Michaelis-Menten kinetics modified to account for competitive inhibition by cells:

$$V = \frac{V_{max}}{1 + \frac{K_m}{[Fe^{2+}]} + \frac{K_m}{K_{ci}} \frac{c_X}{[Fe^{2+}]}} \quad (2\text{-}48)$$

Subsequent work by Lizama and Suzuki (1989) led these researchers to conclude that the rate at which ferrous-iron was oxidised by these strains was also competitively inhibited by ferric-iron. Furthermore, although binding of one inhibitor was inhibited by the other, *i.e.* the apparent inhibition constant increased with an increase in the concentration of the other inhibitor, it did not exclude binding of the other. Where both inhibitors bind the ferrous-iron oxidising system simultaneously, a stronger inhibitory effect is observed than by each separately, *i.e.* it results in synergistic inhibition by the inhibitors. The synergistic inhibition of ferrous-iron oxidation by ferric-iron and cells could be modelled using a model based on Michaelis-Menten kinetics:

$$V = \frac{V_{max}}{1 + \frac{K_m}{[Fe^{2+}]} + \frac{K_m}{K_i} \frac{[Fe^{3+}]}{[Fe^{2+}]} + \frac{K_m}{K_{ci}} \frac{c_X}{[Fe^{2+}]} + \frac{K_m}{\chi K_{ci} K_i} \frac{c_X [Fe^{3+}]}{[Fe^{2+}]}} \quad (2\text{-}49)$$

Nemati and Webb (1997) used initial ferrous-iron oxidation rates and redox potential measurement to determine the kinetics of bacterial ferrous-iron oxidation by *T. ferrooxidans*. Their approach was based on Michaelis-Menten kinetics and the model developed included terms to include the effects of temperature, ferrous-iron and bacterial concentration. It also included terms to account for inhibition by both substrate and cells. The resulting model was successfully used to simulate the full range of experimental data obtained:

$$q_{Fe^{2+}} = \frac{K_0 e^{-\frac{E_a}{RT_{abs}}}}{1 + \frac{K_m}{[Fe^{2+}]} + \frac{K_m}{K_{ci}} \frac{c_X}{[Fe^{2+}]} + \frac{[Fe^{2+}]}{\delta} + \frac{c_X [Fe^{2+}]}{\delta \varepsilon}} \quad (2\text{-}50)$$

In contrast to most research on the kinetics of bacterial ferrous-iron oxidation performed during the last decade, the model proposed by Nemati and Webb (1997) does not include parameters to account for inhibition by ferric-iron. Furthermore, the use of artificially high cell concentrations (as a result of cells having been harvested from batch culture) and the use of high initial ferrous-iron oxidation concentrations (relative to those observed in chemostat culture)* may have contributed to the ferrous-iron oxidation kinetics being inhibited by these parameters. Furthermore, if the cycling of iron occurs in the micro-environment, or EPS, between the mineral surface and the bacteria (Hansford and Vargas, 1999; Sand *et al.*, 1999; Tributsch, 1999), then inhibition by cells is also unlikely to influence the kinetics of the process.

Boon (1996) investigated the kinetics of bacterial ferrous-iron oxidation by *T. ferrooxidans* in batch and continuous culture and the kinetics of bacterial ferrous-iron oxidation by *Leptospirillum*-like bacteria in continuous culture. The growth, concentration and activity of the bacteria were determined by measuring the rate at which carbon dioxide and oxygen were utilised.† A modified Michaelis-Menten-type model, which incorporated terms for both ferric-iron inhibition and a threshold ferrous-iron concentration, was derived in terms of the bacterial specific oxygen utilisation rate:

* During the bioleaching of sulfide minerals the ferrous-iron concentration is usually in the region of 5 mmol $Fe^{2+}.\ell^{-1}$, hence inhibition by ferrous-iron is unlikely.

† The manner in which the ferrous-iron and oxygen and carbon dioxide utilisation rates, and the ferric/ferrous-iron ratio, *i.e.* redox potential, are used to determine the bacterial ferrous-iron oxidation kinetics is covered in detail in Chapter Four.

$$q_{O_2} = \frac{-r_{O_2}}{c_x} = \frac{q_{O_2}^{max}}{1 + \frac{K_s}{[Fe^{2+}] - [Fe^{2+}]_t} + \frac{K_s}{K_i}\frac{[Fe^{3+}]}{[Fe^{2+}] - [Fe^{2+}]_t}} \quad (2\text{-}51)$$

Boon (1996) also showed that the ferrous-iron saturation term and the threshold ferrous-iron concentration could be neglected, hence Equation 2-51 could be simplified to give:

$$q_{O_2} = \frac{q_{O_2}^{max}}{1 + K\frac{[Fe^{3+}]}{[Fe^{2+}]}} \quad (2\text{-}52)$$

This simplified model assumes that the ferrous-iron oxidation kinetics are proportional to the ferric/ferrous-iron ratio, *i.e.* the redox potential, which is consistent with the chemiosmotic theory proposed by Ingledew (1986). Equation 2.52 can also be written in terms of the bacterial specific ferrous-iron oxidation rate:

$$q_{Fe^{2+}} = \frac{q_{Fe^{2+}}^{max}}{1 + K\frac{[Fe^{3+}]}{[Fe^{2+}]}} \quad (2\text{-}53)$$

Equations 2-52 and 2-53 have been found to give a satisfactory fit to experimental data obtained during the oxidation of ferrous-iron by both *T. ferrooxidans* (Boon, 1996) and a *Leptospirillum*–like bacterium (Boon, 1996; Van Scherpenzeel, 1996).

An important feature of Equations 2-52 and 2-53 is that the ferric/ferrous-iron ratio can be related to the solution redox potential via the Nernst Equation:*

$$E_h = E_0 + \frac{R\,T_{abs}}{z\,F}\ln\left(\frac{a_{Fe^{3+}}}{a_{Fe^{2+}}}\right) \quad (2\text{-}54)$$

Furthermore, the reverse sigmoidal shape of the curves predicted by Equations 2-52 and 2-53 are consistent with the shapes obtained if the ferrous-iron oxidation models reviewed above, with substrate inhibition excluded, are plotted as a function of the ferric/ferrous-iron ratio, *i.e.* redox potential.

2.9 Nomenclature

a	constant	dimensionless
$a_{Fe^{2+}}$	activity of ferrous-iron species	dimensionless
$a_{Fe^{3+}}$	activity of ferric-iron species	dimensionless
A	elecrode surface area	cm^{-2}
[As(III)]	concentration of arsenite	mmol As(III).ℓ^{-1}

* The manner in which the ferric/ferrous-iron ratio can be related to the solution redox potential via the Nernst Equation is covered in greater detail in Section 3.2.1.4.

[As(V)]	concentration of arsenate	mmol As(V).ℓ^{-1}
b	stoichiometric coefficient	dimensionless
B	kinetic constant in chemical (ferric) pyrite oxidation	dimensionless
c_X	concentration of bacteria	mmol C.ℓ^{-1}
[Cl^-]	concentration of chloride	mmol Cl^-.ℓ^{-1}
C_X	population of active micro-organisms	mg.cm^{-3}
C_X^{max}	saturation population of active micro-organisms	mg.cm^{-3}
E	redox potential of the solution (Pt-Ag/AgCl)	mV
E′	mineral rest potential	mV
E_0	redox potential of the solution at equilibrium	mV
E_a	activation energy	kJ.$mole^{-1}$
E_h	redox potential of the solution (Pt-SHE)	mV
F	Faraday constant	C.mol^{-1}
[Fe^{2+}]	concentration of ferrous-iron	mmol Fe^{2+}.ℓ^{-1}
[Fe^{3+}]	concentration of ferric-iron	mmol Fe^{3+}.ℓ^{-1}
[Fe^{2+}]$_t$	threshold concentration of ferrous-iron	mmol Fe^{2+}.ℓ^{-1}
[FeS_2]	concentration of pyrite	mmol FeS_2.ℓ^{-1}
i	current	A
k	kinetic constant	mmol FeS_2.ℓ^{-1}.h^{-1}
k′	kinetic constant	g FeAsS.ℓ^{-1}.h^{-1}
k″	kinetic constant	mV^{-1}
k_1	constant	dimensionless
k_2	constant	dimensionless
k_3	constant	dimensionless
k_4	constant	dimensionless
K	kinetic constant in bacterial ferrous-iron oxidation	dimensionless
K_0	frequency factor	mmol Fe^{2+}.(mmol C)$^{-1}$.h^{-1}
$K_{As(V)}$	Monod equation inhibition constant for arsenate	mmol As(V).ℓ^{-1}
k_M	rate constant in logistic equation	h^{-1}
$K_{As(III)}$	Monod equation inhibition constant for arsenite	mmol As(III).ℓ^{-1}
K_{ci}	Michaelis-Menten inhibition constant for cells	mmol C.ℓ^{-1}
K_i	Michaelis-Menten product (ferric-iron) inhibition constant	mmol Fe^{3+}.ℓ^{-1}
K_m	Michaelis-Menten substrate (ferrous-iron) saturation constant	mmol.ℓ^{-1}
K_{O_2}	Michaelis-Menten equation saturation constant for oxygen	mmol O_2.ℓ^{-1}
K_p	Monod equation product (ferric-iron) inhibition constant	mmol Fe^{3+}.ℓ^{-1}
K_s	Monod equation substrate (ferrous-iron) saturation constant	mmol Fe^{2+}.ℓ^{-1}
K_s'	Monod equation saturation constant for oxygen	mmol O_2.ℓ^{-1}
K_{si}	Monod equation substrate (ferrous-iron) inhibition constant	mmol Fe^{2+}.ℓ^{-1}
m	numerical parameter	dimensionless
M	molar weight	g.mol^{-1}
n	numerical parameter	h^{-1}
[NaCl]	concentration of sodium chloride	mmol NaCl.ℓ^{-1}
[O_2]	concentration of oxygen	mmol O_2.ℓ^{-1}
[O_2]$_t$	threshold concentration of oxygen	mmol O_2.ℓ^{-1}
pH_{opt}	optimal pH for growth	pH units

$q_{Fe^{2+}}$	bacterial specific ferrous-iron utilisation rate	mmol Fe^{2+}.(mmol C)$^{-1}$.h^{-1}
$q^{max}_{Fe^{2+}}$	maximum bacterial specific ferrous-iron utilisation rate	mmol Fe^{2+}.(mmol C)$^{-1}$.h^{-1}
q_{O_2}	bacterial specific oxygen utilisation rate	mmol O_2.(mmol C)$^{-1}$.h^{-1}
$q^{max}_{O_2}$	maximum bacterial specific oxygen utilisation rate	mmol O_2.(mmol C)$^{-1}$.h^{-1}
R	Universal gas constant	kJ.K^{-1}.mol^{-1}
R_0	initial particle radius	cm
r_{FeAsS}	arsenopyrite production rate	g FeAsS.ℓ^{-1}.h^{-1}
r_{FeS_2}	pyrite production rate	mmol FeS_2.ℓ^{-1}.h^{-1}
r_{O_2}	oxygen production rate	mmol O_2.ℓ^{-1}.h^{-1}
R_{FeAsS}	arsenopyrite leaching rate	cm.day^{-1}
t	time	h
t_g	mean bacterial generation time	h
T	temperature	°C
T_{abs}	absolute temperature	K
T_{max}	maximum temperature for growth	°C
T_{opt}	optimal temperature for growth	°C
V	ferrous-iron utilisation rate	mmol Fe^{2+}.h^{-1}
V_{max}	maximum ferrous-iron utilisation rate	mmol Fe^{2+}.h^{-1}
w	stoichiometric coefficient	dimensionless
x	stoichiometric coefficient	dimensionless
X	fraction of sulfide oxidised	dimensionless
X_0	fraction of sulfide oxidised at t = 0	dimensionless
X_M	maximum fraction of sulfide that can be oxidised	dimensionless
y	stoichiometric coefficient	dimensionless
$Y_{Fe^{2+}X}$	bacterial yield on ferrous-iron	mmol C.(mmol Fe^{2+})$^{-1}$
z	number of electrons involved in the reaction	dimensionless
α	fraction of mineral reacted at time, t	dimensionless
β	$\frac{zF}{RT_{abs}}$	dimensionless
χ	constant	dimensionless
δ	constant	mmol Fe^{2+}.ℓ^{-1}
ΔG^0_f	Gibbs free energy of formation	kJ.mol^{-1}
ε	constant	mmol C.ℓ^{-1}
μ	bacterial specific growth rate	h^{-1}
μ^{max}	maximum bacterial specific growth rate	h^{-1}
ρ	density	g.cm^{-3}
ρ_{pulp}	solids concentration	% (m.v^{-1})
υ_0	kinetic constant in chemical (ferric-iron) pyrite oxidation	mmol Fe^{2+}.(mmol FeS_2)$^{-1}$.h^{-1}
$\upsilon_{Fe^{2+}}$	pyrite specific ferrous-iron production rate	mmol Fe^{2+}.(mmol FeS_2)$^{-1}$.h^{-1}
υ_{FeS_2}	pyrite specific oxidation rate	mmol FeS_2.(mmol FeS_2)$^{-1}$.h^{-1}
$\upsilon^{max}_{FeS_2}$	maximum pyrite specific oxidation rate	mmol FeS_2.(mmol FeS_2)$^{-1}$.h^{-1}
υ_{O_2}	pyrite specific oxygen utilisation rate	mmol O_2.(mmol FeS_2)$^{-1}$.h^{-1}
$\xi_{Fe^{2+}}$	pyrite specific ferrous-iron production rate	mmol Fe^{2+}.m^{-2}.h^{-1}

2.10 References

Abdrashitova, S.A., Ilyaletdinov, A.N., Mynbaeva, B.N. and Abdulina, G.G. 1982. The catalase activity of *Pseudomonas putida* strain oxidizing arsenic. Mikrobiologiya **51**: 34-37.

Aposhian, H.V. and Aposhian, M.M. 1989. Newer developments in arsenic toxicity. Journal of the American College of Toxicology **8**(7): 1297-1305.

Asai, S., Konishi, Y. and Yoshida, K. 1992. Kinetic model for batch bacterial dissolution of pyrite particles by *Thiobacillus ferrooxidans*. Chemical Engineering Science **47**(1): 133-139.

Bailey, A.D. and Hansford, G.S. 1993. Factors affecting bio-oxidation of sulphide minerals at high solids concentrations: a review. Biotechnology and Bioengineering **42**: 1181-1189.

Bailey, A.D. and Hansford, G.S. 1994. Oxygen mass transfer limitation of batch bio-oxidation at high solids concentration. Minerals Engineering **7**(2/3): 293-304.

Barrett, J. 1991. Understanding Inorganic Chemistry. Ellis Horwood, New York.

Barrett, J. and Hughes, M.N. 1993. The mechanism of the bacterial oxidation of arsenopyrite-pyrite mixtures: the identification of plant control parameters. Minerals Engineering **6**(8-10): 969-975.

Barrett, J., Ewart, D.K., Hughes, M.N. and Poole, R.K. 1993(b). Chemical and biological pathways in the bacterial oxidation of arsenopyrite. FEMS Microbiology Reviews **11**: 57-62.

Barrett, J., Ewart, D.K., Hughes, M.N., Nobar, A.M. and Poole, R.K. 1989. The oxidation of arsenic in arsenopyrite: the toxicity of As(III) to a moderately thermophilic mixed culture, pp. 49-57. In: J. Salley, R.G.L. McCready and P.L. Wichlacz (eds.), Proc. Biohydrometallurgy-89. Jackson Hole, July 1989.

Barrett, J., Hughes, M.N. and Russell, A. 1990. Oxidation of arsenopyrite by iron(III), pp. 135–136. In: Proc. Randol Gold Forum. Squaw Valley.

Barrett, J., Hughes, M.N., Karavaiko, G.I. and Spencer, P.A. 1993(a). Metal extraction by bacterial oxidation of minerals. Ellis Horwood, New York.

Beattie, M.J.V. and Poling, G.W. 1987. A study of the surface oxidation of arsenopyrite using cyclic voltametry. International Journal of Minerals Processing **20**: 87-108.

Boogerd, F.C., Van den Beemd, C., Stoelwinder, T., Bos, P. and Kuenen, J.G. 1991. Relative contributions of biological and chemical reactions to the overall rate of pyrite oxidation at temperatures between 30°C and 70°C. Biotechnology and Bioengineering **38**: 109-115.

Boon, M. 1996. Theoretical and experimental methods in the modelling of bio-oxidation kinetics of sulfide minerals. Ph.D. Thesis. Delft University of Technology, Delft.

Boon, M., Hansford, G.S. and Heijnen, J.J. 1995. The role of bacterial ferrous-iron oxidation in the bio-oxidation of pyrite, pp. 153-163. In: T. Vargas, C.A. Jerez, J.V. Wiertz and H. Toledo (eds.), Biohydrometallurgical Processing **1**. University of Chile, Santiago.

Boon, M., Hansford, G.S. and Heijnen, J.J. 1998. The mechanism and kinetics of bioleaching sulphide minerals. Min. Pro. Ext. Met. Rev. **19**: 107-115.

Braddock, J.F., Luong, H.V. and Brown, E.J. 1984. Growth kinetics of *Thiobacillus ferrooxidans* isolated from arsenic mine drainage. Applied and Environmental Microbiology **48**(1): 48-55.

Brierley, C.L. 1993. Application of biotechnology to the economic recovery of metals from ores and concentrates. Australian Mineral Foundation Course No 827/93, 24-25 March 1993. Australian Mineral Foundation, Adelaide.

Brierley, C.L. 1997. Mining biotechnology: research to commercial development and beyond, pp. 3-17. In: D.E. Rawlings (ed.), Biomining: theory, microbes and industrial processes. Springer-Verlag and Landes Bioscience, Berlin.

Brierley, C.L. and Brierley, J.A. 1982. Anaerobic reduction of molybdenum by *sulfolobus* species. Zentralbl. Bakteriol. Parasitenkd. Infektionskr. Hyg. Abt. **3**(2): 289-294.

Broadhurst, J.L. 1994. Neutralisation of arsenic bearing BIOX® liquors. Minerals Engineering **7**(8): 1029-1038.

Brock, T.D. and Gustafson, J. 1976. Ferric iron reduction by sulphur- and iron-oxidising bacteria. Applied and Environmental Microbiology **32**: 567-571.

Bruhn, D.F. and Roberto, F.F. 1993. Maintenance and expression of enteric arsenic resistance genes in *Acidiphilium*, pp. 745-754. In: A.E. Torma, M.L. Apel and C.L. Brierley (eds.), Biohydrometallurgical Technologies **II**. The Minerals, Metals and Materials Society, Warrendale, Pa..

Buckley, A.N. and Walker, G.W. 1988. The surface composition of arsenopyrite exposed to oxidising environments. Applied Surface Science **35**: 277-240.

Cassity, W.D. and Pesic, B. 1995. Interaction of *Thiobacillus ferrooxidans* with arsenite, arsenate and arsenopyrite, pp. 223-228. In: B.J. Scheiner, T.D. Chatwin, H. El-Shall, S.K. Kawatra and A.E. Torma (eds.), New Remediation Technology in the Changing Environmental Arena. Society for Mining, Metallurgy, and Exploration, Inc., Littleton, Co..

Coddington, K. 1986. A review of arsenicals in biology. Toxicological and Environmental Chemistry **11**: 281-290.

Collinet, M.-N. and Morin, D. 1990. Characterisation of arsenopyrite oxidising *Thiobacillus*. Tolerance to arsenite, arsenate, ferrous and ferric iron. Antonie van Leeuwenhoek **57**: 237-244.

Crundwell, F.K. 1994. Mathematical modelling of batch and continuous bacterial leaching. Chem. Eng. J. **54**: 207-220.

Crundwell, F.K. 1995. Progress in the mathematical modelling of leaching reactors. Hydrometallurgy **39**: 321-335.

Cullen, W.R. and Reimer, K.J. 1989. Arsenic speciation in the environment. Chemical Reviews **89**(4): 713-764.

Dabbs, E.R. and Sole, G.J. 1988. Plasmid-borne resistance to arsenate, arsenate, cadmium, and chloramphenicol in a *Rhodococcus* species. Mol. Gen. Genet. **211**: 148-154.

Dew, D.W. 1995. Comparison of performance for continuous bio-oxidation of refractory gold ore flotation concentrates, pp. 239-251. In: T. Vargas, C.A. Jerez, J.V. Wiertz and H. Toledo (eds.), Biohydrometallurgical Processing **I**. University of Chile, Santiago.

Dew, D.W., Lawson, E.N. and Broadhurst, J.L. 1997. The BIOX® process for biooxidation of gold-bearing ores or concentrates, pp. 45-80. In: D.E. Rawlings (ed.), Biomining: theory, microbes and industrial processes. Springer-Verlag and Landes Bioscience, Berlin.

Dew, D.W., Miller, D.M. and Van Aswegen, P.C. 1993. GENMIN's commercialisation of the bacterial oxidation process for the treatment of refractory gold concentrates, pp. 229-237. In: Randol Gold Forum, Randol International.

Dunn, J.G., Fernandez, P.G., Hughes, H.C. and Linge, H.G. 1989. Aqueous oxidation of arsenopyrite in acid, pp. 217-220. In: Proc. Austral. Inst. Min. Metall. Annual Conference. Australasian Institute of Mining and Metallurgy, Glenside, SA.

Eary, L.E. and Schramke, J.A. 1990. Rates of inorganic oxidation reactions involving dissolved oxygen, pp. 379-396. In: D.C. Melchior and R.L. Bassett (eds.), Chemical Modelling of Aqueous Systems II. ACS Symposium Series **416**, Washington D.C.

Fernandez, M.G.M., Mustin, C., De Donato, P., Barres, O., Marion, P. and Berthelin, J. 1995. Occurrences at mineral-bacteria interface during oxidation of arsenopyrite by *Thiobacillus ferrooxidans*. Biotechnology and Bioengineering **46**(1): 13-21.

Fernandez, P.G., Linge, H.G. and Wadsley, M.W. 1996. Oxidation of arsenopyrite in acid. Part I: reactivity of arsenopyrite. Journal of Applied Electrochemistry **26:** 575-583.

Garrels, R.M. and Thompson, M.E. 1960. Oxidation of pyrite by iron sulphate solutions. American Journal of Science **258A**: 57-67.

Golovacheva, R.S., Golyshina, O.V., Karavaiko, G.I., Dorofeyev, A.G., Pivovarova, T.A. and Chernych, N.A. 1992. A new iron oxidising bacterium, *Leptospirillum thermoferrooxidans* sp. nov. Mikrobiologiya **61:** 744-750.

Guay, R., Silver, M. and Torma, A.E. 1977. Ferrous iron oxidation and uranium extraction by *Thiobacillus ferrooxidans*. Biotechnology and Bioengineering **XIX**: 727-740.

Haines, A.K. and Van Aswegen, P.C. 1990. Process and engineering challenges in the treatment of refractory gold ores, pp. 103-110. In: Innovations in Metallurgical Plant, Proc. International Deep Mining Conference. SAIMM, Johannesburg.

Hallberg, K.B. 1995. Role of arsenic toxicity to and resistance of thermophilic bioleaching micro-organisms. Ph.D. Thesis, Umeå University, Umeå.

Hallmann, R., Friedrich, A., Koops, H.P., Pommering-Röser, A., Zenneck, C. and Sand, W. 1993. Physicological characteristics of *Thiobacillus ferrooxidans* and *Leptospirillum ferrooxidans* and physicochemical factors influence microbial metal leaching. Geomicrobiology Journal **10**: 193-205.

Hansford, G.S. 1997. Recent developments in modelling the kinetics of bioleaching, pp. 153-175. In: D.E. Rawlings (ed.), Biomining: theory, microbes and industrial processes. Springer-Verlag and Landes Bioscience, Berlin.

Hansford, G.S. and Bailey, A.D. 1992. The logistic equation for modelling bacterial oxidation kinetics. Minerals Engineering **5**: 1355-1364.

Hansford, G.S. and Chapman, J.T. 1992. Batch and continuous bio-oxidation kinetics of a refractory gold-bearing pyrite/arsenopyrite concentrate. Minerals Engineering **5**(6): 597-612.

Hansford, G.S. and Drossou, M. 1988. A propagating pore model for the batch bioleach kinetics of a gold-bearing pyrite, pp. 345-358. In: P.R. Norris and D.P. Kelly (eds.), Biohydrometallurgy. Science and Technology Letters, Kew, Surrey.

Hansford, G.S. and Miller, D.M. 1993. Biooxidation of a gold-bearing pyrite-arsenopyrite concentrate. FEMS Microbiology Reviews **11**: 175-182.

Hansford, G.S. and Vargas, T. 1999. Chemical and electrochemical basis for the bioleaching process, pp. 13-26. In: R. Amils, A. Ballester (eds.), Biohydrometallurgy and the environment toward the mining of the 21st century **A**. Elsevier, Amsterdam.

Harvey, P.I. and Crundwell, F.K. 1997. Growth of *Thiobacillus ferrooxidans*: a novel experimental design for batch growth and bacterial leaching studies. Applied and Environmental Microbiology **63**(7): 2586-2592.

Helle, U. and Onken, U. 1988. Continuous bacterial leaching of pyritic flotation concentrate by mixed cultures, pp. 61-75. In: P.R. Norris and D.P. Kelly (eds.), Biohydrometallurgy. Science and Technology Letters, Kew, Surrey.

Hindmarsh, J.T. and McCurdy, R.F. 1986. Clinical and environmental aspects of arsenic toxicity. CRC Critical Reviews in Clinical Laboratory Sciences **23**(4): 315-347.

Huber, G. and Stetter, K.O. 1991. *Sulfolobus metallicus*, sp. nov., a novel strictly chemolithoautotrophic thermophilic archaeal species of metal-mobilizers. System. Appl. Microbiol. **14**: 372-378.

Huberts, R. 1994. Modelling of ferrous sulphate oxidation by iron oxidizing bacteria – a chemiosmotic and electrochemical approach. Ph.D. Thesis. University of the Witwatersrand, Johannesburg.

Huysmans, K.D. and Frankenberger, W.T. 1992. Microbial resistance to arsenic, pp. 93-116. In: I.K. Iskander and H.M. Selim (eds.), Engineering Aspects of Metal-waste Management. Lewis Publishers, Boca Raton, Fla..

Iglesias, N. and Carranza, F. 1994. Refractory gold-bearing ores: a review of treatment methods and advances in biotechnological techniques. Hydrometallurgy **34**(3): 383-395.

Iglesias, N., Palencia, I. and Carranza, F. 1996. Treatment of a gold bearing arsenopyrite concentrate by ferric sulphate leaching. Minerals Engineering **9**(3): 317-330.

Iglesias, N., Palencia, I. and Carranza, F. 1993. Removal of the refractoriness of a gold bearing pyrite-arsenopyrite ore by ferric sulphate leaching at low concentration, pp. 99-115. In: J.P. Hager (ed.), EPD Congress 1993, The Minerals, Metals and Materials Society, Warrendale, Co..

Ingledew, W.J. 1986. Ferrous iron oxidation by *Thiobacillus ferrooxidans*. Biotechnology and Bioengineering Symposium Series **16**: 23-33.

Ji, G. and Silver, S. 1992. Reduction of arsenate to arsenite by the ArsC protein of the arsenic resistance operon of *Staphylococcus aureus* plasmid pI258. Proc. Natl. Acad. Sci. USA **89**: 9474-9478.

Jin, Z.M., Warre,n G.W. and Henein, H., 1984. Reaction kinetics of the ferric chloride leaching of sphalerite - an experimental study. Metallurgical Transactions B, **15B**: 5-12.

Jones, C.A. and Kelly, D.P. 1983. Growth of *Thiobacillus ferrooxidans* on ferrous iron in chemostat culture: influence of product and substrate inhibition. Journal of Chemical Technology and Biotechnology **33B**(4): 241-261.

Karavaiko, G.I., Golovacheva, R.S., Pivovarova, T.A., Tzaplina, I.A. and Vartanjan, N.S. 1988. Thermophilic bacteria of the genus *Sulfobacillus*, pp. 29-41. In: P.R. Norris and D.P. Kelly (eds.), Biohydrometallurgy. Science and Technology Letters, Kew, Surrey.

Kawakami, K., Sato, J., Kusunoke, K., Kusokabe, K. and Morooka, S. 1988. Kinetic study of oxidation of a pyrite slurry by ferric chloride. Ind. Eng. Chem. Res. **27**: 571-576

Kelly, D.P. and Jones, C.A. 1978. Factors affecting metabolism and ferrous iron oxidation in suspensions and batch cultures of *Thiobacillus ferrooxidans*: relevance to ferric iron leach solution generation, pp. 19-44. In: L.E. Murr, A.E. Torma and J.A. Brierley (eds.), Metallurgical Applications of Bacterial Leaching and Related Microbiological Phenomena. Academic Press, New York.

Konishi, Y. and Asai, S. 1993. A biochemical engineering approach to the bioleaching of pyrite in batch continuous tank reactors. In: A.E. Torma, J.E. Wey, V.I. Lakshmanan (eds.), Biohydrometallurgical Technologies **I**. The Minerals, Metals and Materials Society, Warrendale, Pa..

Konishi, Y., Asai, S. and Katoh, H. 1990. Bacterial dissolution of pyrite by *Thiobacillus ferrooxidans*. Bioprocess Engineering **5**: 231-237.

Konishi, Y., Kubo, H. and Asai, S. 1992. Bioleaching of zinc sulfide concentrate by *Thiobacillus ferrooxidans*. Biotechnology and Bioengineering **39**(1): 66-74.

Konishi, Y., Takasaka, Y. and Asai, S. 1994. Kinetics of growth and elemental sulfur oxidation in batch culture of *Thiobacillus ferrooxidans*. Biotechnology and Bioengineering **44**(6): 667-673.

Kostina, G.M. and Chernyak, A.S. 1976. Electrochemical conditions for the oxidation of pyrite and arsenopyrite in alkaline and acid solutions. Zhurnal Prikladnoi Khimii **49**(7): 1534-1570.

La Motta, E.J. 1976. Kinetics of continuous growth cultures using the logistic growth curve. Biotechnology and Bioengineering **XVIII**: 1029-1032.

Lacey, D.T. and Lawson, F. 1970. Kinetics of the liquid-phase oxidation of acid ferrous sulphate by the bacterium *Thiobacillus ferrooxidans*. Biotechnology and Bioengineering **12**: 29-50.

Lawson, E.N. 1993. Arsenic toxicity, bacterial resistance and bacterial oxidation/reductions. Phase 1: literature review. Report No. PR 93/109C of Project No. PR 93/132. GENMIN Process Research, Johannesburg.

Lawson, E.N., Nicholas, C.N. and Pellat, H. 1995. The toxic effects of chloride ions on *Thiobacillus ferrooxidans*, pp. 165-174. In: T. Vargas, C.A. Jerez, J.V. Wiertz and H. Toledo (eds.), Biohydrometallurgical Processing **I**. University of Chile, Santiago.

Lázaro, I., Cruz, R., González, I. and Monroy, M. 1997. Electrochemical oxidation of arsenopyrite in acidic media. International Journal of Minerals Processing **50**(1-2): 63-75.

Lázaro, I., Martinez-Medina, N., Arce, E., Rodriguez, I. and Gonzalez, I. 1995. The use of carbon paste electrodes with non conducting binder to the study of minerals: chalcopyrite. Hydrometallurgy, **38**(3): 275-285.

Lindström, E.B. and Sehlin, H.M. 1989. Toxicity of arsenic compounds to the sulphur- dependent archaebacterium *Sulfolobus*, pp. 59-70. In: J. Salley, R.G.L. McCready and P.L. Wichlacz (eds.), Proc. Biohydrometallurgy-89. Jackson Hole, July 1989.

Linge, H.G. and Jones, W.G. 1993. Electrolytic oxidation of arsenopyrite slurries. Minerals Engineering **6**(8-10): 873-882.

Liu, M.S., Branion, R.M.R. and Duncan, D.W. 1988. The effects of ferrous iron, dissolved oxygen, and inert solids concentration on the growth of *Thiobacillus ferrooxidans*. The Canadian Journal of Chemical Engineering **66** (June): 445-451.

Lizama, H.M. and Suzuki, I. 1989. Synergistic competitive inhibition of ferrous iron oxidation by *Thiobacillus ferrooxidans* by increasing concentrations of ferric iron and cells. Applied and Environmental Microbiology **55**(10): 2588-2591.

Lundgren, D. and Tano, T. 1978. Structure-function relationships of *Thiobacillus* relative to ferrous iron and sulfide oxidations, pp. 151-166. In: L.E. Murr, A.E. Torma and J.A. Brierley (eds.), Metallurgical Applications of Bacterial Leaching and Related Microbiological Phenomena. Academic Press, New York.

MacDonald, D.G. and Clarke, R.H. 1970. The oxidation of aqueous ferrous sulphate by *Thiobacillus ferrooxidans*. The Canadian Journal of Chemical Engineering **48**(December): 669-676.

Madgewick, J. 1989. Bacterial pretreatment of refractory gold ores. Australian Journal of Biotechnology **3**(4): 255-257.

Malatt, K. 1998. The bacterial oxidation of gold-bearing pyrite/arsenopyrite concentrates. Ph.D. Thesis, Curtin University of Technology, Perth, WA.

Mandl, M., Matulová, P. and Docekalová, H. 1992. Migration of arsenic(III) during bacterial oxidation of arsenopyrite in chalcopyrite concentrate by *Thiobacillus ferrooxidans*. Applied Microbiology and Biotechnology **38**: 429-431.

Mathews, C.T. and Robins, R.G. 1972. The oxidation of iron disulfide by ferric sulphate. Australian Journal of Chemical Engineering **August**: 21-25.

May, N. 1997. The ferric leaching of pyrite. M. App. Sc. Dissertation. University of Cape Town, Cape Town.

May, N., Ralph, D.E. and Hansford, G.S. 1997. Dynamic redox potential measurement for determining the ferric leach kinetics of pyrite. Minerals Engineering **10**(11): 1279-1290.

McKibben, M.A. and Barnes, H.L. 1986. Oxidation of pyrite in low temperature acidic solutions. Geochem. et Cosmochim. Acta. **50**: 1509-1520.

Miller, D.M. 1991. Effect of temperature on BIOX® operations. In: Proc. Bacterial Oxidation Colloquium, The South African Institute of Mining and Metallurgy, Johannesburg.

Miller, D.M. and Hansford, G.S. 1992(a). Batch biooxidation of a gold-bearing pyrite-arsenopyrite concentrate. Minerals Engineering **5**(6): 613-629.

Miller, D.M. and Hansford, G.S. 1992(b). The use of the logistic equation for modelling the performance of a biooxidation pilot plant treating a gold-bearing arsenopyrite-pyrite concentrate. Minerals Engineering **5**(7): 737-749.

Miller, P.C. 1997. The design and operating practice of bacterial oxidation plant using moderate thermophiles (the BacTech process), pp. 81-102. In: D.E. Rawlings (ed.), Biomining: theory, microbes and industrial processes. Springer-Verlag and Landes Bioscience, Berlin.

Mobley, H.T. and Rosen, B.P. 1982. Energetics of plasmid-mediated arsenate resistance in *Escherichia coli*. Proc. Natl. Acad. Sci. USA **79**: 6119-6122.

Morin D., Ollivier P., Toromanoff, I. and Letestu, A. 1991. Bioleaching of gold refractory arsenopyrite rich sulfide concentrate: laboratory and pilot case studies, pp. 577-589. In: D.R. Gaskell (ed.), Proc. EPD Congress '91. The Minerals, Metals & Materials Society, Warrendale, Co..

Moses, C.O., Nordstrom, D.K., Herman, J.S. and Mills, A.L. 1987. Aqueous pyrite oxidation by dissolved oxygen and ferric iron. Geochem. et Cosmochim. Acta. **51**: 2502-2509.

Nagpal, S., Dahlstrom, D. and Oolman, T. 1994. A mathematical model for the bacterial oxidation of a sulfide ore concentrate. Biotechnology and Bioengineering **43**(5): 357-364.

Nagpal, S., Oolman, T., Free, M.L., Palmer, B. and Dahlstrom, D. 1991. Biooxidation of a refractory pyrite-arsenopyrite-gold ore concentrate, pp. 469-483. In: R.W. Smith and M. Misra (eds.), Mineral Bioprocessing. The Minerals, Metals & Materials Society, Warrendale, Co..

Natarajan, K.A. 1988. Electrochemical aspects of bioleaching multisulfide minerals. Materials and Metallurgical Processing **May**: 61-65.

Natarajan, K.A. and Iwasaki, I. 1985. Microbe-mineral interactions in the leaching of complex sulfide, pp. 1-13. In: J.A. Clum and L.A. Haas (eds.), Microbiological effects on metallurgical processes. TMS/AIME, Pennsylvania.

Nemati, M. and Webb, C. 1997. A kinetic model for biological oxidation of ferrous iron by *Thiobacillus ferrooxidans*. Biotechnology and Bioengineering **53**(5): 478-486.

Nemati, M., Harrison, S.T.L., Webb, C. and Hansford, G.S. 1998. Biological oxidation of ferrous sulphate by *Thiobacillus ferrooxidans*: a review on the kinetic aspects. Biochemical Engineering Journal **1**: 171-190.

Nicolau, C. and Raimond, J. 1983. As cited by Lawson, E.N. 1993. Arsenic toxicity, bacterial resistance and bacterial oxidation/reductions. Phase 1: literature review. Report No. PR 93/109C of Project No. PR 93/132. GENMIN Process Research, Johannesburg.

Nikolov, L.N. and Karamanev, D.G. 1992. Kinetics of the ferrous-iron oxidation by resuspended cells of *Thiobacillus ferrooxidans*. Biotechnology Progress **8**(3): 252-255.

Norris, P.R. 1997. Thermophiles and bioleaching, pp. 247-258. In: D.E. Rawlings (ed.), Biomining: theory, microbes and industrial processes. Springer-Verlag and Landes Bioscience, Berlin.

Norris, P.R. and Barr, D.W. 1985. Growth and iron oxidation by acidophilic thermophiles. FEMS Microbiology Letters **28:** 221-224.

Norris, P.R. and Kelly, D.P. 1978. Toxic metals in leaching systems, pp. 83-102. In: L.E. Murr, A.E. Torma, J.A. Brierley (eds.), Metallurgical applications of bacterial leaching and related microbiological phenomena. Academic Press, New York.

Norris, P.R., Barr, D.W. and Hinson D. 1988. Iron and mineral oxidation by acidophilic bacteria: affinities for iron and attachment to pyrite, pp. 43-59. In: P.R. Norris and D.P. Kelly (eds.), Biohydrometallurgy. Science and Technology Letters, Kew, Surrey.

Novick, R.P. and Roth, C. 1968. Plasmid-linked resistance to inorganic salts in *Staphylococcus aureus*. Journal of Bacteriology **95**(4): 1335-1342.

Osborne, F.H. and Ehrlich, H.L. 1976. Oxidation of arsenite by a soil isolate of *Alcaligenes*. Journal of Applied Bacteriology **41**: 295-305.

Panin, V.V., Karavaiko, G.I. and Pol'kin, S.I. 1985. Mechanism and kinetics of bacterial oxidation of sulfide minerals, pp. 197-215. In: Biotechnology of Metals, G.I. Karavaiko and S.N. Groudev (eds.). Centre of International Projects, Moscow.

Phillips, S.E. and Taylor, M.L. 1976. Oxidation of arsenite to arsenate by *Alcaligenes faecalis*. Applied and Environmental Microbiology **32**(3): 392-399.

Pinches, A., Chapman, J.T., Te Riele, W.A.M. and Van Staden, M. 1988. The performance of bacterial leach reactors for the pre-oxidation of refractory gold-bearing sulfide concentrates, pp. 329-344. In: P.R. Norris and D.P. Kelly (eds.), Biohydrometallurgy. Science and Technology Letters, Kew, Surrey.

Pirt, S.J. 1975. Principles of microbe and cell cultivation. John Wiley and Sons Inc., New York.

Pletcher, D. 1984. Industrial Electrochemistry. Chapman and Hall, New York.

Pol'kin, S.I., Panin, V.V., Adamov, E.V., Karavaiko, G.I. and Chernyak, A.S. 1975. Theory and practice of utilizing micro-organisms in difficult-to-dress ores and concentrates, pp. 901-923. In: Proc. 11th International Mineral Processing Congress. Cagliari, 20-26 April 1975.

Pronk, J.T., De Bruyn, J.C., Bos, P. and Kuenen, J.G. 1992. Anaerobic growth of *Thiobacillus ferrooxidans*. Applied and Environmental Microbiology **58**: 2227-2230.

Rawlings, D.E. 1995. Restriction enzyme analysis of 16S rDNA genes for the rapid identification of *Thiobacillus ferrooxidans, Thiobacillus thiooxidans* and *Leptospirillum ferrooxidans* strains in leaching environments, pp. 9-17. In: T. Vargas, C.A. Jerez., J.V. Wiertz and H. Toledo (eds.), Biohydrometallurgical Processing **1**. University of Chile, Santiago.

Rawlings, D.E. 1997(b). Mesophilic, autotrophic bioleaching bacteria: description, physiology and role, pp. 229-245. In: D.E. Rawlings (ed.), Biomining: theory, microbes and industrial processes. Springer-Verlag and Landes Bioscience, Berlin.

Rawlings, D.E. (ed.). 1997(a). Biomining: theory, microbes and industrial processes. Springer-Verlag and Landes Bioscience, Berlin.

Rawlings, D.E., Coram, N.J., Gardner, M.N. and Deane, M.N. 1999(a). *Thiobacillus caldus* and *Leptospirillum ferrooxidans* are widely distributed in continuous flow biooxidation tanks used to treat a variety of metal containing ores and concentrates, pp. 777-786. In: R. Amils, A. Ballester (eds.), Biohydrometallurgy and the environment toward the mining of the 21st century **A**. Elsevier, Amsterdam.

Rawlings, D.E., Tributsch, H. and Hansford, G.S. 1999(b). Reasons why *Thiobacillus ferrooxidans* is not the dominant iron-oxidising bacterium in many commercial processes for the biooxidation of pyrite and related ores. Microbiology **145**(1): 5-13.

Rimstidt, J.D., Chermak, J.A. and Gagen, P.M. 1994. Rates of reaction of galena, sphalerite, chalcopyrite and arsenopyrite with Fe(III) in acidic solutions, pp. 2-13. In: C.N. Alpers and D.W. Blowes (eds.), Environmental Geochemistry of sulfide oxidation. ACS Symposium Series **550**, Washington D.C.

Rinderle, S.J., Schrier, J. and Williams, J.W. 1984. Purification and properties of arsenite oxidase (abstract). Fed. Proc. **43**: 2060.

Rosen, B.P., Hsu, C.M., Karkaria, C.E., Owolabi, J.B. and Tisa, L.S. 1990. Molecular analysis of an ATP-dependent anion pump. Phil. Trans. R. Soc. Lond. B **326**: 455-463.

Rosenstein, R., Paschel, A., Wieland, B. and Götz, F. 1992. Expression and regulation of the antimonite, arsenite and arsenate resistance operon of *Staphylococcus xylosus* plasmid pSX267. Journal of Bacteriology **174**(11): 3676-3683.

Rossi, G. 1990. Biohydrometallurgy. McGraw-Hill Book Company GmbH, Hamburg.

Sanchez, V.M. and Hiskey, J.B. 1991. Electrochemical behaviour of arsenopyrite in alkaline media. Minerals and Metallurgical Processing **February**: 1-6.

Sand, W., Gehrke, T., Josza, P.-G. and Schippers, A. 1999. Direct versus indirect bioleaching, pp. 27-49. In: R. Amils, A. Ballester (eds.), Biohydrometallurgy and the environment toward the mining of the 21st century **A**. Elsevier, Amsterdam.

Sand, W., Rohde, K., Sobotke, B. and Zenneck, C. 1992. Evaluation of *Leptospirillum ferrooxidans* for leaching. Applied and Environmental Microbiology **58**(1): 85-92.

Schippers, A. and Sand, W. 1999. The bioleaching of sulfide minerals proceeds via two indirect mechanisms: via thiosulfate or via polysulfides and sulfur. Applied and Environmental Microbiology **65**: 319-321.

Schnaitman, C.A., Korzynski, M.S. and Lundgren, D.G. 1969. Kinetic studies of ferrous iron oxidation by whole cells of *Ferrobacillus ferrooxidans*. Journal of Bacteriology **99**(8): 552-557.

Schnell, H.A. 1997. Bioleaching of copper, pp. 21-43. In: D.E. Rawlings (ed.), Biomining: theory, microbes and industrial processes. Springer-Verlag and Landes Bioscience, Berlin.

Sehlin, H.M. and Lindström, E.B. 1992. Oxidation and reduction of arsenic by *Sulfolobus acidocaldarius* strain BC. FEMS Microbiology Letters **93**: 87-92.

Shrestha, G.N. 1988. Microbial leaching of refractory gold ores. Australian Mining **October**: 48-51.

Shuey, T.T. 1975. Semiconducting Ore Minerals. Elsevier Scientific Publishing Company, Amsterdam.

Silver, S. 1978. Transport of cations and anions, pp. 221-324. In: B.P. Rosen (ed.), Bacterial Transport, Marcel Dekker Inc., New York.

Silver, S. and Keach, D. 1982. Energy-dependent arsenate efflux: the mechanism of plasmid-mediated resistance. Proc. Natl. Acad. Sci. USA **79**: 6114-6118.

Silver, S. and Misra, T.K. 1988. Plasmid-mediated heavy metal resistances. Ann. Rev. Microbiol. **42**: 717-743.

Silver, S. and Nakahara, H. 1983. Bacterial resistance to arsenic compounds, pp. 190-198. In: W.H. Lederer and R.J. Fensterheim (eds.), Arsenic: Industrial, Biomedical, Environmental Perspectives. Van Nostrand Reinhold, New York.

Silver, S., Budd, K., Leahy, K.M., Shaw, W.V., Hammond, D., Novick, R.P., Willsky, G.R., Malamy, M.H. and Rosenberg, H. 1981. Inducible plasmid-determined resistance to arsenate, arsenite and antimony(III) in *Escherichia coli* and *Staphylococcus aureus*. Journal of Bacteriology **146**(3): 983-996.

Suzuki, I. and Lizama, H.M. 1989. Synergistic inhibition of ferrous iron oxidation by *Thiobacillus ferrooxidans* by increasing concentrations of cells. Applied and Environmental Microbiology **55**(5): 1117-1121.

Tal, P. 1986. The effect of the iron(III) to iron(II) ratio on the rate of dissolution of pyrite. Technical Memorandum No: 18255. Council for Mineral Technology: Hydrometallurgy Division, Johannesburg.

Torma, A.E. and Oolman, T. 1992. Bioliberation of gold. International Materials Reviews **37**(4): 187-193.

Trevors, J.T., Oddie, K.M. and Belliveau, B.H. 1985. Metal resistance in bacteria. FEMS Microbiology Reviews **32**: 39-54.

Tributsch, H. 1999. Direct versus indirect bioleaching, pp. 51-60. In: R. Amils, A. Ballester (eds.), Biohydrometallurgy and the environment toward the mining of the 21st century **A**. Elsevier, Amsterdam.

Tuovinen, O.H., Niemelä, S.I. and Gyllenberg, H.G. 1971. Tolerance of *Thiobacillus ferrooxidans* to some metals. Antonie van Leeuwenhoek **37**: 489-496.

Van Aswegen, P.C. 1993. Bio-oxidation of refractory gold ores. the GENMIN experience, pp. 15.1-15.14. In: Biomine '93. Australian Mineral Foundation, Glenside, SA.

Van Scherpenzeel, D.A. 1996. The kinetics of ferrous-iron oxidation by *Leptospirillum*-like bacteria in absence and in presence of pyrite and pyrite/arsenopyrite mixtures in continuous and batch cultures. M.Sc. Dissertation, University of Cape Town, Cape Town.

Vargas, T. 2000. Private communication.

Wakao, N., Koyatsu, H., Komai, Y., Shimokawara, H., Sakurai, Y. and Shiota, H. 1988. Microbial oxidation of arsenite and occurrence of arsenite-oxidising bacteria in acid mine water from a sulphur-pyrite mine. Geomicrobiology Journal **6**: 11-24.

Welham, N.J. 1994. As cited by Malatt, K. 1998. The bacterial oxidation of gold-bearing pyrite/arsenopyrite concentrates. Ph.D. Thesis, Curtin University of Technology, Perth, WA.

Welham, N.J. and Linge, H.G. 1994. As cited by Malatt, K. 1998. The bacterial oxidation of gold-bearing pyrite/arsenopyrite concentrates. Ph.D. Thesis, Curtin University of Technology, Perth, WA.

Whitlock, J.L. 1997. Biooxidation of refractory gold ores (the geobiotics process), pp. 117-127. In: D.E. Rawlings (ed.), Biomining: theory, microbes and industrial processes. Springer-Verlag and Landes Bioscience, Berlin.

Wiersma, C.L. and Rimstidt, J.D. 1984. Rates of reaction of pyrite and marcasite with ferric iron at pH 2. Geochem. et Cosmochim. Acta. **48**: 85-92.

Williams, J.W. and Silver, S. 1984. Bacterial resistance and detoxification of heavy metals. Enzyme. Microb. Technol. **6**: 530-537.

Williamson, M.A. and Rimstidt, J.D. 1994. The kinetics and electrochemical rate-determining step of aqueous pyrite oxidation. Geochem. et Cosmochim. Acta. **58**: 5443-5454.

Willsky, G.R. and Malamy, M.H. 1980. Effect of arsenate on inorganic phosphate transport in *Escherichia coli*. Journal of Bacteriology **144**(1): 366-374.

Zheng, C.Q., Allen, C.C. and Bautista, R.G. 1986. Kinetic study of the oxidation of pyrite in aqueous ferric sulfate. Ind. Eng. Chem. Process. Des. Dev. **23**: 308-317.

Zhukov, I.A. and Smagunov, V.N. 1971. Oxidation mechanism of arsenopyrite. Journal of Applied Chemistry of the USSR **44**(8): 1680-1688.

For Darren

Argue
for your limitations,
and sure enough,
they're
yours.

ILLUSIONS – Richard Bach

Chapter Three

The Ferric Leaching of Arsenopyrite

As stated in the literature review, the rate at which both pyrite and arsenopyrite are leached by ferric-iron has been found to increase with an increase in the ferric/ferrous-iron ratio, or redox potential (Malatt, 1998; May *et al.*, 1997). This suggests that these minerals undergo dissolution by electrochemical means. However, although many researchers have identified the redox potential as being an important parameter during the ferric leaching of sulfide minerals, apart from the model proposed by May *et al.* (1997), few workers have attempted to formulate models based on electrochemical/corrosion theory to describe the kinetics.

The work presented in this chapter was therefore aimed at determining whether or not the ferric leaching rate of arsenopyrite could be described using a mechanistically based kinetic model, such as the Butler-Volmer based model proposed by May *et al.* (1997) for the leaching of pyrite.

However, before this could be done it was necessary to establish the stoichiometry of the reaction by which arsenopyrite is degraded by ferric-iron. Although considerable work on the ferric leaching of pyrite has been performed, to date very little work on the ferric leaching of arsenopyrite has been reported. This has resulted in the literature having conflicting reports with regard to the stoichiometry by which arsenopyrite is leached by ferric-iron. Therefore, an initial investigation was performed in an attempt to determine the stoichiometry of this reaction. However, because of difficulties encountered with regard to obtaining samples of pure arsenopyrite, this work was performed using an arsenopyrite/pyrite flotation concentrate.

A further objective of the work described in this chapter was to determine the effect of various parameters (*viz.* $E_{initial}$, $[Fe]_{tot}$, ρ_{pulp} and pH) on the ferric leaching kinetics of arsenopyrite.

3.1 Ferric Leaching of an Arsenopyrite/pyrite Flotation Concentrate*

3.1.1 Materials and Methods

3.1.1.1 Experimental equipment

The experiments were carried out in sealed, baffled, agitated 2 ℓ, glass Quickfit culture vessels. These vessels are 220 mm in height and have an internal diameter of 116 mm. Quickfit flat flange lids, 100 mm in diameter, were used in an attempt to reduce evaporative losses. Two of the three sampling ports were sealed; the third was fitted with a Quickfit reflux condenser through which cooling water was passed.

The slurry was suspended by 4-bladed pitched blade impellers rotating at 600 rev.min^{-1} by Heidolph RZR 50 105/38W variable speed overhead motors. The impellers were 70 mm in diameter and were located 40 mm from the base of the reactor. The impeller blades were 20 mm wide and had a pitch of 45°.

Four stainless steel baffles located at 90° to one another ensured uniform suspension of the slurry. The baffles were 14 mm wide and extended from 7 mm above the reactor base to a height of 15 mm above the slurry surface. The baffles were held in place by means of two 10 mm wide, flexible, stainless steel bands to which they were welded, 12 mm from the top and base, respectively.

The slurry temperature in the reactors was controlled at 40°C by placing the reactors in a water bath. The temperature of the water in the water bath was maintained at 40°C using a 2 kW Labotec Model 101 water heater.

The redox potential of the slurry in the reactors was monitored continuously by direct millivolt measurement using an ASI OR101431 Pt combination, double junction Ag/AgCl ORP electrode and a Hitech Micro Systems UCT Redox Controller.

3.1.1.2 Mineral used

The arsenopyrite/pyrite flotation concentrate used was obtained from Fairview Gold Mine in Barberton, South Africa. The size distribution was determined using a Malvern Laser Master-Sizer. This method utilises the fact that particles suspended in water passing through the measuring cell diffract the laser beam at angles which correspond to the diameter of the particles. The size analysis of the concentrate sample is listed in Table 3-1 and indicates that 86.35 % of the material was finer than 75 micron and 70.07 % was finer than 25 micron.

---

* Breed, A.W., Harrison, S.T.L. and Hansford, G.S. 1997. A preliminary investigation of the ferric leaching of a pyrite/arsenopyrite flotation concentrate. Minerals Engineering **10**(9): 1023-1030.

Table 3-1: Size analysis of Fairview flotation concentrate sample

Size fraction (μm)	Mass percent (%)
+ 106	1.73
- 106 + 75	5.16
- 75 + 38	10.07
- 38 + 25	6.21
- 25	70.07

The total iron and arsenic content of the concentrate was determined by digesting a representative sample of known mass in hydrofluoric, nitric and perchloric acid (Bailey, 1993). The amount of iron and arsenic solubilised was then determined by Flame Atomic Adsorption Spectroscopy (FAAS). The sulfur content of the sample was determined using a Leco SC32 sulfur analyser. The elemental analysis of the concentrate is listed in Table 3-2.

Table 3-2: Elemental analysis of Fairview flotation concentrate sample

Element	Mass Percent (%)
As	5.84
S	21.71
Fe	24.01

The mineral analysis of the concentrate was estimated from the elemental analysis; it is listed in Table 3-3.

Table 3-3: Mineral analysis of Fairview flotation concentrate sample

Mineral	Mass Percent (%)
Arsenopyrite (FeAsS)	12.68
Pyrite (FeS_2)	37.18

3.1.1.3 Ferric/ferrous-iron ratio determination

The ferric/ferrous-iron ratio can be related to the solution redox potential, using the Nernst equation:

$$E_h = E_0 + \frac{RT}{zF}\ln\left(\frac{a_{Fe^{+3}}}{a_{Fe^{+2}}}\right) \quad (3\text{-}1)$$

Equation 3-1 can be rewritten as:

$$E_h = E_0' + \frac{RT}{zF}\ln\left(\frac{[Fe^{+3}]}{[Fe^{+2}]}\right) \quad (3\text{-}2)$$

where:

$$E_0' = E_0 + \frac{R\,T}{z\,F}\ln\left(\frac{\gamma_{Fe^{+3}}}{\gamma_{Fe^{+2}}}\right) \tag{3-3}$$

Equation 3-2 can also be written for redox potential measurements in which the reference electrode is not the standard hydrogen electrode (SHE):

$$E = E_0'' + \frac{R\,T}{z\,F}\ln\left(\frac{[Fe^{+3}]}{[Fe^{+2}]}\right) \tag{3-4}$$

The measured solution redox potential and a calibration curve for the redox probe can then be used to determine the ferric/ferrous-iron ratio. The ferric/ferrous-iron ratio and the total iron concentration can in turn be used to calculate the concentrations of both ferrous- and ferric-iron:

$$[Fe^{2+}] = \frac{[Fe]_{tot}}{1 + \frac{[Fe^{3+}]}{[Fe^{2+}]}} \tag{3-5}$$

$$[Fe^{3+}] = \frac{[Fe]_{tot}\frac{[Fe^{3+}]}{[Fe^{2+}]}}{1 + \frac{[Fe^{3+}]}{[Fe^{2+}]}} \tag{3-6}$$

3.1.1.4 Redox probe calibration

The total iron concentration, the counter-ions present, and the temperature of the solution influence the activities of the dissolved ferric and ferrous-iron species, hence these parameters affect the measured value of the redox potential at a particular ferric/ferrous-iron ratio. It was therefore necessary to calibrate the redox probe at the conditions to be employed before using it to determine the dissolved ferrous- and ferric-iron concentrations. However, as previous work has shown that arsenic concentrations below 13 mmol.ℓ^{-1} have little effect on the relationship between the redox potential and the ferric/ferrous-iron ratio (Breed and Hansford, unpublished data), its effect was not considered during the redox probe calibration.

The redox probe was calibrated as follows. Ferrous- and ferric sulfate solutions of similar concentrations were made up, and the concentrations thereof determined by titration with potassium dichromate, $K_2Cr_3O_7$ (Jeffrey *et al.*, 1989). A known volume of ferric sulfate was added to a jacketed vessel, the redox probe inserted and the solution agitated. The temperature in the reactor was maintained at the required temperature by circulating water from a Grant Y6 constant temperature bath through the reactor jacket. Once thermal equilibrium had been

achieved an aliquot of ferrous sulfate* was added and the redox potential of the solution recorded.† This procedure was continued until the solution contained equal volumes of ferric- and ferrous sulfate. Thereafter the measured redox potential values were plotted against $\ln([Fe^{3+}]/[Fe^{2+}])$, and the Nernst parameters, *viz.* RT/zF (slope) and E_0'' (intercept), determined.

The raw data and results of a typical redox probe calibration are shown in the Appendix to this Chapter.

3.1.1.5 Experimental procedure

The experiments were begun by filling the reactors to be used with distilled water and placing them in the waterbath. The temperature of the waterbath was adjusted to ensure that the temperature in the reactors was 40°C, and the system left overnight to reach thermal equilibrium. The following day the water lost due to evaporation was replaced and the required quantity of ferric sulfate was added to the reactors.‡ The initial ferric-iron concentrations in the batch reactors are listed in Table 3-4 below.

Table 3-4: Initial ferric-iron concentration in the batch reactors

Reactor	$[Fe^{3+}]_{initial}$ (mmol $Fe^{3+}.\ell^{-1}$)
1	0
2	90
3	180
5	360
6	450
7	540

The reactors were left to condition for 2 hours, a sample of the leach liquor was taken and the quantity of arsenopyrite/pyrite flotation concentrate required to ensure a solids concentration of 1 %, was added. The experiments were continued for a further 48 hours. During this time, the leaching rate was monitored by observing the variation in the redox potential of the slurry. In addition, periodic samples of the leach liquor were taken, filtered through an 8 micron Millipore filter and the concentrations of iron and arsenic determined by Flame Atomic Adsorption Spectroscopy (FAAS).

The pH of the slurry was not controlled§, nor was water added to account for evaporative and sampling losses.

* The ferrous sulfate solution was placed in the constant temperature bath used to control the temperature of the solution in which the probe was calibrated. This ensured that the addition of the ferrous sulfate solution did not result in fluctuations in the temperature of the solution used to calibrate the redox probe.

† The response of the logging system was rapid and the readings were found to be stable over long periods of time, *e.g.* a stable reading was achieved 2 s after a 30 mV step change in the solution redox potential.

‡ Because of uncertainty concerning the degree of hydration of the ferric sulfate, its molecular mass was determined by dissolving a known mass in water and determining the iron content using FAAS.

§ The initial pH in the reactors was between pH 1.10 and pH 1.80, depending on the amount of ferric sulfate added to the reactor. During the experiment performed in the absence of ferric sulfate, the initial pH was adjusted to pH 1.75. The pH was not controlled. However, it did not vary by more than 0.10 during the course of an experiment.

3.1.2 Results and Discussion

The total iron concentration of the supernatant in the reactors with initial ferric-iron concentrations of 0, 90, 180, 450 and 540 mmol.ℓ^{-1} did not vary significantly during the course of the experiment. However, the total iron concentration of the supernatant in the reactor with an initial concentration of 360 mmol $Fe^{3+}.\ell^{-1}$, decreased during the course of the experiment (data not shown).

The variation in the measured redox potential of the supernatant during the course of the experiments is shown in Figure 3.1. From Figure 3.1, it is clear that the redox potential of the slurry in all the reactors decreased with time.

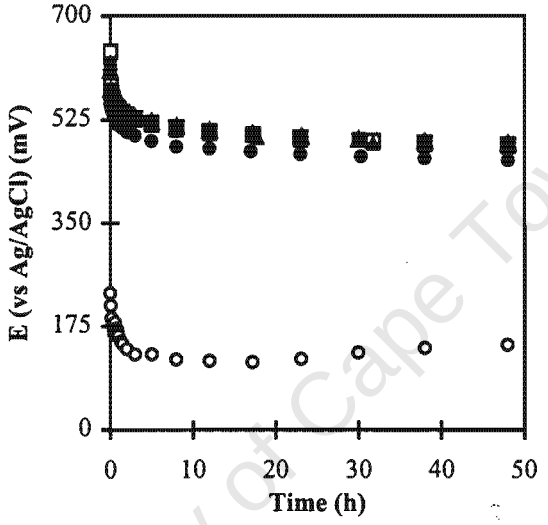

Figure 3.1: Variation in the redox potential of the slurry with time at different initial ferric-iron concentrations. [o] 0 mmol $Fe^{3+}.\ell^{-1}$; [•] 90 mmol $Fe^{3+}.\ell^{-1}$; [□] 180 mmol $Fe^{3+}.\ell^{-1}$; [▲] 360 mmol $Fe^{3+}.\ell^{-1}$; [Δ] 450 mmol $Fe^{3+}.\ell^{-1}$; [■] 540 mmol $Fe^{3+}.\ell^{-1}$.

The decrease in the redox potential of the slurry in the reactor to which no ferric-iron was added can be attributed to the dissolution of trace quantities of ferrous-iron present on the surface of the mineral. This resulted in a significant change in the redox potential because of the very low overall iron concentration in this reactor, *viz.* $[Fe]_{tot} \leq 4$ mmol.ℓ^{-1}.

However, the decrease in the redox potential of the slurry in the reactors to which ferric-iron was added indicates that ferric-iron was consumed and ferrous-iron generated, according to;

$$Fe^{3+} + e^{-} \rightarrow Fe^{2+} \qquad (3\text{-}7)$$

It is also evident from Figure 3.1 that the shape of the redox potential versus time curves were similar in all the reactors to which ferric-iron was added. This suggests that the rate at which arsenopyrite is solubilised may be a

function of the solution redox potential, and not of the absolute ferric-iron concentration, which is consistent with the results of recent research using pyrite (May, 1997).*

Figure 3.2 shows the variation in the arsenic concentration of the supernatant during the course of the experiment. It is apparent from Figure 3.2 that no arsenic was solubilised in the absence of added ferric-iron. However, significant leaching of arsenic occurred in the reactors to which ferric-iron was added.

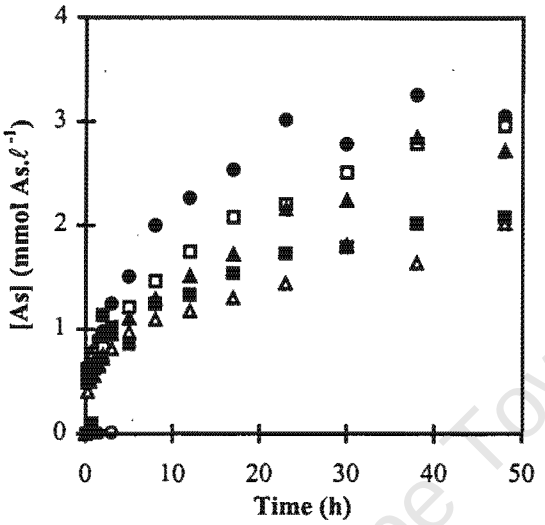

Figure 3.2: Variation in the arsenic concentration of the supernatant with time at different initial ferric-iron concentrations. [○] 0 mmol $Fe^{3+}.\ell^{-1}$; [•] 90 mmol $Fe^{3+}.\ell^{-1}$; [□] 180 mmol $Fe^{3+}.\ell^{-1}$; [▲] 360 mmol $Fe^{3+}.\ell^{-1}$; [Δ] 450 mmol $Fe^{3+}.\ell^{-1}$; [■] 540 mmol $Fe^{3+}.\ell^{-1}$.

The results shown in Figures 3.1 and 3.2 therefore suggest that the chemical leaching of arsenopyrite occurs according to;

$$FeAsS + (x-1)\,Fe^{3+} \rightarrow \text{Sulphur species} + \text{Arsenic species} + x\,Fe^{2+} \qquad (3\text{-}8)$$

It is also apparent from Figure 3.2 that the final arsenic concentration of the supernatant decreased with an increase in the initial ferric-iron concentration. This trend was not anticipated; it suggests that the arsenopyrite conversion, *i.e.* the proportion of arsenopyrite in the feed that was solubilised, decreases with an increase in the leachate concentration.† The conversions calculated in this manner are listed in Table 3-5.

The decrease in the final arsenic concentration of the supernatant with an increase in the initial ferric-iron concentration shown in Figure 3-2, and the results shown in Table 3-5 suggest that high concentrations of ferric-iron in the leaching medium result in either:

i) passivation of the mineral surface, or
ii) co-precipitation of iron and arsenic.

* Although the chemical leaching of the pyrite portion of the concentrate cannot be disregarded, it has been found that the bioleaching of arsenopyrite precedes the bioleaching of pyrite (Miller and Hansford, 1992). For this reason, it was assumed that the data obtained could be interpreted assuming that the sample consisted only of arsenopyrite.

† The assumption that the proportion of arsenic solubilised is equivalent to the conversion of arsenopyrite was based on the fact that it has been reported that arsenopyrite undergoes stoichiometric dissolution in ferric sulfate media (Malatt, 1998).

Table 3-5: Arsenopyrite conversion based on the assumption that all the arsenic remained in solution

$[Fe^{3+}]_{initial}$ (mmol $Fe^{3+}.\ell^{-1}$)	X_{FeAsS} (%)
90	40
180	38
360	35
450	26
540	27

In an attempt to determine the reason(s) for the apparent decrease in conversion with an increase in the initial ferric-iron concentration, the variation in the measured arsenic concentration of the supernatant was plotted as a function of the calculated ferrous-iron concentration.* This data is shown in Figure 3.3 together with similar data obtained during the ferric leaching of pure arsenopyrite (Iglesias *et al.*, 1993). Linear regression of the results shown in Figure 3.3 was carried out to determine the stoichiometric coefficient of Fe^{2+}, *viz.* "x", in Equation 3-8. These results are shown in Table 3-6.

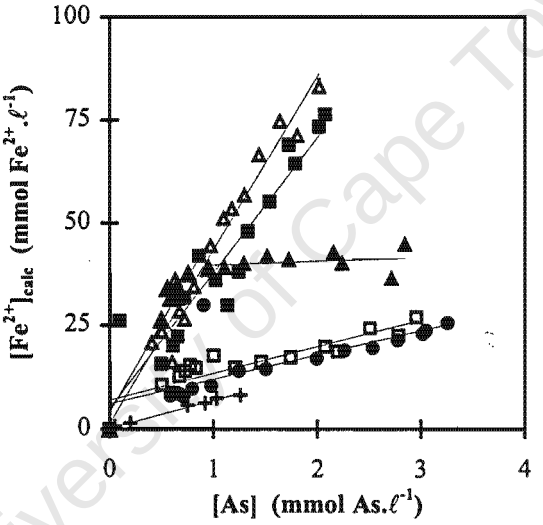

Figure 3.3: Variation in the ferrous-iron concentration of the supernatant as a function of the arsenic concentration at different initial ferric-iron concentrations. [o] 0 mmol $Fe^{3+}.\ell^{-1}$; [•] 90 mmol $Fe^{3+}.\ell^{-1}$; [□] 180 mmol $Fe^{3+}.\ell^{-1}$; [▲] 360 mmol $Fe^{3+}.\ell^{-1}$; [Δ] 450 mmol $Fe^{3+}.\ell^{-1}$; [■] 540 mmol $Fe^{3+}.\ell^{-1}$; [+] Iglesias *et al.* (1993).

It is apparent from Figure 3.3 and Table 3-6 that at concentrations of 90 and 180 mmol $Fe^{3+}.\ell^{-1}$, the results obtained are in agreement with the stoichiometry previously reported for the ferric leaching of pure arsenopyrite (Iglesias *et al.*, 1993):

$$FeAsS + 5\,Fe^{3+} \rightarrow S^0 + As^{3+} + 6\,Fe^{2+} \qquad (3\text{-}9)$$

However, at initial concentrations of 360, 450 and 540 mmol $Fe^{3+}.\ell^{-1}$ the results of this investigation differ significantly from the stoichiometry indicated in Equation 3-9.

* The ferrous-iron concentration was calculated from the solution redox potential (see Section 3.1.1.3).

Table 3-6: Results of the linear regression analysis carried out to determine the stoichiometric coefficient of Fe^{2+} in Equation 3-8

$[Fe^{3+}]_{initial}$ (mmol $Fe^{3+}.\ell^{-1}$)		Constant	R^2	Coefficient of Fe^{2+}
90		6.1	0.58	5.8
180		7.0	0.81	6.4
360	[As] ≤ 1 mmol.ℓ^{-1}	4.1	0.90	43.2
360	[As] ≥ 1 mmol.ℓ^{-1}	36.5	0.70	2.5
450		1.4	0.96	41.9
540		5.0	0.89	32.7
Iglesias *et al.* (1993)		0.2	0.99	6.6

The large variation in the stoichiometric coefficient calculated for Fe^{2+} suggests that, in addition to being affected by the leaching of arsenopyrite, the $[Fe^{2+}]/[As]$ ratio in the supernatant is also affected by one or more of the following:

i) the oxidation of arsenite, As(III), to arsenate, As(V), by ferric-iron (Mandl and Vyškovský, 1994; Iglesias *et al.*, 1993) according to;

$$As^{3+} + 2Fe^{3+} \rightarrow As^{5+} + 2Fe^{2+} \quad (3\text{-}10)$$

ii) the precipitation of ferric arsenate (Fernandez *et al.*, 1995) according to;

$$H_3AsO_4 + Fe^{3+} + nH_2O \rightarrow FeAsO_4.nH_2O\downarrow + 3H^+ \quad (3\text{-}11)$$

iii) the ferric leaching of pyrite (Mathews and Robins, 1972; Garrels and Thompson, 1960) according to;

$$FeS_2 + 14Fe^{3+} + 8H_2O \rightarrow 2SO_4^{2-} + 15Fe^{2+} + 16H^+ \quad (3\text{-}12)$$

In other words the ferric leaching of arsenopyrite, the oxidation of arsenite to arsenate by ferric-iron, the precipitation of ferric arsenate and (possibly) the ferric leaching of pyrite compete for the available ferric-iron. Therefore, the rate at which each of these reactions occurs will depend on the concentrations of arsenopyrite, arsenite, arsenate and ferric-iron in solution.*

This phenomenon is responsible for the total iron concentration of the supernatant in the reactor, in which the initial ferric-iron concentration was 360 mmol.ℓ^{-1}, decreasing during the course of the experiment, and for the resulting curve of [As] vs. $[Fe^{2+}]_{calc}$ having two distinct regions, *i.e.* it displays mixed kinetics. At [As] ≤ 1 mmol.ℓ^{-1} the slope of the curve is similar to the slope obtained at initial ferric-iron concentrations of 450 and 540 mmol.ℓ^{-1}. However, at [As] ≥ 1 mmol.ℓ^{-1} the slope is similar to the slope obtained at initial ferric-iron concentrations of 90 and 180 mmol .ℓ^{-1}.

* The hypothesis of competing reactions is consistent with the stoichiometry of Equation 2-26, and may have contributed to the controversy surrounding the stoichiometry of the reaction involving arsenopyrite and ferric-iron.

This "competing reactions" hypothesis also suggests that the assumption that all the arsenic remained in solution may have resulted in an underestimation of the arsenopyrite conversion. For this reason the arsenopyrite conversion was also calculated using the ferrous-iron concentration determined from the final redox potential of the solution and the assumption that the only reaction occurring was the ferric leaching of arsenopyrite (according to the reaction stoichiometry shown in Equation 3-9). The values of the arsenopyrite conversion calculated in this way are listed in Table 3-7.

From Table 3-7, it is apparent that the above assumption results in an overestimation of the arsenopyrite conversion. In spite of this limitation however, whereas the results listed in Table 3-5 suggest that the arsenopyrite conversion decreases with an increase in the initial ferric-iron concentration, those listed in Table 3-7 suggest that the arsenopyrite conversion actually increases with an increase in the initial ferric-iron concentration.

Table 3-7: Arsenopyrite conversion calculated using the final redox potential and Equation 3-9

$[Fe^{3+}]_{initial}$ (mmol $Fe^{3+}.\ell^{-1}$)	X_{FeAsS} (%)
90	51
180	58
360	78
450	178
540	163

Averaging the conversions listed in Tables 3-5 and 3-7 also suggests that the arsenopyrite conversion increases with an increase in the initial ferric-iron concentration. Furthermore, averaging of the conversions listed in Tables 3-5 and 3-7 suggests that a relatively large proportion of the mineral (45-100 %) was solubilised during the 48 hours over which the experiments were performed. In contrast to this observation, previous research reported arsenic extractions of (only) about 25 % in 24 hours (Iglesias *et al.*, 1993).

3.2 THE FERRIC LEACHING KINETICS OF ARSENOPYRITE*

3.2.1 Materials and Methods

3.2.1.1 Experimental equipment

The experiments and the redox probe calibration were performed in a 100 mℓ jacketed glass vessel. The reactor had a h/d ≈ 1 and a working volume of 75 mℓ. The temperature in the reactor was maintained at 25°C by

* Ruitenberg, R., Hansford, G.S., Reuter, M.A. and Breed, A.W. 1999. The ferric leaching kinetics of arsenopyrite. Hydrometallurgy 52(1): 37-53.

circulating water from a Grant Y6 constant temperature bath through the reactor jacket. Mixing was achieved by rotating a flat glass impeller using a variable speed Heidolph RZR 50 105/38 W overhead motor.

The redox potential of the leaching solution was measured using a Crison platinum wire-Ag/AgCl electrode filled with 3 mol LiCl.ℓ^{-1} (198 mV vs. SHE). The redox electrode was connected via an optically isolated amplifier and an analogue to digital converter (ADC) on a single board microcomputer to a personal computer (Randall *et al.*, 1993). This allowed the redox potential of the leaching solution to be recorded continuously. A diagrammatic representation of the experimental equipment is shown in Figure 3.4.

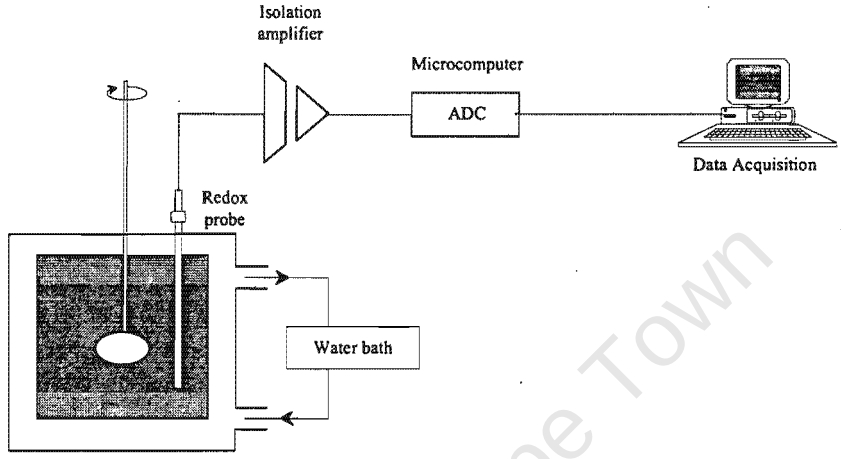

Figure 3.4: Diagrammatic representation of the experimental equipment.

3.2.1.2 Mineral used

The arsenopyrite used was obtained from Wards' (USA). Handpicked arsenopyrite crystals were ground using a pestle and mortar until the entire sample passed through a 100 micron sieve. The ultra-fine material was removed by suspending the ground mineral in distilled water, allowing it to settle for a few minutes and then decanting the ultra-fines with the liquid.

The size analysis of the material used during the experimental work was determined using a Malvern Laser Master-Sizer. This showed that 92.61 % of the ground ore was finer than 75 micron, and 63.27 % was finer than 25 micron. The complete size analysis of the mineral is shown in Table 3-8.

Table 3-8: Size analysis of ground Wards' arsenopyrite mineral

Size fraction (μm)	Mass percent (%)
+ 106	3.34
- 106 + 75	4.08
- 75 + 53	9.95
- 53 + 38	7.89
- 38 + 25	11.50
- 25	63.27

The specific surface area of the ground material, as determined using the Malvern Laser Master-Sizer, was 0.384 $m^2.g^{-1}$. The BET surface area was found to be 1.9675 $m^2.g^{-1}$.

A representative sample of the ground mineral was digested in hydrofluoric, nitric and perchloric acid (Bailey, 1993) to determine its elemental composition. The elemental analysis of the mineral sample is listed in Table 3-9. The presence of the elements listed in Table 3-9 was confirmed by means of scanning electron microscopy (SEM). In addition, SEM analysis indicated that the chief gangue mineral was quartz.

Table 3-9: Elemental analysis of Wards' arsenopyrite mineral

Element	Mass Percent (%)
As	25.4
S	19.7
Fe	16.5
Pb	1.0
Zn	0.5
Gangue	36.9

The mineral analysis of the sample was estimated from the elemental analysis; the iron, lead and zinc were assumed to be present as arsenopyrite, galena and sphalerite, respectively.* The mineral analysis estimated in this manner is listed in Table 3-10.

Table 3-10: Mineral analysis of Wards' arsenopyrite mineral

Mineral	Mass Percent (%)
Arsenopyrite (FeAsS)	48.03
Galena (PbS)	1.15
Sphalerite (ZnS)	0.75

3.2.1.3 Redox probe calibration

As stated previously the solution conditions influence the measured value of the redox potential at a particular ferric/ferrous-iron ratio. It was therefore necessary to calibrate the redox probe prior to using it to determine the dissolved ferrous- and ferric-iron concentrations; the calibration method used is described in Section 3.1.1.4.

The values of the Nernst equation parameters, E_0'' and RT/zF, for the Crison platinum wire-Ag/AgCl electrode filled with 3 mol LiCl.ℓ^{-1} (198 mV vs. SHE) at 25°C and varying total iron concentrations are listed in Table 3-11 below. From Table 3-11 it is apparent that, at 25°C and overall iron concentrations ranging from 143 to 573 mmol Fe.ℓ^{-1}, the total iron concentration did not have a significant effect on the values of either E_0'' or RT/zF.

* The assumption that all the Fe was present in the form of arsenopyrite resulted in a lower estimate of the arsenopyrite content than the assumption that all the As was present in the form of arsenopyrite.

Table 3-11: Comparison between the measured and theoretical Nernst equation parameters

$[Fe]_{tot}$ (mmol Fe.ℓ^{-1})	RT/zF (mV)	E_0'' (mV)
143	25.78	430.9
287	27.21	430.0
573	28.38	431.9
Theoretical value	25.70	572.0

3.2.1.4 Experimental procedure

As in the ferric leaching experiments performed using Fairview concentrate, distilled water and analytical grade laboratory chemicals were used for all the experiments. A ferric sulfate solution of the required concentration was made up and added to the jacketed vessel. The redox probe, which had been calibrated as described in Section 3.1.1.4, was inserted into the solution and the solution agitated. Once thermal equilibrium was achieved a known quantity of ore was added, and the redox potential was monitored for the duration of the experiment, *viz.* between one and two hours.

A number of parameters were varied during the course of the experimental program; these were the initial redox potential of the solution, $E_{initial}$, the total iron concentration, $[Fe]_{tot}$, the solids concentration, ρ_{pulp}, and the pH of the solution. However, a set of standard conditions was used in an attempt to reduce confounding of the results. The chosen standard ferric leaching conditions are shown in Table 3-12.

The concentrations of arsenic and ferrous- and ferric-iron in the leach solutions and spent leach liquor were determined by Flame Atomic Adsorption Spectroscopy (FAAS), and titration with potassium dichromate, respectively. However, the arsenic and iron concentrations of the leach solution were not measured during the experiment. Furthermore, although no attempt was made to confirm the reaction stoichiometry, upon completion of each experiment, the spent leach liquor was titrated with cerium sulfate and the presence of arsenite confirmed.*

Table 3-12: Standard conditions for the ferric leaching of arsenopyrite

Parameter	Level
volume (mℓ)	75
$[Fe]_{tot}$ (mmol Fe.ℓ^{-1}))	287
pH	1.1
ρ_{pulp} (%)	1
agitator speed (rev.min^{-1})	1500
Temperature (°C)	25
$E_{initial}$ (vs. Ag/AgCl) (mV)	615

* The method used was developed at Gencor Process Research in Johannesburg, South Africa. It is described in detail in the Appendix to Chapter Five.

3.2.1.5 Rate determination

The leaching rate was determined using the Nernst equation, the reaction stoichiometry of Equation 3-9 and the variation in the redox potential of the slurry measured during the course of the experiment. The decision to use the reaction stoichiometry of Equation 3-9 during the arsenopyrite leaching rate calculation was based on the following:

i) the stoichiometry of Equation 3-9 is consistent with the stoichiometry for the dissolution of (pure) arsenopyrite determined during a previous investigation (Iglesias *et al.*, 1993), and
ii) the stoichiometry of Equation 3-9 has arsenite and elemental sulfur as its final products which is consistent with the ferric leaching mechanism proposed as a result of a review of the literature (see Section 2.3).

In addition, changes in the redox potential resulting from the leaching of sulfides other than arsenopyrite were found to be negligible (see Section 3.2.2.1).

As stated previously the ferric/ferrous-iron ratio can be related to the solution redox potential using the Nernst equation. Differentiating the Nernst equation written for redox potential measurements in which the reference electrode is not the SHE, *i.e.* Equation 3-4, yields:

$$\frac{dE}{dt} = \frac{RT}{zF}\frac{d}{dt}\ln\left(\frac{[Fe^{3+}]}{[Fe^{2+}]}\right) \tag{3-13}$$

$$\frac{dE}{dt} = \frac{RT}{zF}\left(\frac{1}{[Fe^{3+}]}\frac{d[Fe^{3+}]}{dt} - \frac{1}{[Fe^{2+}]}\frac{d[Fe^{2+}]}{dt}\right) \tag{3-14}$$

If it is assumed that arsenopyrite undergoes stoichiometric dissolution in ferric sulfate media then the rate of arsenopyrite dissolution can be defined as:

$$r_{FeAsS} = \frac{d[FeAsS]}{dt} = -\frac{d[Fe]_{tot}}{dt} = -\frac{d\left([Fe^{3+}]+[Fe^{2+}]\right)}{dt} \tag{3-15}$$

Combining Equation 3-14 with Equation 3-15 and the reaction stoichiometry given in Equation 3-9, yields:

$$\frac{dE}{dt} = \frac{RT}{zF}r_{FeAsS}\left(\frac{5}{[Fe^{3+}]} + \frac{6}{[Fe^{2+}]}\right) \tag{3-16}$$

Rearranging Equation 3-16 yields an expression for the rate of arsenopyrite leaching:

$$r_{FeAsS} = \frac{\frac{zF}{RT}\frac{dE}{dt}}{\frac{5}{[Fe^{3+}]} + \frac{6}{[Fe^{2+}]}} \tag{3-17}$$

Substituting Equations 3-5 and 3-6 into Equation 3-17 yields an expression for the rate of arsenopyrite leaching in terms of the variation in the redox of the solution, the total iron concentration and the ferric/ferrous-iron ratio:

$$r_{FeAsS} = \frac{[Fe]_{tot}\,\frac{zF}{RT}\,\frac{dE}{dt}}{\left(1+\frac{[Fe^{3+}]}{[Fe^{2+}]}\right)\left(\frac{5}{\frac{[Fe^{3+}]}{[Fe^{2+}]}}+6\right)} \tag{3-18}$$

Before calculating the rate of arsenopyrite leaching using Equation 3-18 it was necessary to smooth the raw redox potential vs. time data in order to eliminate the scatter resulting from the differentiation of a noisy electronic signal. The general form of the smoothing equation found to give the best fit was:

$$E_{fit} = a\,t^{b} + c \tag{3-19}$$

The constants "a", "b" and "c" were found by minimising the sum of the squared errors between the measured redox potential and the redox potential predicted by Equation 3-19. Differentiating Equation 3-19, with respect to time, yields:

$$\frac{dE_{fit}}{dt} = a\,b\,t^{b-1} \tag{3-20}$$

Therefore, substitution of Equation 3-20 into Equation 3-18 yields an equation in which all the parameters can be determined. This means that it is possible to calculate the variation in the rate of arsenopyrite dissolution with time using the measured variation in the redox potential and the total iron concentration*, *viz.*:

$$r_{FeAsS} = \frac{[Fe]_{tot}\,\frac{zF}{RT}\,a\,b\,t^{b-1}}{\left(1+\frac{[Fe^{3+}]}{[Fe^{2+}]}\right)\left(\frac{5}{\frac{[Fe^{3+}]}{[Fe^{2+}]}}+6\right)} \tag{3-21}$$

3.2.2 Results and Discussion

3.2.2.1 General behaviour

Figure 3.5 shows the variation in the redox potential of the solution observed during the course of a typical experiment. In all the experiments, raw data similar in shape to the data shown in Figure 3.5 was obtained.

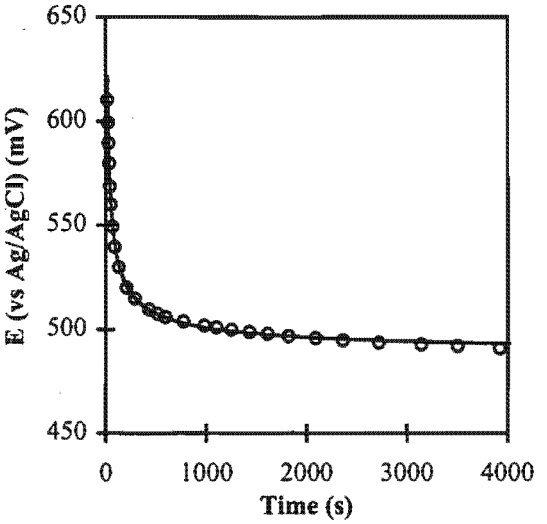

Figure 3.5: Typical example of the [o] observed variation in the redox potential with time and a [——] curve fit ($E_{fit} = 679.6t^{-0.56} + 486.6$; $R^2 = 0.998$) to the experimental data.

From Figure 3.5 it is apparent that during the first few minutes of leaching there was a rapid drop in the redox potential of the solution. This rapid change in the initial redox potential was also observed during the experiments performed using Fairview flotation concentrate (Figure 3.1), and can be explained as follows. At high total iron concentrations and ferric/ferrous-iron ratios, even a small increase in the ferrous-iron concentration will result in a large change in the ferric/ferrous-iron ratio, and hence a large change in the redox potential.

After smoothing the raw data, the resulting equation was used to calculate the rate of ferrous-iron production as a function of the redox potential of the leaching solution.

Ferric leaching rate

The variation in the (calculated) rate of arsenopyrite leaching (expressed as the specific rate of ferrous-iron production) with changing solution redox potential for a typical experiment is shown in Figure 3.6. From Figure 3.6 it is apparent that the rate of ferrous-iron production initially increases with a decrease in the redox potential of the solution. It appears to pass through a maximum and then decreases rapidly with a further decrease in the redox potential of the solution.

An increase in the initial ferric leaching rate with decreasing redox potential was also observed during the ferric leaching of pyrite (May *et al.*, 1997). It is suggested that this is a transient phenomenon, and can be attributed to the rearrangement of the ions on the surface and in the electrical double layer surrounding the mineral, *i.e.* it is not a result of leaching of the mineral. The following support this postulate:

i) the maximum rate shown in Figure 3.6 was reached within 20 s of beginning the experiment (as stated previously each experiment took about 1 to 2 hours),

(..continued)

* Although the increase in the total iron concentration during the course of the experiments was small, *viz.* ± 5 % of the initial iron

Continued overleaf...

ii) the electrophoretic mobility of arsenopyrite has been shown to be influenced by the ferric-iron concentration (MacDonald and Hansford, unpublished data), and

iii) no surface products responsible for passivation of the mineral surface were observed.

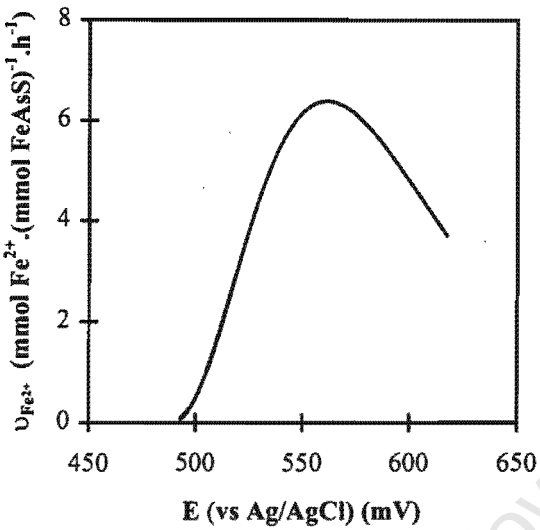

Figure 3.6: Variation in the (calculated) specific ferrous-iron production rate as a function of the solution redox potential for a typical experiment.

In spite of the initial increase in the ferrous-iron production rate with a decrease in the redox potential of the solution, it is apparent that for most of the experiment, the rate of leaching decreased with a decrease in the redox potential of the solution. This decrease in the leaching rate with a decrease in the redox potential is in agreement with the results presented in Section 3.1, and with previously reported trends for the ferric leaching of other sulfide minerals (May *et al.*, 1997; Verbaan and Huberts, 1988; Jorge and Martins, 1986; Crundwell, 1986). Furthermore, the dependence of the rate on the redox potential of the leaching solution in turn suggests that an electrochemical model be used to describe the leaching kinetics.

During this investigation a maximum ferric leaching rate of about 6.8 mmol Fe^{2+}.(mmol FeAsS)$^{-1}$.h^{-1} was observed (see Figure 3.8). This represents a surface area of 0.58 g FeAsS.m^{-2}.h^{-1} (BET based) and 2.95 g FeAsS.m^{-2}.h^{-1} (Malvern based), which is comparable with the rates of ferric leaching reported previously (see Table 2-6).

Error analysis

The contribution of ferrous-iron oxidation by dissolved oxygen to the ferric-iron concentration, and hence the observed rate of ferric-iron leaching, was determined in an air-sparged CSTR. The feed to the reactor consisted of a salt solution containing 215 mmol $Fe^{2+}.\ell^{-1}$. The temperature, pH and residence time of the solution in the reactor were maintained at 40°C, pH 1.75 and 100 h, respectively. Sparging compressed air at 100 mℓ.min^{-1} into the solution ensured that the liquid was saturated with oxygen.

(..continued)
concentration, it was taken into consideration during the calculation of the leaching rate.

The measured variation in the ferrous-iron concentration of the reactor outlet with elapsed time is shown in Figure 3.7, together with the predicted variation in the ferrous-iron concentration of the reactor outlet if no reaction and ideal CSTR behaviour is assumed.

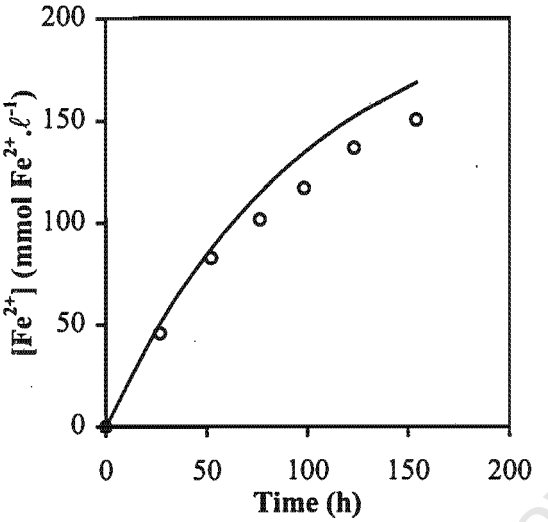

Figure 3.7: Variation in the [o] measured and [—] predicted variation in the outlet ferrous-iron with time.

The data shown in Figure 3.7 was used to determine the approximate rate at which ferrous-iron is oxidised to ferric-iron by oxygen. It was found to be in the region of 6.33×10^{-5} mmol $Fe^{2+}.\ell^{-1}.s^{-1}$. In comparison, the rate of ferrous-iron production observed during the ferric leaching experiments ranged from a maximum of 5.57×10^{-2} mmol $Fe^{2+}.\ell^{-1}.s^{-1}$ to a minimum of about 8.10×10^{-4} mmol $Fe^{2+}.\ell^{-1}.s^{-1}$, measured at the end of the experiment. This suggested that the oxidation of ferrous-iron by oxygen could be ignored during the analysis of the experiments carried out to determine the ferric leaching kinetics of arsenopyrite. This result is consistent with those of previous work.* Therefore, no attempt was made to exclude oxygen from the solution during the ferric leaching experiments.

Calculations indicated that complete dissolution of the galena and sphalerite content of the mineral would result in the ferrous-iron concentration increasing by 1.25 mmol.ℓ^{-1} (*i.e.* ΔFe^{2+} = 177.93 mmol.ℓ^{-1}) whereas complete dissolution of the mineral would result in the ferrous-iron concentration increasing by 177.93 mmol.ℓ^{-1}. During the ferric leaching experiments, the maximum change in the ferrous-iron concentration, calculated from the change in the redox potential, was 23.82 mmol.ℓ^{-1}. In the event of complete dissolution of the galena and sphalerite content of this mineral, this change in the overall ferrous-iron concentration thus indicates a change in the ferrous-iron concentration, as a result of arsenopyrite dissolution, of 22.37 mmol.ℓ^{-1}, which in turn corresponds to 12.77 % dissolution of the arsenopyrite and 8.03% dissolution of the (entire) mineral sample.

Less than 10 % dissolution of the (entire) mineral sample is unlikely to influence the integrity of the mineral particles themselves. Thus, as it is unlikely that the liberation characteristics of the minerals differed to any great degree, it is also unlikely that complete dissolution of the galena and sphalerite content of the mineral

* Singer and Stumm (1970) reported the ferric leaching of pyrite to be independent of the oxygen concentration; Barrett *et al.* (1993) used the data obtained by Singer and Stumm (1970) and calculated the half reaction time for the oxidation of ferrous-iron by oxygen to be about 24 000 days.

would have occurred.* The above therefore suggests that the dissolution could be assumed to occur via a shrinking core type mechanism, which in turn implies that the dissolution of the minerals occurred according to the proportion in which they were present in the sample. Calculations based on this assumption indicated that the contribution of the dissolution of the galena and sphalerite content of the mineral to the change in the ferrous-iron concentration was in the region of 1%.†

Therefore, as the experimental reproducibility was found to be in the region of 8 %, it was possible to disregard the errors introduced as a result of ignoring the contribution of the leaching of the sphalerite and galena to the changes in the redox potential of the solution. Furthermore, acid leaching tests performed in the absence of ferric-iron were found to have little effect on the redox potential, hence its effect was also ignored.

In addition to the error analyses described above, a series of experiments were performed at impeller speeds ranging from 1250 to 1800 rev.min^{-1}. Increasing the impeller speed from 1250 to 1800 rev.min^{-1} yielded no trend in the rate of arsenopyrite leaching, which suggests that, under the conditions employed, the rate of reaction was not mass transfer limited. This observation is consistent with the results of previous research performed at the same temperature (Iglesias *et al.*, 1996).

3.2.2.2 Effect of initial redox potential, $E_{initial}$

The influence of the initial redox potential of the solution on the rate of arsenopyrite leaching was investigated at initial redox potentials ranging from 470-625 mV.‡ These results are shown in Figure 3.8. In Figure 3.8 the experiments performed at $E_{initial}$ = 613 and 625 mV and at $E_{initial}$ = 558 and 561 mV indicate the reproducibility of the experiments. Although the difference between $E_{initial}$ = 613 and $E_{initial}$ = 625 mV appears to be significant in Figure 3.8, at an overall iron concentration of 287 mmol.ℓ^{-1}, this difference in the redox potential indicates a concentration difference of only 0.09 mmol $Fe^{2+}.\ell^{-1}$. At an overall iron concentration of 287 mmol.ℓ^{-1}, the difference between $E_{initial}$ = 558 and $E_{initial}$ = 561 mV indicates a concentration difference of 0.21 mmol $Fe^{2+}.\ell^{-1}$.

It is apparent from Figure 3.8 that the initial increase in the leaching rate apparent in Figure 3.6 was not apparent at low initial redox potentials, *viz.* $E_{initial} < 550$. Instead, the rate of leaching decreased with a decrease in the redox potential of the solution, across the entire range of redox potentials encountered. This result is consistent with the hypothesis that the increase in the initial rate of ferrous-iron production with a decrease in the redox potential is the result of rearrangement of the ions within the electrical double-layer. At low redox potentials less time is required to achieve equilibrium within the electrical double layer. Therefore, as the initial redox potential decreases, so does the period for which the leaching rate increases with a decrease in the redox potential.

* The low proportion of sphalerite and galena present in the sample would result in most of these minerals being occluded by the gangue and arsenopyrite fractions of the sample.

† Although Flame Atomic Absorption Spectroscopy (FAAS) analyses performed to determine the Pb and Zn content of the supernatant did not provide conclusive results possibly as a result of the low concentrations of Pb and Zn in the supernatant, they did suggest that the above assumptions were in fact valid.

‡ As stated previously (see Section 3.2.1.4) a set of standard conditions were chosen in an attempt to reduce confounding of the results. Thus, during the experiments performed at different initial redox potentials, the desired initial redox potential was attained by mixing ferric- and ferrous-iron solutions, both of which had an iron concentration of 287 mmol.ℓ^{-1}. This ensured that the initial redox potential and the total iron concentration were not varied simultaneously. The chosen standard ferric leaching conditions are shown in Table 3-12.

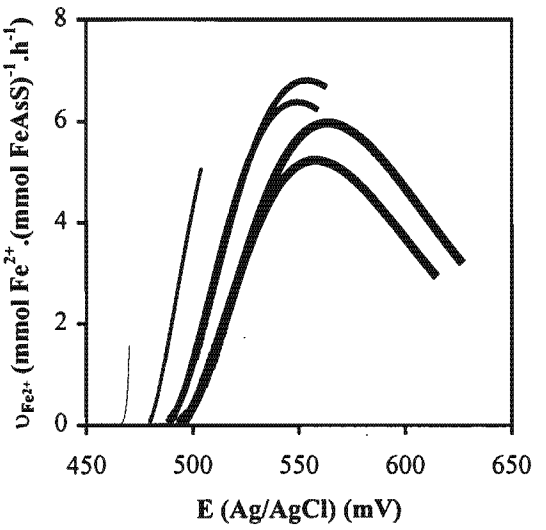

Figure 3.8: Variation in the specific ferrous-iron production rate with changing redox potential at different values of the initial solution redox potential. [——] $E_{initial}$ = 470 mV; [——] $E_{initial}$ = 503 mV; [——] $E_{initial}$ = 558 mV; 561 mV; [——] $E_{initial}$ = 613; 625 mV.

It is also apparent from Figure 3.8 that a higher initial redox potential resulted in the leaching of the mineral stopping at a higher redox potential. In an attempt to determine whether or not this phenomenon was a result of the formation of a passivating layer, the change in the amount of ferrous-iron in solution was calculated from the change in the redox potential during each experiment. The results of these calculations are presented in Table 3-13.

Table 3-13: Change in the ferrous-iron concentration of the supernatant during the experiments performed at different values of the initial solution redox potential

$E_{initial}$ (mV)	E_{final} (mV)	ΔFe^{2+} (mmol $Fe^{2+}.\ell^{-1}$)
470	466	6.17
503	479	19.56
558	489	22.74
561	488	23.82
613	494	20.54
625	494	20.63

The results listed in Table 3-13 suggest that the experiments performed at initial redox potentials in excess of 500 mV resulted in similar quantities of ferrous-iron being produced, irrespective of the value of $E_{initial}$. This observation, together with the fact that the rest potential of the mineral increased with an increase in $E_{initial}$, suggests that the extent of leaching is influenced by the formation of a passivating layer.* On the other hand, the results obtained at $E_{initial}$ = 470 mV suggest that the rest potential of the mineral is in the region of 465 mV.

Scanning electron microscopy (SEM) was used in an attempt to confirm the existence of a passivating layer. Although previous workers have detected a sulfur layer on the mineral surface after both the acid, and ferric

* The "rest potential" is defined as the solution redox potential at which leaching of the mineral stops.

leaching of arsenopyrite, it has not been found to hinder the dissolution reaction (Iglesias *et al.*, 1993; Dunn *et al.*, 1989; Kostina and Chernyak, 1976; Lázaro *et al.*, 1997). However, neither jarosite nor elemental sulfur was visible on the surface of a mineral sample that had been leached for one hour. However, as the stoichiometry by which arsenopyrite is leached by ferric-iron predicts the formation of elemental sulfur (Equation 3-9), its "absence" suggests that the sulfur layer formed after an hour was too thin to be observed by scanning electron microscopy (Vargas, 2000).

In addition to the SEM investigation, mineral that had been leached for one hour was dried and leached again, using fresh leaching solution. The results of the experiment performed using "leached" arsenopyrite and the results of an experiment performed using unleached mineral, at the same conditions, are shown in Figure 3.9.

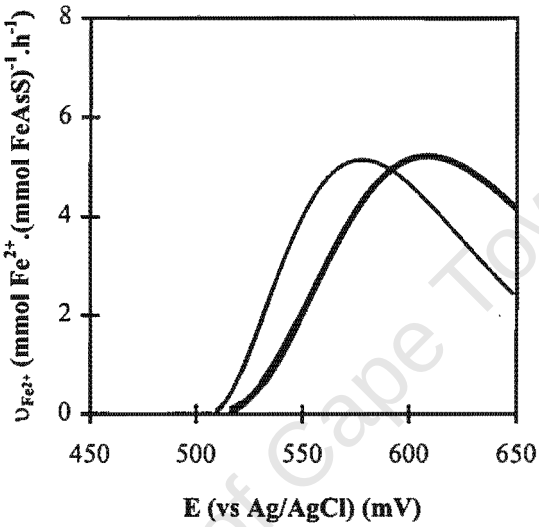

Figure 3.9: Comparison between the variation in the specific ferrous-iron production rate during the ferric leaching of [—] unleached and [▬] leached arsenopyrite, as a function of the redox potential of the solution.

From Figure 3.9 it is apparent that although the trends in the leaching rates of the "leached" and "unleached" material were similar, the rate at which "leached" mineral was degraded appeared to be reduced relative to the rate at which "unleached mineral" was leached at the same redox potential. However, a comparison between the changes in the amount of ferrous-iron solubilised during the leaching of "leached" and "unleached" material indicated that a greater proportion of the mineral that had been leached previously was solubilised.

The above therefore suggests that although the rate of leaching may be influenced by the formation of a product layer consisting of elemental sulfur, this layer does not influence the extent to which leaching occurs. The latter may however also be a result of the time-scale used during the leaching experiments, *i.e.* both the extent and rate of leaching would be expected to decrease during long term ferric leaching experiments performed at constant (high) redox potentials.

3.2.2.3 Effect of initial ferric-iron concentration, $[Fe^{3+}]_{initial}$

The effect of the ferric-iron concentration on the kinetics was investigated at initial ferric-iron concentrations of 143, 286 and 573 mmol.ℓ^{-1}. These results are shown in Figure 3.10 and show that an increase in the initial ferric-iron concentration had the same effect as an increase in the initial redox potential, *i.e.* it resulted in the

ferric leaching reaction stopping at a higher value of the solution redox potential. It is also apparent from Figure 3.10 that the maximum leaching rate observed at an initial concentration of 143 mmol $Fe^{3+}.\ell^{-1}$ was significantly lower than at higher overall iron concentrations. Although this effect was reproducible, it was not supported by other findings.

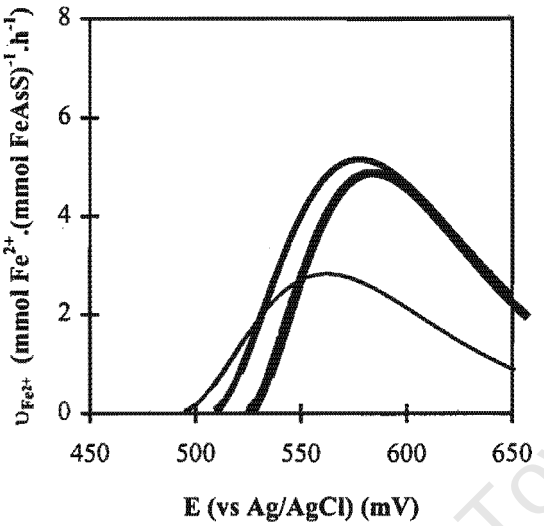

Figure 3.10: Variation in the specific ferrous-iron production rate as a function of the solution redox potential at different initial ferric-iron concentrations. [—] 143 mmol $Fe^{3+}.\ell^{-1}$; [—] 286 mmol $Fe^{3+}.\ell^{-1}$; [—] 571 mmol $Fe^{3+}.\ell^{-1}$.

Furthermore, although there was no obvious trend in the variation in the leaching rate with increasing initial ferric-iron concentration, the degree of leaching, calculated from the change in the ferrous-iron concentration and shown in Table 3-14, increased with an increase in the initial ferric-iron concentration.

Table 3-14: Change in the ferrous-iron concentration of the supernatant during the experiments performed at different values of the initial ferric-iron concentration

$[Fe^{3+}]_{initial}$	$E_{initial}$ (mV)	E_{final} (mV)	ΔFe^{2+} (mmol $Fe^{2+}.\ell^{-1}$)
143	650	509	6.17
286	646	495	19.56
571	655	525	22.74

3.2.2.4 Effect of solids concentration, ρ_{pulp}

Figure 3.11 shows the influence of the mineral concentration, at concentrations of 0.5, 1.0 and 2.0 % solids, on the ferric leaching kinetics. The results shown in Figure 3.11 suggest that the arsenopyrite concentration affects the redox potential at which the leaching of the mineral stops. However, it does not appear to have a significant effect on either the maximum leaching rate or the rate at which the leaching rate varied, *i.e.* the slope of the curve. Although the curves shown in Figure 3.11 display similar trends, they do not suggest that the leaching rate at a particular redox potential is independent of the solids concentration, *i.e.* that the surface area based rate is constant. However, they do suggest that the leaching rate may be dependent on the solids conversion.

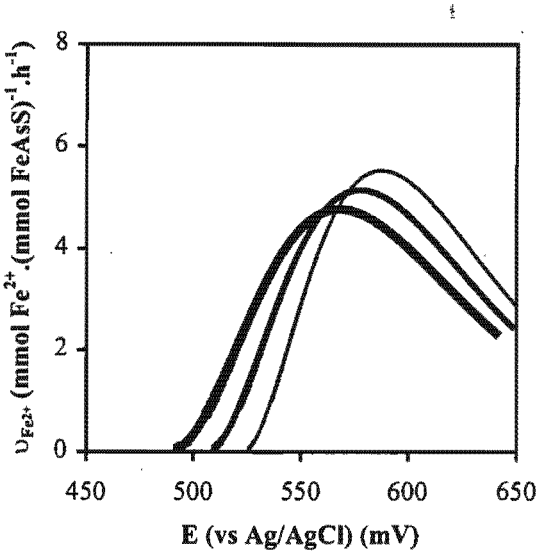

Figure 3.11: Variation in the specific ferrous-iron production rate with changing solution redox potential at different solids concentrations. [—] 0.5 %; [▬] 1.0 %; [▬] 2.0 %.*

Calculations performed to determine the effect of the solids concentration on the degree of leaching suggested that the amount of arsenopyrite solubilised was directly proportional to the arsenopyrite concentration. In other words, the amount of ferrous-iron solubilised divided by the pulp density did not vary significantly with changes in the solids concentration, which is consistent with the suggestion that the leaching rate may be dependent on the solids conversion. The results of these calculations are shown in Table 3.15.

Table 3-15: Effect of solids concentration on the change in the ferrous-iron concentration of the supernatant

ρ_{pulp}	$E_{initial}$ (mV)	E_{final} (mV)	ΔFe^{2+} (mmol $Fe^{2+}.\ell^{-1}$)	$\Delta Fe^{2+}/\rho_{pulp}$ (mmol $Fe^{2+}.\ell^{-1}.\%^{-1}$)
0.5	660	525	6.73	13.46
1.0	647	509	12.07	12.07
2.0	640	492	22.11	11.06

3.2.2.5 Effect of pH

The effect of pH (sulfuric acid) on the ferric leaching of arsenopyrite was investigated at pH 1.10, pH 1.36 and pH 1.45. The results of these experiments are shown in Figure 3.12, and suggest that the mineral is more active at higher pH values, *i.e.* lower concentrations of H_2SO_4. Although a similar trend has been previously reported for arsenopyrite (Malatt, 1998), this result appears to contradict the suggestion that the bioleaching of arsenopyrite occurs via the polysulfide mechanism proposed by Sand *et al.* (1999). According to the polysulfide mechanism proposed by Sand *et al.* (1999), the mineral is leached by both protons and ferric iron, hence an increase in the proton concentration would be expected to increase the rate and degree of mineral dissolution.

* The experiments performed at different solids concentrations were carried out using the same leaching medium. Although the difference between the initial redox potentials appears to be significant, at an overall iron concentration of 287 mmol.ℓ^{-1}, this difference in the initial redox potential indicates a concentration difference of less than 0.07 mmol $Fe^{2+}.\ell^{-1}$.

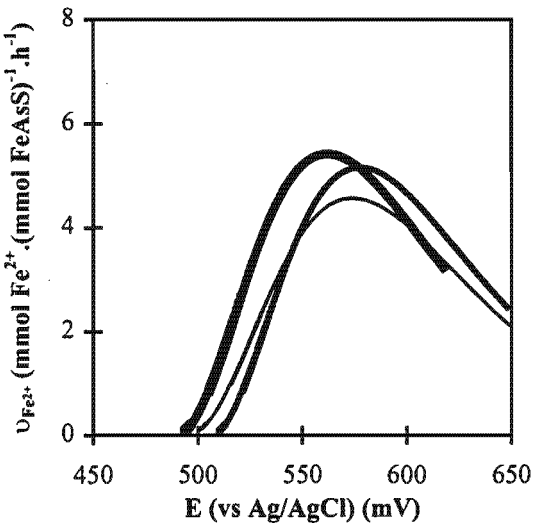

Figure 3.12: Variation in the specific ferrous-iron production rate with redox potential of the solution at different values of the solution pH. [—] pH 1.10; [▬] pH 1.36; [▬] 1.45.

In addition, the proportion of mineral solubilised, as measured by the change in the dissolved ferrous-iron concentration, increased with an increase in the pH. The results of these calculations are shown in Table 3.16.

Table 3-16: Effect of pH on the degree of arsenopyrite solubilisation

pH	$E_{initial}$ (mV)	E_{final} (mV)	ΔFe^{2+} (mmol $Fe^{2+}.\ell^{-1}$)
1.10	650	509	12.08
1.36	647	497	17.93
1.45	617	493	21.22

3.2.2.6 Ferric leaching kinetics

If it is assumed that the increase in the initial leaching rate with a decrease in the redox potential can be attributed to rearrangement of the ions comprising the electrical double layer, and not the leaching of the mineral, then the results obtained indicate that the rate of mineral leaching decreases with a decrease in the redox potential of the solution. This trend is consistent with previous research and suggests that the ferric leaching mechanism is electrochemical in nature.

It has been suggested that an electrochemically driven reaction should exhibit a half-order dependence on the ferric-iron concentration (Pletcher, 1984). However, this dependence has not been reported for the ferric leaching of arsenopyrite. Furthermore, May *et al.* (1997) found the ferric leaching rate of pyrite to be independent of the total iron concentration, for iron concentrations ranging from 50 to 500 mmol Fe.ℓ^{-1}.

Although the ferric leaching rate of arsenopyrite did not exhibit a half order dependence on the ferric-iron concentration, it was not found to be independent of the total iron concentration either. Furthermore, it was not possible to fit the electrochemically-based model proposed by Verbaan and Crundwell (1986), nor the Monod-

type model proposed by Boon (1996). However, it was possible to model the kinetics using the Butler-Volmer based model suggested by May *et al.* (1997):

$$\upsilon_{Fe^{2+}} = \upsilon_0 \left(e^{\alpha\beta(E - E')} - e^{(1-\alpha)\beta(E - E')} \right) \tag{3-22}$$

The values of υ_0, α, β and E' were determined by minimising the sum of the squared errors between the values of $\upsilon_{Fe^{2+}}$ calculated using Equation 3-6 and the values predicted by Equation 3-22:

$$\sum e^2 = \sum_{p=1}^{p=n} \left(\frac{7.335\times10^5 [Fe]_{tot} \frac{zF}{RT} a b t^{b-1}}{\left(1 + \frac{[Fe^{3+}]}{[Fe^{2+}]}\right)\left(\frac{5}{\frac{[Fe^{3+}]}{[Fe^{2+}]}} + 6\right)} - \upsilon_0 \left(e^{\alpha\beta(E - E')} - e^{(1-\alpha)\beta(E - E')} \right) \right)^2 \tag{3-23}^*$$

A comparison between the specific rate of ferrous-iron production predicted using the Butler-Volmer based model and a typical set of experimental results is shown in Figure 3.13. From Figure 3.13 it is apparent that, in the region in which the specific rate of ferrous-iron production, *i.e.* the leaching rate, decreased with a decrease in the redox potential, the agreement between the model and the experimental results is good.

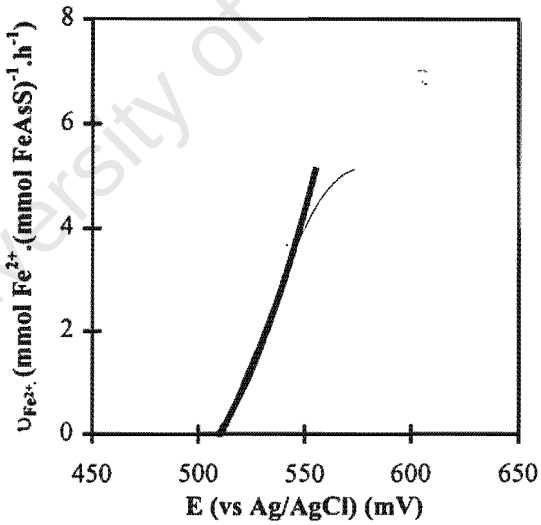

Figure 3.13: Comparison between the [——] measured variation in the specific ferrous-iron production rate and the variation in the specific ferrous-iron production rate [▬] predicted by the Butler-Volmer based model ($\upsilon_0 = 603.72$, $\alpha = 0.497$, $\beta = 0.01847$, $E' = 510.39$).

It is clear from Figure 3.13 that the Butler–Volmer based model does not predict a "maximum" or "limiting" ferric leaching rate, irrespective of the redox potential of the leaching solution†. However, even the proponents of the Butler-Volmer model, *viz.* May *et al.* (1997), encountered a "maximum" leaching rate during the ferric

* The value 7.335×10^5 is a conversion factor: mol FeAsS.ℓ^{-1}.s^{-1} to mmol Fe^{2+}.(mmol FeAsS)$^{-1}$.h^{-1}.

† The model proposed by Tal (1991), for the ferric leaching of pyrite, also suggests that no "limiting" ferric leaching rate exists.

leaching of pyrite. Although a "limiting" leaching rate is feasible, possibly because of mass transfer limitations, the reasons therefore have yet to be conclusively identified. Furthermore, to date, most of the proposed ferric leaching models have included term(s) which suggest that a maximum leach rate exists (Boon, 1996; Boogerd *et al.*, 1991; McKibben and Barnes, 1986; Zheng *et al.*, 1986).

3.3 Chapter Summary

The results performed using a sample of arsenopyrite/pyrite flotation concentrate from the Fairview Gold Mine in Barberton, South Africa showed that no leaching occurred in the absence of ferric-iron. However, considerable leaching of arsenic occurred in the presence of ferric-iron. The degree of leaching increased with an increase in the initial ferric-iron concentration. However, the rate of leaching appeared to be dependent on the redox potential of the slurry, and not on the absolute ferric-iron concentration. In addition, the results obtained using the arsenopyrite/pyrite flotation concentrate suggested that the leaching of arsenopyrite, the oxidation of arsenite to arsenate, the leaching of pyrite and the precipitation of ferric arsenate compete for the available ferric-iron.

Although the competitive nature of these reactions prevented reliable determination of either the rate or degree of leaching, both were estimated to be greater than previously reported. Furthermore, although the competing reactions influenced the observed stoichiometry of the ferric leaching reaction, the results obtained were consistent with the stoichiometry postulated previously by Iglesias *et al.* (1993):

$$FeAsS + 5Fe^{3+} \rightarrow S^0 + As^{3+} + 6Fe^{2+} \qquad (3\text{-}24)$$

The ferric leaching rate of pure arsenopyrite was also found to decrease with a decrease in the redox potential of the leaching solution and, in the region in which the specific rate of ferrous-iron production decreased with a decrease in the redox potential, the results could be accurately described using the Butler-Volmer based model suggested by May *et al.* (1997):

$$\upsilon_{Fe^{2+}} = \upsilon_0 \left(e^{\alpha\beta(E - E')} - e^{(1-\alpha)\beta(E - E')} \right) \qquad (3\text{-}25)$$

However, a limitation of the model appears to be its dependence on the "rest potential" of the mineral, *i.e.* the redox potential of the solution at which the mineral dissolution stops. The "rest potential" was found to increase with an increase in either the ferric-iron or the proton concentration, or when the solids concentration was reduced. As no occluding sulfur layer could be detected on the surface of leached mineral particles, the results obtained suggest that the reactivity of the mineral is determined by the ferric-iron and proton concentration based on the arsenopyrite surface area. An increase in the (surface area based) concentration of either ferric-iron or protons resulted in a decrease in the reactivity of the mineral. This is regarded as highly unusual as most reaction mechanisms are favoured by an increase in the reactant concentration. In spite of the above limitations, the ability of the model to predict the leaching rate of both pyrite and arsenopyrite, across a range of operating conditions, suggest that the Butler-Volmer model has potential for predicting the rate by which sulfide minerals are degraded by ferric-iron.

In order to achieve this goal it is however necessary to determine the mechanism by which the ferric leaching of arsenopyrite and other sulfide minerals occurs so that the influence of parameters such as pH *etc.*, can be incorporated into the model. This may yield a mechanistically based model capable of predicting the ferric leaching rate of sulfide minerals over a range of operating conditions.

3.4 Nomenclature

a	constant	dimensionless
$a_{Fe^{2+}}$	activity of ferrous-iron species	dimensionless
$a_{Fe^{3+}}$	activity of ferric-iron species	dimensionless
[As]	arsenic concentration	mmol As.ℓ^{-1}
b	constant	dimensionless
c	constant	dimensionless
d	reactor diameter	m
e	error	varies
E	redox potential of the solution (Pt-Ag/AgCl)	mV
E′	mineral rest potential	mV
E_0	redox potential of the solution at equilibrium	mV
E_0'	value of $E_0 + \frac{RT}{zF}\ln\left(\frac{\gamma_{Fe^{+3}}}{\gamma_{Fe^{+2}}}\right)$ for SHE	mV
E_0''	value of $E_0 + \frac{RT}{zF}\ln\left(\frac{\gamma_{Fe^{+3}}}{\gamma_{Fe^{+2}}}\right)$ for Ag/AgCl electrode	mV
E_{final}	redox potential of the solution at the end of the experiment (Pt-Ag/AgCl)	mV
E_{fit}	redox potential of the solution calculated from the smoothing equation (Pt-Ag/AgCl)	mV
E_h	redox potential of the solution (Pt-SHE)	mV
$E_{initial}$	redox potential of the solution at the beginning of the experiment (Pt-Ag/AgCl)	mV
F	Faraday constant	C.mol^{-1}
$[Fe^{2+}]$	concentration of ferrous-iron	mmol $Fe^{2+}.\ell^{-1}$
$[Fe^{3+}]$	concentration of ferric-iron	mmol $Fe^{3+}.\ell^{-1}$
$[Fe^{2+}]_{calc}$	concentration of ferrous-iron calculated from the redox potential	mmol $Fe^{2+}.\ell^{-1}$
$[Fe^{3+}]_{initial}$	initial concentration of ferric-iron	mmol $Fe^{3+}.\ell^{-1}$
[FeAsS]	concentration of arsenopyrite	mmol FeAsS.ℓ^{-1}
$[Fe]_{tot}$	concentration of iron	mmol Fe.ℓ^{-1}
h	reactor height	m
r_{FeAsS}	arsenopyrite production rate	mmol FeAsS.ℓ^{-1}.h^{-1}
R	Universal gas constant	kJ.K^{-1}.mol^{-1}
R^2	correlation coefficient	dimensionless
t	time	s

T	absolute temperature	K
x	stoichiometric coefficient	dimensionless
X_{FeAsS}	arsenopyrite conversion	%
z	number of electrons involved in reaction	dimensionless
Σe^2	sum of the squared errors	varies
α	fraction of mineral reacted at time, t	dimensionless
β	$\frac{zF}{RT}$	dimensionless
ΔFe^{2+}	change in the concentration of ferrous-iron calculated from the redox potential	mmol $Fe^{2+}.\ell^{-1}$
$\gamma_{Fe^{2+}}$	activity coefficient of ferrous-iron	dimensionless
$\gamma_{Fe^{3+}}$	activity coefficient of ferric-iron	dimensionless
ρ_{pulp}	solids concentration	% ($m.v^{-1}$)
υ_0	kinetic constant in chemical (ferric-iron) arsenopyrite oxidation	mmol Fe^{2+}.(mmol FeAsS)$^{-1}.h^{-1}$
$\upsilon_{Fe^{2+}}$	arsenopyrite specific ferrous-iron production rate	mmol Fe^{2+}.(mmol FeAsS)$^{-1}.h^{-1}$

3.5 References

Bailey, A.D. 1993. An assessment of oxygen availability, iron build-up and the relative significance of free and attached bacteria, as factors affecting bio-oxidation of refractory gold-bearing sulfides at high solids concentrations. Ph.D. Thesis, University of Cape Town, Cape Town.

Barrett, J., Hughes, M.N., Karavaiko, G.I. and Spencer, P.A. 1993. Metal extraction by bacterial oxidation of minerals. Ellis Horwood, New York.

Boogerd, F.C., Van den Beemd, C., Stoelwinder, T., Bos, P. and Kuenen, J.G. 1991. Relative contributions of biological and chemical reactions to the overall rate of pyrite oxidation at temperatures between 30°C and 70°C. Biotechnology and Bioengineering **38**: 109-115.

Boon, M. 1996. Theoretical and experimental methods in the modelling of bio-oxidation kinetics of sulfide minerals. Ph.D. Thesis. Delft University of Technology, Delft.

Crundwell, F.K. 1986. Kinetics and mechanism of the oxidative dissolution of a zinc sulfide concentrate in ferric sulphate solutions. Hydrometallurgy **19**(2): 227-242.

Dunn, J.G., Fernandez, P.G., Hughes, H.C. and Linge, H.G. 1989. Aqueous oxidation of arsenopyrite in acid, pp. 217-220. In: Proc. Austral. Inst. Min. Metall. Annual Conference. Australasian Institute of Mining and Metallurgy, Glenside, SA.

Fernandez, M.G.M., Mustin, C., De Donato, P., Barres, O., Marion, P. and Berthelin, J. 1995. Occurrences at mineral-bacteria interface during oxidation of arsenopyrite by *Thiobacillus ferrooxidans*. Biotechnology and Bioengineering **46**(1): 13-21.

Garrels, R.M. and Thompson, M.E. 1960. Oxidation of pyrite by iron sulphate solutions. American Journal of Science **258A**: 57-67.

Iglesias, N., Palencia, I. and Carranza, F. 1996. Treatment of a gold bearing arsenopyrite concentrate by ferric sulphate leaching. Minerals Engineering **9**(3): 317-330.

Iglesias, N., Palencia, I. and Carranza, F. 1993. Removal of the refractoriness of a gold bearing pyrite-arsenopyrite ore by ferric sulphate leaching at low concentration, pp. 99-115. In: J.P. Hager (ed.), EPD Congress 1993, The Minerals, Metals and Materials Society, Warrendale, Co..

Jeffrey, G.H., Bassett, J., Mendham, J. and Denney, R.C. 1989. Vogel's Textbook of Quantitative Chemical Analysis. 5th edition, Longman Scientific & Technical, New York.

Jorge, P.F. and Martins, G.P. 1986. Electrochemical and other aspects of indirect electrooxidation process for the leaching of molybdenite by hyperchloride, pp. 263-292. In: R.G. Bautista, R.J. Wesely and G.W. Warren (eds.), Hydrometallurgical reactor design and kinetics. The Metallurgical Society, Warrendale, Pa..

Kostina, G.M. and Chernyak, A.S. 1976. Electrochemical conditions for the oxidation of pyrite and arsenopyrite in alkaline and acid solutions. Zhurnal Prikladnoi Khimii **49**(7): 1534-1570.

Lázaro, I., Cruz, R., González, I. and Monroy, M. 1997. Electrochemical oxidation of arsenopyrite in acidic media. International Journal of Minerals Processing **50**(1-2): 63-75.

Malatt, K. 1998. The bacterial oxidation of gold-bearing pyrite/arsenopyrite concentrates. Ph.D. Thesis, Curtin University of Technology, Perth, WA.

Mandl, M. and Vyškovský, M. 1994. Kinetics of arsenic(III) oxidation by iron(III) catalysed by pyrite in the presence of *Thiobacillus ferrooxidans*. Biotechnology Letters **16**(11): 1199-1204.

Mathews, C.T. and Robins, R.G. 1972. The oxidation of iron disulfide by ferric sulphate. Australian Journal of Chemical Engineering **August**: 21-25.

May, N. 1997. The ferric leaching of pyrite. M. App. Sc. Dissertation. University of Cape Town, Cape Town.

May, N., Ralph, D.E. and Hansford, G.S. 1997. Dynamic redox potential measurement for determining the ferric leach kinetics of pyrite. Minerals Engineering **10**(11): 1279-1290.

McKibben, M.A. and Barnes, H.L. 1986. Oxidation of pyrite in low temperature acidic solutions. Geochem. et Cosmochim. Acta. **50**: 1509-1520.

Miller, D.M. and Hansford, G.S. 1992. The use of the logistic equation for modelling the performance of a biooxidation pilot plant treating a gold-bearing arsenopyrite-pyrite concentrate. Minerals Engineering **5**(7): 737-749.

Pletcher, D. 1984. Industrial Electrochemistry. Chapman and Hall, New York.

Randall, E.W., Moon, P. and Gavin, A.D.M. 1993. Dynamically extendable communications protocol for a serial input/output system. Journal of Microcomputer applications **16**: 385-393.

Sand, W., Gehrke, T., Josza, P.-G. and Schippers, A. 1999. Direct versus indirect bioleaching, pp. 27-49. In: R. Amils and A. Ballester (eds.), Biohydrometallurgy and the environment toward the mining of the 21st century **A**. Elsevier, Amsterdam.

Shuey, T.T. 1975. Semiconducting Ore Minerals. Elsevier Scientific Publishing Company, Amsterdam.

Singer, P.C. and Stumm, W. 1970. Acidic mine drainage: rate determining step. Science **167**: 1121-1123.

Tal, P. 1986. The effect of the iron(III) to iron(II) ratio on the rate of dissolution of pyrite. Technical Memorandum No: 18255. Council for Mineral Technology: Hydrometallurgy Division, Johannesburg.

Vargas, T. 2000. Private communication.

Verbaan, B. and Crundwell, F.K. 1986. An electrochemical model for the leaching of a sphalerite concentrate. Hydrometallurgy **16**(3): 345-359.

Verbaan, B. and Huberts, R. 1988. An electrochemical study of the bacterial leaching of synthetic nickel sulfide (Ni_3S_2). International Journal of Mineral Processing **24**(3-4): 185-202.

Zheng, C.Q., Allen, C.C. and Bautista, R.G. 1986. Kinetic study of the oxidation of pyrite in aqueous ferric sulfate. Ind. Eng. Chem. Process. Des. Dev. **23**: 308-317.

3.6 Appendix

As stated in Section 3.1.1.4, the total iron concentration, the counter-ions present, and the temperature of the solution influence the activities of the dissolved ferric and ferrous-iron species, hence these parameters affect the measured value of the redox potential at a particular ferric/ferrous-iron ratio. It was therefore necessary to calibrate the redox probe at the conditions to be employed before using it to determine the dissolved ferrous- and ferric-iron concentrations.

3.6.1 Calibration Method

i) Ferrous- and ferric sulfate solutions of similar concentrations were made up, and the concentrations thereof determined by titration with potassium dichromate, $K_2Cr_3O_7$ (Jeffrey *et al.*, 1989).

ii) A known volume of ferric sulfate was added to a jacketed vessel, the redox probe inserted and the solution agitated. The temperature in the reactor was maintained at the required temperature by circulating water from a Grant Y6 constant temperature bath through the reactor jacket.

iii) Once thermal equilibrium had been achieved an aliquot of ferrous sulfate was added and the redox potential of the solution recorded. This procedure was continued until the solution contained approximately equal volumes of ferric- and ferrous sulfate.

iv) The measured redox potential values were plotted against $\ln([Fe^{3+}]/[Fe^{2+}])$, and the Nernst parameters, *viz.* RT/zF (slope) and E_0'' (intercept), determined.

3.6.2 Raw Data

The raw data listed in Table 3A was obtained during the calibration of a Metrohm Pt-Ag/AgCl redox electrode, at 40°C, pH 1.70 and a total iron concentration of about 12 $g.\ell^{-1}$.

$[Fe^{3+}] = 11.54\ g.\ell^{-1}$

$[Fe^{2+}] = 12.00\ g.\ell^{-1}$.

$[V_{Fe^{3+}}]_{initial} = 400\ m\ell$

Table 3A: Raw data obtained during the calibration of a Metrohm Pt-Ag/AgCl redox electrode, at 40°C, pH 1.70 and a total iron concentration of about 12 $g.\ell^{-1}$.

Aliquot Volume ($m\ell$)	Cumulative volume ($m\ell$)	$[Fe^{3+}]$ (g/ℓ)	$[Fe^{2+}]$ (g/ℓ)	$[Fe^{3+}]/[Fe^{2+}]$	E (mV)
	400.00	11.5400	0.0000		664.40
0.02	400.02	11.5394	0.0006	19233.33	663.30

0.02	400.04	11.5388	0.0012	9616.67	662.00
0.02	400.06	11.5383	0.0018	6411.11	661.80
0.02	400.08	11.5377	0.0024	4808.33	661.20
0.02	400.10	11.5371	0.0030	3846.67	659.00
0.02	400.12	11.5365	0.0036	3205.56	658.30
0.02	400.14	11.5360	0.0042	2747.62	657.00
0.02	400.16	11.5354	0.0048	2404.17	656.20
0.02	400.18	11.5348	0.0054	2137.04	655.00
0.05	400.23	11.5334	0.0069	1672.46	652.80
0.05	400.28	11.5319	0.0084	1373.81	650.40
0.05	400.33	11.5305	0.0099	1165.66	649.00
0.05	400.38	11.5290	0.0114	1012.28	647.50
0.05	400.43	11.5276	0.0129	894.57	645.60
0.05	400.48	11.5262	0.0144	801.39	644.30
0.05	400.53	11.5247	0.0159	725.79	643.00
0.05	400.58	11.5233	0.0174	663.22	641.50
0.05	400.63	11.5219	0.0189	610.58	640.00
0.05	400.68	11.5204	0.0204	565.69	639.10
0.05	400.73	11.5190	0.0219	526.94	638.00
0.05	400.78	11.5175	0.0234	493.16	637.00
0.10	400.88	11.5147	0.0263	437.12	635.90
0.10	400.98	11.5118	0.0293	392.52	633.80
0.10	401.08	11.5089	0.0323	356.17	631.70
0.10	401.18	11.5061	0.0353	325.99	630.00
0.10	401.28	11.5032	0.0383	300.52	628.50
0.10	401.38	11.5003	0.0413	278.74	627.70
0.10	401.48	11.4975	0.0442	259.91	626.00
0.50	401.98	11.4832	0.0591	194.28	620.70
0.50	402.48	11.4689	0.0739	155.11	615.00
0.50	402.98	11.4547	0.0887	129.08	612.00
0.50	403.48	11.4405	0.1035	110.54	607.50
0.50	403.98	11.4263	0.1182	96.65	605.00
0.50	404.48	11.4122	0.1329	85.86	602.60
0.50	404.98	11.3981	0.1476	77.24	600.00
0.50	405.48	11.3840	0.1622	70.19	598.00
0.50	405.98	11.3700	0.1768	64.33	595.90
0.50	406.48	11.3560	0.1913	59.36	593.80
0.50	406.98	11.3421	0.2058	55.11	591.20
0.50	407.48	11.3282	0.2203	51.43	589.10
0.50	407.98	11.3143	0.2347	48.20	588.00
0.50	408.48	11.3004	0.2491	45.36	586.40
0.50	408.98	11.2866	0.2635	42.84	585.40
0.50	409.48	11.2728	0.2778	40.58	583.00
1.00	410.48	11.2454	0.3064	36.70	581.00
1.00	411.48	11.2180	0.3348	33.51	578.90
1.00	412.48	11.1908	0.3631	30.82	577.00

1.00	413.48	11.1638	0.3912	28.54	574.00
1.00	414.48	11.1368	0.4192	26.57	572.00
1.00	415.48	11.1100	0.4471	24.85	571.00
1.00	416.48	11.0834	0.4748	23.34	570.60
2.50	418.98	11.0172	0.5436	20.27	566.40
2.50	421.48	10.9519	0.6116	17.91	562.70
2.50	423.98	10.8873	0.6787	16.04	560.10
2.50	426.48	10.8235	0.7451	14.53	555.90
5.00	431.48	10.6981	0.8755	12.22	551.70
5.00	436.48	10.5755	1.0029	10.54	546.90
5.00	441.48	10.4557	1.1275	9.27	543.30
5.00	446.48	10.3386	1.2492	8.28	538.50
5.00	451.48	10.2242	1.3683	7.47	535.00
5.00	456.48	10.1122	1.4848	6.81	532.20
5.00	461.48	10.0026	1.5987	6.26	529.80
10.00	471.48	9.7904	1.8193	5.38	525.00
10.00	481.48	9.5871	2.0307	4.72	520.60
10.00	491.48	9.3920	2.2336	4.20	518.00
10.00	501.48	9.2048	2.4283	3.79	514.30
10.00	511.48	9.0248	2.6155	3.45	512.70
10.00	521.48	8.8517	2.7954	3.17	510.50
20.00	541.48	8.5248	3.1354	2.72	505.40
20.00	561.48	8.2211	3.4512	2.38	501.10
20.00	581.48	7.9384	3.7452	2.12	496.40
20.00	601.48	7.6744	4.0197	1.91	492.70
20.00	621.48	7.4274	4.2765	1.74	487.00
50.00	671.48	6.8744	4.8516	1.42	477.60
50.00	721.48	6.3980	5.3470	1.20	474.00
50.00	771.48	5.9833	5.7782	1.04	471.70

3.6.3 Determination of Nernst Equation Parameters

The variation in the measured redox potential, E, with changes in the natural logarithm of the ferric/ferrous-iron ratio observed during the calibration of a Metrohm Pt-Ag/AgCl redox electrode, at 40°C, pH 1.75 and a total iron concentration of about 12 g.ℓ^{-1} is shown in Figure 3A, together with a fit of the Nernst equation curve fit to the experimental data.

The values of the Nernst equation parameters determined from Figure 3A were:

RT/zF (slope) = 29.604 mV, and
E_0'' (y-intercept) = 474.29 mV

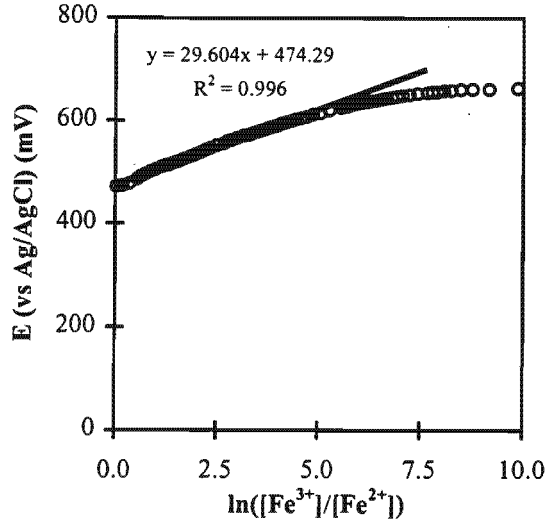

Figure 3A: Variation in the measured redox potential with changes in the ferric/ferrous-iron ratio observed during the calibration of a Metrohm Pt-Ag/AgCl redox electrode, at 40°C, pH 1.75 and a total iron concentration of about 12 g.ℓ^{-1} and [——] Nernst equation curve fit to the experimental data.

3.6.4 Sample Calculation

The measured redox potential of the solution, a calibration curve for the redox probe, *i.e.* the values of the Nernst equation parameters RT/zF and E_0'', and the total iron concentration of the solution can be used to determine the ferrous- and ferric-iron concentration of the solution as shown below.

The Nernst equation, written for redox potential measurements in which the reference electrode is not the standard hydrogen electrode (SHE) (Equation 3-4) may be rearranged to give:

$$\frac{[Fe^{3+}]}{[Fe^{2+}]} = e^{\left(\frac{E-E_0''}{\frac{RT}{zF}}\right)} \qquad (3A\text{-}26)$$

Substituting the value of the Nernst equation parameters determined from Figure 3A, *viz.* RT/zF = 29.604 mV, E_0'' = 474.29 mV, and the redox potential measured at a residence time of 71 hours during a ferrous iron oxidation experiment performed at 40°C and pH 1.70, *viz.* E = 670 mV, into Equation 3A-26 yields:

$$\frac{[Fe^{3+}]}{[Fe^{2+}]} = 743.175$$

Substituting the calculated value of the ferric/ferrous-iron ratio, *viz.* $[Fe^{3+}]/[Fe^{2+}] = 743.175$, and the total iron concentration measured at a residence time of 71 hours during a ferrous iron oxidation experiment performed at

40°C and pH 1.70, *viz.* $[Fe]_{tot} = 10.19\ g.\ell^{-1}$ into Equations 3-5 and 3-6 yields the ferrous- and ferric-iron concentrations:

$[Fe^{2+}] = 0.0137\ g.\ell^{-1}$

$[Fe^{3+}] = 10.1763\ g.\ell^{-1}$

For Melanie

The
simplest questions
are the most profound.

Where were you born? Where is your home?
Where are you going?
What are you doing?

Think about
these once in a while, and
watch your answers
change.

ILLUSIONS – Richard Bach

Chapter Four

The Effect of Temperature* and pH† on the Continuous Ferrous-iron Oxidation Kinetics of a Predominantly *Leptospirillum ferrooxidans* Culture

As stated in the literature review, the bacteria most commonly isolated from inorganic mining environments are *Thiobacillus ferrooxidans, Leptospirillum ferrooxidans* and *Thiobacillus thiooxidans.* Until recently, *T. ferrooxidans* was considered to be the micro-organism primarily responsible for the bioleaching of sulfide ores and concentrates. For this reason, most bioleaching research performed to date has been carried out using *T. ferrooxidans*. Recent research has however shown that *L. ferrooxidans* is at least as important, if not more important, than *T. ferrooxidans* (Rawlings *et al.*, 1999(a); Rawlings *et al.*, 1999(b); Dew *et al.*, 1997; Boon, 1996; Rawlings, 1995; Hallmann *et al.*, 1993; Sand *et al.*, 1992; Norris *et al.*, 1988; Helle and Onken, 1988) and that the micro-organism thought to have been *T. thiooxidans* may in fact have been *Thiobacillus caldus* (Rawlings *et al.*, 1999(a)).

In addition to using *T. ferrooxidans*, most bioleaching research performed to date has been carried out in batch culture, at temperatures and pH values in the region of 30°C and pH 1.8-2.0, respectively; these conditions are similar to those that have been reported to be the optimum conditions for *T. ferrooxidans*. However, most

---

* Breed, A.W., Dempers, C.J.N., Searby, G.E., Gardner, M.N., Rawlings, D.E. and Hansford, G.S. 1999. The effect of temperature on the continuous ferrous-iron oxidation kinetics of a predominantly *Leptospirillum ferrooxidans* culture. Biotechnology and Bioengineering 65(1): 44-53.

† Breed, A.W. and Hansford, G.S. 1999. Effect of pH on ferrous-iron oxidation kinetics of *Leptospirillum ferrooxidans* in continuous culture. The Biochemical Engineering Journal 1(3): 193-201.

commercial bioleaching operations using mesophilic bacteria are continuous processes and operate at about 40°C and pH 1.2-1.8.

Apart from the work performed by Nemati and Webb (1997), the effect of temperature on the kinetics of bacterial ferrous-iron oxidation has not been studied extensively. Furthermore, there is currently little information available on the effect of pH on the ferrous-iron oxidation kinetics of either *T. ferrooxidans* or *L. ferrooxidans*. In general, however, the growth and substrate (CO_2, O_2, Fe^{2+}) utilisation kinetics of the ferrous-iron oxidising species encountered in bioleaching operations have been found to follow a reverse sigmoidal curve with increasing ferric/ferrous-iron ratio. This trend is consistent with chemiosmotic potential theory (Ingledew, 1986) and suggests that the kinetics of these micro-organisms is a function of the redox potential of the solution. The dependence of the kinetics on the ferric/ferrous-iron ratio (redox potential) in turn suggests that they may be described using kinetic models such as the Michaelis-Menten based model proposed by Boon (1996).

The work presented below was performed in an attempt to determine the effect of temperature and pH on the ferrous-iron oxidation kinetics of the ferrous-iron oxidising species encountered in a mixed bacterial culture from a continuous bioleaching mini-plant oxidising an arsenopyrite/pyrite flotation concentrate, at conditions ranging from 30 to 40°C and pH 1.10 to pH 1.70.

4.1 Theoretical Aspects

Several researchers have reported the stoichiometric formula of bacteria (Roels, 1983), including *T. ferrooxidans* (Jones and Kelly, 1983), to be approximately $CH_{1.8}O_{0.5}N_{0.2}$. If the carbon and nitrogen sources are limited to CO_2 and NH_4^+ the formation of biomass occurs according to;

$$CO_2 , NH_4^+ , H_2O \rightarrow CH_{1.8}O_{0.5}N_{0.2} \tag{4-1}$$

The steady-state carbon dioxide utilisation rate can be used to estimate the bacterial concentration and growth rate (Boon, 1996):*

$$r_X = -r_{CO_2} \tag{4-2}$$

If it is assumed that the bacteria follow Monod growth kinetics:

$$c_X = \frac{r_X}{\mu} = \frac{-r_{CO_2}}{D} \tag{4-3}$$

Energy for bacterial growth and maintenance is obtained from the oxidation of ferrous-iron according to;

* Braddock *et al.* (1984) reported that the average carbon content of *T. ferrooxidans* cells decreased during the course of a batch experiment and with an increase in the dilution rate during growth in continuous culture, *i.e.* the size of the micro-organisms is not constant but is a function of the conditions under which they are grown. These results therefore suggest that the carbon dioxide utilisation rate or protein (N) concentration are better measures of the bacterial growth rate than the number of cells.

$$4Fe^{2+} + O_2 + 4H^+ \rightarrow 4Fe^{3+} + 2H_2O \quad (4\text{-}4)$$

Performing a mass balance on each of the elements, an overall charge balance and solving the resulting equations in terms of r_{O_2} and r_{CO_2}, yields a degree of reduction balance, *viz.*:

$$-r_{Fe^{2+}} = -4r_{O_2} - 4.2\,r_{CO_2} \quad (4\text{-}5)$$

Substitution and simplification yields the overall stoichiometry for the biooxidation of ferrous-iron (Boon, 1996), *viz.*:

$$CO_2 + 0.2\,NH_4^+ + \left[\frac{1 - 4.2\,Y_{Fe^{2+}X}}{4\,Y_{Fe^{2+}X}}\right]O_2 + \frac{1}{Y_{Fe^{2+}X}}Fe^{2+} + \left[\frac{1}{Y_{Fe^{2+}X}} - 0.2\right]H^+ \rightarrow CH_{1.8}O_{0.5}N_{0.2} + \frac{1}{Y_{Fe^{2+}X}}Fe^{3+} + \left[\frac{1}{2\,Y_{Fe^{2+}X}} - 0.6\right]H_2O \quad (4\text{-}6)$$

In Equation 4-6 the bacterial yield on ferrous-iron, $Y_{Fe^{2+}X}$, is defined as the amount of biomass, as moles carbon, produced per mole of ferrous-iron oxidised, *i.e.*:

$$Y_{Fe^{2+}X} = \frac{r_X}{-r_{Fe^{2+}}} \quad (4\text{-}7)$$

The bacterial yield on oxygen, Y_{O_2X}, is similarly defined:

$$Y_{O_2X} = \frac{r_X}{-r_{O_2}} \quad (4\text{-}8)$$

The relationship between the amount of substrate consumed by the biomass for bacterial growth and maintenance is described by means of the Pirt Equation (Pirt, 1982), *viz.*:

$$-r_{Fe^{2+}} = \frac{r_X}{Y^{max}_{Fe^{2+}X}} + m_{Fe^{2+}}\,c_X \quad (4\text{-}9)$$

If it is assumed that the bacteria follow Monod growth kinetics, dividing Equation 4-9 by the bacterial production rate, r_X, and combining the result with Equation 4-7 gives:

$$\frac{1}{Y_{Fe^{2+}X}} = \frac{1}{Y^{max}_{Fe^{2+}X}} + \frac{m_{Fe^{2+}}}{D} \quad (4\text{-}10)$$

Equation 4-10 can also be written in terms of the bacterial yield on oxygen:

$$\frac{1}{Y_{O_2X}} = \frac{1}{Y^{max}_{O_2X}} + \frac{m_{O_2}}{D} \quad (4\text{-}11)$$

Therefore, from steady-state continuous culture data, plotting the values of $Y_{Fe^{2+}X}$ or Y_{O_2X} against 1/D can be used to determine the values of $Y^{max}_{Fe^{2+}X}$ and $m_{Fe^{2+}}$ or $Y^{max}_{O_2X}$ and m_{O_2}. The validity of the values determined in this manner can be checked using the degree of reduction balance, Equation 4-5:

$$Y^{max}_{O_2X} = \frac{4\,Y^{max}_{Fe^{2+}X}}{1 - 4.2\,Y^{max}_{Fe^{2+}X}} \tag{4-12}$$

$$m_{O_2} = \frac{m_{Fe^{2+}}}{4} \tag{4-13}$$

The bacterial specific ferrous-iron utilisation rate, $q_{Fe^{2+}}$, is defined as the rate of ferrous-iron oxidation per mole of biomass (*i.e.* per mole of carbon), *i.e.*:

$$q_{Fe^{2+}} = \frac{-r_{Fe^{2+}}}{c_X} \tag{4-14}$$

Therefore, division of Equation 4-9 by the bacterial concentration and substitution assuming Monod growth kinetics (Equation 4-3) and combining the result with Equation 4-14 yields:

$$q_{Fe^{2+}} = \frac{D}{Y^{max}_{Fe^{2+}X}} + m_{Fe^{2+}} \tag{4-15}$$

Equation 4-15 can also be written in terms of the bacterial specific oxygen utilisation rate, q_{O_2}:

$$q_{O_2} = \frac{D}{Y^{max}_{O_2X}} + m_{O_2} \tag{4-16}$$

Therefore, plotting the values of $q_{Fe^{2+}}$ or q_{O_2}, measured during chemostat operation, versus D can also be used to determine the values of $Y^{max}_{Fe^{2+}X}$ and $m_{Fe^{2+}}$ or $Y^{max}_{O_2X}$ and m_{O_2}.

Boon (1996) suggested that the ferrous-iron oxidation kinetics could be described using a simplified form of the Michaelis-Menten model in which the bacterial specific ferrous-iron utilisation rate, $q_{Fe^{2+}}$, is proportional to the ferric/ferrous-iron ratio:

$$q_{Fe^{2+}} = \frac{q^{max}_{Fe^{2+}}}{1 + K_{Fe^{2+}}\dfrac{[Fe^{3+}]}{[Fe^{2+}]}} \tag{4-17}$$

The values of the maximum bacterial specific ferrous-iron utilisation rate, $q^{max}_{Fe^{2+}}$, and the kinetic constant in bacterial ferrous-iron oxidation, $K_{Fe^{2+}}$, in Equation 4-17 can be determined by means of a Lineweaver-Burke plot, *i.e.* inverting Equation 4-17 and simplifying yields:

$$\frac{1}{q_{Fe^{2+}}} = \frac{1}{q^{max}_{Fe^{2+}}} + \frac{K_{Fe^{2+}}}{q^{max}_{Fe^{2+}}} \frac{[Fe^{3+}]}{[Fe^{2+}]} \tag{4-18}$$

Hence, from steady-state chemostat data, plotting the values of $1/q_{Fe^{2+}}$ against $[Fe^{3+}]/[Fe^{2+}]$ can be used to determine the values of $q^{max}_{Fe^{2+}}$ and $K_{Fe^{2+}}$. Furthermore, because the ferrous-iron, oxygen and carbon dioxide utilisation rates are related via the degree of reduction balance, *viz.* Equation 4-5, the value of $q^{max}_{Fe^{2+}}$ can be used to calculate the value of $q^{max}_{O_2}$. Alternatively, the equations described above can be defined and written in terms of the bacterial specific oxygen utilisation rate:

$$q_{O_2} = \frac{q^{max}_{O_2}}{1 + K_{Fe^{2+}} \frac{[Fe^{3+}]}{[Fe^{2+}]}} \tag{4-19}$$

The oxygen based kinetic constants, *viz.* $q^{max}_{O_2}$ and K_{O_2}, can then be determined by means of a Lineweaver-Burke plot:

$$\frac{1}{q_{O_2}} = \frac{1}{q^{max}_{O}} + \frac{K_{O_2}}{q^{max}_{O_2}} \frac{[Fe^{3+}]}{[Fe^{2+}]} \tag{4-20}$$

If the Pirt Equation applies, Equations 4-15 and 4-16 may also be written in terms of $q^{max}_{Fe^{2+}}$ and $q^{max}_{O_2}$:

$$q^{max}_{Fe^{2+}} = \frac{\mu^{max}}{Y^{max}_{Fe^{2+}X}} + m_{Fe^{2+}} \tag{4-21}$$

$$q^{max}_{O_2} = \frac{\mu^{max}}{Y^{max}_{O_2X}} + m_{O_2} \tag{4-22}$$

The values of $q^{max}_{Fe^{2+}}$, $Y^{max}_{Fe^{2+}X}$ and $m_{Fe^{2+}}$, or $q^{max}_{O_2}$, $Y^{max}_{O_2X}$ and m_{O_2}, determined as described above, may be used to determine the maximum bacterial specific growth rate, μ^{max}. Alternatively, substitution of Equations 4-15 and 4-21 into Equation 4-18 and rearranging yields:

$$\frac{1}{D + m_{Fe^{2+}} Y^{max}_{Fe^{2+}}} = \frac{1}{\mu^{max} + m_{Fe^{2+}} Y^{max}_{Fe^{2+}}} + \frac{K_{Fe^{2+}}}{\mu^{max} + m_{Fe^{2+}} Y^{max}_{Fe^{2+}}} \frac{[Fe^{3+}]}{[Fe^{2+}]} \tag{4-23}$$

Similarly, substitution of Equations 4-16 and 4-22 into Equation 4-20 and rearranging yields:

$$\frac{1}{D + m_{O_2} Y^{max}_{O_2}} = \frac{1}{\mu^{max} + m_{O_2} Y^{max}_{O_2}} + \frac{K_{O_2}}{\mu^{max} + m_{O_2} Y^{max}_{O_2}} \frac{[Fe^{3+}]}{[Fe^{2+}]} \tag{4-24}$$

Hence, plotting $1/(D+ m_{Fe^{2+}} Y^{max}_{Fe^{2+}X})$ or $1/(D+ m_{O_2} Y^{max}_{O_2X})$ vs. $[Fe^{3+}]/[Fe^{2+}]$ and using the values of $Y^{max}_{Fe^{2+}X}$ and $m_{Fe^{2+}}$, or $Y^{max}_{O_2X}$ and m_{O_2}, determined as described above, may be used to determine the maximum bacterial specific growth rate, μ^{max}.

In addition to the methods described above, the maximum bacterial specific growth rate, μ^{max}, can be determined using an equation analogous to Equations 4-17 and 4-19, written in terms of the bacterial specific growth rate, μ, *viz.*:

$$\mu = \frac{\mu^{max}}{1 + K_\mu \frac{[Fe^{3+}]}{[Fe^{2+}]}} \tag{4-25}$$

As in the case of Equations 4-17 and 4-19, inverting Equation 4-25 and simplifying yields:

$$\frac{1}{\mu} = \frac{1}{\mu^{max}} + \frac{K_\mu}{\mu^{max}} \frac{[Fe^{3+}]}{[Fe^{2+}]} \tag{4-26}$$

During chemostat operation, the bacterial growth rate is determined by the residence time, *i.e.* $\mu = D$, hence plotting the values of $1/D$ against $[Fe^{3+}]/[Fe^{2+}]$ can be used to determine the values of μ^{max} and K_μ.*

The effect of temperature can be incorporated into the kinetic model suggested by Boon (1996) (Equation 4-17) by replacing the maximum bacterial specific ferrous-iron utilisation rate with a temperature dependent function. The form of this function can be established by evaluating the maximum bacterial specific ferrous-iron utilisation rate at a number of different temperatures and plotting the values of $q^{max}_{Fe^{2+}}$ against temperature. Nemati and Webb (1997) proposed that the effect of temperature on the ferrous-iron oxidation kinetics of *T. ferrooxidans* could be described using the Arrhenius equation, *viz.*:

$$q^{max}_{Fe^{2+}} = A\, e^{-\frac{E_a}{RT}} \tag{4-27}$$

Linearisation of Equation 4-27 yields:

$$\ln\left(q^{max}_{Fe^{2+}}\right) = \ln A - \frac{E_a}{RT} \tag{4-28}$$

Therefore, if plotting $\ln\left(q^{max}_{Fe^{2+}}\right)$ vs. $1/T$ produces a straight line, the values of the activation energy, E_a, and the frequency factor, A, can be determined from the slope and $y_{intercept}$. These values can in turn be substituted into Equation 4-17 to yield a model that predicts the specific rate of bacterial ferrous-iron utilisation as a function of the ferric/ferrous-iron ratio, across a range of temperatures, *i.e.*:

* It is important to recognise that the values of $q_{Fe^{2+}}$, q_{O_2} and μ are related via the degree of reduction balance, Equation 4-5; the degree of reduction balance, written in terms of $q^{max}_{Fe^{2+}}$, $q^{max}_{O_2}$ and μ^{max}, can be used to show that $K_{Fe^{2+}} = K_{O_2} = K_\mu$.

$$q_{Fe^{2+}} = \frac{A e^{-\frac{E_a}{RT}}}{1 + K_{Fe^{2+}} \frac{[Fe^{3+}]}{[Fe^{2+}]}} \quad (4\text{-}29)$$

Equation 4-29 can also be written in terms of the bacterial specific rate of oxygen utilisation:

$$q_{O_2} = \frac{B e^{-\frac{E_a}{RT}}}{1 + K_{O_2} \frac{[Fe^{3+}]}{[Fe^{2+}]}} \quad (4\text{-}30)$$

The value of "B" in Equation 4-30 could be calculated from the value of "A" in Equation 4-29. Alternatively, the values of both B and E_a in Equation 4-30 could be determined from the slope and $y_{intercept}$ of a plot of $\ln\left(q_{O_2}^{max}\right)$ vs. 1/T. It is however obvious that the activation energy, E_a, will be the same irrespective of whether it is determined using the ferrous-iron or oxygen based data and equations.* Furthermore, it is clear that in both cases, the ferric/ferrous-iron ratio can be related to the solution redox potential via the Nernst Equation.

4.2 Materials and Methods

4.2.1 Continuous-flow Bioreactors

The experiments described below were carried out in 2 ℓ jacketed Z61104CT04 Applikon® autoclavable bioreactors made of borosilicate glass. The bioreactors had a h/d ≈ 1.32 and a working volume of 1 ℓ. The head plates were constructed of 316 stainless steel and contained a number of ports for baffles, probes and other auxiliaries. Three baffles, 10 mm wide, 220 mm long and constructed of 316 stainless steel were located at 120 degrees to one another. A diagrammatic representation of a single bioreactor is shown in Figure 4.1.

The bioreactors were maintained at the required temperature by circulating water from Grant Y6 constant temperature baths through the bioreactor jackets. The pH of the solution in the bioreactors was not controlled directly. However, it was maintained at the desired pH by adjusting the pH of the feed to the reactor using sulphuric acid. The actual pH of the feed solution depended on both the target pH within the bioreactor and the prevailing dilution rate.

The inorganic nutrient medium was fed to the bioreactors by Masterflex® Model 7521-57 L/S™ Variable-Speed Drives fitted with L/S™ 7013-20 Standard Pump Heads and L/S™ 13 Norprene® Food Tubing. A chemostat tube made of 316 stainless steel was used to maintain a constant volume within the reactor. The liquid was removed from the bioreactor by means of a L/S™ 7014-20 Standard Pump Head and L/S™ 14 Norprene® Food Tubing fitted on a Masterflex® Model 7521-57 L/S™ Fixed-Speed Drive.

---

* Although the stoichiometry of Equation 4-6 is not constant, and although the Y_{O_2X}:$Y_{Fe^{2+}X}$ ratio is not constant, the errors introduced by ignoring these changes are small relative to the other errors involved. The stoichiometry of Equation 4-6 will vary with changes in the yield on ferrous-iron, *i.e.* with changes in the dilution rate.

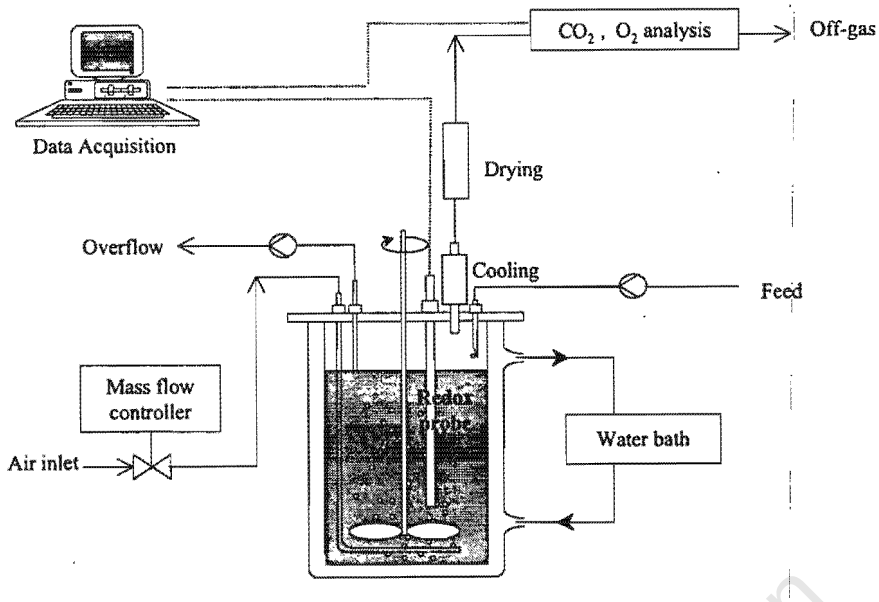

Figure 4.1: Diagrammatic representation of a single bioreactor.

Mixing and gas dispersion was achieved by a pitched (45°) six-blade 316 stainless steel turbine impeller located 2 cm from the base of the reactor. It was rotated at 600 rev.min^{-1} via a flexible coupling linked to an Applikon® P100 motor and an Applikon® 1012 stand alone speed controller.

Inlet gas was supplied by a Peak Scientific OAG2000DA Oilless Air Generator. The flow rate to the bioreactors was controlled at the required rate using Brooks Model 5850S Mass Flow Controllers and a Brooks Model 0154 Microprocessor Control and Read Out Unit. Air was introduced via an air-inlet pipe located under the impeller. The holes in the air-inlet pipe were located at the bottom to minimise blockages. The off-gas was dried using a reflux condenser through which an ethylene/glycol mixture (75 %/25 %) from a Grant LTD6G low temperature bath was circulated. The low temperature bath maintained the coolant at 6°C. Before entering the gas analysers, the off-gas was also passed through a cloth filter and a Hartmann & Braun CGEK Sample Gas Conditioner fitted with a CGKA 1 Automatic Condensate Outlet.

The carbon dioxide and oxygen concentrations in the bioreactor off-gas were determined by means of a Hartmann & Braun Uras 4 NDIR (non-dispersive infrared) Industrial Photometer and a Magnos 6 G Oxygen Analyser, respectively. The carbon dioxide and oxygen concentrations of the off-gas from each bioreactor and the inlet air were alternately logged by computer. A six-minute sampling period was used for each bioreactor. The switching and data logging hardware and software used were designed, built, and written, within the Department of Chemical Engineering at the University of Cape Town.

The ferrous-iron oxidation kinetics were investigated at dilution rates ranging from 0.01 to 0.10 h^{-1}, *i.e.* $\tau \approx 100$ to 10 h. The bioreactor was operated at each dilution rate, D, for at least three residence times before steady-state was assumed. Furthermore, steady-state was assumed only once the oxygen and carbon dioxide concentrations in the off-gas, and the redox potential in the bioleaching liquor, were constant. Each steady-state was maintained for at least one residence time.

Wall growth was minimised by shutting down the reactor once a day and scrubbing the walls of the bioreactors and all available surfaces with a bottle brush and metal scourer.

4.2.2 Bacterial Culture

The bacterial culture used was obtained from a vat-type two-stage (2×20 ℓ) continuous bioleaching mini-plant* treating an arsenopyrite/pyrite concentrate from Fairview Gold Mine in Barberton, South Africa. Although it was originally reported to consist primarily of *T. thiooxidans* and *L. ferrooxidans* (Rawlings, 1995), more recent work has shown that it consists primarily of *T. caldus* and *L. ferrooxidans* (Rawlings *et al.*, 1999(a)).

The ferrous-iron oxidising species was isolated from the mixed culture by placing 1 ℓ of slurry from the continuous bioleaching mini-plant into a 1 ℓ continuous-flow bioreactor operating at a residence time of 100 h.† Aeration and agitation of the bioreactor was stopped for a short period each day and the solids allowed to settle. The supernatant was decanted from the settled solids and returned to the bioreactor; the solids were discarded. Thus, the use of a nutrient medium that did not contain sulfur and the removal of solids that may have contained sulfur resulted in a gradual washout of the sulfur oxidising species. This procedure was repeated five times (*i.e.* for 5 residence times) before the supernatant was used the as the inoculum for the continuous ferrous-iron oxidation experiments.‡

4.2.3 Preparation of Chromosomal DNA from Bioreactor Biomass§

The biomass was harvested by centrifugation. The recovered biomass was washed using acidified water, at pH 1.80, and resuspended in 560 µℓ TE (10 mmol.ℓ^{-1} Tris, 1 mmol.ℓ^{-1} EDTA)-150 mmol.ℓ^{-1} NaCl pH 7.6 buffer. After heating the cells to 70°C for 15 minutes, 15 µℓ of a 20 g.ℓ^{-1} solution of Proteinase K and 30 µℓ of 10 % SDS were added to the sample. Thereafter it was incubated at 42°C for 30 minutes to ensure complete lysis of the recovered cells and the DNA precipitated using 10 % (v.v^{-1}) 3 mol.ℓ^{-1} Kac, at pH 5.2, and two volumes of ethanol. The precipitated DNA was washed with 70 % ethanol, air-dried and resuspended in pH 7.6 TE buffer before amplification using the polymerase chain reaction (PCR).

The polymerase chain reaction (PCR) was carried out in 100 µℓ total volume using universal primers, designed from conserved regions of bacterial 16S rDNA genes (bold), as shown below (Rawlings, 1995).

primer fDD2 5' CC *GGATCCGTCGAC***AGATTTGATCITGGCTCAG** 3' 34-mer
primer rPP2 5' CC *AAGCTTCTAGA***CGGITACCTTGGTTACGACTT** 3' 33-mer

The recovered 16S rDNA was amplified in a Biometra® Personal Cycler using 1 µℓ genomic DNA, 0.25 µmol.ℓ^{-1} of each primer, 2.5 mmol.ℓ^{-1} $MgCl_2$, 0.25 mmol.ℓ^{-1} dNTPs and 1 unit Redhot polymerase (Boeringher-Mannheim). After initial denaturation for 60 s at 94°C, 25 cycles of amplification were carried out as follows: 30 s at 94°C, 30 s at 52°C, 90 s at 72°C. A final elongation step of 120 s at 72°C followed by a

* The bioleaching mini-plant is described in detail in Chapter Six.

† The nutrient solution fed to the bioreactor contained approximately 12 g.ℓ^{-1} ferrous-iron, but no sulfur (see Table 4-1).

‡ Although the inoculum volume used was the same for each experiment, ensuring that the number of bacteria inoculated remained constant was not necessary owing to the fact that the steady-state bacterial concentration was determined by means of off-gas analysis (see Section 4.1).

§ The preparation of the chromosomal DNA and the identification of the bacterial species in the bioreactors were done by Mr. M.N. Gardner, of the Department of Microbiology at the University of Cape Town.

cooling step for 60 s at 25°C ended the reaction. Restriction enzyme analysis for the identification of species as described by Rawlings (1995) was utilised to determine the dominant species in the bioreactors.

4.2.4 Growth Medium

In addition to sulphide mineral or ferrous-iron substrate, oxygen and carbon dioxide, the bacteria used in bioleaching require nitrogen*, potassium and phosphorous and trace metals such as zinc and manganese. Nitrogen, potassium and phosphorous are usually supplied as ammonium, NH_4^+, K_2SO_4 and $(NH_4)_2HPO_4$, respectively. In the case of mineral bioleaching, the required trace elements are usually present in the mineral in sufficient quantity. However, if ferrous-iron is the substrate trace elements need to be supplied.

The composition of the nutrient solution used in this investigation is listed in Table 4-1. It was adjusted to between pH 0.95 and pH 1.30 using concentrated sulfuric acid.

Table 4-1: Inorganic nutrient medium composition

Compound	Concentration
$(NH_4)_2SO_4$	1.83 $g.\ell^{-1}$
$(NH_4)_2HPO_4$	1.11 $g.\ell^{-1}$
K_2SO_4	0.53 $g.\ell^{-1}$
$FeSO_4.7H_2O$	59.74 $g.\ell^{-1}$
trace metal solution†	10 $m\ell.\ell^{-1}$

No attempt was made to maintain sterility.

4.2.5 Ferric/Ferrous-Iron Ratio Determination

The redox potential in the bioreactors was measured using Metrohm redox electrodes (Pt-Ag/AgCl) and logged by computer. The total iron concentration in solution was determined by both Flame Atomic Adsorption Spectroscopy (FAAS) and titration with potassium dichromate (Jeffrey *et al.*, 1989). This enabled the ferric/ferrous-iron ratio and the ferrous and ferric-iron concentrations to be determined using a calibration curve for the specific electrode and the Nernst equation (see Section 3.1.1.3). The ferrous-iron concentration was also determined by titration with cerium(IV) sulfate (see Appendix to Chapter Five).

* Although *L. ferrooxidans*, *T. ferrooxidans* and *T. thiooxidans* have the genes required to fix atmospheric nitrogen, to date only *L. ferrooxidans* and *T. ferrooxidans* have been shown capable of doing so (Dew *et al.*, 1997).

† Ethylenediamine tetra-acetic acid 50.0 $g.\ell^{-1}$, $ZnSO_4.7H_2O$ 22.0 $g.\ell^{-1}$, $CaCl_2$ 5.54 $g.\ell^{-1}$, $MnCl_2.4H_2O$ 5.06 $g.\ell^{-1}$, $FeSO_4.7H_2O$ 4.99 $g.\ell^{-1}$, $(NH_4)_6Mo_7O_{24}.4H_2O$ 1.10 $g.\ell^{-1}$, $CuSO_4.5H_2O$ 1.57 $g.\ell^{-1}$, $CoCl_2.6H_2O$ 1.61 $g.\ell^{-1}$ adjusted to pH 6.0 using KOH (Vishniac and Santer, 1957).

4.3 Results and Discussion

During the experiments carried out to determine the effect of temperature on the ferrous-iron oxidation kinetics, the pH in each of the bioreactors was maintained at pH 1.70. Single bioreactors were maintained at 30 and 35°C, respectively, and duplicate bioreactors were maintained at 40°C. However, in the figures shown below the results obtained at 40°C have been combined.

During the experiments carried out to determine the effect of pH on the ferrous-iron oxidation kinetics, the bioreactors were all maintained at a temperature of 40°C, and pH 1.10, 1.30 and 1.50, respectively.

4.3.1 Identification of Bacterial Species*

The restriction enzyme banding patterns of PCR amplified 16S rDNA from the chromosomal DNA of pure cultures of *T. ferrooxidans* ATCC 33020, *L. ferrooxidans* DSM 2705 and the biomass harvested from the bioreactor maintained at 35°C and one of the bioreactors maintained at 40°C, while both were operating at a residence time of 70 hours, are shown in Figure 4.2.

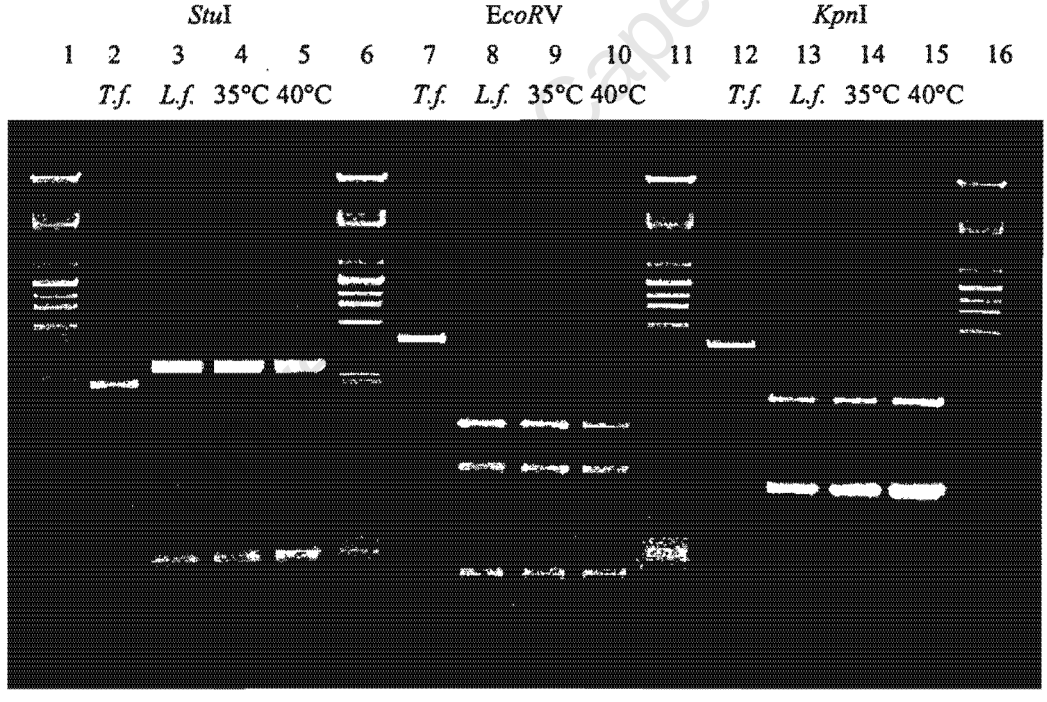

Figure 4.2: Restriction enzyme analysis of PCR amplified 16S rDNA from pure cultures of *T. ferrooxidans* and *L. ferrooxidans* and the ferrous-iron oxidising bacterial species obtained from the bioleaching mini-plant. Lanes 1, 6, 11and 16 are size markers obtained by digestion of phage λ with *Pst*I.

Three restriction enzymes were used: *Stu*I (lanes 2 to 5), *Eco*RV (lanes 7 to 10) and *Kpn*I (lanes 12 to 15). From Figure 4.2 it is clear that the sizes of the bands obtained from the biomass in the two bioreactors are identical, irrespective of which restriction enzyme was used. In addition, they are also identical to those obtained for

* As stated previously this was performed by Mr. M.N. Gardner, of the Department of Microbiology at the University of Cape Town.

L. ferrooxidans DSM 2705 (lanes 3, 8 and 13) and different from *T. ferrooxidans* ATCC 33020 (lanes 2, 7 and 12), irrespective of which restriction enzyme was used.

Similar banding patterns were obtained after restriction enzyme digestion of the PCR products amplified from the biomass in the other bioreactors (data not shown). This indicated that *L. ferrooxidans* was the only bacterial species detected in the four bioreactors.

Restriction enzyme analysis of PCR amplified genomic DNA from the bioreactors and of pure cultures of *T. ferrooxidans* and *L. ferrooxidans* was repeated at each steady-state, and the same result obtained. As bacterial species present in low concentrations may not have been detected using the above method, the results cannot be considered evidence that the culture in the bioreactors consisted solely of *L. ferrooxidans*. In spite of this limitation, however, the results do indicate that *L. ferrooxidans* was present in numbers far exceeding any other bacterial species. It was therefore possible to assume that any variations in the measured parameters, *viz.* ferrous-iron, carbon dioxide and oxygen utilisation rates, could be directly attributed to changes in the concentration and metabolic activity of *L. ferrooxidans*.

A scanning electron micrograph (SEM) of the ferrous-iron oxidising bacteria obtained from one of the bioreactors maintained at 40°C, while operating at a residence time of 25 hours, is shown in Figure 4.3. The coccoid shape of many of the bacteria apparent in Figure 4.3 can be attributed to the high levels of ferric-iron in the bioreactors (Barrett *et al.*, 1993).

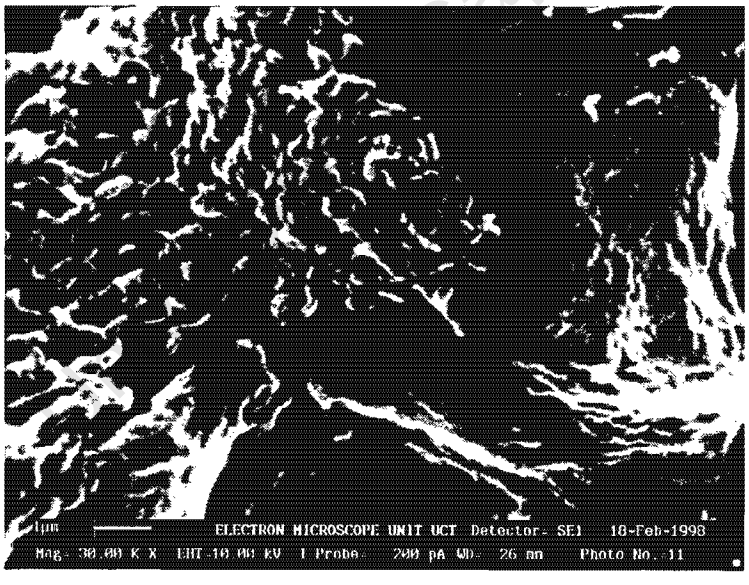

Figure 4.3: Scanning electron micrograph of the ferrous-iron oxidising bacterial species obtained from one of the bioreactors maintained at 40°C.

4.3.2 Validation of Raw Data

Prior to performing any kinetic analysis, the validity of the data obtained was checked by comparing trends in the redox potential and the rates of ferrous-iron, oxygen and carbon dioxide utilisation with changing dilution rate, with the expected trends. This was done as follows:

The variation in the substrate (ferrous-iron) concentration with changes in the dilution rate was calculated from the measured variation in the redox potential with changes in the dilution rate. This allowed the validity of the redox potential data to be checked by comparing the variation in the calculated ferrous-iron concentration with changes in the dilution rate with the variation in the substrate concentration with changes in the dilution rate observed during previous investigations performed in continuous-flow bioreactors.

The validity of the calculated rates of ferrous-iron, oxygen and carbon dioxide utilisation with changing dilution rate were checked by comparing the relationship between the measured values of these parameters and the relationship predicted by the degree of reduction balance, Equation 4-5.

4.3.2.1 Substrate concentration versus dilution rate

The variation in the measured redox potential, E, and ferrous-iron concentration, $[Fe^{2+}]$, in the bioreactors as a function of the dilution rate, D, at temperatures ranging from 30 to 40°C and pH values ranging from pH 1.10 to pH 1.70, are shown in Figures 4.4(a) and (b), respectively.

From Figure 4.4(a), it is clear that the redox potential decreased with increasing dilution rate. This reflected an increase in the ferrous-iron concentration, apparent in Figure 4.4(b), with increasing dilution rate. This trend is typical for substrate concentration versus dilution rate in a continuous-flow bioreactor (van Scherpenzeel *et al.*, 1998; Boon, 1996; Schlegel, 1986).

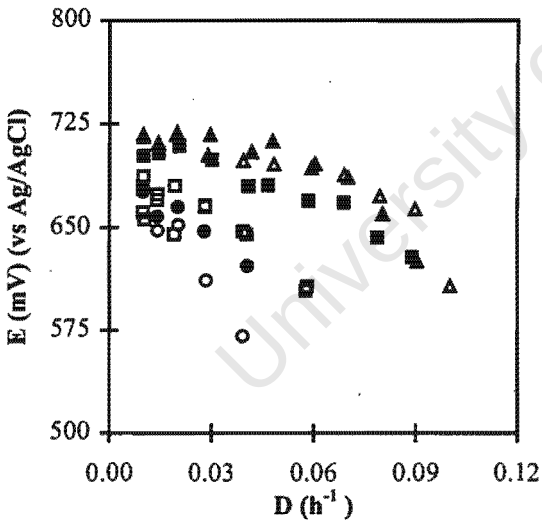

Figure 4.4(a): Variation in the measured redox potential with changes in the dilution rate.

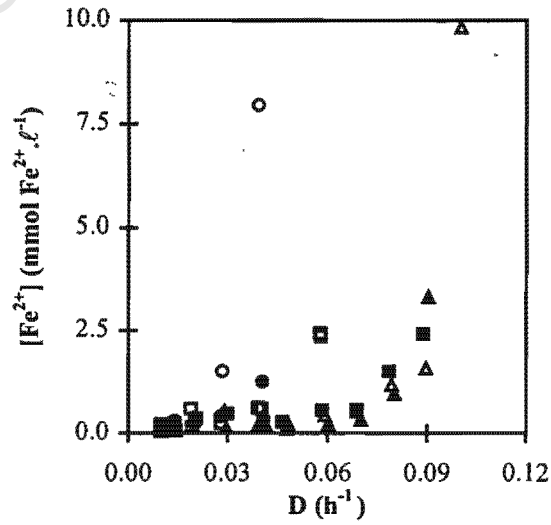

Figure 4.4(b): Variation in the ferrous-iron concentration with changes in the dilution rate.

[○] 30°C, pH 1.70; [●] 35°C, pH 1.70; [□] 40°C, pH 1.70; [▲] 40°C, pH 1.10; [△] 40°C, pH 1.30; [■] 40°C, pH 1.50.

4.3.2.2 Ferrous-iron, oxygen and carbon dioxide utilisation rates versus dilution rate

The variation in the measured ferrous-iron, $-r_{Fe^{2+}}$, oxygen, $-r_{O_2}$, and carbon dioxide, $-r_{CO_2}$, utilisation rates with changes in the dilution rate, D, at temperatures ranging from 30 to 40°C and pH values ranging from pH 1.10 to pH 1.70 are shown in Figures 4.5(a), (b) and (c), respectively.

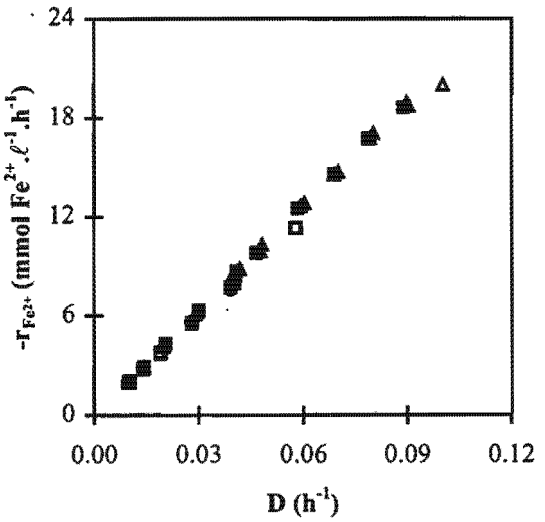

Figure 4.5(a): Variation in the ferrous-iron utilisation rate with changes in the dilution rate.

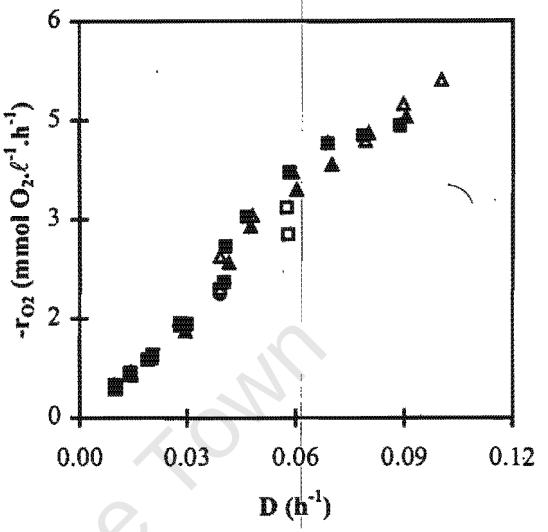

Figure 4.5(b): Variation in the oxygen utilisation rate with changes in the dilution rate.

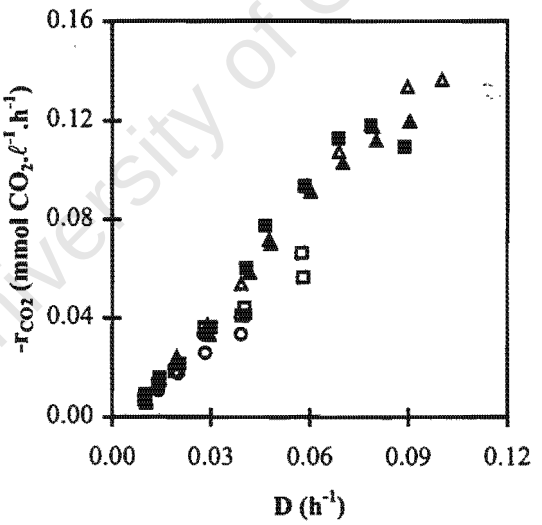

Figure 4.5(c): Variation in the carbon dioxide utilisation rate with changes in the dilution rate.
[○] 30°C, pH 1.70; [●] 35°C, pH 1.70; [□] 40°C, pH 1.70; [▲] 40°C, pH 1.10; [Δ] 40°C, pH 1.30; [■] 40°C, pH 1.50.

From Figures 4.5(a) to (c) it is clear that a linear relationship exists between the measured ferrous-iron, oxygen and carbon dioxide utilisation rates and the dilution rate. This therefore suggests that a linear relationship exists between the respective utilisation rates. However, as the rates shown are not based on the biomass concentration it is not possible to determine whether either temperature or pH has an effect on the bacterial specific ferrous-iron, oxygen and carbon dioxide utilisation rates.

4.3.2.3 Degree of reduction balance

The measured ferrous-iron, oxygen and carbon dioxide utilisation rates shown in Figures 4.5(a) to (c) are related via the degree of reduction balance, Equation 4-5. A comparison of the predicted and measured relationship between these parameters is shown in Figure 4.6 where it can be seen that the agreement is good.

Therefore, although the results shown in Figures 4.4 to 4.6 do not give any indication with regard to the effect of either temperature or pH on the ferrous-iron oxidation kinetics of *L. ferrooxidans*, they do demonstrate the trends anticipated, which in turn suggests that the measured values of $-r_{Fe^{2+}}$, $-r_{O_2}$ and $-r_{CO_2}$ were valid.

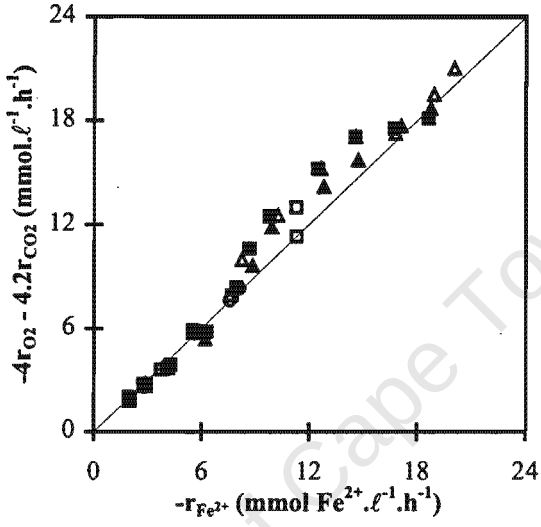

Figure 4.6: Comparison between the predicted and experimental relationship between the ferrous-iron, oxygen and carbon dioxide utilisation rates. [○] 30°C, pH 1.70; [●] 35°C, pH 1.70; [□] 40°C, pH 1.70; [▲] 40°C, pH 1.10; [Δ] 40°C, pH 1.30; [■] 40°C, pH 1.50.

4.3.3 Concentration of Biomass

The biomass concentration, c_X, in the bioreactors was calculated from the carbon dioxide utilisation rate using Equation 4-3. Figure 4.7 shows the variation in the biomass concentration in the bioreactors, at temperatures ranging from 30 to 40°C and pH values ranging from pH 1.10 to pH 1.70, with changes in the dilution rate.

From Figure 4.7 it is apparent that the highest biomass concentrations were achieved at intermediate residence times, irrespective of the temperature and pH maintained within the bioreactor. The reduced biomass concentration at low dilution rates can be attributed to an increased maintenance requirement at long residence times and is consistent with both Equation 4-10, and the results of previous research (Van Scherpenzeel *et al.*, 1998; Boon, 1996).

However, the reduced biomass concentration at high dilution rates may have been a result of progressive washout caused by a reduction in ferric-iron inhibition (Jones and Kelly, 1983), or due to a decrease in the yield with increasing growth rate. The former is unlikely as there was little variation in the ferric-iron concentration

between dilution rates of 0.06 and 0.09 h^{-1};* whereas the latter implies that the Pirt equation may not be applicable.†

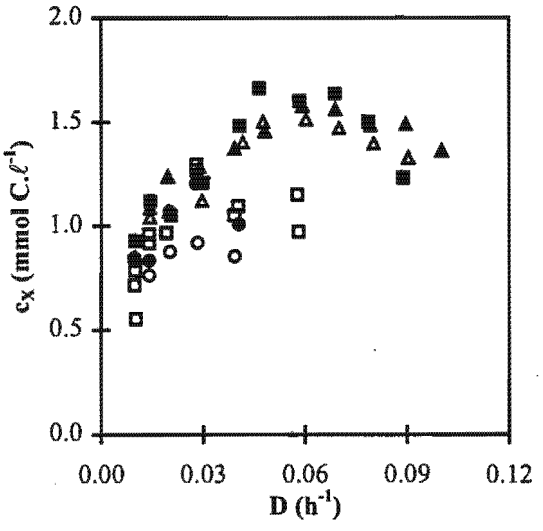

Figure 4.7: Variation in the biomass concentration with changes in the dilution rate. [○] 30°C, pH 1.70; [●] 35°C, pH 1.70; [□] 40°C, pH 1.70; [▲] 40°C, pH 1.10; [Δ] 40°C, pH 1.30; [■] 40°C, pH 1.50.

It is also apparent that c_X increased with increasing temperature, at all dilution rates, and that the bioreactors maintained at 40°C were less subject to washout. Furthermore, although the bacterial culture maintained at 40°C and pH 1.30 "washed out" at the highest dilution rate, at pH values below pH 1.70, the biomass concentration did not appear to be significantly affected by pH.

4.3.4 Pirt Equation Parameters

The values of the maximum bacterial yield on ferrous-iron, $Y^{max}_{Fe^{2+}X}$, and the maintenance coefficient on ferrous-iron, $m_{Fe^{2+}}$, were determined at pH 1.70 and 30, 35 and 40°C, by linear regression using Equations 4-10 and 4-15. Although it was possible to use the values of $Y^{max}_{Fe^{2+}X}$ and $m_{Fe^{2+}}$, and Equations 4-12 and 4-13 to calculate the values of the maximum bacterial yield on oxygen, $Y^{max}_{O_2X}$, and the maintenance coefficient on oxygen, m_{O_2}, they were determined by linear regression, using Equations 4-11 and 4-16, instead.

The average values of the maximum yields on ferrous-iron and oxygen and their respective maintenance coefficients are listed in Table 4-2, together with the average correlation coefficient, R^2.‡ The greatest significance level at which the null hypothesis is accepted, α^{max}, is also listed. The null hypothesis is that temperature does not affect the values of the maximum biomass yield on either ferrous-iron or oxygen, nor their respective maintenance coefficients. However, the low values of α^{max} listed in Table 4-2 suggest that $Y^{max}_{Fe^{2+}X}$,

* At D ≈ 0.06 h^{-1}, $[Fe^{3+}] \approx 214$ mmol $Fe^{3+}.\ell^{-1}$ whereas $[Fe^{3+}] \approx 204$ mmol $Fe^{3+}.\ell^{-1}$ at D ≈ 0.09 h^{-1}.

† The Pirt equation assumes that the yield increases with an increase in the dilution rate.

‡ The "average values" listed in Table 4-2 are the averages of the values obtained using Equations 4-10 and 4-15, in the case of the ferrous-iron based parameters and Equations 4-11 and 4-16 in the case of the oxygen based parameters, at each set of experimental conditions used.

$Y^{max}_{O_2/X}$, $m_{Fe^{2+}}$ and m_{O_2} are all influenced by temperature, *i.e.* $Y^{max}_{Fe^{2+}/X}$, $Y^{max}_{O_2/X}$, $m_{Fe^{2+}}$ and m_{O_2} all increase with increasing temperature across the range from 30 to 40°C.

Table 4-2: Average values of the maximum biomass yields on ferrous-iron and oxygen and their respective maintenance coefficients at pH 1.70 and temperatures ranging from 30 to 40°C

	Temperature			*t*-test H_0: $\bar{x}_T = \bar{x}_{T=40°C}$
	30°C	35°C	40°C	α^{max}
$Y^{max}_{Fe^{2+}/X}$	0.0047	0.0060	0.0068	0.20
$m_{Fe^{2+}}$	0.3587	0.7221	1.0578	0.20
R^2	0.6546	0.8031	0.8185	
$Y^{max}_{O_2/X}$	0.0185	0.0246	0.0251	0.10
m_{O_2}	0.0132	0.1719	0.2053	0.20
R^2	0.5329	0.7897	0.7806	

The procedure detailed above was also carried out using the data obtained at 40°C and pH 1.10, 1.30, 1.50 and 1.70. The resulting average values of $Y^{max}_{Fe^{2+}/X}$, $Y^{max}_{O_2/X}$, $m_{Fe^{2+}}$, m_{O_2} and R^2 are listed in Table 4-3, together with the greatest significance level at which the null hypothesis is accepted. In this case the null hypothesis is that pH does not affect the maximum biomass yields on either ferrous-iron or oxygen, nor their respective maintenance coefficients. As in the case of Table 4-2 however, the low values of α^{max} listed in Table 4-3 suggest that $Y^{max}_{Fe^{2+}/X}$, $Y^{max}_{O_2/X}$, $m_{Fe^{2+}}$ and m_{O_2} are also influenced by pH. From Table 4-3 it appears as though both $Y^{max}_{Fe^{2+}/X}$ and $Y^{max}_{O_2/X}$ achieve maximum values between pH 1.30 and pH 1.50 while $m_{Fe^{2+}}$ and m_{O_2} achieve minimum values within the same pH range.

Table 4-3: Average values of the maximum biomass yield on ferrous-iron and oxygen and their respective maintenance coefficients at 40°C and pH values ranging from pH 1.10 to pH 1.70

	pH				*t*-test H_0: $\bar{x}_{pH} = \bar{x}_{pH\,1.70}$
	pH 1.10	pH 1.30	pH 1.50	pH 1.70	α^{max}
$Y^{max}_{Fe^{2+}/X}$	0.0073	0.0076	0.0074	0.0068	0.20
$m_{Fe^{2+}}$	0.8943	0.7440	0.6629	1.0578	0.20
R^2	0.9244	0.9758	0.8044	0.8185	
$Y^{max}_{O_2/X}$	0.0277	0.0280	0.0272	0.0251	0.20
m_{O_2}	0.1377	0.1578	0.1247	0.2053	0.20
R^2	0.9516	0.7838	0.8624	0.7806	

Although the statistical analysis of the regression data suggested that the maximum yields on ferrous-iron and oxygen and their respective maintenance coefficients were all affected by both temperature and pH, the techniques used did not take into account the poor correlation coefficients obtained during the regression analysis. For this reason, average values of the maximum yields on ferrous-iron and oxygen and their respective

maintenance coefficients were determined based on the assumption that neither temperature, nor pH, has an effect on the values of these parameters.

The data used to calculate the average values of the ferrous-iron based parameters, based on this assumption, are shown in Figures 4.8 and 4.9 and the data used to calculate the average values of the oxygen based parameters, based on the assumption that neither temperature, nor pH, has an effect on the values of these parameters, are shown in Figures 4.10 and 4.11.

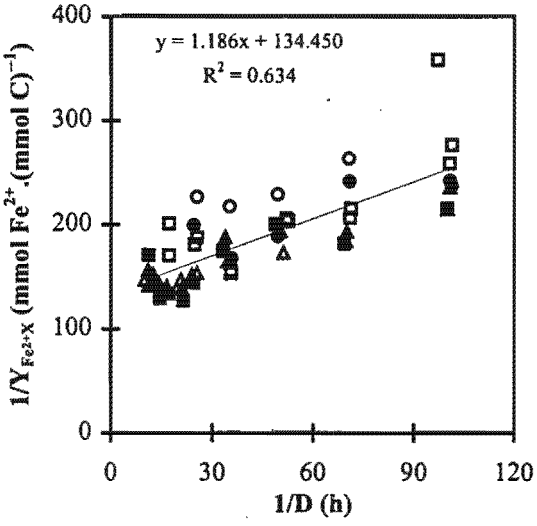

Figure 4.8: Data used to determine the maximum biomass yield on ferrous-iron and the maintenance coefficient on ferrous-iron using Equation 4-10.

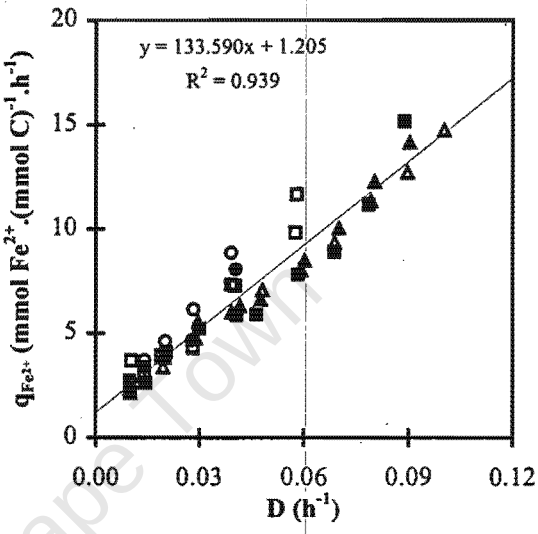

Figure 4.9: Data used to determine the maximum biomass yield on ferrous-iron and the maintenance coefficient on ferrous-iron using Equation 4-15.

[○] 30°C, pH 1.70; [•] 35°C, pH 1.70; [□] 40°C, pH 1.70; [▲] 40°C, pH 1.10; [Δ] 40°C, pH 1.30; [■] 40°C, pH 1.50.

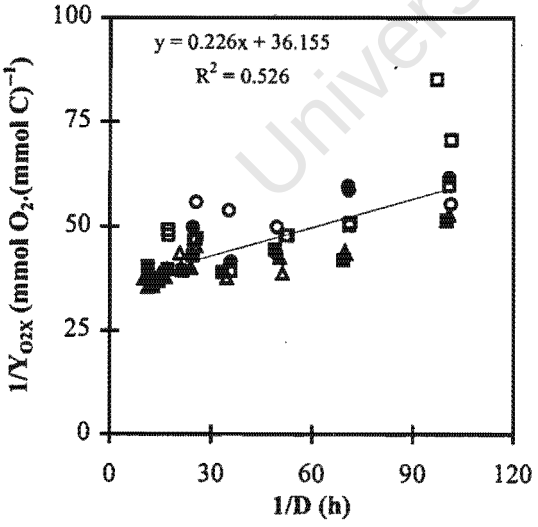

Figure 4.10: Data used to determine the maximum biomass yield on oxygen and the maintenance coefficient on oxygen using Equation 4-11.

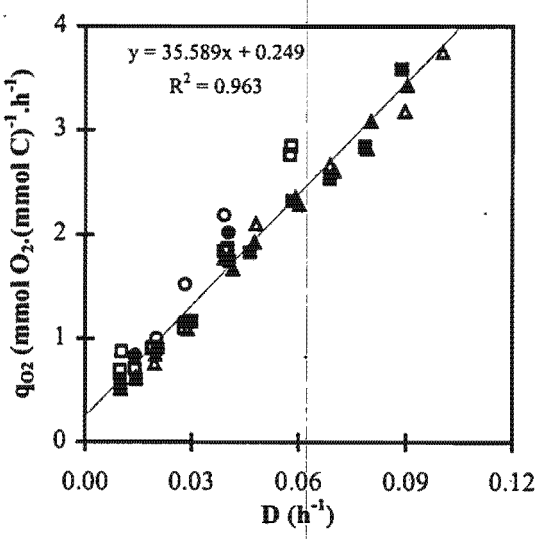

Figure 4.11: Data used to determine the maximum biomass yield on oxygen and the maintenance coefficient on oxygen using Equation 4-16.

[○] 30°C, pH 1.70; [•] 35°C, pH 1.70; [□] 40°C, pH 1.70; [▲] 40°C, pH 1.10; [Δ] 40°C, pH 1.30; [■] 40°C, pH 1.50.

Comparison of the regression coefficients obtained in Figures 4.8 and 4.10 with those obtained in Figures 4.9 and 4-11 suggested that the "fits" obtained using Equations 4-15 and 4-16 were considerably better than those obtained using Equations 4-10 and 4-11. This can be attributed to the emphasis that Equations 4-10 and 4-11 place on the experimental data obtained at long residence times. In general, operating small-scale continuous bioreactors at long residence times produces the poorest (most variable) data because of difficulties involved in maintaining steady-state operation. In spite of this limitation however, the values of the maximum yields on ferrous-iron and oxygen and their respective maintenance coefficients determined by linear regression of the data in Figures 4.8 and 4.9, and Figures 4.10 and 4.11, were similar.

For this reason, the average values of the maximum yields on ferrous-iron and oxygen and their respective maintenance coefficients, determined assuming neither temperature, nor pH has an effect on them, are listed in Tables 4-4 and 4-5.* The values reported previously for *T. ferrooxidans* (Boon, 1996) and a *Leptospirillum*-like bacterium (Van Scherpenzeel *et al.*, 1998) are also listed in these tables. From Tables 4-4 and 4-5, it is clear that the values of the maximum yields on ferrous-iron and oxygen and their respective maintenance coefficients determined during this investigation are similar to those reported previously for both *T. ferrooxidans* and a *L. ferrooxidans*-like bacterium.

Table 4-4: Average values of the maximum biomass yield and maintenance coefficient on ferrous-iron calculated assuming neither are functions of temperature or pH, together with previously reported values

Bacterial Culture	Temperature, pH	$Y^{max}_{Fe^{2+}X}$ (mmol C.(mmol Fe^{2+})$^{-1}$)	$m_{Fe^{2+}}$ (mmol Fe^{2+}.(mmol C)$^{-1}$.h^{-1})
Predominantly *L. ferrooxidans*	30-40°C, pH 1.10-1.70	0.0075	1.1956
Leptospirillum-like (Van Scherpenzeel *et al.*, 1998)	30°C, pH 1.5-1.6	0.0105	0.3355
T. ferrooxidans (Boon, 1996)	30°C, pH 1.8-1.9	0.0121 ± 0.0007†	0.40 ± 0.2‡

In addition to the values listed in Table 4-4, values of the maximum biomass yield on ferrous-iron ranging from 0.01 to 0.1667 mmol C.(mmol Fe^{2+})$^{-1}$ have been reported for *T. ferrooxidans* (Liu *et al.*, 1988; Braddock *et al.*, 1984). Braddock *et al.* (1984) also calculated the theoretical yield on ferrous-iron at 22.5°C and pH 1.80; it was found to be 0.0442 mmol C.(mmol Fe^{2+})$^{-1}$.

Table 4-5: Average values of the maximum biomass yield and maintenance coefficient on oxygen calculated assuming neither are functions of temperature or pH, together with previously reported values

Bacterial Culture	Temperature, pH	$Y^{max}_{O_2X}$ (mmol C.(mmol O_2)$^{-1}$)	m_{O_2} (mmol C.(mmol O_2)$^{-1}$.h^{-1})
Predominantly *L. ferrooxidans*	30-40°C, pH 1.10-1.70	0.0279	0.2376
Leptospirillum-like (Van Scherpenzeel *et al.*, 1998)	30°C, pH 1.5-1.6	0.046	0.0425
T. ferrooxidans (Boon, 1996)	30°C, pH 1.8-1.9	0.051 ± 0.003	0.1 ± 0.05

* The "average values" listed in Tables 4-4 and 4-5 were calculated in the same way as the parameters listed in Tables 4-2 and 4-3.
† Calculated using Equation 4-12.
‡ Calculated using Equation 4-13.

In addition to the values listed in Table 4-5, Liu *et al.* (1988) reported a maximum biomass yield on oxygen of 0.0493 mmol C.(mmol O_2)$^{-1}$ for *T. ferrooxidans*. However, as no values were reported for the maintenance coefficients on ferrous-iron and oxygen, the values of the maximum biomass yields determined during these investigations were not included in the respective tables.

In general, however, it appears as though the maximum yield on ferrous-iron is lower than the maximum yield on oxygen, whereas the maintenance coefficient on ferrous-iron is greater than the maintenance coefficient on oxygen. These observations are clearly consistent with the predictions of Equations 4-12 and 4-13.

In addition, the relationship between the values of the ferrous-iron and oxygen based parameters listed in Tables 4-4 and 4-5 were compared with the relationship predicted by the degree-of-reduction balance, *viz.* Equations 4-12 and 4-13. These comparisons are shown in Figure 4.12, from which it is apparent that the correlation is good.

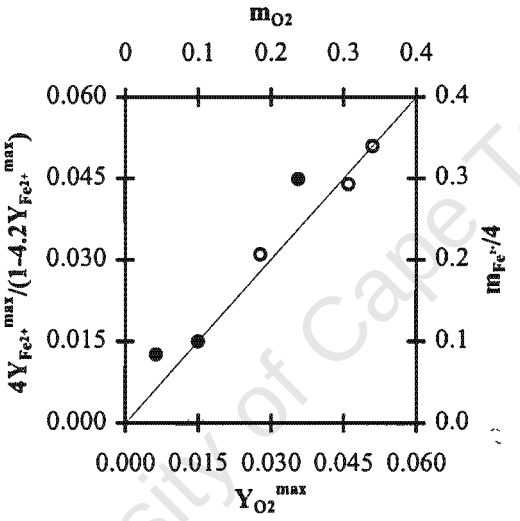

Figure 4.12: Comparison of the predicted and experimental relationships between the [o] maximum yield and [•] maintenance coefficients for the data listed in Tables 4-4 and 4-5.

4.3.5 Maximum Bacterial Specific Utilisation Rates

4.3.5.1 Ferrous-iron based parameters

The values of the maximum bacterial specific ferrous-iron utilisation rate, $q_{Fe^{2+}}^{max}$, and the kinetic constant in bacterial ferrous-iron oxidation, $K_{Fe^{2+}}$, at each set of experimental conditions were initially determined by means of Lineweaver-Burke plots. However, this method yielded poor correlation coefficients, $R_{avrg}^2 \approx 0.789$, and values of $q_{Fe^{2+}}^{max}$, which were significantly lower than the maximum values observed during the experiments. For this reason, the values of $q_{Fe^{2+}}^{max}$ and $K_{Fe^{2+}}$ were determined by minimising the sum of the square of the errors, Σe^2, between the values of $q_{Fe^{2+}}$ determined experimentally and the values predicted by Equation 4-17, *i.e.* by minimising the value of Σe^2 in:

$$\sum e^2 = \sum_{p=1}^{p=n} \left(\frac{q_{Fe^{2+}}^{max}}{1 + K_{Fe^{2+}} \frac{[Fe^{3+}]}{[Fe^{2+}]}} - q_{Fe^{2+},exp} \right)^2 \quad (4\text{-}31)$$

The values of $q_{Fe^{2+}}^{max}$ and $K_{Fe^{2+}}$ determined in this manner are listed in Table 4-6, together with the values determined previously for a *Leptospirillum*-like bacterium (Van Scherpenzeel *et al.*, 1998) and *T. ferrooxidans* (Boon, 1996). From Table 4-6, it is apparent that the value of the maximum bacterial specific ferrous-iron utilisation rate of the predominantly *L. ferrooxidans* culture increased with increasing temperature. However, although the results suggest that $q_{Fe^{2+}}^{max}$ achieved a maximum value at pH 1.50, no simple relationship between $q_{Fe^{2+}}^{max}$ and pH is apparent. It is also apparent from the results listed in Table 4-6 that the value of the kinetic constant, $K_{Fe^{2+}}$, increased with an increase in either temperature or pH.

Table 4-6: Values of the maximum bacterial specific ferrous-iron utilisation rate and the kinetic constant in bacterial ferrous-iron oxidation, at temperatures ranging from 30 to 40°C and pH values ranging from pH 1.10 to pH 1.70

Bacterial Culture	Temperature (°C)	pH	$q_{Fe^{2+}}^{max}$ (mmol Fe^{2+}.(mmol C)$^{-1}$.h^{-1})	$K_{Fe^{2+}}$
Predominantly *L. ferrooxidans*	30	1.70	8.65	0.0018
	35	1.70	11.01	0.0023
	40	1.70	13.62	0.0034
Predominantly *L. ferrooxidans*	40	1.10	15.26	0.0010
	40	1.30	15.57	0.0022
	40	1.50	19.02	0.0037
Leptospirillum-like (Van Scherpenzeel *et al.*, 1998)	30	1.5-1.6	7.09*	0.0004†
T. ferrooxidans (Boon, 1996)	30	1.8-1.9	9.2†	0.05‡

Comparison of the results obtained for the predominantly *L. ferrooxidans*, the *Leptospirillum*-like and the *T. ferrooxidans* species suggests that, at 30°C, there is little difference in the ferrous-iron oxidising ability of these cultures. However, the results listed in Table 4-6 indicate that the optimum conditions for the predominantly *L. ferrooxidans* culture (40°C and pH 1.50) are different from those reported previously for *L. ferrooxidans* (35°C and pH 1.50-2.0) and *T. ferrooxidans* (28-35°C and pH 2-2.5). This suggests that the maximum bacterial specific ferrous-iron utilisation rate of *L. ferrooxidans* may be greater than that of *T. ferrooxidans*, if both species are cultivated under optimal conditions.

It is also apparent from the results listed in Table 4-6 that the values of $K_{Fe^{2+}}$ listed for the predominantly *L. ferrooxidans* culture and the *Leptospirillum*-like bacterium are significantly smaller than the value reported for *T. ferrooxidans*. This difference has been observed during previous investigations and has been attributed to

* Calculated using the degree-of-reduction balance, *viz.* Equation 4-5.
† The values listed were calculated from oxygen utilisation rate data and reported as K_s/K_i.

L. ferrooxidans having a greater affinity for ferrous-iron than *T. ferrooxidans* (Boon, 1996; Norris *et al.*, 1988). The differences between the two *Leptospirillum* species may be attributed to differences between different sub-species; the predominantly *L. ferrooxidans* culture originated from the Fairview Gold Mine in Barberton, whereas the *Leptospirillum*-like bacterium originated from Gamsberg in Namaqualand.

A comparison between the experimentally determined values of $q_{Fe^{2+}}$ and the prediction of Equation 4-17, using the values of $q^{max}_{Fe^{2+}}$ and $K_{Fe^{2+}}$ listed in Table 4-6, is shown in Figure 4.13. From Figure 4.13, it can be seen that the agreement is good.

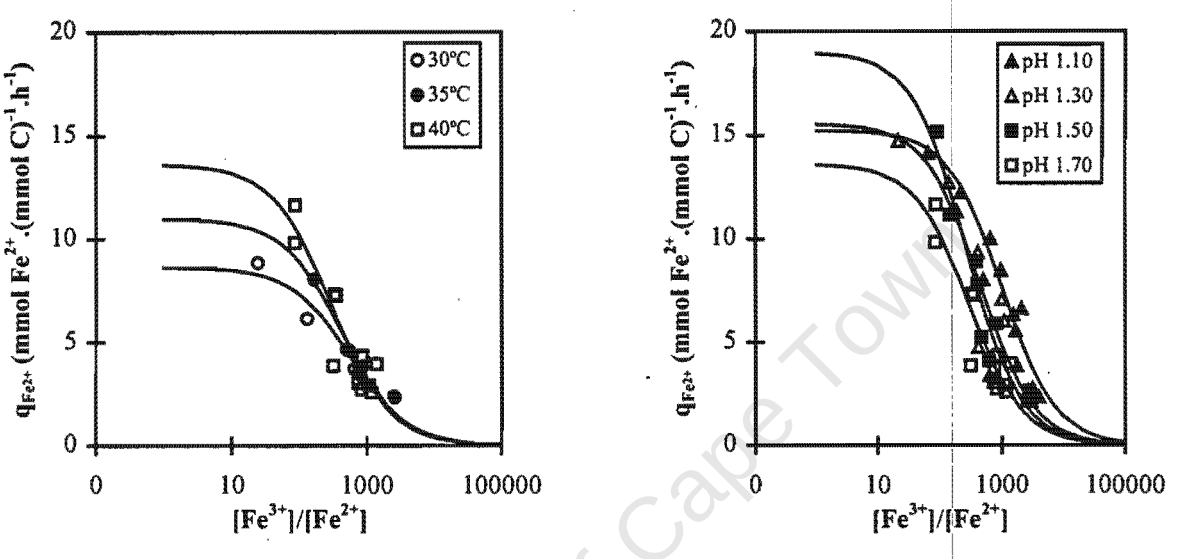

Figure 4.13: Comparison between the experimental and predicted variation in the bacterial specific ferrous-iron utilisation rate with changing ferric/ferrous-iron ratio.

It is also apparent from the results shown in Figure 4.13 that there are a number of data points at ferric/ferrous-iron ratios in the region of 800 to 4000, *i.e.* at redox potential values in the region of 660 to 680 mV. It has been suggested that these represent the threshold ferrous-iron concentration, *i.e.* the ferrous-iron concentration below which no further ferrous-iron utilisation occurs (Braddock *et al.*, 1984).

However, the agreement between the model and the experimentally determined values of $q_{Fe^{2+}}$ shown in Figure 4.13 suggests that the ferrous-iron oxidation kinetics are a function of the ferric/ferrous-iron ratio, or redox potential. This in turn suggests that these points represent a threshold redox potential, which is consistent with the chemiosmotic potential theory proposed by Ingledew (1986). At a total iron concentration of 214 mmol.ℓ^{-1}, this threshold redox potential corresponds to ferrous-iron concentrations in the region of 0.054-0.268 mmol $Fe^{2+}.\ell^{-1}$. This ferrous-iron concentration is greater than the 0.005 mmol $Fe^{2+}.\ell^{-1}$ reported for a *Leptospirillum*-like bacteria isolated from the Gamsberg deposit in South Africa (van Scherpenzeel, 1996), but less than the 0.5 mmol $Fe^{2+}.\ell^{-1}$ reported for *T. ferrooxidans* (Boon, 1996); in both cases the threshold ferrous-iron concentrations were also determined at a total iron concentration of about 214 mmol.ℓ^{-1}. In other words, the *Leptospirillum* species are less subject to inhibition by higher ferric/ferrous-iron ratios (*i.e.* redox potentials) than *T. ferrooxidans*; this results in the *Leptospirillum* species having lower values of $K_{Fe^{2+}}$ than *T. ferrooxidans*.

In addition to the above observations, the results shown in Figure 4.13 suggest that the threshold redox potential is influenced by the pH of the medium; a decrease in the pH of the solution results in an increase in the threshold

redox potential. This can possibly be attributed to the speciation of the iron sulfate complexes being affected by the pH of the liquor (Barrett *et al.*, 1993).

4.3.5.2 Oxygen based parameters

Although it is possible to calculate the values of the maximum bacterial specific oxygen utilisation rate, $q_{O_2}^{max}$, and the kinetic constant, K_{O_2}, from the values of $q_{Fe^{2+}}^{max}$ and $K_{Fe^{2+}}$, using the degree of reduction balance, the oxygen-based parameters were initially determined by means of Lineweaver-Burke plots instead. However, as in the case of the ferrous-iron based parameters, this method yielded poor correlation coefficients, $R^2_{avrg} \approx 0.748$, and values of $q_{O_2}^{max}$ which were significantly lower than the observed maximum values. For this reason, the values of $q_{O_2}^{max}$ and K_{O_2} were also determined by minimising the sum of the square of the errors between the experimental results and the values of q_{O_2} predicted by Equation 4-19.

The values of $q_{O_2}^{max}$ and K_{O_2} determined in this manner are listed in Table 4-7, together with the values determined previously for *T. ferrooxidans* (Boon, 1996; Norris *et al.*, 1988), *L. ferrooxidans* (Norris *et al.*, 1988) and a *Leptospirillum*-like bacterium (Van Scherpenzeel *et al.*, 1998).

Table 4-7: Values of the maximum bacterial specific oxygen utilisation rate and the kinetic constant in bacterial ferrous-iron oxidation, at temperatures ranging from 30 to 40°C and pH values ranging from pH 1.10 to pH 1.70

Bacterial Culture	Temperature (°C)	pH	$q_{O_2}^{max}$ (mmol O_2.(mmol C)$^{-1}$.h^{-1})	K_{O_2}
Predominantly *L. ferrooxidans*	30	1.70	2.19	0.0023
	35	1.70	2.85	0.0026
	40	1.70	3.67	0.0038
Predominantly *L. ferrooxidans*	40	1.10	3.77	0.0009
	40	1.30	3.83	0.0019
	40	1.50	4.23	0.0026
Leptospirillum-like (Van Scherpenzeel *et al.*, 1998)	30	1.5-1.6	1.7	0.0004*
L. ferrooxidans (Norris *et al.*, 1988)	32	1.7	1.2	0.400*
T. ferrooxidans (Boon, 1996)	30	1.8-1.9	2.2	0.05*
T. ferrooxidans (Norris *et al.*, 1988)	32	1.7	0.43	0.006*

From Table 4-7 it is apparent that the values of $q_{O_2}^{max}$ and K_{O_2} follow the same trends as $q_{Fe^{2+}}^{max}$ and $K_{Fe^{2+}}$ with respect to both temperature and pH. This was anticipated as the ferrous-iron and oxygen based parameters are

* Reported as K_s/K_i.

related via the degree of reduction balance, Equation 4-5. Furthermore, the degree of reduction balance results in the relationships between the oxygen-based parameters of the various species being similar to the ferrous-iron based relationships. It is suggested that the low value of the maximum bacterial specific oxygen utilisation rate reported for *L. ferrooxidans* (Norris *et al.*, 1988) may have been because of the conditions used. It is however interesting to note that in spite of the low value of $q_{O_2}^{max}$ reported for *L. ferrooxidans*, the value reported was still higher than the value reported for *T. ferrooxidans* (Norris *et al.*, 1988).

A comparison between the experimental results and the prediction of Equation 4-19, using the values of $q_{O_2}^{max}$ and K_{O_2} listed in Table 4-7 is shown in Figure 4.14. From Figure 4.14 it is apparent that, as in the case of the ferrous-iron based parameters, the agreement between the model and the experimental data is good.

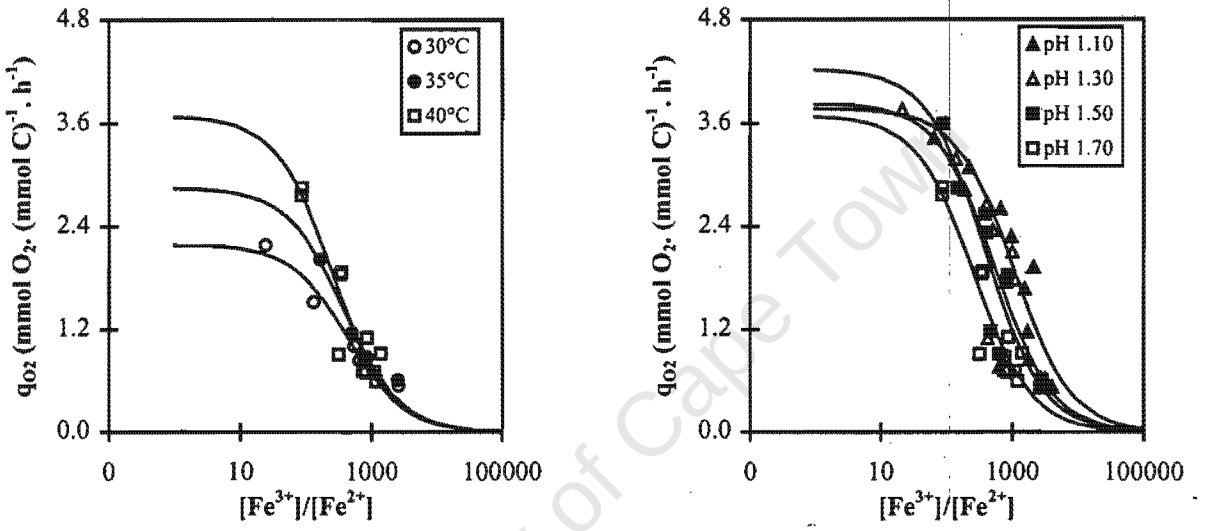

Figure 4.14: Comparison between the experimental and predicted variation in the bacterial specific oxygen utilisation rate with changing ferric/ferrous-iron ratio.

4.3.6 Maximum Specific Growth Rate

Values of the maximum specific growth rate, μ^{max}, at temperatures ranging from 30 to 40°C and pH values ranging from pH 1.10 to pH 1.70, were calculated using Equations 4-21 and 4-22. The values of the maximum yield on ferrous-iron and oxygen and their respective maintenance coefficients were obtained from Tables 4-2 and 4-3, whereas the values of the maximum bacterial specific utilisation rates were obtained from Tables 4-6 and 4-7, respectively.

The average values of μ^{max} calculated using the ferrous-iron and oxygen-based parameters, *i.e.* using Equations 4-21 and 4-22, respectively, and the dilution rate at which washout was observed to occur, D_w, are listed in Table 4-8. The values of μ^{max} reported previously for *T. ferrooxidans* (Boon, 1996) and a *Leptospirillum*-like bacterium (Van Scherpenzeel *et al.*, 1998) are also listed.

Although the bacterial culture maintained at 40°C and pH 1.30 "washed out" at the highest dilution rate, the highest calculated maximum specific growth rate, μ^{max} was obtained at 40°C and pH 1.50. In spite of this inconsistency in the results, it is apparent from Table 4-8 that the values of μ^{max} are in reasonable agreement with

the dilution rate at which washout was observed to occur. It is also apparent from the results listed in Table 4-8 that, at similar conditions of temperature and pH, the maximum specific growth rate of *T. ferrooxidans* is greater than that of the *Leptospirillum* species. Although this observation is consistent with previous results (Boon, 1996; Norris *et al.*, 1988), the difference in the maximum specific growth rates of the *Leptospirillum* species and *T. ferrooxidans* does not appear to be as great as previously reported. As stated previously, this may be a result of most work using *L. ferrooxidans* performed to date having been carried out at sub-optimal growth conditions.

Table 4-8: Values of the (calculated) average maximum specific growth rate and the dilution rate at which washout was observed to occur

Bacterial Culture	Temperature, °C	pH	μ^{max} (h^{-1})	D_w (h^{-1})
Predominantly *L. ferrooxidans*	30	1.70	0.0397	$0.059 < D_w < 0.040$
	35	1.70	0.0638	$0.059 < D_w < 0.040$
	40	1.70	0.0862	$D_w < 0.059$
Predominantly *L. ferrooxidans*	40	1.10	0.1027	$0.09 < D_w < 0.10$
	40	1.30	0.1077	$0.10 < D_w$
	40	1.50	0.1238	$0.09 < D_w < 0.10$
Leptospirillum-like (Van Scherpenzeel *et al.*, 1998)	30	1.5-1.6	0.069	0.077
T. ferrooxidans (Boon, 1996)*	30	1.8-1.9	0.14	0.096

The values of μ^{max} could also have been calculated by linear regression using Equation 4-23 and/or 4-24, or by minimising the sum of the squared errors between the experimentally determined values of μ, *i.e.* D, and the values predicted by Equation 4-25.

4.3.7 Kinetic Modelling

4.3.7.1 Effect of temperature

The variation in the maximum bacterial specific ferrous-iron and oxygen utilisation rates, $q^{max}_{Fe^{2+}}$ and $q^{max}_{O_2}$, with changes in temperature across the range from 30 to 40°C, is shown in Figure 4.15(a). The variation in the kinetic constants, $K_{Fe^{2+}}$ and K_{O_2}, with changes in temperature, across the range from 30 to 40°C, is shown in Figure 4.15(b). From Figure 4.15(a) it is apparent that the relationship between the maximum bacterial specific utilisation rates and temperature can be described using the Arrhenius equation, whereas the results shown in Figure 4.15(b) suggest that a linear relationship exists between the values of the kinetic constants and temperature.

* In addition to the values listed in Table 4-8, values of the maximum specific growth rate ranging from 0.089 to 0.143 h^{-1} and 0.07 to 1.78 h^{-1} have been reported for *T. ferrooxidans*, for growth in batch and continuous culture, respectively (Liu *et al.*, 1988; Braddock *et al.*, 1984; Jones and Kelly, 1983; Kelly and Jones, 1978; MacDonald and Clarke, 1970; Lacey and Lawson, 1970).

The values of the activation energy calculated using the maximum bacterial specific ferrous-iron and oxygen utilisation rate data shown in Figure 4.15(a) were 35.62 and 40.56 kJ.mol^{-1}, respectively. These values fall at the bottom of the range 33-96 kJ.mol^{-1} reported previously for bacterial ferrous-iron oxidation and are significantly lower than the value of 68.4 kJ.mol^{-1} reported for *T. ferrooxidans* (Nemati and Webb, 1997). The difference between the values determined during this investigation and the value reported by Nemati and Webb (1997) may be attributed to differences between the bacterial species, or to the fact that Nemati and Webb (1997) used initial rate data.

The ferrous-iron and oxygen-based values of the frequency factor, A and B, were calculated to be 1.326×10^{7} mmol Fe^{2+}.(mmol C)$^{-1}$.h^{-1} and 2.522×10^{7} mmol O_2.(mmol C)$^{-1}$.h^{-1}, respectively.

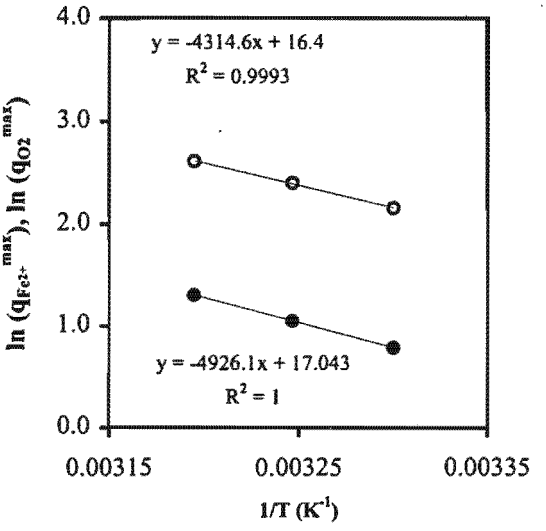

Figure 4.15(a): Effect of temperature on the maximum bacterial specific [o] ferrous-iron and [•] oxygen utilisation rates.

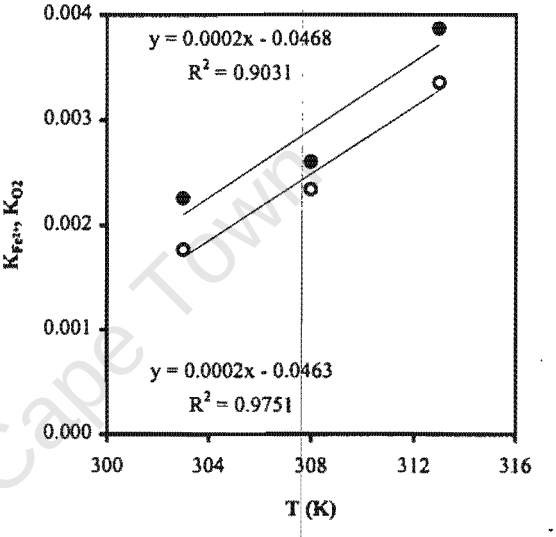

Figure 4.15(b): Effect of temperature on the [o] ferrous-iron and [•] oxygen based kinetic constants in bacterial ferrous-iron oxidation.

The relationships between the kinetic constants, $K_{Fe^{2+}}$ and K_{O_2}, and temperature determined from the data shown in Figure 4.15(b) were found to be:

$$K_{Fe^{2+}} = 1.585\times10^{-4}\,T - 0.0463 \qquad (4\text{-}32)$$

$$K_{O_2} = 1.613\times10^{-4}\,T - 0.0468 \qquad (4\text{-}33)$$

As stated previously, substituting the ferrous-iron based values of E_a, A, and the expression for $K_{Fe^{2+}}$, into Equation 4-29 should yield a model which predicts $q_{Fe^{2+}}$, at pH 1.70, across the range of temperatures from 30 to 40°C, as a function of the ferric/ferrous-iron ratio:

$$q_{Fe^{2+}} = \frac{1.326\times10^{7}\, e^{-\frac{35.87}{RT}}}{1+\left(1.585\times10^{-4}\,T-0.0463\right)\frac{[Fe^{3+}]}{[Fe^{2+}]}} \qquad (4\text{-}34)$$

Using Equation 4-34 resulted in the sum of the squared errors, Σe^2, being 1.30 % greater than if the values of $q_{Fe^{2+}}^{max}$ and $K_{Fe^{2+}}$ listed in Table 4-6 were used.

Similarly, substituting the oxygen based values of E_a, B, and the expression for K_{O_2} into Equation 4-30 should yield a model that predicts q_{O_2}, at pH 1.70, across the same temperature range:

$$q_{O_2} = \frac{2.522 \times 10^7 \, e^{-\frac{40.96}{RT}}}{1 + \left(1.613 \times 10^{-4} \, T - 0.0468\right)\frac{[Fe^{3+}]}{[Fe^{2+}]}} \qquad (4\text{-}35)$$

Using Equation 4-35 resulted in the sum of the squared errors, Σe^2, being 2.62 % greater than if the values of $q_{O_2}^{max}$ and K_{O_2} listed in Table 4-6 were used.

The above results therefore suggest that the effect of temperature on the maximum specific ferrous-iron and oxygen utilisation rates, $q_{Fe^{2+}}^{max}$ and $q_{O_2}^{max}$, can be described using the Arrhenius Equation, whereas the kinetic constants, $K_{Fe^{2+}}$ and K_{O_2}, increase linearly with increasing temperature.

4.3.7.2 Effect of pH

The relationship between the solution pH and the maximum bacterial specific ferrous-iron and oxygen utilisation rates, $q_{Fe^{2+}}^{max}$ and $q_{O_2}^{max}$, is shown in Figure 4.16(a). The relationship between the solution pH and the kinetic constants in bacterial ferrous-iron oxidation, $K_{Fe^{2+}}$ and K_{O_2}, is shown in Figure 4.16(b).

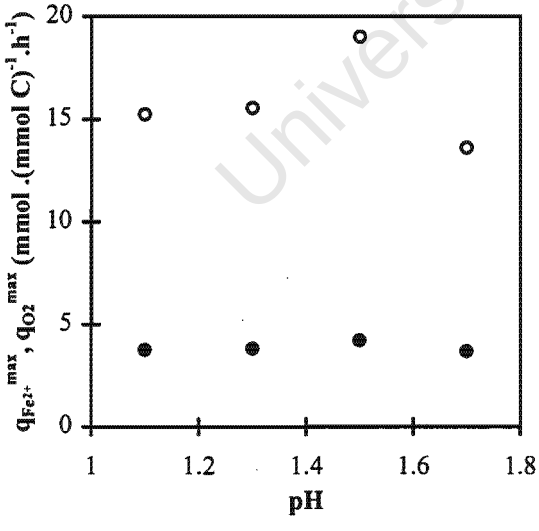

Figure 4.16(a): Effect of pH on the maximum bacterial specific [o] ferrous-iron and [•] oxygen utilisation rates.

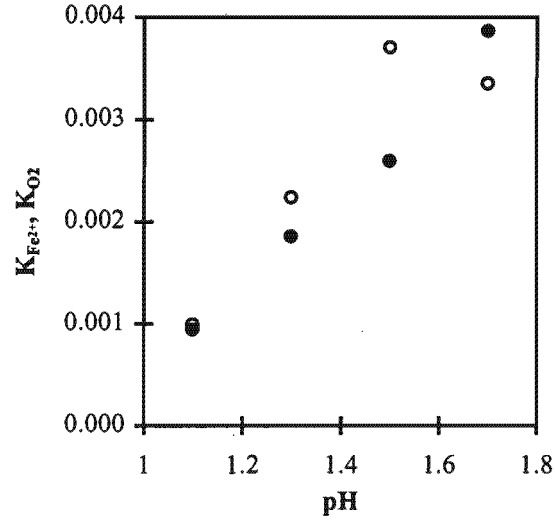

Figure 4.16(b): Effect of pH on the [o] ferrous-iron and [•] oxygen based kinetic constants in bacterial ferrous-iron oxidation.

Although the results shown in Figure 4.16(a) suggest that the maximum bacterial specific ferrous-iron utilisation rate achieved a maximum value at pH 1.50, no simple relationship between $q^{max}_{Fe^{2+}}$ and the solution pH is evident. The results also suggest that the maximum bacterial specific oxygen utilisation rate is not influenced by changes in the pH across the range from pH 1.10 to pH 1.70.

It is however apparent from the results shown in Figure 4.16(b) that an increase in the pH across the range from pH 1.10 to pH 1.70 resulted in a proportional increase in the kinetic constants, $K_{Fe^{2+}}$ and K_{O_2}.

For the reasons listed above, the variation in the ferrous-iron and oxygen utilisation rates with changing ferric/ferrous-iron ratio were modelled assuming that the kinetics constants, $K_{Fe^{2+}}$ and K_{O_2}, were directly proportional to the pH. The resulting functions were derived by minimising the sum of the squared errors, Σe^2, between the values of $q_{Fe^{2+}}$ and q_{O_2} determined experimentally, and the values predicted by the resulting models:

$$\sum e^2 = \sum_{pH=1.10}^{pH=1.70} \left(\frac{q^{max}_{Fe^{2+}}}{1 + (a\,pH + b)\dfrac{[Fe^{3+}]}{[Fe^{2+}]}} - q_{Fe^{2+},exp} \right)^2 \qquad (4\text{-}36)$$

$$\sum e^2 = \sum_{pH=1.10}^{pH=1.70} \left(\frac{q^{max}_{O_2}}{1 + (a\,pH + b)\dfrac{[Fe^{3+}]}{[Fe^{2+}]}} - q_{O_2,exp} \right)^2 \qquad (4\text{-}37)$$

Using a constant value of $q^{max}_{Fe^{2+}}$ for all pH values, *i.e.* assuming $q^{max}_{Fe^{2+}}$ to be independent of pH, and assuming a linear relationship between pH and $K_{Fe^{2+}}$ resulted in Σe^2 being 15.79 % greater than if the values of $q^{max}_{Fe^{2+}}$ and $K_{Fe^{2+}}$ listed in Table 4-6 were used. Assuming a linear relationship between pH and $K_{Fe^{2+}}$ and using the values of $q^{max}_{Fe^{2+}}$ listed in Table 4-6 resulted in Σe^2 being 15.60 % greater than if the values of $q^{max}_{Fe^{2+}}$ and $K_{Fe^{2+}}$ listed in Table 4-6 were used. These results therefore suggest that the errors introduced can be primarily attributed to the assumption of a linear relationship between pH and $K_{Fe^{2+}}$. Thus, the assumption that $q^{max}_{Fe^{2+}}$ is independent of pH appears to contribute to a simpler model, without resulting in a significant increase in the error.

The variation in $q_{Fe^{2+}}$, at 40°C, and pH values ranging from pH 1.10 to 1.70, with changes in $[Fe^{3+}]/[Fe^{2+}]$ can therefore be described using:

$$q_{Fe^{2+}} = \frac{15.53}{(0.0048\,pH - 0.0043)\dfrac{[Fe^{3+}]}{[Fe^{2+}]}} \qquad (4\text{-}38)$$

A similar procedure performed using a constant value of $q^{max}_{O_2}$ for all pH values and assuming a linear relationship between pH and $K_{Fe^{2+}}$, resulted in Σe^2 being 8.27 % greater than if the values of $q^{max}_{O_2}$ and K_{O_2} listed in Table 4-7 were used. Assuming a linear relationship between pH and K_{O_2} and using the values of $q^{max}_{O_2}$ listed in Table 4-7 resulted in Σe^2 being 0.46 % greater than if the values of $q^{max}_{Fe^{2+}}$ and $K_{Fe^{2+}}$ listed in Table 4-7 were

used. These results therefore suggest that the variation in the bacterial specific oxygen utilisation rate, at 40°C and pH values ranging from pH 1.10 to 1.70, with changes in the ferric/ferrous-iron ratio can be adequately described using:

$$q_{O_2} = \frac{3.85}{(0.0043\,pH - 0.0037)\frac{[Fe^{3+}]}{[Fe^{2+}]}} \qquad (4\text{-}39)$$

The above results therefore suggest that, at 40°C and pH values ranging from pH 1.10 to 1.70, $q_{Fe^{2+}}^{max}$ and $q_{O_2}^{max}$ can be considered to be independent of pH whereas $K_{Fe^{2+}}$ and K_{O_2} appear to increase linearly with increasing pH, across the same range of pH values.

4.3.7.3 Overall Kinetic Model

The apparent lack of interaction between the effect of temperature and pH on the ferrous-iron oxidation kinetics of the predominantly *L. ferrooxidans* species suggests that the effect of temperature and pH may be combined to produce a model which predicts the variation in $q_{Fe^{2+}}$ with changes in $[Fe^{3+}]/[Fe^{2+}]$, across the range of temperatures and pH values used in the investigation. However, inspection of Equations 4-34 and 4-35 and Equations 4-38 and 4-39 also indicates a few inconsistencies in the results presented thus far:

i) the values of the activation energy, E_a, should be the same,*
ii) the values of the frequency factors, A and B, should be related via the stoichiometry of the reaction, *viz.* Equation 4-6, and
iii) the kinetic constants, $K_{Fe^{2+}}$ and K_{O_2}, are related via the degree of reduction balance, Equation 4-5, hence they should exhibit the same dependence on both temperature and pH.†

In other words, it should be possible to describe the variation in the bacterial specific ferrous-iron and oxygen utilisation rates, $q_{Fe^{2+}}$, and q_{O_2}, at temperatures and pH values ranging from 30 to 40°C and pH 1.10 to pH 1.70, with changes in the ferric/ferrous-iron ration, $[Fe^{3+}]/[Fe^{2+}]$, using:

$$q_{Fe^{2+}} = \frac{Ae^{-\frac{E_a}{RT}}}{1 + (a\,pH + b + c\,T)\frac{[Fe^{3+}]}{[Fe^{2+}]}} \qquad (4\text{-}40)$$

$$q_{O_2} = \frac{A\left(\frac{1 - Y_{Fe^{2+}}^{max}}{4}\right)e^{-\frac{E_a}{RT}}}{1 + (a\,pH + b + c\,T)\frac{[Fe^{3+}]}{[Fe^{2+}]}} \qquad (4\text{-}41)$$

* As stated previously, although the stoichiometry of Equation 4-6 and the Y_{O_2X}:$Y_{Fe^{2+}X}$ ratio are not constant, the errors introduced by ignoring these changes are small relative to the other errors involved.

† The degree of reduction balance, written in terms of $q_{Fe^{2+}}^{max}$, $q_{O_2}^{max}$ and μ^{max}, can be used to show that $K_{Fe^{2+}} = K_{O_2} = K_\mu$.

The values of A, E_a, a, b and c, in Equations 4-40 and 4-41, were determined by simultaneously minimising the sum of the squared errors between the predicted and experimentally determined values of $q_{Fe^{2+}}$ and q_{O_2}. This yielded:

$$q_{Fe^{2+}} = \frac{1.204 \times 10^{7}\, e^{-\frac{35.33}{RT}}}{1 + \left(7.530 \times 10^{-7}\, T + 0.0043\, pH - 0.0040\right)\frac{[Fe^{3+}]}{[Fe^{2+}]}} \quad (4\text{-}42)$$

$$q_{O_2} = \frac{2.915 \times 10^{6}\, e^{-\frac{35.33}{RT}}}{1 + \left(7.530 \times 10^{-7}\, T + 0.0043\, pH - 0.0040\right)\frac{[Fe^{3+}]}{[Fe^{2+}]}} \quad (4\text{-}43)$$

A comparison between the variation in the specific ferrous-iron utilisation rate with changes in the ferric/ferrous-iron ratio predicted using Equation 4-42, and the experimentally determined values is shown in Figure 4.17(a). A comparison between the variation in the specific oxygen utilisation rate with changes in the ferric/ferrous-iron ratio predicted using Equation 4-43, and the experimentally determined values is shown in Figure 4.17(b). From Figures 4.17(a) and (b) it is apparent that the agreement between the experimental data and the predicted values is adequate.

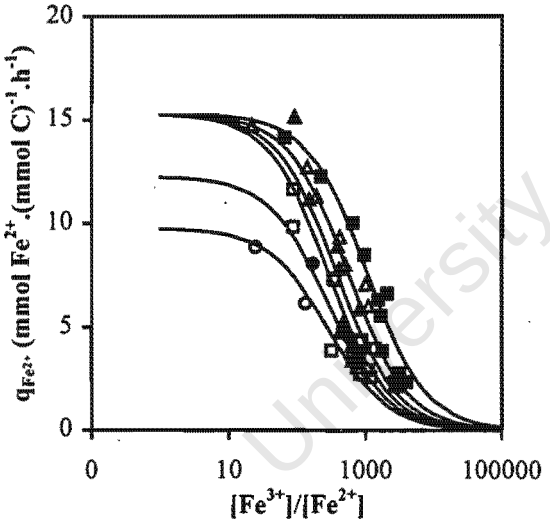

Figure 4.17(a): Comparison between the variation in the specific ferrous-iron utilisation rate with changes in the ferric/ferrous-iron ratio predicted using Equation 4-42, and the experimentally determined values.

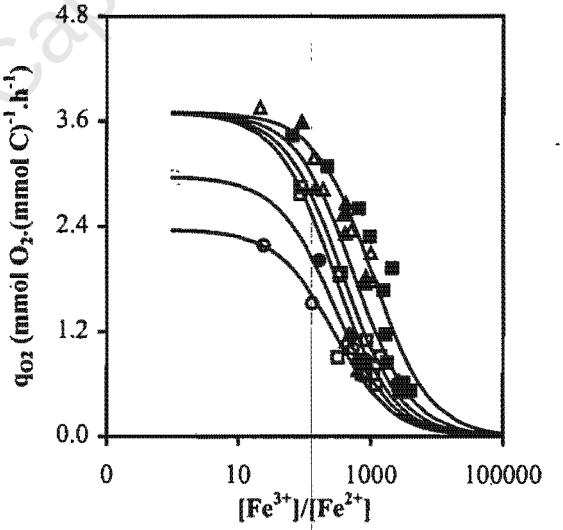

Figure 4.17(b): Comparison between the variation in the specific oxygen utilisation rate with changes in the ferric/ferrous-iron ratio predicted using Equation 4-43, and the experimentally determined values.

[○] 30°C, pH 1.70; [●] 35°C, pH 1.70; [□] 40°C, pH 1.70; [▲] 40°C, pH 1.10; [Δ] 40°C, pH 1.30; [■] 40°C, pH 1.50.

The values of the maximum specific ferrous-iron and oxygen utilisation rates and their respective kinetic constants predicted by Equations 4-42 and 4-43 are shown in Table 4-9.

Table 4-9: Values of the maximum specific ferrous-iron and oxygen utilisation rates and their respective kinetic constants predicted by Equations 4-42 and 4-43

Temperature, °C	pH	$q_{Fe^{2+}}^{max}$	$q_{O_2}^{max}$	K
30	1.70	9.77	2.37	0.0035
35	1.70	12.27	2.97	0.0035
40	1.70	15.29	3.70	0.0035
40	1.10	15.29	3.70	0.0010
40	1.30	15.29	3.70	0.0018
40	1.50	15.29	3.70	0.0027

From the results shown in Figures 4.17(a0 and (b), and the results tabulated in Table 4-9 it is apparent that, across the ranges used in this investigation, the effect of temperature and pH on the ferrous-iron oxidation kinetics of the predominantly *L. ferrooxidans* culture can be summarised as follows:

i) an increase in temperature results in an increase in the maximum specific ferrous-iron and oxygen utilisation rates, $q_{Fe^{2+}}^{max}$ and $q_{O_2}^{max}$, respectively, and

ii) an increase in the pH results in an increase in the kinetic constant, K.

4.4 Chapter Summary

The ferrous-iron oxidation kinetics of a predominantly *L. ferrooxidans* culture were studied in continuous-flow bioreactors at dilution rates ranging from 0.01 to 0.10 h^{-1}, temperatures ranging from 30 to 40°C and pH values ranging from pH 1.10 to pH 1.70. The growth and oxygen and ferrous-iron utilisation rates of the bacteria were monitored by means of off-gas analysis and redox potential measurement. Analysis of the rates of ferrous-iron, oxygen and carbon dioxide utilisation showed that they could be accurately related via a degree of reduction balance.

The biomass concentration in the bioreactors increased with increasing temperature; the greatest biomass concentrations were achieved at intermediate residence times irrespective of the temperature and/or pH in the bioreactor. Although the biomass concentration in the bioreactors appeared to be independent of the pH, the bacterial culture maintained at 40°C and pH 1.30 "washed out" at the highest dilution rate. However, the highest calculated maximum specific growth rate, $\mu^{max} = 0.1238\ h^{-1}$, was calculated from the data obtained at 40°C and pH 1.50.

Statistical analysis suggested that the values of the maximum bacterial yields on ferrous-iron and oxygen and their respective maintenance coefficients are functions of both temperature and pH. However, because the statistical techniques employed did not take into account the poor correlation coefficients obtained during the regression analysis, average values of the yield and maintenance parameters were also determined assuming that neither temperature, nor pH, has an effect. The values of $Y_{Fe^{2+}X}^{max}$, $Y_{O_2X}^{max}$, $m_{Fe^{2+}}$ and m_{O_2}, calculated in this manner were similar to those reported previously for both *L. ferrooxidans* and *T. ferrooxidans*.

The maximum bacterial specific ferrous-iron and oxygen utilisation rates and their respective kinetic constants increased with increasing temperature. The temperature dependence of the maximum bacterial specific ferrous-iron and oxygen utilisation rates could be described using the Arrhenius Equation whereas the relationship between temperature and the kinetic constants appeared to be linear. The kinetic constants also increased linearly with increasing pH. Although both the maximum bacterial specific ferrous-iron and oxygen utilisation rates appeared to achieve maximum values at pH 1.50, no simple relationship between these parameters and pH was evident. Therefore, in an attempt to simplify the modelling, it was assumed that pH had no effect on the either $q_{Fe^{2+}}^{max}$ or $q_{O_2}^{max}$.

The above trends and assumptions were incorporated into the Michaelis-Menten based model proposed by Boon (1996). This resulted in models capable of predicting the bacterial specific ferrous-iron and oxygen utilisation rates as a function of the ferric/ferrous-iron ratio, for temperatures ranging from 30 to 40°C and pH values ranging from pH 1.10 to pH 1.70. Comparison of the variation in the specific ferrous-iron and oxygen utilisation rates with changes in the ferric/ferrous-iron ratio predicted by the resulting model with the experimentally obtained data showed good agreement. It is therefore possible to depict the primary differences in the effect of temperature and pH on the ferrous-iron oxidation kinetics of the predominantly *L. ferrooxidans* culture as indicated in Figure 4.18.

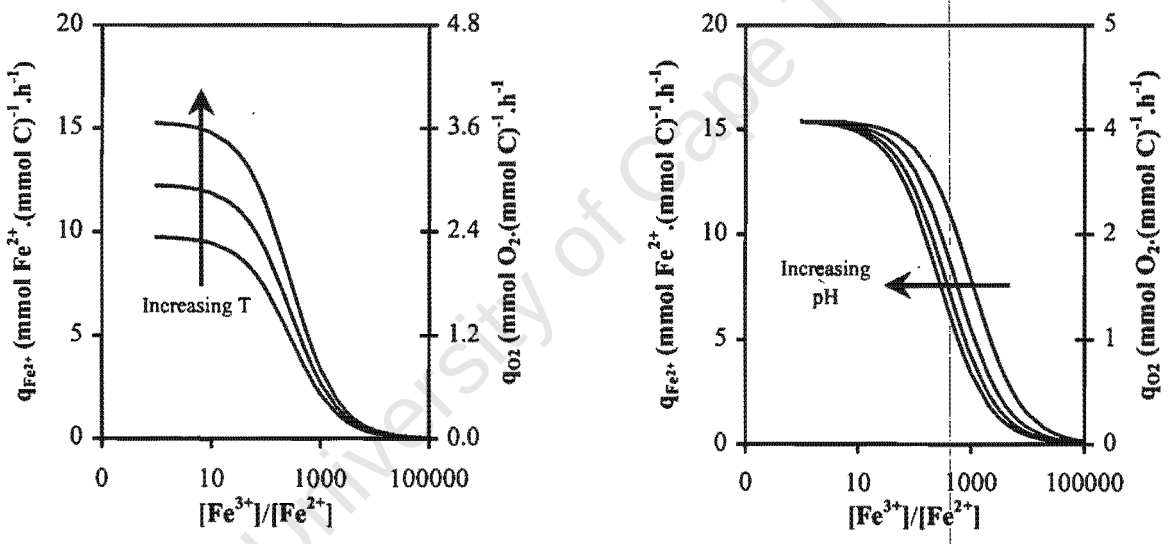

Figure 4.18: Effect of temperature and pH on the bacterial specific ferrous-iron and oxygen utilisation rates.

4.5 Nomenclature

a	constant	(pH units)$^{-1}$
A	ferrous-iron based frequency factor in bacterial ferrous-iron oxidation	mmol Fe^{2+}.(mmol C)$^{-1}$.h^{-1}
b	constant	dimensionless
B	oxygen based frequency factor in bacterial ferrous-iron oxidation	mmol O_2.(mmol C)$^{-1}$.h^{-1}
c	constant	K^{-1}
c_x	concentration of bacteria	mmolC.ℓ^{-1}

d	diameter	mm
D	dilution rate	h^{-1}
D_w	dilution rate at which washout occurs	h^{-1}
e	error	varies
E	redox potential of the solution (Pt-Ag/AgCl)	mV
E_a	activation energy	$kJ.mol^{-1}$
$[Fe^{2+}]$	concentration of ferrous-iron	mmol $Fe^{2+}.\ell^{-1}$
$[Fe^{3+}]$	concentration of ferric-iron	mmol $Fe^{3+}.\ell^{-1}$
h	height	mm
K	kinetic constant in bacterial ferrous-iron oxidation	dimensionless
$K_{Fe^{2+}}$	ferrous-iron based kinetic constant in bacterial ferrous-iron oxidation	dimensionless
K_i	Michaelis-Menten product (ferric-iron) inhibition constant	mmol $Fe^{3+}.\ell^{-1}$
K_{O_2}	oxygen based kinetic constant in bacterial ferrous-iron oxidation	dimensionless
K_s	Monod equation substrate (ferrous-iron) saturation constant	mmol $Fe^{2+}.\ell^{-1}$
K_μ	growth based kinetic constant in bacterial ferrous-iron oxidation	dimensionless
$m_{Fe^{2+}}$	maintenance coefficient on ferrous-iron	mmol Fe^{2+}.(mmol C)$^{-1}$.h^{-1}
m_{O_2}	maintenance coefficient on oxygen	mmol O_2.(mmol C)$^{-1}$.h^{-1}
$q_{Fe^{2+}}$	bacterial specific ferrous-iron utilisation rate	mmol Fe^{2+}.(mmol C)$^{-1}$.h^{-1}
$q_{Fe^{2+},\,exp}$	measured bacterial specific ferrous-iron utilisation rate	mmol Fe^{2+}.(mmol C)$^{-1}$.h^{-1}
q_{O_2}	bacterial specific oxygen utilisation rate	mmol O_2.(mmol C)$^{-1}$.h^{-1}
$q_{O_2,\,exp}$	measured bacterial specific oxygen utilisation rate	mmol O_2.(mmol C)$^{-1}$.h^{-1}
$q_{Fe^{2+}}^{max}$	maximum bacterial specific ferrous-iron utilisation rate	mmol Fe^{2+}.(mmol C)$^{-1}$.h^{-1}
$q_{O_2}^{max}$	maximum bacterial specific oxygen utilisation rate	mmol O_2.(mmol C)$^{-1}$.h^{-1}
$r_{Fe^{2+}}$	ferrous-iron production rate	mmol $Fe^{2+}.\ell^{-1}.h^{-1}$
r_{CO_2}	carbon dioxide production rate	mmol $CO_2.\ell^{-1}.h^{-1}$
r_{O_2}	oxygen production rate	mmol $O_2.\ell^{-1}.h^{-1}$
r_X	biomass production rate	mmol $C.\ell^{-1}.h^{-1}$
R	Universal gas constant	$kJ.K^{-1}.mol^{-1}$
R^2	correlation coefficient	dimensionless
R^2_{avrg}	average value of the correlation coefficient	dimensionless
T	absolute temperature	K
$\bar{x}_{pH}$	mean value of the parameter at a particular pH	varies
$\bar{x}_{pH\,1.70}$	mean value of the parameter at a pH 1.70	varies
$\bar{x}_T$	mean value of the parameter at a particular temperature	varies
$\bar{x}_{T\,=\,40°C}$	mean value of the parameter at a temperature of 40°C	varies
$Y_{Fe^{2+}X}$	bacterial yield on ferrous-iron	mmol C.(mmol Fe^{2+})$^{-1}$
$Y_{Fe^{2+}X}^{max}$	maximum bacterial yield on ferrous-iron	mmol C.(mmol Fe^{2+})$^{-1}$
Y_{O_2X}	bacterial yield on oxygen	mmol O_2.(mmol C)$^{-1}$
$Y_{O_2X}^{max}$	maximum bacterial yield on oxygen	mmol O_2.(mmol C)$^{-1}$

Σe^2	sum of the squared errors	varies
α^{max}	maximum significance level at which the null hypothesis is accepted	dimensionless
μ	bacterial specific growth rate	h^{-1}
μ^{max}	maximum bacterial specific growth rate	h^{-1}

References

Barrett, J., Hughes, M.N., Karavaiko, G.I. and Spencer, P.A. 1993. Metal extraction by bacterial oxidation of minerals. Ellis Horwood, New York.

Boon, M. 1996. Theoretical and experimental methods in the modelling of bio-oxidation kinetics of sulfide minerals. Ph.D. Thesis. Delft University of Technology, Delft.

Braddock, J.F., Luong, H.V. and Brown, E.J. 1984. Growth kinetics of *Thiobacillus ferrooxidans* isolated from arsenic mine drainage. Applied and Environmental Microbiology **48**(1): 48-55.

Dew, D.W., Lawson, E.N. and Broadhurst, J.L. 1997. The BIOX® process for biooxidation of gold-bearing ores or concentrates, pp. 45-80. In: D.E. Rawlings (ed.), Biomining: theory, microbes and industrial processes. Springer-Verlag and Landes Bioscience, Berlin.

Hallmann, R., Friedrich, A., Koops, H.P., Pommering-Röser, A., Zenneck, C. and Sand, W. 1993. Physicological characteristics of *Thiobacillus ferrooxidans* and *Leptospirillum ferrooxidans* and physicochemical factors influence microbial metal leaching. Geomicrobiology Journal **10**: 193-205.

Helle, U. and Onken, U. 1988. Continuous bacterial leaching of pyritic flotation concentrate by mixed cultures, pp. 61-75. In: P.R. Norris and D.P. Kelly (eds.), Biohydrometallurgy. Science and Technology Letters, Kew, Surrey.

Ingledew, W.J. 1986. Ferrous iron oxidation by *Thiobacillus ferrooxidans*. Biotechnology and Bioengineering Symposium Series **16**: 23-33.

Jeffrey, G.H., Bassett, J., Mendham, J. and Denney, R.C. 1989. Vogel's Textbook of quantitative chemical analysis. 5th edition, Longman Scientific & Technical, New York.

Jones, C.A. and Kelly, D.P. 1983. Growth of *Thiobacillus ferrooxidans* on ferrous iron in chemostat culture: influence of product and substrate inhibition. Journal of Chemical Technology and Biotechnology **33B**(4): 241-261.

Kelly, D.P. and Jones, C.A. 1978. Factors affecting metabolism and ferrous iron oxidation in suspensions and batch cultures of *Thiobacillus ferrooxidans*: relevance to ferric iron leach solution generation, pp. 19-44. In: L.E. Murr, A.E. Torma and J.A. Brierley (eds.), Metallurgical Applications of Bacterial Leaching and Related Microbiological Phenomena. Academic Press, New York.

Lacey, D.T. and Lawson, F. 1970. Kinetics of the liquid-phase oxidation of acid ferrous sulphate by the bacterium *Thiobacillus ferrooxidans*. Biotechnology and Bioengineering **12**: 29-50.

Liu, M.S., Branion, R.M.R. and Duncan, D.W. 1988. The effects of ferrous iron, dissolved oxygen, and inert solids concentration on the growth of *Thiobacillus ferrooxidans*. The Canadian Journal of Chemical Engineering **66**(June): 445-451.

MacDonald, D.G. and Clarke, R.H. 1970. The oxidation of aqueous ferrous sulphate by *Thiobacillus ferrooxidans*. The Canadian Journal of Chemical Engineering **48**(December): 669-676.

Nemati, M. and Webb, C. 1997. A kinetic model for biological oxidation of ferrous iron by *Thiobacillus ferrooxidans*. Biotechnology and Bioengineering **53**(5): 478-486.

Norris, P.R., Barr, D.W. and Hinson, D. 1988. Iron and mineral oxidation by acidophilic bacteria: affinities for iron and attachment to pyrite, pp. 43-59. In: P.R. Norris and D.P. Kelly (eds.), Biohydrometallurgy. Science and Technology Letters, Kew, Surrey.

Pirt, S.J. 1982. Maintenance energy: a general model for energy limited and energy sufficient growth. Arch. Microbiol. **133**: 300-302.

Rawlings, D.E. 1995. Restriction enzyme analysis of 16S rDNA genes for the rapid identification of *Thiobacillus ferrooxidans*, *Thiobacillus thiooxidans* and *Leptospirillum ferrooxidans* strains in leaching environments, pp. 9-17. In: T. Vargas, C.A. Jerez., J.V. Wiertz and H. Toledo (eds.), Biohydrometallurgical Processing **1**. University of Chile, Santiago.

Rawlings, D.E., Coram, N.J., Gardner, M.N. and Deane, M.N. 1999(a). *Thiobacillus caldus* and *Leptospirillum ferrooxidans* are widely distributed in continuous flow biooxidation tanks used to treat a variety of metal containing ores and concentrates, pp. 777-786. In: R. Amils, A. Ballester (eds.), Biohydrometallurgy and the environment toward the mining of the 21st century **A**. Elsevier, Amsterdam.

Rawlings, D.E., Tributsch, H. and Hansford, G.S. 1999(b). Reasons why *Thiobacillus ferrooxidans* is not the dominant iron-oxidising bacterium in many commercial processes for the biooxidation of pyrite and related ores. Microbiology **145**(1): 5-13.

Roels, J.A. 1983. Energetics and Kinetics in Biotechnology. Elsevier Biomedical Press, Amsterdam.

Sand, W., Rohde, K., Sobotke, B. and Zenneck, C. 1992. Evaluation of *Leptospirillum ferrooxidans* for leaching. Applied and Environmental Microbiology **58**(1): 85-92.

Schlegel, H.G. 1986. General Microbiology. 6th edition, Cambridge University Press.

Van Scherpenzeel, D.A., Boon, M., Hansford, G.S. and Heijnen, J.J. 1998. Kinetics of ferrous iron oxidation by *Leptospirillum* bacteria in continuous cultures. Biotechnology Progress **14**: 425-433.

Van Scherpenzeel, D.A. 1996. The kinetics of ferrous-iron oxidation by *Leptospirillum*-like bacteria in absence and in presence of pyrite and pyrite/arsenopyrite mixtures in continuous and batch cultures. M.Sc. Dissertation, University of Cape Town, Cape Town.

Vishniac, W. and Santer, M. 1957. The thiobacilli. Bacterial Revs. **21**: 195-213.

For Kevin

You are
never given a wish
without also being given the
power to make it true.
You may
have to work for it,
however.

ILLUSIONS – Richard Bach

Chapter Five

The Effect of As(III) and As(V) on the Batch Bioleaching of an Arsenopyrite/pyrite Concentrate*

The bioleaching of arsenopyrite solubilises the arsenic in the mineral as arsenite, As(III). Depending on the conditions employed, its dissolution may be followed by the oxidation of arsenite to arsenate, As(V), followed by the precipitation of ferric arsenate (Dew *et al.*, 1997). Arsenite is alleged to be more toxic than arsenate, hence the conditions affecting its oxidation will also affect the overall process. Although there is currently a lack of consensus in the literature with regard to the mechanism whereby this occurs, the results of previous research suggest that ferric-iron is the oxidising agent and that the reaction requires both a high redox potential and a mineral capable of acting as a conduit of charge.

The micro-organisms used in bioleaching are characterised by their resistance to metal ions. In spite of this inherent resistance however, the toxicity of arsenic to life, and the fact that arsenopyrite is often associated with sulfide minerals containing valuable metals, means that the toxic nature of-, and mechanisms of resistance to-, arsenic, are of considerable importance.

Arsenite is alleged to be the most toxic form of arsenic. It inactivates enzymes with thiol (HS) groups at their active centre by binding to two different groups on the enzyme (Coddington, 1986). In contrast to arsenite, arsenate is the least toxic form of inorganic arsenic. The toxicity of arsenate is related to its similarity to phosphate (phosphate and arsenate are analogs); arsenate replaces the phosphate in ATP to form an unstable ADP-arsenate complex (Coddington, 1986).

There are two main forms of arsenic resistance in bacteria; plasmid determined arsenic resistance and chromosomal arsenate resistance (Cullen and Reimer, 1989; Coddington, 1986; Silver and Nakahara, 1983; Novick and Roth, 1968). Chromosomal arsenate resistance reduces the amount of arsenate entering the cell via the phosphate transport system (Cullen and Reimer, 1989; Coddington, 1986; Silver and Nakahara, 1983; Silver, 1978) whereas plasmid-encoded resistance protects the micro-organism by pumping arsenic from the cells via an energy dependent membrane pump (Huysmans and Frankenberger, 1992; Cullen and Reimer, 1989; Coddington, 1986; Silver and Nakahara, 1983; Mobley and Rosen, 1982; Silver and Keach, 1982). Other proposed mechanisms of arsenic resistance include the oxidation of arsenite to arsenate (Lindström and Sehlin, 1989; Cullen and Reimer, 1989; Williams and Silver, 1984; Silver and Nakahara, 1983; Abdrashitova *et al.*, 1982) and the reduction of arsenate to arsenite followed by excretion of the arsenite ion (Sehlin and Lindström, 1992; Cullen and Reimer, 1989; Wakao *et al.*, 1988).

Resistance to arsenite, antimony and arsenate may be induced by growing *Thiobacillus caldus* in the presence of non lethal concentrations of any one of these ions (Hallberg, 1995). This resistance is conferred, *i.e.* it is not a result of natural selection, but is a result of reduced cellular accumulation of these ions, coupled to an energy dependent efflux of the species taken up (Hallberg, 1995). However, although it has been claimed that arsenic resistance in *Thiobacillus ferrooxidans* is plasmid borne (Nicolau and Raimond, 1993), the mechanism of arsenic resistance in acidophilic chemoautotrophs other than *T. caldus* has not been determined. However, the fact that arsenite is more toxic to the micro-organisms used in bioleaching than arsenate suggests that arsenate resistance may be attributed to chromosomal mutations, *i.e.* natural selection (Lawson, 1993).

As stated earlier, the initial objective of the work presented in this thesis was to determine the relationship between perturbations in the aeration and agitation of bioleaching reactors and arsenic toxicity. Although the emphasis of the thesis was changed, because of the high concentrations of arsenic encountered during the bioleaching of arsenopyrite, some work on the effect of arsenic was deemed necessary. The work presented in this chapter was therefore aimed at establishing the relative effect of arsenite and arsenate on the activity of a mixed culture from a continuous bioleaching mini-plant, in batch culture.

5.1 Materials and Methods

5.1.1 Experimental Equipment

The experiments were carried out in baffled, agitated, aerated bioreactors. The bioreactors were 25 cm high, 18.5 cm in diameter and had a working volume of 5.6 ℓ. The baffles were 2 cm wide and extended from 2 cm above the bioreactor base to 2 cm above the slurry surface. The slurry was agitated by 6-bladed, pitched blade impellers rotating at 610 rev.min^{-1}. The impellers were 9.5 cm in diameter and located 2 cm from the base of the bioreactor.

Compressed air, at a pressure of 200 kPa, was used to aerate the slurry. The sparger outlet was located below the impeller. This aided the dispersion of the gaseous phase.

* Breed, A.W., Glatz, A., Hansford, G.S. and Harrison, S.T.L. 1996. The effect of As(III) and As(V) on the batch bioleaching of a pyrite-arsenopyrite concentrate. Minerals Engineering 9(12): 1235-1252.

The temperature in the bioreactors was maintained at 40°C by placing the bioreactors in a water bath.

5.1.2 Bacterial Culture

The bacterial culture was obtained from the two-stage continuous bioleaching mini-plant described in detail in Chapter Six. As stated previously it has been reported to consist primarily of *T. caldus* and *Leptospirillum ferrooxidans* (Rawlings *et al.*, 1999).

5.1.3 Mineral Used

The flotation concentrate used was the same as the flotation concentrate used in the bioleaching mini-plant and the initial ferric leaching work (see Section 3.1). It originated from the Fairview Gold Mine in Barberton, South Africa. The size, elemental and mineral analysis of the flotation concentrate are listed in Tables 3-1, 3-2 and 3-3, respectively.

5.1.4 Nutrient Medium

The nutrient solution used was similar in composition to the nutrient solution used during the investigation into the effect of temperature and pH on the ferrous-iron oxidation kinetics of the predominantly *L. ferrooxidans* culture. However, as the substrate used in the work was flotation concentrate, the ferrous-iron source, *viz.* $FeSO_4.7H_2O$, and the trace element solution were not added to the nutrient medium. The composition of the inorganic nutrient solution is listed in Table 5-1.

Table 5-1: Inorganic nutrient medium composition

Compound	Concentration
$(NH_4)_2SO_4$	1.83 $g.\ell^{-1}$
$(NH_4)_2HPO_4$	1.11 $g.\ell^{-1}$
K_2SO_4	0.53 $g.\ell^{-1}$

5.1.5 Experimental Procedure

The experiments were begun by dissolving the required quantity of either arsenite or arsenate in the nutrient solution. The arsenite and arsenate were added as arsenic trioxide (As_2O_3) and sodium arsenate ($Na_2HAsO_4.7H_2O$), respectively. Once the arsenic had been dissolved, the concentrate was added to the

solution, the pH adjusted and the slurry left overnight to attain thermal equilibrium. The pH was adjusted before the addition of the inoculii; the inoculii were obtained from the continuous bioleaching mini-plant and resulted in an initial cell concentration of about 10^8 cells.ℓ^{-1} in each of the bioreactors.

The pH was adjusted daily; it was maintained at between pH 1.6 and pH 1.8 by addition of either 98 % H_2SO_4 or 10 mol NaOH.ℓ^{-1}.

Water was added before sampling to account for losses due to evaporation.

The arsenite and arsenate concentrations used in this investigation are listed in Tables 5-2 and 5-3, respectively. The concentrations chosen were based on:

i) the arsenite and arsenate concentrations used during previous research,
ii) the solubility of arsenic trioxide (As_2O_3) and sodium arsenate ($Na_2HAsO_4.7H_2O$) in water, and
iii) the steady-state arsenite concentrations measured in the continuous bioleaching mini-plant from which the culture was obtained.

Table 5-2: Initial arsenite concentration in the batch bioreactors

Reactor	$[As(III)]_{initial}$ g.ℓ^{-1}	$[As(III)]_{initial}$ mmol As(III). ℓ^{-1}
Control 1	0.0	0
Control 2	0.0	0
Low As(III)	1.5	20
High As(III)	3.0	40

Table 5-3: Initial arsenate concentration in the batch bioreactors

Reactor	$[As(V)]_{initial}$ g.ℓ^{-1}	$[As(V)]_{initial}$ mmol As(V). ℓ^{-1}
Control 1	0.0	0
Control 2	0.0	0
Low As(V)	8.0	107
High As(V)	16.5	220

5.1.6 Analyses

The total iron and arsenic concentrations were determined by Flame Atomic Absorption Spectroscopy (FAAS). The ferrous-iron and arsenite concentrations in solution were determined by titration with $Ce(SO_4)_2$.* This allowed the ferric-iron and arsenate concentrations to be determined by difference.

* This method was developed at Gencor Process Research in Johannesburg, South Africa. It is described in detail in the Appendix to this Chapter.

The oxygen utilisation rate, $-r_{O_2}$, was determined by monitoring the rate at which oxygen was consumed by the bacteria in an air-saturated bioleaching slurry. A Yellow Springs Instrument Model 5739 Oxygen Temperature Probe and a Hitech Micro Systems Dissolved Oxygen/Utilisation Rate Meter were used.

The redox potential was obtained by direct millivolt measurement using an ASI OR101431 Pt-Ag/AgCl ORP electrode and a Hitech Micro Systems UCT Redox Controller.

5.2 Results and Discussion

During the investigations into the effect of arsenite and arsenate on the bacterial culture from the continuous bioleaching mini-plant, the values of the measured parameters in the bioreactors to which no arsenic was added were similar. For this reason, only the average values of the respective parameters are shown in the figures.

5.2.1 The Effect of Arsenite, As(III)

Figure 5.1 indicates the variation in the oxygen utilisation rate, $-r_{O_2}$, of the bacterial cultures during the course of the arsenite tolerance investigation. The low oxygen utilisation rates apparent during the first 6 days of the experiment suggest that no significant bacterial activity occurred in any of the bioreactors during this time.

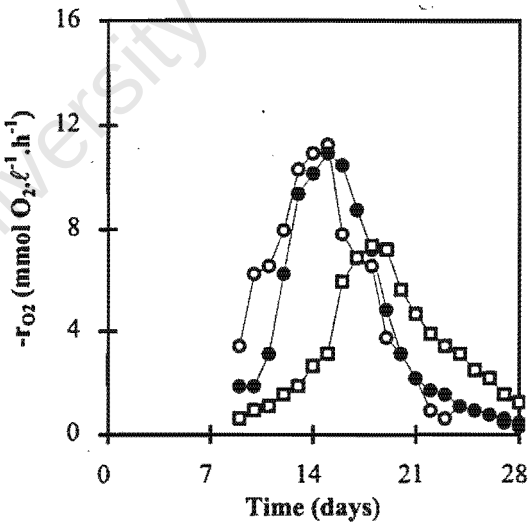

Figure 5.1: Variation in the oxygen utilisation rate of the bacterial cultures at different initial arsenite concentrations with time. [○] 0 mmol As(III).ℓ$^{-1}$; [●] 20 mmol As(III).ℓ$^{-1}$; [□] 40 mmol As(III).ℓ$^{-1}$.

In the case of the bacterial cultures to which 0 and 20 mmol As(III).ℓ$^{-1}$ was added, the initial lag phase was followed by a sharp increase in the oxygen utilisation rate. These cultures both achieved a maximum oxygen utilisation rate, $-r_{O_2}^{max}$, of about 11.3 mmol O_2.ℓ$^{-1}$.h^{-1}. However, although the bacterial culture to which

20 mmol As(III).ℓ^{-1} was added appeared to follow normal exponential growth, the oxygen utilisation rate of this culture appeared to "lag" that of the of the culture to which no arsenite was added by about 2 days.

In contrast to the above, the oxygen utilisation rate of the culture exposed to an initial concentration of 40 mmol As(III).ℓ^{-1} did not increase as rapidly as the oxygen utilisation rates of the cultures in the other bioreactors. In addition, the oxygen utilisation rate of the culture in this bioreactor only achieved a maximum oxygen utilisation rate of about 7.4 mmol $O_2.\ell^{-1}.h^{-1}$, *i.e.* about 62% of the maximum oxygen utilisation rate achieved by the bacterial cultures to which 0 and 20 mmol As(III).ℓ^{-1} was added.

The cumulative amount of oxygen consumed by the bacteria during the experiment, η_{O_2}, expressed as a percentage of the total amount of oxygen consumed by the bacteria grown in the absence of arsenite is shown in Figure 5.2. It was calculated using:

$$\eta_{O_2,i} = \frac{\int_0^t r_{O_2,i}\,dt}{\int_0^T r_{O_2,control}\,dt} 100 \qquad (5\text{-}1)$$

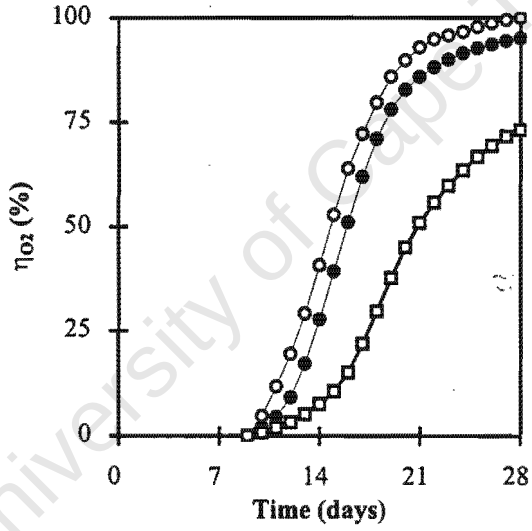

Figure 5.2: Variation in the amount of oxygen consumed by the bacterial cultures relative to the total amount consumed by the culture to which no arsenic was added, with time. [o] 0 mmol As(III).ℓ^{-1}; [•] 20 mmol As(III).ℓ^{-1}; [□] 40 mmol As(III).ℓ^{-1}.

The results shown in Figure 5.2 confirm that the activity of the culture exposed to an initial concentration of 20 mmol As(III).ℓ^{-1} lagged that of the culture to which no arsenite was added by about 2 days. In addition, the overall oxygen consumption of the culture exposed to an initial concentration of 20 mmol As(III).ℓ^{-1} was in the region of 95 % of that of the culture to which no arsenite was added.

Figure 5.2 also shows that the overall oxygen consumption of the culture exposed to an initial concentration of 40 mmol As(III).ℓ^{-1} was only about 72 % of that of the culture to which no arsenite was added.

The rate at which oxygen is utilised by the bacteria is a function of both their concentration and activity:

$$-r_{O_2} = q_{O_2} c_x \tag{5-2}$$

As demonstrated in Chapter Four, the bacterial specific oxygen utilisation rate, q_{O_2}, can be described using an equation of the form:

$$q_{O_2} = \frac{q_{O_2}^{max}}{1 + K\dfrac{[Fe^{3+}]}{[Fe^{2+}]}} \tag{5-3}$$

It was therefore not possible to ascertain whether the elevated arsenite concentration inhibits bacterial oxidation (*i.e.* it affects bacterial activity via $q_{O_2}^{max}$) or whether it is toxic to the bacteria (*i.e.* it restricts growth and therefore affects c_X).

The variation in the ferrous-iron concentration, $[Fe^{2+}]$, in each of the bioreactors during the course of the experiments is shown in Figure 5.3. From Figure 5.3 it is apparent that the ferrous-iron concentration of the slurry in all the bioreactors followed the same trend; it increased during the lag phase, decreased once aerobic activity commenced, and then remained low for the remainder of the experiment.

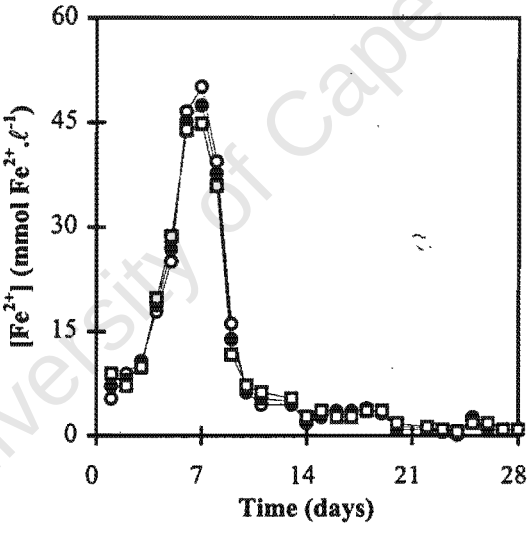

Figure 5.3: Variation in the ferrous-iron concentration of the slurry in the bioreactors during the course of the arsenite tolerance investigation. [o] 0 mmol As(III).ℓ^{-1}; [•] 20 mmol As(III).ℓ^{-1}; [□] 40 mmol As(III).ℓ^{-1}.

The initial increase in the ferrous-iron concentration during the period prior to the commencement of aerobic activity can be attributed to one or more of the following phenomena:

i) the dissolution of surface ferrous-iron species as a result of the low pH, *i.e.* as a result of acid leaching of the mineral,
ii) the (anaerobic) reduction of ferric-iron by the micro-organisms,
iii) the ferric leaching of the mineral (FeAsS and/or FeS_2), and
iv) the oxidation of arsenite to arsenate by ferric-iron.

The rapid decrease in the ferrous-iron concentration subsequent to the commencement of aerobic (bacterial) activity and the low ferrous-iron concentration maintained in the bioreactors for the remainder of the experiment, can be attributed to bacterial ferrous-iron oxidation, presumably by *L. ferrooxidans*:

$$4Fe^{2+} + O_2 + 4H^+ \rightarrow 4Fe^{3+} + 2H_2O \quad (5\text{-}4)$$

The above therefore suggests that the ferrous-iron produced during the lag phase serves as the initial energy source for the bacteria.

The variation in the arsenite concentration, [As(III)], of the slurry in the bioreactors during the course of the experiment is shown in Figure 5.4. From Figure 5.4 it is evident that the arsenite concentration of the slurry in the bioreactors to which 0 and 20 mmol As(III).ℓ^{-1} was added increased during the bacterial lag phase, whereas the arsenite concentration in the bioreactor to which 40 mmol As(III).ℓ^{-1} was added, decreased during the same period. However, the arsenite concentration in all the bioreactors decreased rapidly once the metabolic activity of the bacteria increased, and remained low for the remainder of the experiment.

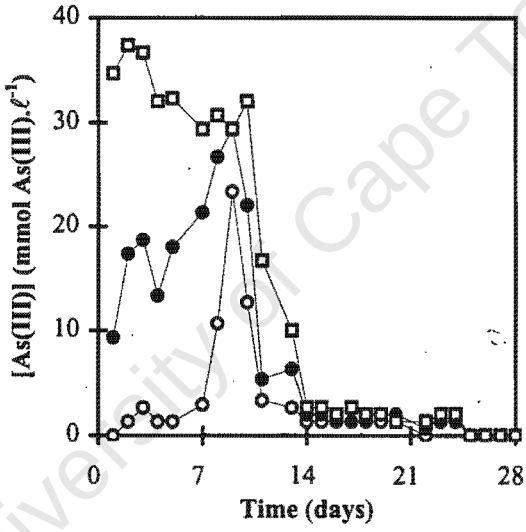

Figure 5.4: Variation in the arsenite concentration of the slurry in the bioreactors during the course of the experiment. [o] 0 mmol As(III).ℓ^{-1}; [•] 20 mmol As(III).ℓ^{-1}; [□] 40 mmol As(III).ℓ^{-1}.

The simultaneous increase in the ferrous-iron (see Figure 5.3) and arsenite concentrations of the slurry in the bioreactors to which 0 and 20 mmol As(III).ℓ^{-1} was added, observed during the bacterial lag phase, suggests that these species were produced by the chemical (ferric) leaching of the arsenopyrite:

$$FeAsS + 5Fe^{3+} \rightarrow 6Fe^{2+} + As(III) + S^0 \quad (5\text{-}5)$$

However, the increase in the ferrous-iron concentration of the slurry in the bioreactor to which 40 mmol As(III).ℓ^{-1} was added was associated with a decrease in the arsenite concentration. This in turn suggests that the dominant reaction occurring during this period was the chemical ferric oxidation of the arsenite to arsenate:

$$2Fe^{3+} + As(III) \rightarrow 2Fe^{2+} + As(V) \quad (5\text{-}6)$$

Comparison of the relative changes in the ferrous-iron and arsenite concentrations observed during the bacterial lag phase with the stoichiometries of Equations 5-5 and 5-6 are in agreement with the above suggestions.*

The decrease in the arsenite concentration, which accompanied the increase in aerobic activity, can be attributed to the oxidation of the arsenite to arsenate by ferric-iron. The increased availability of ferric-iron can in turn be attributed to the increased rate of bioleaching, *i.e.* the increased rate of both chemical ferric leaching of the mineral and bacterial ferrous-iron oxidation. This increased availability of ferric-iron is also responsible for the low arsenite concentration observed in the bioreactors for the remainder of the experiment.

Figure 5.5 shows the variation in the arsenate concentration, [As(V)], in the bioleaching slurry for the duration of the experiment. From Figure 5.5, it is evident that the variation in the arsenate concentration in all the bioreactors displayed the same trends. It did not vary significantly until the onset of bacterial activity,† at this stage the arsenate concentration increased rapidly to a maximum value of about 120 mmol As(V).ℓ^{-1}, and remained at this level for the remainder of the experiment‡.

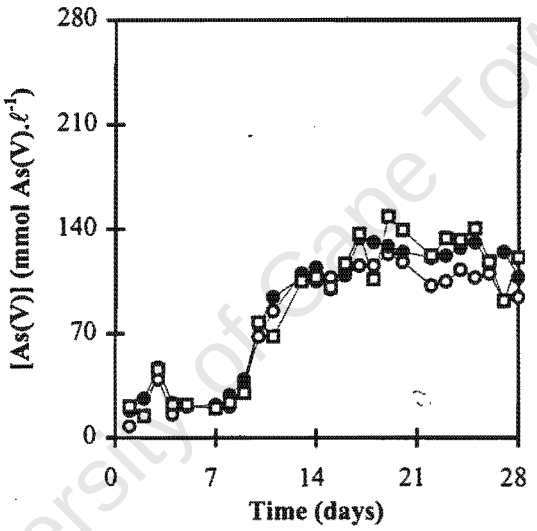

Figure 5.5: Variation in the arsenate concentration of the slurry in the bioreactors during the arsenite tolerance experiments. [o] 0 mmol As(III).ℓ^{-1}; [•] 20 mmol As(III).ℓ^{-1}; [□] 40 mmol As(III).ℓ^{-1}.

Comparison of Figure 5.5 with Figures 5.1 and 5.4 indicates that the increase in the arsenate concentration coincided with the increase in the oxygen utilisation rates, and a decrease in the arsenite concentration. The increase in the arsenate concentration can therefore be attributed to the oxidation of arsenite produced during the bioleaching of the mineral, to arsenate. As stated previously, under normal conditions the rate at which arsenite is oxidised to arsenate is in the region of 10 times the rate at which arsenopyrite is oxidised. This results in a low arsenite concentration in solution during periods of rapid bacterial growth (metabolic activity).

* From Figure 5.3, it is apparent that the increase in the ferrous-iron concentration was similar in all the bioreactors. In addition, the change in the arsenite concentration in the bioreactors to which 0 and 20 mmol As(III).ℓ^{-1} was added, was similar, and greater than the change in the arsenite concentration in the bioreactor to which 40 mmol As(III).ℓ^{-1} was added. For the same increase in the ferrous-iron concentration, the ratio between the increase, and decrease, in the arsenite concentration predicted by Equations 5-5 and 5-6, respectively, is 3:1. The ratio determined from Figures 5.3 and 5.4 was in the region of 2:1.

† From the results shown in Figure 5.5, it seems as though the arsenate concentration in all the bioreactors achieved a local maximum on the 3rd day of the experiment. However, because the concentrations in the bioreactors increased and decreased by the same amount over a 24-hour period, this phenomenon is most likely the result of errors in the sample analysis.

‡ The fluctuations in the arsenate concentrations in the bioreactors after day 15 can be attributed to analytical errors and the precipitation and dissolution of ferric arsenate caused by routine pH adjustments.

It is also apparent that the results shown in Figures 5.1 to 5.5 are consistent with the hypothesis that the ferric leaching of arsenopyrite, the ferric oxidation of arsenite to arsenate and the precipitation of ferric arsenate are competing reactions. In other words, the rate and extent to which each of these reactions occurs depends on both the absolute and relative concentrations of arsenopyrite, arsenite and arsenate in solution and the availability of ferric-iron. The availability of ferric-iron is related to both the ferric-iron concentration and the redox potential of the solution. It is therefore determined by the activity of the bacteria.

At low ferric-iron concentrations (low redox potentials) (*i.e.* prior to rapid bacterial activity) and in the absence of added arsenite, the chemical leaching of arsenopyrite (Equation 5-5) is the dominant reaction.* However, at low ferric-iron concentrations (low redox potentials) and high arsenite concentrations, the relative abundance of arsenite substrate in solution causes the oxidation of arsenite (Equation 5-6) to dominate. However, at high ferric-iron concentrations (high redox potentials) (*i.e.* during periods of rapid bacterial growth), there is sufficient ferric-iron available for oxidation of both the suspended arsenopyrite and the dissolved arsenite, and for the precipitation of ferric arsenate. This results in the low arsenite and high, but relatively constant, arsenate concentrations observed during the latter stages of the experiments.

5.2.2 The Effect of Arsenate, As(V)

The variation in the oxygen utilisation rates, $-r_{O_2}$, of the cultures in the bioreactors during the course of the arsenate tolerance experiments is shown in Figure 5.6.

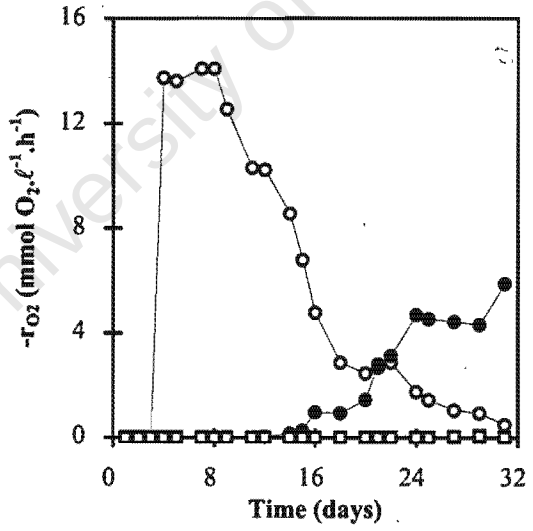

Figure 5.6: Variation in the oxygen utilisation rate of the bacterial cultures at different initial arsenate concentrations with time. [o] 0 mmol As(V).ℓ^{-1}; [•] 107 mmol As(V).ℓ^{-1}; [□] 220 mmol As(V).ℓ^{-1}.

From Figure 5.6 it is apparent that the culture to which no arsenate was added experienced a lag phase of 3 days; this lag phase was followed by normal metabolic activity. In comparison, the bacterial culture to which no arsenite was added experienced a lag phase of 8 days. This difference can be attributed to differences in the

* A requirement for the ferric leaching of arsenopyrite would of course be that the redox potential is greater than the rest potential of the mineral.

activities of the inoculii used in the respective experiments.* Comparison of Figures 5.1 and 5.6 also indicates that the culture in the bioreactor to which no arsenate was added achieved a higher maximum oxygen utilisation rate, $-r_{O_2}^{max}$, than the culture in the bioreactor to which no arsenite was added. If it is assumed that the maximum bacterial specific oxygen utilisation rates, $q_{O_2}^{max}$, of the inoculii were similar, then, according to Equations 5-2 and 5-3, the difference in the maximum oxygen utilisation rates can be attributed to differences in the sizes of the bacterial populations in the respective bioreactors.

Exposure to an initial concentration of 107 mmol As(V).ℓ^{-1} resulted in an increase in the lag phase from 3 to 15 days. Subsequent metabolic activity of this culture was also significantly reduced in comparison with that of the culture in the bioreactor to which no arsenate was added. The bacterial culture in the bioreactor to which no arsenate was added achieved a maximum oxygen utilisation rate of 14 mmol O_2.ℓ^{-1}.h^{-1} whereas the culture exposed to an initial concentration of 107 mmol As(V).ℓ^{-1} achieved a maximum oxygen utilisation rate of about 7.4 mmol O_2.ℓ^{-1}.h^{-1}. However, the oxygen utilisation rate of the bacterial culture in the bioreactor to which 107 mmol As(V).ℓ^{-1} was added was still increasing when the experiment was stopped.

In contrast to the above, however, it is apparent from Figure 5.6 that the bacterial culture exposed to an initial arsenate concentration of 220 mmol As(V).ℓ^{-1} showed no measurable aerobic activity for the duration of the experiment.

The cumulative amount of oxygen consumed by the bacterial cultures at various stages of the experiment relative to the total amount of oxygen consumed by the culture in the bioreactor to which no arsenate was added, η_{O_2}, is shown in Figure 5.7.

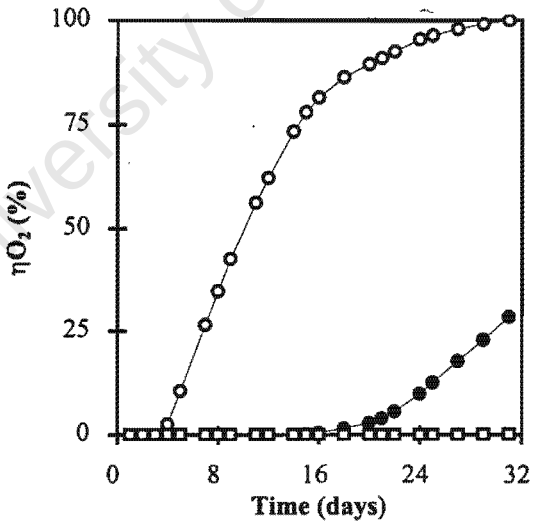

Figure 5.7: Variation in the cumulative amount of oxygen consumed by the bacterial cultures with time.
[o] 0 mmol As(V).ℓ^{-1}; [•] 107 mmol As(V).ℓ^{-1}; [□] 220 mmol As(V).ℓ^{-1}.

The results shown in Figure 5.7 confirm that the metabolic activity of the culture exposed to an initial concentration of 107 mmol As(V).ℓ^{-1} lagged the culture to which no arsenate was added by 12 days. It is also

* The inoculii used in the arsenite tolerance investigation were taken from the mini-plant while it was operating in batch mode whereas the inoculii used in the arsenate tolerance investigation were taken when the mini-plant was operating continuously, at a

apparent from Figure 5.7 that the overall oxygen consumption of the bacterial culture exposed to an initial concentration of 107 mmol As(V).ℓ^{-1} was only about 29 % of that of the culture to which no arsenate was added. As stated above, the oxygen utilisation rate of the bacterial culture exposed to an initial concentration of 107 mmol As(V).ℓ^{-1} was increasing when the experiment was stopped, hence the overall oxygen consumption of this culture would have increased further had the experiment been continued. In spite of this however, the results obtained suggest that elevated arsenate concentrations influence either the bacterial activity, *i.e.* it affects $q_{O_2}^{max}$, or their viability, *i.e.* it restricts growth and therefore affects c_X.

The variations in the ferrous-iron concentrations, [Fe^{2+}], measured in the bioreactors during the arsenate tolerance experiments are shown in Figure 5.8. Comparison of Figures 5.8 and 5.3 indicates that the variation in the ferrous-iron concentration in the bioreactors to which no arsenic was added followed the same trends. The trends observed in Figure 5.8 can therefore be explained in the same way as those in Figure 5.3. However, although these bioreactors displayed the same trends in the ferrous-iron concentration, the maximum ferrous-iron concentration achieved in the bioreactor to which no arsenate was added was considerably lower than that of the bioreactor to which no arsenite was added. This difference can again be attributed to differences in the activities of the respective inoculii. The more active inoculii used in the arsenate tolerance investigation resulted in a shorter lag phase, *i.e.* a shorter chemical leaching phase, which in turn resulted in a lower maximum ferrous-iron concentration. In spite of this difference, however, in both cases the rates of ferrous-iron production were similar.

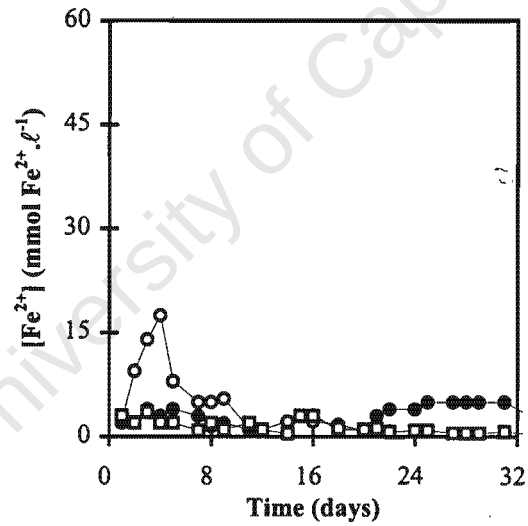

Figure 5.8: Variation in the ferrous-iron concentration with time for the duration of the experiment.
[o] 0 mmol As(V).ℓ^{-1}; [•] 107 mmol As(V).ℓ^{-1}; [□] 220 mmol As(V).ℓ^{-1}.

It is however clear from Figure 5.8 that the ferrous-iron concentration in the bioreactors to which 107 and 220 mmol As(V).ℓ^{-1} was added followed different trends, with respect to both the bioreactor to which no arsenate was added, and one another.

The ferrous-iron concentration of the slurry in the bioreactor in which the bacterial culture was exposed to an initial concentration of 107 mmol As(V).ℓ^{-1} did not vary significantly during the first 20 days of the experiment, which suggests that no ferric leaching of the mineral occurred during this period. The onset of bacterial activity

plant residence time of 15 days. This resulted in the inoculii used in the arsenate tolerance investigation being more active than

was however followed by a slight increase, and subsequent decrease, in the ferrous-iron concentration, similar to that observed in the arsenite tolerance experiments and the bioreactor to which no arsenate was added. However, the rate, and degree, to which the ferrous-iron concentration increased and decreased was reduced in comparison to the bioreactor to which no arsenate was added. These differences can be attributed to the inhibitory effect of the added arsenate on the bacteria.

In contrast to the above, no change in the ferrous-iron concentration, other than because of experimental error, was observed in the bioreactor to which 220 mmol As(V).ℓ^{-1} was added.

The variations in the arsenite concentrations, [As(III)], in the bioreactors observed during the arsenate tolerance experiments are shown in Figure 5.9. From Figure 5.9, it is apparent that the arsenite concentrations in the bioreactors to which 0 and 107 mmol As(V).ℓ^{-1} was added followed the same trends as the bioreactor to which no arsenite was added. The onset of bacterial activity was accompanied by an increase and subsequent decrease in the arsenite concentration, after which the concentration remained low for the remainder of the experiment. The increase in the arsenite concentration can be attributed to the increased rate of arsenopyrite leaching associated with the increase in aerobic activity. The decrease in the arsenite concentration after the onset of metabolic activity can be attributed to the oxidation of arsenite to arsenate resulting from the increased availability of ferric-iron.

In spite of displaying similar trends with regard to the arsenite concentration, the rate of production and consumption of arsenite in the bioreactor to which 107 mmol As(V).ℓ^{-1} was added was reduced in comparison with the bioreactors to which no arsenic was added. These differences can be explained in terms of the availability of ferric-iron, which in turn can be attributed to one or both of the following:

i) the inhibitory effect of arsenate with regard to the bacterial oxidation of ferrous-iron, and/or
ii) the precipitation of the ferric-iron added with the inoculii and the added arsenate as insoluble ferric arsenate.

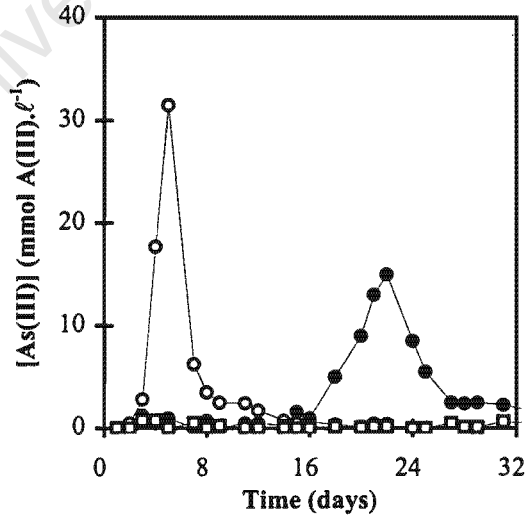

Figure 5.9: Variation in the arsenite concentration with time for the duration of the experiment.
[o] 0 mmol As(V).ℓ^{-1}; [•] 107 mmol As(V).ℓ^{-1}; [□] 220 mmol As(V).ℓ^{-1}.

the inoculii used in the arsenite tolerance investigation.

It is also evident from Figure 5.9 that no variation in the arsenite concentration was observed in the bioreactor to which 220 mmol As(V).ℓ^{-1} was added. This can also be attributed to the reduced availability of ferric-iron.

Figure 5.10 shows the variation in the arsenate concentration, [As(V)], observed in the bioreactors during the arsenate tolerance experiments. As expected, the variation in the arsenate concentration in the bioreactor to which no arsenate was added was similar to the variation in the arsenate concentration in the bioreactor to which no arsenite was added (see Figure 5.5). The observed trends can therefore be explained in the same way.

It is also apparent from Figure 5.10 that the arsenate concentration in the bioreactors to which 107 and 220 mmol As(V).ℓ^{-1} was added, decreased linearly, and at a similar rate, during the first 15 days of the experiments. No changes in the ferrous-iron or arsenite concentrations were observed during this period, nor was any aerobic activity measured.* This suggests that the reduction in the arsenate concentration was caused by the precipitation of ferric arsenate, according to (Fernandez *et al.*, 1995);

$$H_3AsO_4 + Fe^{3+} + n\,H_2O \rightarrow FeAsO_4.n\,H_2O\downarrow + 3\,H^+ \qquad (5.7)$$

The arsenate concentration in the bioreactor to which 220 mmol As(V).ℓ^{-1} was added, continued to decrease for the remainder of the experiment. However, the arsenate concentration in the bioreactor to which 107 mmol As(V).ℓ^{-1} was added appeared to stabilise at a concentration of about 50-70 mmol As(V).ℓ^{-1}, before increasing to about 140 mmol As(V).ℓ^{-1}, once aerobic bacterial activity commenced. As explained previously, the increase in the arsenate concentration can be attributed to the oxidation of arsenite produced as a result of the increased rate of mineral leaching associated with the increased level of bacterial activity.

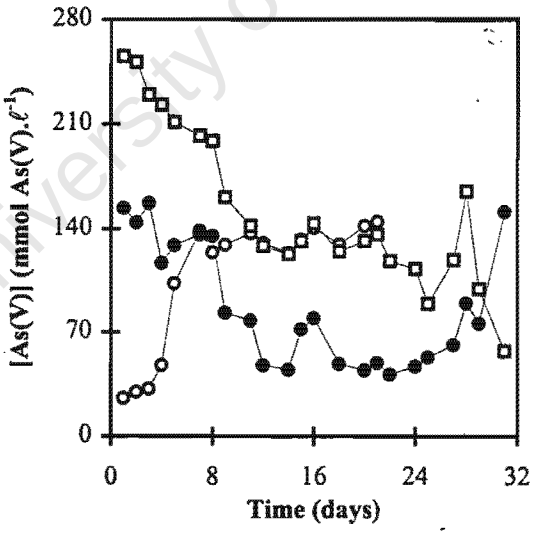

Figure 5.10: Variation in the arsenate concentration in the bioreactors with time for the duration of the experiment. [o] 0 mmol As(V).ℓ^{-1}; [•] 107 mmol As(V).ℓ^{-1}; [□] 220 mmol As(V).ℓ^{-1}.

* Although the lag time observed during the experiments performed at elevated arsenate concentrations may have been influenced by the a diffusional barrier resulting from the co-precipitation of adapted bacteria, the fact that similar amounts of precipitate were formed (based on the fact that the arsenate concentration in the bioreactors to which 107 and 220 mmol As(V).ℓ^{-1} was added decreased linearly and at a similar rate during this period) but different lag times observed, suggests that this phenomenon was not the sole reason for the observed lag phases.

The above trends, and those observed in Figures 5.6 to 5.9, are thus also consistent with the suggestion that the ferric leaching of arsenopyrite, the ferric oxidation of arsenite to arsenate and the precipitation of ferric arsenate are competing reactions.

5.2.3 Comparison of the Effects of Arsenite and Arsenate

Figure 5.11 illustrates the relative effect of different levels of arsenite and arsenate on the cumulative amount of oxygen consumed by the bacterial cultures at varying stages of the arsenite and arsenate tolerance investigations. In both sets of experiments, the lag phases were eliminated to facilitate comparison of the results.

It is apparent from Figure 5.11 that elevated arsenite concentrations did not result in a significant increase in the lag phase. Furthermore, although exposure to an initial concentration of 20 mmol As(III).ℓ^{-1} retarded the initial rate of bacterial metabolism, the bacteria appeared to recover from the effect of the added arsenite. This effect was more pronounced when 40 mmol As(III).ℓ^{-1} was added; this culture did not achieve the same maximum oxygen utilisation rate as the cultures exposed to initial concentrations of 0 and 20 mmol As(III).ℓ^{-1}, and showed a lower cumulative oxygen usage.

Exposure to an initial concentration of 107 mmol As(V).ℓ^{-1} resulted in a significant lag phase and retarded the initial rate of bacterial metabolism. Furthermore, the culture did not appear to recover from the effect of the added arsenate over the 31-day period for which the experiment was performed. Exposure to an initial concentration of 220 mmol As(V).ℓ^{-1} had an even more severe effect on the bacterial culture; this culture showed no measurable aerobic activity for the duration of the experiment.

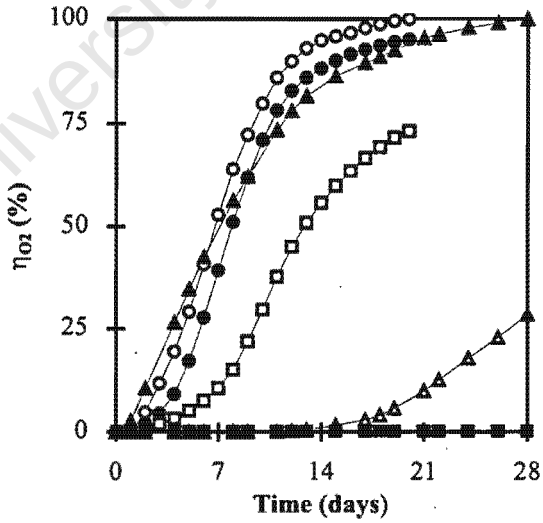

Figure 5.11: Variation in the cumulative amount of oxygen consumed by the bacterial cultures with time at different initial arsenite and arsenate concentrations. [○] 0 mmol As(III).ℓ^{-1}; [●] 20 mmol As(III).ℓ^{-1}; [□] 40 mmol As(III).ℓ^{-1}; [▲] 0 mmol As(V).ℓ^{-1}; [Δ] 107 mmol As(V).ℓ^{-1}; [■] 220 mmol As(V).ℓ^{-1}.

In contrast to the above trends, previous workers have reported that elevated arsenate levels result in a reduction in the maximum growth capacity (Lindström and Sehlin, 1989) whereas elevated arsenite concentrations result

in an extended lag phase (Cassity and Pesic, 1995; Collinet and Morin, 1990; Barrett *et al.*, 1989; Lindström and Sehlin, 1989; Pol'kin *et al.*, 1975).

It is important to note that the levels of arsenite used during this investigation were in the region of 10 times those observed during routine operation of a continuous bioleaching mini-plant oxidising the same flotation concentrate.* In spite of this, where an inhibitory effect was observed, the bacterial culture exhibited the ability to recover. In contrast to the above, the initial arsenate concentrations of the bioreactors to which arsenate was added were similar to those observed during routine operation of the mini-plant, yet the effect of the added arsenate was severe. The above therefore suggests that both the nature of- and the resistance mechanisms to- arsenite and arsenate are different.

Although concentrations of up to 145 mmol As(III).ℓ^{-1} have been reported in actively growing cultures accustomed to high arsenite concentrations (Morin *et al.*, 1991), most researchers have found arsenite to be inhibitory at concentrations similar to those used in this investigation (Barrett *et al.*, 1989; Pol'kin *et al.*, 1975). Furthermore, although some researchers have suggested that arsenite is in the region of two to three times more toxic than arsenate (Barrett *et al.*, 1989; Pol'kin *et al.*, 1975), during this investigation exposure to 107 mmol As(V).ℓ^{-1} had a far more pronounced effect than 40 mmol As(III).ℓ^{-1}. It should however be noted that most researchers have performed toxicity experiments in media supplemented with ferrous-iron, which is the most easily used source of energy for iron-oxidising bacteria. This may well have influenced the results obtained by them. Although the inhibitory effect of arsenic is more pronounced if ferrous-iron is the substrate; *cf.* sulfide mineral,† it is likely that the inhibitory effect would be least apparent if the medium contained both suspended mineral particles and added ferrous-iron.

The results of this research therefore suggest that the mechanism of arsenate resistance in the mixed (mesophilic) culture may be attributed to (chromosomal) Pst^+Pit^- mutations, *i.e.* natural selection, and an energy dependent efflux pump. The Pst^+Pit^- mutations result in a reduced uptake of arsenate, which enables the bacteria to survive in bioleaching solutions in which the arsenate concentration is significantly higher than the arsenite concentration. However, the excretion of arsenate that enters the cell, presumably via the phosphate uptake system, requires energy. Therefore, during periods of reduced bacterial activity, *e.g.* prior to exponential growth, the inhibitory effect of arsenate may manifest at arsenate concentrations to which the culture has previously been adapted.

As stated previously, the mixed culture used in this work has been reported to consist (predominantly) of *L. ferrooxidans* and *T. caldus*. The proposed resistance mechanism described is therefore in partial disagreement with the results of previous work. Hallberg (1995) reported the resistance mechanism to arsenite and arsenate in *T. caldus* to be the result of a reduced cellular accumulation of these ions and an energy dependent efflux of the accumulated ions.

However, Hallberg (1995) also suggested that the resistance to arsenite, arsenate and antimony is conferred, *i.e.* it is not due to chromosomal mutations, but is induced by growth in the presence of non lethal concentrations of any of these ions. Although this suggestion is in disagreement with the mechanism of arsenate resistance proposed for the mixed culture, it is not necessarily in disagreement with the results obtained during the current (or previous) investigations. It is possible that the ability of bioleaching micro-organisms to survive in solutions in which the arsenate concentrations are significantly higher than the arsenite concentrations may be attributed to

* These results are presented in Chapter Six.

† It is also possible that this phenomenon extends to the inhibitory effect of other elements.

these ions entering the micro-organisms via different pathways. These pathways would be expected to have different affinities for arsenite and arsenate; hence, the solution concentration at which each of these ions become inhibitory would also be different.

5.3 Chapter Summary

Batch bioleaching experiments were carried out over periods of about one month. Varying quantities of arsenite or arsenate were added to slurries consisting of 20 % arsenopyrite/pyrite flotation concentrate in an inorganic nutrient solution. The slurry was inoculated with a culture from a continuous bioleaching mini-plant treating the same concentrate; subsequent research has shown that the inoculii consisted primarily of *L. ferrooxidans* and *T. caldus*. The effect of the added arsenic was determined by comparing the variation in the concentrations and speciation of iron and arsenic in solution, and the oxygen utilisation rate of the bacterial cultures in the bioreactors to which arsenic had been added, with the results obtained in the absence of added arsenic.

In the absence of bacterial activity and at "low" concentrations of arsenate, and/or arsenite, the ferric leaching of arsenopyrite resulted in the solubilisation of iron and arsenic as ferrous-iron and arsenite, respectively. However, at "high" concentrations of arsenite, the oxidation of arsenite to arsenate predominated, and at "high" arsenate concentrations, the precipitation of ferric arsenate predominated. These results are consistent with the postulate that the oxidation of arsenopyrite and arsenite, by ferric-iron, and the precipitation of ferric arsenate, are competing reactions. Their rates are therefore influenced by the relative concentrations of arsenopyrite, arsenite and arsenate in the bioleaching slurry and the availability of ferric-iron. The availability of ferric-iron is indicated by the redox potential of the solution (a high redox potential represents a high availability of ferric-iron and *vice versa*) and is in turn determined by the activity of the bacteria.

Exposure to an initial concentration of 20 mmol As(III).ℓ^{-1} did not have a significant effect on the performance of the bacterial culture. However, exposure to an initial concentration of 40 mmol As(III).ℓ^{-1} reduced both the initial and maximum oxygen utilisation rates of the bacterial culture. In neither case was the lag phase affected to a significant degree.

In contrast to the above, exposure to an initial concentration of 107 mmol As(V).ℓ^{-1} increased the lag phase of the bacterial culture by 12 days and reduced both the initial and maximum oxygen utilisation rates of the bacterial culture. The addition of 220 mmol As(V).ℓ^{-1} to the bacterial culture resulted in a lag phase that lasted for more than 31 days.

The arsenite levels used during this investigation were in the region of 10 times those observed during routine operation of the mini-plant from which the inoculii were obtained (whilst oxidising the same concentrate), yet where an inhibitory effect was observed, the bacterial culture exhibited the ability to recover. In contrast to the above, the arsenate concentrations used were similar to those observed in the mini-plant, yet the effect on the bacteria in batch culture was severe.

The results obtained, together with those of previous workers, therefore suggest that arsenate toxicity, and the relative toxicity of arsenite and arsenate to the culture used in this investigation is affected by the activity of the micro-organisms and the availability of ferrous-iron (substrate). In other words, the mechanism of bacterial arsenate resistance may be attributed to an energy dependent efflux pump and a membrane system which

influences the (relative) rates at which arsenite and arsenate are able to enter the micro-organisms. The latter resistance mechanism may or may not be attributable to $Pst^+ Pit^-$ (chromosomal) mutations.

5.4 Nomenclature

$[As(III)]$	arsenite concentration	mmol As(III).ℓ^{-1}
$[As(III)]_{initial}$	initial arsenite concentration	mmol As(III).ℓ^{-1}
$[As(V)]$	arsenate concentration	mmol As(V).ℓ^{-1}
$[As(V)]_{initial}$	initial arsenate concentration	mmol As(V).ℓ^{-1}
c_X	concentration of bacteria	mmolC.ℓ^{-1}
$[Ce^{4+}]$	concentration of cerium(IV)	mmol Ce^{4+}.ℓ^{-1}
E^0	standard redox potential	V
$[Fe^{2+}]$	concentration of ferrous-iron	mmol Fe^{2+}.ℓ^{-1}
$[Fe^{3+}]$	concentration of ferric-iron	mmol Fe^{3+}.ℓ^{-1}
K	kinetic constant in bacterial ferrous-iron oxidation	dimensionless
q_{O_2}	bacterial specific oxygen utilisation rate	mmol O_2.(mmol C)$^{-1}$.h^{-1}
$q_{O_2}^{max}$	maximum bacterial specific oxygen utilisation rate	mmol O_2.(mmol C)$^{-1}$.h^{-1}
r_{O_2}	oxygen production rate	mmol O_2.ℓ^{-1}.h^{-1}
$r_{O_2, control}$	oxygen production rate of the culture in the 'control'	mmol O_2.ℓ^{-1}.h^{-1}
$r_{O_2, i}$	oxygen production rate of the culture in bioreactor 'i'	mmol O_2.ℓ^{-1}.h^{-1}
$r_{O_2}^{max}$	maximum rate of oxygen production	mmol O_2.ℓ^{-1}.h^{-1}
t	time	days
$V_{As(III)}$	"theoretical" arsenite titration volume	mℓ
$V_{(As(III) + Fe^{2+})}$	"combined" ferrous-iron and arsenite titration volume	mℓ
$V_{Fe^{2+}}$	ferrous-iron titration volume	mℓ
V_{sol}	solution aliquot volume	mℓ
V_t	titration volume	mℓ
$\eta_{O_2, i}$	cumulative proportion of oxygen consumed by the bacterial culture in bioreactor 'i' relative to the total amount consumed by the culture in the 'control'	%

5.5 References

Abdrashitova, S.A., Ilyaletdinov, A.N., Mynbaeva, B.N. and Abdulina, G.G. 1982. The catalase activity of *Pseudomonas putida* strain oxidizing arsenic. Mikrobiologiya **51**: 34-37.

Barrett, J., Ewart, D.K., Hughes, M.N., Nobar, A.M. and Poole, R.K. 1989. The oxidation of arsenic in arsenopyrite: the toxicity of As(III) to a moderately thermophilic mixed culture, pp. 49-57. In: J. Salley, R.G.L. McCready and P.L. Wichlacz (eds.), Proc. Biohydrometallurgy-89. Jackson Hole, July 1989.

Broadhurst, J.L. 1993. Determination of arsenic and iron, and their oxidation states, in BIOX® process liquors. Report No. PR 93/85C of Project No. PR 93/128, GENMIN Process Research, Johannesburg.

Cassity, W.D. and Pesic, B. 1995. Interaction of *Thiobacillus ferrooxidans* with arsenite, arsenate and arsenopyrite, pp. 223-228. In: B.J. Scheiner, T.D. Chatwin, H. El-Shall, S.K. Kawatra and A.E. Torma (eds.), New Remediation Technology in the Changing Environmental Arena. Society for Mining, Metallurgy, and Exploration, Inc., Littleton, Co..

Coddington, K. 1986. A review of arsenicals in biology. Toxicological and Environmental Chemistry **11**: 281-290.

Collinet, M.-N. and Morin, D. 1990. Characterisation of arsenopyrite oxidising *Thiobacillus*. Tolerance to arsenite, arsenate, ferrous and ferric iron. Antonie van Leeuwenhoek **57**: 237-244.

Cullen, W.R. and Reimer, K.J. 1989. Arsenic speciation in the environment. Chemical Reviews **89**(4): 713-764.

Dew, D.W., Lawson, E.N. and Broadhurst, J.L. 1997. The BIOX® process for biooxidation of gold-bearing ores or concentrates, pp. 45-80. In: D.E. Rawlings (ed.), Biomining: theory, microbes and industrial processes. Springer-Verlag and Landes Bioscience, Berlin.

Fernandez, M.G.M., Mustin, C., De Donato, P., Barres, O., Marion, P. and Berthelin, J. 1995. Occurrences at mineral-bacteria interface during oxidation of arsenopyrite by *Thiobacillus ferrooxidans*. Biotechnology and Bioengineering **46**(1): 13-21.

Hallberg, K.B. 1995. Role of arsenic toxicity to and resistance of thermophilic bioleaching micro-organisms. Ph.D. Thesis, Umeå University, Umeå.

Huysmans, K.D. and Frankenberger, W.T. 1992. Microbial resistance to arsenic, pp. 93-116. In: I.K. Iskander and H.M. Selim (eds.), Engineering Aspects of Metal-waste Management. Lewis Publishers, Boca Raton, Fla..

Jeffrey, G.H., Bassett, J., Mendham, J. and Denney, R.C. 1989. Vogel's Textbook of Quantitative Chemical Analysis. 5th edition, Longman Scientific & Technical, New York.

Lawson, E.N. 1993. Arsenic toxicity, bacterial resistance and bacterial oxidation/reductions. Phase 1: literature review. Report No. PR 93/109C of Project No. PR 93/132. GENMIN Process Research, Johannesburg.

Lindström, E.B. and Sehlin, H.M. 1989. Toxicity of arsenic compounds to the sulphur- dependent archaebacterium *Sulfolobus*, pp. 59-70. In: J. Salley, R.G.L. McCready and P.L. Wichlacz (eds.), Proc. Biohydrometallurgy-89. Jackson Hole, July 1989.

Mobley, H.T. and Rosen, B.P. 1982. Energetics of plasmid-mediated arsenate resistance in *Escherichia coli*. Proc. Natl. Acad. Sci. USA **79**: 6119-6122.

Morin, D., Ollivier, P., Toromanoff, I. and Letestu, A. 1991. Bioleaching of gold refractory arsenopyrite rich sulfide concentrate: laboratory and pilot case studies, pp. 577-589. In: D.R. Gaskell (ed.), Proc. EPD Congress '91. The Minerals, Metals & Materials Society, Warrendale, Co..

Nicolau, C. and Raimond, J. 1983. As cited by Lawson, E.N. 1993. Arsenic toxicity, bacterial resistance and bacterial oxidation/reductions. Phase 1: literature review. Report No. PR 93/109C of Project No. PR 93/132. GENMIN Process Research, Johannesburg.

Novick, R.P. and Roth, C. 1968. Plasmid-linked resistance to inorganic salts in *Staphylococcus aureus*. Journal of Bacteriology **95**(4): 1335-1342.

Pol'kin, S.I., Panin, V.V., Adamov, E.V., Karavaiko, G.I. and Chernyak, A.S. 1975. Theory and practice of utilizing micro-organisms in difficult-to-dress ores and concentrates, pp. 901-923. In: Proc. 11th International Mineral Processing Congress. Cagliari, 20-26 April 1975.

Rawlings, D.E., Coram, N.J., Gardner, M.N. and Deane, M.N. 1999. *Thiobacillus caldus* and *Leptospirillum ferrooxidans* are widely distributed in continuous flow biooxidation tanks used to treat a variety of metal containing ores and concentrates, pp. 777-786. In: R. Amils, A. Ballester (eds.), Biohydrometallurgy and the environment toward the mining of the 21st century A. Elsevier, Amsterdam.

Sehlin, H.M. and Lindström, E.B. 1992. Oxidation and reduction of arsenic by *Sulfolobus acidocaldarius* strain BC. FEMS Microbiology Letters **93**: 87-92.

Silver, S. and Keach, D. 1982. Energy-dependent arsenate efflux: the mechanism of plasmid-mediated resistance. Proc. Natl. Acad. Sci. USA **79**: 6114-6118.

Silver, S. and Nakahara, H. 1983. Bacterial resistance to arsenic compounds, pp. 190-198. In: W.H. Lederer and R.J. Fensterheim (eds.), Arsenic: Industrial, Biomedical, Environmental Perspectives. Van Nostrand Reinhold, New York.

Silver, S. 1978. Transport of cations and anions, pp. 221-324. In: B.P. Rosen (ed.), Bacterial Transport. Marcel Dekker Inc., New York.

Wakao, N., Koyatsu, H., Komai, Y., Shimokawara, H., Sakurai, Y. and Shiota, H. 1988. Microbial oxidation of arsenite and occurrence of arsenite-oxidising bacteria in acid mine water from a sulphur-pyrite mine. Geomicrobiology Journal **6**: 11-24.

Williams, J.W. and Silver, S. 1984. Bacterial resistance and detoxification of heavy metals. Enzyme. Microb. Technol. **6**: 530-537.

5.6 Appendix

The standard method for the determination of the ferrous-, ferric- and total iron concentrations in bioleaching slurries involves the titration of the slurry filtrate with potassium dichromate solution of known concentration, using diphenylamine sulphonate redox indicator to detect the end-point. However, in the presence of more than 1 $g.\ell^{-1}$ arsenite, As(III), the arsenite interferes with the determination of both the ferrous- and total iron concentrations (Broadhurst, 1993). The relative error in the determination of ferrous-iron, at ferrous-iron concentrations ranging from 0.5 to 1.9 $g.\ell^{-1}$, was found to increase from < 2 % to between 145 and 240 % in the presence of 5.27 $g.\ell^{-1}$ arsenite (Broadhurst, 1993). The degree of interference during the determination of the total iron concentration was significantly lower, presumably because of the higher $[Fe^{2+}]/As(III)]$ ratio (Broadhurst, 1993). At a total iron concentration of 25 $g.\ell^{-1}$ the error ranged from < 2 % to between 9 and 14 % in the presence of 5.27 $g.\ell^{-1}$ arsenite (Broadhurst, 1993). The above phenomenon was attributed to the partial oxidation of arsenite by dichromate:

$$Cr_2O_7^{2-} + 3\,As(III) + 14\,H^+ \rightarrow 2\,Cr^{3+} + 3\,As(V) + 7\,H_2O \qquad \text{(A-1)}$$

The above led to the development of a titrimetric method for the determination of the ferrous-iron and arsenite concentrations in bioleaching slurries using cerium(IV) sulfate.

Cerium(IV) sulfate is a powerful oxidising agent. It is capable of oxidising ferrous-iron, Fe^{2+}, to ferric-iron, Fe^{3+}, and arsenite, As(III), to arsenate, As(V), in acidic solutions:

$$Ce^{4+} + Fe^{2+} \rightarrow Ce^{3+} + Fe^{3+} \quad \text{(A-2)}$$

$$2\,Ce^{4+} + As(III) \rightarrow 2\,Ce^{3+} + As(V) \quad \text{(A-3)}$$

However, under normal conditions, the oxidation of arsenite to arsenate is extremely slow. This allows the ferrous-iron concentration to be determined by titration with cerium(IV) sulfate, at normal atmospheric conditions, without encountering interference from the oxidation of arsenite to arsenate. After the determination of the ferrous-iron concentration, titration with cerium(IV) sulfate solution in the presence of a catalyst, *viz.* osmium tetroxide, enables the arsenite concentration to be determined:

$$V_{As(III)} = V_{(As(III)+Fe^{2+})} - V_{Fe^{2+}} \quad \text{(A-4)}$$

In both instances, the titration end-point is detected using ferroin indicator, *viz.* 1,10-phenanthroline-ferrous complex solution.

If the total iron and arsenic concentrations in solution are determined by Flame Atomic Adsorption Spectroscopy (FAAS), the ferric-iron and arsenate concentrations can be calculated by difference.

The standard titrimetric methods for the determination of the ferrous-iron and arsenite concentrations in bioleaching liquors, using cerium(IV) sulfate as suggested by Broadhurst (1993), are described in detail below.

5.6.1 Standard Titrimetric Methods for the Determination of Fe^{2+} and As(III) in Bioleaching Liquors using Cerium(IV) Sulfate

5.6.1.1 Reagents

As(III) standard solution (0.05 mol .ℓ^{-1})

i) Dry about 5 g of AR grade arsenic trioxide, As_2O_3, in an oven at 105 to 110°C for 1 to 2 hours. Allow the dry As_2O_3 to cool to room temperature in a desiccator.

ii) Accurately weigh out 2.470 g of the cool As_2O_3 into a 100 mℓ beaker.

iii) Using distilled water, quantitatively transfer the 2.470 g of As_2O_3 into a 500 mℓ beaker.

iv) Add 400 mℓ of distilled water and agitate on a magnetic stirrer/heater.

v) Adjust the pH of the solution to pH 1.6 using 1 mol $H_2SO_4.\ell^{-1}$.

vi) Heat to about 60°C and agitate until the salt has dissolved completely. Allow to cool to room temperature.

vii) Using distilled water, quantitatively transfer the solution into a 500 mℓ volumetric flask. Fill the flask to the 500 mℓ mark using distilled water and mix the solution thoroughly.

The arsenite concentration, in mol As(III).ℓ^{-1}, is calculated according to;

$$[\text{As(III)}] = \frac{\text{mass } As_2O_3 \times 4}{197.84} \qquad \text{(A-5)}$$

Cerium(IV) sulfate solution (0.05 mol .ℓ^{-1})

Standardised cerium(IV) sulfate solution is commercially available. However, solutions may also be prepared by dissolving cerium(IV) sulfate in dilute sulfuric acid (Jeffrey *et al.*, 1989).

Spekker acid solution

i) Agitate 1.2 ℓ of distilled water in a 5 ℓ beaker.
ii) Slowly, and carefully, add 600 mℓ of concentrated sulfuric acid (*viz.* 98 % H_2SO_4).
iii) Add 600 mℓ of concentrated phosphoric acid (*viz.* 85 % HPO_4).
iv) Allow the spekker acid solution to cool before transferring it to a storage bottle.

Osmium tetroxide solution (~ 0.01 mol $OsO_4.\ell^{-1}$)

i) Using distilled water quantitatively transfer 1 g of osmium tetroxide, OsO_4, from the glass ampoule into a 500 mℓ beaker.
ii) Add 250 mℓ distilled water and 20 mℓ of a 1 mol $H_2SO_4.\ell^{-1}$ solution and agitate until the OsO_4 crystals have dissolved.
iii) Make up to 400 mℓ with distilled water and store in a glass bottle with a glass stopper.

Ferroin indicator solution

Ferroin indicator solution, 1,10-phenanthroline-ferrous complex solution, with an E^0 value of 1.06 V in 1 mol $H_2SO_4.\ell^{-1}$, is commercially available.

5.6.1.2 Procedures

Titrations must be carried out on clear aliquots of the solutions. Slurries must be allowed to either settle, or must be filtered, before titration. The latter is the preferred option. Titrations are generally carried out using a 5 mℓ aliquot. For greater accuracy at concentrations of less than 1 g.ℓ^{-1}, a 10 mℓ aliquot may be used.

Standardisation of cerium(IV) sulfate solution

Although commercially available cerium(IV) sulfate solutions have been standardised using sodium oxalate, the concentrations of the supplied solutions have been found to vary significantly, hence they should therefore be standardised using As(III).

i) Pipette 5 mℓ of the 0.05 mol As(III).ℓ^{-1} standard solution into a 100 mℓ conical flask.
ii) Add 10 mℓ spekker acid solution and 3 drops osmium tetroxide solution.
iii) Add 1-2 drops ferroin indicator solution.
iv) Titrate with 0.05 mol.ℓ^{-1} cerium(iv) sulfate solution until the first permanent colour change from orange/red to blue is observed.

The cerium(IV) concentration, in mol $Ce^{4+}.\ell^{-1}$, is calculated according to;

$$[Ce^{4+}] = \frac{[As(III)]V_{sol} \times 2}{V_t} \quad \text{(A-6)}$$

Determination of ferrous-iron concentration, $[Fe^{2+}]$

i) Pipette the required solution aliquot into a 100 mℓ conical flask.
ii) Add 10 mℓ spekker acid solution and 1-2 drops ferroin indicator solution.
iii) Titrate with the standardised cerium(iv) sulfate solution until the first permanent colour change from orange/red to blue is observed.

The ferrous-iron concentration, in mol $Fe^{2+}.\ell^{-1}$, is calculated according to;

$$[Fe^{2+}] = \frac{[Ce^{4+}]V_t \times 55.847}{V_{sol}} \quad \text{(A-7)}$$

Determination of arsenite concentration, [As(III)]

i) Pipette the required solution aliquot into a 100 mℓ conical flask.
ii) Add 10 mℓ spekker acid solution, 3 drops of osmium tetroxide solution and 1-2 drops ferroin indicator solution.
iii) Titrate with the standardised cerium(iv) sulfate solution until the first permanent colour change from orange/red to blue is observed.

The arsenite concentration, in mol As(III).ℓ^{-1}, is calculated according to;

$$[As(III)] = \left(V_t - \frac{[Fe^{2+}]V_{sol}}{[Ce^{4+}] \times 55.847}\right)\left(\frac{[Ce^{4+}] \times 74.92}{V_{sol} \times 2}\right) \quad \text{(A-8)}$$

For Cheye

You are led
through your lifetime
by the inner learning creature,
the playful spiritual being
that is your real self.

Don't turn away
from possible futures
before you're certain you don't have
anything to learn from them.

You're always free
to change your mind and
choose a different future, or
a different
past.

ILLUSIONS – Richard Bach

Chapter Six

Steady-state Operation and Aeration Perturbations of a Continuous Bioleaching Mini-plant Treating an Arsenopyrite/pyrite Flotation Concentrate*

During continuous bioleaching operations, disruptions in the aeration and agitation of the bioreactors may occur as a result of either power or equipment failures. These perturbations will result in a reduction in the level of bacterial activity for the duration of the perturbation. During this period, the continued (ferric) leaching of the mineral may result in an increase in the rate of arsenite production, relative to its conversion to arsenate. This may in turn result in the concentration of arsenite reaching levels that are inhibitory to the micro-organisms. Furthermore, the toxic effect of the arsenite may persist once aeration and agitation are restored; this may result in significant losses in production. It is therefore apparent that knowledge of what changes occur during and after disruptions in the aeration and agitation of the bioreactors may allow measures to be taken during, and/or after the disruptions, to ensure rapid recovery of the bioleaching plant.

The work presented in this chapter was therefore aimed at determining the relationship between perturbations in the aeration and agitation of the mixed culture from the Fairview BIOX® plant, while oxidising a sample of arsenopyrite/pyrite flotation concentrate from the Fairview Gold Mine, and arsenic toxicity. A further aim of the work was to determine whether the performance of the mini-plant was consistent with the hypothesis that the bioleaching of arsenopyrite occurs via a multiple sub-process mechanism.

---

* Breed, A.W., Harrison, S.T.L. and Hansford, G.S. 1997. The bioleaching of a pyrite-arsenopyrite flotation concentrate in a continuous bioleaching mini-plant. Steady-state operation and behaviour during periods without aeration and agitation, pp. M.8.3.1-M.8.3.10. In: Biotechnology Comes of Age, Proceedings of IBS-BIOMINE 97. AMF, Glenside, SA.

6.1 Materials and Methods

6.1.1 Continuous Bioleaching Mini-plant

The continuous bioleaching mini-plant consisted of two baffled, agitated, aerated bioreactors operating in series under controlled conditions of temperature, pH, dissolved oxygen and solids concentration and nutrient supply. The bioreactors were fed from a baffled, agitated conditioning vessel, to which the nutrient solution and (dry) concentrate were added. A general view of the mini-plant is shown in Figure 6.1.

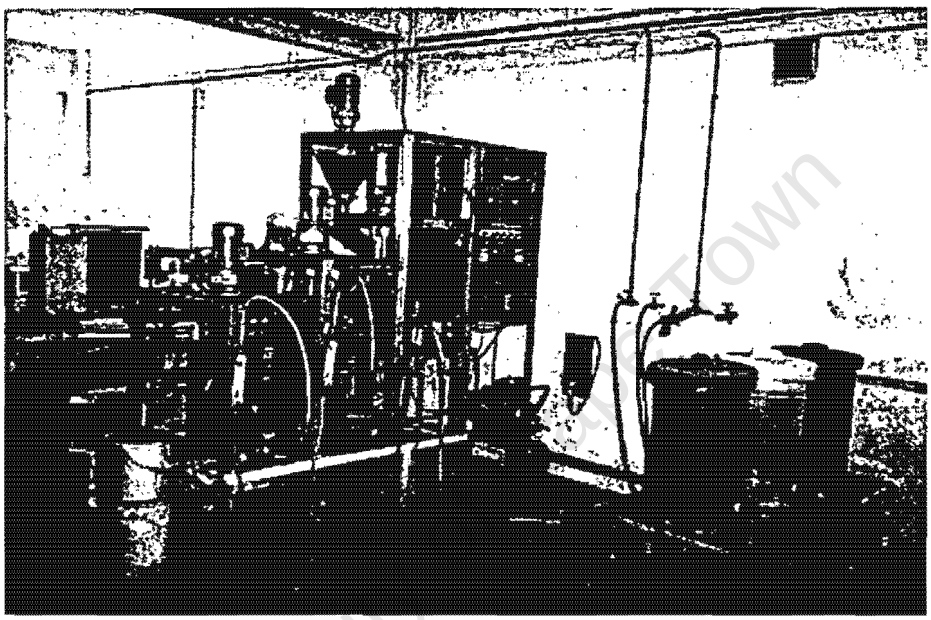

Figure 6.1: General view of the continuous bioleaching mini-plant.

6.1.1.1 Bioreactors

The bioreactors were constructed from PVC tubing with an internal diameter of 300 mm. They were 500 mm high and had a working volume of about 20 ℓ. The slurry was agitated by 6-bladed, pitched blade impellers, 140 mm in diameter and located 110 mm from the base of the bioreactor. The impellers were rotated at 570 rev.min^{-1} by 0.37 kW Flender Himmel motors. The agitator shafts and impellers were constructed from stainless steel owing to the corrosive nature of the bioleaching slurry.

Air operated Wilden® M-1® double diaphragm pumps were used to circulate the slurry from the base to the top of the bioreactors. This prevented settling in the conical base of the bioreactors and ensured a uniform slurry concentration within the bioreactors.

6.1.1.2 Temperature control system

Because the heat duty is affected by the activity of the culture and the atmospheric conditions (*e.g.* temperature and relative humidity), the temperature in each of the bioreactors was controlled separately. The temperature control system consisted of Electrolink LM 35 temperature sensors, a Hitech Micro Systems Temperature Controller and separate heating and cooling circuits.* The temperature sensors were located in a hollow tube in each bioreactor. These tubes were located at a height of 230 mm from the base of the bioreactors, and extended into the bioreactors to a depth of 100 mm.

The heating circuit consisted of a stainless steel heating tank (in which water was maintained at about 60°C), a centrifugal pump, stainless steel U-tubes mounted inside the bioreactors and ASCO® 8210 solenoid valves. The stainless steel U-tubes were 8 mm in diameter and had a submerged length of 46 mm. The hot water was continually pumped from the heating tank through a ring-main configuration and back to the heating tank. The slurry in the bioreactors was heated by opening the required solenoid valve and allowing the hot water to pass through the stainless steel U-tubes before returning to the heating tank.

The cooling circuit consisted of a (tap) water source (at municipal supply temperature and pressure), stainless steel U-tubes (identical to those used in the heating circuit) and ASCO® 8210 solenoid valves. The slurry in the bioreactors was cooled by opening the required solenoid valve and allowing the (tap) water to pass through the (cooling) stainless steel U-tubes, before being discharged to the municipal drainage system.

6.1.1.3 pH control system

During normal operation, the bioleaching of the arsenopyrite/pyrite flotation concentrate used in this investigation is acid producing. However, during the bacterial lag phase the concentrate is acid consuming. In addition, variations in the pH of the slurry may occur as a result of variations in the activity of the bacterial population. For the above reasons, automated acid and base circuits were commissioned to maintain the pH in each of the bioreactors within the desired pH range.

The pH in the bioreactors was monitored and controlled by means of Foxboro® 871PH pH and ORP sensors and Foxboro® 873PH pH/ORP Electrochemical Analysers in which the saturated KCl solution had been replaced with 1 mol LiCl.ℓ^{-1}.

The acid addition circuit consisted of a PVC tank, a Prominent® gamma/ 4 0216 diaphragm metering pump and Bürkert type 121 solenoid valves. The sulfuric acid solution (9.8 % H_2SO_4) was continually pumped from the PVC tank through a ring-main configuration, and back to the tank. The pH of the slurry in the bioreactors was reduced by opening the required solenoid valve and allowing the sulfuric acid solution to flow into the bioreactor.

The base circuit consisted of a PVC tank, a MFG® EV 3000 4 peristaltic pump and Bürkert type 121 solenoid valves. The sodium hydroxide solution (10 mol NaOH.ℓ^{-1}) was also pumped through a ring-main configuration. The pH of the slurry in the bioreactors was increased by opening the necessary solenoid valve, thereby allowing the NaOH solution to flow into the bioreactor.

---

* Hitech Micro Systems equipment are designed and manufactured in the Department of Chemical Engineering at the University of Cape Town.

6.1.1.4 Aeration system

The aeration system consisted of a compressed air source, a pressure regulator, rotameters and removable stainless steel rod spargers. The air feed rate to the bioreactors was controlled using the pressure regulator and rotameters. It was sparged into the centre of each bioreactor, at a height of 40 mm from the bioreactor base (*i.e.* below the impeller blades), through a 1 mm discharge angled towards the base of the bioreactor.

Dissolved oxygen measurements, using a YSI Model 5739 dissolved oxygen probe and a Hitech Micro Systems Dissolved Oxygen / Utilisation Rate Meter, were carried out periodically to ensure that the bacterial culture was not oxygen limited.

6.1.1.5 Feed control system

The feed control system consisted of a conditioning vessel with an external recycle stream, and separate (dry) concentrate and nutrient feed systems. This allowed the overall plant (hydraulic) residence time, $\tau_{overall}$, and the solids concentration, ρ_{pulp}, to be individually controlled.

The conditioning vessel was constructed from PVC tubing with an internal diameter of 240 mm. It was 330 mm high and had a working volume of about 10 ℓ. The slurry was agitated by a 4-bladed pitched blade impeller, 110 mm in diameter and located 80 mm from the base of the vessel. The impeller was rotated at 570 rev.min^{-1} by a 0.37 kW Flender Himmel motor. The agitator shaft and impeller were constructed from stainless steel.

A MFG EV 3000 4 peristaltic pump withdrew slurry from the base of the conditioning vessel and delivered it into a launder located below the dry concentrate feeder. The launder in turn discharged the slurry into the top of the conditioning vessel. The purpose of the recycle stream was threefold:

i) it prevented settling in the (conical) base of the conditioning vessel,
ii) it washed the fresh (dry concentrate) feed into the conditioning vessel, and
iii) it ensured a uniform slurry composition within the conditioning vessel.

The dry solids were introduced into the recycle stream by means of a screw feeder located in a conical hopper; both were constructed from stainless steel. The screw feeder was rotated at 38 rev.min^{-1} by a 0.18 kW Flender Himmel motor and was operated on a semi-continuous basis by means of a digital on/off timer.

Nutrients at the required concentration were supplied to the conditioning vessel at a constant rate by means of ProMinent® gamma/ 4 0216 diaphragm metering pump. The nutrient solution feed rate depended on the prevailing mini-plant retention time and included a fixed amount of water to account for evaporative losses.

Manual monitoring of the solid and liquid feed rates was carried out periodically and the rates adjusted as required.

6.1.2 Mini-plant Monitoring

The performance of the bioleaching mini-plant was monitored by measuring the variation in the concentrations of the iron and arsenic species, the oxygen utilisation rate of the bacterial culture and the pH and redox potential of the slurry in each of the bioreactors.

The ferrous-iron and arsenite concentrations in solution were determined by titration with cerium(IV) sulfate, as detailed in the Appendix to Chapter Five. The total iron and arsenic concentrations in solution were determined by Flame Atomic Adsorption Spectroscopy (FAAS). This enabled the ferric-iron and arsenate concentrations to be calculated by difference.

The oxygen utilisation rate of the culture in the bioreactors was measured off-line, in a sealed 1 ℓ vessel, using a Yellow Springs Instrument Model 5739 dissolved oxygen probe and a Hitech Micro Systems Dissolved Oxygen / Utilisation Rate Meter. A slurry sample was saturated with oxygen and the oxygen utilisation rate of the bacterial culture was determined by measuring the rate at which the dissolved oxygen concentration decreased.

The pH and redox potential of the bioleaching slurry were obtained by direct measurement using the Foxboro pH/ORP sensor and analyser.

6.1.3 Bacterial Culture

The mixed culture used in the bioleaching mini-plant originated from the Fairview Gold Mine in Barberton, South Africa. As stated previously, although it was originally reported to consist primarily of *Leptospirillum ferrooxidans* and *Thiobacillus thiooxidans* (Rawlings, 1995), it has subsequently been found to consist primarily of *L. ferrooxidans* and *Thiobacillus caldus* (Rawlings *et al.*, 1999).

6.1.4 Nutrient Medium

The composition of the nutrient solution used in the continuous bioleaching mini-plant was the same as that used during the investigation into the effect of arsenic on the batch bioleaching of an arsenopyrite/pyrite flotation concentrate (see Chapter Five). The composition of the nutrient solution is listed in Table 5-1.

6.1.5 Mineral Used

The mineral used in the continuous bioleaching mini-plant originated from the Fairview Gold Mine in Barberton, South Africa. The same flotation concentrate was also used in the initial ferric leaching work (see Section 3.1), and during the arsenic tolerance investigation (see Chapter Five).

Particle size analysis of a representative sub-sample of the concentrate indicated that it was within the size range recommended for the BIOX® process, *i.e.* 85 % passing 75 micron. The complete size, elemental and mineral analyses of the flotation concentrate are listed in Tables 3-1, 3-2 and 3-3, respectively.

6.1.6 Operating Conditions

The operating conditions used in the continuous bioleaching mini-plant are listed in Table 6-1.

Table 6-1: Bioleaching mini-plant operating conditions

Parameter		Level
T:	Primary	$40.0°C \leq T \leq 40.5$
	Secondary	$40.5°C \leq T \leq 41.0$
pH:	Primary	$1.65°C \leq pH \leq 1.75$
	Secondary	$1.65°C \leq pH \leq 1.75$
$[O_2]$:	Primary	± 6 mg.ℓ^{-1}
	Secondary	± 6 mg.ℓ^{-1}
ρ_{pulp} (feed)		± 20 % solids
$\tau_{overall}$ (hydraulic)		8, 7, 6, 5, 4.5 and 4 days

6.2 Results and Discussion

The mini-plant was operated at overall residence times of 4, 8 and 15 days for 5 tank residence times and at overall residence times of 4½, 5, 6 and 7 days for one plant residence time. During these periods the variation in the controlled variables, *viz.* T, $[O_2]$, pH, $\tau_{overall}$, ρ_{pulp}, and the resulting variations in the redox potential, E, oxygen utilisation rate, $-r_{O_2}$, and the ferrous-, $[Fe^{2+}]$, and ferric-iron, $[Fe^{3+}]$, and arsenite [As(III)] and arsenate [As(V)] concentrations in the primary and secondary bioreactors were monitored. This allowed the degree of control attained within the bioreactors to be assessed and enabled the effect of the overall residence time on the activity of the bacterial culture and the concentrations of the iron and arsenic species to be determined.

Perturbations in the agitation and aeration of the culture in the bioleaching mini-plant were carried out in an attempt to simulate power and/or equipment failures. Two disruption tests were performed; both were carried out while the mini-plant was operating at an overall residence time of 4 days. The first test consisted of a 15-minute interruption in the agitation and aeration of the secondary bioreactor and the second test consisted of a 17-hour interruption in the agitation and aeration of the primary bioreactor. One litre slurry samples were taken from the bioreactor at regular intervals during the disruption tests, and the oxygen utilisation rate of the bacterial culture determined. About 50 mℓ of the sample was retained for iron and arsenic analyses. This allowed the effect of the perturbation on both the activity of the bacterial cultures and the concentrations of the iron and arsenic species to be determined. The remainder of the sample was returned to the bioreactor.

6.2.1 Steady-state Results

6.2.1.1 Steady-state mini-plant performance

The performance of the continuous bioleaching mini-plant at a residence time of 8 days, with regard to the variation in the controlled variables, *viz.* temperature, dissolved oxygen concentration, pH, redox potential, residence time and feed pulp density, is illustrated in Figures 6.2 to 6.4.

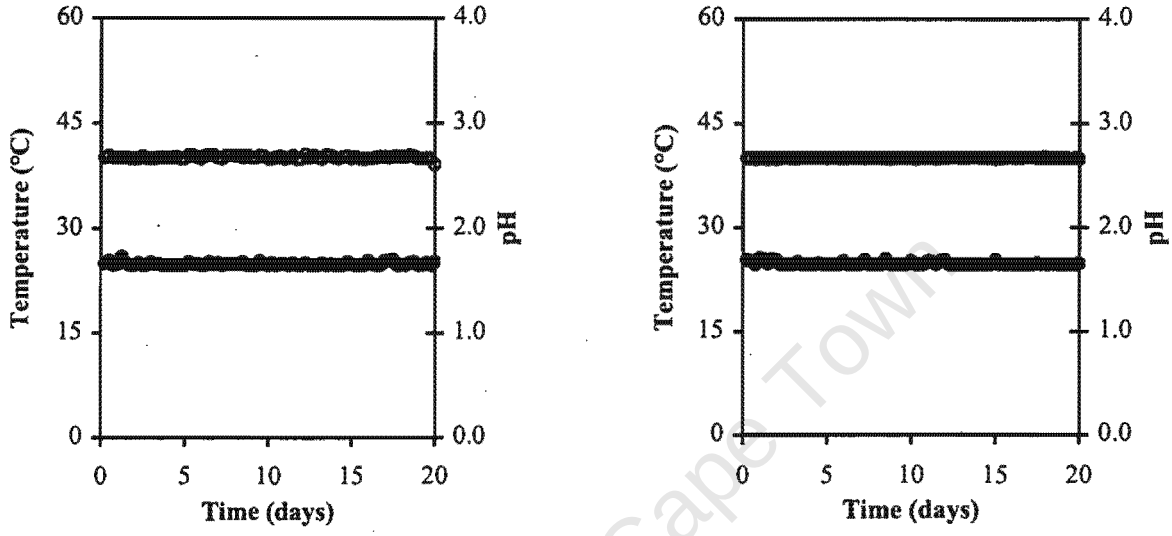

Figure 6.2: Variation in the [o] temperature and [•] pH of the slurry in the primary and secondary bioreactors at an overall residence time of 8 days.

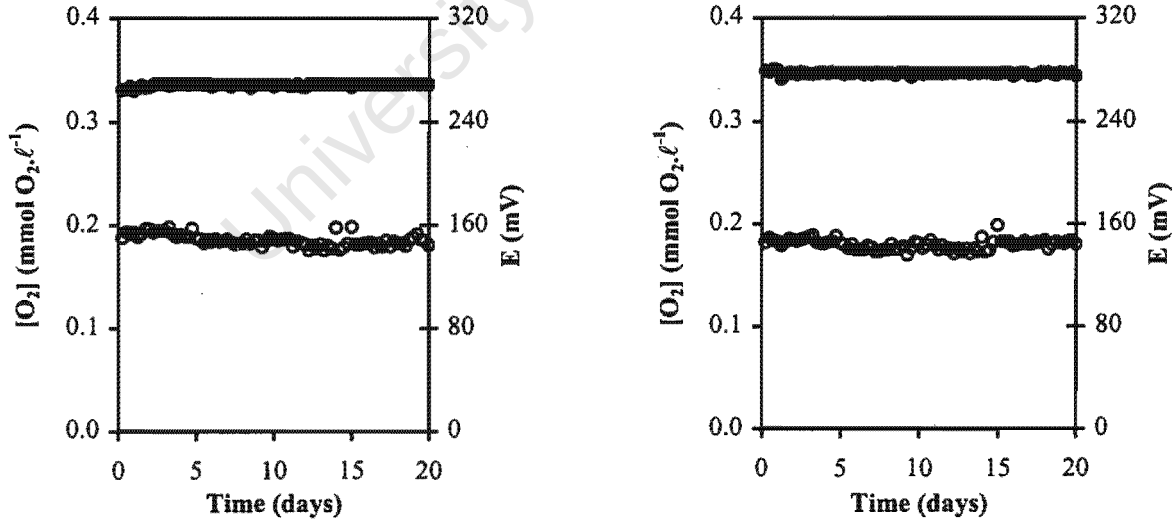

Figure 6.3: Variation in the [o] dissolved oxygen concentration and [•] redox potential of the slurry in the primary and secondary bioreactors at an overall residence time of 8 days.

From Figures 6.2 and 6.3, it is apparent that the range within which the controlled variables, *e.g.* T, pH and $[O_2]$, varied was narrow. From Figure 6.4 it is apparent that although there was some fluctuation in the values of m_{solids} and Q_{liquid}, the average values of these parameters was reasonably constant. This resulted in the average

values of ρ_{pulp} and $\tau_{overall}$ being fairly close to the target values, *viz.* 20 % and 8 days for the data shown in Figure 6.4.

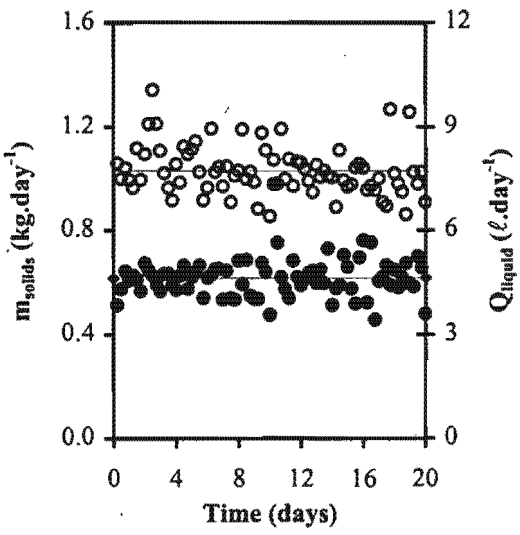

Figure 6.4(a): Variation in the [o] (dry) concentrate and [•] nutrient medium flow rates into the conditioning vessel at a residence time of 8 days.

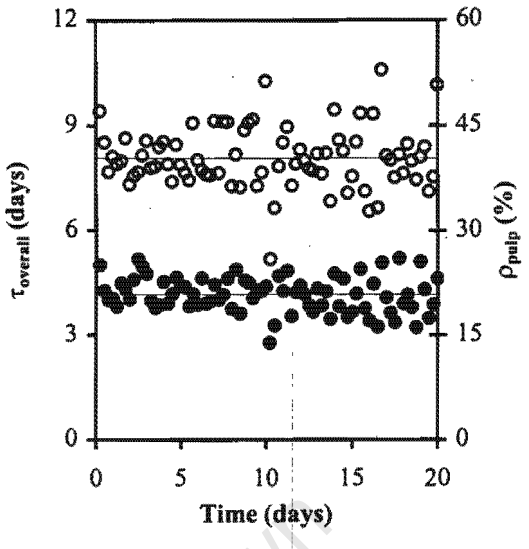

Figure 6.4(b): Variation in the [o] residence time and [•] feed pulp density (based on the dry concentrate and nutrient feed rates) of the bioleaching mini-plant at a residence time of 8 days.

The resulting variations in the ferrous- and ferric-iron and arsenite and arsenate concentrations measured in the conditioning vessel (feed), primary and secondary bioreactors, are shown in Figures 6.5 and 6.6.

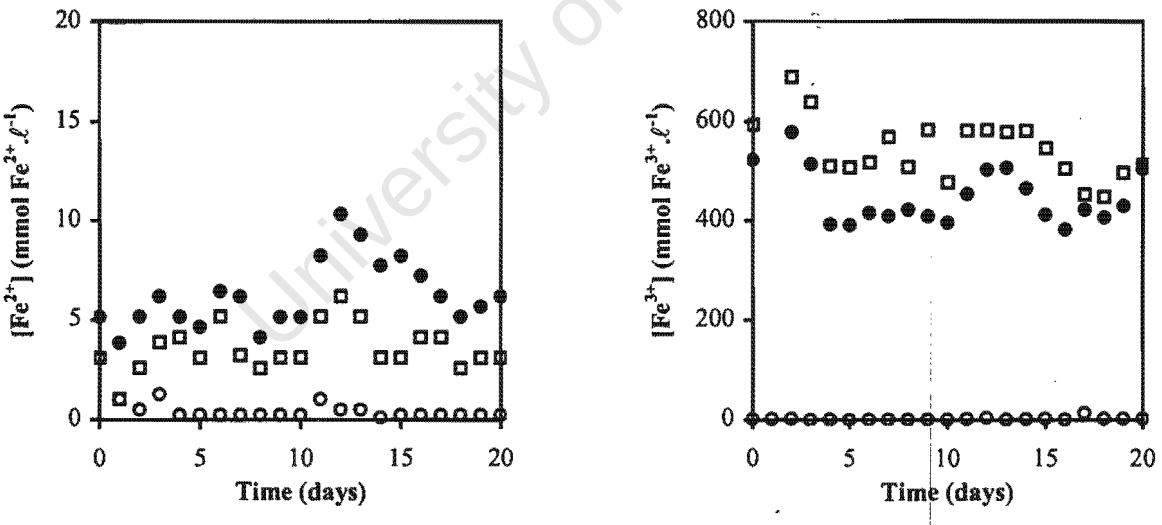

Figure 6.5: Variation in the ferrous- and ferric-iron concentrations measured in the [o] feed and the [•] primary and [□] secondary bioreactors of the bioleaching mini-plant at a residence time of 8 days.

From Figures 6.5 and 6.6 it is evident that, in spite of satisfactory operation and control of the mini-plant, the values of the ferrous- and ferric-iron and arsenite and arsenate concentrations measured in the primary and secondary bioreactors varied considerably from day to day. These variations are typical of continuous processes involving micro-organisms and were therefore anticipated.

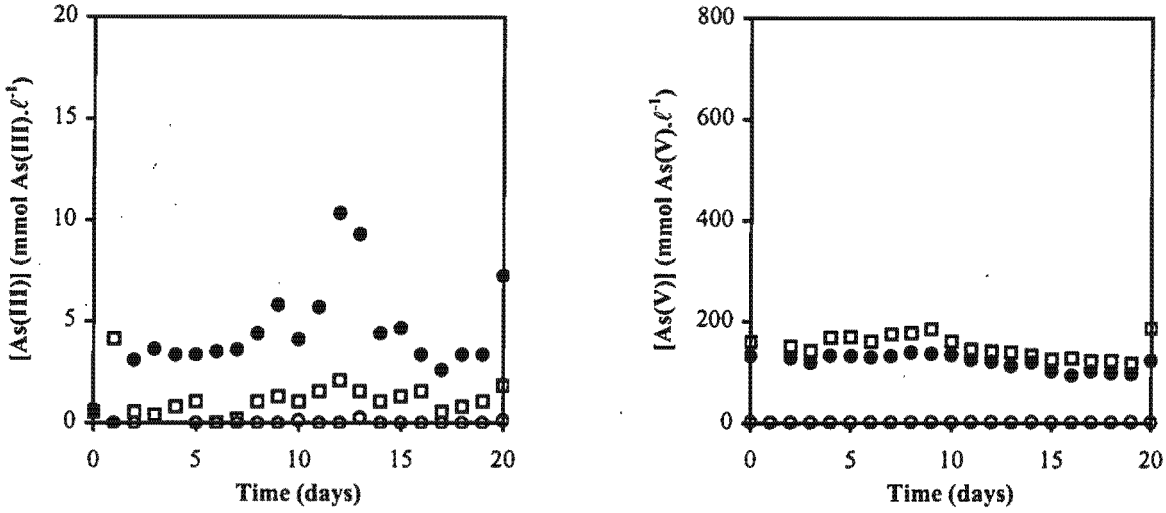

Figure 6.6: Variation in the arsenite and arsenate concentration measured in the [o] feed and the [•] primary and [□] secondary bioreactors of the bioleaching mini-plant at a residence time of 8 days.

Similar degrees of variation in the controlled variables and in the redox potential, oxygen utilisation rate and the iron and arsenic concentration and speciation were observed at the other residence times used (data not shown).

6.2.1.2 Steady-state oxygen utilisation rate, $-r_{O_2}$

The steady-state oxygen utilisation rate, $-r_{O_2}$, measured in the conditioning vessel (feed) and the primary and secondary bioreactors, at overall residence times of 4 and 15 days, is indicated in Table 6-2.

Table 6-2: Oxygen utilisation rate measured in the conditioning vessel (feed) and the primary and secondary bioreactors

$\tau_{overall}$ (days)	$-r_{O_2}$ (mmol $O_2.\ell^{-1}.h^{-1}$)		
	Conditioning vessel (feed)	Primary bioreactor	Secondary bioreactor
4	0	57	12
15	0	11	5

As expected the results shown in Table 6-2 confirm that the conditioning vessel (feed) did not contain aerobic bacteria. The results listed in Table 6-2 also indicate that the bacterial culture in the primary bioreactor was more active than the culture in the secondary bioreactor. This phenomenon can be attributed to substrate depletion. At the residence times used in this investigation most of the easily oxidisable ore was leached in the primary bioreactor.* This resulted in a "low" substrate concentration in the feed to the secondary bioreactor, which in turn resulted in the culture in the secondary bioreactor growing under substrate limiting conditions relative to the culture in the primary bioreactor.

* During a previous investigation using the same concentrate and an overall residence time of 4 days, 55 % of the pyritic sulfur was oxidised in the first stage and the overall sulfide conversion was in the region of 82 % (Miller and Hansford, 1992).

In addition, at "long" residence times, *viz.* 15 days, the cultures in the bioreactors were substrate limited relative to the cultures in the same bioreactor at "short" residence times, *viz.* 4 days. This resulted in the activities of the cultures in both bioreactors, increasing with decreasing residence time.

6.2.1.3 Steady-state ferrous-, Fe^{2+}, and ferric-iron, Fe^{3+}, and arsenite, As(III), and arsenate, As(V), concentrations

The average (steady-state) ferrous-, Fe^{2+}, and ferric-iron, Fe^{3+}, and arsenite, As(III), and arsenate, As(V), concentrations in the conditioning vessel and the primary and secondary bioreactors, at the residence times employed, are listed in Table 6-3 and indicated in Figures 6.7 and 6.8, respectively. The error bars in Figures 6.7 and 6.8 indicate the mean concentration ± the standard error of the concentrations measured at the respective residence time.

Table 6-3: Steady-state ferrous-iron, ferric-iron, arsenite and arsenate concentrations in the conditioning vessel (feed) and the primary and secondary bioreactors at the residence times employed

Bioreactor	τ (days)	$[Fe^{2+}]$ (mmol.ℓ^{-1})	$[Fe^{3+}]$ (mmol.ℓ^{-1})	[As(III)] (mmol.ℓ^{-1})	[As(V)] (mmol.ℓ^{-1})
Conditioning Vessel	4	0.63	10.04	0.41	1.48
	6	0.48	1.05	0.19	1.86
	7	0.39	0.09	0.04	2.36
	8	0.55	2.69	-0.03	2.19
	15	1.66	-0.91	0.20	2.78
Primary Bioreactor	4	2.14	337	3.58	107
	6	2.95	369	3.58	127
	7	2.90	418	3.44	111
	8	6.26	456	4.51	121
	15	3.01	296	4.32	62
Secondary Bioreactor	4	1.92	396	0.71	130
	6	1.55	369	0.46	153
	7	1.32	435	0.97	153
	8	3.56	547	1.15	150
	15	1.97	392	2.22	69

If it is assumed that no precipitation occurs, then at a feed pulp density, ρ_{pulp}, of 20 %, complete dissolution of the flotation concentrate (FeAsS = 12.68 %, FeS_2 = 37.18 %) within one residence time should result in $[As]_t \approx 156$ mmol.ℓ^{-1} and $[Fe]_t \approx 776$ mmol.ℓ^{-1} (in the secondary bioreactor).

If it is assumed that no precipitation occurred during the steady-state investigation, or if equimolar precipitation of ferric-iron and arsenate is assumed, then it is apparent that the results listed in Table 6-3 are consistent with the suggestion that the dissolution of arsenopyrite precedes that of pyrite (Miller and Hansford, 1992). If no precipitation is assumed, then the results listed in Table 6-3 suggest that the conversions of arsenopyrite and pyrite, at an overall residence time of 4 days, were in the region of 84 % and 39 %, respectively.

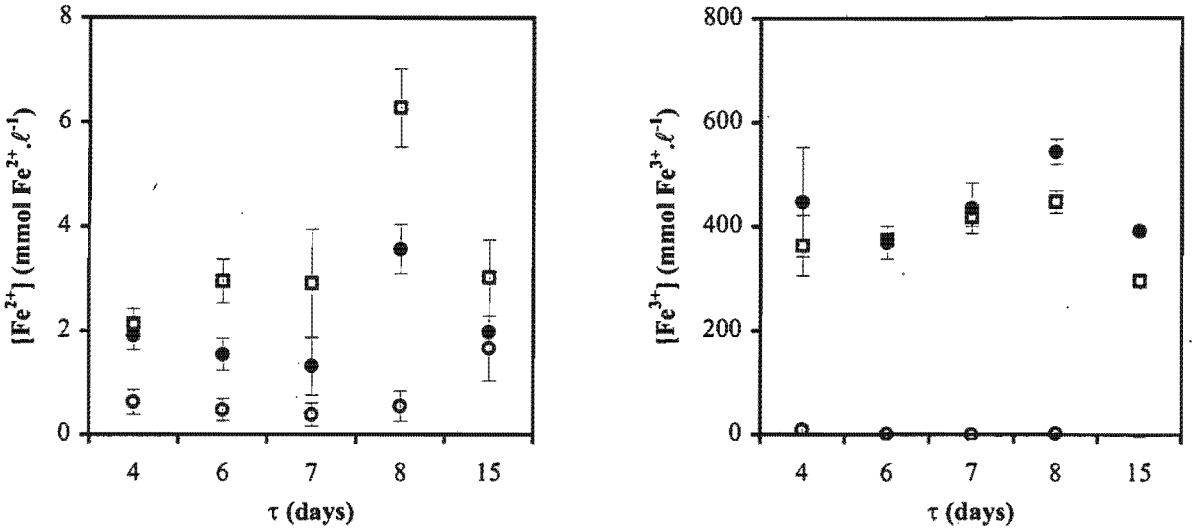

Figure 6.7: Variation in the concentrations of ferrous- and ferric-iron in the [o] conditioning vessel and the [•] primary and [□] secondary bioreactors with overall residence time.

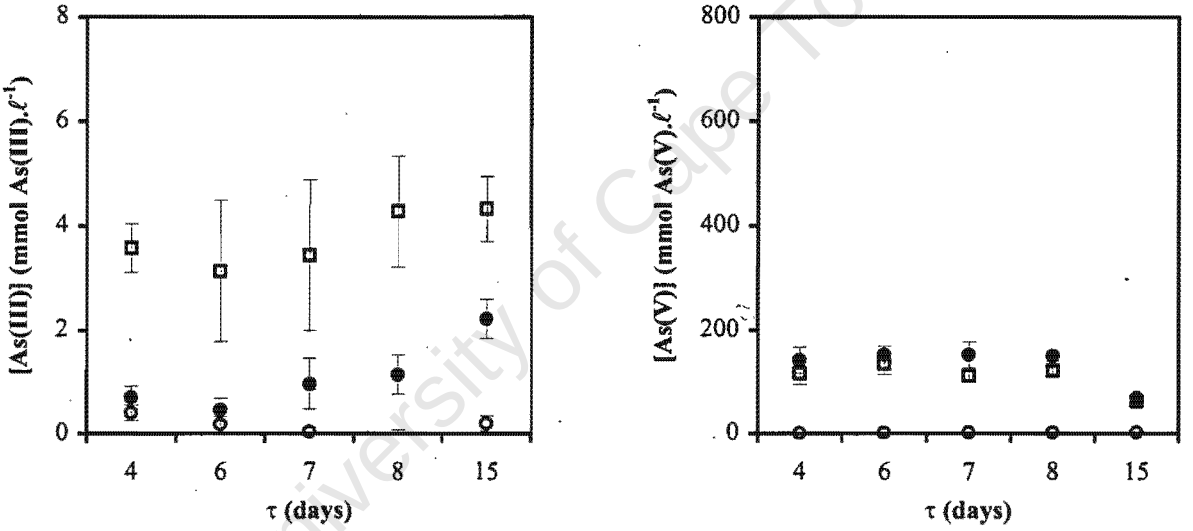

Figure 6.8: Variation in concentrations of arsenite and arsenate in the [o] conditioning vessel and the [•] primary and [□] secondary bioreactors with overall residence time.

A statistical analysis (Kruskal-Wallis test) of the results listed in Table 6-3 and shown in Figures 6.7 and 6.8 was performed in an attempt to determine whether or not the concentrations of the iron and arsenic species were dependent on the prevailing residence time.* The results of the statistical analysis are shown in Table 6-4. The null hypothesis, H_0, is that all the groups have the same mean and the alternative hypothesis, H_1, is that some, or all, of the means differ.† From Table 6-4 it is apparent that the results of the statistical analysis suggested that the Fe^{2+}, Fe^{3+} and As(V) concentrations in all the vessels and the As(III) concentration in the conditioning vessel and secondary bioreactor were influenced by changes in the overall residence time.

* The statistical analysis was performed with the assistance of Prof. T. Dunne of the Department of Statistical Sciences at the University of Cape Town.

† The groups referred to in Table 6-4 are the sets of data obtained for each ionic species at each of the residence times employed during the investigation.

Table 6-4: Results of the Kruskal-Wallis test

		N	Test Statistic	p-value	Result
Conditioning Vessel	Fe^{2+}	59	29.05	$p < 0.0005$	reject H_0
	Fe^{3+}	53	36.10	$p < 0.0005$	reject H_0
	As(III)	59	21.40	$p < 0.0005$	reject H_0
	As(V)	53	35.57	$p < 0.0005$	reject H_0
Primary Bioreactor	Fe^{2+}	60	35.17	$p < 0.0005$	reject H_0
	Fe^{3+}	55	37.19	$p = 0.1338$	**cannot reject H_0**
	As(III)	60	7.04	$p < 0.0005$	reject H_0
	As(V)	55	32.85	$p < 0.0005$	reject H_0
Secondary Bioreactor	Fe^{2+}	54	34.32	$p < 0.0005$	reject H_0
	Fe^{3+}	60	31.16	$p < 0.0005$	reject H_0
	As(III)	60	27.82	$p < 0.0005$	reject H_0
	As(V)	54	2.58	$p < 0.0005$	reject H_0

Although the results listed in Table 6-4 suggest that the Fe^{2+}, Fe^{3+} and As(V) concentrations in all the vessels, and the As(III) concentration in the conditioning vessel and secondary bioreactor were influenced by changes in the overall residence time, no clear relationships between these parameters and the residence time were evident.*

From the results listed in Table 6-3 and shown in Figures 6.7 and 6.8 it is however apparent that the ferric-iron and arsenate concentrations in the bioreactors were significantly higher than the ferrous-iron and arsenite concentrations. It is also evident from Table 6-3 and Figures 6.7 and 6.8 that the ferrous-iron and arsenite concentrations were higher in the primary bioreactor than in the secondary bioreactor. On the other hand, the ferric-iron and arsenate concentrations were higher in the secondary bioreactor than in the primary bioreactor. These observations are clearly consistent with the hypothesis that the bioleaching of arsenopyrite occurs via the multiple sub-process mechanism. According to this mechanism the arsenopyrite is chemically leached by ferric-iron (Iglesias *et al.*, 1993):

$$FeAsS + 5\,Fe^{3+} \rightarrow S^0 + As^{3+} + 6\,Fe^{2+} \qquad (6\text{-}1)$$

The ferrous-iron produced by this reaction is subsequently oxidised to ferric-iron by *L. ferrooxidans*:

$$4\,Fe^{2+} + O_2 + 4\,H^+ \rightarrow 4\,Fe^{3+} + 2\,H_2O \qquad (6\text{-}2)$$

The elemental sulfur produced during the (chemical) ferric leaching of the arsenopyrite is oxidised to sulfate by *T. caldus* (Pol'kin *et al.*, 1975):

$$2S + 3O_2 + 2H_2O \rightarrow 2H_2SO_4 \qquad (6\text{-}3)$$

Depending on the conditions in the bioreactors, the arsenite formed during the dissolution of the arsenopyrite may be oxidised to arsenate by ferric-iron (Shrestha, 1988):

* An increase in the residence time was expected to result in an increase in the ferric-iron and arsenate concentrations. Although the ferric-iron and arsenate concentrations in the bioreactors may have been influenced by the precipitation of ferric arsenate, the lack of trends in the concentrations of the iron and arsenic species suggests that the variations detected by the statistical analysis may have been erroneous. For this reason, no attempt was made to interpret the variations in the concentrations of these species with changes in the overall residence time.

$$H_3AsO_3 + 2Fe^{3+} + H_2O \rightarrow H_3AsO_4 + 2Fe^{2+} + 2H^+ \quad (6\text{-}4)$$

As suggested in Section 2.3, the above reaction requires the presence of a suitable catalytic surface and may in turn be followed by the precipitation of ferric arsenate (Dew *et al.*, 1997; Fernandez *et al.*, 1995):

$$2H_3AsO_4 + Fe_2(SO_4) \rightarrow 2FeAsO_4 + 3H_2SO_4 \quad (6\text{-}5)$$

It is also apparent from the results obtained that the long residence times used during the steady-state investigation, relative to washout (see Chapter Four), resulted in most of the mineral being oxidised in the primary bioreactor. This resulted in the ferric-iron and arsenate concentrations in both bioreactors being significantly higher than the respective ferrous-iron and arsenite concentrations. Furthermore, although most of the oxidation occurred in the primary bioreactor, further oxidation of the concentrate in the secondary bioreactor resulted in the ferric-iron and arsenate concentrations in the secondary bioreactor being greater than in the primary bioreactor.

In addition to the above, it is also apparent from the results listed in Table 6-3 and shown in Figures 6.7 and 6.8 that the concentrations of the iron and arsenic species in the conditioning vessel (feed) were low at all residence times. This observation is consistent with the oxygen utilisation rate data shown in Table 6-2 and was expected as the conditioning vessel contained neither bacteria, nor acid, nor added ferric-iron.

6.2.2 Secondary Bioreactor Disruption Test

As stated previously, the disruption test using the secondary bioreactor was carried out while the mini-plant was operating at an overall residence time of 4 days. At t = 0, aeration and agitation of the slurry in the secondary bioreactor was stopped and the overflow from the primary bioreactor diverted. In addition, the pH control was disabled to ensure that the pH was not adjusted based on readings obtained in the presence of settled ore. After 15 minutes, *i.e.* at t = 0.25 hours, aeration and agitation was resumed. pH control was enabled 15 minutes after agitation had been restored, *i.e.* at t = 0.50 hours, and continuous operation was resumed 90 minutes later, *i.e.* at t = 2 hours.

The variation in the oxygen utilisation rate, $-r_{O_2}$, measured during the disruption test carried out using the secondary bioreactor is shown in Figure 6.9 below. The error bars in Figure 6.9 indicate the mean oxygen utilisation rate ± standard deviation of the values shown in Figure 6.9.

From Figure 6.9, it appears as though the 15-minute interruption in the aeration and agitation of the slurry in the secondary bioreactor may have resulted in a slight decrease in the activity of the bioleaching culture. The oxygen utilisation rate before the interruption was 12.1 mmol $O_2.\ell^{-1}.h^{-1}$, after 15 minutes without aeration and agitation it was 11.8 mmol $O_2.\ell^{-1}.h^{-1}$. The activity of the culture continued to decrease once aeration and agitation had been restored; 15 minutes after aeration and agitation had been restored the oxygen utilisation rate had decreased to 10.9 mmol $O_2.\ell^{-1}.h^{-1}$. However, the "recovery" of the bioleaching culture in the secondary bioreactor was rapid; 45 minutes after the aeration and agitation had been restored the oxygen utilisation rate had increased to 12.2 mmol $O_2.\ell^{-1}.h^{-1}$.

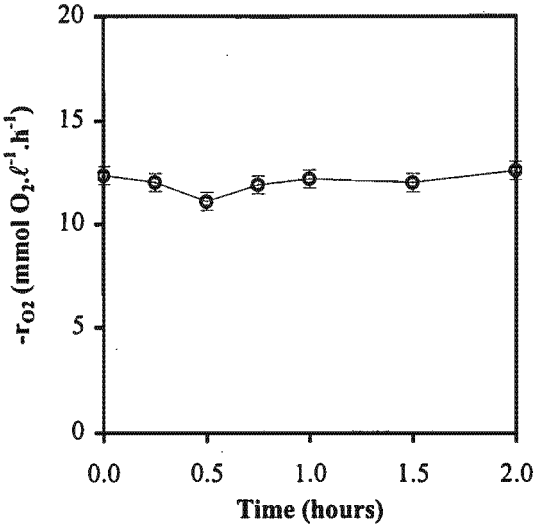

Figure 6.9: Variation in the oxygen utilisation rate during the disruption test carried out using the secondary bioreactor.

The measured variation in the ferrous- and ferric-iron concentrations observed during the disruption test are presented in Figure 6.10(a). The measured variations in the arsenite and arsenate concentrations are shown in Figure 6.10(b). The error bars in Figures 6.10(a) and (b) indicate the measured concentration ± standard error.*

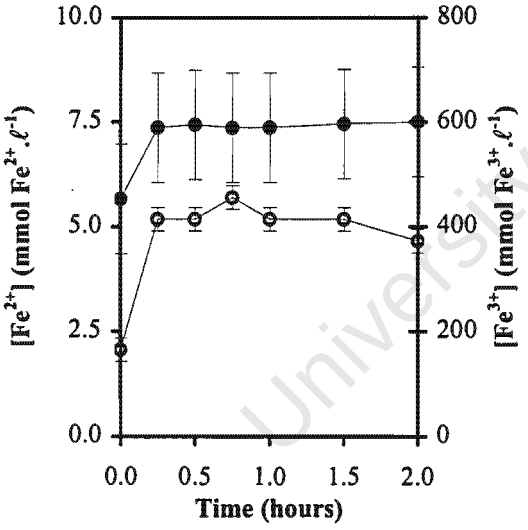

Figure 6.10(a): Variation in the concentrations of [o] ferrous- and [•] ferric-iron during the disruption test carried out using the secondary bioreactor.

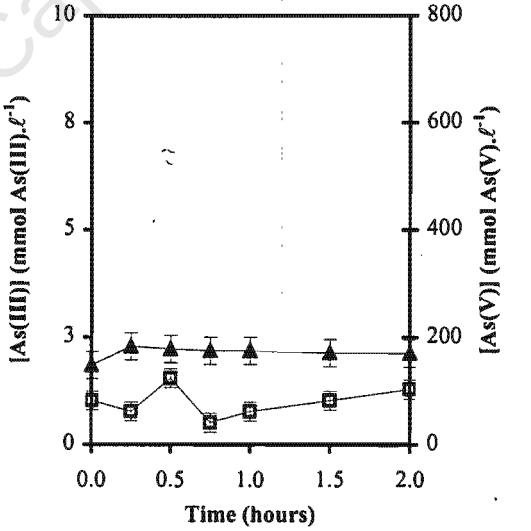

Figure 6.10(b): Variation in the concentrations of [□] arsenite and [▲] arsenate during the disruption test carried out using the secondary bioreactor.

From Figure 6.10(a), it is apparent that the ferrous-iron concentration increased during the period in which aeration and agitation were stopped. This increase in the ferrous-iron concentration may have been caused by one or more of the following:

* The values of the standard error determined during the steady-state investigation were used during the analysis of the perturbation results.

i) experimental error,
ii) the ferric leaching of arsenopyrite according to Equation 6-1,
iii) the oxidation of arsenite to arsenate by ferric-iron according to Equation 6-4, and/or
iv) the anaerobic reduction of ferric-iron by bacteria.

However, it is also apparent from Figure 6.10(a) that no significant variation in the ferrous-iron concentration was observed upon resumption of aeration and agitation. It is therefore suggested that the variations in the ferrous-iron concentration apparent in Figure 6.10(a) can be attributed to experimental error.

It is also apparent from Figures 6.10(a) and (b) that the ferric-iron and arsenate concentrations in the secondary bioreactor increased by about 135 and 35 mmol.ℓ^{-1}, respectively, during the period in which aeration and agitation of the culture in the secondary bioreactor was stopped. These changes in the ferric-iron and arsenate concentrations were too rapid to be a result of the ferric leaching of the flotation concentrate, nor were they consistent with the stoichiometry of ferric arsenate formation (dissolution) (Equation 6-5).* The above therefore suggest that the variations in the ferric-iron and arsenate concentrations apparent in Figures 6.10(a) and (b) were due to experimental error. This suggestion is supported by the fact that the concentrations of ferric-iron and arsenate did not change upon resumption of aeration and agitation, but remained at this "elevated level".

The variations in the arsenite concentration shown in Figure 6.10(b) could be explained in terms of variations of the relative rates of arsenite production by the leaching of arsenopyrite, and its subsequent oxidation to arsenate, by ferric-iron. However, the observations with regard to the variations in the ferrous- and ferric-iron and arsenate concentrations described above suggest that the variations in the arsenite concentration were most likely to be the result of experimental error.

The above therefore suggest that the variation in the oxygen utilisation rate shown in Figure 6.9 may also have been a result of experimental errors. In spite of this limitation, the results obtained do suggest that a 15-minute interruption in the aeration and agitation had no significant effect on the long or short term activity and viability of the bacterial culture. In addition, it is likely that a similar result would have been achieved had the disruption test been carried out using the culture in the primary bioreactor.

6.2.3 Primary Bioreactor Disruption Test

The disruption test performed using the primary bioreactor was also carried out while the mini-plant was operating at an overall residence time of 4 days. At t = 0, aeration and agitation of, and the feed to, the bacterial culture in the primary bioreactor was stopped and the pH control disabled. Aeration and agitation of the slurry in the primary bioreactor was resumed seventeen hours later, *i.e.* at t = 17 hours. pH control was enabled 15 minutes after aeration and agitation had been restored, *i.e.* at t = 17¼ hours. Continuous operation, at an overall residence time of 4 days, was begun 6½ hours after aeration and agitation had been restored, *i.e.* at t = 23½ hours. 26½ hours after aeration and agitation had been restored, *i.e.* at t = 43½ hours, the overall residence time was increased to 6 days. 56¾ hours after aeration and agitation had been restored, *i.e.* at t = 73¾ hours, problems were encountered with the solids feeder and continuous operation of the mini-plant was no longer possible.

* At τ = 2 days, ρ_{pulp} = 20 % (m/v), FeS_2 = 37.18 %, FeAsS = 12.68 %, complete dissolution of the arsenopyrite within one residence time results in $r_{As} \approx 3.25$ mmol.ℓ^{-1}.h^{-1}, $r_{Fe} \approx 16.125$ mmol.ℓ^{-1}.h^{-1}, *i.e.* the rate of precipitate dissolution necessary to account for the observed changes in the ferric-iron and arsenate concentrations would have been in the region of 33-43 times the rate of concentrate (bioleaching) dissolution.

As stated previously, one litre samples were taken from the bioreactor at regular intervals during the disruption test and the oxygen utilisation rate, $-r_{O_2}$, thereof determined. The values of the oxygen utilisation rate measured during the course of the disruption test performed using the primary bioreactor are shown in Figure 6.11.*

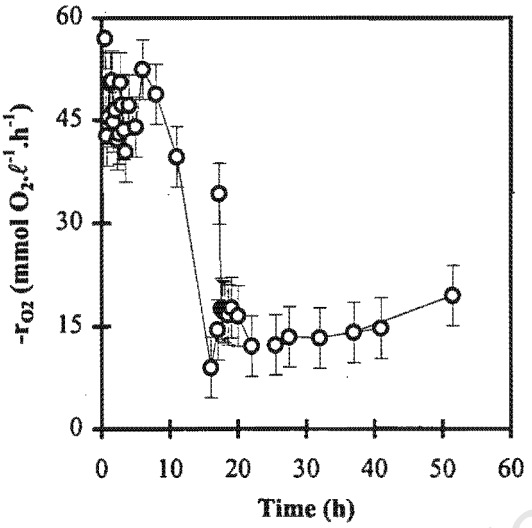

Figure 6.11: Variation in the oxygen utilisation rate during the disruption test carried out using the primary bioreactor.

From Figure 6.11, it is apparent that the oxygen utilisation rate of the bacterial culture did not decrease during the first 8 hours of the experiment. This was attributed to the intermittent sparging of a portion of the bacterial culture and led to the intervals between oxygen utilisation rate determinations being increased. The oxygen utilisation rate was measured at 15-minute intervals during the first 3½ hours of the disruption test, and at 30-minute intervals for the following hour. This was followed by intervals of 1½ and 2 hours between measurements. Increasing the intervals between successive oxygen utilisation rate measurements, to 3 and 5 hours, respectively, resulted in a decreasing trend in the activity of the culture becoming apparent; 16 hours after aeration and agitation had been stopped, the oxygen utilisation rate, had decreased to 9.0 mmol $O_2.\ell^{-1}.h^{-1}$, *i.e.* to about 20 % of its steady-state value of 46.1 mmol $O_2.\ell^{-1}.h^{-1}$.†

Aeration and agitation of the culture in the primary bioreactor was resumed an hour later, *i.e.* at t = 17 hours. However, the feed to the primary bioreactor remained diverted. Fifteen minutes after the resumption of aeration and agitation the oxygen utilisation rate of the bacterial culture in the primary bioreactor had increased from 14.5 to 34.3 mmol $O_2.\ell^{-1}.h^{-1}$. However the bacterial culture did not maintain this level of activity; 15 minutes later the oxygen utilisation rate had decreased to 17.5 mmol $O_2.\ell^{-1}.h^{-1}$. The activity of the culture continued to decrease for the following 4½ hours; 5 hours after aeration and agitation had been restored, *i.e.* at t = 22 hours, the oxygen utilisation rate had decreased to 12.1 mmol $O_2.\ell^{-1}.h^{-1}$.

It was thought that this gradual reduction in the oxygen utilisation rate was caused by arsenic toxicity and/or nutrient and substrate depletion. For this reason feeding of the mini-plant, at an overall residence time of 4 days, was begun 6½ hours after aeration and agitation had been restored, *i.e.* at t = 23½ hours. This resulted in a gradual increase in the oxygen utilisation rate, from 12.3 to 14.7 mmol $O_2.\ell^{-1}.h^{-1}$ over the following 8½ hours.

* The erratic nature of the oxygen utilisation rate values determined during the period in which the slurry was not aerated and agitated can be attributed to the lack of mixing.

† Although aerating some of the culture was expected to result in a longer period before a decrease in the activity of the culture was observed, as only 4.4 % of the culture was aerated this effect was expected to be small. However, the results obtained suggest that it might be possible to sustain the bacterial culture during power or equipment failures by intermittent aeration of small amounts of the culture in the bioreactors.

This relatively slow increase in the oxygen utilisation rate was attributed to washout Therefore, 26½ hours after aeration and agitation had been restored, *i.e.* at t = 43½ hours, the overall residence time was increased to 6 days. This resulted in an increase in the oxygen utilisation rate, from 14.7 to 19.5 mmol $O_2.\ell^{-1}.h^{-1}$, during the following 8 hours. At this stage, problems were encountered with the solids feeder and continuous operation of the mini-plant was no longer possible. For this reason, complete recovery of the mini-plant was not observed.

The variation in the measured ferrous-, [Fe^{2+}], and ferric-iron, [Fe^{3+}], concentrations during the disruption test performed using the primary bioreactor are shown in Figure 6.12(a). The variation in the measured arsenite, [As(III)], and arsenate, [As(V)], concentrations during the disruption test are shown in Figure 6.12(b).

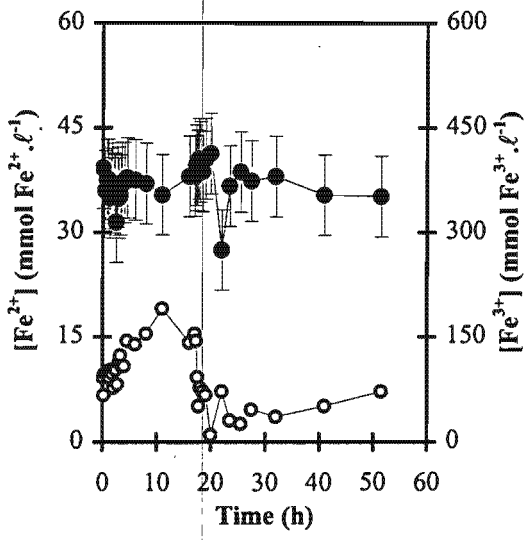

Figure 6.12(a): Variation in the concentrations of [○] ferrous- and [●] ferric-iron during the disruption test carried out using the primary bioreactor.

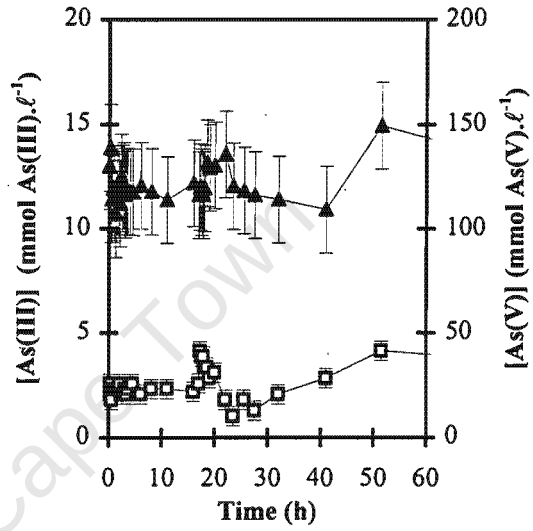

Figure 6.12(b): Variation in the concentrations of [□] arsenite and [▲] arsenate during the disruption test carried out using the primary bioreactor.

From Figure 6.12(a) it is apparent that the ferrous-iron concentration in the primary bioreactor increased during the 17 hours in which the slurry in the bioreactor was not aerated. It is also apparent from Figure 6.12(b) that the increase in the ferrous-iron concentration was not accompanied by an increase in the arsenite concentration. This suggests that the increase in the ferrous-iron concentration was a result of anaerobic ferric-iron respiration (Pronk *et al.*, 1992), rather than the ferric leaching of arsenopyrite. However, the rapid increase in the arsenite concentration once aeration and agitation was restored suggests that the arsenite produced by the chemical leaching of the arsenopyrite, according to Equation 6-1, was masked by the absence of agitation, *i.e.* the samples used for the determination of the iron and arsenic concentration and speciation were not representative of the slurry in the bioreactor.

Comparison of Figures 6.11 and 6.12(a) and (b) shows that the increase in the oxygen utilisation rate (once aeration and agitation of the slurry was restored) was accompanied by a rapid decrease in the ferrous-iron and arsenite concentrations. This can be attributed to bacterial ferrous-iron oxidation by *L. ferrooxidans*, according to Equation 6-2, and the oxidation of arsenite to arsenate by ferric-iron, according to Equation 6-4. The above observations are thus also consistent with the suggestion that the ferric leaching of arsenopyrite and the oxidation of arsenite by ferric-iron are competing reactions. During periods of reduced bacterial activity, the leaching of arsenopyrite predominates whereas during periods of rapid bacterial oxidation, the increased availability of

ferric-iron results in both the leaching of arsenopyrite and the oxidation of arsenite.* However, because the arsenate and ferric-iron concentrations in the primary bioreactor were approximately 30 and 160 times the ferrous-iron and arsenite concentrations, respectively, corresponding changes in their concentrations were not observed.

It is apparent from the results shown in Figures 6.12(a) and (b) that the ferric-iron and arsenate concentrations in the primary bioreactor varied significantly during the disruption test.† However, these variations in the ferric-iron and arsenate concentrations were too rapid to be the result of either the ferric leaching of the flotation concentrate or the dissolution of the ferric arsenate precipitate. Furthermore, the changes in the ferric-iron and arsenate concentrations were not consistent with the stoichiometry of ferric arsenate formation (dissolution) (Equation 6-5). The above therefore suggests that, as in the perturbation test performed using the secondary bioreactor, the observed variations in the ferric-iron and arsenate concentrations were due to experimental error.

From Figures 6.12(a) and (b), it is also apparent that both the ferrous-iron and arsenite concentrations increased once continuous operation, at an overall residence time of 4 days, was begun. This can be attributed to the increased availability of substrate and the "low" metabolic activity of the bacteria relative to the activity observed at the same residence time during the steady-state investigation. Although increasing the residence time to 6 days resulted in an increase in the oxygen utilisation rate, it had no apparent effect on the trends in the ferrous-iron and arsenite concentrations; both increased with an increase in the residence time. These trends in the oxygen utilisation rate, and the ferrous-iron and arsenite concentrations indicate that, although the bacterial culture was beginning to recover from the perturbation, its activity was still significantly reduced relative to its activity before the perturbation.‡ However, neither the oxygen utilisation rate of the bacterial culture, nor the ferrous-iron and arsenite concentrations reached levels comparable with those observed before the interruption. This suggests that long perturbations in the aeration and agitation of the bacterial culture have a long-term effect on the activity of the bacteria, *viz. L. ferrooxidans* and *T. caldus*.

In addition, comparison of the results obtained during the perturbation test with those presented in Chapter Five suggest that the slow recovery of the culture in the mini-plant may be a result of the bacteria being unable to protect themselves from the arsenate (and possibly the arsenite) concentrations present during routine mini-plant operation, rather than as a result of elevated concentrations caused by the perturbation itself, *i.e.* from the chemical leaching of arsenopyrite during the period of reduced bacterial activity.§ This may in turn be attributed to the arsenic tolerance mechanism being energy dependent. Therefore, during periods in which they have no energy source, the bacteria are unable to protect themselves from the toxic effects of the arsenic. This may apply to a lack of either oxygen or ferrous-iron, or both.

As stated previously, 56¾ hours after aeration and agitation had been restored, *i.e.* at t = 73¾ hours, problems were encountered with the solids feeder and continuous operation of the mini-plant was no longer possible. For this reason, complete recovery of the continuous bioleaching mini-plant was not observed. However, the bioreactor was operated in batch mode for a further 52 hours. During this time the ferrous-iron and arsenite concentrations decreased. The decrease in the ferrous-iron concentration can be attributed to substrate depletion whereas the decrease in the arsenite concentration can be attributed to an increase in its rate of oxidation, to

* As stated previously, under normal conditions the rate at which As(III) is oxidised to As(V) is in the region of 10 times the rate at which As(III) is produced by the bioleaching of arsenopyrite.

† A similar phenomenon was observed during the disruption test performed using the secondary bioreactor (see Figure 6.10).

‡ During the initial stages of recovery, the ferrous-iron concentration would be expected to be higher than during steady-state operation at the same residence time. However, the increased oxygen utilisation rate observed during the latter stages of recovery would be expected to be accompanied by a decrease in the ferrous-iron concentration. Furthermore, the resulting increased availability of ferric-iron would be expected to result in a reduction in the arsenite concentration.

§ During the period in which the aeration and agitation of the culture in the primary bioreactor was stopped, the arsenite concentration achieved a maximum concentration of about 5 mmol.ℓ^{-1}. In comparison, an initial arsenite concentration of 20 mmol.ℓ^{-1} had little effect on the batch bioleaching performance of the bacterial culture from the continuous bioleaching mini-plant.

arsenate, relative to its rate of production. The latter can in turn be attributed to the increased availability of ferric-iron.

6.3 Chapter Summary

The steady-state performance of a (mixed) mesophilic culture oxidising a sample of arsenopyrite/pyrite flotation concentrate from the Fairview Gold Mine in Barberton, South Africa, was investigated at residence times ranging from 4 to 15 days. Statistical analysis of the steady-state concentrations of the iron and arsenic species suggested that the arsenate and the ferric- and ferrous-iron concentrations in all the vessels, and the arsenite concentration in the conditioning vessel and secondary bioreactor, were influenced by changes in the overall residence time. However, no trends in the concentrations of these species with changes in the residence time were apparent; hence no attempt was made to interpret the variations in their concentration with changes in the residence time.

It was however apparent that the steady-state ferrous-iron and arsenite concentrations were higher in the primary bioreactor than in the secondary bioreactor, whereas the steady-state ferric-iron and arsenate concentrations were higher in the secondary bioreactor than in the primary bioreactor. These trends in the concentrations of the iron and arsenic species are consistent with the hypothesis that the bioleaching of arsenopyrite occurs via a multiple sub-process mechanism. According to this mechanism the mineral is chemically leached by ferric-iron; this solubilises the iron, arsenic and sulfur as ferrous-iron, arsenite and elemental sulfur, respectively. The arsenite, sulfur and ferrous-iron are subsequently oxidised to arsenate, sulfate and ferric-iron, presumably by ferric-iron, *L. ferrooxidans* and *T. caldus*, respectively. Thus, the primary role of the bacteria is the oxidation of the ferrous-iron to the ferric form; this maintains a high redox potential within the bioreactor which in turn ensures the continued leaching of the mineral.

In addition to the above, the results of the steady-state investigation indicated that, at the residence times used in this investigation, substrate depletion was responsible for the bacterial culture in the primary bioreactor being more active than the culture in the secondary bioreactor, and in the oxygen utilisation rate of the cultures in both bioreactors increasing with a decrease in the residence time.

Two disruption tests were carried out in an attempt to determine the effect of power or equipment failures on the performance of the continuous bioleaching mini-plant. The first test comprised of a 15-minute interruption in the agitation and aeration of the secondary bioreactor and the second test consisted of a 17-hour interruption in the agitation and aeration of the primary bioreactor. The response of the mini-plant to the perturbations was assessed by monitoring the oxygen utilisation rate of the bacterial culture and the concentrations of the iron and arsenic species, *viz.* $[Fe^{2+}]$, $[Fe^{3+}]$, [As(III)] and [As(V)].

Although it was possible to interpret the variations in the oxygen utilisation rate and the concentrations of the iron and arsenic species observed during the perturbation test performed using the secondary bioreactor in terms of the sub-processes involved, the results obtained suggested that they were probably the result of experimental errors. In spite of this limitation the results obtained suggest that short interruptions in the aeration and agitation do not have a significant effect on the activity of the bacteria, nor on the concentrations of the iron and arsenic species.

During the perturbation test performed using the primary bioreactor, the oxygen utilisation rate of the bacterial culture decreased during the period in which aeration and agitation was stopped. This decrease in the oxygen utilisation rate was accompanied by an increase in the ferric-iron and arsenic concentrations. The resumption of aeration and agitation resulted in an increase in the oxygen utilisation rate of the bacterial culture and a decrease in the ferric-iron and arsenic concentrations.

The trends in the oxygen utilisation rate and the ferrous-iron and arsenite concentrations observed during the perturbation experiments are thus consistent with the hypothesis that the bioleaching of arsenopyrite occurs via a multiple sub-process mechanism. They are also consistent with the hypothesis that the oxidation of arsenopyrite and arsenite, by ferric-iron, and the precipitation of ferric arsenate are competing reactions and that their respective rates depend on the absolute and relative concentrations of arsenopyrite, arsenite and arsenate in solution, and on the concentration and availability of ferric-iron. The concentration and availability of ferric-iron is in turn determined by the activity of the bacteria. During periods of reduced bacterial activity, the chemical leaching of arsenopyrite is the dominant reaction. However, during periods of rapid metabolic activity, the increased availability of ferric-iron in solution results in the oxidation of both arsenopyrite and arsenite.

Although the oxygen utilisation rate of the bacterial culture in the primary bioreactor increased upon resumption of aeration and agitation, it did not achieve the level of bacterial activity exhibited before the interruption. This suggests that a 17 hour perturbation in the aeration and agitation of the bacterial culture has a long term effect on the activity of the bacteria, *viz. L. ferrooxidans* and/or *T. caldus*.

Furthermore, comparison of the perturbation results with the results presented in Chapter Five suggests that the slow recovery of the mini-plant could be attributed to the bacteria being unable to protect themselves from the toxic effects of the arsenic concentration and speciation present during routine mini-plant operation. This can be attributed to the arsenic tolerance mechanism being energy dependent.

In addition to the above it is important to note that the oxygen utilisation rate of the bacterial culture in the primary bioreactor did not decrease significantly during the period in which small quantities of the culture was intermittently aerated. This suggests that it may be possible to sustain the bacterial culture during power and equipment failures by making use of "undersized" standby compressors.

6.4 Nomenclature

$[As(III)]$	concentration of arsenite	mmol As(III).ℓ^{-1}
$[As(V)]$	concentration of arsenate	mmol As(V).ℓ^{-1}
$[As]_t$	concentration of arsenic	mmol As.ℓ^{-1}
$[Fe^{2+}]$	concentration of ferrous-iron	mmol Fe^{2+}.ℓ^{-1}
$[Fe^{3+}]$	concentration of ferric-iron	mmol Fe^{3+}.ℓ^{-1}
$[Fe]_t$	concentration of iron	mmol Fe.ℓ^{-1}
E	redox potential of the solution	mV
m_{solids}	solids feed rate	kg.day^{-1}
$[O_2]$	concentration of oxygen	mmol O_2.ℓ^{-1}
p	significance level at which null hypothesis is accepted	dimensionless
Q_{liquid}	liquid feed rate	ℓ.day^{-1}

r_{O_2}	oxygen production rate	mmol $O_2.\ell^{-1}.h^{-1}$
t	time	h
T	temperature	°C
ρ_{pulp}	solids concentration	% ($m.v^{-1}$)
$\tau_{overall}$	overall (plant) residence time	day

6.5 References

Dew, D.W., Lawson, E.N. and Broadhurst, J.L. 1997. The BIOX® process for biooxidation of gold-bearing ores or concentrates, pp. 45-80. In: D.E. Rawlings (ed.), Biomining: theory, microbes and industrial processes. Springer-Verlag and Landes Bioscience, Berlin.

Fernandez, M.G.M., Mustin, C., De Donato, P., Barres, O., Marion, P. and Berthelin, J. 1995. Occurrences at mineral-bacteria interface during oxidation of arsenopyrite by *Thiobacillus ferrooxidans*. Biotechnology and Bioengineering **46**(1): 13-21.

Iglesias, N., Palencia, I. and Carranza, F. 1993. Removal of the refractoriness of a gold bearing pyrite-arsenopyrite ore by ferric sulphate leaching at low concentration, pp. 99-115. In: J.P. Hager (ed.), EPD Congress 1993, The Minerals, Metals and Materials Society, Warrendale, Co..

Miller, D.M. and Hansford, G.S. 1992. The use of the logistic equation for modelling the performance of a biooxidation pilot plant treating a gold-bearing arsenopyrite-pyrite concentrate. Minerals Engineering **5**(7): 737-749.

Pol'kin, S.I., Panin, V.V., Adamov, E.V., Karavaiko, G.I. and Chernyak, A.S. 1975. Theory and practice of utilizing micro-organisms in difficult-to-dress ores and concentrates, pp. 901-923. In: Proc. 11th International Mineral Processing Congress. Cagliari, 20-26 April 1975.

Pronk, J.T., De Bruyn, J.C., Bos, P. and Kuenen, J.G. 1992. Anaerobic growth of *Thiobacillus ferrooxidans*. Applied and Environmental Microbiology **58**: 2227-2230.

Rawlings, D.E. 1995. Restriction enzyme analysis of 16S rDNA genes for the rapid identification of *Thiobacillus ferrooxidans, Thiobacillus thiooxidans* and *Leptospirillum ferrooxidans* strains in leaching environments, pp. 9-17. In: T. Vargas, C.A. Jerez., J.V. Wiertz and H. Toledo (eds.), Biohydrometallurgical Processing **1**. University of Chile, Santiago.

Rawlings, D.E., Coram, N.J., Gardner, M.N. and Deane, M.N. 1999. *Thiobacillus caldus* and *Leptospirillum ferrooxidans* are widely distributed in continuous flow biooxidation tanks used to treat a variety of metal containing ores and concentrates, pp. 777-786. In: R. Amils, A. Ballester (eds.), Biohydrometallurgy and the environment toward the mining of the 21st century **A**. Elsevier, Amsterdam.

Shrestha, G.N. 1988. Microbial leaching of refractory gold ores. Australian Mining **October**: 48-51.

For Beth

Every person,
all the events of your life
are there because you have
drawn them there.
What you choose
to do with them is
up to you.

ILLUSIONS – Richard Bach

Chapter Seven

Modelling Continuous Bioleach Reactors*

Although the bioleaching of sulfide minerals has found widespread application for the recovery of copper, and the pre-treatment of refractory gold ores and concentrates, there are currently no mechanistic models that can be used to predict the performance of continuous bioleach reactors. This can be attributed to the complex nature of microbial interactions and difficulties encountered when attempting to measure the biomass concentration and growth rate, and the ferric and ferrous-iron concentrations in a 3-phase system.

The above difficulties have resulted in the logistic equation being the rate expression that has found the most widespread application to date. Because the logistic equation is not mechanistically based, it does not require knowledge of the bacterial concentration, or their activity. However, the lack of a mechanistic basis means that it cannot be used to predict the performance of bioleaching operations for different micro-organism/mineral combinations or across a range of operating conditions. In spite of this limitation, it has however proved useful in the modelling of batch and continuous laboratory, pilot and full-scale plant data for several pyrite and arsenopyrite/pyrite flotation concentrates (Crundwell, 1994; Dew *et al.*, 1993; Hansford and Miller, 1993; Hansford and Bailey, 1992; Hansford and Chapman, 1992; Miller and Hansford, 1992(a); Miller and Hansford, 1992(b); Pinches *et al.*, 1988).

The results of recent work on the bioleaching of pyrite (Boon *et al.*, 1995), the identification of *Leptospirillum ferrooxidans* and *Thiobacillus caldus* as the dominant species in continuous bioleaching plants (Rawlings *et al.*, 1999(a)) and the results presented in the preceding Chapters suggest that the bioleaching of sulfide mineral occurs via a multiple sub-process mechanism. According to this mechanism, the sulfide mineral is chemically oxidised by the ferric-iron present in the bioleaching medium. The ferrous-iron produced by this reaction is

---

* Breed, A.W. and Hansford, G.S. 1999. Studies on the mechanism and kinetics of bioleaching. Minerals Engineering **12**(4): 383-392.
Breed, A.W. and Hansford, G.S. 1999. Modelling continuous bioleach reactors. Biotechnology and Bioengineering **65**(1): 44-53.

subsequently oxidised to the ferric form by the bacteria; this serves to maintain a high redox potential in the bioreactors, thereby ensuring the continued leaching of the mineral.

As stated previously, the existence of a multiple sub-process mechanism implies that the kinetics of the respective sub-processes may be determined separately, and then combined to produce a model that predicts the performance of a continuous bioleach reactor. This is the approach followed below.

7.1 Steady-state Bacterial Ferrous-iron Oxidation

A schematic representation of steady-state mineral bioleaching in a continuous bioreactor is shown in Figure 7.1.

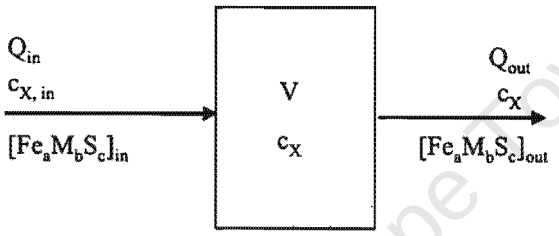

Figure 7.1: Schematic representation of steady-state mineral bioleaching in a continuous bioreactor.

During steady-state mineral bioleaching in a continuous bioreactor with volume, V, a bacterial mass balance yields:

$$Q_{in}\, c_{X,in} + V r_X = Q_{out}\, c_X \tag{7-1}$$

If the change in the volume resulting from the formation of biomass and the solubilisation of the mineral is assumed negligible:

$$Q_{in} = Q_{out} = Q \tag{7-2}$$

If the feed to the bioreactor is sterile:

$$c_{X,in} = 0 \tag{7-3}$$

Substituting Equations 7-2 and 7-3 into Equation 7-1 yields:

$$V r_X = Q c_X \tag{7-4}$$

If it is assumed that the bacteria follow Monod growth kinetics:

$$r_X = \mu c_X \tag{7-5}$$

Substituting Equation 7-5 into Equation 7-4, re-arranging and simplifying gives:

$$\mu = \frac{Q}{V} = \frac{r_X}{c_X} = D = \frac{1}{\tau} \tag{7-6}$$

In other words, the bacterial specific growth rate is inversely proportional to the hydraulic residence time.

It is assumed that both the maximum yield and maintenance coefficient on ferrous-iron, *viz.* $Y^{max}_{Fe^{2+}X}$ and $m_{Fe^{2+}}$, are energetic parameters which are constant for a particular bacterial species/substrate combination, they can be related via the empirical Pirt equation (Pirt, 1982):

$$-r^{bact}_{Fe^{2+}} = \frac{r_X}{Y^{max}_{Fe^{2+}X}} + m_{Fe^{2+}}\, c_X \tag{7-7}$$

Dividing Equation 7-7 by the concentration of biomass, c_X, yields:

$$-\frac{r^{bact}_{Fe^{2+}}}{c_X} = \frac{r_X}{Y^{max}_{Fe^{2+}X} c_X} + m_{Fe^{2+}} \tag{7-8}$$

The bacterial specific ferrous-iron oxidation rate, $q_{Fe^{2+}}$, is defined as the rate of ferrous-iron utilisation per mole of biomass:

$$q_{Fe^{2+}} = \frac{-r^{bact}_{Fe^{2+}}}{c_X} \tag{7-9}$$

Substitution of Equation 7-9 into Equation 7-8 and simplifying using Equation 7-6 yields:

$$q_{Fe^{2+}} = \frac{1}{Y^{max}_{Fe^{2+}X}\,\tau} + m_{Fe^{2+}} \tag{7-10}$$

The results of previous research (Van Scherpenzeel, 1996; Boon, 1996) and the results presented in Chapter Four have demonstrated that the bacterial specific ferrous-iron utilisation rate, $q_{Fe^{2+}}$, can be expressed as a function of the ferric/ferrous-iron ratio, $[Fe^{3+}]/[Fe^{2+}]$, using a simplified form of the equation suggested by Braddock *et al.* (1984):

$$q_{Fe^{2+}} = \frac{q^{max}_{Fe^{2+}}}{1 + K\dfrac{[Fe^{3+}]}{[Fe^{2+}]}} \tag{7-11}$$

Substituting Equation 7-11 into Equation 7-10 yields:

$$\frac{q^{max}_{Fe^{2+}}}{1 + K\dfrac{[Fe^{3+}]}{[Fe^{2+}]}} = \frac{1}{Y^{max}_{Fe^{2+}X}\,\tau} + m_{Fe^{2+}} \tag{7-12}$$

Equation 7-12 can be rearranged to give:

$$\frac{[Fe^{3+}]}{[Fe^{2+}]} = \frac{\left(\dfrac{\tau q^{max}_{Fe^{2+}} Y^{max}_{Fe^{2+}X}}{1+m_{Fe^{2+}}\tau Y^{max}_{Fe^{2+}X}}\right)-1}{K} \qquad (7\text{-}13)$$

Equation 7-13 shows that the ferric/ferrous-iron ratio (redox potential) is only a function of:*

i) the residence time, and
ii) a group of constants, the values of which are determined by the characteristics of the bacterial species (kinetic parameters) being used.

In other words, the ferric/ferrous-iron ratio, or redox potential of the bioleaching solution is not a function of either the pyrite concentration, or the total or ferrous-iron concentrations:

$$\frac{[Fe^{3+}]}{[Fe^{2+}]} = f(\tau) \neq f\left([FeS_2]_{in}, [Fe]_{tot}, [Fe^{2+}]\right) \qquad (7\text{-}14)$$

Although the above is not an intuitive result, it is expected from the assumption of Monod or Michaelis-Menten type kinetics.

Figure 7.2 shows the variation in the predicted ferric/ferrous-iron ratio and redox potential for *T. ferrooxidans*, a *Leptospirillum*–like bacterium and a predominantly *L. ferrooxidans* culture during steady-state bioreactor operation, at 30°C, for residence times ranging from 0 to 20 days.

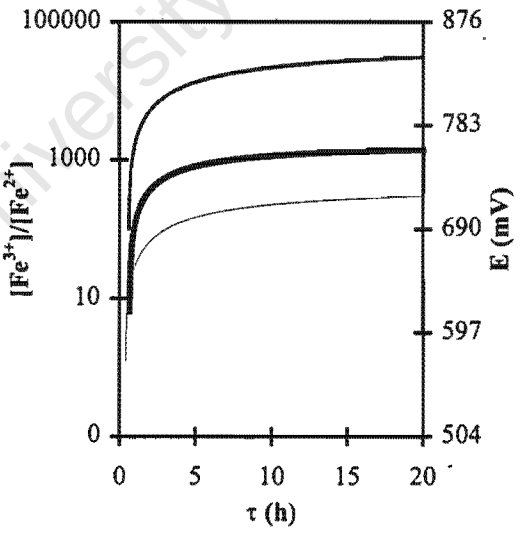

Figure 7.2: Variation in the predicted ferric/ferrous-iron ratio and redox potential with changing residence time, for [——] *T. ferrooxidans*, a [——] *Leptospirillum*-like bacterium and a [▬] predominantly *L. ferrooxidans* culture, at 30°C. Data were calculated using $E^{\circ\prime}_0$ = 572 mV, RT/zF = 26.13 (determined by probe calibration).

* It is important to note that values of the residence time lower than the residence time at which washout occurs result in negative values of the ferric/ferrous-iron ratio. Therefore, Equations 7-13 is only valid for $\tau > \tau_{washout}$. Furthermore, although Equation 7-13 indicates that the mineral conversion is not influenced by the pyrite concentration in the feed, high solids concentrations have been shown to result in oxygen transfer limitations (Bailey and Hansford, 1993). Equation 7-13 is therefore (also) only valid at solids concentrations at which mass transfer is not limiting.

In Figure 7.2, the values of the kinetic parameters for *T. ferrooxidans*, the *Leptospirillum*–like bacterium and the predominantly *L. ferrooxidans* culture were obtained from Boon (1996), Van Scherpenzeel *et al.* (1998) and the results presented in Chapter Four, respectively.

From Figure 7.2 it is clear that at residence times greater than about 1 day, the solution redox potential will be higher if the bacteria present are *Leptospirillum*–like as opposed to *T. ferrooxidans*. Therefore, at residences of more than 1 day, *L. ferrooxidans* will be the dominant micro-organism. This result is consistent with the results presented in Chapter Four, and those of previous research (Rawlings *et al.*, 1999(a); Rawlings *et al.*, 1999(b); Dew *et al.*, 1997; Rawlings, 1995; Boon, 1996; Hallmann *et al.*, 1993; Helle and Onken, 1988; Norris *et al.*, 1988).

7.2 Steady-state Bioleaching of Pyrite

During the steady-state leaching of pyrite in a continuous bioreactor performing a pyrite mass balance yields:

$$Q_{in}\left[FeS_2\right]_{in} + V\, r_{FeS_2} = Q_{out}\left[FeS_2\right]_{out} \tag{7-15}$$

If the change in the volumetric flow rate resulting from the formation of biomass and the dissolution of solids is neglected, Equation 7-15 can be simplified to give:

$$\left[FeS_2\right]_{in} - \left[FeS_2\right]_{out} = -\tau\, r_{FeS_2} \tag{7-16}$$

The reaction stoichiometry for the chemical (ferric) leaching of pyrite is:

$$FeS_2 + 14\,Fe^{3+} + 8\,H_2O \rightarrow 15\,Fe^{2+} + 16\,H^{+} + 2\,SO_4^{2-} \tag{7-17}$$

Therefore, for every mole of pyrite oxidised, 15 moles of ferrous-iron are produced:

$$15\, r_{FeS_2} = -\, r_{Fe^{2+}}^{chem} \tag{7-18}$$

Hence:

$$r_{FeS_2} = -\frac{r_{Fe^{2+}}^{chem}}{15} \tag{7-19}$$

Substituting Equation 7-19 into Equation 7-16 yields:

$$\left[FeS_2\right]_{in} - \left[FeS_2\right]_{out} = \frac{\tau\, r_{Fe^{2+}}^{chem}}{15} \tag{7-20}$$

By definition:

$$r_{Fe^{2+}}^{chem} = \upsilon_{Fe^{2+}} [FeS_2]_{out} \tag{7-21}$$

Boon (1996) suggested that the rate at which pyrite is degraded by ferric-iron could be described by an equation of the form:

$$\upsilon_{Fe^{2+}} = \frac{\upsilon_{Fe^{2+}}^{max}}{1 + B\frac{[Fe^{2+}]}{[Fe^{3+}]}} \tag{7-22}$$

Substitution of Equation 7-22 into Equation 7-21 yields:

$$r_{Fe^{2+}}^{chem} = \frac{\upsilon_{Fe^{+2}}^{max} [FeS_2]_{out}}{1 + B\frac{[Fe^{2+}]}{[Fe^{3+}]}} \tag{7-23}$$

Substituting Equation 7-23 into Equation 7-20 gives:

$$[FeS_2]_{in} - [FeS_2]_{out} = \frac{\frac{\tau}{15}\upsilon_{Fe^{2+}}^{max} [FeS_2]_{out}}{1 + B\frac{[Fe^{2+}]}{[Fe^{3+}]}} \tag{7-24}$$

Equation 7-24 may be simplified to yield:

$$[FeS_2]_{in} = [FeS_2]_{out}\left(1 + \frac{\frac{\tau}{15}\upsilon_{Fe^{2+}}^{max}}{1 + B\frac{[Fe^{2+}]}{[Fe^{3+}]}}\right) \tag{7-25}$$

Rearranging Equation 7-25 gives:

$$\frac{[FeS_2]_{in}}{[FeS_2]_{out}} = 1 + \frac{\frac{\tau}{15}\upsilon_{Fe^{2+}}^{max}}{1 + B\frac{[Fe^{2+}]}{[Fe^{3+}]}} \tag{7-26}$$

The conversion, or fraction of pyrite leached, X, is defined as:

$$X = \frac{[FeS_2]_{in} - [FeS_2]_{out}}{[FeS_2]_{in}} = 1 - \frac{[FeS_2]_{out}}{[FeS_2]_{in}} \tag{7-27}$$

Therefore, substitution of Equation 7-27 into Equation 7-26 and rearranging yields the following expression for the conversion of pyrite:

$$X = \frac{\frac{\tau}{15}\upsilon_{Fe^{2+}}^{max}}{1 + B\frac{[Fe^{2+}]}{[Fe^{3+}]} + \frac{\tau}{15}\upsilon_{Fe^{2+}}^{max}} \quad (7\text{-}28)^*$$

From Equation 7-28 it is clear that the fraction of mineral leached, *i.e.* the mineral conversion, is only a function of the ferric/ferrous-iron ratio or redox potential, the residence time and the characteristics of the pyrite itself. In other words, the conversion is not a function of the mineral concentration. As stated above, although this may not be an intuitive result, it is expected from the assumption of Monod or Michaelis-Menten type kinetics:

$$X = g\left(\frac{[Fe^{3+}]}{[Fe^{2+}]}\right) \neq f\left([FeS_2]_{in}\right) \quad (7\text{-}29)$$

According to Equation 7-13, the characteristics of the bacterial species and the prevailing residence time determine the ferric/ferrous-iron ratio. Therefore, substitution of Equation 7-13 into Equation 7-28 yields an expression in which the pyrite is only a function of:

i) the characteristics of the mineral,
ii) the characteristics of the bacterial species, and
iii) the prevailing residence time.

In other words:

$$X = \frac{\frac{\tau}{15}\upsilon_{Fe^{2+}}^{max}}{1 + B\left(\frac{K}{\left(\frac{\tau q_{Fe^{2+}}^{max} Y_{Fe^{2+}X}^{max}}{1 + m_{Fe^{2+}} \tau Y_{Fe^{2+}X}^{max}}\right) - 1}\right) + \frac{\tau}{15}\upsilon_{Fe^{2+}}^{max}} \quad (7\text{-}30)$$

Figure 7.3 shows the predicted variation in the pyrite conversion, using *T. ferrooxidans*, a *Leptospirillum*–like bacterium and a predominantly *L. ferrooxidans* culture in a continuous-flow bioreactor, at a temperature of 30°C and residence times ranging from 0 to 20 days. As in the case of Figure 7.2, the values of the kinetic parameters for *T. ferrooxidans*, the *Leptospirillum*–like bacterium and the predominantly *L. ferrooxidans* culture were obtained from Boon (1996), Van Scherpenzeel *et al.* (1998) and the results presented in Chapter Four, respectively. The kinetic parameters for pyrite were estimated from the results obtained by Boon (1996), *viz.* $\upsilon_{Fe^{2+}}^{max} = 0.0960$ mmol Fe^{2+}.(mmol FeS_2)$^{-1}$.h^{-1} and B = 2439. These predictions are compared with the results of Hansford and Chapman (1992) for the continuous bioleaching of a similar sized euhedral pyrite by an unidentified microbial species.

From Figure 7.3 it is apparent that the data of Hansford and Chapman (1992) follows the trend predicted by the model if the kinetic parameters for the *Leptospirillum*–like bacterium or the predominantly *L. ferrooxidans*

* As in the case of Equation 7-13, Equation 7-28 is only valid for $\tau > \tau_{washout}$ and in the absence of mass transfer limitations. Furthermore, it is only valid at redox potentials that are greater than the rest potential of the mineral.

culture are assumed. Furthermore, the values of the experimental values and those predicted using the kinetic parameters for the *Leptospirillum*–bacterium and the predominantly *L. ferrooxidans* culture are similar.*

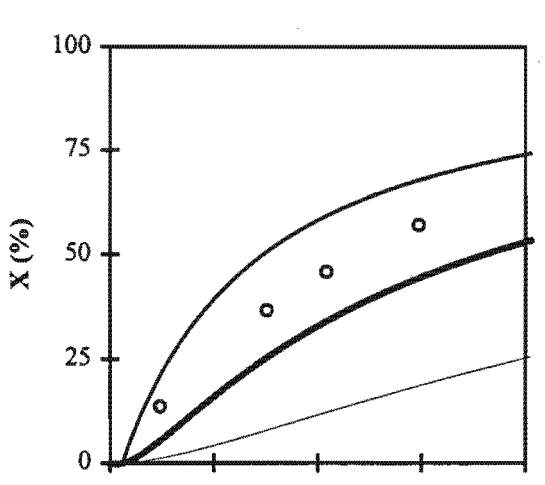

Figure 7.3: Comparison between the predicted variation in the pyrite conversion with changing residence time, at 30°C, for [——] *T. ferrooxidans*, a [▬] *Leptospirillum*-like bacterium, a [▬] predominantly *L. ferrooxidans* culture and the [o] experimental results obtained by Hansford and Chapman (1992).

At this stage, it is important to note that the kinetic parameters of the bacteria were determined at residence times of between 10 and 100 hours, while the kinetic parameters of the pyrite were determined in batch culture. Furthermore, neither the bacterial species, nor the pyrite used to determine the kinetic parameters were the same as those used by Hansford and Chapman (1992). In spite of this it appears as though the model developed is able to predict the performance of a continuous bioleach reactor.

7.3 Steady-state Bioleaching of Arsenopyrite

Performing an arsenopyrite mass balance across a bioleaching reactor operating at steady-state and simplifying yields:

$$[\mathrm{FeAsS}]_{in} - [\mathrm{FeAsS}]_{out} = -\tau r_{\mathrm{FeAsS}} \tag{7-31}$$

The results of previous research (Iglesias *et al.*, 1993) and the results presented in Chapter Three have demonstrated that the chemical (ferric) leaching of arsenopyrite occurs according to;

$$\mathrm{FeAsS} + 5\mathrm{Fe}^{3+} \rightarrow 6\mathrm{Fe}^{2+} + \mathrm{As}^{3+} + \mathrm{S}^{0} \tag{7-32}$$

* Although the microbial species used by Hansford and Chapman (1992) was not identified, the results described in Chapter Four, and those of previous research (Rawlings *et al.*, 1999(a); Rawlings *et al.*, 1999(b); Dew *et al.*, 1997; Boon, 1996; Rawlings, 1995; Hallmann *et al.*, 1993; Helle and Onken, 1988; Norris *et al.*, 1988) suggest that the micro-organism would have been *L. ferrooxidans*.

According to Equation 7-32, the relationship between the rate of mineral leaching and the rate of ferrous-iron production is:

$$r_{FeAsS} = -\frac{r_{Fe^{2+}}^{chem}}{6} \tag{7-33}$$

As in the case of pyrite leaching, the mineral specific ferrous-iron production rate is defined according to;

$$r_{Fe^{2+}}^{chem} = \upsilon_{Fe^{2+}} [FeAsS]_{out} \tag{7-34}$$

Substituting Equations 7.33 into Equation 7-31, and combining the result with Equation 7-34 yields:

$$[FeAsS]_{in} - [FeAsS]_{out} = \frac{\tau \upsilon_{Fe^{2+}} [FeAsS]_{out}}{6} \tag{7-35}$$

Equation 7-35 may be rearranged to yield:

$$\frac{[FeAsS]_{in}}{[FeAsS]_{out}} = 1 + \frac{\tau \upsilon_{Fe^{2+}}}{6} \tag{7-36}$$

The fraction of mineral leached, X, is defined according to Equation 7-27. Therefore, combining Equation 7-27, written in terms of the arsenopyrite concentration, with Equation 7-36 and simplifying yields an expression for the conversion of arsenopyrite:

$$X = \frac{\tau \upsilon_{Fe^{2+}}}{6 + \tau \upsilon_{Fe^{2+}}} \tag{7-37}$$

The results presented in Chapter Three indicated that the Butler-Volmer based model proposed by May *et al.* (1997), written in terms of the mineral specific rate of ferrous-iron production, best described the rate at which arsenopyrite is degraded by ferric-iron over the range of conditions used:

$$\upsilon_{Fe^{2+}}^{chem} = \upsilon_0 \left(e^{\alpha\beta(E - E')} - e^{(1-\alpha)\beta(E - E')} \right) \tag{7-38}$$

Substitution of Equation 7-38 into Equation 7-37 yields an expression for the conversion of arsenopyrite in terms of the redox potential of the bioleaching solution:

$$X = \frac{\tau \upsilon_0 \left(e^{\alpha\beta(E - E')} - e^{(1-\alpha)\beta(E - E')} \right)}{6 + \tau \upsilon_0 \left(e^{\alpha\beta(E - E')} - e^{(1-\alpha)\beta(E - E')} \right)} \tag{7-39}$$

From Equation 7-39 it is clear that, as in the case of pyrite leaching, the arsenopyrite conversion is a function of the redox potential (ferric/ferrous-iron ratio), the residence time and the characteristics of the mineral itself; not of the mineral concentration. As in the case of Equations 7-13 and 7-28, Equation 7-39 is only valid for $\tau > \tau_{washout}$, $E > E'$ and in the absence of mass transfer limitations. Furthermore, it is only valid for values of α and β such that $\alpha \neq \beta$.

As shown previously, the ferric/ferrous-iron ratio is a function of the characteristics of the bacterial species and the residence time. Therefore, substitution of Equation 7-13 into Equation 7-39 yields an expression in which the arsenopyrite conversion is only a function of the characteristics of the bacterial species, the prevailing residence time and the characteristics of the mineral:

$$X = \frac{\tau \upsilon_0 e^{\alpha\beta\left(E_0^* + \frac{RT}{zF}\ln\left(\frac{\left(\frac{\tau q_{Fe^{+2}}^{max} Y_{Fe^{2+}X}^{max}}{1+m_{Fe^{2+}}\tau Y_{Fe^{2+}X}^{max}}\right)-1}{K}\right)-E'\right)} - \tau \upsilon_0 e^{(1-\alpha)\beta\left(E_0^* + \frac{RT}{zF}\ln\left(\frac{\left(\frac{\tau q_{Fe^{+2}}^{max} Y_{Fe^{2+}X}^{max}}{1+m_{Fe^{2+}}\tau Y_{Fe^{2+}X}^{max}}\right)-1}{K}\right)-E'\right)}}{6 + \tau \upsilon_0 e^{\alpha\beta\left(E_0^* + \frac{RT}{zF}\ln\left(\frac{\left(\frac{\tau q_{Fe^{+2}}^{max} Y_{Fe^{2+}X}^{max}}{1+m_{Fe^{2+}}\tau Y_{Fe^{2+}X}^{max}}\right)-1}{K}\right)-E'\right)} - \tau \upsilon_0 e^{(1-\alpha)\beta\left(E_0^* + \frac{RT}{zF}\ln\left(\frac{\left(\frac{\tau q_{Fe^{+2}}^{max} Y_{Fe^{2+}X}^{max}}{1+m_{Fe^{2+}}\tau Y_{Fe^{2+}X}^{max}}\right)-1}{K}\right)-E'\right)}} \qquad (7\text{-}40)$$

Figure 7.4 shows the variation in the solution redox potential predicted by Equation 7-13 for *T. ferrooxidans*, a *Leptospirillum*-like bacterium and a predominantly *L. ferrooxidans* culture during steady-state bioreactor operation, at 38°C and pH 1.8, for residence times ranging from 0 to 5 days. As in the case of previous figures, the values of the kinetic parameters for *T. ferrooxidans*, the *Leptospirillum*-like bacterium and the predominantly *L. ferrooxidans* culture were obtained from Boon (1996), Van Scherpenzeel *et al.* (1998) and the results presented in Chapter Four, respectively. These predictions are compared with the redox potential measured in the 60 ℓ first stage of a continuous BIOX® mini-plant (Dew, 1998) operating at 40°C and pH 1.8.

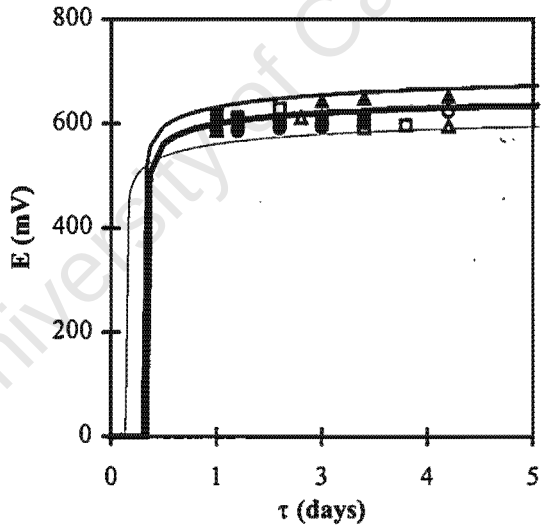

Figure 7.4: Comparison between the predicted and measured variations in the redox potential at different residence times for [——] *T. ferrooxidans*, a [——] *Leptospirillum*-like bacterium and a [▬] predominantly *L. ferrooxidans* culture, at 38°C and pH 1.8, and the redox potential measured in the 60 ℓ first stage of a continuous BIOX® mini-plant. [o] USA; [•] Uzbekistan No. 1; [□] Australia; [▲] Uzbekistan No. 2; [△] Dominican Republic No. 1; [■] Dominican Republic No. 2.

The effect of temperature on the maximum specific bacterial ferrous-iron utilisation rate of *T. ferrooxidans* and the *Leptospirillum*-like bacterium was accounted for by assuming that the relationship between temperature and $q_{Fe^{2+}}^{max}$ could be described using the Arrhenius equation, Equation 4-27. The activation energy determined by Nemati and Webb (1997) was used to account for the effect of temperature on the value of $q_{Fe^{2+}}^{max}$ determined by Boon (1996) for *T. ferrooxidans*. The activation energy determined in Chapter Four was used to account for the

effect of temperature on the value of $q_{Fe^{2+}}^{max}$ determined by Van Scherpenzeel *et al.* (1998) for the *Leptospirillum*-like bacterium. The effect of temperature on the values of K determined for *T. ferrooxidans* and the *Leptospirillum*-like bacterium, by Boon (1996) and Van Scherpenzeel *et al.* (1998), respectively, was accounted for by assuming that the relationship between K and temperature was linear, and could be described using the relationship determined in Chapter Four, *viz.* Equation 4-32.

From Figure 7.4, it is apparent that the variation in the predicted redox potential with changing residence time is similar for all three bacterial cultures. In addition, the redox potential predicted at a particular residence time is similar to the redox potential measured in the mini-plant.

The variation in the arsenopyrite conversion, at 38°C and pH 1.8, for residence times ranging from 0 to 5 days, predicted by Equation 7-40 is shown in Figure 7.5. The kinetic parameters for arsenopyrite were obtained from the results presented in Chapter Three. These predictions are compared with the results measured in the 60 ℓ first stage of a continuous BIOX® mini-plant (Dew, 1998).

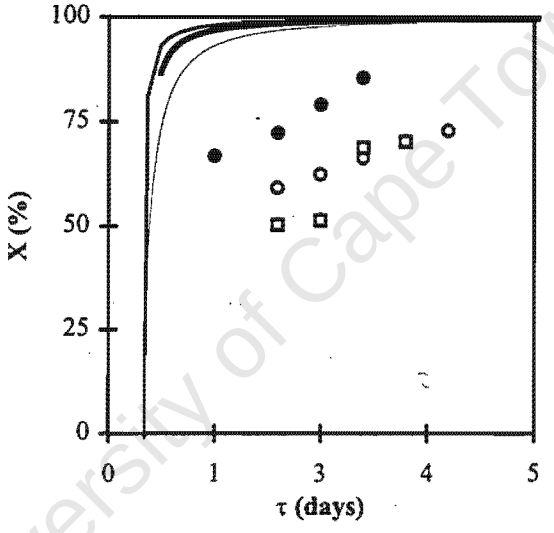

Figure 7.5: Comparison between the predicted and measured arsenopyrite conversion at different residence times for [——] *T. ferrooxidans*, a [——] *Leptospirillum*-like bacterium and a [▬▬] predominantly *L. ferrooxidans* culture, at 38°C, and the conversion measured in the 60 ℓ first stage of a BIOX® mini-plant. [o] USA; [•] Uzbekistan No. 1; [□] Australia.*

Rimstidt *et al.* (1994) reported the optimum temperature for the ferric (chloride) leaching of arsenopyrite to be 25°C; increasing the temperature above this resulted in a reduced rate of mineral dissolution. For this reason, the values of the kinetic parameters, υ_0, E', α and β determined at 25°C where used, *viz.* υ_0, = 900.80, E' = 516.83, α = 0.5029 and β = 0.0096.* In addition, it was assumed that the leaching of arsenopyrite precedes that of pyrite, *i.e.* the ferrous-iron produced was only because of the leaching of arsenopyrite.

From Figure 7.5, it is apparent that although the variation in the predicted arsenopyrite conversion with changing residence time is similar for all three bacterial cultures, the agreement between the predicted conversion and experimental data is poor. This result was however anticipated and can be explained as follows:

* The conversions for the concentrates from Uzbekistan No. 2, Dominican Republic No. 1 and Dominican Republic No. 2 could not be determined as the feed analysis was given in terms of total sulfide not as pyrite and arsenopyrite.

Although galvanic interactions have been shown to result in the leaching of arsenopyrite preceding that of pyrite (Malatt, 1998; Miller and Hansford, 1992(b)), this phenomenon still requires that the arsenopyrite is accessible to the leaching solution. However, this is not possible unless the concentrate is subjected to ultra-fine grinding, thereby ensuring almost complete liberation of the respective minerals. Malatt (1998) reported chemical ferric leaching rates, for pure arsenopyrite, ranging from 0.2 to 29 g $FeAsS.m^{-2}.h^{-1}$. During the investigation into the ferric leaching of arsenopyrite (see Chapter Three) the maximum rate at which pure (high grade and pyrite free) arsenopyrite was leached by ferric-iron was found to be either 0.51 or 2.6 g $FeAsS.m^{-2}.h^{-1}$, depending on the method used to determine the specific surface area of the mineral. In comparison, rates ranging from 0.02 to 0.06 g $FeAsS.m^{-2}.h^{-1}$ have been reported for the bioleaching of arsenopyrite in arsenopyrite/pyrite concentrates (Malatt, 1998; Hansford and Chapman, 1992; Miller and Hansford, 1992(a)). The differences in the chemical and bioleaching rates can thus be attributed to the chemical leaching rate experiments having been performed using high grade arsenopyrite and short time scales, relative to those encountered in bioleaching. For this reason, the measured rates of chemical ferric leaching were not significantly influenced by the liberation characteristics of the mineral. The arsenopyrite and pyrite contents of the concentrates used in the bioleaching mini-plant ranged from 1.2 to 14.8 % and 22.6 to 53.8 %, respectively (Dew, 1998). Therefore, the over-prediction of the model evident in Figure 7.5 can be attributed to some of the arsenopyrite being occluded by pyrite or gangue, or both pyrite and gangue, *i.e.* during the bioleaching of mixed mineral concentrates the liberation characteristics of the mineral will influence rate at which each mineral is leached.

The above explanation is consistent with the results of previous research which has shown that the rate at which sulfide minerals are degraded by both ferric-iron (May *et al.*, 1997) and bacteria (Miller and Hansford, 1992(a); Hansford and Chapman, 1992) is dependent on the surface area of the mineral being leached. It is therefore necessary to base the rate of mineral leaching on the surface area of the mineral that is exposed to the leaching medium, and to incorporate changes in the exposed surface area of the mineral with time.

It is possible to relate the concentration based mineral specific ferrous-iron production rate, $\upsilon_{Fe^{2+}}^{chem}$, to the surface area based mineral specific ferrous-iron production rate, $\xi_{Fe^{2+}}$:

$$\upsilon_{Fe^{2+}}^{chem} = \xi_{Fe^{2+}}\,\delta \tag{7-41}$$

The mineral specific ferrous-iron production rate based on the mineral surface area can in turn be described using equations analogous to Equations 7-22 and/or 7-38:

$$\xi_{Fe^{+2}} = \frac{\xi_{Fe^{+2}}^{max}}{1 + B\dfrac{[Fe^{+2}]}{[Fe^{+3}]}} \tag{7-42}$$

$$\xi_{Fe^{2+}} = \xi_0\left(e^{\alpha\beta(E - E')} - e^{(1-\alpha)\beta(E - E')}\right) \tag{7-43}$$

It is therefore possible to express the rate equations developed in terms of the surface area of the mineral. In addition, the above methodology can be extended to account for the size distribution of the feed, and changes

* The values of υ_0, E', α and β determined for the "leached" mineral were used (see Figure 3.9).

resulting from the leaching process, by means of a population balance model (Crundwell, 1994).* Therefore, although the approach detailed above has yet to be extensively tested and vigorously applied, the results obtained to date suggest that it has potential for predicting the performance of continuous bioleach reactors.

7.4 Chapter Summary

The results of this and previous research have shown that the bioleaching of sulfide minerals occurs via a multiple sub-process mechanism. According to this mechanism, it is possible to determine the kinetics of the chemical and bacterial sub-processes independently and then use the derived kinetic constants to predict the steady-state and dynamic performance of continuous bioleach reactors.

The results of this and other recent work have also shown that the ferric leaching kinetics of sulfide minerals and the kinetics of bacterial ferrous-iron oxidation are both governed by the ferric/ferrous-iron ratio (*i.e.* the redox potential).

The model developed proposes that the residence time and characteristics of the microbial species determine the redox potential of the bioleaching solution. The redox potential of the solution, the characteristics of the mineral being leached and the residence time in turn determine the degree of sulfide mineral leaching, *i.e.* the mineral conversion. A change in the residence time will therefore result in a change in the solution redox potential, and hence in the overall leaching rate of the mineral.

Although sulfur oxidising species have been detected during the bioleaching of mixed mineral concentrates containing arsenopyrite (Rawlings, 1995, Rawlings 1999(a)), chalcopyrite and pentlandite (Rawlings 1999(a)), the model developed, like previous models, does not consider the fate of the sulfur moiety. It is however acknowledged that the fate of the sulfur species may be important in the bioleaching of base metal sulfides as sulfur products may result in passivation of the mineral surface. Although sulfur oxidising bacteria will assist in the solubilisation of this passivating layer, the presence of a passivating layer consisting of sulfur may result in sulfur oxidation, and not ferrous-iron oxidation, being the rate limiting step.

Thus, although the above hypothesis has yet to be extensively tested and vigorously applied, the agreement of the model with the data of Hansford and Chapman (1992) and the results obtained in the 60 ℓ first stage of a continuous BIOX® mini-plant suggests that the model has potential for predicting the performance of continuous bioleach reactors, and hence finding use in engineering and industrial applications.

* Although the population model used by Crundwell (1994) makes use a shrinking particle model and the bioleaching of pyrite has been shown to occur by the formation of pores (Hansford and Drossou, 1988), this approach has proved successful (Crundwell, 1994).

7.5 Nomenclature

B	kinetic constant in chemical (ferric) pyrite oxidation	dimensionless
c_X	concentration of bacteria	mmol C.ℓ^{-1}
$c_{X,in}$	concentration of bacteria in the feed	mmol C.ℓ^{-1}
D	dilution rate	h^{-1}
E	redox potential of the solution (Pt-Ag/AgCl)	mV
E'	mineral rest potential	mV
E_0	redox potential of the solution at equilibrium	mV
E_0''	value of $E_0 + \frac{RT}{zF}\ln\left(\frac{\gamma_{Fe^{+3}}}{\gamma_{Fe^{+2}}}\right)$ for Ag/AgCl electrode	mV
F	Faraday constant	C.mol^{-1}
$[Fe^{2+}]$	concentration of ferrous-iron	mmol $Fe^{2+}.\ell^{-1}$
$[Fe^{3+}]$	concentration of ferric-iron	mmol $Fe^{3+}.\ell^{-1}$
$[Fe]_{tot}$	concentration of iron	mmol Fe.ℓ^{-1}
$[Fe_aM_bS_c]_{out}$	concentration of sulfide in the outlet	mmol $Fe_aM_bS_c.\ell^{-1}$
$[Fe_aM_bS_c]_{in}$	concentration of sulfide in the feed	mmol $Fe_aM_bS_c.\ell^{-1}$
$[FeAsS]_{in}$	concentration of arsenopyrite in the feed	mmol FeAsS.ℓ^{-1}
$[FeAsS]_{out}$	concentration of arsenopyrite in the outlet	mmol FeAsS.ℓ^{-1}
$[FeS_2]_{in}$	concentration of pyrite in the feed	mmol $FeS_2.\ell^{-1}$
$[FeS_2]_{out}$	concentration of pyrite in the outlet	mmol $FeS_2.\ell^{-1}$
K	kinetic constant in bacterial ferrous-iron oxidation	dimensionless
$m_{Fe^{2+}}$	maintenance coefficient on ferrous-iron	mmol Fe^{2+}.(mmol C)$^{-1}.h^{-1}$
$q_{Fe^{2+}}$	bacterial specific ferrous-iron oxidation rate	mmol Fe^{2+}.(mmol C)$^{-1}.h^{-1}$
$q_{Fe^{2+}}^{max}$	maximum bacterial specific ferrous-iron utilisation rate	mmol Fe^{2+}.(mmol C)$^{-1}.h^{-1}$
Q	volumetric flow rate	$m^3.h^{-1}$
Q_{in}	volumetric flow rate into the bioreactor	$m^3.h^{-1}$
Q_{out}	volumetric flow rate out of the bioreactor	$m^3.h^{-1}$
R	Universal gas constant	kJ.$K^{-1}.mol^{-1}$
$r_{Fe^{2+}}$	ferrous-iron production rate	mmol $Fe^{2+}.\ell^{-1}.h^{-1}$
$r_{Fe^{2+}}^{bact}$	bacterial ferrous-iron production rate	mmol $Fe^{2+}.\ell^{-1}.h^{-1}$
$r_{Fe^{2+}}^{chem}$	chemical ferrous-iron production rate	mmol $Fe^{2+}.\ell^{-1}.h^{-1}$
r_{FeAsS}	arsenopyrite production rate	mmol FeAsS.$\ell^{-1}.h^{-1}$
r_{FeS_2}	pyrite production rate	mmol $FeS_2.\ell^{-1}.h^{-1}$
r_X	biomass production rate	mmol C.$\ell^{-1}.h^{-1}$
T	absolute temperature	K
V	volume	m
X	fraction of sulfide oxidised	dimensionless
$Y_{Fe^{2+}X}^{max}$	maximum bacterial yield on ferrous-iron	mmol C.(mmol Fe^{2+})$^{-1}$
z	number of electrons involved in the reaction	dimensionless

α	fraction of mineral reacted at time, t	dimensionless
β	$\frac{zF}{RT}$	dimensionless
δ	specific surface area of sulfide	$m^2.mol^{-1}$
$\gamma_{Fe^{2+}}$	activity coefficient of ferrous-iron	dimensionless
$\gamma_{Fe^{3+}}$	activity coefficient of ferric-iron	dimensionless
μ	bacterial specific growth rate	h^{-1}
$\tau_{washout}$	residence time at which washout occurs	h
τ	residence time	h
υ_0	kinetic constant in chemical (ferric-iron) mineral oxidation	mmol Fe^{2+}.mmol^{-1}.h^{-1}
$\upsilon_{Fe^{2+}}$	pyrite specific ferrous-iron production rate	mmol Fe^{2+}.(mmol FeS_2)$^{-1}$.h^{-1}
$\upsilon_{Fe^{2+}}^{chem}$	specific mineral ferrous-iron production rate	mmol Fe^{2+} mmol.h^{-1}
$\upsilon_{Fe^{+2}}^{max}$	maximum pyrite specific ferrous-iron production rate	mmol Fe^{2+} (mmol FeS_2)$^{-1}$.h^{-1}
$\xi_{Fe^{2+}}$	mineral specific ferrous-iron production rate	mmol Fe^{2+}.m^{-2}.h^{-1}
$\xi_{Fe^{+2}}^{max}$	maximum mineral specific ferrous-iron production rate	mmol Fe^{2+}.m^{-2}.h^{-1}

7.6 References

Bailey, A.D. and Hansford, G.S. 1993. Factors affecting bio-oxidation of sulphide minerals at high solids concentrations: a review. Biotechnology and Bioengineering **42**: 1181-1189.

Boon, M. 1996. Theoretical and experimental methods in the modelling of bio-oxidation kinetics of sulfide minerals. Ph.D. Thesis. Delft University of Technology, Delft.

Boon, M., Hansford, G.S. and Heijnen, J.J. 1995. The role of bacterial ferrous-iron oxidation in the bio-oxidation of pyrite, pp. 153-163. In: T. Vargas, C.A. Jerez, J.V. Wiertz and H. Toledo (eds.), Biohydrometallurgical Processing **1**. University of Chile, Santiago.

Braddock, J.F., Luong, H.V. and Brown, E.J. 1984. Growth kinetics of *Thiobacillus ferrooxidans* isolated from arsenic mine drainage. Applied and Environmental Microbiology **48**(1): 48-55.

Crundwell, F.K. 1994. Mathematical modelling of batch and continuous bacterial leaching. Chem. Eng. J. **54**: 207-220.

Dew, D.W. 1998. Private communication.

Dew, D.W., Lawson, E.N. and Broadhurst, J.L. 1997. The BIOX® process for biooxidation of gold-bearing ores or concentrates, pp. 45-80. In: D.E. Rawlings (ed.), Biomining: theory, microbes and industrial processes. Springer-Verlag and Landes Bioscience, Berlin.

Dew, D.W., Miller, D.M. and Van Aswegen, P.C. 1993. GENMIN's commercialisation of the bacterial oxidation process for the treatment of refractory gold concentrates, pp. 229-237. In: Randol Gold Forum, Randol International.

Hallmann, R., Friedrich, A., Koops, H.P., Pommering-Röser, A., Zenneck, C. and Sand, W. 1993. Physicological characteristics of *Thiobacillus ferrooxidans* and *Leptospirillum ferrooxidans* and physicochemical factors influence microbial metal leaching. Geomicrobiology Journal **10**: 193-205.

Hansford, G.S. and Bailey, A.D. 1992. The logistic equation for modelling bacterial oxidation kinetics. Minerals Engineering **5**: 1355-1364.

Hansford, G.S. and Chapman, J.T. 1992. Batch and continuous bio-oxidation kinetics of a refractory gold-bearing pyrite/arsenopyrite concentrate. Minerals Engineering **5**(6): 597-612.

Hansford, G.S. and Drossou, M. 1988. A propagating pore model for the batch bioleach kinetics of a gold-bearing pyrite, pp. 345-358. In: P.R. Norris and D.P. Kelly (eds.), Biohydrometallurgy. Science and Technology Letters, Kew, Surrey.

Hansford, G.S. and Miller, D.M. 1993. Biooxidation of a gold-bearing pyrite-arsenopyrite concentrate. FEMS Microbiology Reviews **11**: 175-182.

Helle, U. and Onken, U. 1988. Continuous bacterial leaching of pyritic flotation concentrate by mixed cultures, pp. 61-75. In: P.R. Norris and D.P. Kelly (eds.), Biohydrometallurgy. Science and Technology Letters, Kew, Surrey.

Iglesias, N., Palencia, I. and Carranza, F. 1993. Removal of the refractoriness of a gold bearing pyrite-arsenopyrite ore by ferric sulphate leaching at low concentration, pp. 99-115. In: J.P. Hager (ed.), EPD Congress 1993, The Minerals, Metals and Materials Society, Warrendale, Co..

Malatt, K. 1998. The bacterial oxidation of gold-bearing pyrite/arsenopyrite concentrates. Ph.D. Thesis, Curtin University of Technology, Perth, WA.

May, N., Ralph, D.E. and Hansford, G.S. 1997. Dynamic redox potential measurement for determining the ferric leach kinetics of pyrite. Minerals Engineering **10**(11): 1279-1290.

Miller, D.M. and Hansford, G.S. 1992(a). Batch biooxidation of a gold-bearing pyrite-arsenopyrite concentrate. Minerals Engineering **5**(6): 613-629.

Miller, D.M. and Hansford, G.S. 1992(b). The use of the logistic equation for modelling the performance of a biooxidation pilot plant treating a gold-bearing arsenopyrite-pyrite concentrate. Minerals Engineering **5**(7): 737-749.

Nemati, M. and Webb, C. 1997. A kinetic model for biological oxidation of ferrous iron by *Thiobacillus ferrooxidans*. Biotechnology and Bioengineering **53**(5): 478-486.

Norris, P.R., Barr, D.W. and Hinson D. 1988. Iron and mineral oxidation by acidophilic bacteria: affinities for iron and attachment to pyrite, pp. 43-59. In: P.R. Norris and D.P. Kelly (eds.), Biohydrometallurgy. Science and Technology Letters, Kew, Surrey.

Pinches, A., Chapman, J.T., Te Riele, W.A.M. and Van Staden, M. 1988. The performance of bacterial leach reactors for the pre-oxidation of refractory gold-bearing sulfide concentrates, pp. 329-344. In: P.R. Norris and D.P. Kelly (eds.), Biohydrometallurgy. Science and Technology Letters, Kew, Surrey.

Pirt, S.J. 1982. Maintenance energy: a general model for energy limited and energy sufficient growth. Arch. Microbiol. **133**: 300-3-2.

Rawlings, D.E. 1995. Restriction enzyme analysis of 16S rDNA genes for the rapid identification of *Thiobacillus ferrooxidans, Thiobacillus thiooxidans* and *Leptospirillum ferrooxidans* strains in leaching environments, pp. 9-17. In: T. Vargas, C.A. Jerez., J.V. Wiertz and H. Toledo (eds.), Biohydrometallurgical Processing **1**. University of Chile, Santiago.

Rawlings, D.E., Coram, N.J., Gardner, M.N. and Deane, M.N. 1999(a). *Thiobacillus caldus* and *Leptospirillum ferrooxidans* are widely distributed in continuous flow biooxidation tanks used to treat a variety of metal containing ores and concentrates, pp. 777-786. In: R. Amils, A. Ballester (eds.), Biohydrometallurgy and the environment toward the mining of the 21st century **A**. Elsevier, Amsterdam.

Rawlings, D.E., Tributsch, H. and Hansford, G.S. 1999(b). Reasons why *Thiobacillus ferrooxidans* is not the dominant iron-oxidising bacterium in many commercial processes for the biooxidation of pyrite and related ores. Microbiology **145**(1): 5-13.

Rimstidt, J.D., Chermak, J.A. and Gagen, P.M. 1994. Rates of reaction of galena, sphalerite, chalcopyrite and arsenopyrite with Fe(III) in acidic solutions, pp. 2-13. In: C.N. Alpers and D.W. Blowes (eds.), Environmental Geochemistry of sulfide oxidation. ACS Symposium Series **550**, Washington D.C.

Van Scherpenzeel, D.A., Boon, M., Hansford, G.S. and Heijnen, J.J. 1998. Kinetics of ferrous iron oxidation by *Leptospirillum* bacteria in continuous cultures. Biotechnology Progress **14**: 425-433.

Van Scherpenzeel, D.A. 1996. The kinetics of ferrous-iron oxidation by *Leptospirillum*-like bacteria in absence and in presence of pyrite and pyrite/arsenopyrite mixtures in continuous and batch cultures. M.Sc. Dissertation, University of Cape Town, Cape Town.

For my late father, Louis Breed

Don't be
dismayed at good-byes.
A farewell is necessary before
you can meet
again.

And meeting
again, after moments or
lifetimes, is certain for
those who are
friends.

ILLUSIONS – Richard Bach

Chapter Eight

Conclusions and Recommendations

The broad objective of the work presented in this thesis was to attempt to test the applicability of the two-step mechanism for the bioleaching of arsenopyrite, and to provide kinetic data on the chemical and bacterial sub-processes involved. An additional objective of the work was to attempt to gain some insight into the mechanism of arsenic toxicity, and resistance, and to attempt to determine the relationship between arsenic toxicity and perturbations in the aeration and agitation of bioreactors.

8.1 Mechanism of Arsenopyrite Bioleaching

During the steady-state bioleaching of an arsenopyrite/pyrite flotation concentrate in a 2-stage continuous bioleaching mini-plant, the ferrous-iron and arsenite concentrations were higher in the primary than in the secondary bioreactor, irrespective of the residence time employed. On the other hand, the ferric-iron and arsenate concentrations in the secondary bioreactor were higher than in the primary bioreactor, at all residence times.

During the perturbation studies, the ferrous-iron and arsenite concentrations in the bioreactors increased during the period in which the bioreactors were not aerated, *i.e.* in the absence of bacterial activity, and decreased on resumption of aeration and agitation. Similar trends in the concentrations of ferrous-iron and arsenite were observed during the bacterial lag and exponential growth phases of the batch bioleaching experiments performed at elevated arsenite and arsenate concentrations.

These trends are clearly consistent with the hypothesis that the bioleaching of arsenopyrite occurs via a multiple sub-process mechanism. This conclusion is further supported by the identification of *Leptospirillum ferrooxidans*

and *Thiobacillus caldus* as the dominant ferrous-iron and sulfur oxidising species, respectively, present during the continuous bioleaching of this arsenopyrite/pyrite concentrate.

According to the multiple sub-process mechanism, the primary attack of the sulfide mineral is by ferric-iron; for the case of arsenopyrite leaching this occurs according to the stoichiometry proposed by Iglesias *et al.* (1993):

$$FeAsS + 5Fe^{3+} \rightarrow S^0 + As^{3+} + 6Fe^{2+} \quad (8\text{-}1)$$

Greater values of the ferric- and ferrous-iron stoichiometric coefficients determined during previous studies can be attributed to the subsequent oxidation of some, or all, of the sulphur and arsenite species, to sulphate and arsenate, respectively. The ferrous-iron produced by Equation 8-1 is subsequently oxidised to ferric-iron by ferrous-iron oxidising micro-organisms, *viz. L. ferrooxidans*, present in the bioleaching solution according to;

$$4Fe^{2+} + O_2 + 4H^+ \rightarrow 4Fe^{3+} + 2H_2O \quad (8\text{-}2)$$

The oxidation of ferrous-iron to the ferric form maintains a high redox potential within the system thereby ensuring the continued leaching of the mineral. Oxidation of the sulfur moiety proceeds via the formation of polysulfides, and elemental sulphur, with the elemental sulphur being oxidised to sulphate by sulphur oxidising bacteria, *viz. T. caldus*, present in the bioleaching solution:

$$2S + 3O_2 + 2H_2O \rightarrow 2H_2SO_4 \quad (8\text{-}3)$$

Depending on the conditions employed, the dissolution of arsenopyrite may be followed by the oxidation of arsenite to arsenate:

$$H_3AsO_3 + 2Fe^{3+} + H_2O \rightarrow H_3AsO_4 + 2Fe^{2+} + 2H^+ \quad (8\text{-}4)$$

Although the positive free energy value for the reaction shown in Equation 8-4 suggests that it is not thermodynamically possible, the results obtained during the current investigation, together with those of previous research, suggest that sulphide minerals which are more noble than arsenopyrite, can act as conduits of charge, thereby facilitating the transfer of electrons from one arsenite ion to two ferric-iron ions.

The oxidation of arsenite to arsenate may be followed by the precipitation of ferric arsenate (Dew *et al.*, 1997):

$$2H_3AsO_4 + Fe_2(SO_4) \rightarrow 2FeAsO_4 + 3H_2SO_4 \quad (8\text{-}5)$$

In addition to being consistent with the multiple sub-process mechanism, the results obtained suggest that the oxidation of arsenopyrite and arsenite, by ferric-iron, the precipitation of ferric arsenate, and possibly the ferric leaching of pyrite, are competing reactions. Their relative rates are therefore influenced by the concentrations of arsenopyrite, pyrite, arsenite and arsenate, and by the availability of ferric-iron in the bioleaching slurry. The availability of ferric-iron is in turn determined by the activity of the bacteria, and is indicated by the redox potential of the solution.

At high ferric-iron availabilities (*i.e.* at high redox potentials), and in the absence of either a significant level of bacterial activity, or significant quantities of arsenite and/or arsenate, the ferric leaching of arsenopyrite, according to Equation 8-1, is the dominant reaction. This results in a decrease in the concentration of ferric-iron and an increase in the ferrous-iron and arsenite concentrations in the slurry.

In the absence of significant bacterial activity, high ferric-iron availabilities and elevated arsenite concentrations, result in the ferric oxidation of arsenite to arsenate, according to Equation 8-4, being the dominant reaction. This results in a reduction in the concentrations of ferric-iron and arsenite, and an increase in the concentration of arsenate.* In the absence of significant bacterial activity, high ferric-iron availabilities and elevated arsenate concentrations result in the precipitation of ferric arsenate, according to Equation 8-5, being the dominant reaction. This results in a decrease in the concentrations of ferric-iron and arsenate. The decrease in the ferric-iron concentration which accompanies the above reactions results in a decrease in the amount of ferric-iron available for the ferric leaching of arsenopyrite. The reduced rate of mineral leaching in turn results in a reduced availability of ferrous-iron substrate, and may therefore serve to increase the bacterial lag phase.

However, during periods of rapid bacterial oxidation, the high redox potential maintained by the ferrous-iron oxidising species results in sufficient ferric-iron being available for the oxidation of both arsenopyrite, and arsenite, and for the precipitation of ferric arsenate. This results in low ferrous-iron and arsenite concentrations, and high ferric-iron and arsenate concentrations. Furthermore, the concentrations of ferric-iron and arsenate, or possibly the relative concentrations of these species, in solution are limited by the precipitation of ferric arsenate.

8.2 Arsenic Inhibition and Resistance

The results of the batch bioleaching experiments and the steady-state and perturbation studies suggest that the mechanism of arsenic resistance in the mixed culture, *viz. L. ferrooxidans* and *T. caldus*, may be attributed to an energy dependent efflux pump and a membrane system which influences the (relative) rates at which arsenite and arsenate are able to enter the micro-organism. The membrane system, which may or may not be attributable to $Pst^+ Pit^-$ (chromosomal) mutations, enables the bacteria to survive in solutions in which the dissolved arsenate concentration is significantly higher than the dissolved arsenite concentration. Plasmid-encoded resistance, on the other hand, involves the active excretion of arsenic via an energy dependent membrane-bound arsenite pump and may involve the oxidation of arsenite and arsenate. Therefore, in the absence of an energy source, or during periods of reduced bacterial activity, the bacteria are unable to protect themselves from the toxic effects of arsenic, hence the inhibitory effect thereof may manifest at concentrations to which the culture has previously been adapted.

During normal operation of continuous bioleaching operations, neither arsenite, nor arsenate, pose a threat to the culture, provided that it has been adapted to the steady-state arsenic concentration and speciation. However, the overall arsenic concentration, the arsenic speciation, or the ability of the bacteria to protect themselves from the prevailing concentration of the arsenic species may be affected by changes in the mineral composition of the feed or changes in the substrate availability.

Changes in the composition of the feed to the bioreactor may result in an increase in the rate of arsenite formation, relative to its subsequent conversion to arsenate. This could occur as a result of an increase in the arsenopyrite concentration, or a reduction in the availability of a catalytic surface for the oxidation of arsenite to arsenate. This in turn could result in the concentration of arsenite achieving concentrations to which the culture had not been adapted. This may damage or disable the culture.

* Under normal conditions the background arsenate concentration results in the associated increase in the arsenate concentration not being apparent.

The availability of oxygen is influenced by the reliability of the power supply to the compressors, and of the compressors themselves. Loss of aeration will stop the bacterial regeneration of ferric-iron. This will result in an increase in the rate of arsenite formation, relative to its conversion to arsenate, which may damage or disable the culture. However, a more likely scenario is that a loss of aeration will affect the ability of the micro-organisms to protect themselves from the prevailing arsenic concentration and speciation. This may result in an extended lag phase once aeration is restored.

It is, however, important to note that during the perturbation study performed using the primary bioreactor, the oxygen utilisation rate of the culture did not decrease significantly during the period in which a small portion of the culture was intermittently sparged. This suggests that it may be possible to sustain the culture during power, or equipment, failures by intermittent aeration of small amounts of the culture. This could be implemented in the form of "undersized" standby compressors.

8.3 Bacterial Ferrous-iron Oxidation Kinetics

Restriction enzyme analysis of PCR amplified 16S rDNA of the ferrous-iron oxidising micro-organisms isolated from the continuous bioleaching mini-plant was only able to detect the presence of *L. ferrooxidans*. This showed that *L. ferrooxidans*, and not *Thiobacillus ferrooxidans*, is the dominant ferrous-iron oxidising species during the continuous bioleaching of this arsenopyrite/pyrite flotation concentrate.

During the ferrous-iron kinetic studies the cell concentration in the bioreactors increased with increasing temperature, at all dilution rates, and the greatest biomass concentration was achieved at intermediate residence times, irrespective of the temperature and/or pH in the bioreactor. Although the cell concentration in the bioreactors appeared to be independent of both temperature and pH, the bacterial culture maintained at 40°C and pH 1.30 "washed out" at the highest dilution rate. However, the highest calculated maximum specific growth rate, $\mu^{max} = 0.1238\ h^{-1}$, occurred at 40°C and pH 1.50.

Statistical analysis suggested that the maximum bacterial yields on ferrous-iron and oxygen, $Y^{max}_{Fe^{2+}X}$ and $Y^{max}_{O_2X}$, respectively, and their respective maintenance coefficients, $m_{Fe^{2+}}$ and m_{O_2}, increased with increasing temperature across the range from 30 to 40°C. Similar analysis suggested that $Y^{max}_{Fe^{2+}X}$ and $Y^{max}_{O_2X}$, achieved maximum values within the range pH 1.30 to pH 1.50 while $m_{Fe^{2+}}$ and m_{O_2} achieved minimum values within the same pH range. Because the statistical techniques employed did not take into account the poor correlation coefficients obtained during the regression analysis, values of the yield and maintenance parameters were also determined assuming that neither temperature, nor pH has an effect. The "average" values of $Y^{max}_{Fe^{2+}X}$, $Y^{max}_{O_2X}$, $m_{Fe^{2+}}$ and m_{O_2} calculated in this manner were similar to those reported previously for both *L. ferrooxidans* and *T. ferrooxidans*.

The bacterial specific ferrous-iron and oxygen utilisation rates, $q_{Fe^{2+}}$ and q_{O_2}, of the predominantly *L. ferrooxidans* culture increased with a decrease in the ferric/ferrous-iron ratio, $[Fe^{3+}]/[Fe^{2+}]$, (*i.e.* redox potential) and could be accurately described using the modified Michaelis-Menten type model proposed by Boon (1996).

The maximum bacterial specific ferrous-iron and oxygen utilisation rates $q_{Fe^{2+}}^{max}$ and $q_{O_2}^{max}$, and their respective kinetic constants, $K_{Fe^{2+}}$ and K_{O_2}, increased with increasing temperature, across the range from 30 to 40°C. The temperature dependence of $q_{Fe^{2+}}^{max}$ and $q_{O_2}^{max}$ could be accurately described using the Arrhenius Equation whereas the relationship between $K_{Fe^{2+}}$ and K_{O_2} appeared to be linear.

Both $q_{Fe^{2+}}^{max}$ and $q_{O_2}^{max}$ appeared to achieve maximum values at pH 1.50. However, no simple relationship between these parameters and the pH of the solution was apparent. On the other hand the values of the kinetic constants, $K_{Fe^{2+}}$ and K_{O_2}, increased linearly with increasing pH.

In addition to the above, the results indicated that temperature has a far more pronounced effect on $q_{Fe^{2+}}^{max}$ and $q_{O_2}^{max}$ than pH, whereas pH has a far more pronounced effect on $K_{Fe^{2+}}$ and K_{O_2} than temperature.

The assumption that pH has no effect on either $q_{Fe^{2+}}^{max}$ or $q_{O_2}^{max}$ and that the stoichiometry of the overall reaction is constant, *i.e.* E_a and $Y_{Fe^{2+}X}$:Y_{O_2X} is constant, led to a model which predicts the ferrous-iron oxidation kinetics of the predominantly *L. ferrooxidans* species with changes in the ferric/ferrous-iron ratio, across the range 30 to 40°C and pH 1.10 to pH1.70:†

$$q_{Fe^{2+}} = \frac{1.204 \times 10^{7}\, e^{-\frac{35.33}{RT}}}{1 + \left(7.530 \times 10^{-7}\, T + 0.0043\, pH - 0.0040\right)\frac{[Fe^{3+}]}{[Fe^{2+}]}} \qquad (8\text{-}6)$$

$$q_{O_2} = \frac{2.915 \times 10^{6}\, e^{-\frac{35.33}{RT}}}{1 + \left(7.530 \times 10^{-7}\, T + 0.0043\, pH - 0.0040\right)\frac{[Fe^{3+}]}{[Fe^{2+}]}} \qquad (8\text{-}7)$$

A comparison of the predicted variation in the bacterial specific ferrous-iron and oxygen utilisation rates with changes in the ferric/ferrous-iron ratio and the experimental data showed good agreement.

8.4 Chemical Ferric Leaching Kinetics of Arsenopyrite

The ferric leaching rate of both Fairview concentrate and pure arsenopyrite decreased with a decrease in the redox potential of the leaching solution. It was not possible to use the linear model proposed by Nagpal *et al.* (1994), nor the model based on electrochemical theory (Verbaan and Crundwell, 1986), nor the model based on the Monod equation (Boon, 1996) to describe the kinetics. However, it was possible to use the modified form of the Butler-Volmer equation suggested by May *et al.* (1997) to describe the kinetics over the range of operating conditions used:

† The model also takes into account that $K_{Fe^{2+}} = K_{O_2}$.

$$\upsilon_{Fe^{2+}} = \upsilon_0 \left(e^{\alpha\beta(E - E')} - e^{(1-\alpha)\beta(E - E')} \right) \quad (8\text{-}8)$$

A limitation of the model however, appears to be its dependence on the "rest potential" of the mineral, E'. The "rest potential" was found to increase with an increase in the ferric-iron or proton concentration, or when the solids concentration was reduced. No occluding sulphur layer could be detected on the surface of mineral particles that had been leached for an hour, nor was the reactivity of "leached" mineral significantly reduced in comparison to "fresh" mineral.

The results suggest that the reactivity of the mineral is determined by the ferric-iron and proton concentration based on the arsenopyrite surface area. An increase in the concentration of either ferric-iron or protons (based on the arsenopyrite surface area) results in a decrease in the reactivity of the mineral. This is regarded as highly unusual as most reaction mechanisms are favoured by an increase in reactant concentration.

The results obtained therefore indicate that it is necessary to modify the Butler-Volmer based model to include the effect of parameters such as pH and ferric-iron concentration on the leaching rate in order to yield a mechanistically based model capable of predicting the ferric leaching rate of sulfide minerals over a range of operating conditions.

8.5 Modelling Continuous Bioleach Reactors Based on the Multiple Sub-process Mechanism

According to the multiple sub-process mechanism, it is possible to determine the kinetics of the chemical and bacterial sub-processes independently and then use the derived kinetic constants to predict the steady-state and dynamic performance of continuous bioleach reactors.

If, during the steady-state bioleaching of sulfide minerals:

i) the bacteria follow Monod growth kinetics,
ii) the maximum yield and maintenance coefficient on ferrous-iron can be related via the Pirt equation (Pirt, 1982), and
iii) the bacterial specific ferrous-iron utilisation rate can be described can be described as a function of the ferric/ferrous-iron ratio,

then, it can be shown that the resulting ferric/ferrous-iron ratio (*i.e.* the redox potential) of the bioleaching solution is only a function of:

i) the residence time, and
ii) the characteristics of the bacterial species.

If the rate at which the mineral is leached by ferric-iron can be described as a function of the ferric/ferrous-iron ratio, then the mineral conversion during steady-state leaching in a continuous bioreactor is only a function of:

i) the residence time,
ii) the characteristics of the bacterial species, and

iii) the characteristics of the mineral.

Although this may not be an intuitive result, it is expected from the assumption of Monod or Michaelis-Menten type kinetics.

Thus, the model developed proposes that the residence time and characteristics of the microbial species determine the redox potential of the bioleaching solution. The redox potential of the solution, the characteristics of the mineral being leached and the residence time in turn determine the degree of sulphide mineral leaching, *i.e.* the mineral conversion. A change in the residence time will result in a change in the solution redox potential, and hence in the overall leaching rate of the mineral. It may also influence the bacterial speciation.

A comparison of the model prediction with the pyrite conversion measured during a previous investigation showed good agreement if it was assumed that the bacterial species present was *L. ferrooxidans*. However, although the agreement between the redox potential measured in the first stage of a continuous BIOX® mini-plant oxidising a range of arsenopyrite/pyrite concentrates and the redox potential predicted by the model was good, the agreement between the predicted conversion and the experimental data was poor. This was anticipated and can be attributed to the fact that the " relatively low" concentrations of arsenopyrite in the mineral resulted in a large proportion of it being occluded by pyrite and/or gangue. Although galvanic interactions result in the leaching of arsenopyrite preceding that of pyrite, and although the bioleaching of sulfide minerals has been found to occur via the formation of pores, some of the arsenopyrite will still not be immediately accessible to the leaching solution.

The above suggests that the rate of mineral leaching should be based on the exposed surface area of the mineral being leached, and that the model used needs to incorporate changes in the exposed surface area with time. However, it is also apparent that the above methodology can be extended to account for the size distribution of the mineral feed, and changes resulting from the leaching process by means of a population balance model.

The model developed, like previous models, does not consider the fate of the sulphur moiety. However, during the bioleaching of base metal sulfides, sulphur products may result in passivation of the mineral surface. Although sulphur oxidising bacteria should assist in the solubilisation of this passivating layer, sulfur oxidation may be rate limiting during the bioleaching of these minerals. Therefore, refinement of the model to include the kinetics of bacterial sulfur oxidation is also necessary. Other required refinements include the effect of precipitate formation and galvanic interactions on the rate of leaching.

In spite of the above limitations, and although the above hypothesis has yet to be extensively tested, the results obtained to date suggest that the model has potential for predicting the performance of continuous bioleach reactors, and hence finding use in engineering and industrial applications.

8.6 Nomenclature

E	redox potential of the solution (Pt-Ag/AgCl)	mV
E′	rest potential of the mineral	mV
E_a	activation energy	$kJ.mol^{-1}$
F	Farady constant	$C.mol^{-1}$
$[Fe^{2+}]$	concentration of ferrous-iron	mmol $Fe^{2+}.\ell^{-1}$

$[Fe^{3+}]$	concentration of ferric-iron	mmol $Fe^{3+}.\ell^{-1}$
E′	mineral rest potential	mV
K	kinetic constant in bacterial ferrous-iron oxidation	dimensionless
$K_{Fe^{2+}}$	ferrous-iron based kinetic constant in bacterial ferrous-iron oxidation	dimensionless
K_{O_2}	oxygen based kinetic constant in bacterial ferrous-iron oxidation	dimensionless
$m_{Fe^{2+}}$	maintenance coefficient on ferrous-iron	mmol Fe^{2+}.(mmol C)$^{-1}$.h^{-1}
m_{O_2}	maintenance coefficient on oxygen	mmol O_2.(mmol C)$^{-1}$.h^{-1}
$q_{Fe^{2+}}$	bacterial specific ferrous-iron oxidation rate	mmol Fe^{2+}.(mmol C)$^{-1}$.h^{-1}
$q_{Fe^{2+}}^{max}$	maximum bacterial specific ferrous-iron oxidation rate	mmol Fe^{2+}.(mmol C)$^{-1}$.h^{-1}
q_{O_2}	bacterial specific oxygen utilisation rate	mmol O_2.(mmol C)$^{-1}$.h^{-1}
$q_{O_2}^{max}$	maximum bacterial specific oxygen utilisation rate	mmol O_2.(mmol C)$^{-1}$.h^{-1}
R	Universal gas constant	kJ.K^{-1}.mol^{-1}
T	absolute temperature	K
z	number of electrons involved in the reaction	dimensionless
$Y_{Fe^{2+}X}$	bacterial yield on ferrous iron	mmol C.(mmol Fe^{2+})$^{-1}$
$Y_{Fe^{2+}X}^{max}$	maximum bacterial yield on ferrous iron	mmol C.(mmol Fe^{2+})$^{-1}$
Y_{O_2X}	bacterial yield on oxygen	mmol O_2.(mmol C)$^{-1}$
$Y_{O_2X}^{max}$	maximum bacterial yield on oxygen	mmol O_2.(mmol C)$^{-1}$
μ^{max}	maximum bacterial specific growth rate	h^{-1}
α	fraction of mineral reacted at time, t	dimensionless
β	$\frac{zF}{RT}$	dimensionless
υ_0	kinetic constant in chemical (ferric-iron) mineral oxidation	mmol Fe^{2+}.$mmol^{-1}$.h^{-1}
$\upsilon_{Fe^{2+}}$	mineral specific ferrous-iron production rate	mmol Fe^{2+}.$mmol^{-1}$.h^{-1}

8.7 References

Boon, M. 1996. Theoretical and experimental methods in the modelling of bio-oxidation kinetics of sulfide minerals. Ph.D. Thesis. Delft University of Technology, Delft.

Dew, D.W., Lawson, E.N. and Broadhurst, J.L. 1997. The BIOX® process for biooxidation of gold-bearing ores or concentrates, pp. 45-80. In: D.E. Rawlings (ed.), Biomining: theory, microbes and industrial processes. Springer-Verlag and Landes Bioscience, Berlin.

Iglesias, N., Palencia, I. and Carranza, F. 1993. Removal of the refractoriness of a gold bearing pyrite-arsenopyrite ore by ferric sulphate leaching at low concentration, pp. 99-115. In: J.P. Hager (ed.), EPD Congress 1993, The Minerals, Metals and Materials Society, Warrendale, Co..

May, N., Ralph, D.E. and Hansford, G.S. 1997. Dynamic redox potential measurement for determining the ferric leach kinetics of pyrite. Minerals Engineering **10**(11): 1279-1290.

Nagpal, S., Dahlstrom, D. and Oolman, T. 1994. A mathematical model for the bacterial oxidation of a sulfide ore concentrate. Biotechnology and Bioengineering **43**(5): 357-364.

Pirt, S.J. 1982. Maintenance energy: a general model for energy limited and energy sufficient growth. Arch. Microbiol. **133**:300-302.

Verbaan, B. and Crundwell, F.K. 1986. An electrochemical model for the leaching of a sphalerite concentrate. Hydrometallurgy **16**(3): 345-359.

Journal Publications

Pergamon

Minerals Engineering, Vol. 9, No. 12, pp. 1235–1252, 1996

PII:S0892–6875(96)00119–7
0892–6875/96 $15.00+0.00

THE EFFECT OF As(III) AND As(V) ON THE BATCH BIOLEACHING OF A PYRITE-ARSENOPYRITE CONCENTRATE

A.W. BREED§, A. GLATZ†, G.S. HANSFORD§ and S.T.L. HARRISON§

§ Department of Chemical Engineering, University of Cape Town, Rondebosch, 7700, South Africa
† Fachbereich Biotechnologie, Fachhochschule Mannheim,
Hochschule für Gestaltung und Technik, Mannheim, Germany
(Received 10 May 1996; accepted 28 June 1996)

ABSTRACT

The bioleaching of arsenical gold-bearing sulphide ores and concentrates solubilises iron, arsenic and sulphur. Previous work has shown that high concentrations of iron and arsenic in solution inhibit bacterial growth, with As(III) reported to inhibit bacteria to a greater degree than As(V).

Batch bioleaching experiments were carried out over periods of one month. Varying quantities of either 0.020–0.040 M As(III) or 0.107–0.220 M As(V), were added to a slurry, consisting of a pyrite-arsenopyrite concentrate (20% solids ($m.v^{-1}$)) in a nutrient solution. The slurry was inoculated with a culture, consisting primarily of Leptospirillum ferrooxidans and Thiobacillus thiooxidans. The culture was obtained from a continuous bioleaching mini-plant treating the same concentrate. The results obtained were compared with those of a culture to which no arsenic was added. The effect of the added arsenic was determined by monitoring three parameters: the oxygen utilisation rate, r_{O_2}, of the culture, the rate at which the arsenic in the concentrate was solubilised and the speciation of the dissolved arsenic.

The results suggest that the nature of the As(III) and As(V) toxicity is different. The addition of the culture to a slurry containing As(III) resulted in a reduced rate of bacterial oxidation. However, the addition of the culture to a slurry containing As(V) resulted in both a lag phase and a reduced rate of bacterial oxidation. At sufficiently high dosages of As(III) and As(V) the maximum oxygen utilisation rate, $r_{O_2}^{max}$, of the culture was also affected. The results indicate that As(V) toxicity, and the relative toxicity of As(III) and As(V) to a mixed culture, appear to be affected by the availability of an energy source. Hence the toxicity of As(III) is not necessarily in the region of three times that of As(V). Furthermore, the results suggest that the mechanism of arsenic resistance may be attributed to the Pst $^+$ Pit $^-$ mutations and an energy dependent efflux pump.

Keywords
Bacteria; bioleaching; oxidation; sulphide ores; extractive metallurgy

INTRODUCTION

Bioleaching, using mixed cultures of *Thiobacillus ferrooxidans*, *Thiobacillus thiooxidans* and *Leptospirillum ferrooxidans*, is an established method for the pre-treatment of refractory arsenical gold

Presented at *Biotech '96, International Symposium on Biotechnology in Minerals Engineering*, Falmouth, UK, March 1996

ores. It offers an economically feasible alternative to pressure oxidation, at throughputs below 1 200 tons.day $^{-1}$, or it can be used to increase the capacity of pressure oxidation plants [1]. Furthermore it has environmental advantages over roasting with regard to the quality of gaseous and liquid effluent. At present commercial plants in South Africa, Australia, Brazil and Ghana treat arsenopyrite flotation concentrates [1,2], and heap bioleaching is used in the USA [2]. Potential complications in the bioleaching of minerals include the solubilisation of metals to concentrations toxic to the microorganisms [3–6] and the inhibitory effect of reagents used in the flotation of the minerals minerals [3,7]. Furthermore, the adaptation to provide resistance to one metal does not necessarily imply resistance to another metal.

The bioleaching of arsenical gold-bearing sulphide ores and concentrates solubilises iron, arsenic and sulphur. The iron is solubilised as Fe(II), the arsenic as As(III) [3,5,6,8–10] and the sulphur as either S(VI) [5,9,10] or S(0) [3,11]. The bacteria in the bioleaching slurry oxidise the dissolved Fe(II) to Fe(III) and the S(0) to S(VI) [3]. It has been suggested that the As(III) is oxidised to As(V) by either oxygen [12], Fe(III) [5], or by Fe(III) in the presence of both active bacteria and a pyrite [8,9] or chalcopyrite surface [9].

High concentrations of dissolved arsenic inhibit bacterial growth [3,5,8,13]. As(III) has been reported to inhibit a wide range of microorganisms [6,8–10,14–16], including *Thiobacillus ferrooxidans* [3,17,18] and *Thiobacillus thiooxidans* [17], to a greater degree than As(V). The mixed culture used in commercial BIOX ® operations has also been found to be more resistant to arsenate than arsenite [19]. Furthermore, As(III) has a more pronounced effect on *Thiobacillus thiooxidans* than on *Thiobacillus ferrooxidans* whereas As(V) has a similar effect on both *Thiobacillus thiooxidans* and *Thiobacillus ferrooxidans* [17].

The addition of As(III) to thiobacilli results in an increase in the lag time prior to bioleaching of the mineral [3,8,17,18]. During this time the As(III) is oxidised to As(V). It has been suggested that the required membrane-associated enzyme protecting systems develop, or the selection of tolerant cells occurs during the lag period caused by inhibitory substances [20].

As(III) and As(V) are present in the bioleaching medium as $HAsO_2$ [5,8] or H_3AsO_3 [3] (arsenious acid) and H_3AsO_4 [5, 8] or $H_2AsO_4^-$ [3] (arsenic acid), respectively. As(III) concentrations in the region of 0.030 M were found to be toxic to a mixed culture of thiobacilli, not conditioned to high arsenic levels and growing on pyrite. Concentrations in the region of 0.090 M were found in dead cultures of the same bacteria [8]. However, As(III) concentrations of up to 0.145 M have been observed in actively growing cultures accustomed to high As(III) [21]. The As(III) form has been reported to be in the region of three times more toxic than the As(V) form [3,8].

As(III) inactivates enzymes with thiol (HS) groups at the active centre [22], resulting in carbohydrate depletion and diminished glutathione (GSH) [23]. The latter protects cells against radiation effects, oxidative damage and certain toxic compounds [23]. As(V) is the least toxic form of inorganic arsenic [22]. As(V) toxicity is caused by the similarity between As(V) and phosphate [16,22]. *e.g.* phosphate fertilisers mobilise arsenate as a result of competition for adsorption sites [24]. The As(V) replaces the phosphate in ATP to form an unstable ADP–arsenate complex [22].

Bacteria may protect themselves from the toxic effect of metals by the production of polysaccharides (slime) which prevent excessive uptake and by the production of low molecular weight binding peptides (phytochelatins) [25]. Furthermore they may acquire resistance through a process of natural selection.

Arsenic resistance in bacteria may be plasmid-borne or located chromosomally [22,26–28]. Chromosomal arsenate resistance reduces the amount of arsenate entering the cell via the phosphate transport system [22,27–29]. *Escherichia coli* has two active phosphate uptake systems [14,29,30]. The Pst phosphate transport system is specific to phosphate, while the Pit system will transport either phosphate or arsenate [22,29,30]. Chromosomal arsenate resistance occurs with the Pst^+ Pit^- mutation [14, 22, 27, 30]. At present chromosomal arsenite resistance is poorly understood [27,28].

Plasmid-encoded resistance protects bacteria by pumping arsenic from the cells via an energy dependent

membrane pump [16,22,27,28,31,32]. In *Escherichia coli*, the *ars* operon in plasmid R773 contains three reading frames, *arsA*, *arsB* and *arsC*, in addition to an *arsR* regulatory gene [33]. These encode an ATP-binding protein (ArsA), an inner membrane protein (ArsB) and a smaller polypeptide (ArsC), respectively [33]. ArsA appears in solution as a monomeric protein, and is loosely associated with the cell membrane [33]. ArsB is postulated to be both the anion-conducting unit and the membrane anchor for the ArsA protein, hence ArsA and ArsB form a membrane-bound complex [34]. ArsC reduces arsenate to arsenite and is stimulated by the reduced thiol compound, dithioreitol [35]. Therefore, cells expressing only ArsA and ArsB extrude arsenite but not arsenate [34]. The arsenic resistance plasmids of *Staphylococcus aureus* (plasmid pI258) [35] and *Staphylococcus xylosus* (plasmid pSx267) [36] do not have the *arsA* gene. However, it has been suggested that ArsB alone is sufficient for anion (arsenite) conduction in these species [19].

In an attempt to increase the arsenic tolerance levels of bioleaching bacteria arsenic resistance plasmids were transferred into a strain of the acidophilic heterotroph, *Acidiphilium* . Although these plasmids were expressed in subsequent subcultures, they had no effect on the arsenopyrite leaching performance of a mixed culture, which contained *Acidiphilium*, *Thiobacillus ferrooxidans* and *Leptospirillum ferrooxidans* [37].

The oxidation of As(III) to As(V) has also been suggested to be a resistance mechanism towards As(III) [6,27,28,38,39] and has been reported to occur in many microorganisms [6,28,40–43]. However, there is no evidence that the energy of oxidation is used for growth [3,28,42]. An enzyme which oxidises arsenite to arsenate has been isolated and purified from *Alcaligenes faecalis* [44]. However, *Thiobacillus ferrooxidans* [3,42,45,46], *Thiobacillus thiooxidans* [42], and a mixed culture of thiobacilli [8–10] were not capable of oxidising As(III) to As(V), nor could *Thiobacillus ferrooxidans* use As(III) as an energy source [3,46].

To date the mechanism of arsenic resistance in acidophilic chemoautotrophs has not been determined [47] although it has been claimed that arsenic resistance in *Thiobacillus ferrooxidans* is plasmid borne [48]. However, the fact that arsenite is more toxic than arsenate suggests that arsenic resistance can also be attributed to the Pst $^{+}$ Pit $^{-}$ mutations [19].

The aim of this work was to determine the relative effect of As(III) and As(V) on the activity of a mixed culture of thiobacilli, in batch culture, and to determine the effect of these elevated As(III) and As(V) concentrations on the bioleaching of an arsenopyrite-pyrite concentrate.

MATERIALS AND METHODS

The bacterial culture was obtained from a two-stage (2x20 ℓ) continuous bioleaching mini-plant treating a pyrite-arsenopyrite concentrate from Fairview gold mine, in Barberton, South Africa. It consisted primarily of *Thiobacillus thiooxidans* and *Leptospirillum ferrooxidans* [49]. The same concentrate was used in the batch tests. The concentrate sample contained 7.3% As, 25.7% S and 24.0% Fe and 86.35% of the material was finer than 75 micron. The mineral analysis of the concentrate was 15.87% FeAsS and 41.04% FeS_2.

The batch tests were carried out in 5 ℓ baffled, agitated, aerated bioreactors at a solids concentration of 200 g.ℓ^{-1}. The nutrient composition was 1.83 g.ℓ^{-1} $(NH_4)_2SO_4$, 1.11 g.ℓ^{-1} K_2SO_4 and 0.53 g.ℓ^{-1} $(NH_4)_2HPO_4$. The temperature in the bioreactors was maintained at 40°C. The pH was maintained between 1.6 and 1.8 by addition of 98% H_2SO_4 or 10 M NaOH. Water was added prior to sampling to account for losses due to evaporation.

The As(III) and As(V) were added as arsenic trioxide (As_2O_3) and sodium arsenate ($Na_2HAsO_4.7H_2O$), respectively. In both experiments the arsenic was dissolved in the nutrient solution. The concentrate was added to the nutrient solution, the pH adjusted and the slurry was conditioned overnight. The pH was adjusted again prior to the addition of the inoculum. The inoculum, added from the primary bioreactor of

the continuous mini-plant, resulted in an initial cell concentration in the region of 10^8 cells.ℓ^{-1}. The batch tests were carried out at five conditions, detailed in Tables 1 and 2.

TABLE 1 Initial As(III) concentration in the batch bioreactors

Reactor	Initial As(III) concentration	
	g.ℓ^{-1}	M (mole.ℓ^{-1})
Control 1	0.0	0.000
Control 2	0.0	0.000
Low As(III)	1.5	0.020
High As(III)	3.0	0.040

TABLE 2 Initial As(V) concentration in the batch bioreactors

Reactor	Initial As(V) concentration	
	g.ℓ^{-1}	M (mole.ℓ^{-1})
Control 1	0.0	0.000
Control 2	0.0	0.000
Low As(V)	8.0	0.107
High As(V)	16.5	0.220

The Fe(II) and As(III) concentrations in solution were determined by titration with $Ce(SO_4)_2$ [50]. The total iron and arsenic concentrations in solution were determined by atomic adsorption spectroscopy (AA). This allowed the Fe(III) and As(V) concentrations to be calculated by difference. The total iron and arsenic content of solid samples were determined by digesting a known mass of the solid in hydrofluoric (HF), nitric (HNO_3) and perchloric (HCl_4) acid [51]. The iron and arsenic solubilised were then determined by atomic adsorption spectroscopy (AA).

The oxygen utilisation rate, r_{O_2}, was determined by monitoring the rate at which the oxygen was utilised by the bacteria in an air-saturated bioleaching slurry. A Yellow Springs Instrument Model 5739 Oxygen Temperature Probe and a Hitech Micro Systems Dissolved Oxygen / Utilisation Rate Meter were used. The redox potential was obtained by direct millivolt (mv) measurement using a ASI OR101431 Pt combination, double junction Ag/AgCl ORP electrode and a Hitech Micro Systems UCT Redox Controller.

RESULTS AND DISCUSSION

The Effect of As(III)

The As(III) concentrations used in arsenic tolerance studies by previous researchers [8], the limited solubility of As_2O_3 in water and the steady-state As(III) concentrations measured in the continuous bioleaching mini-plant *viz.* 0.00025 to 0.00451 M (0.0187 to 0.3379 g.ℓ^{-1}, respectively) [52] resulted in the effect of As(III) on the culture from the continuous bioleaching mini-plant being investigated at the levels listed in Table 1. The results of the As(III) tolerance investigation are presented in Figures 1-5. The measured parameters of 'Control 1' and 'Control 2' were similar, hence the 'Control' in Figures 1-5 represents the average response of 'Control 1' and 'Control 2'.

Figure 1 indicates the variation in the oxygen utilisation rate, r_{O_2}, of the culture during the course of the experiment. Figure 2 shows the cumulative amount of oxygen consumed by the bacterial culture at various stages of the experiment, as a percentage of the amount of oxygen consumed by the bacterial culture in the 'Control' bioreactor. Figure 3 shows the variation in the Fe(II) concentration in the bioleaching slurry during the course of the experiment. Figures 4 and 5 show the variation in the As(III) and As(V) concentrations in the bioleaching slurry for the duration of the experiment, respectively.

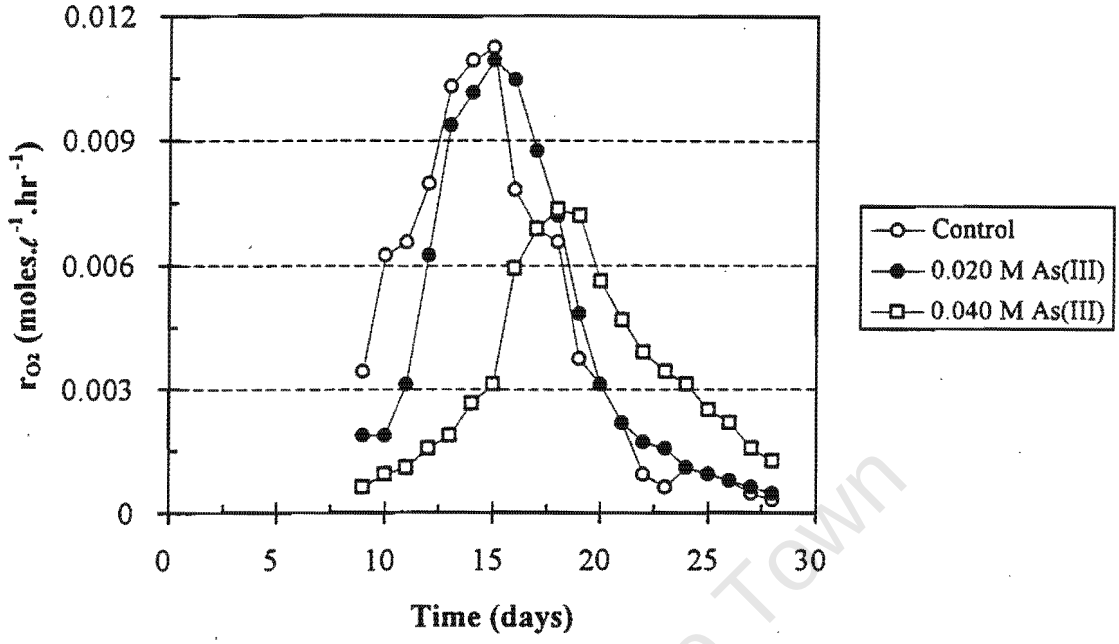

Fig.1 Variation in the oxygen utilisation rate, r_{O_2}, of the bacterial culture with time at different levels of added As(III)

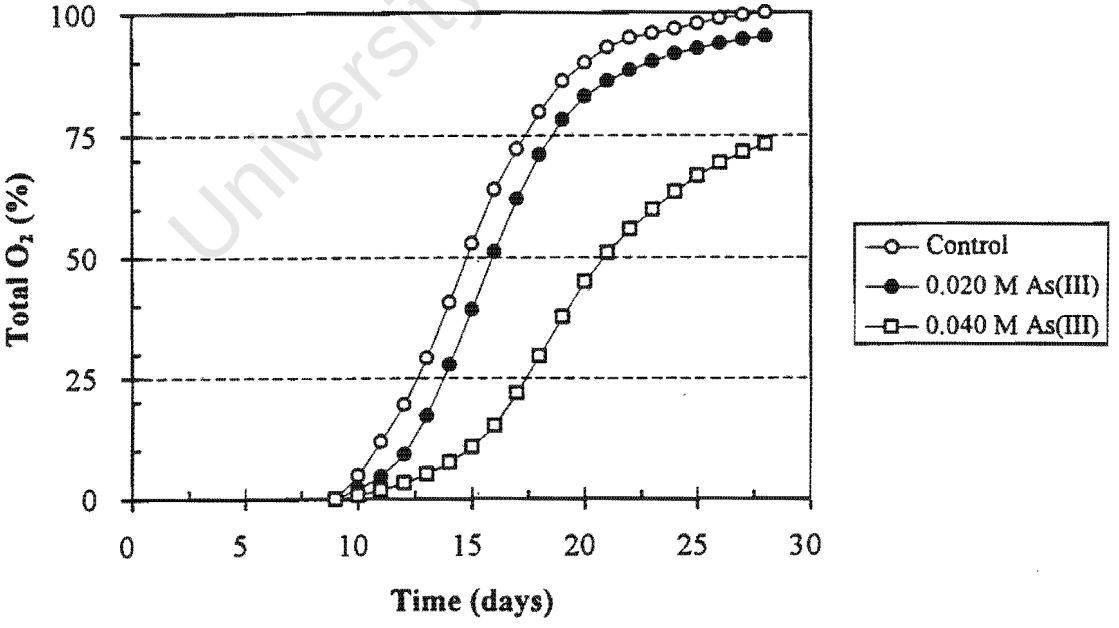

Fig.2 Variation in the cumulative amount of oxygen consumed by the bacterial culture with time at different levels of added As(III)

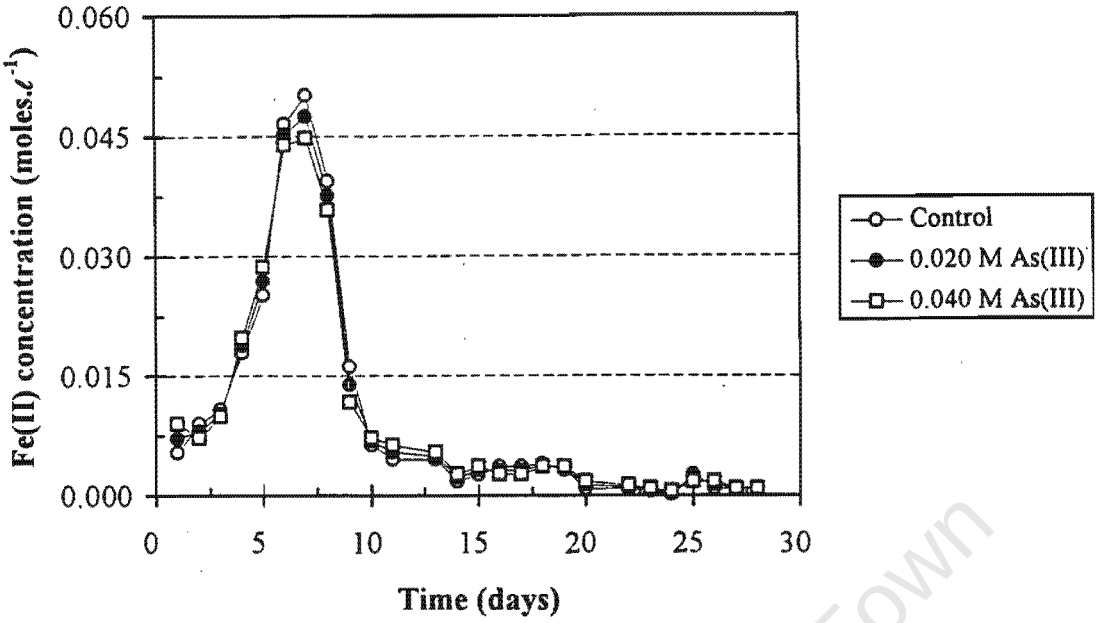

Fig.3 Variation in the Fe(II) concentration of the bioleaching slurry with time at different levels of added As(III)

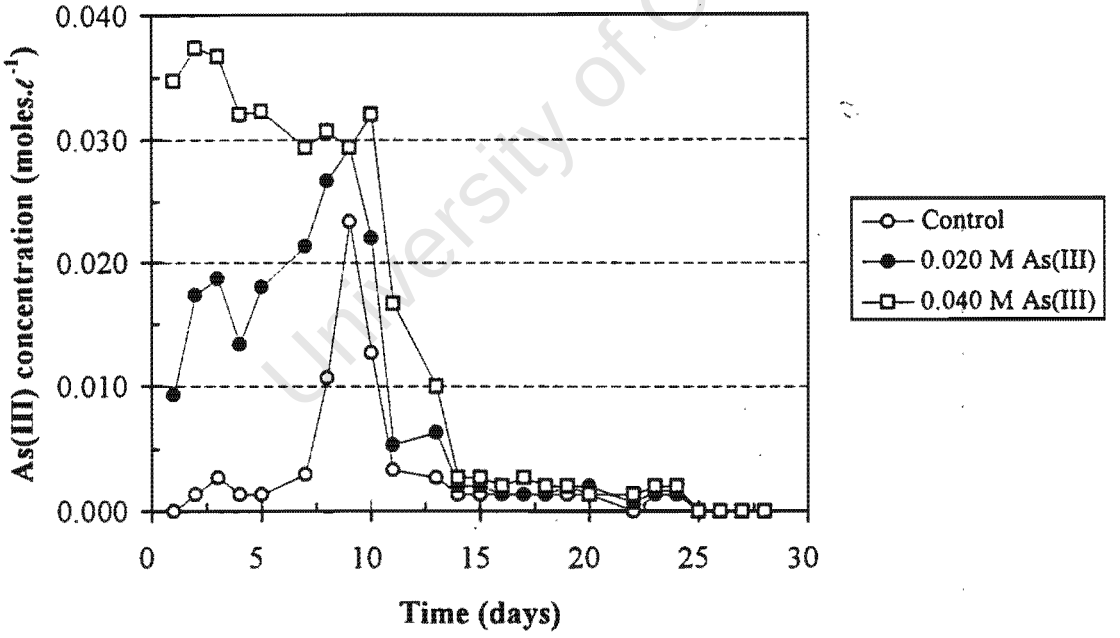

Fig.4 Variation in the As(III) concentration of the bioleaching slurry with time at different levels of added As(III)

From the low initial oxygen utilisation rate, r_{O_2}, shown in Figure 1, it is apparent that no significant bacterial activity occurred during the first 6 days of the experiment *i.e.* only chemical oxidation occurred. This is confirmed in Figure 3 where it can be seen that the Fe(II) concentration of the slurry in all the bioreactors increased during this period. Therefore it is assumed that Fe(III) was reduced according to the

½-reaction shown in Eq. 1:

$$Fe(III) + \acute{e} \rightarrow Fe(II) \quad (1)$$

The initial lag phase of the culture in the 'Control' bioreactor was followed by a sharp increase in r_{O_2} (Figure 1). The initial oxygen utilisation rate, r_{O_2}, of the culture exposed to 0.020 M (1.5 g.ℓ^{-1}) As(III) was lower than that of the culture in the 'Control' bioreactor. This period of reduced metabolic activity lasted for 2 days, but appeared to be followed by normal exponential growth. The 'Control' culture and the culture exposed to an initial As(III) concentration of 0.020 M achieved a maximum oxygen utilisation rate, $r_{O_2}^{max}$, of about 0.0113 moles.ℓ^{-1}.hr^{-1} (0.350 g.ℓ^{-1}.hr^{-1}).

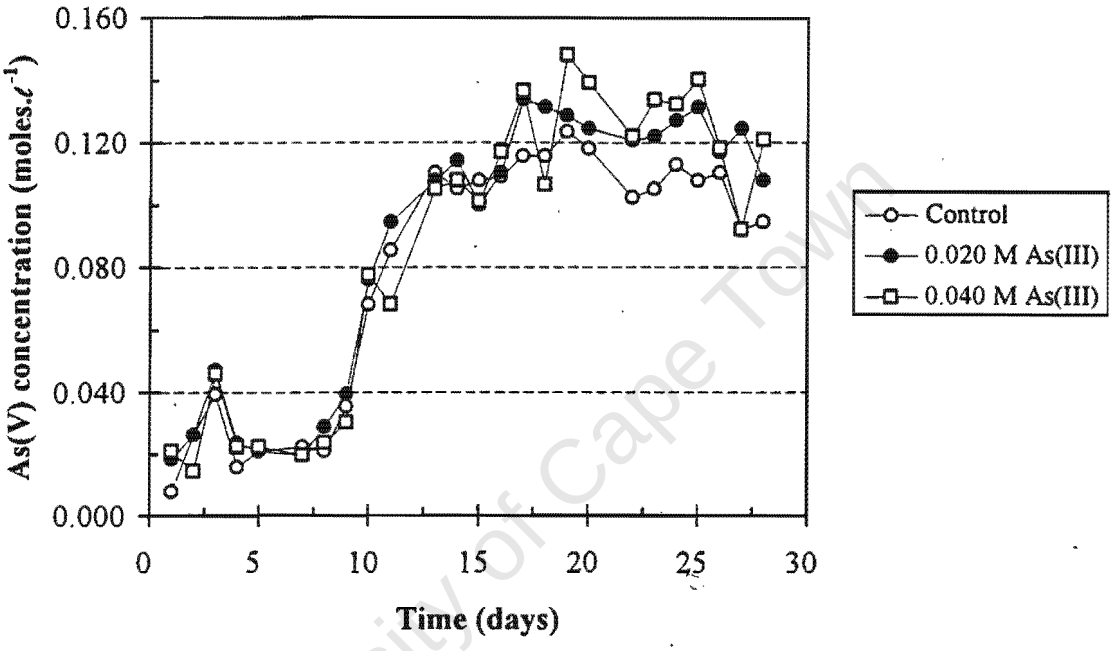

Fig.5 Variation in the As(V) concentration of the bioleaching slurry with time at different levels of added As(III)

The cumulative oxygen consumption data plotted in Figure 2 was calculated according to Eq. 2:

$$\eta_{O_2,\,i} = \frac{\int_0^t r_{O_2,\,i}\,dt}{\int_0^T r_{O_2,\,control}\,dt} \cdot (100) \quad (2)$$

where:

$\eta_{O_2,\,i}$	=	cumulative percent oxygen consumed by the bacterial culture in bioreactor (i) relative to the total amount of oxygen consumed by the bacterial culture in the 'Control' bioreactor,
$r_{O_2,\,i}$	=	oxygen utilisation rate of the bacterial culture in bioreactor (i), and
$r_{O_2,\,control}$	=	oxygen utilisation rate of the bacterial culture in the 'Control' bioreactor.

Figure 2 illustrates that the cumulative oxygen consumption of the culture exposed to an initial As(III) concentration of 0.020 M lagged the cumulative amount of oxygen consumed by the culture in the

'Control' bioreactor by about 2 days. The overall oxygen consumption of the culture exposed to an initial As(III) concentration of 0.020 M was in the region of 95 % of that of the culture in the 'Control' bioreactor.

In Figure 1, it can be seen that the initial oxygen utilisation rate of the culture exposed to an initial As(III) concentration of 0.040 M (3.0 $g.\ell^{-1}$) was reduced in comparison with that of the culture exposed to an initial As(III) concentration of 0.020 M. Furthermore, the culture exposed to 0.040 M As(III) achieved a maximum oxygen utilisation rate of about 0.0074 $moles.\ell^{-1}.hr^{-1}$ (0.230 $g.\ell^{-1}.hr^{-1}$) compared with the 0.0113 $moles.\ell^{-1}.hr^{-1}$ (0.350 $g.\ell^{-1}.hr^{-1}$) achieved by the culture in the 'Control' bioreactor and the culture exposed to an initial As(III) concentration of 0.020 M. Figure 2 also shows that the overall oxygen consumption of the culture exposed to an initial As(III) concentration of 0.040 M was about 72 % of that of the culture in the 'Control' bioreactor.

The rate at which oxygen is utilised by the bacteria is a function of both the bacterial concentration and their activity, as indicated in Eq. 3:

$$r_{O_2} = q_{O_2}^{max} \cdot C_x \qquad (3)$$

where:

r_{O_2}	=	oxygen utilisation rate,
$q_{O_2}^{max}$	=	maximum specific oxygen utilisation rate (*i.e.* metabolic activity), and
C_x	=	size of the bacterial population

Hence, it was not possible to ascertain whether the As(III) inhibits bacterial oxidation of the mineral (*i.e.* it affects bacterial activity and thus the maximum specific oxygen utilisation rate) or whether it is toxic to the bacteria (*i.e.* it restricts growth and therefore affects the bacterial concentration).

Figures 3 and 4 indicate that the Fe(II) and As(III) concentration of the slurry in the 'Control' bioreactor increased during the chemical oxidation period. The above suggests that As(III) was produced by the chemical leaching of the arsenopyrite concentrate by the dissolved Fe(III), as indicated in Eq. 4 [52,53]:

$$FeAsS + 5Fe(III) \rightarrow 6Fe(II) + As(III) + S(0) \qquad (4)$$

Figure 3 shows that the Fe(II) concentration of the slurry in the bioreactor to which 0.040 M As(III) had been added, also increased during the chemical oxidation period. However, from Figure 4 it is apparent that the As(III) concentration of the slurry in the bioreactor decreased during the same period. The above would seem to suggest that the As(III) was oxidised to As(V) by the dissolved Fe(III), as indicated in Eq. 5:

$$2Fe(III) + As(III) \rightarrow 2Fe(II) + As(V) \qquad (5)$$

It is also apparent from Figures 3 and 4 that the Fe(II) and As(III) concentration of the slurry in the bioreactor to which 0.020 M As(III) had been added, increased during the chemical oxidation period. However, the increase in the As(III) concentration was less rapid than the increase in the As(III) concentration observed in the 'Control' bioreactor.

From Figure 1 it is apparent that the bacterial activity in each of the bioreactors increased significantly after the initial period of chemical leaching *i.e.* after 8 days. From Figure 3 it is apparent that this occurred simultaneously with the observed reduction in the Fe(II) concentration of the bioleaching slurry. It is therefore postulated that the Fe(II) produced during the chemical leaching period serves as the initial energy source for the bacteria.

Figures 4 and 5 show that the increased bacterial activity was associated with a reduction in the As(III) concentration, and an increase in the As(V) concentration, in each of the bioreactors. The above can be

attributed to the primary oxidation of arsenopyrite to produce As(III), according to Eq. 4, and the subsequent oxidation of the As(III) to As(V), according to Eq. 5.

These results suggest that the reactions described by Eqs 4 and 5 are competing reactions, and are therefore influenced by the concentrations of As(III), As(V) and Fe(III). At low Fe(III) concentrations (*viz.* prior to rapid bacterial activity) and in the absence of added As(III), the chemical leaching of arsenopyrite (Eq. 4) is the dominant reaction. At low Fe(III) concentrations and high As(III) concentrations, the abundance of As(III) substrate in solution causes the oxidation of As(III) (Eq. 5) to dominate. However, at high Fe(III) concentrations (*i.e.* during rapid bacterial growth), there is sufficient Fe(III) in solution to oxidise both the arsenopyrite and the dissolved As(III). This resulted in the low As(III) and high As(V) concentrations observed during the latter stages of the As(III) tolerance investigation.

The Effect of As(V)

The As(V) concentrations used in arsenic tolerance studies by previous researchers [8], the apparent resistance of the culture from the continuous bioleaching mini-plant to As(III) and the steady-state As(V) concentrations measured in the continuous bioleaching mini-plant *viz.* 0.093 to 0.153 M (6.97 to 11.46 g.ℓ^{-1}, respectively) [52] resulted in the effect of As(V) on the culture from the continuous bioleaching mini-plant being investigated at the levels listed in Table 2. The results of the investigation of As(V) tolerance are presented in Figures 6–10. As in the As(III) tolerance investigation, the profiles of 'Control 1' and 'Control 2' were similar, hence the 'Control' in Figures 6–10 is the average of 'Control 1' and 'Control 2'.

Figure 6 indicates the variation in the oxygen utilisation rate, r_{O_2}, of the culture during the course of the experiment. In Figure 7, the cumulative amount of oxygen consumed by the bacterial cultures at various stages of the experiment, as a percentage of the amount of oxygen consumed by the 'Control' culture is shown. Figure 8 shows the variation in the Fe(II) concentration while Figures 9 and 10 show the variation in the As(III) and As(V) concentrations in the bioleaching slurry for the duration of the experiment, respectively.

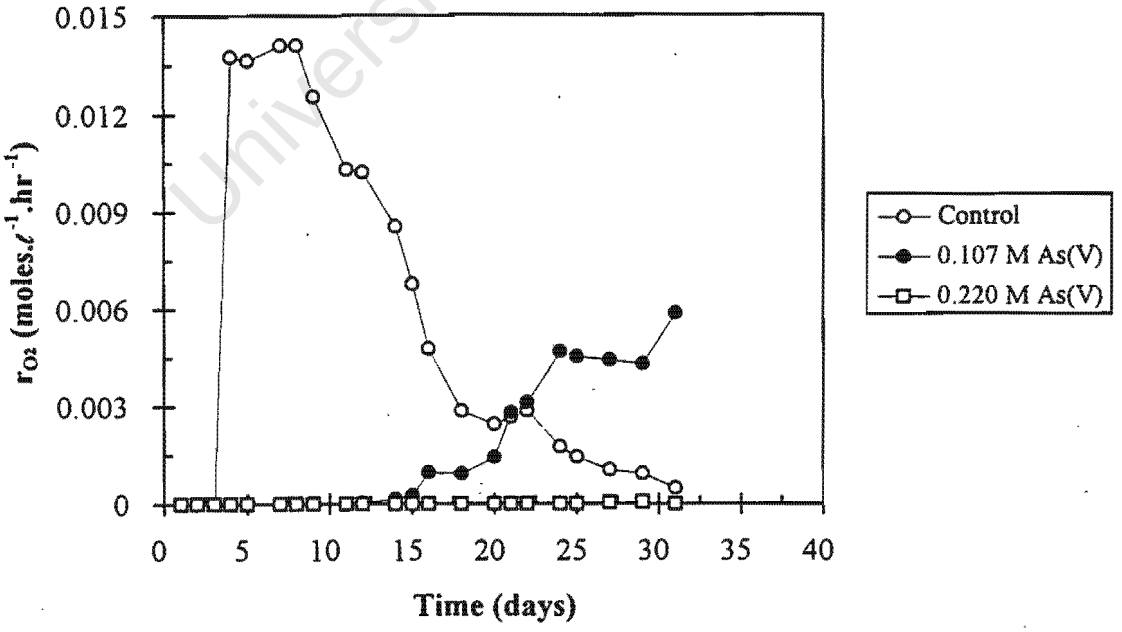

Fig.6 Variation in the oxygen utilisation rate, r_{O_2}, of the bacterial culture with time at different levels of added As(V)

From the variation in the oxygen utilisation rate, r_{O_2}, shown in Figure 6 below, it is apparent that the inoculum used in the As(V) tolerance investigation experienced a lag phase of 3 days. No significant bacterial activity was apparent during this period *i.e.* only chemical oxidation occurred. The Fe(II) concentration of the 'Control' bioreactor increased during this period (Figure 8). It can be assumed that the Fe(III) was being reduced to Fe(II) according to the ½-reaction shown in Eq. 1 above. Figure 6 shows that the initial lag phase of the culture in the 'Control' bioreactor was followed by normal metabolic activity.

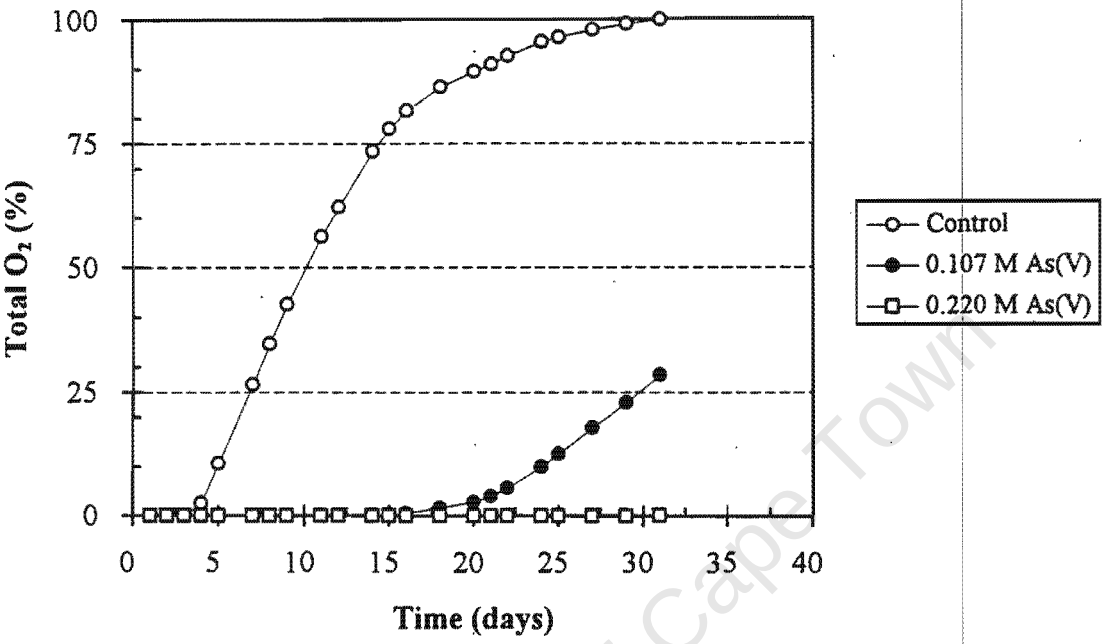

Fig.7 Variation in the cumulative amount of oxygen consumed by the bacterial culture with time at different levels of added As(V)

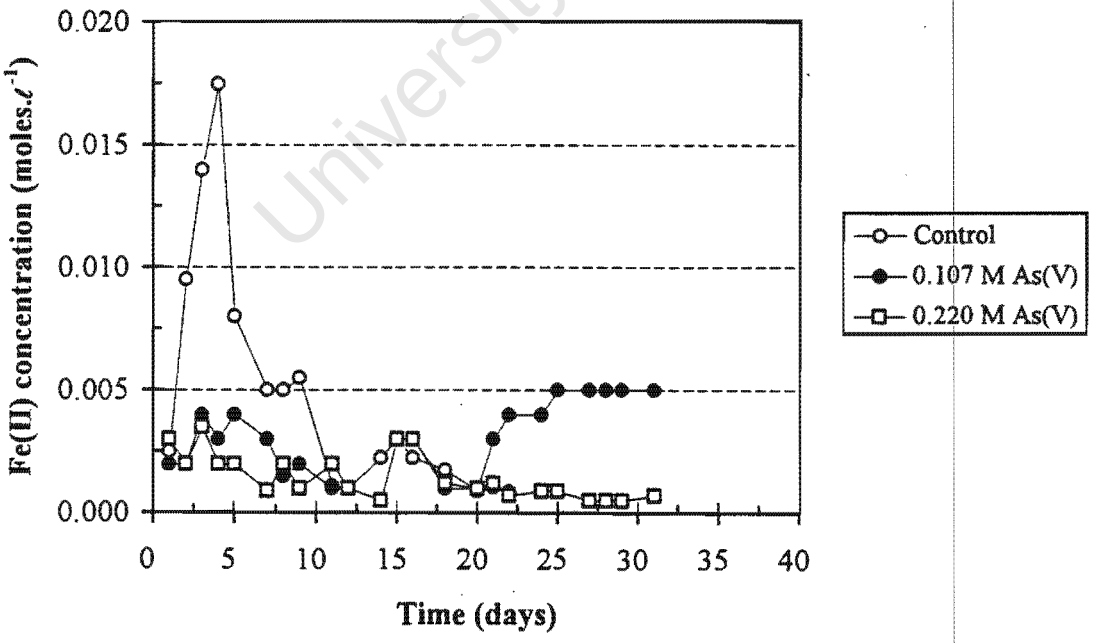

Fig.8 Variation in the Fe(II) concentration of the bioleaching slurry with time at different levels of added As(V)

Exposure to an initial As(V) concentration of 0.107 M (8.0 g.ℓ^{-1}) increased the lag phase of the bacterial culture to 15 days (Figure 6). Subsequent metabolic activity of this culture was significantly reduced in comparison with that of the culture in the 'Control' bioreactor. The bacterial culture in the 'Control' bioreactor achieved a maximum oxygen utilisation rate, $r_{O_2}^{max}$, of about 0.014 moles.ℓ^{-1}.hr^{-1} (0.417 g.ℓ^{-1}.hr^{-1}) whereas the culture at an initial As(V) concentration of 0.107 M achieved a maximum oxygen utilisation rate of about 0.0074 moles.ℓ^{-1}.hr^{-1} (0.187 g.ℓ^{-1}.hr^{-1}) during the 31 day experiment. As the oxygen utilisation rate was increasing at 31 days, it may have increased further had the experiment been continued. However, the bacterial culture exposed to an initial As(V) concentration of 0.220 M (16.5 g.ℓ^{-1}) showed no measurable metabolic activity over the 31 day duration of the experiment (Figure 6).

From Figure 7 it is apparent that the culture exposed to an initial As(V) concentration of 0.107 M began to use oxygen about 12 days after the culture in the 'Control'. The overall oxygen consumption of the culture exposed to an initial As(V) concentration of 0.107 M was in the region of 29 % of that of the 'Control'. As stated previously, the rate at which oxygen is utilised by the bacterial population is a function of the size of the population and its activity (Eq. 3), hence it was not possible to ascertain whether the As(V) affects bacterial activity or whether it affects the ability of the bacteria to grow and reproduce (viability).

From Figures 8 and 9, it is apparent that the chemical leaching of the arsenopyrite resulted in an increase in the Fe(II) and As(III) concentration of the slurry in the 'Control' bioreactor (Eq 4). Figure 6 shows that the onset of bacterial activity (in terms of r_{O_2}) in the 'Control' bioreactor was accompanied by a decrease in the Fe(II) concentration of the slurry. This further supports the postulate that the Fe(II) produced during the chemical leaching phase provides the bacteria with a substrate from which to obtain energy. Figures 9 and 10 indicate that the increased bacterial activity resulted in a reduction in the As(III) concentration, and an increase in the As(V) concentration. As stated previously, this can be attributed to the oxidation of As(III) to As(V) in the presence of Fe(III) *i.e.* the high Fe(III) concentrations caused by rapid bacterial activity result in sufficient Fe(III) being present for the oxidation of both the arsenopyrite and As(III).

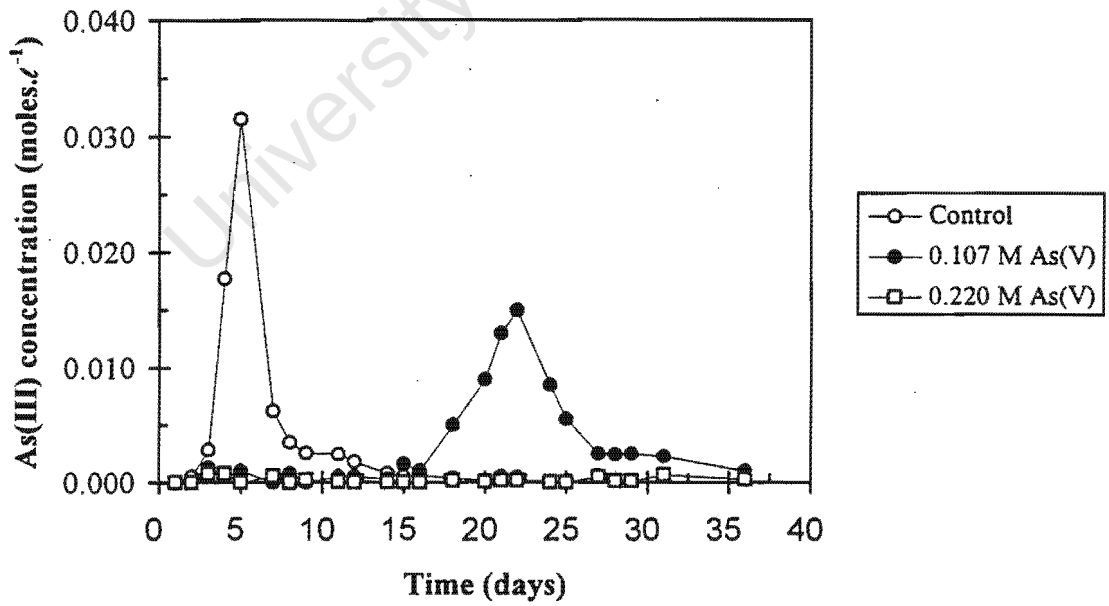

Fig.9 Variation in the As(III) concentration of the bioleaching slurry with time at different levels of added As(V)

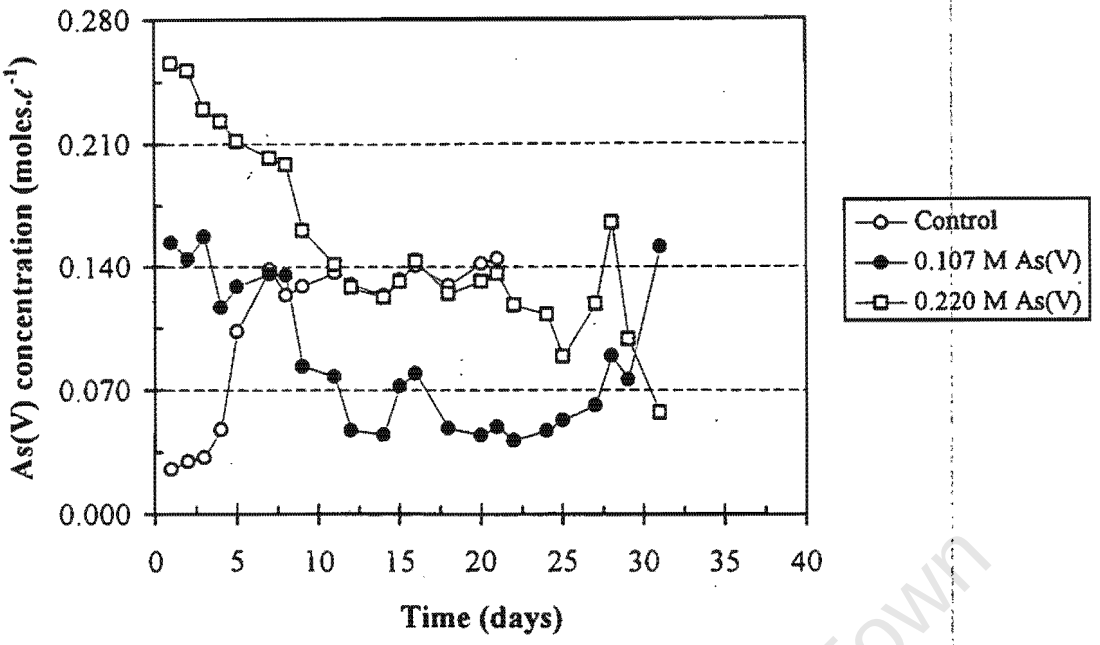

Fig.10 Variation in the As(V) concentration of the bioleaching slurry with time at different levels of added As(V)

Figure 10 indicates that the As(V) concentration of the slurry to which 0.107 M As(V) was added, decreased linearly during the period prior to bacterial activity *i.e.* during the first 15 days. This can be attributed to the As(V) in solution being depleted by formation an insoluble ferric arsenate precipitate, according to Eq. 6 [11]:

$$H_3AsO_4 + Fe(III) + nH_2O \rightarrow FeAsO_4 \cdot nH_2O\downarrow + 3H^+ \quad (6)$$

The precipitation of ferric arsenate resulted in no Fe(III) being available for the chemical leaching of the arsenopyrite, hence no change in the Fe(II) (Figure 8) and As(III) (Figure 9) concentration was observed prior to day 15. These results suggest that the chemical leaching of arsenopyrite (Eq. 4), the chemical oxidation of As(III) (Eq. 5) and the precipitation of ferric arsenate (Eq. 6) are competing reactions, and are therefore influenced by the concentrations of As(III), As(V) and Fe(III).

After 15 days the oxygen utilisation rate, r_{O_2}, of the bacterial culture exposed to an initial As(V) concentration of 0.107 M increased (Figure 6). The increase in the r_{O_2} of the culture was accompanied by an increase in both the Fe(II) (Figure 8) and the As(III) (Figure 9) concentrations. The increase in the Fe(II) and As(III) concentrations can be attributed to the precipitation of ferric arsenate becoming limited by the dissolved As(V) concentration, hence the residual Fe(III) was available for the chemical leaching of arsenopyrite, according to Eq. 4 above. The above observations also support the postulate that the Fe(II) produced during the chemical leaching period serves as the initial energy source for the bacteria.

From Figure 8 it is apparent that the Fe(II) concentration in the bioreactor to which 0.107 M As(V) was added initially did not decrease to the Fe(II) levels observed in the 'Control'. The elevated Fe(II) concentration observed in this bioreactor suggests that the activity of the culture exposed to an initial As(V) concentration of 0.107 M was reduced in comparison with that of the culture in the 'Control'. However, from Figures 9 and 10 it is apparent that the rate of bacterial oxidation was sufficient to ensure that Fe(III) was available for the oxidation of both As(III) and arsenopyrite.

Figure 10 also shows that the As(V) concentration in the bioreactor in which the culture was exposed to 0.220 M As(V) (16.5 g.ℓ^{-1}) decreased linearly as a result of the formation of ferric arsenate precipitate, according to Eq. 6. This precipitation reaction depleted the available Fe(III), inhibiting the chemical

leaching of arsenopyrite, hence no increase in the concentration of either Fe(II) (Figure 8) nor As(III) (Figure 9) was observed. Furthermore, the absence of an initial energy source prevented the bacteria from overcoming the inhibitory effects of the As(V), hence no bacterial activity was observed for the duration of the experiment (31 days).

Comparison of the Effects of As(III) and As(V)

Comparison of Figures 1 and 6 indicates that a shorter lag period was observed in the As(V) tolerance investigation 'Control' bioreactor compared with the As(III) tolerance investigation 'Control'. The inoculum used in the As(III) tolerance investigation was taken from the mini-plant while it was operating in batch mode. However, the mini-plant was operating continuously, at a plant residence time of 15 days, when the inoculum used in the As(V) tolerance investigation was taken. Therefore, the difference in the activity of the inoculi can be attributed to differences in the continuous mini-plant on harvesting of inoculum. Furthermore, it is apparent from Figures 1 and 6 that, the culture in the 'Control' bioreactor of the As(V) tolerance investigation achieved a higher $r_{O_2}^{max}$ compared with the 'Control' of the As(III) tolerance investigation. If it is assumed that the $q_{O_2}^{max}$ of the cultures in the 'Control' bioreactors were similar, then the difference in the $r_{O_2}^{max}$ can be attributed to the bacterial populations in the 'Control' bioreactors being different sizes (Eq. 3).

Figure 11 indicates the relative effect of different levels of added As(III) and As(V) on the cumulative amount of oxygen consumed by the culture from the continuous bioleaching mini-plant at varying stages of the As(III) and As(V) tolerance investigations. The initial (inoculum) lag phase (*i.e.* the chemical leaching phase) observed in the As(III) and As(V) tolerance investigations were eliminated to facilitate comparison of the results.

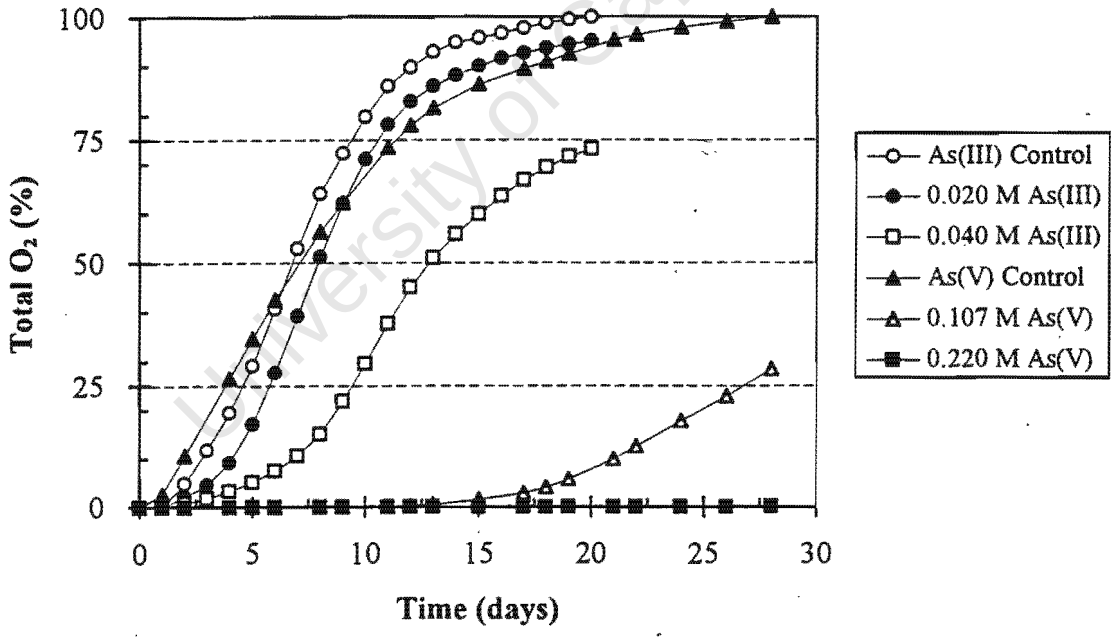

Fig.11 The relative effect of different levels of added As(III) and As(V) on the amount of oxygen consumed by the bacterial culture at varying stages of the As(III) and As(V) tolerance investigations

It is apparent that the addition of As(III) to the nutrient solution prior to the addition of the inoculum from the continuous bioleaching mini-plant did not cause a lag phase *i.e.* there was no period during which bacterial activity was observed in the 'Control' bioreactor but not in the bioreactors to which As(III) was added. However, the addition of 0.107 M (8.0 $g.\ell^{-1}$) As(V) to the nutrient solution prior to the addition of the inoculum resulted in a lag phase of 15 days. During this period no oxygen was consumed by the

bacteria. The addition of 0.220 M (16.5 g.ℓ^{-1}) As(V) to the nutrient solution prior to inoculation resulted in a lag phase which lasted in excess of 31 days. The bacteria exposed to 0.220 M As(V) did not consume any oxygen for the duration of the experiment.

Figure 11 shows that the addition of 0.020 M (1.5 g.ℓ^{-1}) As(III) to the nutrient solution prior to the addition of the inoculum retarded the initial rate of bacterial metabolism. This effect was more pronounced when 0.040 M (3.0 g.ℓ^{-1}) As(III) was added. The culture exposed to an initial As(III) concentration of 0.020 M appeared to recover from the effect of the added arsenic. However, the culture exposed to an initial As(III) concentration of 0.040 M did not achieve an equivalent $r_{O_2}^{max}$ and showed a lower cumulative oxygen usage. The addition of 0.107 M (8.0 g.ℓ^{-1}) As(V) to the nutrient solution prior to the addition of the inoculum resulted in a significant lag phase and retarded the initial rate of bacterial metabolism. The culture did not appear to recover from the effect of the added As(V) over the 31 day period studied.

The above results suggest that the nature of the As(III) and As(V) toxicity is different. The addition of As(III) to the culture from the continuous bioleaching mini-plant resulted in a reduced rate of bacterial oxidation. However, the addition of As(V) to the culture resulted in a lag phase and a reduced rate of bacterial oxidation. At sufficiently high dosages of As(III) and As(V) the maximum oxygen utilisation rate, $r_{O_2}^{max}$, of the culture was also affected.

Although As(III) concentrations of up to 0.145 M have been reported in actively growing cultures accustomed to high As(III) concentrations [21] several researchers have found As(III) to be toxic at concentrations similar to those observed in this investigation [3, 8]. Furthermore, several researchers have suggested that As(III) is in the region of two to three times more toxic than As(V) [3, 8]. It should however be noted that most researchers have performed toxicity experiments in media supplemented with Fe(II). However, the results of this investigation show that the addition of 0.107 M (8 g.ℓ^{-1}) As(V) to an inoculum from a continuous bioleaching mini-plant had a far more pronounced effect than the addition of 0.040 M (3.0 g.ℓ^{-1}) As(III).

The levels of As(III) added in the batch study (0.020 and 0.040 M) were in the region of 10 times those observed during routine operation of the mini-plant (0.00025 to 0.00451 M) [52]. Where an inhibitory effect was observed, the bacterial culture exhibited the ability to recover. In contrast to the above, the levels of As(V) added in the As(V) tolerance investigation (107 and 220 M) were similar to those observed during routine operation of the mini-plant (0.093 to 0.153 M) [52] yet the effect of the added As(V), in batch culture, was severe.

The results of this study, together with the those of previous researchers suggest that the mechanism of arsenic resistance in the (mesophilic) bacteria used in the bioleaching of sulphide minerals may be attributed to the Pst^+ Pit^- mutations and an energy dependent efflux pump. The Pst^+ Pit^- mutations result in a reduced uptake of As(V). This results in the bacteria being able to survive in bioleaching solutions in which the dissolved As(V) concentration is significantly higher than the dissolved As(III) concentration. However, the excretion of As(V) which enters the cell, presumably via the phosphate uptake system, requires energy. Therefore, in the absence of an energy source, *e.g.* Fe(II) and/or O_2, or during periods of reduced bacterial activity, the inhibitory effect of As(V) will exceed that of steady-state bioreactor operation at As(V) concentrations to which the culture has been adapted. Therefore, the tolerance levels reported by previous researchers [3,8,17] may have been influenced by their experiments having been performed in media supplemented with Fe(II), which is the most easily used source of energy for iron-oxidising bacteria.

CONCLUSIONS

The arsenic in the arsenopyrite is solubilised as As(III) by a ferric leach in the absence of bacterial activity *i.e.* lag phase of the batch process. In the presence of Fe(III), the dissolved As(III) is further oxidised to As(V). Excess dissolved As(V) and Fe(III) precipitate as ferric arsenate. The above are competing reactions, and are therefore influenced by the availability of Fe(III), and the concentrations of As(III) and

As(V). The availability of Fe(III) is in turn determined by the activity of the bacteria.

Exposure to initial As(III) concentrations in the region of 0.020 to 0.040 M reduced the initial oxygen utilisation rate, r_{O_2}, and the maximum oxygen utilisation rate, $r_{O_2}^{max}$, of the bacterial culture. Several researchers have found As(III) to be toxic at concentrations similar to those observed in this investigation. Exposure to an initial As(V) concentration of 0.107 M increased the lag phase of the bacterial culture by 12 days and reduced the initial oxygen utilisation rate, r_{O_2}, and the maximum oxygen utilisation rate, $r_{O_2}^{max}$, of the bacterial culture. The addition of 0.220 M As(V) to the nutrient solution prior to inoculation resulted in a lag phase which lasted in excess of 31 days. These bacteria did not consume any oxygen for the duration of the experiment. Because the rate at which oxygen is utilised by the bacterial population is a function of the bacterial concentration, C_x, and their activity, $q_{O_2}^{max}$, it was not possible to ascertain whether the arsenic inhibits bacterial oxidation (*i.e.* it reduces the bacterial activity) or whether it is toxic to the bacteria (*i.e.* it reduces the viability of the bacterial culture).

Comparison of the results of the As(III) and As(V) tolerance investigations suggest that the nature of As(III) and As(V) toxicity is different. Furthermore, the effect of As(V) on the bacterial culture was far more severe than anticipated (based on the As(III) and As(V) concentrations observed during routine operation of the continuous bioleaching mini-plant, and the results of other researchers). Comparison of the results obtained in this investigation with those obtained by other researchers and with the behaviour of the bacterial culture in the continuous mini-plant suggest that As(V) toxicity, and the relative toxicity of As(III) and As(V) to a mixed culture are affected by the availability of an energy source. Therefore, the toxicity of As(III) is not necessarily in the region of three the times that of As(V).

Furthermore, the results of this investigation and those of other researchers suggest that the mechanism of arsenic resistance in the (mesophilic) bacteria used in the bioleaching of sulphide minerals may be attributed to the Pst^+ Pit^- mutations and an energy dependent efflux pump.

ACKNOWLEDGMENTS

The authors would like to thank GENCOR for technical and financial support of the research.

REFERENCES

1. Van Aswegen P.C., Bio-oxidation of Refractory Gold Ores. The GENMIN Experience. *Biomine '93*, Chapter 15, Australian Mineral Foundation, Inc., Glenside, SA (1993).
2. Brierley J.A., Wan R.Y., Hill D.L. & Logan T.C., Biooxidation—Heap Pretreatment Technology for Processing Lower Grade Refractory Gold Ores. *Biohydrometallurgical Processing*, Viña del Mar, Chile, 19–22 November 1995, Vargas T., Jerez C.A., Wiertz J.V. & Toledo H. (eds), **I**, 253, University of Chile (1995).
3. Pol'kin S.I., Panin V.V., Adamov E.V., Karavaiko G.I. & Chernyak A.S., Theory and Practice of Utilizing Microorganisms in Difficult-to-dress Ores and Concentrates. *11th International Mineral Processing Congress*, Cagliari, 901 (20–26 April 1975).
4. Norris P.R. & Kelly D.P., Toxic Metals in Leaching Systems. *Metallurgical Applications of Bacterial Leaching and Related Microbiological Phenomena*, Murr L.E., Torma A.E. & Brierley J.A. (eds), 83, Academic Press, New York (1978).
5. Shrestha G.N., Microbial leaching of refractory gold ores. *Australian Mining* **October**, 48 (1988).
6. Lindström E.B. & Sehlin H.M. Toxicity of Arsenic Compounds to the Sulphur-Dependent Archaebacterium *Sulfolobus*. *Biohydrometallurgy—89*, Jackson Hole, July 1989, Salley J., McCready R.G.*l*. & Wichlacz P.L. (eds), 59 (1989).
7. Lan X., Jia-jun K. & Rong-qing Q., Effect of Flotation Reagents on the Growth of Bacteria and the Bioleaching of Arsenic-bearing Gold Concentrate. *EPD Congress '91*, Gaskell D.R.(ed), 59, The Minerals, Metals & Materials Society (1991).

8. Barrett J., Ewart D.K., Hughes M.N., Nobar A.M. & Poole R.K., The Oxidation of Arsenic in Arsenopyrite: The Toxicity of As(III) to a Moderately Thermophilic Mixed Culture. *Biohydrometallurgy-89*, Jackson Hole, July 1989, Salley J., McCready R.G.L. & Wichlacz P.L. (eds), 49 (1989).
9. Barrett J., Ewart D.K., Hughes M.N. & Poole R.K., Chemical and Biological Pathways in the Bacterial Oxidation of Arsenopyrite. *FEMS Microbiology Reviews* **11**, 57 (1993).
10. Barrett J. & Hughes M.N., The Mechanism of the Bacterial Oxidation of Arsenopyrite-pyrite Mixtures: The Identification of Plant Control Parameters. *Minerals Engineering* **6**(8–10), 969 (1993).
11. Fernandez M.G.M., Mustin C., De Donato P., Barres O, Marion P. & Berthelin J., Occurrences at Mineral–Bacteria Interface During Oxidation of Arsenopyrite by *Thiobacillus ferrooxidans*. *Biotechnol. Bioeng.* **46**(1), 13 (1995).
12. Panin V.V., Karavaiko G.I. & Pol'kin S.I., Mechanism and Kinetics of Bacterial Oxidation of Sulphide Minerals. *Biotechnology of Metals*, Karavaiko G.I. & Groudev S.N. (eds), 197, Centre of International Projects, Moscow (1985) as cited by Barrett J. & Hughes M.N. The Mechanism of the Bacterial Oxidation of Arsenopyrite-pyrite Mixtures: The Identification of Plant Control Parameters. *Minerals Engineering*, **6**(8–10), 969 (1993).
13. Trevors J.T., Oddie K.M. & Belliveau B.H., Metal resistance in bacteria. *FEMS Microbiology Reviews*, **32**, 39 (1985).
14. Silver S., Budd K., Leahy K.M., Shaw W.V., Hammond D., Novick R.P., Willsky G.R., Malamy M.H. & Rosenberr H., Inducible Plasmid-Determined Resistance to Arsenate, Arsenite and Antimony(III) in *Escherichia coli* and *Staphylococcus aureus*. *Journal of Bacteriology* **146**(3), 983 (1981).
15. Dabbs E.R. & Sole G.J. Plasmid-borne resistance to arsenate, arsenate, cadmium, and chloramphenicol in a *Rhodococcus* species. *Mol. Gen. Genet.*, **211**, 148 (1988).
16. Huysmans K.D. & Frankenberger W.T., Microbial Resistance to Arsenic. *Engineering Aspects of Metal-waste Management*, Iskander I.K. & Selim H.M. (eds), 93, Lewis Publishers (1992).
17. Collinet, M-N. & Morin, D., Characterisation of arsenopyrite oxidising *Thiobacillus*. Tolerance to arsenite, arsenate, ferrous and ferric iron. *Antonie van Leeuwenhoek*, **57**, 237 (1990).
18 Cassity W.D. & Pesic B., Interaction of *Thiobacillus ferrooxidans* with Arsenite, Arsenate and Arsenopyrite. *New Remediation Technology in the Changing Environmental Arena*, Scheiner B.J., Chatwin T.D., El-Shall H., Kawatra S.K. & Torma A.E. (eds), 221, Society for Mining, Metallurgy, and Exploration, Inc., Littleon, Colorado (1995).
19. Lawson E.N., Arsenic Toxicity, Bacterial Resistance and Bacterial Oxidation/Reductions. Phase 1: Literature Review. *Report No. PR 93/109C of Project No. PR 93/132*, GENMIN Process Research, Johannesburg, (1 November 1993).
20. Tuovinen O.H., Niemelä S.I. & Gyllenberg H.G., Tolerance of *Thiobacillus ferroxidans* to some metals. *Antonie van Leeuwenhoek*, **37**, 489 (1971).
21. Morin D., Ollivier P., Toromanoff I. & Letestu A., Bioleaching of Gold Refractory Arsenopyrite Rich Sulphide Concentrate Laboratory and Pilot Case Studies. *EPD Congress '91*, Gaskell D.R.(ed), 577, The Minerals, Metals & Materials Society (1991).
22. Coddington K., A Review of Arsenicals in Biology. *Toxicological and Environmental Chemistry* **11**, 281 (1986).
23. Aposhian H.V. & Aposhian M.M., Newer Developments in Arsenic Toxicity. *Journal of the American College of Toxicology*, **8**(7), 1297 (1989).
24. Hindmarsh J.T. & Mc Curdy R.F., Clinical and Environmental Aspects of Arsenic Toxicity. *CRC Critical Reviews in Clinical Laboratory Sciences*, **23**(4), 315 (1986).
25. Angle J.S. & Chaney R.L. Cadmium Resistance Screening in Nitrilotriacetate-Buffered Minimal Media. *Appl. Environ. Microbiol*, **55**(8), 2101 (1989).
26. Novick R.P. & Roth C., Plasmid-linked Resistance to Inorganic Salts in *Staphylococcus aureus*. *J. Bacteriol.* **95**(4), 1335 (1968).
27. Silver S. & Nakahara H., Bacterial Resistance to Arsenic Compounds. *Arsenic: Industrial, Biomedical, Environmental Perspectives*, Lederer, W.H. & Fensterheim, R.J. (eds), 190, Van Nostrand Reinhold, New York (1983).
28. Cullen W.R. & Reimer K.J., Arsenic Speciation in the Environment. *Chem. Rev.*, **89**(4), 713

(1989).
29. Silver S., Transport of Cations and Anions. *Bacterial Transport*, Rosen B.P. (ed), 221, Marcel Dekker Inc., New York (1978).
30. Willsky G.R. & Malamy M.H. Effect of Arsenate on Inorganic Phosphate Transport in *Escherichia coli*. *J.Bacteriol.*, **144**(1), 366 (1980).
31. Mobley H.T. & Rosen B.P., Energetics of plasmid-mediated arsenate resistance in *Escherichia coli*. *Proc. Natl. Acad. Sci. U.S.A*, **79**, 6119 (1982).
32. Silver S. & Keach D., Energy-dependent arsenate efflux: The mechanism of plasmid-mediated resistance. *Proc. Natl. Acad. Sci. USA*, **79**, 6114 (1982).
33. Silver S. & Misra T.K., Plasmid-mediated Heavy Metal Resistances. *Ann. Rev. Microbiol.*, **42**, 717 (1988).
34. Rosen, B.P., Hsu, C.M., Karkaria, C.E., Owolabi, J.B. & Tisa L.S., Molecular Analysis of an ATP-dependent Anion Pump. *Phil. Trans. R. Soc. Lond. B*, **326**, 455 (1990).
35. Ji, G. & Silver, S., Reduction of arsenate to arsenite by the ArsC protein of the arsenic resistance operon of *Staphylococcus aureus* plasmid pI258. *Proc. Natl. Acad. Sci. USA*, **89**, 9474 (1992).
36. Rosenstein, R, Paschel, A., Wieland, B. & Götz, F., Expression and Regulation of the Antimonite, Arsenite and Arsenate Resistance Operon of *Staphylococcus xylosus* Plasmid pSX267. *J. Bact.*, **174**(11), 3676 (1992).
37. Bruhn, D.F. & Roberto, F.F., Maintenance and Expression of Enteric Arsenic Resistance Genes in *Acidiphilium*. *Biohydrometall. Technol.*, Torma A.E. (ed), **2**, 745, Miner. Met. Mater. Soc., Warrendale, Pa (1993).
38. Abdrashitova, S.A., Ilyaletdinov, A.N., Mynbaeva, B.N. & Abdulina, G.G., The Catalase Activity of *Pseudomonas putida* Strain Oxidizing Arsenic. *Mikrobiologiya*, **51**, 34 (1982).
39. Williams, J.W. & Silver, S., Bacterial resistance and detoxification of heavy metals. *Enzyme. Microb. Technol.*, **6**, 530 (1984).
40. Osborne, F.H. & Ehrlich, H.L., Oxidation of Arsenite by a Soil Isolate of *Alcaligenes*. *J. Appl. Bacteriol.*, **41**, 295 (1976).
41. Phillips, S.E. & Taylor, M.L., Oxidation of Arsenite to Arsenate by *Alcaligenes faecalis*. *Appl. Environ. Microbiol.*, **32**(3), 392 (1976).
42. Wakao, N., Koyatsu, H., Komai, Y., Shimokawara, H., Sakurai, Y. & Shiota, H., Microbial Oxidation of Arsenite and Occurrance of Arsenite-Oxidising Bacteria in Acid Mine Water from a Sulphur-Pyrite Mine. *Geomicrobiology Journal*, **6**, 11 (1988).
43. Sehlin, H.M. & Lindström, E.B., Oxidation and reduction of arsenic by *Sulfolobus acidocaldarius* strain BC. *FEMS Microbiology Letters*, **93**, 87 (1992).
44. Rinderle, S.J., Schrier, J. & Williams, J.W., Purification and Properties of Arsenite Oxidase (abstract). *Fed. Proc.*, **43**, 2060 (1984).
45. Mandl, M., Matulová, P. & Docekalová, H., Migration of arsenic(III) during bacterial oxidation of arsenopyrite in chalcopyrite concentrate by *Thiobacillus ferrooxidans*. *Appl. Microbiol. Biotechnol.*, **38**, 492 (1992).
46. Braddock, J.F., Luong, H.V. & Brown, E.J., Growth Kinetics of *Thiobacillus ferroxidans* Isolated from Arsenic Mine Drainage. *Appl. Environ. Microbiol.*, **48**(1), 48 (1984).
46. Lindström, E.B., Gunneriusson, E. & Tuovinen, O.H., Bacterial Oxidation of Refractory Sulfide Ores for Gold Recovery. *Critical Reviews in Biotechnology*, **12**(1/2), 133 (1992).
48. Nicolau, C. & Raimond, J., Procedure for the Enhancement of the Resistance to Arsenite and Arsenate of *Thiobacillus ferrooxidans*. *S. African Patent No 833709* (1983) as cited by Lawson E.N. Arsenic Toxicity, Bacterial Resistance and Bacterial Oxidation/Reductions. Phase 1 : Literature Review. *Report No PR 93/109C of Project No PR 93/132*, GENMIN Process Research, Johannesburg (1 November 1993).
49. Rawlings, D.E., Restriction Enzyme Analysis of 16S rRNA Genes for the Rapid Identification of *Thiobacillus ferrooxidans, Thiobacillus thiooxidans* and *Leptospirillum ferrooxidans* Strains in Leaching Environments. *Biohydrometallurgical Processing*, Viña del Mar, Chile, 19–22 November 1995, Vargas T., Jerez C.A., Wiertz J.V. & Toledo H. (eds), **II**, 9, University of Chile (1995).
50. Broadhurst, J.L., Determination of Arsenic and Iron, and their Oxidation States, in BIOX® Process Liquors. *Report No. PR 93/85C of Project No. PR 93/128*, GENMIN Process Research, Johannesburg (4 August 1993).

51. Bailey, A.D., An Assessment of Oxygen Availability, Iron Build-up and the Relative Significance of Free and Attached Bacteria, as Factors Affecting Bio-oxidation of Refractory Gold-bearing Sulphides at High Solids Concentrations. *PhD Thesis*, University of Cape Town (1993).
52. Breed, A.W., Hansford, G.S. & Harrison, S.T.L., Steady-state Operation and Aeration Perturbation Studies of the UCT/GENCOR Continuous Bio-oxidation Mini-plant. *Report submitted to GENCOR Process Research Laboratories*, Department of Chemical Engineering, University of Cape Town (10 August 1995).
53. Iglesias, N., Palencia, I. & Carranz, F., Removal of the Refractoriness of a Gold Bearing Pyrite-Arsenopyrite Ore by Ferric Sulphate Leaching at Low Concentration. *EPD Congress 1993*, Hager J.P.(ed), 99, The Minerals, Metals & Materials Society (1992).

Pergamon

Minerals Engineering, Vol. 10, No. 9, pp. 1023–1030, 1997

0892–6875/97 $17.00+0.00

S0892–6875(97)00081–2

TECHNICAL NOTE
A PRELIMINARY INVESTIGATION OF THE FERRIC LEACHING OF A PYRITE/ARSENOPYRITE FLOTATION CONCENTRATE

A.W. BREED, S.T.L. HARRISON and G.S. HANSFORD

Department of Chemical Engineering, University of Cape Town, Rondebosch 7700, South Africa. E-mail: AWB@chemeng.uct.ac.za
(Received 8 April 1997; accepted 15 May 1997)

ABSTRACT

Although considerable work on the leaching of pyrite using Fe(III) is reported in the literature, to date very little work on the chemical leaching of arsenopyrite, using Fe(III) has been reported.

Batch, ferric leaching experiments, each 48 hours in length, were carried out in sealed, baffled, agitated vessels. Varying quantities of Fe(III), ranging from 0 to 0.54 M were added to a slurry, containing 10 g.ℓ^{-1} concentrate. The redox potential was monitored continuously. Samples were taken at regular intervals and the total iron and arsenic concentration of the supernatant was determined.

The results showed that no leaching occurred in the absence of Fe(III). However, considerable leaching of arsenic occurred in the reactors to which Fe(III) was added. Furthermore the results suggest that the chemical leaching rate may be a function of the redox potential, and not of the absolute Fe(III) concentration. The stoichiometry determined for the ferric leaching of arsenopyrite agreed with the stoichiometry postulated by previous researchers [1], viz.:

$$FeAsS + 5Fe^{3+} \rightarrow S^0 + As^{3+} + 6Fe^{2+}$$

Furthermore, the results obtained are consistent with the hypothesis that the leaching of arsenopyrite, the oxidation of As(III) to As(V), the leaching of pyrite, and the precipitation of ferric arsenate compete for the available Fe(III). © *1997 Elsevier Science Ltd*

Keywords
Gold ores; sulphide ores; leaching; oxidation; extractive metallurgy

INTRODUCTION

Bioleaching is now an established technology for the pre-treatment of refractory gold ores and concentrates. It offers economic, environmental and technical advantages over pressure oxidation and roasting. Furthermore, the spontaneous bioleaching of wastes containing sulphide minerals contributes to acid mine

drainage, and the contamination of ground water by metals trapped within the matrices of these minerals.

Recent research suggests that the bioleaching of sulphide minerals occurs via a two-step mechanism [2], *i.e.* the mineral is leached chemically by Fe(III), and the role of the bacteria is to regenerate Fe(III), thereby maintaining a high redox potential within the system. A potential complication in the bioleaching of minerals is the solubilisation of metals to concentrations toxic to the micro-organisms [3–6], hence knowledge of the stoichiometry and kinetics of both the bacterial and chemical reactions may aid the design and modelling of the overall process.

Although considerable work on the leaching of pyrite using Fe(III) has been reported in the literature [7–9], to date very little work on the leaching of arsenopyrite, using Fe(III) at concentrations and conditions similar to those used in bioleaching, has been reported. For this reason some controversy exists in the literature with regard to the stoichiometry of the leaching reaction. Some of the leaching reactions postulated to date are listed below:

$$FeAsS + 11Fe^{3+} + 7H_2O \rightarrow 12Fe^{2+} + H_3AsO_3 + HSO_4^- + 10H^+ \quad [10] \qquad (1)$$

$$FeAsS + 13Fe^{3+} + 8H_2O \rightarrow 14Fe^{2+} + H_3AsO_4 + SO_4^{2-} + 13H^+ \quad [11] \qquad (2)$$

$$FeAsS + 7Fe^{3+} + 4H_2O \rightarrow 8Fe^{2+} + H_3AsO_4 + S^0 + 5H^+ \quad [11] \qquad (3)$$

$$FeAsS + 5Fe^{3+} \rightarrow S^0 + As^{3+} + 6\,Fe^{2+} \quad [1] \qquad (4)$$

The objective of this work was to determine whether or not a sample of pyrite/arsenopyrite flotation concentrate from the Fairview Gold Mine in Barberton, South Africa, could be leached by Fe(III), at concentrations similar to those observed during normal bioleaching operations. In view of the disparity with regard to the stoichiometry proposed by other workers, a further objective of the work was to attempt to determine the stoichiometry for the ferric leaching of this concentrate.

MATERIALS AND METHODS

The experiments were carried out in sealed, baffled, agitated 2.0 ℓ, glass Quickfit culture vessels. A slurry volume of 1.75 ℓ was used. Varying quantities of Fe(III), ranging from 0 to 0.54 M were added to a slurry, containing 10 $g.\ell^{-1}$ (1% ($m.v^{-1}$)) concentrate. The concentrate sample contained 5.84% As, 21.71% S and 24.01% Fe. 86.35% of the material was finer than 75 micron. The mineral analysis of the concentrate, estimated from the elemental analysis, was 12.70% FeAsS and 37.18% FeS_2. The slurry temperature was controlled at 40°C by placing the reactors in a water bath. However, the pH was not controlled, and the reactors were not aerated. All the leach tests were run for 48 hours.

The leaching rate was monitored by observing the variation in the iron and arsenic concentrations and the redox potential of the slurry. The redox potential of the slurry in the reactors was monitored continuously. It was obtained by direct millivolt measurement using an ASI OR101431 Pt combination, double junction Ag/AgCl ORP electrode and a Hitech Micro Systems UCT Redox Controller. Samples were taken at regular intervals and the total iron and arsenic concentration of the supernatant were determined by Atomic Adsorption Spectroscopy (AA).

RESULTS AND DISCUSSION

The results of this investigation are presented in Figures 1–3. Figure 1 shows the variation in the redox potential of the supernatant during the course of the experiment. Figure 2 shows the variation in the arsenic

concentration of the supernatant during the course of the experiment and Figure 3 shows the arsenic concentration of the supernatant as a function of the Fe(II) concentration calculated using the solution redox potential, the total iron concentration and a calibration curve for the ORP electrode [12].

The total iron concentration of the supernatant in the reactors with initial Fe(III) concentrations of 0.00, 0.09, 0.18, 0.45 and 0.54 M remained constant during the course of the experiment. However, the total iron concentration of the supernatant in the reactor with an initial iron concentration in the region of 0.36 M decreased during the course of the experiment.

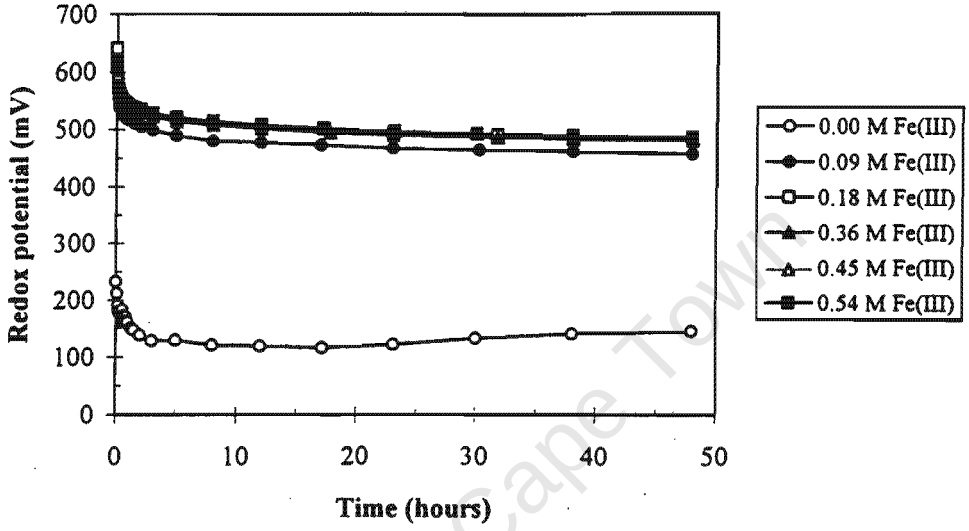

Fig.1 Variation in the redox potential of the slurry with time at different initial Fe(III) concentrations

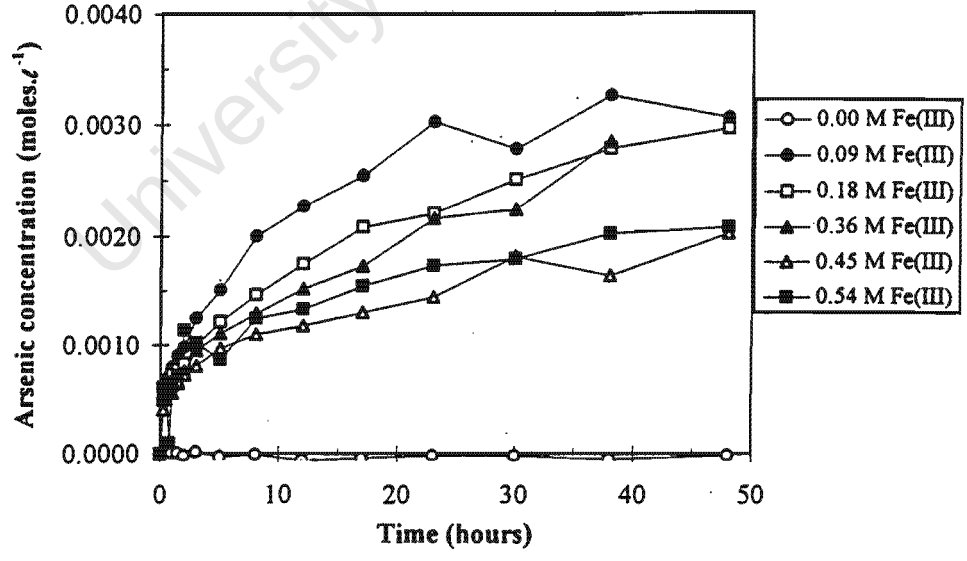

Fig.2 Variation in the arsenic concentration of the supernatant with time at different initial Fe(III) concentrations

It is apparent from Figure 1 that the redox potential of the slurry in all the reactors decreased during the course of the experiments. The decrease in the redox potential of the slurry in the reactor to which no Fe(III) was added can be attributed to the dissolution of trace quantities of Fe(II) present on the surface of

the mineral. This resulted in a significant change in the redox potential as a result of the very low overall iron concentration present, *viz.* $[Fe_{total}] \leq 0.0033$ M. However, the decrease in the redox potential of the slurry in the reactors to which Fe(III) was added indicates that Fe(III) was consumed and Fe(II) generated, according to the half-reaction shown in Eq. 5:

$$Fe(III) + e^- \rightarrow Fe(II) \quad (5)$$

It is also evident from Figure 1 that the shape of the redox potential versus time curves were similar in all the reactors to which Fe(III) was added. This suggests that the leaching rate of arsenopyrite (*i.e.* the rate at which arsenic is solubilised) is a function of the redox potential, and not of the absolute Fe(III) concentration. The above is also consistent with the results of recent research using pyrite [13].

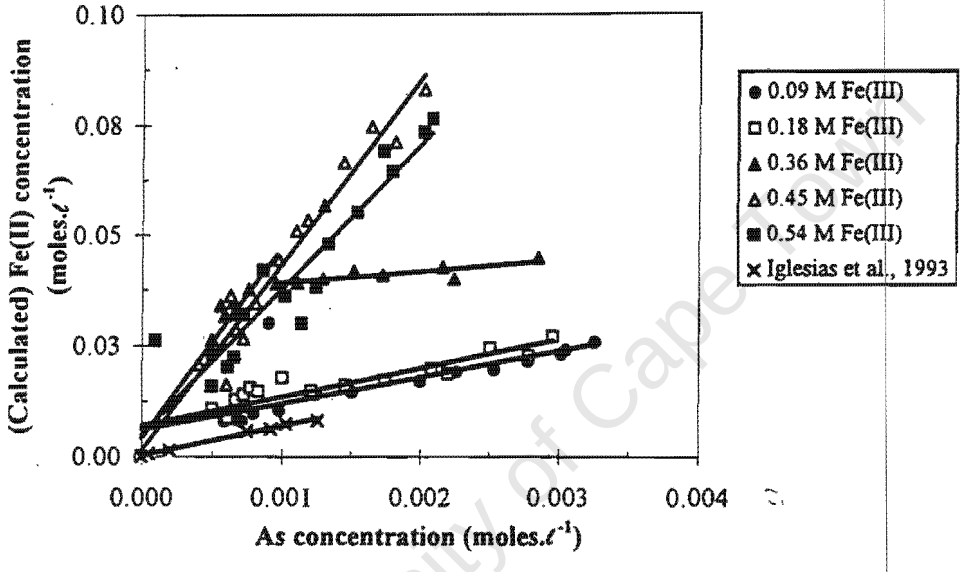

Fig.3 Variation in the Fe(II) concentration of the supernatant as a function of the arsenic concentration at different initial Fe(III) concentrations

Figure 2 indicates that no arsenic was solubilised in the absence of Fe(III). However, significant leaching of arsenic occurred in the reactors to which Fe(III) was added. The results shown in Figures 1 and 2 therefore suggest that the chemical leaching of arsenopyrite occurred in these reactors, according to Eq. 6:

$$FeAsS + (x-1)Fe^{3+} \rightarrow Sulphur\ species + Arsenic\ species + xFe^{2+} \quad (6)$$

Although the chemical leaching of the pyrite portion of the concentrate cannot be disregarded, it has been found that the bioleaching of arsenopyrite precedes the bioleaching of pyrite [14]. For this reason it was initially assumed that the data obtained could be interpreted assuming that the sample consisted of pure arsenopyrite.

It is also apparent from Figure 2 that the arsenic concentration of the supernatant decreased with an increase in the initial Fe(III) concentration. This resulted in the proportion of arsenic (arsenopyrite) solubilised, calculated assuming that all the solubilised arsenic remained in solution, decreasing with an increase in the initial Fe(III) concentration (see Table 2). The above suggests that an excess of Fe(III) in the leaching medium results in either the passivation of the mineral surface, or the co-precipitation of iron and arsenic.

Figure 3 shows the measured arsenic concentration of the supernatant as a function of the Fe(II)

concentration of the supernatant, calculated using the solution redox potential, the total iron concentration and a calibration curve for the ORP electrode, for each of the different initial Fe(II) concentrations, and similar data obtained by previous researchers, using pure arsenopyrite [1].

Linear regression of the results shown in Figure 3 was carried out to determine the stoichiometric coefficient of Fe^{2+}, *viz.* x, in Eq. 6. The results of the linear regression are shown in Table 1. It is clear from Figure 3 and Table 1 that, at initial Fe(III) concentrations of 0.09 and 0.18 M, the results obtained support the stoichiometry shown in Eq. 4. However, at initial Fe(III) concentrations of 0.45 and 0.54 M the results of this investigation differ significantly from the stoichiometry indicated in Eq. 4.

The large variation in the stoichiometric coefficient of Fe^{2+} shown in Table 1 suggests that the Fe^{2+}/As^{3+} ratio is affected by the ferric oxidation of As(III) to As(V) [1], (Eq. 7), the precipitation of ferric arsenate (Eq. 8), and possibly the leaching of pyrite (Eq. 9).

$$As^{3+} + 2Fe^{3+} \rightarrow As^{5+} + 2Fe^{2+} \quad [15] \tag{7}$$

$$2Fe(III) + As(III) \rightarrow 2Fe(II) + As(V) \quad [16] \tag{8}$$

$$FeS_2 + 14Fe^{3+} + 8H_2O \rightarrow 2SO_4^{2-} + 15Fe^{2+} + 16H^+ \quad [7, 8] \tag{9}$$

This is consistent with the postulate that the chemical oxidation of arsenopyrite, the chemical oxidation of As(III) to As(V) and the precipitation of ferric arsenate compete for the available Fe(III) [17]. Therefore, the rate at which each of these reactions occurs depends on the absolute and relative concentrations of arsenopyrite, As(III), As(V)and Fe(III) in solution.

TABLE 1 **Results of the linear regression carried out on the data shown in Figure 3, *viz.* the variation in the Fe(III) concentration of the supernatant as a function of the arsenic concentration of the supernatant at different initial Fe(II) concentrations, and of similar data obtained using pure arsenopyrite [1].**

Fe(III) concentration (moles.ℓ^{-1})	Constant	R^2	Coefficient of Fe(II)
0.09	0.0061	0.5849	5.8218
0.18	0.0070	0.8156	6.4159
0.36 [As≤0.001 M]	0.0041	0.9045	43.2280
0.36 [As≥0.001 M]	0.0365	0.7091	2.5718
0.45	0.0014	0.9604	41.9870
0.54	0.0050	0.8931	32.789
Iglesias *et al.* (1993)	0.0002	0.9900	6.6356

The nature of the competing reactions listed above resulted in the total iron concentration of the supernatant in the reactor with an initial iron concentration of 0.36 M decreasing during the course of the experiment, and in the respective curve obtained (see Figure 3) having two distinct regions. At [As] ≤ 0.001 M the slope of the curve is similar to the slope obtained at initial iron concentrations of 0.45 and 0.54 M. However, at [As] ≥ 0.001 M the slope is similar to the slope obtained at initial iron concentrations of 0.09 and 0.18 M. The above therefore suggests that the rate at which the above reactions occurs depends on the absolute and relative concentrations of arsenopyrite, As(III), As(V)and Fe(III) in solution.

In an attempt to determine whether or not precipitation may have resulted in the *apparent* reduction in the proportion of arsenic (arsenopyrite) solubilised (calculated using the final arsenic concentration of the supernatant), the proportion of arsenic (arsenopyrite) solubilised was also determined using the final Fe(II) concentration (calculated using the solution redox potential, the total iron concentration and a calibration curve for the ORP electrode) and assuming the reaction stoichiometry listed in Eq. 4. The proportion of arsenic (arsenopyrite) solubilised, calculated by both methods, is listed in Table 2.

From Table 2 it is clear that a large discrepancy exists between the two methods employed. However, if it is assumed that the ***actual*** proportion of arsenic solubilised lies somewhere between the proportions calculated by the two methods employed, it is obvious that the proportion of arsenopyrite solubilised increases with an increase in the initial Fe(III) concentration. Furthermore, the above suggests that a large proportion of the mineral is solubilised during the 48 hours over which the experiment was performed. In contrast to these results, previous workers observed about 25% arsenic extraction in 24 hours [1].

TABLE 2 **Calculated proportion of arsenic solubilised based on: (A) the final measured arsenic concentration; and (B) the final Fe(II) concentration determined by redox potential measurement and Eq. 4**

	Proportion of arsenic solubilised(%)	
Initial Fe(III) concentration (M)	(A)	(B)
0.08	40	51
0.16	38	58
0.36	35	78
0.45	26	178
0.54	27	163

CONCLUSIONS

Although the degree of leaching increases with an increase in the initial Fe(III) concentration, the leaching rate of arsenopyrite appears to be dependent on the redox potential of the slurry, and not on the absolute Fe(III) concentration.

The chemical oxidation of arsenopyrite, the chemical oxidation of As(III) to As(V), the precipitation of

ferric arsenate and possibly the chemical oxidation of pyrite, compete for the available Fe(III). Although the above may affect the experimentally determined stoichiometry of the leaching reaction, the stoichiometry determined for the ferric leaching of arsenopyrite agreed with the stoichiometry postulated by previous researchers [1], *viz.*:

$$FeAsS + 5Fe^{3+} \rightarrow S^0 + As^{3+} + 6Fe^{2+}$$

Furthermore, the competitive nature of the above reactions prevent reliable determination of the degree of arsenopyrite oxidation by monitoring the arsenic concentration of the supernatant, or by monitoring the redox potential of the slurry. In spite of the above limitations, the rate, and degree of arsenopyrite solubilisation observed in this investigation was greater than reported previously.

ACKNOWLEDGEMENTS

The authors would like to thank GENCOR Process Research for technical and financial support of the research.

REFERENCES

1. Iglesias, N., Palencia, I. & Carranza, F., Removal of the refractoriness of a gold bearing pyrite-arsenopyrite ore by ferric sulphate leaching at low concentration. In *Proc. EPD Congress 1993*, ed. J.P. Hager. The Minerals, Metals and Materials Society, Warrendale, 1993, pp. 99–115.
2. Boon, M., Hansford, G.S. & Heijnen, J.J., The role of bacterial ferrous iron oxidation in the bio-oxidation of pyrite. In *Proc. Biohydrometallurgical Processing Volume I*, eds. T. Vargas, C.A. Jerez., J.V. Wiertz and H. Toledo. University of Chile, Santiago, 1993, pp. 153–163.
3. Pol'kin, S.I., Panin, V.V., Adamov, E.V., Karavaiko, G.I. & Chernyak, A.S., Theory and practice of utilizing microorganisms in difficult-to-dress ores and concentrates. In *Proc. Eleventh International Mineral Processing Congress*. Instituto di Arte Mineraria e Preparazione dei Minerali, Universita di Cagliari, Cagliari, 1975, pp. 901–923.
4. Norris, P.R. & Kelly, D.P., Toxic metals in leaching systems. In *Metallurgical Applications of* Bacterial *Leaching and Related Microbiological Phenomena*, eds. L.E. Murr, A.E. Torma and J.A. Brierley. Academic Press, New York, 1978, pp. 83–102.
5. Shrestha, G.N., Microbial leaching of refractory gold ores. *Australian Mining*, 1988, October, 48-57.
6. Lindström, E.B. & Sehlin, H.M., Toxicity of arsenic compounds to the sulphur-dependent archaebacterium *Sulfolobus*. In *Proc. Biohydrometallurgy-89*, eds. J. Salley, R.G.L. McCready and P.L. Wichlacz. Canmet, Ottawa, 1989, pp. 59–70.
7. Garrels, R.M. & Thompson, M.E., Oxidation of pyrite by iron sulphate solutions. *American Journal of Science*, 1960, **258-A**, 57–67.
8. Mathews, C.T. & Robins, R.G., The oxidation of iron disulphide by ferric sulphate. *Australian Journal of Chemical Engineering*, 1972, August, 21–25.
9. McKibben, M.A., Kinetics of aqueous oxidation of pyrite by ferric iron, oxygen and hydrogen peroxide from pH 1–4 and 20–40°C. *Ph.D. Thesis*, Pennsylvania State University, 1984.
10. Barrett, J., Hughes, M.N. & Russell, A, Oxidation of Arsenopyrite by Iron(III). In *Proc. Randol Gold Forum*, Squaw Valley, 1990, pp. 135–136.
11. Nagpal, S., Microbial leaching of a mixed sulfide ore concentrate in continuous-flow. *Ph.D. Thesis*, University of Utah, Salt Lake City, 1993.
12. Breed, A.W., and Hansford, G.S., unpublished results, 1995.
13. May, N., The ferric leaching of pyrite. M.Sc. thesis, University of Cape Town, Cape Town, 1997.
14. Miller, D. and Hansford, G.S., Batch biooxidation of a gold-bearing pyrite–arsenopyrite concentrate. *Minerals Engineering*, 1992, 5(6), pp. 613–629.
15. Mandl, M. & Vyškovský, M., Kinetics of arsenic(III) oxidation by iron(III) catalysed by pyrite in

the presence of *Thiobacillus ferrooxidans*. *Biotechnology Letters*, 1994, **16**(11), pp. 1199–1204.
16. Fernandez, M.G.M., Mustin, C., De Donato, P., Barres, O., Marion, P. and Berthelin, J., Occurrences at mineral–bacteria interface during oxidation of arsenopyrite by *Thiobacillus ferrooxidans*. *Biotechnol. Bioeng.*, 1995, **46**(1), pp. 13–21.
17. Breed, A.W., Glatz, A., Harrison, S.T.L. & Hansford, G.S., The effect of As(III) and As(V) on the batch bioleaching of a pyrite–arsenopyrite concentrate. *Minerals Engineering*, 1996, **9**(12), pp. 1235–1252.

Pergamon

Minerals Engineering, Vol. 12, No. 4, pp. 383–392, 1999

0892–6875(99)00018–7
0892–6875/99/$ — see front matter

STUDIES ON THE MECHANISM AND KINETICS OF BIOLEACHING

A.W. BREED[§] and G.S. HANSFORD[†*]

§ Current address: 2 Crown Buildings, 17 Canal Crescent, Perth, PH2 8HT, Scotland.
E-mail: ashli@cableinet.co.uk
† Gold Fields Mineral Bioprocessing Laboratory, Department of Chemical Engineering, University of Cape Town, Rondebosch 7701, South Africa. E-mail: gsh@chemeng.uct.ac.za
* To whom all correspondence should be addressed
(Received 28 September 1998; accepted 17 December 1998)

ABSTRACT

The use of off-gas analysis and redox potential measurement has shown that bioleaching involves at least three important sub-processes. The primary attack of the sulphide mineral is a chemical ferric leach. The role of the bacteria is to convert the iron from the ferrous to the ferric form, thereby maintaining a high redox potential.

The kinetics of bacterial ferrous iron oxidation by Thiobacillus ferrooxidans and a Leptospirillum-like bacterium, and the chemical ferric leach kinetics of pyrite have both been described as functions of the ferric/ferrous-iron ratio. Thus, the chemical ferric leach of the mineral and the bacterial oxidation of the ferrous iron are linked by the redox potential, and are in equilibrium when the rate of iron turnover between the mineral and the bacteria is balanced.

These rate equations have been used to predict the steady state redox potential and sulfide mineral conversion in a continuous bioleach reactor. The model successfully predicts laboratory data and is being tested against data from pilot-plant and full-scale bioleach systems. Furthermore, the model predicts which bacterial species will predominate and which mineral will be preferentially leached under specific operating conditions. Enzyme restriction analysis has shown that in pyrite–arsenopyrite bioleach reactors the dominant iron oxidizer is L. ferrooxidans, which is in agreement with the predictions of the model.

Keywords
Sulfide ores; leaching; reaction kinetics; bioleaching; modeling

INTRODUCTION

The bioleaching of copper from copper-bearing sulfide ore and waste in dumps has been practiced for some time [1]. More recently heap leaching has been used for copper bioleaching and the pretreatment of refractory arsenical gold ores [2,3]. The bioleaching of arsenical gold-bearing concentrates in large stirred tank bioreactors has been practiced since 1984 with several large plants in different parts of the world [4,5]. The design of these has been based on the use of the empirical logistic equation to describe

Presented at *Minerals Engineering '98*, Edinburgh, Scotland, September 1998

the kinetics of bioleaching [6–8]. However recent work by Boon [9] has led to the development of a mechanistically based model for bioleaching [10,11]. This model predicts the kinetics of bioleaching, explains the microbial selection that takes place in bioleach systems and is the basis for the derivation of a performance equation for continuous bioleach reactors. The predictions of the model are in accordance with microbial identification using 16S rDNA techniques and the electrochemistry of the ferric leaching of sulfide minerals [12].

BACKGROUND

The use of degree-of-reduction balances [13] coupled with off-gas analysis for the measurement of oxygen and carbon dioxide utilisation rate has been developed by Boon [9] in order to measure bacterial and pyrite concentrations, in bioleach systems. These measurements have proved difficult in the past. The activity of the bacteria was determined as the specific rate of oxygen utilisation and was either measured in the bioreactors, using off-gas analysis, or off-line in a biological oxygen monitor.

By staged additions of pyrite at four hourly intervals to a batch bioleach, Boon *et al.* [10] were able to measure the specific oxygen utilisation rate as a function of the ferric/ferrous-iron ratio or redox potential. The oxygen utilisation rate was also related to the pyrite concentration via the pyrite specific oxygen utilisation rate. The results of a typical experiment are shown in Figure 1, where it can be seen that the specific rate of oxygen utilisation, decreases with increasing ferric/ferrous-iron ratio while the pyrite specific oxygen utilisation rate increases with increasing ferric/ferrous-iron ratio.

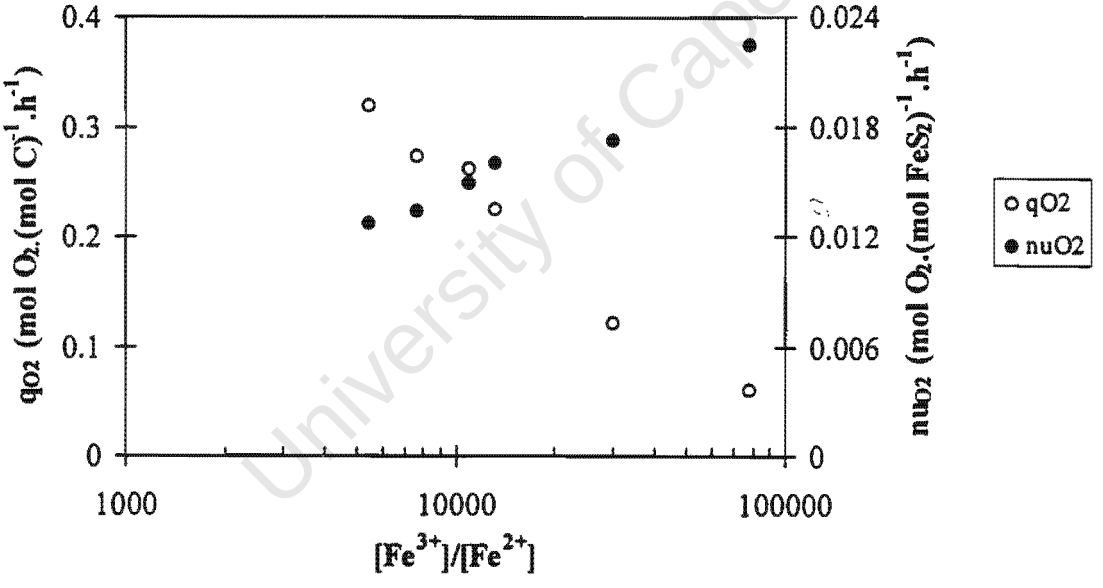

Fig.1 Bacterial and pyrite specific oxygen utilisation rates, q_{O_2} and ν_{O_2}, respectively, as functions of the ferric/ferrous-iron ratio, $[Fe^{3+}]/[Fe^{2+}]$, for the bioleaching of pyrite ($[FeS_2]$ = 2–20 g.ℓ^{-1}) by a *Leptospirillum*-like bacterium (c_X = 25–100 mg C.ℓ^{-1}) at Fe^{tot} = 2.4–5.0 g.ℓ^{-1}, pH 1.6 and T = 30°C. Data was obtained from Boon *et al.* [10].

In addition samples were taken from the batch, the pyrite removed by centrifugation, and the specific oxygen utilisation rate of the bacteria measured in an off-line respirometer, or BOM, using ferrous iron medium. This enabled the specific oxygen utilisation rate to be measured over a wider range of ferric/ferrous-iron ratios than in the pyrite batch. However, in the region where the ranges overlapped, the data for the pyrite- and ferrous iron-grown bacteria coincided, as shown in Figure 2. From this it was concluded that in both cases ferrous iron was the primary substrate, and that the bioleaching of pyrite occurs as a two-step mechanism involving the chemical ferric leaching of the pyrite and the bacterial oxidation of the ferrous iron produced, back to the ferric form.

The reactions involved are:

Chemical: $FeS_2 + 14Fe^{3+} + 8H_2O = 15Fe^{2+} + 2SO_4^{2-} + 16H^+$ (1)

Bacterial: $4Fe^{2+} + O_2 + 4H^+ = 4Fe^{3+} + 2H_2O$ (2)

Overall: $4FeS_2 + 15O_2 + 2H_2O = 4Fe^{3+} + 8SO_4^{2-} + 4H^+$ (3)

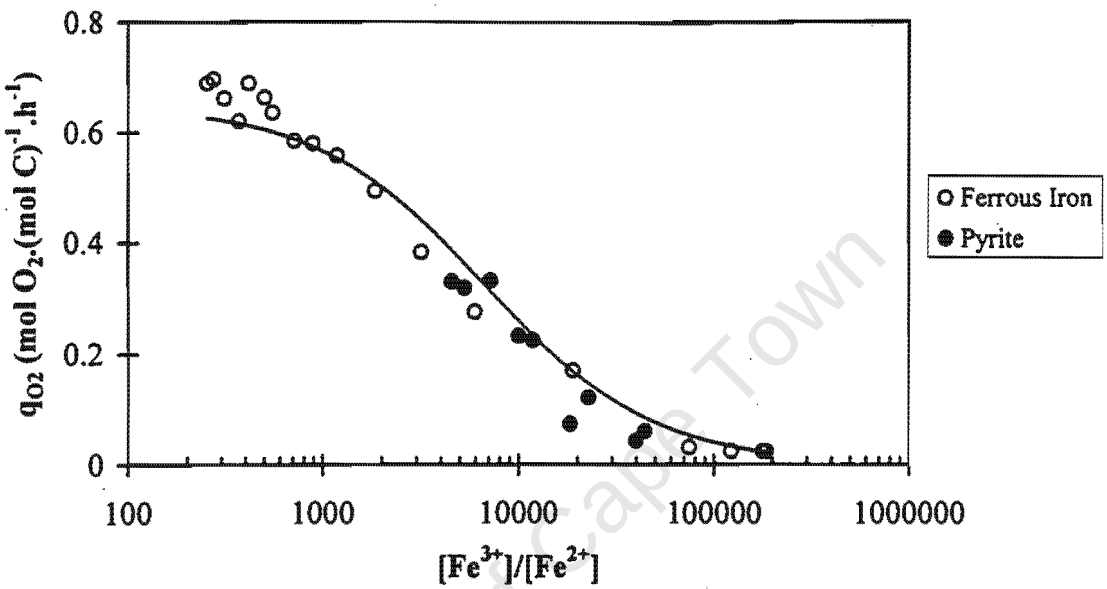

Fig.2 Specific oxygen utilisation rates of pyrite and ferrous iron grown *Leptospirillum*-like bacteria as a function of the ferric/ferrous-iron ratio, together with the prediction of Equation 5. Data was obtained from Boon *et al.* [10].

The existence of a two-step mechanism for the bioleaching of sulphide minerals has a number of important implications for the modelling of bioleaching, *viz.*;

i) the overall process can be reduced to a number of independent sequential and/or parallel sub-processes,

ii) the kinetics of each of these sub-processes can be studied independently, and

iii) the kinetic constants derived during the separate studies can be used to predict both the steady-state and dynamic performance of bioleach systems for a variety of different minerals, bacteria and operating conditions.

A simplified form of a previously used model for inhibited Michaelis-Menten kinetics [14]; can be used to describe the bacterial ferrous iron oxidation sub-process in terms of the specific oxygen utilization rate as a function of the ferrous/ferric-iron ratio [9];

$$q_{O_2} = \frac{-r_{O_2}}{c_X} = \frac{q_{O_2}^{max}}{1 + K\frac{[Fe^{3+}]}{[Fe^{2+}]}} \quad (4)$$

In Eq. 4, q_{O_2} is the bacterial specific oxygen utilization rate (mol O_2.(mol C)$^{-1}$.h^{-1}), r_{O_2} is the rate of oxygen production (mole.ℓ^{-1}.h^{-1}), c_X is the bacterial concentration (mol C.ℓ^{-1}), $q_{O_2}^{max}$ is the maximum bacterial specific oxygen utilization rate (mol O_2.(mol C)$^{-1}$.h^{-1}), K is the kinetic constant in bacterial ferrous iron oxidation (dimensionless), [Fe^{3+}] is the ferric iron concentration (mol.ℓ^{-1}) and [Fe^{2+}] is the ferrous iron concentration (mol.ℓ^{-1}).

The kinetics of the overall process can be described in terms of the pyrite specific oxygen utilisation rate as a function of the ferrous/ferric-iron ratio [9];

$$\nu_{O_2} = \frac{-r_{O_2}}{[FeS_2]} = \frac{\nu_{O_2}^{max}}{1 + B\frac{[Fe^{2+}]}{[Fe^{3+}]}} \quad (5)$$

In Eq. 5, ν_{O_2} is the pyrite specific oxygen utilisation rate (mol O_2.(mol FeS_2)$^{-1}$.h^{-1}), [FeS_2] is the pyrite concentration (mol.ℓ^{-1}), $\nu_{O_2}^{max}$ is the maximum pyrite specific oxygen utilisation rate (mol O_2.(mol FeS_2)$^{-1}$.h^{-1}) and B is the kinetic constant in chemical ferric leaching of pyrite (dimensionless). The following values have been reported for the kinetic constants listed in Eqs. 4 and 5 [9]; $q_{O_2}^{max}$ = 1.7 h^{-1}, K = 0.0005 for the bioleaching of pyrite by *Leptospirillum*-like bacteria, $q_{O_2}^{max}$ =2.2 h^{-1}, K = 0.05 for ferrous iron oxidation by *Thiobacillus ferrooxidans* and $\nu_{O_2}^{max}$ =0.025 h^{-1}, B = 0.00045.

The dependence of the bacterial kinetics on the solution redox potential is consistent with the chemiosmotic theory of Ingledew [15], while the dependence of the ferric leach kinetics on the redox potential is in agreement with electrochemical theory.

THE MECHANISM AND KINETICS OF SULFIDE MINERAL BIOLEACHING

The two sub-processes are linked at pseudo steady state by equating the rate of ferrous iron production from the chemical ferric leach reaction to the rate of consumption of ferrous iron by the bacteria. In order to do this, the kinetics of the two sub-processes must be rewritten for ferrous iron production and utilization in terms of the rate of ferrous iron production per unit surface area of the pyrite particles, *viz.*;

$$\xi_{Fe^{2+}} = \frac{-r_{Fe^{2+}}}{\alpha[FeS_2]} = \frac{\xi^{max}_{Fe^{2+}}}{1+B\dfrac{[Fe^{2+}]}{[Fe^{3+}]}} \quad (6)$$

In Eq. 6, $\xi_{Fe^{2+}}$ is the pyrite specific ferrous iron production rate (mol $Fe^{2+}.m^{-2}.h^{-1}$), $r_{Fe^{2+}}$ is the rate of ferrous iron production (mol.$\ell^{-1}.h^{-1}$), α is the specific surface area of the pyrite particles ($m^2.mol^{-1}$) and $\xi^{max}_{Fe^{2+}}$ is the maximum pyrite specific ferrous iron production rate (mol $Fe^{2+}.m^{-2}.h^{-1}$). The specific surface area of pyrite particles, ξ, enables the sulphide mineral concentration, particle size and roughness to be taken into account.

The bacterial ferrous iron oxidation sub-process can also be expressed in terms of the specific rate of bacterial ferrous iron utilisation [9];

$$q_{Fe^{2+}} = \frac{-r_{Fe^{2+}}}{c_X} = \frac{q_{Fe^{2+}}}{1+K\dfrac{[Fe^{3+}]}{[Fe^{2+}]}} \quad (7)$$

In Eq. 7, $q_{Fe^{2+}}$ is the bacterial specific ferrous iron utilisation rate (mol Fe^{2+}.(mol C)$^{-1}.h^{-1}$) and $q^{max}_{Fe^{2+}}$ is the maximum bacterial specific ferrous iron utilisation rate (mol Fe^{2+}.(molC)$^{-1}.h^{-1}$).

At a particular pyrite and bacterial concentration the pseudo steady state will be defined by;

$$\frac{\xi^{max}_{Fe^{2+}}\alpha[FeS_2]}{1+B\dfrac{[Fe^{2+}]}{[Fe^{3+}]}} = r^{chem}_{Fe^{2+}} = -r^{bact}_{Fe^{2+}} = \frac{q^{max}_{Fe^{2+}}c_X}{1+K\dfrac{[Fe^{3+}]}{[Fe^{2+}]}} \quad (8)$$

In Eq. 8, $r^{chem}_{Fe^{2+}}$ is the chemical ferrous iron production rate (mol $Fe^{2+}.\ell^{-1}.h^{-1}$) and $r^{bact}_{Fe^{2+}}$ is the bacterial ferrous iron production rate (mol $Fe^{2+}.\ell^{-1}.h^{-1}$).

It is possible to express the ferric/ferrous-iron ratio in Eqs. 4–8 in terms of the redox potential using the Nernst equation;

$$\frac{[Fe^{3+}]}{[Fe^{2+}]} = \exp\left(\frac{E_h - E_0}{\dfrac{RT}{nF}}\right) \quad (9)$$

In Eq. 9, E_h is the redox potential (mV), E_0 is the standard redox potential (mV), R is the universal gas constant ($J.K^{-1}.mol^{-1}$), T is the absolute temperature (K), n is the number of electrons in transferred in the redox reaction (dimensionless) and F is the Faraday constant ($C.mol^{-1}$).

Using the stoichiometry of Eqs. 1 and 2, the following values for the ferrous iron based kinetic constants

can be obtained from Boon's oxygen based values [9]; $\xi_{Fe^{2+}}^{max}$ =0.0067 h^{-1}, B = 0.00045, $q_{Fe^{2+}}^{max}$ =6.8 h^{-1}, K = 0.0005 for the bioleaching of pyrite by *Leptospirillum*-like bacteria and $q_{Fe^{2+}}^{max}$ = 8.8 h^{-1}, K = 0.05 for ferrous iron oxidation by *T. ferrooxidans*. Recent work on the chemical ferric leaching of pyrite [16] has shown that the values for $\xi_{Fe^{2+}}^{max}$ and B agree with those obtained from the data of Boon *et al.* [10], for the bioleaching of pyrite.

Although *T. ferrooxidans* can also oxidize sulphur and sulphur moieties, for the purpose of simulation, it is assumed that this is not the rate controlling sub-process in this system.

Figure 3 shows the predicted rate of ferrous iron generation by the ferric leaching of pyrite and the predicted rates of ferrous iron consumption by a *Leptospirillum*-like bacterium and *T. ferrooxidans*, as a function of the redox potential, at a total iron concentration of 12 $g.\ell^{-1}$. The point of intersection of the curves depends on both the concentration of bacteria and the active surface area concentration of the pyrite. It represents a pseudo-steady state from which the rate of ferrous iron turnover and the redox potential can be determined. Furthermore, the point of intersection of the chemical and bacterial curves can be related stoichiometrically to the rate of pyrite bioleaching. In this way the model presented here can be related to those models based on a bacteria-to-mineral ratio, *i.e.* $c_X/[FeS_2]$ [9]. As the bacterial concentration and/or the surface area concentration change the redox potential and overall pyrite bioleaching rate will change accordingly.

From Figure 3 it can be seen that for the bioleaching of pyrite the ferric leach curve intersects the bacterial ferrous iron oxidation curve of the *Leptospirillum*-like bacterium at a higher rate of ferrous iron turnover than *T. ferrooxidans*, hence, the *Leptospirillum*-like bacterium will be the dominant species. This has been confirmed by Rawlings [18], who found that *Leptospirillum ferrooxidans* predominates in the bioreactors of the GENCOR BIOX® process treating an arsenopyrite–pyrite concentrate. However, in the bioleaching of sulphide minerals that have lower rest potentials, the ferric leach curve will intersect the bacterial curves at a lower redox potential. If this occurs at a point where the ferrous iron oxidation rate of *T. ferrooxidans* is higher than that of *L. ferrooxidans*, then *T. ferrooxidans* will be the dominant microorganism.

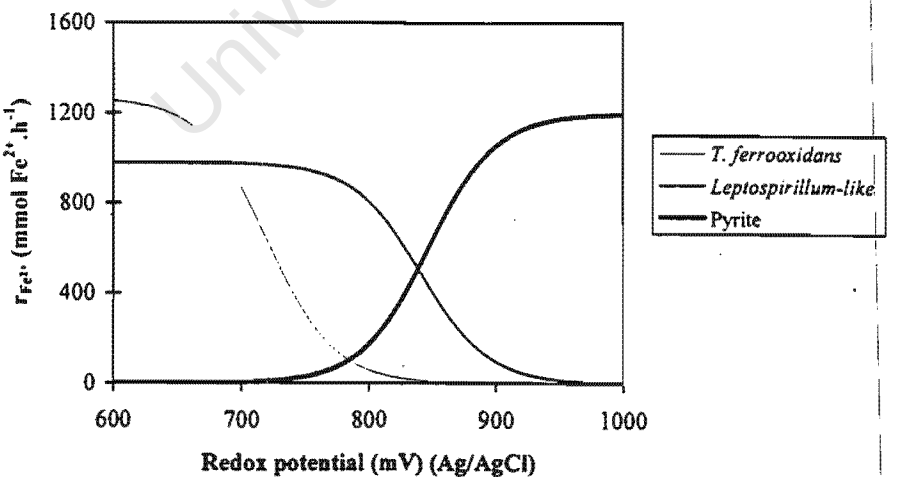

Fig.3 Predicted rate of ferrous iron production by the ferric leaching of −53+75 μm pyrite at 10 $g.\ell^{-1}$ together with the predicted rate of ferrous iron oxidation by a *Leptospirillum*-like bacterium and *T. ferrooxidans* (c_X = 150 mg $C.\ell^{-1}$) as a function of the redox potential. Data for pyrite and *T. ferrooxidans* were obtained from Boon [9] and the data for the *Leptospirillum*-like bacterium were obtained from van Scherpenzeel [17].

MODELLING THE PERFORMANCE OF CONTINUOUS BIOLEACH REACTORS

Bacterial ferrous oxidation

In a continuous bioreactor at steady state it can be shown that the growth rate of the micro-organisms is equal to the dilution rate;

$$\mu = D = \frac{1}{\tau} \tag{10}$$

In Eq. 10, μ is the bacterial specific growth rate (h^{-1}), D is the dilution rate (h^{-1}) and τ is the residence time (h).

If it is assumed that the bacterial specific growth rate is directly related to the specific rate of ferrous iron oxidation then;

$$q_{Fe^{2+}} = \frac{\mu}{Y^{max}_{Fe^{2+}X}} = \frac{D}{Y^{max}_{Fe^{2+}X}} \tag{11}$$

In Eq. 11, $Y^{max}_{Fe^{2+}X}$ is the bacterial yield on ferrous iron (mol C.(mol Fe^{2+})$^{-1}$). Substituting for $q_{Fe^{2+}}$ from Eq. 7 and solving for the ferric/ferrous iron-ratio gives;

$$\frac{[Fe^{3+}]}{[Fe^{2+}]} = \frac{Y^{max}_{Fe^{2+}X} q^{max}_{Fe^{2+}} \tau - 1}{K} \tag{12}$$

The Nernst equation can be used to express Eq. 12 in terms of the solution redox potential.

The above applies to a completely mixed bioreactor at steady state provided there is no retention of biomass within the bioreactor *i.e.* there must be no wall growth. From Eq. 12 it is clear that for the case of a bioreactor with pyrite feed, the steady state ferric/ferrous-iron ratio, or redox potential, is not dependent on the concentration of pyrite in the feed, but only on the residence time. This is analogous to the behaviour of a chemostat [19].

Chemical ferric pyrite leaching

From the stoichiometry of Eq. 1, the rate of pyrite leaching is related to the rate of ferrous iron production rate according to;

$$r_{FeS_2} = \frac{1}{15} r_{Fe^{2+}} = -\frac{1}{15} \xi_{Fe^{2+}} \alpha [FeS_2] \tag{13}$$

In Eq. 13, r_{FeS_2} is the pyrite production rate (mol $FeS_2.\ell^{-1}.h^{-1}$).

A steady state pyrite balance over the bioreactor gives;

$$F([FeS_2]_{in} - [FeS_2]) = -Vr_{FeS_2} \tag{14}$$

In Eq. 14, F is the volumetric flow rate at steady state ($\ell.h^{-1}$), $[FeS_2]_{in}$ is the pyrite concentration in the

feed to the bioreactor (mol $FeS_2.\ell^{-1}$), $[FeS_2]$ is the concentration of pyrite in the bioreactor (mol $FeS_2.\ell^{-1}$) and V is the volume of the bioreactor (ℓ).

Therefore, the pyrite concentration leaving the bioreactor is given by;

$$[FeS_2] = \frac{15[FeS_2]_{in}\left(1+B\frac{[Fe^{2+}]}{[Fe^{3+}]}\right)}{15+15B\frac{[Fe^{2+}]}{[Fe^{3+}]}+\alpha\tau\xi^{max}_{Fe^{2+}}} \quad (15)$$

The pyrite conversion is given by;

$$X_{FeS_2} = \frac{[FeS_2]_{in}-[FeS_2]}{[FeS_2]_{in}} = \frac{\alpha\tau\xi^{max}_{Fe^{2+}}}{15+15B\frac{[Fe^{2+}]}{[Fe^{3+}]}+\alpha\tau\xi^{max}_{Fe^{2+}}} \quad (16)$$

In Eq. 14, X_{FeS_2} is the pyrite conversion (dimensionless).

Substituting the ferric/ferrous-iron ratio from Eq. 12 into Eq. 16 shows that the pyrite conversion is also a function of only the residence time in the bioreactor and the rate constants and particle size distribution of the pyrite.

Figure 4 shows the predicted variation in the pyrite conversion (Eq. 16), using a *Leptospirillum*–like bacterium in a continuous-flow bioreactor, at residence times ranging from 0 to 20 days. The kinetic data for pyrite was obtained from the bioleaching of +53–75 μm size fraction pyrite flotation concentrate from Prieska Copper Mine, Copperton, South Africa [9] and confirmed for the abiotic ferric leaching of the same concentrate [20]. The kinetic data for the *Leptospirillum*–like bacterium was obtained from Van Scherpenzeel [17]. These predictions are compared with the results of Hansford and Chapman [21] for the continuous bioleaching of a similar sized euhedral pyrite in a laboratory-scale, 5-litre continuous bioleach reactor using a culture thought to be *T. ferrooxidans* and a pyrite flotation concentrate from Crown Mines, South Africa. No redox potential data are available. The agreement between the prediction and the experimental data is remarkable, particularly when considering that the pyrite concentrates are from different sources and that the bacteria used by Hansford and Chapman [21] were unidentified and thought to be *T. ferrooxidans*. However in retrospect it is reasonable to assume that the bacteria which would predominate in a continuous culture growing on pyrite would be *L. ferrooxidans*.

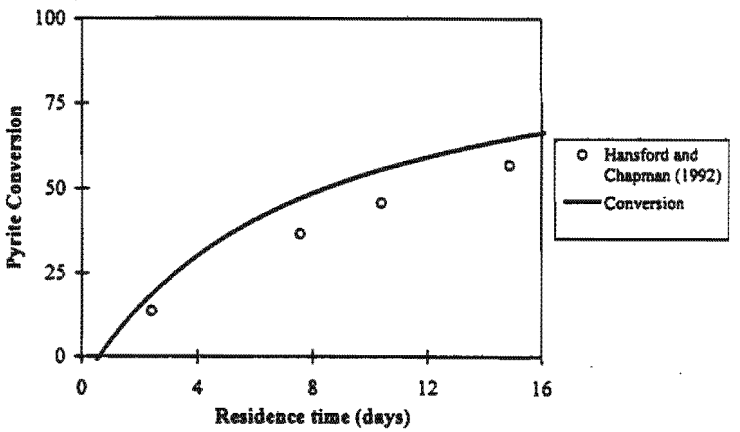

Fig.4 Predicted (Eq. 16) and measured conversions [21] of pyrite in a continuous bioleach reactor.

CONCLUSIONS

The two step mechanism for bioleaching suggests that the kinetics of the two sub-processes can be investigated separately. It provides a basis for predicting the overall rates of bioleaching from the rates of the controlling sub-processes of chemical ferric leaching and bacterial ferrous iron oxidation. These can be conveniently expressed in terms of the ferric/ferrous-iron ratio or redox potential. This approach also predicts which microbial species will predominate.

Further refinement of the approach described is necessary to include changes in size and surface area of the sulphide minerals, the formation of precipitates that could occlude the surface and the bacterial oxidation of the sulphur moiety. However, the model appears to have potential for predicting the performance of continuous bioleach reactors.

REFERENCES

1. Murr, L.E., Theory and practice of copper sulphide leaching in dumps and *in-situ*. *Minerals Science Engineering*, **12**(3), 121–189 (1980).
2. Schnell, H.A., Bioleaching of copper, in *Biomining: Theory, Microbes and Industrial Processes*, ed. D.E. Rawlings, 21–43, Springer, Berlin (1997).
3. Brierley, J.A., Heap leaching of gold-bearing deposits: theory and operational description, *in Biomining: Theory, Microbes and Industrial Processes, ed. D.E. Rawlings*, 103–115, Springer, Berlin (1997).
4. Dew, D.W., Lawson E.N. & Broadhurst, J.L., The BIOX® process for biooxidation of gold-bearing ores or concentrates, in *Biomining: Theory, Microbes and Industrial Processes*, ed. D.E. Rawlings, 45–80, Springer, Berlin (1997).
5. Miller, P.C., The design and operating practice of bacterial oxidation plant using moderate thermophiles (The BACTECH process), in *Biomining: Theory, Microbes and Industrial Processes*, ed. D.E. Rawlings, 81–102, Springer, Berlin (1997).
6. Pinches, A, Chapman, J.T., te Riele, W.A.M. & van Staden, M., The performance of bacterial leach reactors for the pre-oxidation of refractory gold-bearing sulfide concentrates, in *Biohydrometallurgy: Proceedings of International Symposium*, eds. P.R. Norris and D.P. Kelly, 329–344, Science and Technology letters, Kew (1988).
7. Hansford, G.S. & Miller, D.M., Biooxidation of a gold-bearing pyrite arsenopyrite concentrate. *FEMS Microbiology Reviews*, **11**, 175–182 (1993).
8. Dew, D.W., Comparison of performance for continuous bio-oxidation of refractory gold ore flotation concentrates, in *Biohydrometallurgical Processing*, **I**, eds. T. Vargas, C.A. Jerez, J.V. Wiertz and H. Toledo, 239–251, University of Chile, Santiago (1995).
9. Boon, M., Theoretical and Experimental Methods in the Modelling of Bio-oxidation Kinetics of Sulphide Minerals, *PhD Thesis*, Technische Universiteit Delft, Delft (1996).
10. Boon, M., Hansford, G.S. & Heijnen, J.J., The role of bacterial ferrous iron oxidation in the bio-oxidation of pyrite, in *Biohydrometallurgical Processing* **I**, eds. T. Vargas, C.A. Jerez, J.V. Wiertz and H. Toledo, 153–163, University of Chile, Santiago (1995).
11. Hansford, G.S., Recent developments in modeling the kinetics of bioleaching, in *Biomining: Theory, Microbes and Industrial Processes*, ed. D.E. Rawlings, 153–175, Springer, Berlin (1997).
12. Rawlings, D.E., Tributsch, H. & Hansford, G.S., Reasons why *Thiobacillus ferrooxidans* is not the dominant iron-oxidizing bacterium in many commercial processes for the biooxidation of pyrite and related ores. *Microbiology* (in press).
13. Roels, J.A., *Energetics and Kinetics in Biotechnology*, Elsevier Biomedical Press, Amsterdam (1983).
14. Jones, C.A. & Kelly, D.P., Growth of *Thiobacillus ferrooxidans* on ferrous iron in chemostat culture: influence of product and substrate inhibition. *Journal of Chemical Technology and Biotechnology*, **33B**, 241–261 (1983).
15. Ingledew, W.J., *Thiobacillus ferrooxidans;* the bioenergetics of an acidophilic chemolithotroph. *Biochimica Biophysica Acta*, **683**, 89–117 (1982).

In practice, and in this investigation, E_0' and RT/zF are determined by calibrating the redox probe at the conditions used.

Differentiating the Nernst equation (Eq. (5)) yields;

$$\frac{dE}{dt} = \frac{RT}{zF}\frac{d}{dt}\ln\left(\frac{[Fe^{3+}]}{[Fe^{2+}]}\right) \tag{6}$$

$$\frac{dE}{dt} = \frac{RT}{zF}\left(\frac{1}{[Fe^{3+}]}\frac{d[Fe^{3+}]}{dt} - \frac{1}{[Fe^{2+}]}\frac{d[Fe^{2+}]}{dt}\right) \tag{7}$$

The rate of arsenopyrite dissolution can be defined as;

$$r_{FeAsS} = \frac{d[FeAsS]}{dt} = -\frac{d[Fe_{total}]}{dt} = -\frac{d([Fe^{3+}]+[Fe^{2+}])}{dt} \tag{8}$$

Combining Eq. (7) with the reaction stoichiometry and Eq. (8) yields;

$$\frac{dE}{dt} = \frac{RT}{zF} r_{FeAsS}\left(\frac{5}{[Fe^{3+}]} + \frac{6}{[Fe^{2+}]}\right) \tag{9}$$

Rearranging Eq. (9) yields an expression for the rate of arsenopyrite leaching;

$$r_{FeAsS} = \frac{\frac{zF}{RT}\frac{dE}{dt}}{\frac{5}{[Fe^{3+}]} + \frac{6}{[Fe^{2+}]}} \tag{10}$$

The ferric ferrous ratio and the total iron concentration can then be used to determine the concentrations of both Fe^{3+} and Fe^{2+} using;

$$[Fe^{2+}] = \frac{[Fe_{total}]}{1 + \frac{[Fe^{3+}]}{[Fe^{2+}]}} \tag{11}$$

and

$$[Fe^{3+}] = \frac{[Fe_{total}]\frac{[Fe^{3+}]}{[Fe^{2+}]}}{1 + \frac{[Fe^{3+}]}{[Fe^{2+}]}} \tag{12}$$

Substituting Eqs. (11) and (12) into Eq. (10) yields an expression in which all the parameters can be determined. It is therefore possible to determine the variation in the

Table 2
Standard conditions for the ferric leaching of arsenopyrite

Parameter	Level
Volume (mℓ)	75
$[Fe_{total}]$ (g.ℓ^{-1})	16
pH	1.1
Solids concentration (g.ℓ^{-1})	10
Agitator speed (rev.min^{-1})	1500
Temperature (°C)	25
$E_{initial}$ (vs. Ag/AgCl) (mV)	615

rate of arsenopyrite dissolution during the course of the experiment using the measured variation in the redox potential and the initial total iron concentration;

$$r_{FeAsS} = \frac{[Fe_{total}]\dfrac{zF}{RT}\dfrac{dE}{dt}}{\left(1+\dfrac{[Fe^{3+}]}{[Fe^{2+}]}\right)\left(\dfrac{5}{\dfrac{[Fe^{3+}]}{[Fe^{2+}]}}+6\right)} \tag{13}$$

Although the increase in the total iron concentration during the course of the experiments was small, ±5% of the initial iron concentration, it was taken into consideration during the calculation of the leaching rate.

The parameters varied during the course of the experimental program included the initial redox potential, the total iron concentration, the solids concentration and the pH of the solution. The standard ferric leaching conditions are shown in Table 2.

3. Results

3.1. Probe calibration

As the ferric leaching experiments were carried out under nonideal conditions it was necessary to determine the values of E_0' and RT/zF at the conditions used. The values of these parameters at 25°C and varying total iron concentrations are listed in Table 3.

Table 3
Comparison of theoretical and measured Nernst equation parameters (T = 25°C)

$[Fe_{total}]$ (g.ℓ^{-1})	RT/zF (mV)	E_0 (mV)
8	25.78	430.9
16	27.21	430
32	28.38	431.9
Theoretical value	25.70	572

3.2. General behaviour

Although no attempt was made to confirm the reaction stoichiometry, upon completion of each experiment, the spent leach liquor was titrated with cerium sulphate and the presence of As^{3+} confirmed.

Fig. 2 shows the typical variation in the redox potential of the solution observed during the course of an experiment. From Fig. 2 it is apparent that during the first few minutes of leaching there is a rapid drop in the redox potential of the solution.

In all the experiments performed, raw data similar in shape to the data shown in Fig. 2 were obtained. After smoothing the raw data (Eq. (4)) the rate of ferrous iron production as a function of the redox potential of the leaching solution was determined (Eq. (13)) as described in Section 2.6.

3.2.1. Error analysis

The contribution of ferrous iron oxidation, by dissolved oxygen, to the ferric iron concentration, and hence the observed rate of ferric leaching was determined in an air-sparged CSTR. The feed to the reactor consisted of a salt solution containing 12 $g.\ell^{-1}$ ferrous iron. The temperature in the CSTR was maintained at 40°C; the residence time was maintained at 100 h and the pH was maintained at pH 1.75. Sparging compressed air at 100 $m\ell.min^{-1}$ through the solution ensured saturation of the liquid.

Fig. 3 shows the measured variation in the outlet ferrous iron concentration with elapsed time and the predicted variation in the outlet ferrous iron concentration if ideal CSTR behaviour, and no reaction, is assumed. The data in Fig. 3 were used to determine the approximate rate of ferric iron regeneration by oxidation of the ferrous iron. It was found to be in the region of 5.0×10^{-8} mol $Fe^{2+}.\ell^{-1}.s^{-1}$. In comparison, the ferrous iron production rates observed during the ferric leaching experiments ranged from about

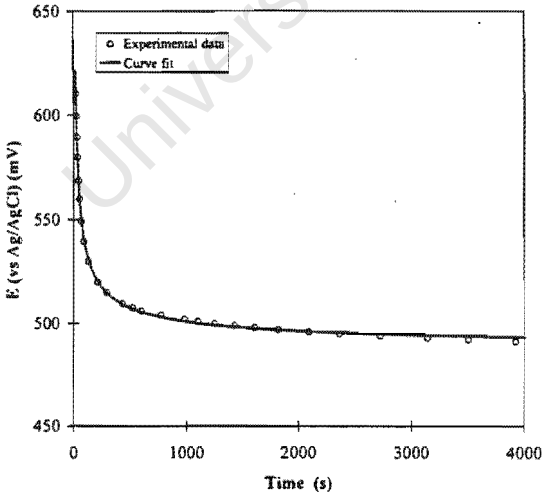

Fig. 2. Typical example of the observed variation in the redox potential with time, and curve fit ($y = 679.6x^{-0.56} + 486.6$; $R^2 = 0.998$) to experimental data.

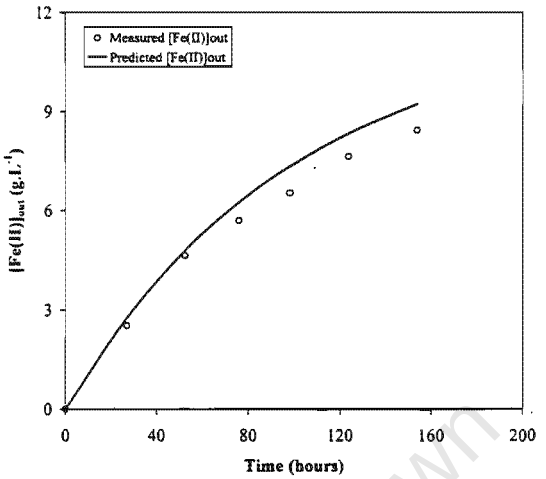

Fig. 3. Variation in the measured outlet ferrous iron concentration and the predicted variation in the outlet ferrous iron concentration if ideal CSTR behaviour and no reaction is assumed, with time.

5.5×10^{-6} mol $Fe^{2+}.\ell^{-1}.s^{-1}$.(g FeAsS)$^{-1}$ at the beginning of the experiment to about 2.7×10^{-8} mol $Fe^{2+}.\ell^{-1}.s^{-1}$.(g FeAsS)$^{-1}$ at the end of the experiment, i.e., from 8.9×10^{-5} to 4.3×10^{-7} mol $Fe^{2+}.\ell^{-1}.s^{-1}$, based on an arsenopyrite concentration of 16 g.ℓ^{-1}.

From the above it is clear that the rate of ferrous iron production during the leaching experiments could be ignored during the analysis of the kinetics of arsenopyrite leaching. For this reason no attempt was made to exclude oxygen from the leaching solution.

In addition to the above, analyses performed to determine the errors introduced as a result of attributing the drop in redox potential to the ferric leaching of arsenopyrite only were found to be in the region of 1%. The reproducibility was found to be in the region of 8%, hence it was possible to ignore the contributions of the ferric leaching of the copper, lead and zinc minerals in the sample to the changes in the redox potential of the solution. Furthermore, acid leaching tests performed in the absence of ferric iron were found to have little effect on the redox potential due to the low rates observed and the stoichiometry of the leaching reaction.

3.2.2. Leaching rate

Fig. 4 shows the specific rate of arsenopyrite leaching (expressed as the ferrous iron production rate per unit mass of arsenopyrite) as a function of the solution redox potential during one run. From Fig. 4 it is apparent that the rate initially increases with a decrease in the redox potential of the solution. It appears to pass through a maximum, and then decreases rapidly with a further decrease in the redox potential of the solution. However, it is clear that for most of the experiment, the rate of leaching decreased with a decrease in the redox potential of the solution.

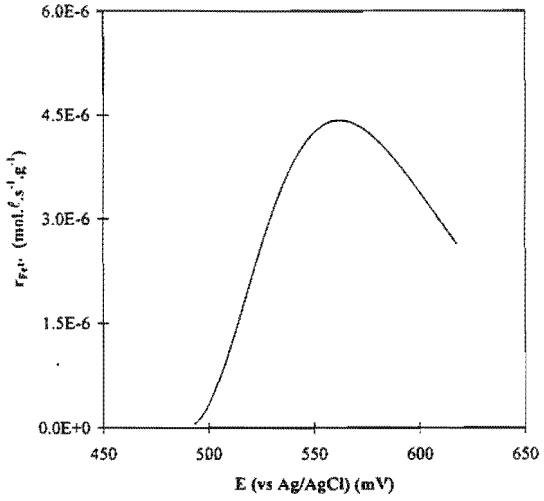

Fig. 4. Variation in the specific ferrous iron production rate during the ferric leaching of arsenopyrite as a function of the solution redox potential during one run.

3.3. Initial redox potential

The influence of the initial solution redox potential on the rate at which arsenopyrite is leached by ferric iron is shown in Fig. 5. From Fig. 5 it is clear that the initial increase in the leaching rate apparent in Fig. 4 is not visible at low initial redox potentials; viz.

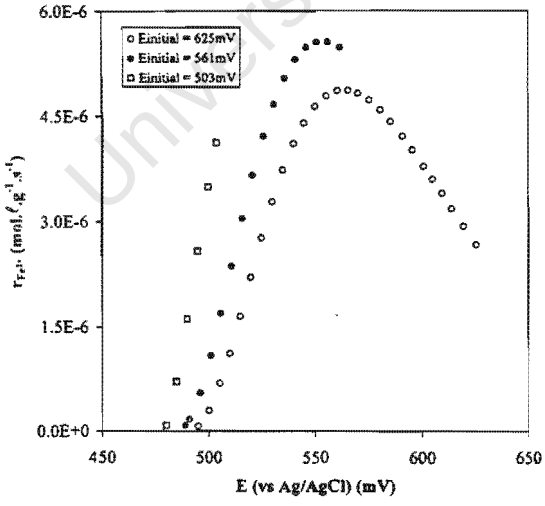

Fig. 5. Influence of the initial solution redox potential on the variation in the specific ferrous iron production rate during the ferric leaching of arsenopyrite, as a function of the solution redox potential.

$E_{initial} < 550$. Instead, the rate of leaching decreased with a decrease in the redox potential of the solution, across the entire range of redox potentials encountered.

3.4. Total iron concentration

The effect of the overall iron concentration on the ferric leaching kinetics of arsenopyrite was investigated at initial ferric iron concentrations of 8, 16 and 32 $g.\ell^{-1}$ (Fig. 6). From Fig. 6 it is apparent that an increase in the total iron concentration resulted in the ferric leaching reaction stopping at a higher value of the solution redox potential. It is also apparent that the maximum leaching rate observed at a total iron concentration of 8 $g.\ell^{-1}$ was significantly lower than at higher overall iron concentrations. Although this effect was reproducible, it was not supported by other findings.

3.5. Mass transfer

The results obtained during the experiments performed at different total iron concentrations suggest that, under the conditions employed, the rate of reaction is not mass-transfer limited. This was confirmed by experiments performed at impeller speeds ranging from 1250 to 1800 $rev.min^{-1}$ and is consistent with the results of previous research performed at the same temperature [17].

3.6. Solids concentration

Fig. 7 shows the influence of the mineral concentration, at concentrations of 5, 10 and 20 $g.\ell^{-1}$, on the ferric leaching of arsenopyrite. As in previous figures, the rate is expressed as the rate of ferrous iron production divided by the solids concentration. This

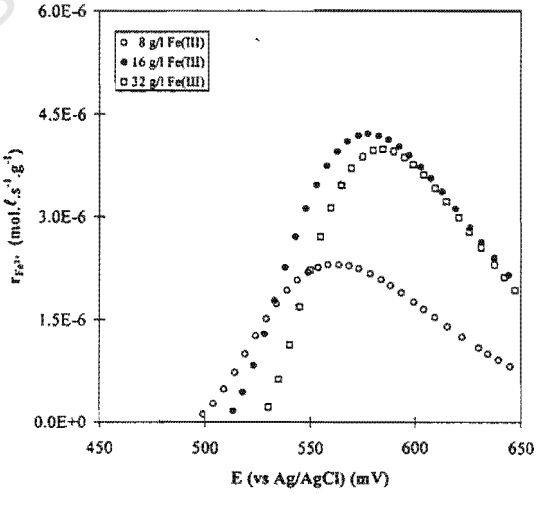

Fig. 6. Influence of the total iron concentration in solution on the variation in the specific ferrous iron production rate during the ferric leaching of arsenopyrite, as a function of the solution redox potential.

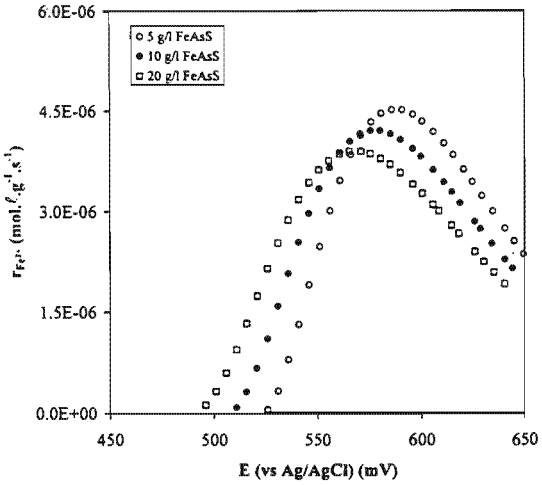

Fig. 7. Influence of the solids (arsenopyrite) concentration on the variation in the specific ferrous iron production rate during the ferric leaching of arsenopyrite, as a function of the redox potential of the solution.

was done in an attempt to eliminate the effect of the increase in the available surface area. From Fig. 7 it is clear that the rate based on the arsenopyrite surface area was not constant. However, the curves obtained show similar trends in the rate with changes in the solution redox potential.

The surface area concentration (arsenopyrite concentration) seems to affect the redox potential at which the leaching stops. It does not appear to have a significant influence on either the rate at which the leaching rate changed (the slope of the curve), or the maximum leaching rate of the arsenopyrite.

3.7. pH

Fig. 8 shows the influence of the solution pH upon the ferric leach rate of arsenopyrite. The mineral seems to be more active at lower acid concentrations.

3.8. Leached vs. unleached ore

Scanning electron microscopy (SEM) was used to determine whether or not the rate of leaching of the mineral used in this investigation was influenced by the formation of an occluding layer consisting of either jarosite or elemental sulphur. However, neither jarosite nor elemental sulphur was visible on the surface of a mineral sample that had been leached for 1 h. In addition, mineral that had been leached for 1 h was dried and leached once again, using fresh leaching solution. The results of the experiment performed using 'leached' arsenopyrite and the results of an experiment performed using unleached mineral, at the same conditions, are shown in Fig. 9. From Fig. 9 it is clear that the ferric leaching rate of 'leached' material is similar to the ferric leaching rate of fresh mineral.

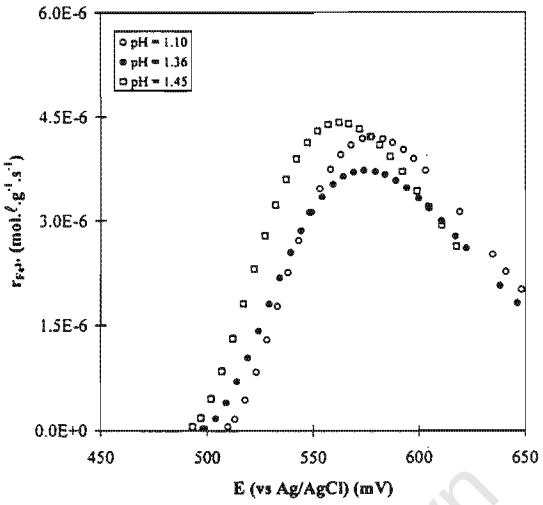

Fig. 8. Influence of the solution pH on the variation in the specific ferrous iron production rate during the ferric leaching of arsenopyrite, as a function of the redox potential of the solution.

3.9. Kinetics

It is apparent from Figs. 4–9 that the relationship between the redox potential of the solution and the specific rate of ferrous iron production is not linear. It was not possible to fit the electrochemically-based model proposed by Verbaan and Crundwell [4], or the Monod-type model proposed by Boon [6]. However, it was possible to model the ferric leach kinetics using the Butler–Volmer-based model suggested by May et al. [7]

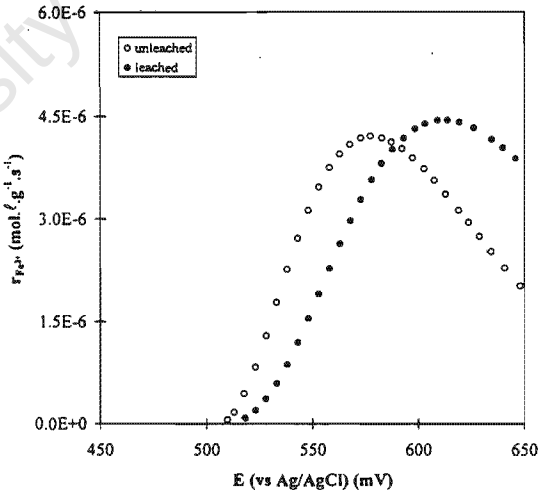

Fig. 9. Comparison between the variation in the specific ferrous iron production rate during the ferric leaching of unleached and leached arsenopyrite, as a function of the redox potential of the solution.

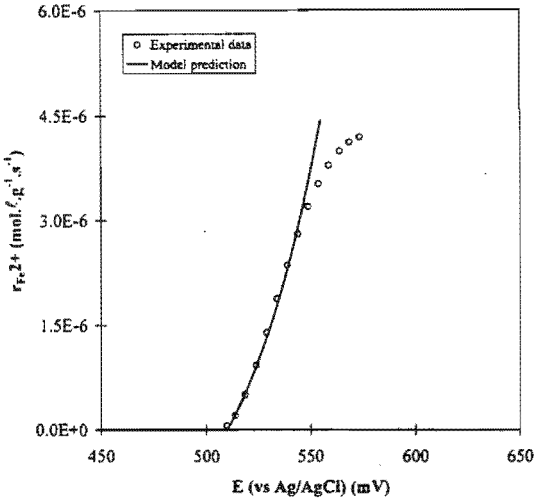

Fig. 10. Comparison between the Butler–Volmer based model prediction ($r_0 = 5 \times 10^4$, $\alpha = 0.498$, $\beta = 0.0272$, $E' = 510$) and the experimental leaching rate data.

(Eq. (2)). Comparison of the Butler–Volmer-based model prediction with a typical set of experimental results is shown in Fig. 10. It is clear from Fig. 10 that the agreement between the model based on the Butler–Volmer equation and the experimental results is good.

4. Discussion

The rapid change in the initial redox potential shown in Fig. 2 was anticipated, and can be explained as follows. At high total iron concentrations and ferric–ferrous ratios, even a small increase in the ferrous iron concentration will result in a large change in the ferric ferrous ratio, and hence a large drop in the redox potential.

In most of the experiments performed the ferric leaching rate of arsenopyrite initially increased with a decrease in the redox potential of the solution (Figs. 4–8). The leaching rate reached a maximum, and then decreased rapidly with a further decrease in the redox potential.

An increase in the initial ferric leaching rate with decreasing redox potential was also observed during the ferric leaching of pyrite [7]. However, although a drop in the ferric leaching rate of arsenopyrite was observed at redox potentials between 600 and 700 mV (vs. SHE) [18], the behaviour apparent in Figs. 4–8 has not been reported previously for arsenopyrite. It is therefore suggested that this *transient* behaviour is a result of the rearrangement of the ions on the surface of the mineral and in the electrical double layer surrounding the mineral; it is not a result of the leaching of the mineral itself. This postulate is supported by observations made during studies on the effect of the ferric iron concentration on the eletrophoretic mobility of arsenopyrite [19], and by the fact that no surface products responsible for passivation of the mineral surface were observed.

Although previous workers have detected a sulphur layer on the mineral surface after both the acid, and the ferric leaching of arsenopyrite, it has not been found to hinder the dissolution reaction [12,18,20,21]. The absence of a surface layer in this investigation may be a result of the high redox potentials used [22]. Furthermore, the reactive nature of the leached mineral suggests that the rate of leaching is not time-dependent and is primarily a function of the redox potential of the leaching solution. The slight increase in the rate of dissolution of the 'leached' mineral can be attributed to the increase in the surface area.

The decrease in the rate of leaching with a decrease in the redox potential of the solution observed for most of the experiment is in agreement with previously reported trends for the ferric leaching of sulphide minerals [7,11,23–25]. This suggests a dependency of the ferric leaching rate on the redox potential of the leaching solution, which in turn suggests that an electrochemical model be used to describe the ferric leaching kinetics of arsenopyrite.

An electrochemically driven reaction should exhibit a half-order dependence on the ferric iron concentration [26]. However, the ferric leaching rate of pyrite was found to be independent of the total iron concentration, for iron concentrations ranging from 0.05 to 0.5 M (2.80 to 28 g.ℓ^{-1}) [7]. Although the leaching rate of arsenopyrite did not exhibit a half-order dependence on the ferric iron concentration it was not found to be independent of the total iron concentration (Fig. 6). In addition, it was not possible to fit the models proposed by either Verbaan and Crundwell [4] or Boon [6].

It was possible to model the ferric leach kinetics of arsenopyrite across a wide range of conditions using the Butler–Volmer based model suggested by May et al. [7] (Eq. (2)). However, a limitation of the model appears to be its dependence on the 'rest potential' of the mineral, i.e., the redox potential of the solution at which at which the dissolution of arsenopyrite stops. This arsenopyrite 'rest potential' was found to increase when:

(i) the starting potential increases,
(ii) the total iron concentration increases,
(iii) the solids concentration decreases, and
(iv) the H^+ concentration increases.

Although pH has been reported to have an effect on the rest potential of molybdenite [23], it is more likely that the effect of pH on the rate of leaching can be attributed to its effect on the speciation of the ferric sulphate complexes. pH has a significant effect on the complexes formed between Fe^{3+} and SO_4^{2-} over the range from pH 1.0 to 2.0 [27]. The different complexes would in turn be expected to have different leaching capabilities.

The results therefore suggest that the reactivity of the mineral is determined by the ferric and proton concentration based on the arsenopyrite surface area. An increase in the concentration of either ferric iron or protons (relative to the arsenopyrite surface area) results in a reduction in the reactivity of the mineral. This is regarded as highly unusual as most reaction mechanisms are favoured by an increase in reactant concentration.

Although the underlying mechanism responsible for the observed influence of the different parameters on the leaching rate is not clear at present, it is suspected that they

affect the speciation of the iron, sulphur and arsenic complexes in the solution. It is therefore necessary to modify the Butler–Volmer-based model to include the effect of parameters such as the pH and the ferric iron concentration on the activity of the ferric and ferrous iron species involved. This may yield a mechanistically based model capable of predicting the ferric leaching rate of minerals over a wide range of conditions.

Acknowledgements

The technical and financial assistance of GENCOR Process Research is gratefully acknowledged.

Appendix A

a	constant in smoothing equation (s^{-1})
B	kinetic constant (dimensionless)
b	constant in smoothing equation (dimensionless)
c	constant in smoothing equation (dimensionless)
E	solution redox potential (mV)
E'	mineral rest potential (mV)
E'_0	constant in Nernst equation (mV)
F	Faraday constant ($C.mol^{-1}$)
$[Fe^{2+}]$	ferrous iron concentration ($mol.\ell^{-1}$)
$[Fe^{3+}]$	ferric iron concentration ($mol.\ell^{-1}$)
$[Fe_{total}]$	total iron concentration ($mol.\ell^{-1}$)
R	universal gas constant ($kJ.K^{-1}.mol^{-1}$)
r_0	kinetic constant in chemical ferric mineral oxidation ($mol.\ell^{-1}.h^{-1}$)
$r_{Fe^{2+}}$	arsenopyrite leaching rate ($mol.\ell.s^{-1}.g^{-1}$)
r_{FeAsS}	arsenopyrite leaching rate ($mol.\ell.s^{-1}.g^{-1}$)
T	absolute temperature (K)
t	time (s)
z	number of electrons involved in a reaction (dimensionless)
α	fraction of mineral reacted at time, t (dimensionless)
β	zF/RT (dimensionless)
$\upsilon_{Fe^{2+}}^{max}$	maximum area specific ferrous iron production rate ($mol.m^{-2}.h^{-1}$)
$\upsilon_{Fe^{2+}}$	area specific ferrous iron production rate ($mol.m^{-2}.h^{-1}$)

References

[1] P.C. Van Aswegen, Commissioning and operation of bio-oxidation plants for the treatment of refractory gold ores, in: J.B. Hiskey, G.W. Warren (Eds.), Hydrometallurgy; Fundamentals, Technology and Innovations, Soc. Min. Metall. Explor. AIME, 1993. pp. 709–725.

[2] R. Poulin, R.W. Lawrence, Economic and environmental niches of biohydrometallurgy, Minererals Engineering 9 (8) (1996) 799–810.

[3] M. Boon, G.S. Hansford, J.J., Heijnen, The role of bacterial ferrous iron oxidation in the bioleaching of pyrite, in: T. Vargas, C.A. Jerez, J.V. Wiertz, H. Toledo (Eds.), Biohydrometallurgical Processing Vol. I, University of Chile, Santiago, 1996, pp. 153–163.
[4] B. Verbaan, F.K. Crundwell, An electrochemical model for the leaching of a sphalerite concentrate, Hydrometallurgy 16 (3) (1986) 345–359.
[5] S. Nagpal, D. Dahlstrom, T. Oolman, A mathematical model for the bacterial oxidation of a sulfide ore concentrate, Biotechnology and Bioengineering 43 (5) (1994) 357–364.
[6] M. Boon, 1996. Theoretical and experimental methods in the modelling of bio-oxidation kinetics of sulphide minerals, Ph.D thesis, Delft University of Technology, The Netherlands.
[7] N. May, D.E. Ralph, G.S. Hansford, Dynamic redox potential measurements for determining the ferric leach kinetics of pyrite, Minerals Engineering 10 (11) (1997) 1279–1290.
[8] R.M. Garrels, M.E. Thompson, Oxidation of pyrite by iron sulphate solutions, American Journal of Science 258A (1960) 57–67.
[9] C.T. Mathews, R.G. Robins, The oxidation of iron disulphide by ferric sulphate, Australian Chemical Engineering (August 1972) 21–25.
[10] M.A. McKibben, H.B. Barnes, Oxidation of pyrite in low temperature acidic solutions: Rate laws and surface textures, Geochimica et Cosmochimica Acta 50 (7) (1986) 1509–1520.
[11] A.W. Breed, S.T.L. Harrison, G.S. Hansford, A preliminary investigation of the ferric leaching of a pyrite/arsenopyrite flotation concentrate, Minerals Engineering 10 (9) (1997) 1023–1030.
[12] N. Iglesias, I. Palencia, F. Carranza, Removal of the refractoriness of a gold bearing pyrite–arsenopyrite ore by ferric sulphate leaching at low concentration, in: J.P. Hager (Ed.), EPD Congress 1993, The Minerals, Metals and Materials Society, 1993, pp. 99–115.
[13] J. Zeman, M. Mandl, P. Mrnustíková, Oxidation of arsenopyrite by *Thiobacillus ferrooxidans* detected by a mineral electrode, Biotechnology Techniques 9 (2) (1995) 111–116.
[14] E.W. Randall, P. Moon, A.D.M. Gavin, Dynamically extendable communications protocol for a serial input/output system, Journal of Microcomputer Applications 16 (1993) 385–393.
[15] A.D. Bailey, An assessment of oxygen availability, iron build-up and the relative significance of free and attached bacteria, as factors affecting bio-oxidation of refractory gold-bearing sulphides at high solids concentrations, PhD thesis, University of Cape Town, South Africa, 1993.
[16] G.H. Jeffrey, J. Bassett, J. Mendham, R.C. Denney, Vogel's Textbook of quantitative chemical analysis, 5th edn., Longman, New York, 1989.
[17] N. Iglesias, I. Palencia, F. Carranza, Treatment of a gold bearing arsenopyrite concentrate by ferric sulphate leaching, Minerals Engineering 9 (3) (1996) 317–330.
[18] J.G. Dunn, P.G. Fernandez, H.C. Hughes, H.G. Linge, Aqueous oxidation of arsenopyrite in acid, Final Proc. Austral. Inst. Min. Metall. Annual Conference, Australasian Institute of Mining and Metallurgy, Carlton, Australia, 1989, pp. 217–220.
[19] A. MacDonald, G.S. Hansford, Zeta potential measurement of Thiobacillus ferrooxidans and Leptospirillum ferrooxidans in the presence of pyrite, Biotech SA '97, Rhodes University, Grahamstown, South Africa, 1997, p. 57.
[20] G.M. Kostina, A.S. Chernyak, Electrochemical conditions for the oxidation of pyrite and arsenopyrite in alkaline and acid solutions, Zhurnal Prikladnoi Khimii 49 (7) (1976) 1534–1570.
[21] I. Lázaro, R. Cruz, I. González, M. Monroy, Electrochemical oxidation of arsenopyrite in acidic media, International Journal of Minerals Processing 50 (1–2) (1997) 63–75.
[22] H. Tributsch, Personal communication, 1997.
[23] P.F. Jorge, G.P. Martins, Electrochemical and other aspects of indirect electrooxidation process for the leaching of molybdenite by hyperchloride, in: R.G. Bautista, R.J. Wesely, G.W. Warren (Eds.), Hydrometallurgical Reactor Design and Kinetics, The Metallurgical Society, 1986, pp. 263–292.
[24] F.K. Crundwell, Kinetics and mechanism of the oxidative dissolution of a zinc sulphide concentrate in ferric sulphate solutions, Hydrometallurgy, 19 (2) 227–242.
[25] B. Verbaan, R. Huberts, An electrochemical study of the bacterial leaching of synthetic nickel sulfide (Ni_3S_2), International Journal of Mineral Processing 24 (3–4) (1988) 185–202.
[26] D. Pletcher, Industrial Electrochemistry, Chapman & Hall, New York, 1984.
[27] J. Barrett, M.N. Hughes, G.I. Karavaiko, P.A. Spencer, Metal extraction by bacterial oxidation of minerals, Ellis Horwood, New York, 1993.

ELSEVIER

Biochemical Engineering Journal 3 (1999) 193–201

Biochemical Engineering Journal

Effect of pH on ferrous-iron oxidation kinetics of *Leptospirillum ferrooxidans* in continuous culture

A.W. Breed, G.S. Hansford*

Gold Fields Minerals Bioprocessing Laboratory, Department of Chemical Engineering, University of Cape Town, Rondebosch 7701, South Africa

Received 7 September 1998; accepted 4 March 1999

Abstract

The ferrous-iron oxidation kinetics of *Leptospirillum ferrooxidans* were studied at dilution rates ranging from 0.01 to 0.10 h^{-1}, and pH values ranging from pH 1.10 to 1.70. The growth rate, and the oxygen and ferrous-iron utilisation rates of the bacteria, were monitored by means of off-gas analysis and redox potential measurement. The degree-of-reduction balance was used to compare the theoretical and experimental values of $-r_{Fe}^{2-}$, $-r_{O_2}$ and r_{CO_2}, and the correlation found to be good. The bacterial culture maintained at pH 1.30 achieved the greatest measured maximum growth rate. An increase in the pH from pH 1.10 to pH 1.70 did not affect the maximum yield and maintenance coefficients, or the maximum specific ferrous-iron and oxygen utilisation rates. However, the kinetic constants in bacterial ferrous-iron oxidation, viz. $K_{Fe^{2+}}$ and K_{O_2}, increased linearly with increasing pH, across the range from pH 1.10 to 1.70. The kinetics could be described in terms of the ferric/ferrous-iron ratio using a Michaelis–Menten based model modified to account for the effect of pH on $K_{Fe^{2+}}$ and K_{O_2}. Furthermore, the threshold concentration of ferrous-iron increased with a decrease in the pH of the solution.

Keywords: *Leptospirillum ferrooxidans*; Ferrous-iron oxidation kinetics; Continuous culture; Off-gas analysis; Redox potential; pH effect

1. Introduction

Bioleaching is now an established technology for the pre-treatment of refractory gold ores and concentrates and the leaching of whole-ore copper heaps. In many cases, it offers economic, environmental and technical advantages over pressure oxidation and roasting [1,2]. However, in order for bioleaching to compete successfully with other pre-treatment processes it needs to be optimised with regard to the parameters that affect the process. Furthermore, there is a need for mechanistically based kinetic models that can be used to derive performance equations for use in the design, optimisation and control of bioleaching processes.

Recent work on the bioleaching of pyrite has provided strong evidence that it occurs via a two-step mechanism [3]. In the two-step mechanism the pyrite is chemically oxidised by the ferric-iron present in the bioleaching medium according to;

$$FeS_2 + 14Fe^{3+} + 8H_2O \rightarrow 15Fe^{2+} + 2SO_4^{2-} + 16H^+ \quad (1)$$

The ferrous-iron produced by this reaction is subsequently oxidised to the ferric form by the bacteria;

$$4Fe^{2+} + O_2 + 4H^+ \rightarrow 4Fe^{3+} + 2H_2O \quad (2)$$

A two-step mechanism suggests that the overall process can be reduced to a number of independent sequential and/or parallel sub-processes. The kinetics of the respective sub-processes may be studied separately, and the results used to predict the performance of bioleach reactors for a variety of different minerals, micro-organisms and operating conditions.

To date a number of kinetic models for bacterial ferrous-iron oxidation have been proposed [4]. These models can be broadly classified as either empirical or Michaelis–Menten/Monod based. Empirical models use tools such as the logistic equation to model the kinetics whereas Michaelis–Menten based models assume that the rate limiting reactions can be described using traditional enzyme kinetics. Lacey and Lawson [5] used the Monod equation to relate the growth of *Thiobacillus ferrooxidans* to the rate of ferrous-iron removal. Jones and Kelly [6] found that both ferrous-iron oxidation and bacterial growth were subject to either competitive or non-competitive product inhibition by ferric-

*Corresponding author. Tel.: +27-21-6502 508; fax: +27-21-6897 579; e-mail: gsh@chemeng.uct.ac.za

1369-703X/99/$ – see front matter
PII: S1369-703X(99)00018-2

iron. However, the effect of non-competitive inhibition proved to be insignificant, compared to competitive inhibition.

Braddock et al. [7] found that the steady-state growth of *T. ferrooxidans* in both batch and continuous culture could be described using a Monod model, in which a threshold concentration of ferrous-iron was included. Boon [8] proposed a modified Michaelis-Menten-type model in terms of the bacterial specific oxygen utilisation rate. It incorporated terms for both ferric-iron inhibition and a threshold ferrous-iron concentration. Boon [8] showed that the kinetics could be related to the ferric/ferrous-iron ratio or redox potential, which is consistent with the chemiosmotic theory proposed by Ingledew [9].

Recent research has shown that *Leptospirillum ferrooxidans* is at least as important, if not more important than *T. ferrooxidans* with regard to the microbial leaching of refractory pyritic ores [3,10–14]. *T. ferrooxidans* and *L. ferrooxidans* are both obligate chemolithoautotrophs, obtaining energy from an inorganic sulphide mineral substrate such as pyrite and carbon from CO_2. Both may be described using similar kinetic models. *T. ferrooxidans* is able to oxidise both the iron and sulphur moieties, whereas *L. ferrooxidans* is only able to oxidise ferrous-iron. This enables *T. ferrooxidans* to produce more energy per mole of pyrite oxidised than *L. ferrooxidans*. However, *L. ferrooxidans* has a greater affinity for ferrous-iron, and is less sensitive to ferric-iron inhibition, hence it will continue to thrive at higher redox potentials than *T. ferrooxidans* [13]. *T. ferrooxidans* grows optimally at a temperature of 30°C and pH 2.2 [13–15], whereas *L. ferrooxidans* grows optimally at a temperature of 40°C [10] and pH 1.6 [13–15].

This paper presents the results of an investigation into the ferrous-iron oxidation kinetics of a *L. ferrooxidans* species, at pH 1.10, 1.30, 1.50 and 1.70 using a modified form of the equation proposed by Boon [8].

2. Materials and methods

2.1. Continuous-flow bioreactors

The experiments were carried out in 2 l air-sparged, agitated bioreactors. The bioreactors had a H/D of 1.32 and a working volume of 1 l. Circulating water from constant temperature baths through the bioreactor jackets controlled the temperature in the bioreactors. The off-gas was dried prior to passing through the CO_2 and O_2 gas analysers. This enabled the oxygen utilisation rate, $-r_{O_2}$, carbon dioxide utilisation rate, $-r_{CO_2}$, and biomass concentration, c_X, to be determined [16]. During the continuous culture experiments the salt medium was fed to, and removed from, the bioreactors by means of variable-speed pumps. A diagrammatic representation of the experimental equipment is shown in Fig. 1 [10].

The pH of the solution in the bioreactors was not controlled directly. However, it was maintained at the required pH by controlling the pH of the feed to the bioreactors using sulphuric acid. The actual pH of the feed solution depended on both the desired solution pH and the prevailing dilution rate.

The ferrous-iron oxidation kinetics were investigated at dilution rates ranging from 0.01 to 0.10 h^{-1}. The bioreactor was operated at each dilution rate, D, for at least three residence times before steady-state was assumed. Furthermore, steady-state was assumed only once the oxygen and

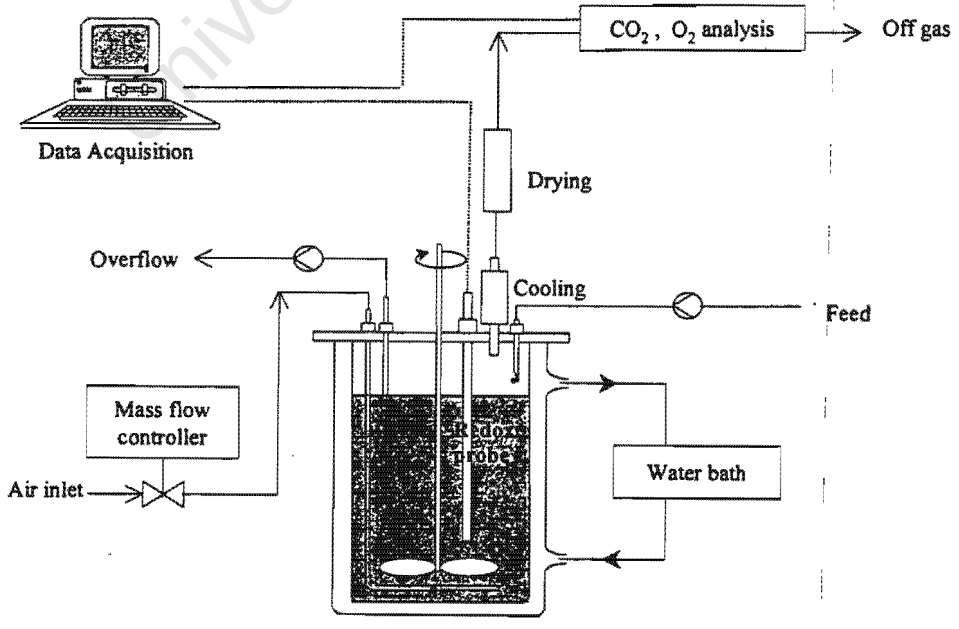

Fig. 1. Diagrammatic representation of the experimental equipment (after Breed et al. [10]).

carbon dioxide concentrations in the off-gas and the redox potential in the bioleaching liquor were constant. The steady state was maintained for at least one residence time.

Wall growth was minimised by shutting down the bioleach reactor once a day and scrubbing the walls of the bioreactors and all available surfaces with a bottle brush and metal scourer.

2.2. Ferric/ferrous-iron ratio determination

The redox potential of the bioleaching solution in the bioreactors was measured continuously using Metrohm redox electrodes (Pt-Ag/AgCl) and logged by computer. The total iron concentration in solution was determined by both atomic adsorption spectroscopy (AAS) and by titration with potassium dichromate [17]. This enabled the ferric/ferrous-iron ratio and the ferrous and ferric-iron concentrations to be determined using a calibration curve for the specific electrode and the Nernst equation [16]. The ferrous-iron concentration in solution was also determined by titration with either cerium (IV) sulphate or potassium dichromate [17]. This enabled the ferrous-iron utilisation rate, r_{Fe}^{2+}, to be calculated [16].

2.3. Bacterial culture

The bacterial culture used was obtained from a vat-type two stage (2×20 l) continuous bioleaching mini-plant treating a pyrite-arsenopyrite concentrate from Fairview gold mine, in Barberton, South Africa [18]. After isolation of the ferrous-iron oxidising species *L. ferrooxidans* was the only bacterial species detected by PCR restriction enzyme analysis [10].

2.4. Growth medium

The ferrous-iron media consisted of 12 g l^{-1} $FeSO_4 \cdot 7H_2O$, 1.11 g l^{-1} K_2SO_4, 0.53 g l^{-1} $(NH_4)_2HPO_4$, 1.83 g l^{-1} $(NH_4)_2SO_4$ and 10 ml l^{-1} trace element solution [19] adjusted to between pH 0.95 and pH 1.30 using $H_2SO_4^{conc}$. No attempt was made to maintain sterile conditions.

3. Theoretical aspects

The theoretical aspects outlined below are described in detail elsewhere [16]. The stoichiometric formula of bacteria is approximately $CH_{1.8}O_{0.5}N_{0.2}$ [6,20]. If the carbon source is limited to CO_2 the steady-state carbon dioxide utilisation rate can be used to estimate the bacterial concentration and growth rate [16]. If it is assumed that energy for bacterial growth and maintenance is obtained from the oxidation of ferrous-iron, performing mass and charge balances and solving in terms of r_{O_2} and r_{CO_2}, yields the degree-of-reduction balance,

$$-r_{Fe^{2+}} = -4r_{O_2} - 4.2r_{CO_2} \quad (3)$$

The relationship between the amount of substrate consumed by the biomass for bacterial growth and maintenance is described by means of the Pirt Equation [21]. If Monod growth kinetics are assumed the Pirt Equation can be manipulated to yield

$$q_{Fe^{2+}} = \frac{D}{Y^{max}_{Fe^{2+}X}} + m_{Fe^{2+}} \quad (4)$$

In Eq. (4) the bacterial specific ferrous-iron oxidation rate, $q_{Fe^{2+}}$, is defined as the rate of ferrous-iron utilisation per mole of biomass (i.e. per mole of carbon). Eq. (4) can also be written in terms of the bacterial specific oxygen utilisation rate, q_{O_2}. Therefore, from steady-state continuous culture data, plotting the values of $q_{Fe^{2+}}$ or q_{O_2} versus D can used to determine the values of $Y^{max}_{Fe^{2+}X}$ and $m_{Fe^{2+}}$ or $Y^{max}_{O_2X}$ and m_{O_2}. The validity of the values determined in this manner can be checked using;

$$Y^{max}_{O_2X} = \frac{4Y^{max}_{Fe^{2+}X}}{1 - 4.2Y^{max}_{Fe^{2+}X}} \quad (5)$$

and

$$m_{O_2} = \frac{m_{Fe^{2+}}}{4} \quad (6)$$

Boon et al. [3] suggested that the ferrous-iron and oxygen utilisation kinetics are proportional to the ferric/ferrous-iron ratio;

$$q_{Fe^{2+}} = \frac{q^{max}_{Fe^{2+}}}{1 + K_{Fe^{2+}}\frac{[Fe^{3+}]}{[Fe^{2+}]}} \quad (7)$$

Hence, $q^{max}_{Fe^{2+}}$ and $K_{Fe^{2+}}$ (and $q^{max}_{O_2}$ and K_{O_2}) may be determined by means of Lineweaver–Burke plots. Eq. (4) may also be written in terms of $q^{max}_{Fe^{2+}}$;

$$q^{max}_{Fe^{2+}} = \frac{\mu^{max}}{Y^{max}_{Fe^{2+}X}} + m_{Fe^{2+}} \quad (8)$$

Hence, the values of $q^{max}_{Fe^{2+}}$, $Y^{max}_{Fe^{2+}X}$ and $m_{Fe^{2+}}$ determined as described above may be used to determine μ^{max}. A similar process could also be performed using $q^{max}_{O_2}$, $Y^{max}_{O_2X}$ and m_{O_2}.

4. Results and discussion

The measured redox potential, E, in the bioreactors decreased with increasing dilution rate, D. This reflected an increase in the ferrous-iron concentration, (Fe^{2+}). This trend is typical for substrate rate concentration versus dilution rate in a continuous-flow bioreactor [10,22,23].

4.1. Degree of reduction balance

A comparison between the predicted and experimental relationship between the ferrous-iron, $-r_{Fe^{2+}}$, oxygen, $-r_{O_2}$, and carbon dioxide, $-r_{CO_2}$, utilisation rates (using Eq. (3)) is shown in Fig. 2. It is clear that the correlation between the

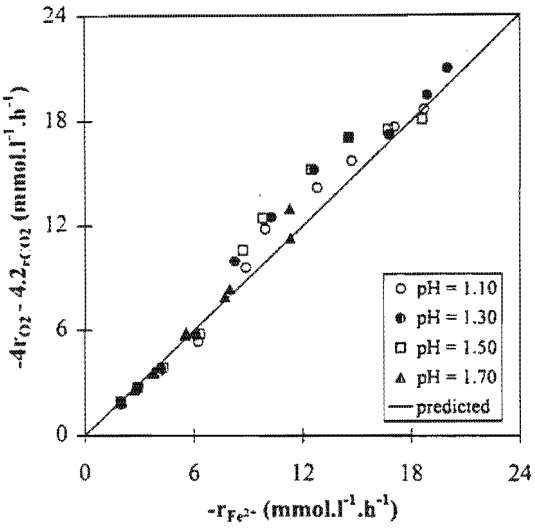

Fig. 2. Comparison between the predicted and experimental relationship between the ferrous-iron $-r_{Fe^{2+}}$, oxygen, $-r_{O_2}$, and carbon $-r_{CO_2}$, utilisation rates.

predicted and experimental relationships is good, thus, it may be assumed that the ferrous-iron, oxygen and carbon dioxide utilisation rates determined were valid.

The biomass concentration, c_X, in the bioreactors was calculated from the carbon dioxide utilisation rate, $-r_{CO_2}$. Although the concentration of bacteria in each of the bioreactors did not vary significantly over the range of dilution rates investigated, the greatest concentration was achieved at intermediate residence times, irrespective of the pH in the bioreactor (data not shown). This result is in agreement with those of the previous researches [10,22]. Furthermore, although the biomass concentration, c_X, did not appear to depend on the pH in the bioreactor, the bacterial culture maintained at pH 1.30 achieved the greatest maximum growth rate; i.e. it 'washed out' at the highest dilution rate.

4.2. Pirt equation parameters

The maximum bacterial yield on ferrous-iron, $Y^{max}_{Fe^{2+}X}$, and the maintenance coefficient on ferrous-iron, $m_{Fe^{2+}}$, were determined using Eq. (4). The data used is shown in Fig. 3. Regression analysis suggested that neither $Y^{max}_{Fe^{2+}X}$ nor $m_{Fe^{2+}}$ were significantly affected by pH, for pH values between pH 1.10 and pH 1.70.

The maximum biomass yield on oxygen, $Y^{max}_{O_2X}$, and the maintenance coefficient on oxygen, m_{O_2}, were determined using an equation of the same form as Eq. (4). The data used is shown in Fig. 4. Regression analysis also suggested that neither $Y^{max}_{O_2X}$ nor m_{O_2} were significantly affected by changes in the pH of the solution, for pH values between pH 1.10 and pH 1.70.

However, the previous work has shown that the dilution rate has an effect on the biomass yield on ferrous-iron, $Y_{Fe^{2+}X}$ and the biomass yield on oxygen, Y_{O_2X} [10]. This

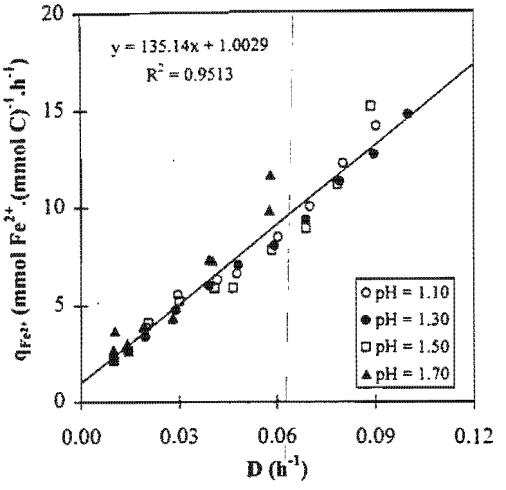

Fig. 3. Data used to determine the maximum bacterial yield on ferrous-iron, $Y^{max}_{Fe^{2+}}$, and the maintenance coefficient on ferrous-iron, $m_{Fe^{2+}}$.

dependence of $Y_{Fe^{2+}X}$ and Y_{O_2X} on the residence time ($\tau = 1/D$) may be a result of either progressive washout [6] or the Pirt Equation not being applicable [8]. For this reason only the average values of $Y^{max}_{Fe^{2+}X}$ and $m_{Fe^{2+}}$, and $Y^{max}_{O_2X}$ and m_{O_2} are listed in Tables 1 and 2, respectively. The average values determined for the same culture during a previous investigation [10] and the values determined for a Leptospirillum-like bacteria [22] are also listed. From Tables 1 and 2 it is clear that the values of $Y^{max}_{Fe^{2+}X}$, $m_{Fe^{2+}}$, $Y^{max}_{O_2X}$ and m_{O_2} determined during the different investigations are reasonably similar.

The validity of the values of $Y^{max}_{Fe^{2+}X}$, $Y^{max}_{O_2X}$, $m_{Fe^{2+}}$ and m_{O_2} determined by linear regression were compared with the values calculated using the degree-of-reduction balance (Eqs. (5) and (6)). Comparisons between the predicted and experimental relationships between the yield and maintenance coefficients are shown in Fig. 5.

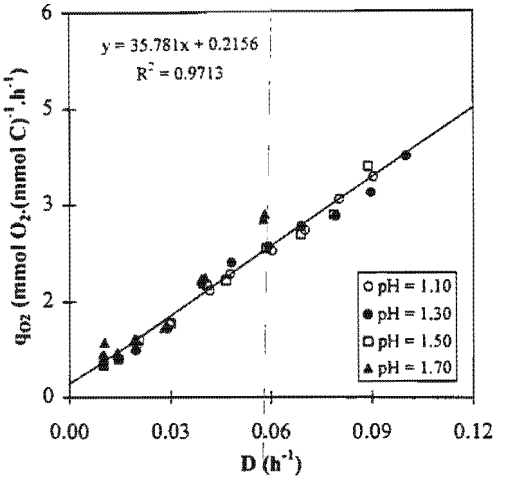

Fig. 4. Data used to determine the maximum bacterial yield on oxygen, $Y^{max}_{O_2}$, and the maintenance coefficient on oxygen, m_{O_2}.

Table 1
Values of the average maximum biomass yield on ferrous-iron, $Y_{Fe^{2+}X_{max}}$ and maintenance coefficient on ferrous-iron, $m_{Fe^{2+}}$

	Fig. 3	Breed et al., [10]	Van Scherpenzeel, [22]
$Y^{max}_{Fe^{2+}X}$	0.0074	0.0059	0.010
$m_{Fe^{2+}}$	1.0029	0.797	0.451
R^2	0.9513	0.9283	0.997

Table 2
Values of the average maximum biomass yield on oxygen, $Y^{max}_{O_2X}$, and maintenance coefficient on oxygen, m_{O_2}

	Fig. 4	Breed et al. [10]	Van Scherpenzeel [22]
$Y^{max}_{O_2X}$	0.0279	0.0220	0.047
m_{O_2}	0.2156	0.1121	0.043
R^2	0.9713	0.9503	0.997

From Fig. 5 it is apparent that the correlation between the predicted and experimental values of $Y^{max}_{Fe^{2+}X}$ and $Y^{max}_{O_2X}$ is good. However, the correlation between the predicted and experimental values of $m_{Fe^{2+}}$ and m_{O^2} is poor. The poor correlation between the predicted and experimental values of the maintenance coefficients, and the effect of the dilution rate on $Y_{Fe^{2+}X}$ and Y_{O_2X} (data not shown) is consistent with the suggestion that the Pirt Equation may not be valid, [8,10].

4.3. Maximum specific growth rate

The average value of the maximum specific growth rate, μ^{max}, calculated from the Pirt Equation, and the dilution rate at which washout was observed to occur, D_w, are listed in Table 3. Although the bacterial culture maintained at pH 1.30 'washed out' at the highest dilution rate, the highest calculated maximum specific growth rate, μ^{max} was obtained at pH 1.50. In spite of this, it is apparent from

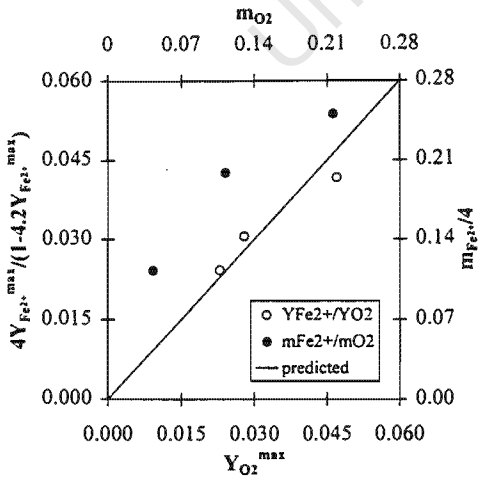

Fig. 5. Comparison of the predicted and experimental relationships between the maximum yield and maintenance coefficients for the data listed in Tables 1 and 2.

Table 3
Values of the average maximum specific growth rate, μ^{max}, calculated from the Pirt Equation, and the dilution rate at which washout was observed, D_w

pH	1.10	1.30	1.50	1.70
μ^{max}	0.1024	0.1043	0.1227	0.0952
D_w	$0.09 < D_w < 0.10$	$0.10 < D_w$	$0.09 < D_w < 0.10$	$0.059 < D_w$

Table 3 that the values of μ^{max} are in reasonable agreement with the dilution rate at which washout was observed to occur.

4.4. Maximum bacterial specific utilisation rates

The variation in the values of the maximum bacterial specific ferrous-iron and oxygen utilisation rates, $q^{max}_{Fe^{2+}}$ and $q^{max}_{O_2}$, and their respective kinetic constants, $K_{Fe^{2+}}$ and K_{O_2}, are shown in Table 4 and Fig. 6(a,b), respectively. Although Fig. 6(a) suggests that $q^{max}_{Fe^{2+}}$ and $q^{max}_{O_2}$ achieved maximum values at pH 1.50, it is clear that no simple relationship between the maximum bacterial specific rates and pH exists. However, from Fig. 6(b), it appears as though $K_{Fe^{2+}}$ ($R^2 = 0.81$) and K_{O_2} ($R^2 = 0.99$) are directly proportional to the pH, across the range pH 1.10 to pH 1.70.

4.5. Kinetic model

For the above reasons the variation in the specific ferrous-iron and oxygen utilisation rates with changes in the ferric/ferrous-iron ratio were modelled assuming that the kinetic constants, $K_{Fe^{2+}}$ and K_{O_2} were directly proportional to the pH. The resulting functions were derived by minimising the sum of the squared errors between the values of $q_{Fe^{2+}}$ and q_{O_2} determined experimentally, and the values predicted by the resulting model, i.e.;

$$\Sigma e^2 = \sum_{pH=1.10}^{pH=1.70} (q_{Fe^{2+}}(\text{predicted}) - q_{Fe^{2+}}(\text{measured}))^2 \qquad (9)$$

and

$$\Sigma e^2 = \sum_{pH=1.10}^{pH=1.70} (q_{O_2}(\text{predicted}) - q_{O_2}(\text{measured}))^2 \qquad (10)$$

Table 4
Values of the maximum bacterial specific ferrous iron and oxygen utilisation rates, $q^{max}_{Fe^{2+}}$ and $q^{max}_{O_2}$, and their respective kinetic constants in bacterial ferrous iron oxidation, $K_{Fe^{2+}}$ and K_{O_2}

pH	1.10	1.30	1.50	1.70
$q^{max}_{Fe^{2+}}$	15.26	15.57	19.02	13.62
$K_{Fe^{2+}}$	0.0010	0.0022	0.0037	0.0034
$q^{max}_{O_2}$	3.77	3.83	4.23	3.69
K_{O_2}	0.0009	0.0019	0.0026	0.0039

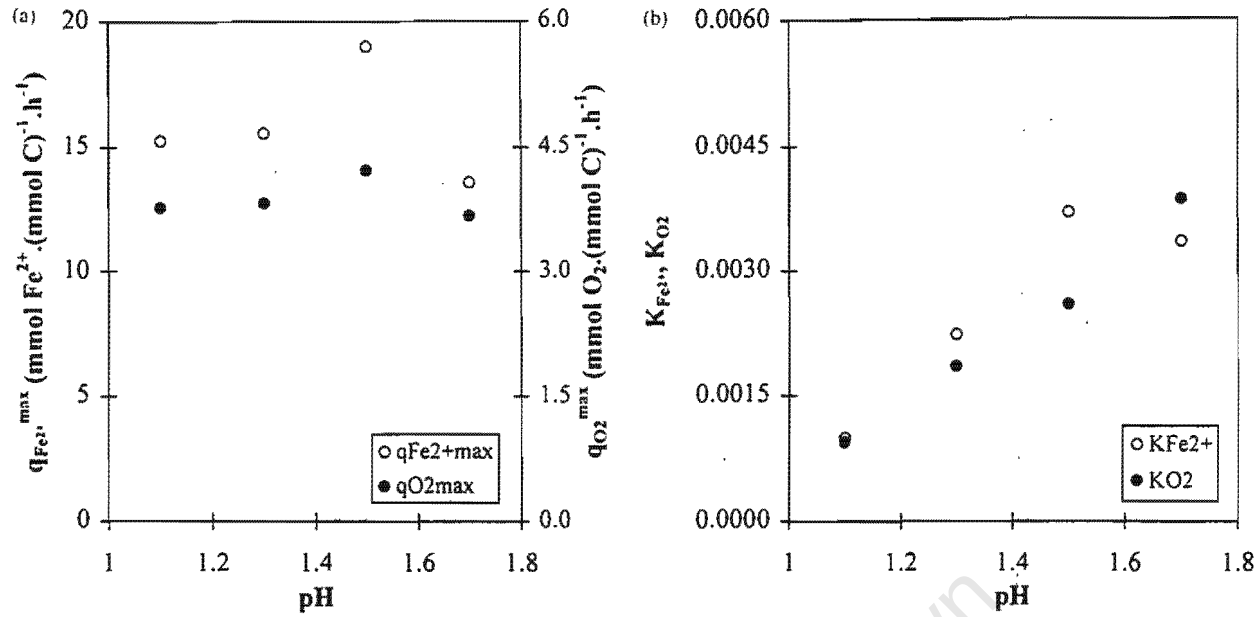

Fig. 6. Effect of pH on the maximum bacterial specific ferrous-iron and oxygen utilisation rates, $q_{Fe^{2+}}^{max}$ and $q_{O_2}^{max}$, and their respective kinetic constants in bacterial ferrous-iron oxidation, $K_{Fe^{2+}}$ and K_{O_2}.

Using a constant value of $q_{Fe^{2+}}$ for all pH values resulted in Σe^2 being 2.6% greater than if the values of $q_{Fe^{2+}}^{max}$ listed in Table 3 were used, and 13.2% greater than if the values of $q_{Fe^{2+}}^{max}$ were determined by minimising the sum of the squared errors; i.e. using Eq. (9). This suggests that using a constant $q_{Fe^{2+}}^{max}$ contributes to a simpler model, without resulting in a significant increase in the error, i.e.,

$$q_{Fe^{2+}}(\text{predicted}) = \frac{15.53}{(0.0048\text{pH} - 0.0043)\dfrac{[Fe^{3+}]}{[Fe^{2+}]}} \quad (11)$$

Fig. 7 shows the predicted variation in the specific ferrous-iron utilisation rate with changes in the ferric/ferrous-iron ratio at pH values ranging from pH 1.10 to pH 1.70, using Eq. (11), and the experimentally determined values. It is clear from Fig. 7 that the agreement between the kinetic model prediction and experimental results is good.

A similar procedure performed using the maximum bacterial specific oxygen utilisation rate, $q_{O_2}^{max}$, resulted in Σe^2 being 7.9% greater than if the values of $q_{O_2}^{max}$ were determined by minimising the sum of the squared errors; i.e., using Eq. (10). This suggests that the bacterial specific oxygen utilisation rate could also be adequately modelled using a constant $q_{O_2}^{max}$, viz.;

$$q_{O_2}(\text{predicted}) = \frac{3.85}{(0.0043\text{pH} - 0.0037)\dfrac{[Fe^{3+}]}{[Fe^{2+}]}} \quad (12)$$

As in the case of $q_{Fe^{2+}}$, the agreement between the kinetic model prediction using Eq. (12) and the experimental results was found to be good (data not shown).

The above results suggest that the ferrous-iron oxidation kinetics of *L. ferrooxidans* are a function of the ferric/ferrous-iron ratio, which is in agreement with the previous researches [8,9,12,22]. Furthermore, it appears as though $q_{Fe^{2+}}^{max}$ and $q_{O_2}^{max}$ are not significantly affected by pH across the range of pH values, from pH 1.10 to 1.70. However, $K_{Fe^{2+}}$ and K_{O_2} appear to be directly proportional to the pH, i.e., they increase linearly with increasing pH, across the range from pH 1.10 to 1.70. It is also apparent from Fig. 7 that there are a large number of data points at ferric/ferrous-iron ratios in the region of 800–4000. These points represent the threshold concentration of ferrous-iron, $[Fe^{2+}]_{thres}$, below which no further ferrous-iron utilisation occurs. This is also consistent with the findings of previous research [7–9]. At a total iron concentration of 12 g l^{-1}, this corresponds to ferrous-iron concentrations in the region of 0.054–0.268 mM. This value is greater than the 0.005 mM reported for a Leptospirillum-like bacteria isolated from the Gamsberg deposit in South Africa [22], but less than the 0.5 mM reported for *T. ferrooxidans* [8]. Furthermore, the value of $[Fe^{2+}]_{thres}$ appears to increase with a decrease in the pH of the solution. This can possibly be attributed to the speciation of the iron sulphate complexes being affected by the pH of the liquor [24].

In contrast to the above, a previous investigation, using the same bacterial culture, showed that both $q_{Fe^{2+}}^{max}$ and $q_{O_2}^{max}$ increased with increasing temperature, across the range from 30 to 40°C [10]. However, the kinetic constants, $K_{Fe^{2+}}$ and K_{O_2} were not significantly affected by temperature, across the range from 30 to 40°C. In addition, the kinetics could be described using a similar model, modified using the Arrhenius equation to account for the effect of temperature.

It is therefore possible to depict the differences in the effect of temperature and pH on the ferrous-iron oxidation kinetics of *L. ferrooxidans* as shown in Fig. 8.

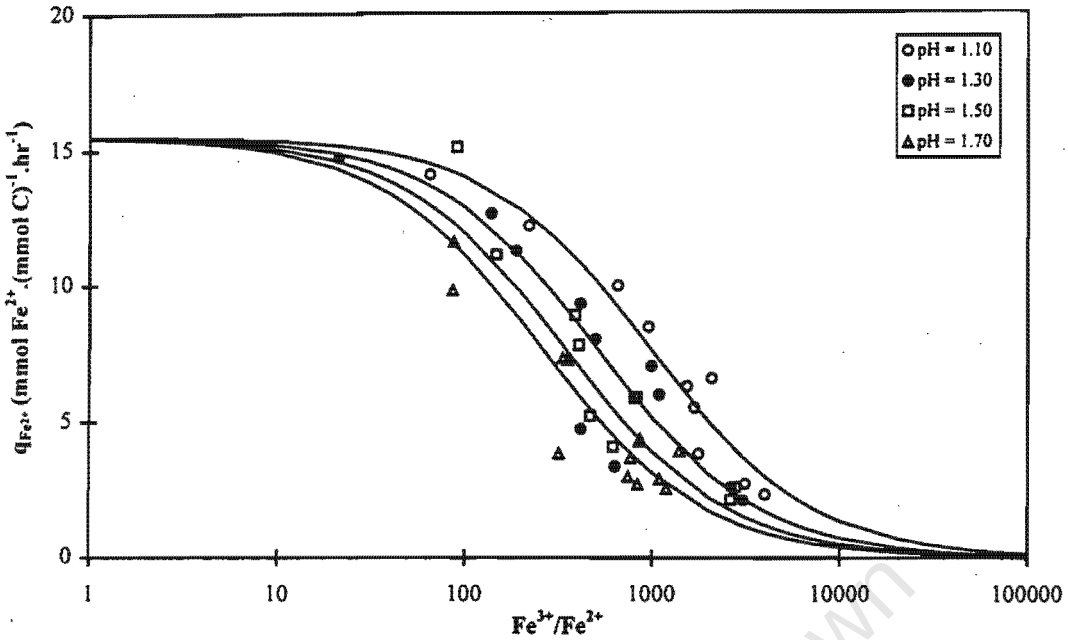

Fig. 7. Comparison between the predicted and experimental variation in the bacterial specific ferrous iron oxidation rate of *L. ferrooxidans* with changes in the ferric/ferrous-iron, at pH 1.10 and 1.70.

5. Conclusions

Analysis of the rates of ferrous-iron, oxygen and carbon dioxide utilisation showed that they could be accurately related via a degree-of-reduction balance. The greatest biomass concentration was achieved at intermediate residence times, irrespective of the pH in the bioreactor. Although the cell concentration in the bioreactors appeared to be independent of the pH in the bioreactor, the bacterial culture maintained at pH 1.30 'washed out' at the highest dilution rate. However, the highest calculated maximum specific growth rate, $\mu^{max} = 0.1024\ h^{-1}$, occurred at pH 1.50.

Although the Pirt Equation may not be valid, the values of $Y^{max}_{Fe^{2+}X}$, $Y^{max}_{O_2X}$, $m_{Fe^{2+}}$ and m_{O_2} determined in this investigation were not significantly different from those determined previously for *L. ferrooxidans*. Changes in the pH across the range pH 1.10–1.70 did not have a marked effect on any of these parameters.

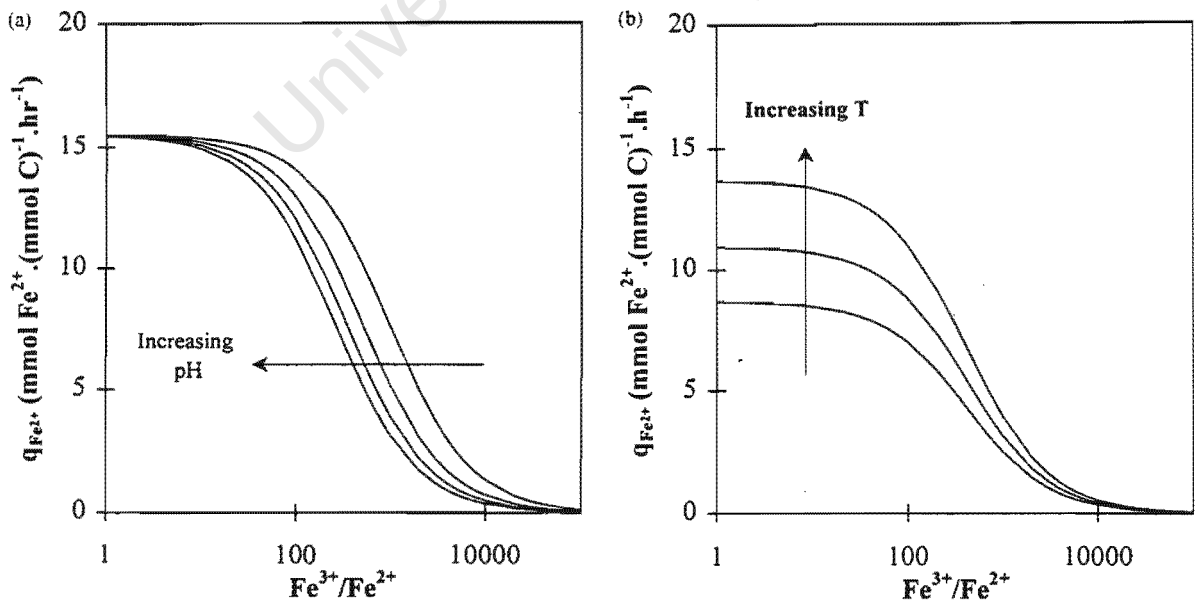

Fig. 8. Comparison between the effect of temperature and pH on the ferrous-iron oxidation kinetics of *L. ferrooxidans* for pH values ranging from pH 1.10 to 1.70 and temperature ranging from 30 to 40°C. Temperature data was obtained from Breed et al. [10].

An increase in the pH from pH 1.10 to 1.70 did not appear to have a significant effect on the maximum specific ferrous-iron and oxygen utilisation rates. However, the kinetic constants in bacterial ferrous-iron oxidation, viz. $K_{Fe^{2+}}$ and K_{O_2}, increased linearly with increasing pH, i.e.,

$$K_{Fe^{2+}}, K_{O_2} = f(\mathrm{pH}) \quad (13)$$

$$q_{Fe^{2+}}, q_{O_2} \neq f(\mathrm{pH}) \quad (14)$$

The ferrous-iron oxidation kinetics could also be described in terms of the ferric/ferrous-iron ratio using the Michaelis-Menten based model proposed by Boon [3], modified to account for the effect of pH on $K_{Fe^{2+}}$ and K_{O_2}.

In contrast to the above, a previous investigation showed that $q^{max}_{Fe^{2+}}$ and $q^{max}_{O_2}$ of *L. ferrooxidans* increased with increasing temperature, whereas $K_{Fe^{2+}}$ and K_{O_2} were not significantly affected by temperature, i.e.,

$$q_{Fe^{2+}}, q_{O_2} = f(T) \quad (15)$$

$$K_{Fe^{2+}}, K_{O_2} \neq f(T) \quad (16)$$

6. Nomenclature

c_X	Concentration of bacteria	mmolC l^{-1}
D	Dilution rate	h^{-1}
D_w	Dilution rate at which washout is observed	h^{-1}
E	Redox potential of the solution (Pt-Ag/AgCl)	mV
$[Fe^{2+}]_{thres}$	Threshold concentration of Fe^{2+}	mmol l^{-1}
$K_{Fe^{2+}}$	Kinetic constant in bacterial ferrous-iron oxidation	dimensionless
K_{O_2}	Kinetic constant in bacterial ferrous-iron oxidation	dimensionless
$m_{Fe^{2+}}$	Maintenance coefficient on Fe^{2+}	mmolFe^{2+} (mmolC)$^{-1}$ h^{-1}
m_{O_2}	Maintenance coefficient on O_2	mmolO_2 (mmolC)$^{-1}$ h^{-1}
$q_{Fe^{2+}}$	Bacterial specific ferrous-iron oxidation rate	mmolFe^{2+} (mmolC)$^{-1}$ h^{-1}
$q^{max}_{Fe^{2+}}$	Maximum bacterial specific ferrous-iron oxidation rate	mmolFe^{2+} (mmolC)$^{-1}$ h^{-1}
q_{O_2}	Bacterial specific oxygen utilisation rate	mmolO_2 (mmolC)$^{-1}$ h^{-1}
$q^{max}_{O_2}$	Maximum bacterial specific oxygen utilisation rate	mmolO_2 (mmolC)$^{-1}$ h^{-1}
r_{CO_2}	Carbon dioxide production rate	mmolCO_2 l^{-1} h^{-1}
$r_{Fe^{2+}}$	Ferrous-iron production rate	mmolFe^{2+} l^{-1} h^{-1}
r_{O_2}	Oxygen production rate	mmolO_2 l^{-1} h^{-1}
r_X	Bacterial production rate	mmolC l^{-1} h^{-1}
$Y_{Fe^{2+}X}$	Bacterial yield on Fe^{2+}	mmolC (mmolFe^{2+})$^{-1}$
$Y^{max}_{Fe^{2+}X}$	Maximum bacterial yield on Fe^{2+}	mmolC (mmolFe^{2+})$^{-1}$
Y_{O_2X}	Bacterial yield on O_2	mmolC (mmolO_2)$^{-1}$
$Y^{max}_{O_2X}$	Maximum bacterial yield on O_2	mmolC (mmolO_2)$^{-1}$
μ^{max}	Maximum bacterial specific growth rate	h^{-1}

Acknowledgements

The financial support from the Gold Fields Foundation, Billiton Process Research and the Foundation for Research Development (South Africa) are gratefully acknowledged.

References

[1] P.C. van Aswegen, Commissioning and operation of bio-oxidation plants for the treatment of refractory gold ores, in: J.B. Hiskey, G.W. Warren (Eds.), Hydrometallurgy; Fundamentals, Technology and Innovations. Soc. Min. Metall. Explor. AIME, 1993, pp. 709–725.

[2] R. Poulin, R.W. Lawrence, Economic and environmental niches of biohydrometallurgy, Miner. Eng. 9(8) (1996) 799–810.

[3] M. Boon, G.S. Hansford, J.J. Heijnen, The role of bacterial ferrous-iron oxidation in the bio-oxidation of pyrite, in: T. Vargas, C.A. Jerez, J.V. Wiertz, H. Toledo (Eds.), Biohydrometallurgical Processing 1. University of Chile, Santiago, Chile, 1995, pp. 153–163.

[4] M. Nemati, S.T.L. Harrison, C. Webb, G.S. Hansford, Biological oxidation of ferrous sulphate by *Thiobacillus ferrooxidans*: A review on the kinetic aspects, Biochem. Eng. J. 1 (1998) 171–190.

[5] D.T. Lacey, F. Lawson, Kinetics of the liquid-phase oxidation of acid ferrous sulphate by the bacterium *Thiobacillus ferrooxidans*, Biotechnol. Bioeng. 12 (1970) 29–50.

[6] C.A. Jones, D.P. Kelly, Growth of *Thiobacillus ferrooxidans* on ferrous-iron in chemostat culture: Influence of product and substrate inhibition, J. Chem. Technol. Biotechnol. 33B(4) (1983) 241–261.

[7] J.F. Braddock, H.V. Luong, E.J. Brown, Growth kinetics of *Thiobacillus ferrooxidans* isolated from arsenic mine drainage, Appl. Environ. Microbiol. 48(1) (1984) 48–55.

[8] M. Boon, Theoretical and experimental methods in the modelling of the bio-oxidation kinetics of sulphide minerals, Ph.D. Thesis, Delft University of Technology, Delft, The Netherlands, 1996.

[9] W.J. Ingledew, Ferrous-iron oxidation by *Thiobacillus ferrooxidans*, Biotechnol. Bioeng. Symp. 16 (1986) 23–33.

[10] A.W. Breed, C. Dempers, G. Searby, M. Gardner, D.E. Rawlings, G.S. Hansford, The effect of temperature on the ferrous-iron oxidation kinetics of *Leptospirillum ferrooxidans*, Biotechnol. Bioeng., 1999, in press.

[11] D.E. Rawlings, Restriction enzyme analysis of 16S rRNA genes for the rapid identification of *Thiobacillus ferrooxidans*, *Thiobacillus thiooxidans* and *Leptospirillum ferrooxidans* strains in leaching environments, in: T. Vargas, C.A. Jerez, J.V. Wiertz, H. Toledo (Eds.), Biohydrometallurgical Processing 1. University of Chile, Santiago, Chile, 1995, pp. 9–17.

[12] W. Sand, K. Rohde, B. Sobotke, C. Zenneck, Evaluation of *Leptospirrillum ferrooxidans* for leaching, Appl. Environ. Microbiol. 58(1) (1992) 85–92.

[13] P.R. Norris, D.W. Barr, D. Hinson, Iron and mineral oxidation by acidophilic bacteria: affinities for iron and attachment to pyrite, in: P.R. Norris, D.P. Kelly (Eds.), Proc. Int. Symp. on Biohydrometallurgy. Science and Technology Letters, Kew, Surrey, 1987, pp. 43–59.

[14] U. Helle, U. Onken, Continuous bacterial leaching of pyritic flotation concentrate by mixed cultures, in: P.R. Norris, D.P. Kelly (Eds.), Proc. Int. Symp. on Biohydrometallurgy. Science and Technology Letters, Kew, Surrey, 1987, pp. 61–75.
[15] R. Hallmann, A. Friedrich, H.P. Koops, A. Pommering-Röser, W. Sand, Physiological characteristics of *Thiobacillus ferrooxidans* and *Leptospirillum ferrooxidans* and physiochemical factors influence on microbial metal leaching, Geomicrobiol. J. 10 (1987) 193–205.
[16] M. Boon, J.J. Heijnen, G.S. Hansford, Recent developments in the modelling of bio-oxidation kinetics and their implications in practice: Part I, measurement methods in bio-oxidation kinetics, in: D. Holmes, R. Smith (Eds.), Minerals Processing II. The Minerals, Metals and Materials Society, Warrendale, PA, 1994, pp. 41–61.
[17] A.I. Vogel, Vogel's Textbook Of Quantitative Chemical Analysis, 5th ed., Longman Group, London, 1989.
[18] A.W. Breed, S.T.L. Harrison, G.S. Hansford, The bioleaching of a pyrite-arsenopyrite flotation concentrate in a continuous bioleaching mini-plant. Steady-state operation and behaviour during periods without aeration and agitation, in: Proc. IBS-BIOMINE 97, Australian Mineral Foundation, Glenside, Australia, 1997.
[19] W. Vishniac, M. Santer, The Thiobacilli. Bacterial Revs. 21 (1957) 195–213.
[20] J.A. Roels, Energetics and Kinetics In Biotechnology, Elsevier, Amsterdam, The Netherlands, 1983.
[21] S.J. Pirt, Maintenance energy: A general model for energy limited and energy sufficient growth, Arch. Microbiol. 133 (1982) 300–302.
[22] D.A. van Scherpenzeel, The kinetics of ferrous-iron oxidation by Leptospirillum-like bacteria in absence and in presence of pyrite and pyrite/arsenopyrite mixtures in continuous and batch cultures, M.Sc. Eng. (Chem.) Thesis, University of Cape Town, Cape Town, South Africa, 1996.
[23] H.G. Schlegel, General Microbiology, 6th ed., Cambridge University Press, 1986.
[24] J. Barrett, M.N. Hughes, G.I. Karavaiko, P.A. Spencer, Metal extraction by bacterial oxidation of minerals, Ellis Horwood, London, 1993.

The Effect of Temperature on the Continuous Ferrous-iron Oxidation Kinetics of a Predominantly *Leptospirillum ferrooxidans* Culture

A.W. Breed,[1] C.J.N. Dempers,[1] G.E. Searby,[1] M.N. Gardner,[2] D.E. Rawlings,[2] G.S. Hansford[1]

[1]*Gold Fields Minerals Bioprocessing Laboratory, Department of Chemical Engineering, University of Cape Town, Rondebosch, 7701, South Africa; telephone: +27 21 6502508; fax: +27 21 6897579; e-mail:gsh@chemeng.uct.ac.za*
[2]*Department of Microbiology, University of Cape Town, Rondebosch, 7701, South Africa*

Received 20 August 1998; accepted 23 March 1999

Abstract: The ferrous-iron oxidation kinetics of a bacterial culture consisting predominantly of *Leptospirillum ferrooxidans* were studied in continuous-flow bioreactors. The bacterial culture was fed with a salts solution containing 12 g/L ferrous-iron, at dilution rates ranging from 0.01 to 0.06 l/h, and temperatures ranging from 30 to 40°C, at a pH of 1.75. The growth rate, and the oxygen and ferrous-iron utilization rates of the bacteria, were monitored by means of off-gas analysis and redox-potential measurement. The degree-of-reduction balance was used to compare the theoretical and experimental values of $-r_{CO_2}$, $-r_{O_2}$ and $-r_{Fe^{+2}}$, and the correlation found to be good.

The maximum bacterial yield on ferrous-iron and the maintenance coefficient on ferrous-iron, were determined using the Pirt equation. An increase in the temperature from 30 to 40°C did not appear to have an effect on either the maximum yield or maintenance coefficient on ferrous-iron. The average maximum bacterial yield and maintenance coefficient on ferrous-iron were found to be 0.0059 mmol C/mmol Fe^{2+} and 0.7970 mmol Fe^{2+}/mmol C)/h, respectively. The maximum specific growth rate was found to be 0.077 l/h.

The maximum specific ferrous-iron utilization rate increased from 8.65 to 13.58 mmol Fe^{2+}/mmol C/h across the range from 30 to 40°C, and could be described using the Arrhenius equation. The kinetic constant in bacterial ferrous-iron oxidation increased linearly with increasing temperature. The ferrous-iron kinetics could be accurately described in terms of the ferric/ferrous-iron ratio by means of a Michaelis–Menten-based model modified to account for the effect of temperature.

A threshold ferrous-iron level, below which no further ferrous-iron utilization occurred, was found at a ferric/ferrous-iron ratio of about 2500. At an overall iron concentration of 12 g/L, this value corresponds to a threshold ferrous-iron concentration of 78.5×10^{-3} m*M*. *Biotechnol Bioeng* 65: 44–53, 1999.

Correspondence to: G.S. Hansford

Contracts sponsors: Gold Fields Foundation; Billiton Process Research; Foundation for Research Development (South Africa)

Keywords: *Leptospirillum ferrooxidans*; ferrous-iron oxidation kinetics; continuous culture; off-gas analysis; redox potential; effect of temperature; Arrhenius equation

INTRODUCTION

Bioleaching is now an established technology for the pretreatment of refractory gold ores and concentrates and the leaching of whole-ore copper heaps. In many cases, it offers economic, environmental and technical advantages over pressure oxidation and roasting (Poulin and Lawrence, 1996; Van Aswegen, 1993). However, for bioleaching to compete successfully with other pretreatment processes it needs to be optimized with regard to the parameters that affect the bioleaching reactions, and the growth of the microorganism involved. Thus, there is a growing need for mechanistically based kinetic models that can be used to derive performance equations for use in the design, optimization, and control of bioleaching processes.

Recent work on the bioleaching of pyrite has provided strong evidence that it occurs via a two-step mechanism (Boon et al., 1995). In the two-step mechanism the pyrite is chemically oxidized by the ferric-iron present in the bioleaching medium according to

$$FeS_2 + 14Fe^{3+} + 8H_2O \rightarrow 15Fe^{2+} + 2SO_4^{2-} + 16H^+ \quad (1)$$

The ferrous-iron produced by this reaction is subsequently oxidized to the ferric form by the bacteria

$$4Fe^{2+} + O_2 + 4H^+ \rightarrow 4Fe^{3+} + 2H_2O \quad (2)$$

A two-step mechanism suggests that the overall process can be reduced to a number of independent sequential and/or parallel subprocesses. The kinetics of the respective subprocesses may be studied separately, and the results used to predict the performance of bioleach reactors for a variety of different minerals, microorganisms and operating conditions.

CCC 0006-3592/99/010044-10

To date a number of kinetic models for bacterial ferrous-iron oxidation by *Thiobacillus ferrooxidans* have been proposed (Nemati et al., 1998). Although no model yet describes the process overall-operating conditions, it has been shown that a rate equation of the form

$$q_{Fe^{2+}} = \frac{-r_{Fe^{2+}}}{c_X} = \frac{q^{max}_{Fe^{2+}}}{1 + K_{Fe^{2+}} \dfrac{[Fe^{3+}]}{[Fe^{2+}]}} \quad (3)$$

successfully describes the kinetics within the range of ferric/ferrous-iron ratios found in bioleach systems (Boon et al., 1995; Hansford, 1997; van Scherpenzeel et al., 1998). This equation assumes that the kinetics are proportional to the ferric/ferrous-iron ratio (i.e., the redox potential), which is consistent with the chemiosmotic theory proposed by Ingledew (1986).

Furthermore, the relationship between the amount of ferrous-iron substrate consumed by the biomass for bacterial growth and maintenance is described by means of the Pirt equation (Pirt, 1982), viz.,

$$-r_{Fe^{2+}} = \frac{r_X}{Y^{max}_{Fe^{2+}X}} + m_{Fe^{2+}} c_X \quad (4)$$

Although most commercial bioleaching operations using mesophilic bacteria are carried out at temperatures in the region of 40°C, most research performed to date has been carried out at temperatures in the region of 30°C. Apart from the work of Nemati and Webb (1997), the effect of temperature has not been studied extensively. In addition, it has been shown that *T. ferrooxidans* is unlikely to predominate in commercial bioleach reactors (Boon et al., 1995; Hallmann et al., 1987; Helle and Onken, 1987; Norris et al., 1987; Rawlings, 1995). An explanation for the above has been suggested by Rawlings et al. (1999).

This article presents the results of an investigation into the ferrous-iron oxidation kinetics of a bacterial culture consisting predominantly of *Leptospirillum ferrooxidans*, at 30, 35, and 40°C. A modified form of the equation proposed by Boon (1996) to describe the kinetics in terms of the ferric/ferrous-iron ratio (Hansford, 1997) was used.

MATERIALS AND METHODS

Continuous-Flow Bioreactors

A diagrammatic representation of a single bioreactor is shown in Figure 1. Experiments were carried out in 2L jacketed Z61104CT04 Applikon® autoclavable bioreactors made of borosilicate glass. The bioreactors had a H/D ≈ 1.32 and a working volume of 1L. The bioreactors were maintained at constant temperatures of 30, 35 and 40°C by circulating water from Grant Y6 constant temperature baths through the bioreactor jackets. The pH of the solution in the bioreactors was maintained at 1.75 by adjusting the pH of the feed to the bioreactor using sulphuric acid.

The nutrient medium was fed to the bioreactors by Masterflex® model 7521-57 L/S™ variable-speed drives fitted with L/S™ 7013-20 standard pump heads and L/S™ 13 Norprene® food tubing. A chemostat tube was used to maintain a constant volume within the bioreactor. The liquid was removed from the bioreactor by means of a L/S™ 7014-20 standard pump head and L/S™ 14 Norprene® food tubing fitted on a Masterflex® model 7521-57 L/S™ fixed-speed drive.

Mixing and gas dispersion was achieved by a pitched

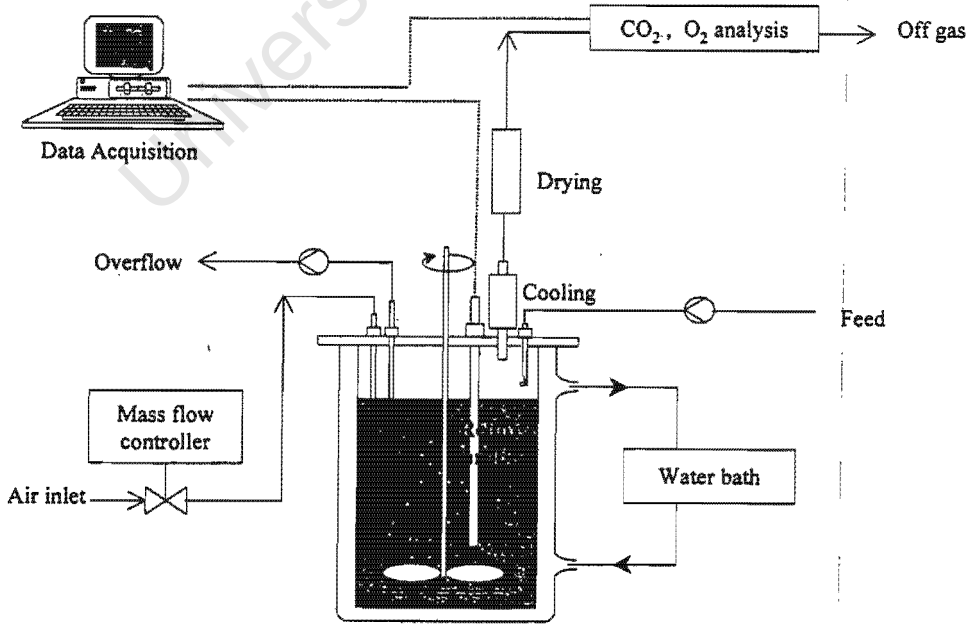

Figure 1. Diagrammatic representation of a single bioreactor.

(45°) six-blade turbine impeller rotating at 600 rpm, located 2 cm from the base of the bioreactor, via a flexible coupling, linked to an Applikon P100 motor and an Applikon 1012 stand-alone speed controller.

Inlet gas was supplied by a Peak Scientific OAG2000DA oilless air compressor. The flow rate to the bioreactors was controlled at the required rate using a Brooks model 5850S mass flow controller and a Brooks model 0154 microprocessor control and read out unit. The off-gas was dried using a reflux condenser using an ethylene/glycol mixture from a Grant LTD6G low-temperature bath, at 6°C. Prior to entering the gas analyzers, the off-gas was passed through a cloth filter and a Hartmann & Braun CGEK sample gas conditioner fitted with a CGKA 1 automatic condensate outlet.

The CO_2 concentration of the bioreactor off-gas was determined using a Hartmann & Braun Uras 4 NDIR (nondispersive infrared) industrial photometer and the O_2 concentration using a Hartmann & Braun Magnos 6 G oxygen analyzer. The CO_2 and O_2 concentrations for each bioreactor and the inlet air were alternately logged by computer.

The ferrous-iron oxidation kinetics were investigated at dilution rates ranging from 0.01 to 0.06/h. The bioreactor was operated at each dilution rate for at least three residence times before steady state was assumed. Furthermore, steady state was assumed only once the oxygen and carbon dioxide concentrations in the off-gas and the redox potential in the bioleaching liquor, were constant. The steady state was maintained for at least one residence time.

Wall growth was minimized by shutting down the bioreactor once a day and scrubbing the walls of the bioreactors and all available surfaces with a bottle brush and metal scourer.

Bacterial Culture

The inoculum was obtained from a vat-type two-stage (2 × 20L) continuous bioleaching mini-plant treating a pyrite-arsenopyrite concentrate from Fairview gold mine, in Barberton, South Africa. It was previously reported to consist primarily of *L. ferrooxidans* and *Thiobacillus thiooxidans* (Rawlings, 1995).

Growth Medium

The ferrous-iron media consisted of 12 g/L Fe^{2+} (added as $FeSO_4 \cdot 7H_2O$), 1.11 g/L K_2SO_4, 0.53 g/L $(NH_4)_2HPO_4$, 1.83 g/L $(NH_4)_2SO_4$ and 10 mL trace element solution (Vishniac and Santer, 1957), adjusted to between pH 0.95 and pH 1.30 using $H_2SO_4^{conc}$. No attempt was made to maintain sterile conditions.

Preparation of Chromosomal DNA from Bioreactor Biomass

The biomass was harvested by centrifugation. The cells were washed in acid water pH 1.80, and resuspended in 560μL TE (0.01*M* Tris, 0.001*M* EDTA)–0.15*M* NaCl pH 7.6 buffer. After heating the cells to 70°C for 15 min, 15μL of a 20 mg/mL solution of Proteinase K and 30μL of 10% SDS was added to the sample and incubated at 42°C for 30 min until cell lysis was complete. The DNA was precipitated using 10% (v/v) 3*M* KAc pH 5.2 and two volumes of ethanol, washed with 70% ethanol, air dried, and resuspended in TE buffer pH 7.6.

Polymerase Chain Reaction (PCR)

The polymerase chain reaction (PCR) was carried out in 100μL total volume using universal primers, designed from conserved regions of bacterial 16S rRNA genes (bold), as shown below (Rawlings, 1995):

primer fDD2 5′ CC *GGATCCGTCGAC***AGATTTGATCITGGCTCAG** 3′ 34-mer

primer rPP2 5′ CC *AAGCTTCTAGA***CGGITACCTTGGTTACGACTT** 3′ 33-mer

16S rDNA was amplified from the sample in a Biometra personal cycler using 1μL genomic DNA, 0.25μ*M* of each primer, 2.5m*M* $MgCl_2$, 0.25m*M* dNTPs, and 1 unit Redhot polymerase (Boehringer-Mannheim Germany). After initial denaturation for 60s at 94°C, 25 cycles of amplification were carried out as follows: 30s at 94°C, 30s at 52°C, 90s at 72°C. A final elongation step of 120s at 72°C followed by a cooling step for 60s at 25°C ended the reaction.

PCR-restriction enzyme analysis for the identification of species was utilized to determine the dominant species in the bioreactors as described by Rawlings (1995).

Ferric/Ferrous-iron Ratio Determination

The redox potential of the bioleaching solution in the bioreactors was measured continuously using Metrohm redox electrodes (Pt-Ag/AgCl) and logged by computer. The total iron concentration in solution was determined by both atomic adsorption spectroscopy (AAS) and by titration with potassium dichromate (Vogel, 1989). This enabled the ferric/ferrous-iron ratio and the ferrous and ferric-iron concentrations to be determined using a calibration curve for the specific electrode and the Nernst equation (Boon et al., 1994). The ferrous-iron concentration in solution was also determined by titration with potassium dichromate (Vogel, 1989). This enabled the ferrous-iron utilization rate, $r_{Fe^{2+}}$, to be calculated (Boon et al., 1994).

THEORETICAL ASPECTS

Several researchers have reported the stoichiometric formula of bacteria (Roels, 1983), including *T. ferrooxidans* (Jones and Kelly, 1983), to be approximately $CH_{1.8}O_{0.5}N_{0.2}$. If the carbon and nitrogen sources are limited to CO_2 and NH_4^+ the formation of biomass occurs according to

$$CO_2, NH_4^+, H_2O \rightarrow CH_{1.8}O_{0.5}N_{0.2} \quad (5)$$

The steady-state carbon dioxide utilization rate can be

used to estimate the bacterial growth rate and concentration (Boon et al., 1994):

$$r_X = -r_{CO_2} \tag{6}$$

$$c_X = \frac{-r_{CO_2}}{D} \tag{7}$$

If it is assumed that energy for bacterial growth and maintenance is obtained from the oxidation of ferrous-iron [Equation (2)], element and charge balances can be used to relate the rates of ferrous-iron, oxygen, and carbon dioxide consumption:

$$-r_{Fe^{2+}} = -4r_{O_2} - 4.2\, r_{CO_2} \tag{8}$$

The bacterial yield on ferrous-iron, $Y_{Fe^{2+}X}$, is defined as the amount of biomass, as moles carbon, produced per mole of ferrous-iron oxidized, i.e.,

$$Y_{Fe^{2+}X} = \frac{r_X}{-r_{Fe^{2+}}} \tag{9}$$

Dividing the Pirt equation [Equation (4)] (Pirt, 1982) by the bacterial production rate, r_X, and combining the result with Equation (9) gives

$$\frac{1}{Y_{Fe^{2+}X}} = \frac{1}{Y^{max}_{Fe^{2+}X}} + \frac{m_{Fe^{2+}}}{D} \tag{10}$$

Therefore, from steady-state continuous culture data, plotting the values of $1/Y_{Fe^{2+}X}$ vs. $1/D$ can be used to determine the values of $Y^{max}_{Fe^{2+}X}$ and $m_{Fe^{2+}}$.

The bacterial specific ferrous-iron oxidation rate, $q_{Fe^{2+}}$, is defined as the rate of ferrous-iron utilization per mole of biomass (i.e., per mole of carbon):

$$q_{Fe^{2+}} = \frac{-r_{Fe^{2+}}}{c_X} \tag{11}$$

Hence, division of the Pirt equation [Equation (4)] (Pirt, 1982) by the bacterial concentration, c_X, yields

$$q_{Fe^{2+}} = \frac{D}{Y^{max}_{Fe^{2+}X}} + m_{Fe^{2+}} \tag{12}$$

Therefore, from steady-state continuous culture data, plotting the values of $q_{Fe^{2+}}$ vs. D can also be used to determine the values of $Y^{max}_{Fe^{2+}X}$ and $m_{Fe^{2+}}$.

If it is assumed that the ferrous-iron oxidation kinetics are proportional to the ferric/ferrous-iron ratio [Equation (3)], $q^{max}_{Fe^{2+}}$ and $K_{Fe^{2+}}$ can be determined by means of Lineweaver-Burke plots, i.e., inverting Equation (3) gives

$$\frac{1}{q_{Fe^{2+}}} = \frac{1}{q^{max}_{Fe^{2+}}} + \frac{K_{Fe^{2+}}}{q^{max}_{Fe^{2+}}} \frac{[Fe^{3+}]}{[Fe^{2+}]} \tag{13}$$

and linear regression of $1/q_{Fe^{2+}}$ versus $[Fe^{3+}]/[Fe^{2+}]$ can be used to determine $q^{max}_{Fe^{2+}}$ and $K_{Fe^{2+}}$.

Equation 12 may also be written in terms of $q^{max}_{Fe^{2+}}$, i.e.;

$$q^{max}_{Fe^{2+}} = \frac{\mu^{max}}{Y^{max}_{Fe^{2+}X}} + m_{Fe^{2+}} \tag{14}$$

Hence, the values of $q^{max}_{Fe^{2+}}$, $Y^{max}_{Fe^{2+}X}$, and $m_{Fe^{2+}}$ determined as described above, may be used to calculate μ^{max}.

The effect of temperature can be incorporated into the kinetic model suggested by Boon et al. (1995) [Equation (3)], by replacing $q^{max}_{Fe^{2+}}$ with a function of temperature. The form of this function can be established by evaluating $q^{max}_{Fe^{2+}}$ at a number of different temperatures and plotting $q^{max}_{Fe^{2+}}$ vs. temperature. Nemati and Webb (1997) proposed that the effect of temperature on the ferrous-iron oxidation kinetics of *T. ferrooxidans* could be described using the Arrhenius equation, viz.,

$$q^{max}_{Fe^{2+}} = K_0 e^{-\frac{E_a}{RT}} \tag{15}$$

Linearization of Equation 15 yields;

$$\ln q^{max}_{Fe^{2+}} = \ln K_0 - \frac{E_a}{R}\frac{1}{T} \tag{16}$$

Therefore, if plotting $\ln(q^{max}_{Fe^{2+}})$ vs. $1/T$ produces a straight line, the values of the activation energy, E_a, and the frequency factor, K_0, can be determined. Substitution of the values of E_a and K_0 into Equation (3) yields a model which predicts $q_{Fe^{2+}}$ as a function of the ferric/ferrous-iron ratio (redox potential), across a range of temperatures, viz.,

$$q_{Fe^{2+}} = K_0 \frac{e^{-\frac{E_a}{RT}}}{1 + K_{Fe^{2+}} \frac{[Fe^{3+}]}{[Fe^{2+}]}} \tag{17}$$

Because the ferrous-iron, oxygen, and carbon dioxide utilization rates are related via Equation (8) the values of the ferrous-iron-based parameters can be used to calculate the oxygen-based parameters. Alternatively, the equations described above can be defined and written in terms of the rate of oxygen utilization by the bacteria, and the parameters determined in the same manner as the ferrous-iron-based parameters.

RESULTS AND DISCUSSION

Single bioreactors were maintained at 30 and 35°C, respectively, and duplicate bioreactors were maintained at 40°C. Steady states were obtained at dilution rates of 0.010, 0.014, 0.020, 0.028, 0.039, and 0.059/h respectively. At each steady state, the bacterial species present and ferrous-iron, oxygen, and carbon dioxide utilization rates of the bacteria, were determined.

The restriction-enzyme banding patterns of PCR amplified bacterial 16S rDNA from the chromosomal DNA of pure cultures of *T. ferrooxidans* ATCC 33020, *L. ferrooxidans* DSM 2705 (controls), and the biomass harvested from bioreactors R2 and R4 are shown in Figure 2.

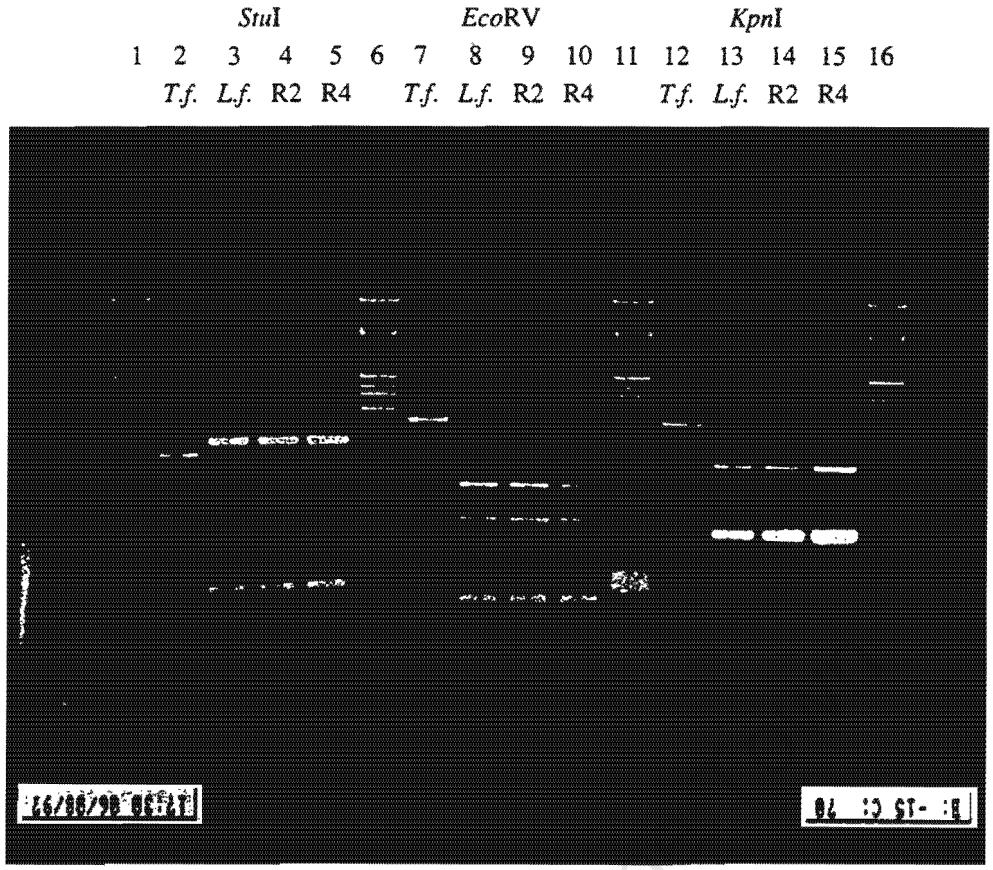

Figure 2. Restriction enzyme analysis of PCR amplified 16S rDNA from pure culture of *L. ferrooxidans* and *T. ferrooxidans* and the ferrous-oxidising bacterial species obtained from the bioleaching mini-plant. Lanes 1, 6, 11 and 16 are size markers obtained by digestion of phage λ with *PstI*.

Three restriction enzymes were used; *StuI* (lanes 2 to 5), *EcoRV* (lanes 7 to 10), and *KpnI* (lanes 12 to 15). The sizes of the bands obtained from the biomass were identical to those obtained for *L. ferrooxidans* DSM 2705 (lanes 3, 8, and 13), but different from *T. ferrooxidans* ATCC 33020 (lanes 2, 7, and 12) irrespective of which restriction enzyme was used. Similar banding patterns were obtained after restriction enzyme digestion of the PCR products amplified

Figure 3. Scanning electron micrograph of ferrous-oxidising bacterial species obtained from Bioreactor 3.

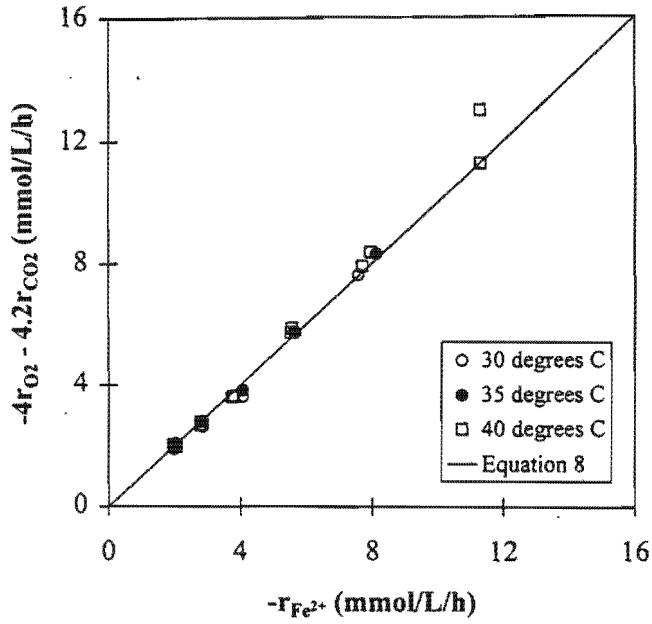

Figure 4. Comparison between the experimental relationship between the ferrous-iron, $-r_{Fe^{+2}}$, oxygen, $-r_{O_2}$, and carbon dioxide, $-r_{CO_2}$, utilisation rates, and the prediction of Equation 8.

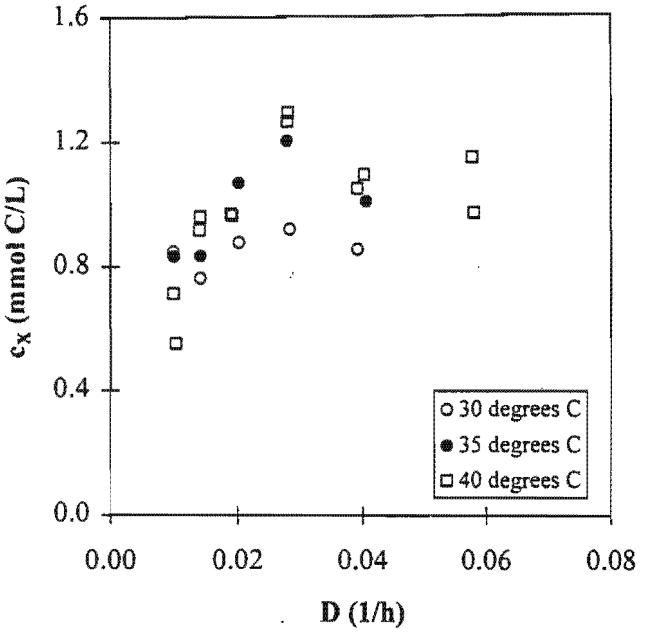

Figure 5. Variation in the concentration of bacteria, c_X, in the bioreactors with changes in the dilution rate, D.

from the biomass in bioreactors R1 and R3 (data not shown). This indicated that *L. ferrooxidans* was the only bacterial species detected in the four bioreactors.

The above result was achieved at each steady state. However, as bacterial species present in low concentrations may not have been detected, the results cannot be considered evidence that the culture in the bioreactors consisted solely of *L. ferrooxidans*. Despite this limitation, the results suggest that *L. ferrooxidans* was present in numbers far exceeding any other species. For this reason, it is logical to assume that any changes in the measured parameters, viz., ferrous-iron, carbon dioxide, and oxygen utilization, can be directly attributed to variations in the concentration and metabolic activity of *L. ferrooxidans*. A scanning electron micrograph of the bacteria is shown in Figure 3.

Prior to performing any kinetic analysis, the validity of the obtained data was checked by comparing the relationship between the measured ferrous-iron, oxygen, and carbon dioxide utilization rates and the theoretical prediction of Equation (8). This comparison is shown in Figure 4 where it can be seen that good agreement was obtained, thereby confirming the validity of the data.

The biomass concentration, c_X, in the bioreactors was calculated from the carbon dioxide utilization rate, $-r_{CO_2}$, using Equation (7). Figure 5 shows the variation in c_X in the bioreactors with changes in the dilution rate, D. It was not possible to maintain a stable steady state at 30 or 35°C above a dilution rate of 0.04/h, while at 40°C it was possible to maintain a steady state up to a dilution rate of 0.06/h; i.e., at 40°C the bioreactors were less subject to washout at low residence times. Furthermore, below a dilution rate of 0.02/h the steady-state biomass concentration decreased in all the bioreactors, indicating a significant maintenance requirement. This trend is in agreement with those of Boon et al. (1995) and Van Scherpenzeel et al. (1998).

The maximum bacterial yield on ferrous-iron, $Y^{max}_{Fe^{2+}X}$, and the maintenance coefficient on ferrous-iron, $m_{Fe^{2+}}$, were determined using Equations (10) and (12). The data used is shown in, Figures 6a and 6b, respectively. Regression analysis of the data obtained at the various temperatures suggested that the maximum bacterial yield on ferrous-iron, $Y^{max}_{Fe^{2+}X}$, might increase with an increase in temperature from

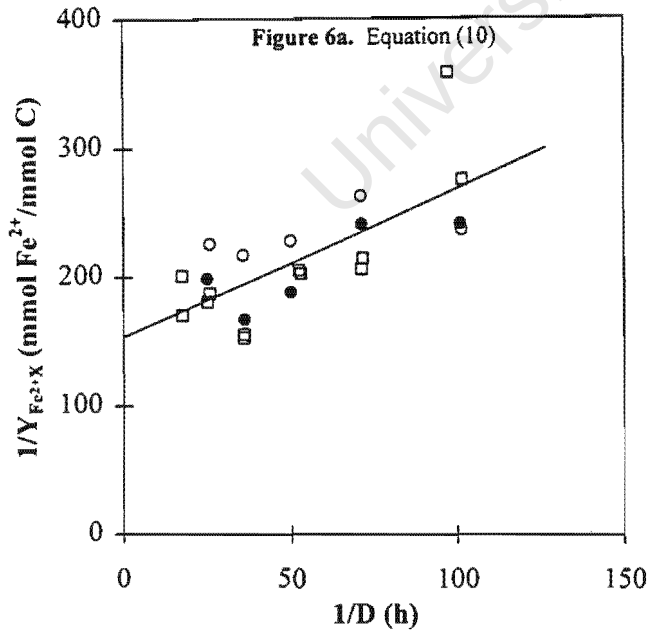

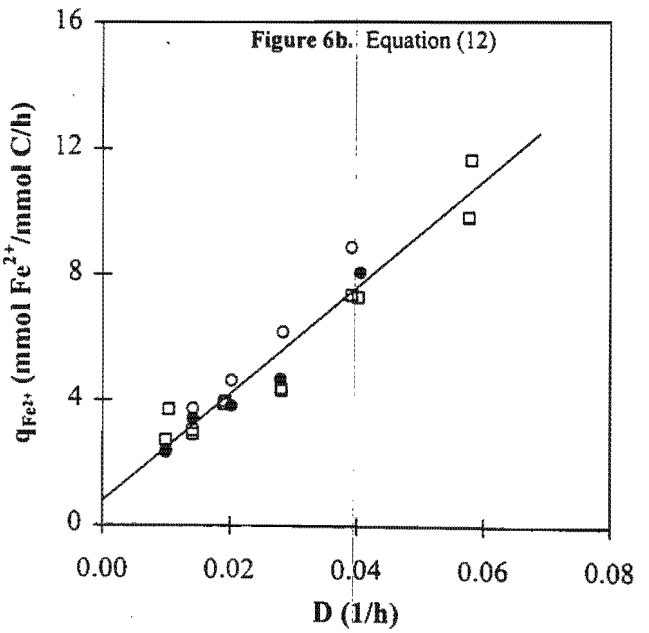

Figure 6. Data used to determine the biomass yield on ferrous-iron, $Y^{max}_{Fe^{2+}}$, and the maintenance coefficient on ferrous-iron, $m_{Fe^{2+}}$ (T = 30°C [○], T = 35°C [●] and T = 40°C [□]).

Table I. Average values of the maximum biomass yield on ferrous-iron, $Y^{max}_{Fe^{2+}X}$, and the maintenance coefficient on ferrous-iron, $m_{Fe^{2+}}$.

	Temperature (°C)	$Y^{max}_{Fe^{2+}X}$ (mmol C/mmol Fe^{2+})	$m_{Fe^{2+}}$ (mmol Fe^{2+}/mmol C/h)
Predominantly *L. ferrooxidans*	30 to 40	0.0059	0.797
Leptospirillum-like	30	0.011	0.444
T. ferrooxidans	30	0.012	0.080

30 to 40°C. However, there was no discernible variation in the maintenance coefficient on ferrous-iron, $m_{Fe^{2+}}$, with changes in temperature.

However, from Figure 6a it appears as though the dilution rate has an effect on $Y_{Fe^{2+}X}$. The dependence of $Y_{Fe^{2+}X}$ on the residence time ($\tau = 1/D$) may be a result of either progressive washout (Jones and Kelly, 1983), or the Pirt equation not being applicable (Boon, 1996). The above, coupled with the scatter obtained in the replicates suggests that the trends observed during the regression analysis may not be statistically significant.

For this reason, the values of $Y^{max}_{Fe^{2+}X}$ and $m_{Fe^{2+}}$ listed in Table I were determined by regression of all the data shown in Figure 6b (i.e., assuming that temperature has no effect on either $Y^{max}_{Fe^{2+}X}$ or $m_{Fe^{2+}}$). Table I also lists the values of $Y^{max}_{Fe^{2+}X}$ and $m_{Fe^{2+}}$ determined previously for *T. ferrooxidans* (Boon, 1996) and a *Leptospirillum*-like bacterium (Van Scherpenzeel et al., 1998). From Table I it is clear that the values obtained in the current investigation are of the same order of magnitude as those determined for a *Leptospirillum*-like bacterium. It is also apparent that they agree more closely with those determined for the *Leptospirillum*-like bacterium than those determined for *T. ferrooxidans*.

The bacterial specific ferrous-iron oxidation rate, $q_{Fe^{2+}}$, was determined at each steady state using Equation (11). The values of $q_{Fe^{2+}}$ and the corresponding ferric/ferrous-iron ratio were, in turn, used to determine the values $q^{max}_{Fe^{2+}}$ and $K_{Fe^{2+}}$ at 30, 35, and 40°C, using Equation (13). The values of $q^{max}_{Fe^{2+}}$ and $K_{Fe^{2+}}$ determined in this manner are shown in Table II together with those determined previously, at 30°C, for a *Leptospirillum*-like bacterium (Van Scherpenzeel et al., 1998) and *T. ferrooxidans* (Boon, 1996).

From Table II, it is apparent that the values of $q^{max}_{Fe^{2+}}$ and $K_{Fe^{2+}}$ determined in this investigation increased with increasing temperature. It is also clear that the value of $K_{Fe^{2+}}$ for *T. ferrooxidans* is an order of magnitude greater than the values of $K_{Fe^{2+}}$ for the *Leptospirillum*-like species and the bacterial culture consisting predominantly of *L. ferrooxidans*. This difference has been reported previously, and has been attributed to *L. ferrooxidans* having a greater affinity for ferrous-iron than *T. ferrooxidans* (Boon, 1996; Norris et al., 1987). However, it may be a result of *L. ferrooxidans* being less subject to inhibition by higher ferric/ferrous-iron ratios (i.e., redox potential). The differences between the two *Leptospirillum* species can be attributed to differences between different subspecies. The culture used in the current investigation originated from the Fairview mine in Barberton, while the culture used by Van Scherpenzeel et al. (1998) originated from Gamsberg in Namaqualand; thus, some strain variation may be expected.

The predicted variation in $q_{Fe^{2+}}$ of the bacterial culture consisting predominantly of *L. ferrooxidans* with changes in the ferric/ferrous-iron ratio at 30, 35, and 40°C are shown in Figure 7 together with the experimentally determined values. It is clear from Figure 7 that the agreement between the predicted and experimental results is good. This suggests that the kinetics of bacterial ferrous-iron oxidation by *L. ferrooxidans* is not a function of the ferric or ferrous-iron concentration, individually, but of the redox potential. This is in agreement with the results of van Scherpenzeel et al. (1998), Boon et al. (1995), and the chemiosmotic model for bacterial ferrous-iron oxidation proposed by Ingledew (1986).

From Figure 7 it is also apparent that there are a large number of data points at ferric/ferrous-iron ratios in the region of 800 to 2500; i.e., at redox potential values in the region of 660 to 680mV. These points represent the threshold ferrous-iron concentration, below which no further ferrous-iron utilization occurs (Braddock et al., 1984; Boon et al., 1995), which is also consistent with the chemiosmotic potential theory proposed by Ingledew (1986). At a total iron concentration of 12 g/L this corresponds to threshold

Table II. Values of the maximum bacterial specific ferrous-iron utilization rates, $q^{max}_{Fe^{2+}}$, and their respective kinetic constants in bacterial ferrous-iron oxidation, $K_{Fe^{2+}}$.

	Temperature (°C)	$q^{max}_{Fe^{2+}}$ (mmol Fe^{2+}/mmol C/h)	$K_{Fe^{2+}}$ (dimensionless)
Predominantly *L. ferrooxidans*	30	8.65	0.0018
	35	11.01	0.0023
	40	13.58	0.0033
Leptospirillum-like	30	6.8	0.0005
T. ferrooxidans	30	8.8	0.05

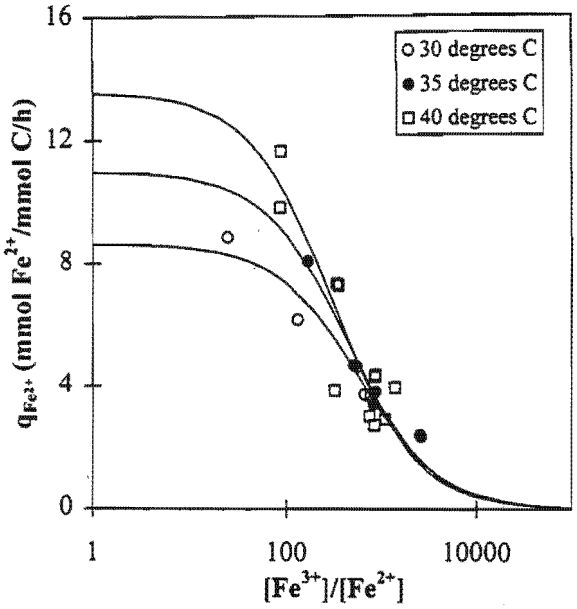

Figure 7. Comparison between the experimental variation in the bacterial specific ferrous-iron oxidation rate of the bacterial culture consisting predominantly of *L. ferrooxidans* with changes in the ferric/ferrous-iron ratio at 30, 35 and 40°C and the prediction of Equation 3 using the data shown in Table II.

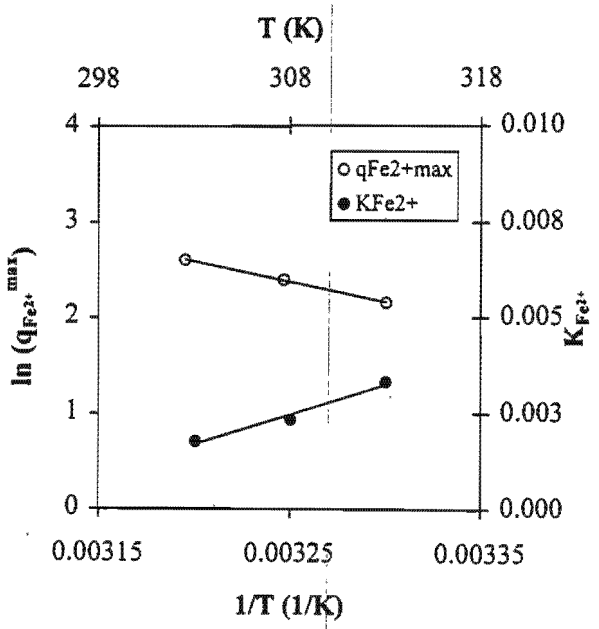

Figure 8. Effect of temperature on the maximum bacterial specific ferrous-iron oxidation rate, $q_{Fe^{2+}}^{max}$, and the kinetic constant in bacterial ferrous-iron oxidation, $K_{Fe^{2+}}$. The variation in $q_{Fe^{2+}}^{max}$ with T is plotted using the linearised form of the Arrhenius equation whereas the variation in $K_{Fe^{2+}}$ is plotted using a linear scale.

ferrous-iron concentrations in the region of 0.086–0.268 m*M*. This concentration is greater than the 0.005m*M* reported for a *Leptospirillum*-like bacterium (van Scherpenzeel et al., 1998), but less than the 0.5m*M* reported for *T. ferrooxidans* (Boon, 1996).

The average value of the maximum specific growth rate, μ^{max}, at each temperature, calculated from Equation (14), and the dilution rate at which washout was observed to occur, D_w, are listed in Table III. From Table III it is apparent that the calculated values of μ^{max} are consistent with the dilution rate at which washout was observed.

Figure 8 shows the variation in the maximum bacterial specific ferrous-iron oxidation rate, $q_{Fe^{2+}}^{max}$, and the kinetic constant in bacterial ferrous-iron oxidation, $K_{Fe^{2+}}$, with changes in temperature. From Figure 8, it is clear that the variation of $q_{Fe^{2+}}^{max}$ and $K_{Fe^{2+}}$ with temperature can be accurately described using a linearized form of the Arrhenius equation and a linear plot, respectively.

The activation energy for the maximum bacterial specific ferrous-iron oxidation rate was calculated to be 35.63 kJ/mol. This value is significantly lower than the value of 68.4 kJ/mol reported for *T. ferrooxidans* (Nemati and Webb, 1997). This difference may be attributed to differences between the bacterial species used, or because Nemati and Webb (1997) used initial rate and not steady-state rate data. The frequency factor for the maximum bacterial spe-

Table III. Values of the average maximum specific growth rate, μ^{max}, and the dilution rate at which washout was observed, D_w, at 30, 35, and 40°C.

Temperature	30°C	35°C	40°C
μ^{max} (h)	0.046	0.060	0.077
D_w (h)	$0.059 < D_w < 0.040$	$0.059 < D_w < 0.040$	$D_w < 0.059$

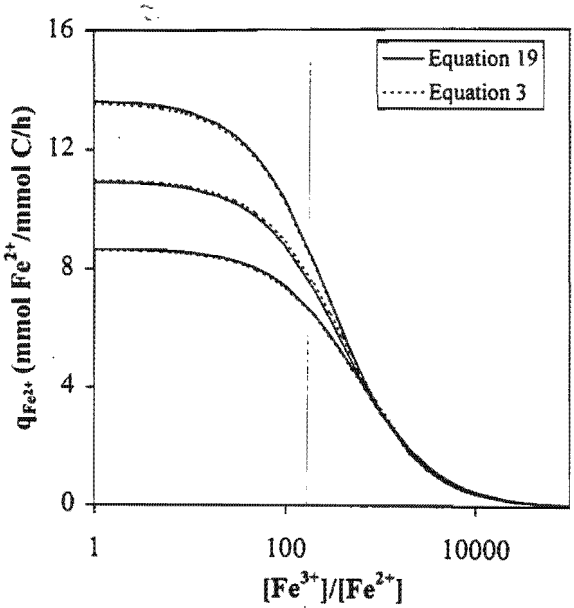

Figure 9. Predicted variation in the bacterial specific ferrous-iron oxidation rate of the bacterial culture consisting predominantly of *L. ferrooxidans* with changes in the ferric/ferrous-iron ratio, at temperatures ranging from 30 to 40°C. The solid lines represent the variation predicted using Equation 19 and the dashed lines represent the variation predicted by Equation 3 and the data listed in Table II.

cific ferrous-iron oxidation rate was calculated to be 1.204×10^7 mmol Fe^{2+}/mol C/h.

The relationship between $K_{Fe^{2+}}$ and absolute temperature was found to be

$$K_{Fe^{2+}} = 0.0002T - 0.0453 \quad (18)$$

Substituting the values of E_a and K_0, and the relationship between $K_{Fe^{2+}}$ and absolute temperature into Equation (16) yields a model which predicts the bacterial specific ferrous-iron oxidation rate from 30 to 40°C, as a function of the ferric/ferrous-iron ratio

$$q_{Fe^{2+}} = 1.204 \times 10^7 \frac{e^{-\frac{35.63}{RT}}}{1 + (0.0002T - 0.0453)\frac{[Fe^{3+}]}{[Fe^{2+}]}} \quad (19)$$

Figure 9 shows the predicted variation in the specific ferrous-iron utilization rate with changes in the ferric/ferrous-iron ratio at temperatures ranging from 30 to 40°C, using the data in Table II and Equation (3), and Equation (19), respectively. It is apparent from Figure 9 that the agreement between the model proposed by Boon et al. (1995) and Equation (19) is excellent.

CONCLUSIONS

At each steady state, total genomic DNA was extracted from the bioreactor biomass, and restriction enzyme analysis of PCR amplified 16S rDNA showed that *L. ferrooxidans* was the only ferrous-iron oxidizing species that could be detected.

Analysis of the relationship between the rates of ferrous-iron, oxygen, and carbon dioxide utilization confirmed that the experimental data was valid. The bacteria in the bioreactors maintained at 40°C achieved the highest growth rate; the maximum bacterial specific growth rate was calculated to be 0.077/h. Below a dilution rate of about 0.02/h the biomass concentration in the bioreactors decreased. This suggests a significant maintenance requirement at high-redox potentials.

Although the results suggest that the Pirt equation may not be valid, the values of $Y^{max}_{Fe^{2+}X}$ and $m_{Fe^{2+}}$ were of the same order of magnitude as those determined previously for a *Leptospirillum*-like bacterium. Increasing the temperature from 30 to 40°C did not have a marked effect on any of these parameters.

The maximum specific ferrous-iron utilization rate, $q^{max}_{Fe^{2+}}$, and the kinetic constant in bacterial ferrous-iron oxidation, $K_{Fe^{2+}}$, both increased with increasing temperature, across the range from 30 to 40°C. The effect of temperature on the maximum specific ferrous-iron utilization rate could be described using the Arrhenius equation, whereas the kinetic constant in bacterial ferrous-iron oxidation increased linearly with increasing temperature. The ferrous-iron kinetics could be accurately described in terms of the ferric/ferrous-iron ratio by means of a Michaelis–Menten-based model modified to account for the effect of temperature.

The financial support from the Gold Fields Foundation, Billiton Process Research and the Foundation for Research Development (South Africa) are gratefully acknowledged.

NOMENCLATURE

c_X	Concentration of bacteria (mmol C/L)
D	dilution rate (1/h)
D_w	dilution rate at which washout is observed (1/h)
E_a	activation energy (kJ/mol)
$[Fe^{2+}]$	concentration of Fe^{2+} (mmol Fe^{2+}/L)
$[Fe^{3+}]$	concentration of Fe^{3+} (mmol Fe^{2+}/L)
K_0	frequency factor (mmol Fe^{2+}/mmolC/h)
$K_{Fe^{2+}}$	kinetic constant in bacterial ferrous-iron oxidation (Dimensionless)
$m_{Fe^{2+}}$	maintenance coefficient on Fe^{2+} (mmol Fe^{2+}/mmolC/h)
$q_{Fe^{2+}}$	bacterial specific ferrous-iron oxidation rate (mmol Fe^{2+}/mmol C/h)
$q^{max}_{Fe^{2+}}$	maximum bacterial specific ferrous-iron oxidation rate (mmol Fe^{2+}/mmolC/h)
R	universal gas constant (J/mol/K)
r_{CO_2}	carbon dioxide production rate (mmol CO_2/L/h)
$r_{Fe^{2+}}$	ferrous-iron production rate (mmol Fe^{2+}/L/h)
r_{O_2}	oxygen production rate (mmol O_2/L/h)
r_X	bacterial production rate (mmol C/L/h)
T	absolute temperature (K)
$Y_{Fe^{2+}X}$	bacterial yield on Fe^{2+} (mmol C/mmol Fe^{2+})
$Y^{max}_{Fe^{2+}X}$	maximum bacterial yield on Fe^{2+} (mmol C/mmol Fe^{2+})
μ^{max}	maximum bacterial specific growth rate (1/h)

References

Boon M. 1996. Theoretical and experimental methods in the modelling of the bio-oxidation kinetics of sulphide minerals. Ph.D. thesis, Delft University of Technology, The Netherlands.

Boon M, Hansford GS, Heijnen JJ. 1995. The role of bacterial ferrous-iron oxidation in the bio-oxidation of pyrite. In: T Vargas, CA Jerez, JV Wiertz, and H Toledo, editors. Biohydrometallurgical Processing I. Santiago: University of Chile. p 153–163.

Boon M, Heijnen JJ, Hansford GS. 1994. Recent developments in the modelling of bio-oxidation kinetics and their implications in practice: Part I, Measurement methods in bio-oxidation kinetics. In: D Holmes and R. Smith, editors. Minerals Processing II. Warrendale, PA: The Minerals, Metals and Materials Society. p 41–61.

Braddock JF, Luong HV, Brown EJ. 1984. Growth kinetics of *Thiobacillus ferrooxidans* isolated from arsenic mine drainage. Appl Environ Microbiol 48(1):48–55.

Hallman R, Friedrich A, Koops HP, Pommering-Röser A, Sand W. 1987. Physiological characteristics of *Thiobacillus ferrooxidans* and *Leptospirillum ferrooxidans* and physiochemical factors influence on microbial metal leaching. Geomicrobiol J 10:193–205.

Hansford GS. 1997. Recent developments in modelling the kinetics of bioleaching. In: DE Rawlings, editor. Biomining: Theory, microbes and industrial processes. Austin, TX: Springer, Berlin and Landes Bioscience. p 153–176.

Helle U, Onken U. 1987. Continuous bacterial leaching of pyritic flotation concentrate by mixed cultures. In: PR Norris and DP Kelly, editors. Proc Int Symp on Biohydrometallurgy. Kew, Surrey: Science and Technology Letters. p 61–75.

Ingledew WJ. 1986. Ferrous-iron oxidation by *Thiobacillus ferrooxidans*. Biotechnol Bioeng Symp 16:23–33.

Jones CA, Kelly DP. 1983. Growth of *Thiobacillus ferrooxidans* on fer-

rous-iron in chemostat culture: Influence of product and substrate inhibition. J Chem Technol Biotechnol 33B(4):241–261.

Nemati M, Harrison STL, Webb Hansford GSC. 1998. Biological oxidation of ferrous sulphate by *Thiobacillus ferrooxidans:* A review on the kinetic aspects. Biochem Eng J 1:171–190.

Nemati M, Webb C. 1997. A kinetic model for biological oxidation of ferrous-iron by *Thiobacillus ferrooxidans*. Biotechnol Bioeng 53: 478–486.

Norris PR, Barr DW, Hinson D. 1987. Iron and mineral oxidation by acidophilic bacteria: Affinities for iron and attachment to pyrite. In: PR Norris and DP Kelly, editors. Proc Int Symp on Biohydrometallurgy. Kew, Surrey: Science and Technology Letters. p 43–59.

Pirt SJ. 1982. Maintenance energy: A general model for energy limited and energy sufficient growth. Arch Microbiol 133:300–302

Poulin R, Lawrence RW. 1996. Economic and environmental niches of biohydrometallurgy. Miner Eng 9(8):799–810.

Rawlings DE. 1995. Restriction enzyme analysis of 16S rRNA genes for the rapid identification of *Thiobacillus ferrooxidans*, *Thiobacillus thiooxidans* and *Leptospirillum ferrooxidans* strains in leaching environments In: T Vargas, CA Jerez, JV Wiertz, and H Toledo, editors. Biohydrometallurgical processing 2. Santiago: University of Chile. p 9–17.

Rawlings DE, Tributsch H, Hansford GS. 1999. Reasons why *Thiobacillus ferrooxidans* is not the dominant iron-oxidising bacterium in many commercial processes for the biooxidation of pyrite and related ores. Microbiol 145(1):5–13.

Roels JA. 1983. Energetics and kinetics in biotechnology. Amsterdam: Elsevier Biomedical Press.

Van Aswegen PC. 1993. Commissioning and operation of bio-oxidation plants for the treatment of refractory gold ores. In: JB Hiskey and GW Warren, editors. Hydrometallurgy; fundamentals, technology and innovations. Littleton, Colorado: Soc Min Metall Explor p 709–725.

Van Scherpenzeel DA, Boon M, Ras C, Hansford GS, Heijnen JJ. 1998. The kinetics of ferrous-iron oxidation by *Leptospirillum* bacteria in continuous cultures. Biotechnol Prog 14:425–433.

Vishniac W, Santer M. 1957. The *Thiobacilli*. Bacterial Revs 21:195–213.

Vogel AI. 1989. Vogel's textbook of quantitative chemical analysis, 5th edition. London: Longman Group.

Modeling Continuous Bioleach Reactors

A. W. Breed, G. S. Hansford

Gold Fields Minerals Bioprocessing Laboratory, Department of Chemical Engineering, Private Bag, University of Cape Town, Rondebosch 7701, South Africa; e-mail: awb@chemeng.uct.ac.za.uct

Received 31 July 1998; accepted 22 February 1999

Abstract: The results of recent research have shown that the bioleaching of sulfide minerals occurs via a two-step mechanism. In this mechanism, the sulfide mineral is chemically oxidized by the ferric-iron in the bioleaching liquor. The ferrous-iron produced is subsequently oxidized to ferric-iron by the microorganism. Further research has shown that the rates of both the ferric leaching and ferrous-iron oxidation are governed by the ferric/ferrous-iron ratio (i.e., the redox potential). During the steady-state operation of a bioleach reactor, the rate of iron turnover between the chemical ferric leaching of the mineral and the bacterial oxidation of the ferrous-iron will define the rate and the redox potential at which the system will operate. The balance between the two rates will in turn depend on the species used, the microbial concentration, the residence time employed, the nature of the sulfide mineral being leached, and its active surface area. The model described proposes that the residence time and microbial species present determine the microbial growth rate, which in turn determines the redox potential in the bioleach liquor. The redox potential of the solution, in turn, determines the degree of leaching of the mineral; that is, conversion in the bioleach reactor. © 1999 John Wiley & Sons, Inc. *Biotechnol Bioeng* 64: 671–677, 1999.

Keywords: *Thiobacillus ferrooxidans; Leptospirillum ferrooxidans;* bioleaching; continuous culture; modeling

INTRODUCTION

Bioleaching of sulfide minerals is a well-known phenomenon, and has found widespread application in the recovery of copper, and the pretreatment of refractory gold ores. Furthermore, it has significant potential for the extraction of nickel, cobalt, and other base metals. However, in order for bioleaching to compete successfully with other pretreatment processes, such as pressure leaching and roasting, it needs to be optimized with regard to the parameters that affect the bioleaching reactions, and the growth of the microorganism involved. Thus, there is a growing need for mechanistically based kinetic models for the operation, optimization, and control of bioleaching processes and the use of these models in deriving the performance equations of continuous bioleach reactors.

In spite of the increased commercial application of bioleaching, at present there are currently no mechanistic models that can be used to predict the performance of bioleach reactors. This can be attributed to the fact that modeling bioleach reactors has been complicated by the complex nature of microbial interactions and difficulties encountered when attempting to measure the biomass concentration and growth rate, and the ferric and ferrous-iron concentrations. The analyses are further complicated by the presence of solids within the system. This has resulted in the models used in the bioleaching of minerals being empirical, in spite of the large amount of research performed thus far.

To date, the logistic equation is the rate expression that has found the most widespread application, with regard to the modeling of both batch and continuous bioleach reactors (Pinches et al., 1988). Although the logistic equation is not mechanistically based it has proved useful in modeling batch and continuous laboratory-, pilot-, and full-scale plant data for several pyrite and pyrite–arsenopyrite flotation concentrates (Dew, private communication, 1993; Hansford and Chapman, 1992; Miller and Hansford, 1992a, 1992b).

The results of recent research have provided strong evidence that the bioleaching of sulfide minerals occurs via a two-step mechanism (Boon et al., 1995). In this mechanism, the sulfide mineral is chemically oxidized by ferric-iron. The ferrous-iron produced by this ferric leaching of the mineral is subsequently oxidized to ferric-iron by the microorganisms, thus maintaining a high redox potential within the system. Of course, for this reaction to be carried out the microorganisms require a source of oxygen, carbon dioxide, and other nutrients.

The existence of a two-step mechanism is supported by the isolation and identification of *Leptospirillum ferrooxidans* (Breed et al., in press) and *Thiobacillus caldus* (Rawlings and Gardner, unpublished results) from a mixed culture oxidizing a pyrite–arsenopyrite flotation concentrate in a continuous bioleaching miniplant, and by observations made by Boon (1996). Diagrammatic representations of the bioleaching of both pyrite and arsenopyrite via the two-step mechanism are shown in Figure 1a and b, respectively.

A two-step mechanism suggests that the overall process can be reduced to a number of independent sequential and/or parallel subprocesses. The kinetics of the respective subprocesses may be studied separately, and the results used to predict the steady-state and continuous performance of bioleach reactors for a variety of different minerals, microor-

Correspondence to: A. W. Breed

Contract grant sponsors: Billiton Process Research; Gold Fields Foundation (South Africa); Foundation for Research Development (South Africa)

CCC 0006-3592/99/060671-07

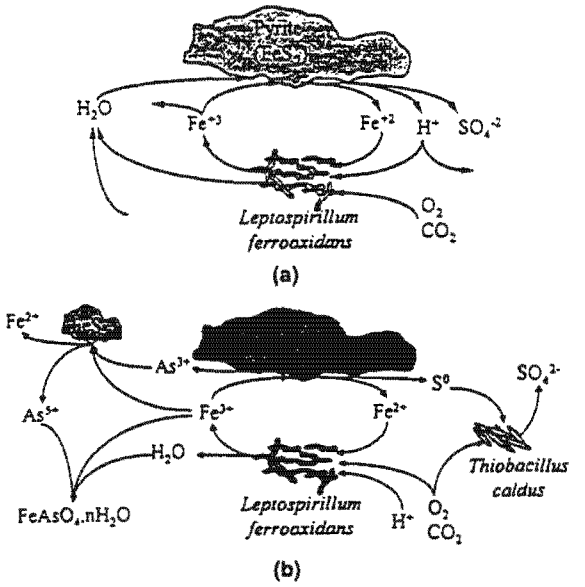

Figure 1. Diagrammatic representation of the bioleaching of pyrite (a) and arsenopyrite (b) via the two-step mechanism.

ganisms, and operating conditions (e.g., pH, T, inhibitory ion concentration).

The purpose of this study is to use the mechanism and kinetics for bioleaching proposed by Boon et al. (1995) (also Hansford, 1997) and to develop a model to predict the steady-state performance of a continuous bioleach reactor.

BACKGROUND

A number of researchers have shown that the ferrous-iron oxidation kinetics of the bacteria involved in bioleaching may be modeled assuming Michaelis–Menten kinetics and a Monod-type equation, modified to account for ferric-iron (product) inhibition (Nemati et al., 1998). A simplified form of the equation suggested by Braddock et al. (1984), written in terms of the specific rate of ferrous-iron utilization, $q_{Fe^{2+}}$, and neglecting the ferrous-iron saturation and threshold ferrous-iron concentration terms, has been used successfully to describe the ferrous-iron oxidation kinetics of *Thiobacillus ferrooxidans* and *Leptospirillum ferrooxidans* (Hansford, 1997):

$$q_{Fe^{2+}} = \frac{q^{max}_{Fe^{2+}}}{1 + K\dfrac{[Fe^{3+}]}{[Fe^{2+}]}} \tag{1}$$

An important feature of Eq. (10) is that the ferric/ferrous-iron ratio can in turn be related to the solution redox potential via the Nernst equation:

$$E_h = E_0^{'} + \frac{RT}{nF}\ln\left(\frac{[Fe^{3+}]}{[Fe^{2+}]}\right) \tag{2}$$

The values of the maximum bacterial-specific ferrous-iron oxidation rate, $q^{max}_{Fe^{2+}}$, and the kinetic constant in bacterial ferrous-iron oxidation, K, determined for *T. ferrooxidans* (Boon et al., 1995) and a *Leptospirillum*-like bacterium (Van Scherpenzeel, 1996) are listed in Table I. The resulting predicted variation in $q_{Fe^{2+}}$, with changing ferric/ferrous-iron ratio, is shown in Figure 2.

From Figure 2, it is clear that, at low ferric/ferrous-iron ratios (i.e., at low redox potentials), *T. ferrooxidans* has a greater specific ferrous-iron oxidation rate than the *Leptospirillum*-like bacterium, hence it will be the dominant species in the bioleaching medium. However, at high redox potentials, the *Leptospirillum*-like bacterium has a greater specific ferrous-iron oxidation rate than *T. ferrooxidans*, hence it will be the dominant species. These predictions are in agreement with the results of previous research (Lawson, private communication, 1997; Norris et al., 1987; Rawlings, 1995). Norris et al. (1987) found that *L. ferrooxidans* had a greater affinity for ferrous-iron than *T. ferrooxidans*. Lawson (private communication, 1997) found that *L. ferrooxidans*, and not *T. ferrooxidans*, was the dominant microorganism during the normal operation of a continuous bioleaching system oxidizing a pyrite flotation concentrate. Rawlings (1995) reported a similar phenomenon for the bioleaching of a pyrite–arsenopyrite concentrate.

Recent research has shown that the ferric leaching of sulfide minerals is dependent on the redox potential (ferric/ferrous-iron ratio) of the bioleaching solution (Boon, 1996; Breed et al., 1997; May et al., 1997; Ruitenberg et al., 1999). Boon (1996) suggested that the ferric leaching of pyrite could be described by an equation of the form:

$$\upsilon_{Fe^{2+}} = \frac{\upsilon^{max}_{Fe^{2+}}}{1 + B\dfrac{[Fe^{2+}]}{[Fe^{3+}]}} \tag{3}$$

For pyrite, the average values of $\upsilon^{max}_{Fe^{2+}}$ and B were calculated to be 0.096 mol Fe^{2+}/mol FeS_2 and 2439 respectively (Boon, 1996). The predicted variation in the pyrite-specific ferrous-iron production rate, $\upsilon_{Fe^{2+}}$, with changing ferric/ferrous-iron ratio, is shown in Figure 3.

If it is assumed that the bioleaching of sulfide minerals occurs via the two-step mechanism, then, at steady-state, the chemical ferrous-iron production rate from the chemical ferric leaching of the sulfide mineral, $r^{chem}_{Fe^{2+}}$, is equal to the bacterial ferrous-iron consumption rate, $-r^{bact}_{Fe^{2+}}$:

Table I. Maximum bacterial specific ferrous-iron oxidation rate, $q^{max}_{Fe^{2+}}$, and bacterial ferrous-iron oxidation kinetic constant, K, at 30°C, for *T. ferrooxidans* and a *Leptospirillum*-like bacterium.[a]

Bacterial species	$q^{max}_{Fe^{2+}}$	K
T. ferrooxidans	8.80	0.05
Leptospirillum-like	6.80	0.0005

[a]Data obtained from Boon (1996) and Van Scherpenzeel (1996), respectively.

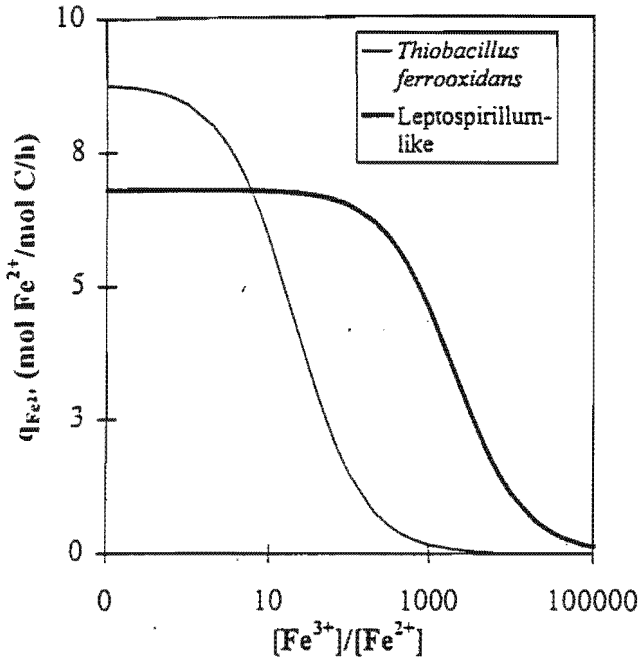

Figure 2. Variation in the bacterial specific ferrous-iron oxidation rate, $q_{Fe^{2+}}$, with changing ferric/ferrous-iron ratio, $[Fe^{3+}]/[Fe^{2+}]$, at 30°C, for *T. ferrooxidans* and a *Leptospirillum*-like bacterium. Data were calculated from the results of Boon (1996) and Van Scherpenzeel (1996).

$$-r^{bact}_{Fe^{2+}} = r^{chem}_{Fe^{2+}} \quad (4)$$

Therefore, in systems containing both bacteria and pyrite, the bacterial and chemical subprocesses are linked by the rate at which the iron is turned over in the system.

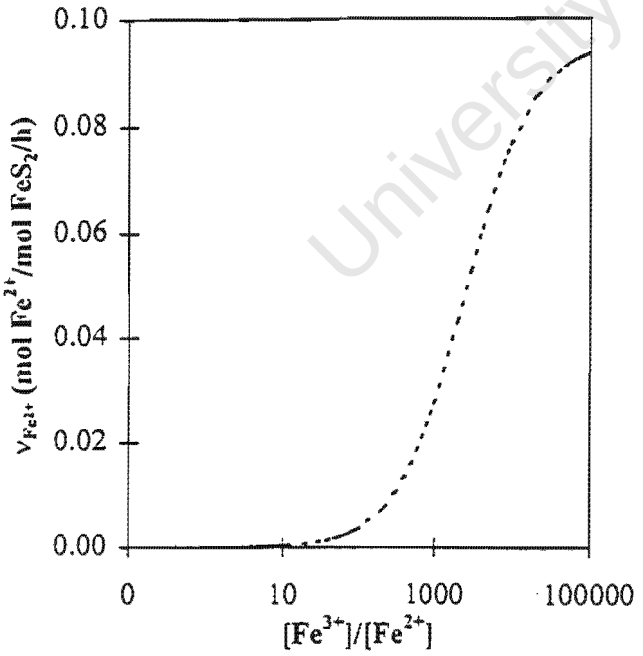

Figure 3. Variation in the pyrite specific ferrous-iron production rate, $v_{Fe^{2+}}$, with changing ferric/ferrous-iron ratio, $[Fe^{3+}]/[Fe^{2+}]$. Data were calculated from the results of Boon (1996).

Figure 4 shows the chemical ferrous-iron production rate from the chemical ferric leaching of pyrite and the bacterial ferrous-iron consumption rate by *T. ferrooxidans* and a *Leptospirillum*-like bacterium as a function of the ferric/ferrous-iron ratio (redox potential), using the kinetic constants determined by Boon (1996) and Van Scherpenzeel (1996). The curves shown were plotted assuming a solids concentration of 100 g/L (94.0% FeS_2), a bacterial concentration of 2.0×10^{-3} mol C/L, and an overall iron concentration of 12 g/L. The point of intersection of the curves represents the steady-state rate of iron turnover. It represents both the rate of mineral leaching and the steady-state ferric/ferrous-iron ratio, or redox potential of the system; hence, it is the point that a model of the system must be able to predict.

From Figure 4 it is apparent that the chemical ferrous-iron production rate curve for pyrite intersects the bacterial ferrous-iron consumption rate curve of the *Leptospirillum*-like bacterium at a higher rate of iron turnover than that of *T. ferrooxidans*. This suggests that the *Leptospirillum*-like bacterium will be the dominant organism in the bioleaching of pyrite. This result is consistent with the findings of previous research (Lawson, private communication, 1997; Boon, 1996).

MODEL DEVELOPMENT

In modeling the bioleaching of pyrite in a continuous bioleach reactor, assumption of the two-step mechanism al-

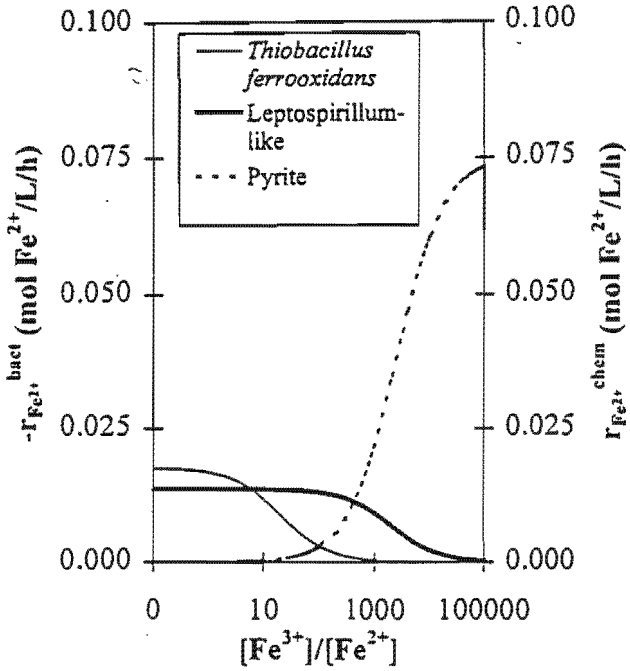

Figure 4. Variation in the ferrous-iron production rate during the ferric leaching of pyrite, $r^{chem}_{Fe^{2+}}$, and the bacterial ferrous-iron consumption rate during the biooxidation of ferrous-iron by *T. ferrooxidans* and a *Leptospirillum*-like bacterium, $-r^{bact}_{Fe^{2+}}$, as a function of the ferric/ferrous-iron ratio, $[Fe^{3+}]/[Fe^{2+}]$ (redox potential). Data were calculated from the results of Boon (1996) and Van Scherpenzeel (1996).

lows each of the rate-controlling subprocesses to be treated separately. First, the steady-state ferric/ferrous-iron ratio or redox potential is determined from the kinetics of the bacterial ferrous-iron oxidation and then the conversion of the pyrite from the chemical leach kinetics.

A schematic representation of steady-state pyrite bioleaching in continuous culture is shown in Figure 5.

Steady-State Bacterial Ferrous-Iron Oxidation

At steady-state:

$$Q_{in} = Q_{out} = Q \tag{5}$$

Using a bioreactor with volume V, and sterile feed (i.e., $c_{X,\,in} = 0$), a bacterial mass balance yields:

$$Vr_X = Qc_X \tag{6}$$

If it is assumed that

$$\mu = \frac{\mu^{max}}{1 + \frac{K_s}{C_s}} \tag{7}$$

then the bacterial production rate, r_X, is directly proportional to the bacterial concentration;

$$r_X = \mu c_X \tag{8}$$

Substituting Equation 8 into Equation 6, re-arranging and simplifying gives;

$$\mu = \frac{Q}{V} = D = \frac{1}{\tau} \tag{9}$$

that is, the bacterial specific growth rate is inversely proportional to the bioreactor residence time.

If it is assumed that maintenance requirements and biomass decay are insignificant the bacterial production rate is directly related to the bacterial ferrous-iron production rate; that is:

$$r_X = -Y_{Fe^{2+}X} r^{bact}_{Fe^{2+}} \tag{10}$$

The bacterial yield on ferrous-iron, $Y_{Fe^{2+}X}$, is defined as the moles of biomass, c_X, produced per mole of Fe^{2+} oxidized.

Rearranging, and dividing by the concentration of bacteria, c_X, yields:

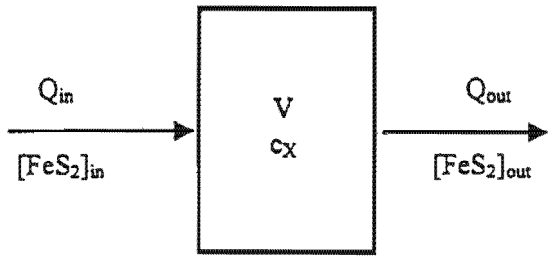

Figure 5. Schematic representation of steady-state pyrite bioleaching in continuous culture.

$$\frac{r_X}{c_X} = \frac{-r^{bact}_{Fe^{2+}} Y_{Fe^{2+}X}}{c_X} \tag{11}$$

Combining Equations 8 to 11;

$$\frac{r_X}{c_X} = \frac{1}{\tau} = \frac{-r^{bact}_{Fe^{2+}} Y_{Fe^{2+}X}}{c_X} \tag{12}$$

The bacterial specific ferrous-iron oxidation rate, $q_{Fe^{2+}}$, is defined as the bacterial ferrous-iron consumption rate, $r_{Fe^{2+}}$, per mole of biomass, c_X; that is:

$$q_{Fe^{+2}} = \frac{-r^{bact}_{Fe^{2+}}}{c_X} \tag{13}$$

Hence substitution of Equation 13 into Equation 12 yields;

$$\frac{1}{\tau} = q_{Fe^{2+}} Y_{Fe^{2+}X} \tag{14}$$

If it is assumed that the bacteria-specific ferrous-iron oxidation rate, $q_{Fe^{2+}}$, can be related to ferric/ferrous-iron ratio using Eq. (1), then substituting Eq. (1) into Eq. (14), and rearranging, gives:

$$\frac{[Fe^{3+}]}{[Fe^{2+}]} = \frac{\tau q^{max}_{Fe^{2+}} Y_{Fe^{2+}} - 1}{K} \tag{15}$$

Eq. (15) shows that the ferric/ferrous-iron ratio (redox potential) is a function only of the residence time and a group of constants, the values of which are determined by the characteristics of the bacterial species (kinetic parameters) being used. The ferric/ferrous-iron ratio and redox potential are not functions of either the mineral concentration, or the total or ferrous-iron concentrations; that is:

$$\frac{[Fe^{3+}]}{[Fe^{2+}]} = f(\tau) \neq f([FeS_2]_{in}, [Fe_T], [Fe^{2+}]) \tag{16}$$

Although this is not an intuitive result, it is expected from the assumption of Monod or Michaelis–Menten-type kinetics.

Figure 6 shows the variation in the predicted ferric/ferrous-iron ratio and redox potential for both *T. ferrooxidans* and a *Leptospirillum*-like bacterium during steady-state bioreactor operation, at 30°C, for residence times ranging from 0 to 20 days. The values of K, $q^{max}_{Fe^{2+}}$, and $Y_{Fe^{2+}X}$ were obtained from Boon (1996) and Van Scherpenzeel (1996), respectively. From Figure 6, it is clear that, at residence times greater than about 1 day, the solution redox potential will be higher if the bacteria present are *Leptospirillum*-like as opposed to *T. ferrooxidans*.

Steady-State Chemical (Ferric) Pyrite Leaching

A number of researchers have reported that both the chemical ferric leaching (May et al., 1998; Ruitenberg et al., 1999) and the bioleaching (Hansford and Chapman, 1992;

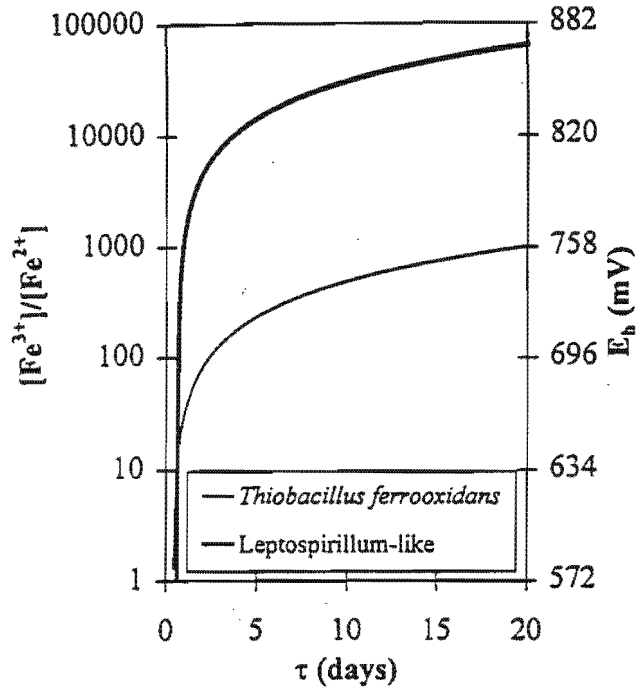

Figure 6. Variation in the predicted ferric/ferrous-iron ratio, $[Fe^{3+}]/[Fe^{2+}]$, and redox potential, E_h, with changing residence time, τ, for *T. ferrooxidans* and a *Leptospirillum*-like bacterium. Data were calculated from the results of Boon (1996) and Van Scherpenzeel (1996), and using E_0 = 572 mV, RT/nF = 26.99.

Miller and Hansford, 1992b) of sulfide minerals is dependent on the surface area of the mineral present. This has led to the use of a population balance model (Crundwell, 1994) to account for the size distribution of the mineral feed, and changes resulting from the leaching process. This approach has proved successful using a shrinking particle model, even though the bioleaching of pyrite has been shown to occur by the formation of pores (Hansford and Drossou, 1988). However, to simplify matters, this study is limited to the use of a global rate for the initial size fraction used.

During the steady-state chemical ferric leaching of pyrite in a continuous reactor, performing a pyrite mass balance yields:

$$Q_{in}[FeS_2]_{in} + Vr_{FeS_2} = Q_{out}[FeS_2]_{out} \quad (17)$$

which can be simplified to give;

$$[FeS_2]_{in} - [FeS_2]_{out} = -\tau r_{FeS_2} \quad (18)$$

The reaction stoichiometry for the chemical (ferric) leaching of pyrite is:

$$FeS_2 + 14Fe^{3+} + 8H_2O \rightarrow 15Fe^{2+} + 16H^+ + 2SO_4^{2-} \quad (19)$$

From Equation 19 it is apparent that for every mole of pyrite oxidised, 15 moles of ferrous-iron are produced i.e.;

$$15r_{FeS_2} = -r_{Fe^{2+}}^{chem} \quad (20)$$

Hence

$$r_{FeS_2} = -\frac{r_{Fe^{2+}}^{chem}}{15} \quad (21)$$

Substituting Equation 21 into Equation 18 yields;

$$[FeS_2]_{in} - [FeS_2]_{out} = \frac{\tau r_{Fe^{2+}}^{chem}}{15} \quad (22)$$

By definition;

$$r_{Fe^{2+}}^{chem} = \upsilon_{Fe^{2+}}[FeS_2]_{out} \quad (23)$$

If the ferric leaching of pyrite can be described by an equation of the form suggested by Boon (1996), viz. Equation 3, substitution of Equation 3 into Equation 23 yields;

$$r_{Fe^{2+}}^{chem} = \frac{\upsilon_{Fe^{2+}}^{max}[FeS_2]_{out}}{1 + B\dfrac{[Fe^{2+}]}{[Fe^{3+}]}} \quad (24)$$

Substituting Equation 24 into Equation 22 gives;

$$[FeS_2]_{in} - [FeS_2]_{out} = \frac{\dfrac{\tau}{15}\upsilon_{Fe^{2+}}^{max}[FeS_2]_{out}}{1 + B\dfrac{[Fe^{2+}]}{[Fe^{3+}]}} \quad (25)$$

which may be simplified to give;

$$[FeS_2]_{in} = [FeS_2]_{out}\left(1 + \frac{\dfrac{\tau}{15}\upsilon_{Fe^{2+}}^{max}}{1 + B\dfrac{[Fe^{2+}]}{[Fe^{3+}]}}\right) \quad (26)$$

Rearranging Equation 26 yields;

$$\frac{[FeS_2]_{in}}{[FeS_2]_{out}} = 1 + \frac{\dfrac{\tau}{15}\upsilon_{Fe^{2+}}^{max}}{1 + B\dfrac{[Fe^{2+}]}{[Fe^{3+}]}} \quad (27)$$

The fraction of mineral leached, X, is defined as;

$$X = \frac{[FeS_2]_{in} - [FeS_2]_{out}}{[FeS_2]_{in}} = 1 - \frac{[FeS_2]_{out}}{[FeS_2]_{in}} \quad (28)$$

Hence

$$X = \frac{\dfrac{\tau}{15}\upsilon_{Fe^{2+}}^{max}}{1 + B\dfrac{[Fe^{2+}]}{[Fe^{3+}]} + \dfrac{\tau}{15}\upsilon_{Fe^{2+}}^{max}} \quad (29)$$

From Eq. (29) it is clear that the fraction of mineral leached (i.e., mineral conversion) is a function of the ferric/ferrous-iron ratio (redox potential), the residence time, and the characteristics of the pyrite itself. However, as shown previously

[see Eq. (16)], the residence time and the bacterial species present determine the ferric/ferrous-iron ratio; hence:residence time and the bacterial species present determine the ferric/ferrous-iron ratio, hence;

$$X = g\left(\frac{[Fe^{3+}]}{[Fe^{2+}]}\right) = f(\tau) \neq f([FeS_2]_{in}) \qquad (30)$$

Figure 7 shows the predicted variation in the pyrite conversion [Eq. (29)], using *T. ferrooxidans* and a *Leptospirillum*-like bacterium in a continuous-flow bioreactor, at residence times ranging from 0 to 20 days. The kinetic data for *T. ferrooxidans* and pyrite were obtained from Boon (1996) and the kinetic data for the *Leptospirillum*-like bacterium was obtained from Van Scherpenzeel (1996). These predictions are compared with the results of Hansford and Chapman (1992) for the continuous bioleaching of a similar sized euhedral pyrite by an unidentified microbial species.

From Figure 7 it is apparent that the data of Hansford and Chapman (1992) follows the trend predicted by the model if the kinetic parameters for the *Leptospirillum*-like bacterium are assumed. Furthermore, the values of the predicted and experimental values are similar. Although the microbial species used by Hansford and Chapman (1992) was not identified, previous research (Lawson, private communication, 1997; Boon, 1996) suggests that the microorganism would have been *L. ferrooxidans*.

At this stage it is important to note that the kinetic parameters of the bacteria were determined at residence times of between 10 and 100 h, whereas the kinetic parameters of the pyrite were determined in batch culture. Furthermore, neither the bacterial species, nor the pyrite used to determine the kinetic parameters, were the same as those used by Hansford and Chapman (1992). In spite of this it appears that the model developed is able to predict the performance of a continuous bioleach reactor.

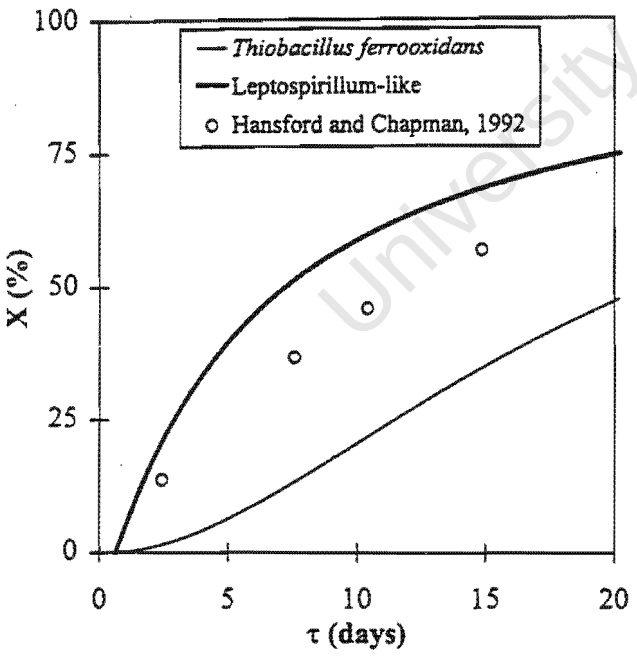

Figure 7. Comparison between the predicted variation in the pyrite conversion, X, with changing residence time, τ, for *T. ferrooxidans* and a *Leptospirillum*-like bacterium and the experimental results obtained by Hansford and Chapman (1992). Data were calculated from the results of Boon (1996) and Van Scherpenzeel (1996).

CONCLUSIONS

According to the two-step mechanism for the bioleaching of sulfide minerals it is possible to determine the kinetics of the chemical and bacterial processes independently and then use the derived kinetic constants of the respective subprocesses to predict the steady-state and dynamic performance of continuous bioleaching operations.

Furthermore, if the two-step mechanism is assumed to be valid, then, at steady-state, the chemical ferrous-iron production rate, $r_{Fe^{2+}}^{chem}$, is equal to the bacterial ferrous-iron consumption rate, $-r_{Fe^{2+}}^{bact}$. The point of intersection of the chemical and bacterial oxidation curves defines the pseudo-steady-state redox potential and ferric–ferrous-iron turnover, and can be stoichiometrically related to the rate of leaching of the mineral. It depends on the characteristics of the bacterial species used, the residence time employed, the characteristics of the mineral being used, and its active surface area.

The model used in this study proposes that the residence time determines the bacterial growth rate, which in turn determines the redox potential of the bioleaching solution. The redox potential in turn determines the degree of sulfide mineral leaching; that is, the mineral conversion. A change in the residence time and/or surface area of the mineral will result in a change in the solution redox potential, and hence the overall leaching rate of the mineral. A change in the mineral being leached may result in a change in the dominant ferrous-iron oxidizing bacterial species. Although the bacterial yield on ferrous-iron, $Y_{Fe^{2+}}$, is assumed to be constant in order to simplify the algebra, it may be incorporated by relating it to the prevailing residence time in the bioreactor, and the ferrous-iron maintenance requirement, via the Pirt equation, or a similar relationship.

Like previous models, this model does not consider the fate of the sulfur moiety of the mineral, although sulfur-oxidizing species have been detected during the bioleaching of mixed mineral concentrates (Rawlings and Gardner, unpublished results; Rawlings, 1995). The fate of sulfur species may be important in the bioleaching of base metals as sulfur products may result in passivation of the mineral surface. Sulfur-oxidizing bacteria should assist in the solubilization of this passivation layer.

Although this hypothesis has yet to be extensively tested and vigorously applied, the agreement of the data of Hansford and Chapman (1992) with the model for a continuous bioleach reactor and pyrite based on the two-step mechanism clearly demonstrates that the model developed has potential for predicting the performance of continuous bioleach reactors, and thus finding use in engineering and industrial applications.

NOMENCLATURE

B	kinetic constant in chemical ferric leaching (–)
C_s	concentration of growth-limiting substrate (mol/L)
c_X	concentration of bacteria (mol/L)
$c_{X,in}$	concentration of bacteria in feed (mol/L)
D	dilution rate (1/h)
E_0	redox potential of the solution at equilibrium (mV)
E_h	redox potential of the solution (mV)
E'_0	value of $E_0 + \frac{RT}{nF}\ln\left(\frac{\gamma_{Fe^{3+}}}{\gamma_{Fe^{2+}}}\right)$ (mV)
F	Faraday constant (C/mol)
$[Fe^{2+}]$	concentration of Fe^{2+} (mol/L)
$[Fe^{3+}]$	concentration of Fe^{3+} (mol/L)
$[FeS_2]_{in}$	concentration of FeS_2 in the feed (mol/L)
$[FeS_2]_{out}$	concentration of FeS_2 in the outlet (mol/L)
$[Fe_T]$	concentration of total iron (mol/L)
K	kinetic constant in bacterial ferrous-iron oxidation (–)
K_s	substrate saturation constant (mol/L)
n	number of electrons involved in a reaction (–)
Q	volumetric flow rate (L/h)
Q_{in}	volumetric flow rate into the bioreactor (L/h)
Q_{out}	volumetric flow rate out of the bioreactor (L/h)
$q_{Fe^{2+}}$	bacterial specific ferrous-iron oxidation rate (mol Fe^{2+}/mol C/h)
$q^{max}_{Fe^{2+}}$	maximum bacterial specific ferrous-iron oxidation rate (mol Fe^{2+}/mol C/h)
R	universal gas constant (kJ/mol/K)
$r^{bact}_{Fe^{2+}}$	bacterial ferrous-iron production rate (mol Fe^{2+}/L/h)
$r^{chem}_{Fe^{2+}}$	chemical ferrous-iron production rate (mol Fe^{2+}/L/h)
r_{FeS_2}	pyrite production rate (mol FeS_2/L/h)
r_X	bacterial production rate (mol C/L/h)
T	absolute temperature (K)
$Y_{Fe^{2+}/X}$	bacterial yield on ferrous-iron (mol C/mol Fe^{2+})
V	bioreactor volume (L)
X	fraction of mineral leached (–)

Greek letters

$\gamma_{Fe^{2+}}$	ferrous-iron activity coefficient (–)
$\gamma_{Fe^{3+}}$	ferric-iron activity coefficient (–)
μ	bacterial specific growth rate (1/h)
μ^{max}	maximum bacterial specific growth rate (1/h)
$\upsilon_{Fe^{2+}}$	pyrite-specific ferrous-iron production rate (mol Fe^{2+}/mol FeS_2/h)
$\upsilon^{max}_{Fe^{2+}}$	maximum pyrite specific ferrous-iron production rate (mol Fe^{2+}/mol FeS_2/h)
τ	residence time (h)

References

Boon M. 1996. Theoretical and experimental methods in the modelling of the bio-oxidation kinetics of sulphide minerals. PhD thesis. Delft University of Technology, Delft, The Netherlands.

Boon M, Hansford GS, Heijnen JJ. 1995. The role of bacterial ferrous iron oxidation in the bio-oxidation of pyrite. In: Vargas T, Jerez CA, Wiertz JV, Toledo H, editors. Biohydrometallurgical processing I. Santiago: University of Chile. p 153–163.

Braddock JF, Luong HV, Brown EJ. 1984. Growth kinetics of *Thiobacillus ferrooxidans* isolated from arsenic mine drainage. Appl Environ Microbiol 48:48–55.

Breed AW, Dempers CJN, Searby GE, Gardner MN, Rawlings DE, Hansford GS. In press. The effect of temperature on the continuous ferrous-iron oxidation kinetics of a predominantly *Leptospirillum ferrooxidans* culture.

Breed AW, Harrison STL, Hansford GS. 1997. A preliminary investigation of the ferric leaching of a pyrite/arsenopyrite flotation concentrate. Miner Eng 10:1023–1030.

Crundwell FK. 1994. Mathematical modelling of batch and continuous bacterial leaching. Chem Eng J 54:207–220.

Hansford GS. 1997. Recent developments in modelling the kinetics of bioleaching. In: Rawlings DE, editor. Biomining: Theory, microbes and industrial processes. Berlin: Springer. p 153–176.

Hansford GS, Chapman JT. 1992. Batch and continuous bio-oxidation kinetics of a refractory gold-bearing pyrite/arsenopyrite concentrate. Miner Eng 5:597–612.

Hansford GS, Drossou M. 1988. A propagating pore model for the batch bioleach kinetics of a gold-bearing pyrite. In: Norris PR, Kelly DP, editors. Proceedings of the International Symposium on Biohydrometallurgy. Science and Technology Letters Kew, Surrey, UK. p 345–358.

May N, Ralph DE, Hansford GS. 1997. Dynamic redox potential measurement for determining the ferric leach kinetics of pyrite. Miner Eng 10:1279–1290.

Miller DM, Hansford GS. 1992a. Batch bio-oxidation of a gold-bearing pyrite/arsenopyrite concentrate. Miner Eng 5:613–629.

Miller DM, Hansford GS. 1992b. The use of the logistic equation for modelling the performance of a bio-oxidation plant treating a gold-bearing pyrite-arsenopyrite concentrate. Miner Eng 5:737–749.

Nemati M, Harrison STL, Webb C, Hansford GS. 1998. Biological oxidation of ferrous sulphate b *Thiobacillus ferrooxidans:* a review on the kinetic aspects. Biochemical Engineering Journal 1:171–190.

Norris PR, Barr DW, Hinson D. 1988. Iron and mineral oxidation by acidophilic bacteria: affinities for iron and attachment to pyrite. In: Norris PR, Kelly DP, editors. Proceedings of the International Symposium on Biohydrometallurgy. Science and Technology Letters Kew, Surrey, UK. p 43–59.

Pinches A, Chapman JT, te Riele WAM, van Staden M. 1988. The performance of bacterial leach reactors for the pre-oxidation of refractory gold-bearing sulphide concentrates. In: Norris PR, Kelly DP, editors. Proceedings of the International Symposium on Biohydrometallurgy. Surrey, UK: Kew. p 329–344.

Rawlings DE. 1995. Restriction enzyme analysis of 16S rRNA genes for the rapid identification of *Thiobacillus ferrooxidans, Thiobacillus thiooxidans* and *Leptospirillum ferrooxidans* strains in leaching environments. In: Vargas T, Jerez CA, Wiertz JV, Toledo H, editors. Biohydrometallurgical processing I. Santiago: University of Chile. p 9–17.

Ruitenberg R, Hansford GS, Reuter MA, Breed AW. 1999. The ferric leaching kinetics of arsenopyrite. Hydrometallurgy 52(1):37–55.

Van Scherpenzeel DA. 1996. The kinetics of ferrous iron oxidation by *Leptospirillum*-like bacteria in absence and in presence of pyrite and pyrite/arsenopyrite mixtures in continuous and batch cultures. MSc dissertation, University of Cape Town, Cape Town, South Africa.

Conference Publications (Refereed)

THE BIOLEACHING OF A PYRITE-ARSENOPYRITE FLOTATION CONCENTRATE IN A CONTINUOUS BIOLEACHING MINI-PLANT. STEADY-STATE OPERATION AND BEHAVIOUR DURING PERIODS WITHOUT AERATION AND AGITATION

Ashley W Breed, Susan T L Harrison & Geoff S Hansford

Department of Chemical Engineering, University of Cape Town, RONDEBOSCH, 7700

Abstract - Steady-state operation of a continuous bioleaching mini-plant, at residence times ranging from 4 to 15 days, showed that the As(III) and Fe(II) levels in the primary bioreactor were higher than in the secondary bioreactor, at all residence times. On the other hand the As(V) and Fe(III) levels in the secondary bioreactor were higher than those in the primary bioreactor, at all residence times. Aeration and agitation perturbation studies showed that both the Fe(II) and As(III) concentrations increased in the absence of bacterial activity, and decreased on resumption of aeration and agitation.

These results are consistent with the hypothesis of chemical leaching of the arsenopyrite by Fe(III) followed by the oxidation of the As(III) by Fe(III) to As(V) and Fe(II), and the oxidation of Fe(II) and S(0), presumably by Thiobacilli, to Fe(III) and S(VI). Redox measurements were also consistent with this hypothesis.

INTRODUCTION

Bioleaching is now an established technology for the pre-treatment of refractory gold ores and concentrates. It offers potential economic, environmental and technical advantages over pressure oxidation and roasting. However, a potential complication in the bioleaching of minerals is the solubilisation of metals to concentrations toxic to the micro-organisms (Pol'kin *et al.*, 1975; Shrestha, 1988). Furthermore, the adaptation to provide resistance to one metal does not necessarily imply resistance to another metal.

The results of recent research suggests that the bioleaching of sulphide minerals occurs via a two-step mechanism (Boon *et al.*, 1995), *i.e.* the mineral is leached chemically by Fe(III) and the role of the bacteria is to regenerate Fe(III), thereby maintaining a high redox potential within the system.

The bioleaching of arsenical sulphides solubilises iron, arsenic and sulphur. The iron is solubilised as Fe(II), the arsenic as As(III) (Pol'kin *et al.*, 1975; Shrestha, 1988; Barrett *et al.*, 1989; Barrett *et al.*, 1993) and the sulphur as either S(VI) (Shrestha, 1988; Barrett *et al.*, 1993; Barrett & Hughes, 1993) or S(0) (Pol'kin *et al.*, 1975). The bacteria in the bioleaching slurry oxidise the dissolved Fe(II) to Fe(III) and the S(0) to S(VI) (Pol'kin *et al.*, 1975). It has been suggested that the As(III) is oxidised to As(V) by either oxygen (Panin *et al.*, 1985), Fe(III) (Shrestha, 1988), or by Fe(III) in the presence of both active bacteria and a pyrite (Barrett *et al.*, 1989; Barrett *et al.*, 1993) or chalcopyrite (Barrett *et al.*, 1993) surface. Excess dissolved As(V) and Fe(III) may precipitate as ferric arsenate.

The bioleaching of arsenopyrite, the oxidation of As(III) to As(V), and the precipitation of ferric arsenate are competing reactions, and are therefore influenced by the concentrations of As(III), As(V) and Fe(III) (Breed *et al.*, 1996). The availability of Fe(III) is in turn determined by the activity of the bacteria, which in turn depends on the availability of O_2.

High concentrations of dissolved arsenic inhibit bacterial growth (Pol'kin *et al.*, 1975; Shrestha, 1988; Barrett *et al.*, 1989). Furthermore, As(III) has been reported to inhibit a wide range of micro-organisms (Barrett *et al.*, 1989; Barrett *et al.*, 1993; Silver *et al.*, 1981), including *Thiobacillus ferrooxidans* (Pol'kin *et al.*, 1975; Collinet & Morin, 1990) and *Thiobacillus thiooxidans* (Collinet & Morin, 1990) to a greater degree than As(V).

Recent research has suggested that the mechanism of As(V) resistance in the (mesophilic) bacteria used in the bioleaching of sulphide minerals may be attributed to chromosomal mutations and an energy dependent efflux pump (Breed *et al.*, 1996). Although the oxidation of As(III) to As(V) has been suggested to be a resistance mechanism of bacteria towards As(III), none of the (mesophilic) bacteria used in bioleaching has been found to be capable of oxidising As(III) to As(V). Therefore, As(V) toxicity, and the relative toxicity of As(III) and As(V) to a mixed culture may be affected by the availability of an energy source, *viz.* O_2 and/or Fe(II).

The aim of this work was to determine whether the performance of a continuous bioleaching mini-plant was consistent with the hypothesis of indirect bioleaching, *viz.* the two-step mechanism, and to determine the effect of interruptions in the O_2 supply on the subsequent performance of the continuous bioleaching mini-plant.

MATERIALS AND METHODS

The bioleaching mini-plant consists of two, 23 ℓ, baffled, agitated, aerated bioreactors operating in series under controlled conditions of temperature, pH, dissolved oxygen concentration, solids concentration and nutrient supply. The bioreactors are fed from a 10 ℓ, baffled, agitated conditioning vessel, to which the nutrient solution and (dry) solid concentrate are added. The mixed culture consisted primarily of *Thiobacillus thiooxidans* and *Leptospirillum ferrooxidans* (Rawlings, 1995).

The temperature of the slurry in the bioreactors was controlled at 40°C. The pH was maintained between 1.6 and 1.8 by addition of 98% H_2SO_4 or 10M NaOH. A dissolved oxygen concentration in the region of saturation, *viz.* 6.5 mg.ℓ^{-1}, was ensured by using air flow rates in the region of 10 to 15 ℓ.min^{-1}. The solids concentration in the bioreactors was 200 g.ℓ^{-1} and the nutrient solution contained $(NH_4)_2SO_4$, K_2SO_4 and $(NH_4)_2HPO_4$. The pyrite-arsenopyrite flotation concentrate sample, from Fairview gold mine (Barberton, South Africa) contained 7.3% As, 25.7% S and 24.0% Fe. 86.35% of the material was finer than 75 micron. The mineral analysis of the concentrate, estimated from the elemental analysis, was 15.87% FeAsS and 41.04% FeS_2.

The performance of the bioleaching mini-plant was monitored by measuring the oxygen utilisation rate, r_{O_2}, of the bacterial culture, the variation in the concentrations and speciation of iron and arsenic, and the pH and redox potential of the slurry in each of the bioreactors.

The oxygen utilisation rate, r_{O_2}, of the bacterial culture in the bioreactors was measured off-line, in a sealed 1 ℓ vessel, using a Yellow Springs Instrument Model 5739 dissolved oxygen probe and a Hitech Micro Systems Dissolved Oxygen / Utilisation Rate Meter. The Fe(II) and As(III)

concentrations in solution were determined by titration with $Ce(SO_4)_2$. The total iron and arsenic concentrations in solution were determined by Atomic Adsorption Spectroscopy (AA). This enabled the Fe(III) and As(V) concentrations to be calculated by difference. The pH and redox potential of the slurry in the bioreactors was continuously monitored using Foxboro 871PH pH sensors and Foxboro 873pH/ORP Electrochemical Analysers.

RESULTS AND DISCUSSION

Steady-State Operation

The mini-plant was operated at residence times ranging from 4 days to 15 days, for periods ranging from 5 tank residence times, at plant residence times of 4, 8 and 15 days, to one plant residence time, at plant residence times of 4½, 5, 6 and 7 days.

The oxygen utilisation rate, r_{O_2}, of the bacterial culture in the primary and secondary bioreactors, at plant residence times of 15 and 4 days, is indicated in Table I. From Table I it is apparent that the conditioning vessel (feed) did not contain aerobic bacteria, and that the bacterial culture in the primary bioreactor was more active than the culture in the secondary bioreactor. Furthermore, it is evident that the r_{O_2} of the cultures in both bioreactors, indicating metabolic activity, increased with decreasing residence time.

Table I: Oxygen utilisation rate, r_{O_2}, of the bacterial culture in the primary and secondary bioreactors, at residence times of 15 and 4 days

Plant residence time (days)	r_{O_2} (moles.(ℓ.hr)$^{-1}$)		
	Conditioning vessel (feed)	Primary bioreactor	Secondary bioreactor
15	0	0.011	0.005
4	0	0.057	0.012

The above can be attributed to substrate depletion, *i.e.* at the residence times used in this investigation, most of the soluble nutrients are consumed by the bacteria in the primary bioreactor, and most of the easily oxidisable ore (*viz.* arsenopyrite) is leached in the primary bioreactor. This results in the culture in the secondary bacteria growing under substrate limiting conditions. However, the above limitations are reduced by a reduction in the overall residence time.

The average Fe(II) and As(III), and Fe(III) and As(V) concentrations in the conditioning vessel (feed) and the primary and secondary bioreactors at the different residence times are indicated in Figures 1 and 2, respectively. Statistical analysis (Kruskal-Wallis test; $p = 0.0005$) suggested that the steady-state concentrations of Fe(II), Fe(III) and As(V) in all vessels, and the As(III) concentration in the feed and secondary bioreactor varied with changes in the plant residence time. However, the As(III) concentration in the primary bioreactor did not appear to be a function of the plant residence time.

The absence of bacteria, acid or added Fe(III) in the feed resulted in low Fe(II), As(III), Fe(III) and As(V) concentrations in the conditioning vessel (see Figs. 1 and 2). The slight variation in the above concentrations can be attributed to the increased solubilisation of surface species as a result of the increased residence time.

From Figure 1 it is apparent that the Fe(II) concentration of the bioreactors was not significantly affected by the plant residence time, at residence times below 8 days. Furthermore, at a plant residence time of 15 days the Fe(II)

concentration in both the primary and secondary bioreactors was significantly lower than at a residence time of 8 days. The above is consistent with the r_{O_2} results listed in Table I. At a residence time of 15 days substrate depletion results in a reduced Fe(II) concentration in both the bioreactors while at short residence times (*viz.* τ_{plant} < 8 days) the increased bacterial activity results in a reduced Fe(II) concentration in both the bioreactors. This results in a (local) maximum Fe(II) concentration at intermediate residence times *viz.* 8 days. It is also apparent that the As(III) concentration in the secondary bioreactor increased slightly with increasing residence time, probably as a result of the increased overall degree of arsenopyrite leaching.

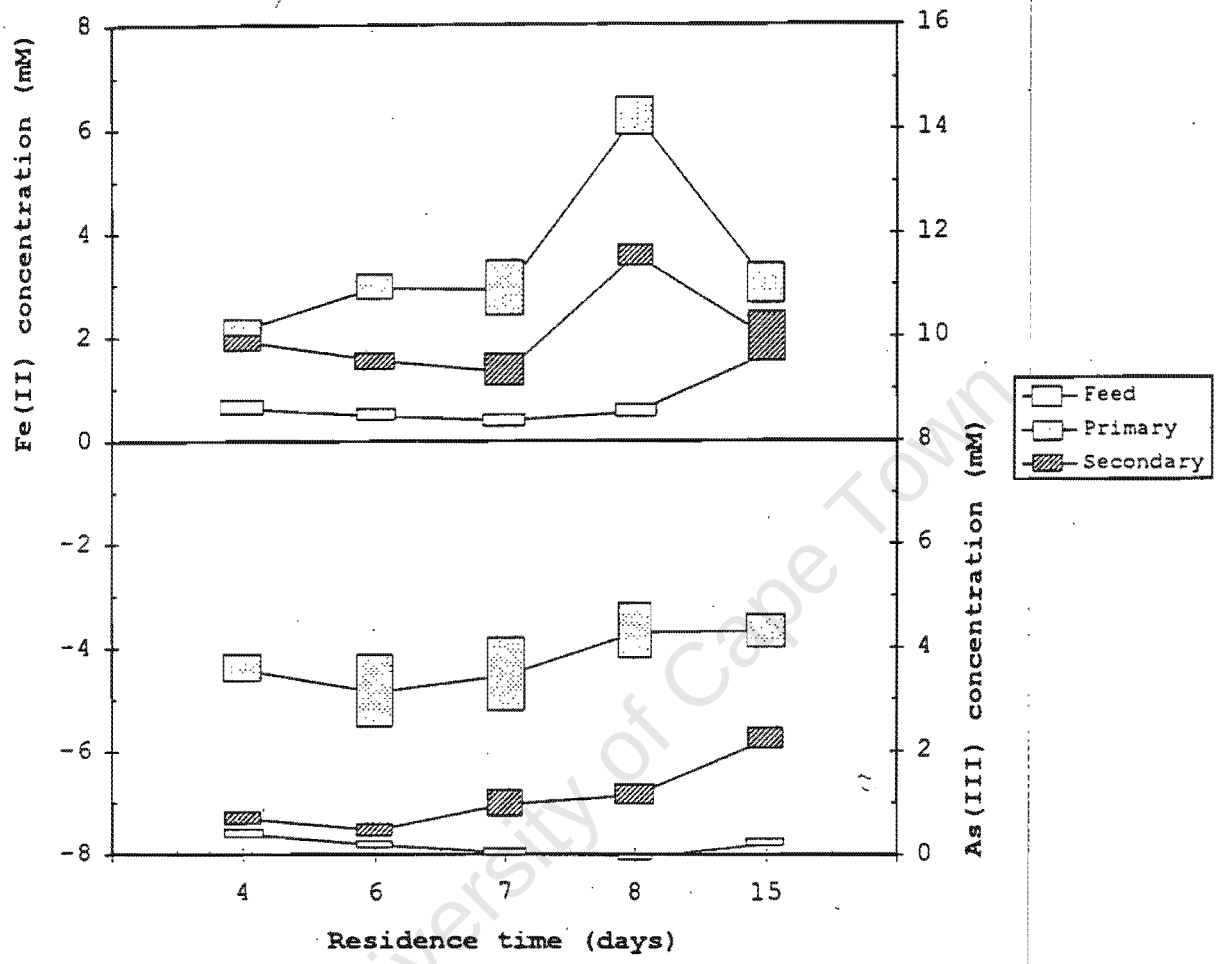

Figure 1: Fe(II) and As(III) concentrations in the conditioning vessel (feed) and the primary and secondary bioreactors as a function of the plant residence time (The box indicates: mean concentration - standard error; mean concentration + standard error)

Figure 2 shows that at residence times below 8 days, the Fe(III) and As(V) concentrations in both the primary and secondary bioreactors decreased slightly with decreasing residence time, probably as a result of the reduced overall degree of leaching. However, at a residence time of 15 days the Fe(III) and As(V) concentrations in both the primary and secondary bioreactors were significantly lower than at residence time of 8 days. This can be attributed to the precipitation of ferric arsenate, and suggests that the steady-state concentrations of Fe(III) and As(V) are determined by the kinetics of the precipitation reaction. Furthermore, the reduced availability of Fe(III) is responsible for the increased As(III) concentration apparent at a residence time of 15 days (see Figure 1).

The above is consistent with the postulate that the oxidation of arsenopyrite and As(III), by Fe(III), and the precipitation of ferric arsenate, are competing reactions and therefore depend on the relative concentrations of Fe(III), arsenopyrite, As(III) and As(V) (Breed *et al.*,

1996). Furthermore, Breed *et al.* (1996) suggested that the rate at which, and degree to which, precipitation occurs is a function of the absolute and relative amounts of Fe(III) and As(V) in the bioleaching slurry. The Fe(III) concentration is in turn determined by the activity of the bacteria.

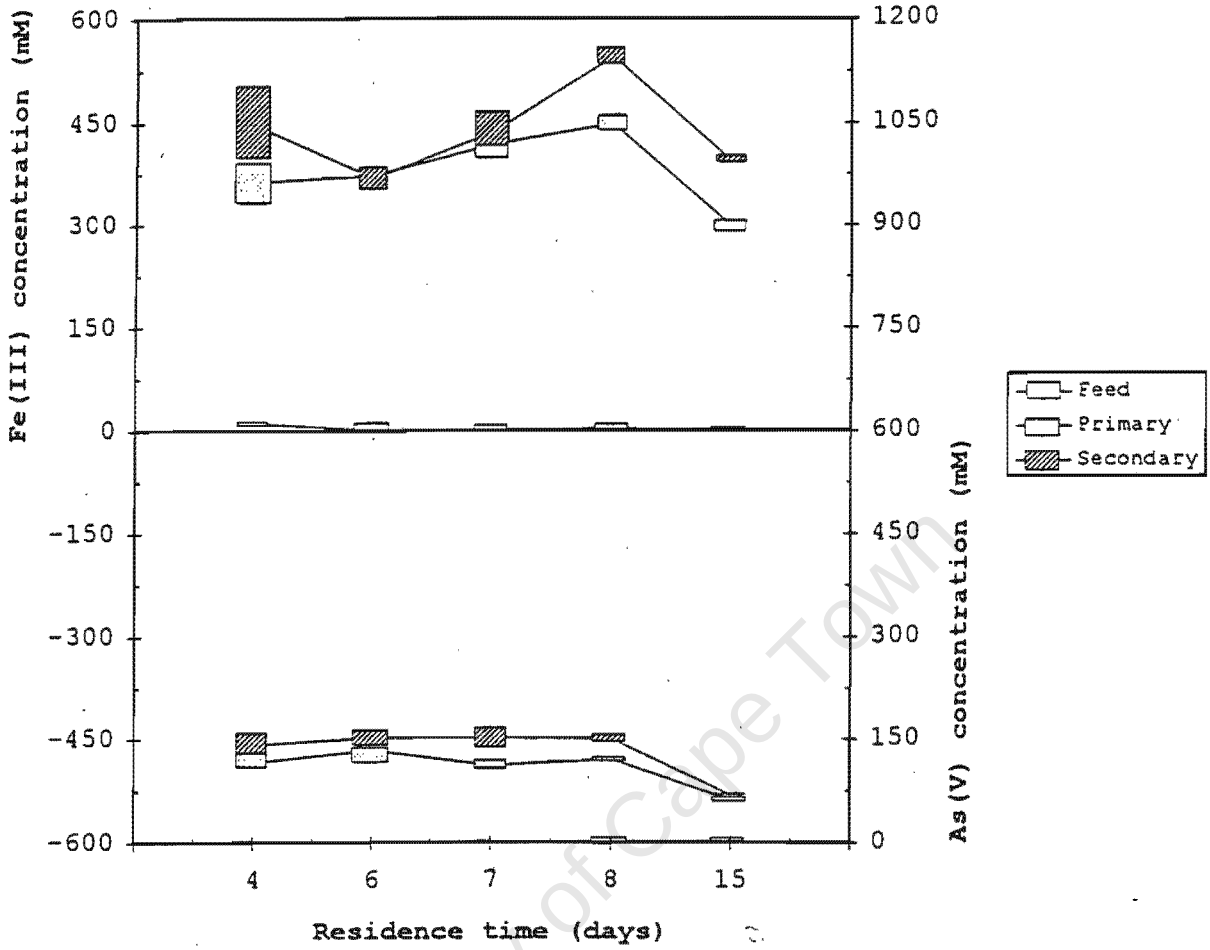

Figure 2: Fe(III) and As(V) concentrations in the conditioning vessel (feed) and the primary and secondary bioreactors as a function of the plant residence time (The box indicates: mean concentration - standard error; mean concentration + standard error)

It is apparent that the Fe(II) and As(III) concentrations were higher in the primary bioreactor than in the secondary bioreactor (Figure 1) and that the Fe(III) and As(V) concentrations were higher in the secondary bioreactor than in the primary bioreactor (Figure 2). Furthermore, comparison of Figures 1 and 2 shows that the Fe(III) and As(V) concentrations were significantly higher than the Fe(II) and As(III) concentrations, in both reactors. This suggests that the bioleaching of arsenopyrite solubilises iron and arsenic as Fe(II) and As(III), respectively. The Fe(II) and As(III) are subsequently oxidised to Fe(III) and As(V), respectively.

The above results are consistent with the hypothesis of indirect bioleaching; *viz.* the arsenopyrite is chemically leached by Fe(III), solubilising As(III), Fe(II) and S(0). This is followed by the oxidation of As(III) to As(V) by Fe(III), and the oxidation of Fe(II) and S(0), presumably by *Leptospirillum ferrooxidans* and *Thiobacillus thiooxidans*, respectively, to Fe(III) and S(VI). Therefore, the oxidation of arsenopyrite predominates in the primary reactor, whereas the oxidation of As(III) to As(V) predominates in the secondary bioreactor. Redox measurements (275 mV in the primary bioreactor; 280 mV in the secondary bioreactor) were also consistent with this hypothesis.

Perturbation Tests

The effect of loss of aeration and agitation on the performance of continuous bioleaching operations was studied. Two disruption tests were carried out at an overall plant residence time of 4 days. The first test consisted of a 15 minute interruption in the agitation and aeration of the secondary bioreactor and the second test consisted of a 17 hour interruption in the agitation and aeration of the primary bioreactor.

During the interruption, the feed to the respective bioreactor was stopped and the pH control disabled. The oxygen utilisation rate, r_{O_2}, was measured at varying intervals. It was anticipated that aerating a sample of the culture from the primary bioreactor during r_{O_2} measurement might affect the response of the bioreactor to the interruption. As only about 4.4% of the total slurry volume in the bioreactor was aerated, this effect was expected to be small.

Analysis of the results obtained during the perturbation test carried out using the secondary bioreactor suggested that short interruptions in the aeration and agitation of bioreactors used for the bioleaching of this concentrate did not have a significant effect on the bacterial activity (*i.e.* the oxygen utilisation rate, r_{O_2}) in the bioreactor. Furthermore, no significant variation in the Fe(II), As(III), Fe(III) or As(V) concentrations was observed during or after the perturbation (results not shown).

However, a 17 hour interruption in the agitation and aeration of the primary bioreactor had a significant effect on both the activity of the bacterial culture and on the concentrations of Fe(II) and As(III) observed in the primary bioreactor. The variation in the oxygen utilisation rate, r_{O_2}, and the Fe(II) and As(III) concentrations are shown in Figures 3 and 4, respectively.

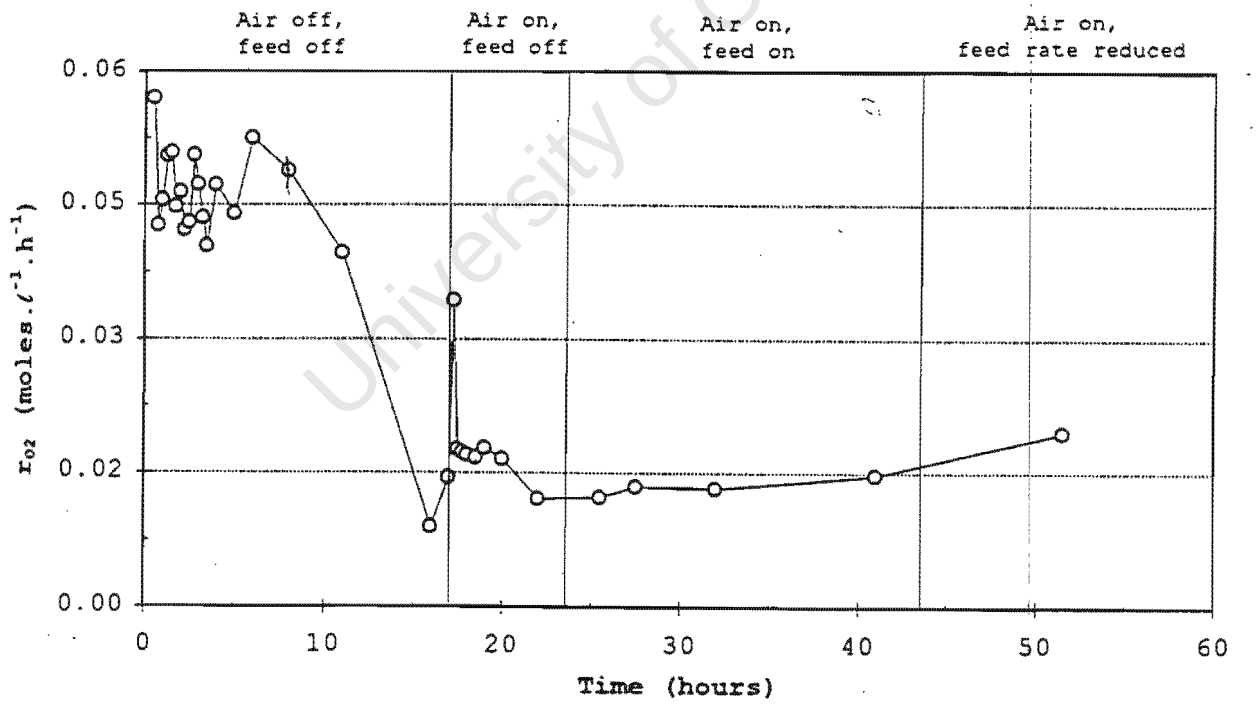

Figure 3: Variation in the oxygen utilisation rate, r_{O_2}, observed during the disruption test carried out using the primary bioreactor

From Figure 3 it is apparent that the potential oxygen utilisation rate, r_{O_2}, of the culture did not decrease significantly during the first 11 hours of the experiment. This may be a consequence of the intermittent sparging of 1 ℓ of

the culture. To avoid this possibility, the intervals between subsequent r_{O_2} measurements were increased. Furthermore, the erratic nature of the r_{O_2} measurements can be attributed to absence of agitation. However, 16 hours after the aeration and agitation of the culture in the primary bioreactor had been stopped, the r_{O_2} of the culture in the bioreactor had decreased from 0.0461 moles.ℓ^{-1}.hr^{-1} to 0.0145 moles.ℓ^{-1}.hr^{-1}.

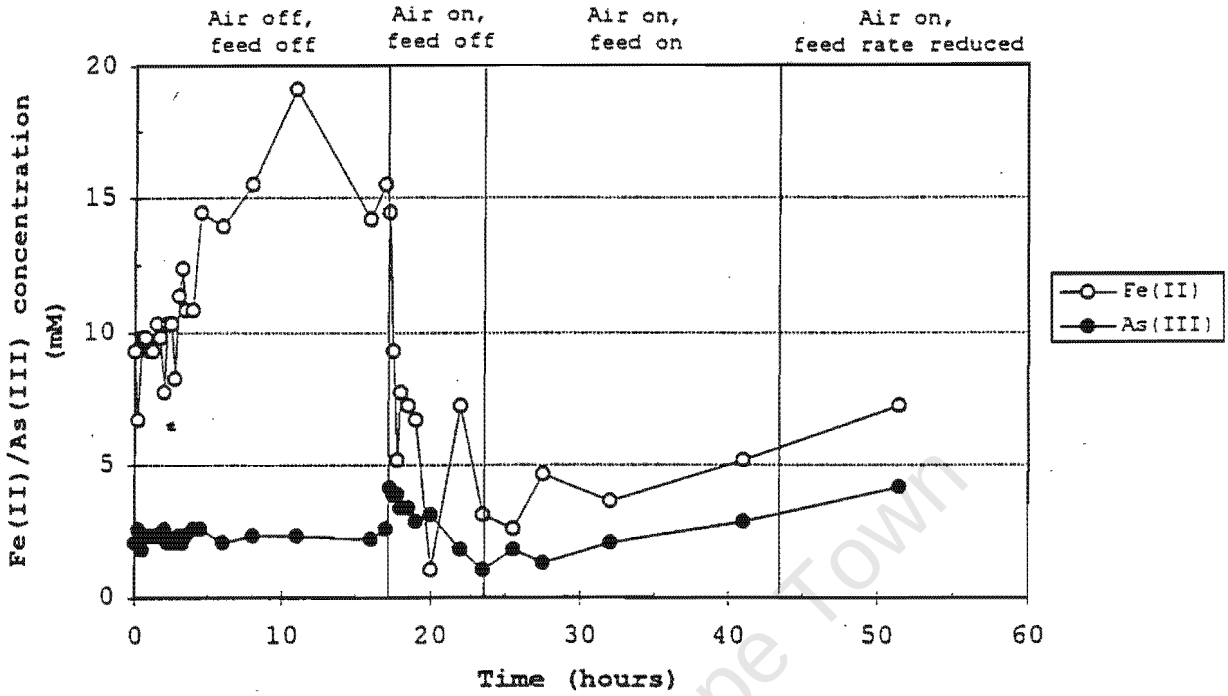

Figure 4: Variation in the Fe(II) and As(III) concentrations during the disruption test carried out using the primary bioreactor

The Fe(II) concentration in the primary bioreactor increased from 9.29 to 15.48 mM during the 17 hours in which the air was off (Figure 4). The increase in the Fe(II) concentration was not accompanied by an increase in the As(III) concentration, suggesting that this increase could be attributed to anaerobic ferric iron respiration (Pronk *et al.*, 1991). However, the rapid increase in the As(III) concentration, from 2.58 to 4.18 mM, once agitation was restored suggests that the As(III) produced by the chemical leaching of the arsenopyrite in the region of settled or settling solids, according to Eq. 1 (Iglesias *et al.*, 1993; Breed *et al.*, 1997), was masked by the absence of agitation:

$$FeAsS + 5Fe^{3+} \rightarrow S^{0} + As^{3+} + 6Fe^{2+} \quad (1)$$

The aeration and agitation of the culture in the primary bioreactor was resumed 17 hours after the initial interruption in the aeration and agitation. However, the feed to the primary bioreactor remained diverted.

From Figure 3 it is apparent that the oxygen utilisation rate, r_{O_2}, of the bacteria in the primary bioreactor increased rapidly once aeration and agitation of the slurry was restored. Comparison of Figures 3 and 4 show that the increase in the r_{O_2} was accompanied by a rapid decrease in the Fe(II) concentration. The above suggests that the Fe(II) was oxidised to Fe(III) by the bacterial culture, according to Eq. 2 (Boon *et al.*, 1994):

$$2Fe^{2+} + 0.5O_2 + 2H^{+} \rightarrow 2Fe^{3+} + H_2O \quad (2)$$

However, the culture did not maintain this level of activity. The r_{O_2} of the culture decreased gradually, until the feed stream to the primary bioreactor was restored (Figure 3). The reduction in the oxygen utilisation rate observed was attributed to arsenic toxicity or substrate depletion. Continuous

operation of the mini-plant, at a plant residence time in the region of 4 days was continued 6.5 hours after aeration and agitation had been restored. This resulted in a gradual increase in the r_{O_2} over the following 8.5 hours.

It is also apparent from Figure 4 that the As(III) concentration decreased once aeration and agitation of the slurry in the bioreactor was resumed, probably as a result of it being oxidised to As(V) by Fe(III), according to Eq. 3 (Mandl and Vyškovský, 1994):

$$As^{3+} + 2Fe^{3+} \rightarrow As^{5+} + 2Fe^{2+} \quad (3)$$

The above is consistent with the postulate of Breed *et al.* (1996), who suggested that the oxidation of arsenopyrite by Fe(III) and the oxidation of As(III) by Fe(III) are competing reactions, and are therefore influenced by the concentration and availability of Fe(III). The Fe(III) concentration is in turn determined by the activity of the bacteria. Furthermore, Breed *et al.* (1996) suggested that the oxidation of arsenopyrite predominates at "low" Fe(III) concentrations. Therefore, during periods of no bacterial activity the chemical leaching of arsenopyrite (Eq. 1) will be the dominant reaction. However, during periods of rapid bacterial oxidation, the abundance of Fe(III) in solution will result in the oxidation of both arsenopyrite (Eq. 1) and As(III) (Eq. 3) occurring.

Because the As(V) and Fe(III) concentrations in the primary bioreactor were approximately 30 and 160 times the As(III) and Fe(II) concentrations in the primary bioreactor, respectively, corresponding changes in the As(V) and Fe(III) concentrations were not observed. Furthermore, the precipitation of ferric arsenate may mask fluctuations in the As(V) and Fe(III) concentrations. The net result of the above was that the Fe(III) and As(V) concentrations did not vary significantly during the course of the experiment.

From Figure 4 it is apparent that once continuous operation of the mini-plant, at a plant residence time of 4 days, was begun, both the Fe(II) and As(III) concentrations increased, probably as a result of the increased availability of substrate and the low metabolic activity of the bacteria (in comparison with the bacterial activity observed at a plant residence time of 4 days during the steady-state investigation). Increasing the residence time to 6 days, at t = 43.5 hours, had no apparent affect on the above trends.

Unfortunately, 51 hours after aeration and agitation of the primary bioreactor had been stopped, problems were encountered with the solids feeder and continuous operation of the mini-plant was no longer possible. For this reason complete recovery was not observed.

CONCLUSIONS

The results of the steady state investigation suggest that substrate depletion is responsible for the bacterial culture in the primary bioreactor being more active than the culture in the secondary bioreactor, and in the oxygen utilisation rate, r_{O_2}, of the cultures in both bioreactors increasing with decreasing residence time.

Furthermore, the steady-state results showed that the As(III) and Fe(II) levels in the primary bioreactor were higher than in the secondary bioreactor and the As(V) and Fe(III) levels in the secondary bioreactor were higher than in the primary bioreactor. These results, and redox measurements, are consistent with the hypothesis of direct chemical leaching of the arsenopyrite by Fe(III) followed by the oxidation of the As(III) by Fe(III) to As(V) and Fe(II), and the oxidation of Fe(II) and S(0), presumably by Thiobacilli, to Fe(III) and S(VI).

In the perturbation studies both the Fe(II) and As(III) concentrations increased in the absence of bacterial activity, and decreased on resumption of aeration and agitation. These results are also consistent with the hypothesis that the bioleaching of arsenopyrite occurs via the indirect, or two-step, mechanism and with the postulate that the oxidation of arsenopyrite and As(III) and the precipitation of ferric arsenate compete for the available Fe(III).

It is also apparent that perturbations in the aeration and agitation of continuous bioleaching operations result in reduced bacterial activity during the perturbation. This reduced activity may persist once aeration and agitation of the bioreactors is restored. Furthermore, comparison of the above results with those of a previous investigation by Breed *et al.* (1996) suggest that the slow recovery of the mini-plant after perturbations in the air supply, may be the result of the bacteria being unable to protect themselves from the toxic effects of the As(III) and As(V), present during routine mini-plant operation, during periods in which they have no energy source. This may apply to a lack of either O_2 or Fe(II), or both.

In conclusion, it is important to note that despite a 17 hour disruption in the feed and air supply, and the agitation of the primary bioreactor, maximum feed rate to the mini-plant was attained within 7 hours of restoring aeration and agitation.

ACKNOWLEDGEMENTS

The authors would like to thank GENCOR for technical and financial support of the research and Professor T. Dunne of the Department of Statistical Sciences at the University of Cape Town for assistance with the statistical analysis.

REFERENCES

Bailey, A.D., 1993 - An assessment of oxygen availability, iron build-up and the relative significance of free and attached bacteria, as factors affecting bio-oxidation of refractory gold-bearing sulphides at high solids concentrations. PhD Thesis, Cape Town, South Africa: *University of Cape Town*.

Barrett, J., Ewart, D.K., Hughes, M.N., Nobar, A.M. & Poole, R.K., 1989 - The oxidation of arsenic in arsenopyrite: The toxicity of As(III) to a moderately thermophilic mixed culture. In Proc. Biohydrometallurgy 1989, Salley, J., McCready, R.G.L. & Wichlacz, P.L. (eds). Jackson Hole, USA: *Canmet*, 49-57.

Barrett, J., Ewart, D.K., Hughes, M.N. & Poole, R.K., 1993 - Chemical and biological pathways in the bacterial oxidation of arsenopyrite. *FEMS Microbiology Reviews* 11, 57-62.

Boon, M., Hansford, G.S. and Heijnen, J.J., 1993 - The role of bacterial ferrous iron oxidation in the bio-oxidation of pyrite. In Proc. Biohydrometallurgical Processing Volume 1. Vargas, T., Jerez., C.A., Wiertz, J.V. and Toledo, H.(eds). Santiago, Chile: *University of Chile*, 153-163.

Breed, A.W., Glatz, A., Harrison, S.T.L. and Hansford, G.S., 1996 - The effect of As(III) and As(V) on the batch bioleaching of a pyrite-arsenopyrite concentrate. *Minerals Engineering*, 9(12), 1235-1252.

Breed, A.W., Harrison, S.T.L. and Hansford, G.S., 1997 - A preliminary investigation of the ferric leaching of a pyrite/arsenopyrite concentrate. Technical note submitted to *Minerals Engineering*.

Collinet, M-N & Morin, D., 1990 - Characterisation of arsenopyrite oxidising *Thiobacillus*. Tolerance to arsenite, arsenate, ferrous and ferric iron. *Antonie van* Leeuwenhoek 57, 237-244.

Iglesias, N., Palencia, I & Carranza, F., 1993 - Removal of the refractoriness of a gold bearing pyrite-arsenopyrite ore by ferric sulphate leaching at low concentration. In Proc. EPD Congress 1993, Hager, J.P.(ed). Warrendale, USA: *The Minerals, Metals & Materials Society*, 99-115.

Mandl, M. and Vyškovský, M., 1994 - Kinetics of arsenic(III) oxidation by iron(III) catalysed by pyrite in the presence of *Thiobacillus ferrooxidans*. *Biotechnology Letters*, 16(11), 1199-1204.

Panin, V.V., Karavaiko, G.I. & Pol'kin, S.I., 1985 - Mechanism and kinetics of bacterial oxidation of sulphide minerals. In Biotechnology of Metals, Karavaiko, G.I. & Groudev, S.N. (eds). Moscow, USSR: *Centre of International Projects*, 197-215.

Pol'kin, S.I., Panin, V.V., Adamov, E.V., Karavaiko, G.I. & Chernyak, A.S., 1975 - Theory and practice of utilizing microorganisms in difficult-to-dress ores and concentrates. In Proc. Eleventh International Mineral Processing Congress. Cagliari, Italy: *Regione Autonoma Della Sardegna*, 901-923.

Pronk, J.T., Liem, K., Bos, P. & Kuenen, J.G., 1991 - Anaerobic growth of *Thiobacillus ferrooxidans*. *Applied and Environmental Microbiology* 58(7), 2227-2230.

Rawlings, D.E., 1995 - Restriction enzyme analysis of 16S rDNA genes for the rapid identification of *Thiobacillus ferrooxidans*, *Thiobacillus thiooxidans* and *Leptospirillum ferrooxidans* strains in leaching environments. In Proc. Biohydrometallurgical Processing Volume 1, Vargas, T., Jerez., C.A., Wiertz, J.V. and Toledo, H.(eds). Santiago, Chile: *University of Chile*, 9-17.

Shrestha, G.N., 1988 - Microbial leaching of refractory gold ores. *Australian Mining* October, 48-57.

Silver, S., Budd, K., Leahy, K.M., Shaw, W.V., Hammond, D., Novick, R.P., Willsky, G.R., Malamy, M.H. & Rosenberr, H., 1981 - Inducible plasmid-determined resistance to arsenate, arsenite and antimony(III) in *Escherichia coli* and *Staphylococcus aureus*. *Journal of Bacteriology* 146(3), 983-996.

Wallis, W.A. & Roberts, H.V., 1963 - Statistics: A new approach. New York, USA: *The Free Press of Glencoe Inc.*.

BREED, A.W., DEMPERS, C.J.N., and HANSFORD, G.S. Studies on the bioleaching of refractory gold concentrates. *Extraction Metallurgy 1999*. Johannesburg, South African Institute of Mining and Metallurgy, 1999.

Studies on the bioleaching of refractory gold concentrates

A.W. BREED, C.J.N. DEMPERS, and G.S. HANSFORD
Gold Fields Minerals Bioprocessing Laboratory, Department of Chemical Engineering, University of Cape Town

The bioleaching of arsenopyrite, the oxidation of arsenate and the precipitation of ferric arsenate are competing reactions, hence their rates depend on the relative concentrations of the respective species, and the activity of the bacterial culture. Arsenic resistance may be attributed to the Pst+Pit- mutation and an energy dependent efflux pump. Pst+Pit- mutations result in a reduced uptake of arsenate. This enables the bacteria to survive in solutions in which the arsenate concentration is significantly higher than the arsenite concentration. However, the excretion of arsenate requires energy. Therefore, in the absence of an energy source or during periods of reduced bacterial activity, the inhibitory effect of arsenate may manifest at concentrations to which the culture has been adapted.

The chemical ferric leaching rate of pyrite and arsenopyrite decreases with a decrease in the solution redox and may be described using a modified Butler-Volmer equation. The bacterial ferrous-iron oxidation kinetics of *L. ferrooxidans* also depend on the redox potential, and can be described using a Michaelis-Menten type model modified to account for both temperature and pH.

During steady-state bioleaching the rate of iron turnover between the chemical ferric leaching of the mineral and the bacterial oxidation of the ferrous-iron will define the rate and the redox potential at which the system will operate. A model developed using the independently determined ferric leaching, and ferrous-iron oxidizing kinetics, has been shown to compare well with the experimental data for the continuous bioleaching of pyrite.

Keywords: *Leptospirillum ferrooxidans*, arsenopyrite, bioleaching, sulphide minerals ferrous-iron oxidation kinetics, ferric leaching kinetics, redox potential.

Introduction

Bioleaching is now an established technology for the pre-treatment of refractory gold ores and concentrates and the leaching of whole-ore copper heaps. In many cases, it offers economic, environmental and technical advantages over pressure oxidation and roasting[1,2]. However, in order for bioleaching to compete successfully with other pre-treatment processes it needs to be optimized with regard to the parameters that affect the process. Furthermore, there is a need for mechanistically based kinetic models that can be used to derive performance equations for use in the design, optimization and control of bioleaching processes.

The modelling of bioleach reactors is complicated by difficulties encountered when attempting to measure the biomass concentration and growth rate in the presence of solids, and the ferric and ferrous-iron concentrations. This has resulted in the logistic equation being the rate expression that has found the most widespread application to date. Although not mechanistically based the logistic equation[3] has proved useful in modelling batch, continuous pilot and full-scale plant data for several pyrite and pyrite-arsenopyrite flotation concentrates[4-9].

Recent research has provided strong evidence that the bioleaching of sulphide minerals occurs via a multiple sub-process mechanism[10]. By staged additions of pyrite to a batch bioleach, these workers were able to measure the specific oxygen utilization rate as a function of the ferric/ferrous-iron ratio or redox potential. The oxygen utilization rate was also related to the pyrite concentration via the pyrite specific oxygen utilization rate. The results showed that the bacterial specific rate of oxygen utilization decreased with increasing ferric/ferrous-iron ratio while the pyrite specific oxygen utilization rate increased with increasing ferric/ferrous-iron ratio.

In addition, samples were taken from the batch, the pyrite removed by centrifugation, and the specific oxygen utilization rate of the bacteria measured in an off-line respirometer, using ferrous-iron medium. This enabled the specific oxygen utilization rate to be measured over a wider range of ferric/ferrous-iron ratios than in the pyrite batch. However, in the region where the ranges overlapped, the data for the pyrite- and ferrous iron-grown bacteria coincided. From this it was concluded that in both cases ferrous-iron was the primary substrate, and that the bioleaching of pyrite occurs via a multiple sub-process mechanism. Therefore, for the case of pyrite bioleaching the primary role of the bacteria is the oxidation of the ferrous-iron to the ferric form, thereby maintaining a high redox potential within the system and ensuring the continued leaching of the mineral.

This mechanism suggests that the overall process can be reduced to a number of independent sequential and/or parallel sub-processes. The kinetics of these sub-processes may be studied separately, and the results used to predict the performance of bioleach reactors for a variety of operating conditions.

The existence of a multiple sub-process mechanism for the bioleaching of sulphide minerals is supported by;

- the identification of *Leptospirillum ferrooxidans* as the dominant ferrous-iron oxidizing species in a continuous bioleaching mini-plant oxidizing an arsenopyrite/pyrite flotation[11], and
- the identification of *L. ferrooxidans* and *Thiobacillus caldus* in continuous flow bioleaching oxidation tanks used to treat a variety of metal containing ores and concentrates[12].

According to this mechanism the sulphide mineral is chemically oxidized by ferric-iron *i.e.*:

$$FeS_2 + 14Fe^{3+} + 8H_2O \rightarrow 15Fe^{2+} + 2SO_4^{2-} + 16H^{+}\ ^{13} \qquad [1]$$

$$FeAsS + 5Fe^{3+} \rightarrow As^{3+} + 6Fe^{2+} + S^{o}\ ^{14-16} \qquad [2]$$

The ferrous-iron produced by these reactions is subsequently oxidized to ferric-iron by the micro-organizms.

$$4Fe^{2+} + O_2 + 4H^{+} \rightarrow 4Fe^{3+} + 2H_2O\ ^{17} \qquad [3]$$

Polysulphides and sulphur or thiosulphate produced by the ferric leaching reactions are oxidized to sulphate by sulphur oxidizing micro-organizms[18]. Diagrammatic representations of the bioleaching of both pyrite and arsenopyrite are shown in Figure 1.

The bioleaching of arsenopyrite

From Equation [2] it is clear that the bioleaching of arsenopyrite solubilizes the arsenic as arsenite and iron, As^{3+}, and ferrous-iron, Fe^{2+}, respectively. Depending on the conditions employed, the dissolution of arsenopyrite may be followed by the oxidation of arsenite to arsenate, As^{5+}, according to;

$$H_3AsO_3 + 2Fe^{3+} + H_2O \rightarrow H_3AsO_4 + 2Fe^{2+} + 2H^{+}\ ^{20} \qquad [4]$$

The oxidation of arsenite to arsenate may in turn be followed by the precipitation of ferric arsenate, according to:

$$2H_3AsO_4 + Fe_2(SO_4)_3 \rightarrow 2FeAsO_4 + 3H_2SO_4\ ^{9} \qquad [5]$$

High concentrations of dissolved arsenic have been shown to inhibit bacteria[20–23]. Therefore, the relative rates at which the reactions shown in Equations [2], [4] and [5] occur may influence the activity of the bacterial culture, and hence the rate of bioleaching. Recent work has shown that the reactions shown in Equations [2], [4] and [5] are competing reactions, and are influenced by the concentrations of arsenite, arsenate, ferric-iron and arsenopyrite. Furthermore, the oxidation of arsenite to arsenate requires the presence of a mineral less noble than arsenopyrite[24].

At low ferric-iron concentrations (viz. prior to rapid bacterial activity) and low arsenite concentrations, the chemical leaching of arsenopyrite (Equation 2) is the dominant reaction. At low ferric-iron concentrations and high arsenite concentrations, the abundance of arsenite in solution causes the oxidation of arsenite (Equation 5) to dominate. However, at high ferric-iron concentrations (i.e. during periods of rapid bacterial growth), there is sufficient ferric-iron in solution to oxidize both the arsenopyrite and the dissolved arsenite. This results in the low arsenite and high arsenate concentrations observed during continuous bioleaching operations[25].

Arsenite has been reported to inhibit a wide range of microorganizms[23,26–29], including *Thiobacillus ferrooxidans* [21,30–31], *T. thiooxidans*[30], and the mixed culture used in BIOX® operations to a greater degree than arsenate[32]. Arsenite inactivates enzymes with thiol (HS) groups at the active centre[33]. Arsenate toxicity is caused by its similarity to phosphate[29,33]; arsenate replaces the phosphate in ATP to form an unstable ADP-arsenate complex[33].

The two main forms of arsenic resistance in bacteria are chromosomal arsenate resistance and plasmid determined arsenic resistance[33–36]. Chromosomal arsenate resistance reduces the amount of arsenate entering the cell via the phosphate transport system[33,35–37]. The Pst phosphate transport system is specific to phosphate, while the Pit system will transport either phosphate or arsenate[33,37,38], hence chromosomal arsenate resistance occurs with the $Pst^{+}Pit^{-}$ mutation[26,33,35,38].

Plasmid-encoded resistance protects bacteria by pumping arsenic from the cells via an energy dependent membrane pump[29,33,35,36,39,40]. In bacteria which exhibit this type of resistance, plasmids encode proteins which form a membrane-bound complex, and interact to form an arsenite pump[41–43]. In some species, the membrane-bound complex is able to reduce arsenate to arsenite, which results in resistance to both arsenate and arsenite. A diagrammatic representation of the phosphate (arsenate) transport system

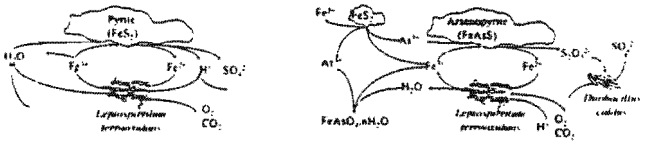

Figure 1. Diagrammatic representation of the bioleaching of pyrite and arsenopyrite via the two-step mechanism. The bacteria shown are planktonic (i.e., unattached) for reasons of clarity; however, the mechanism is the same for both attached and unattached microorganisms (after Breed *et al.*[19])

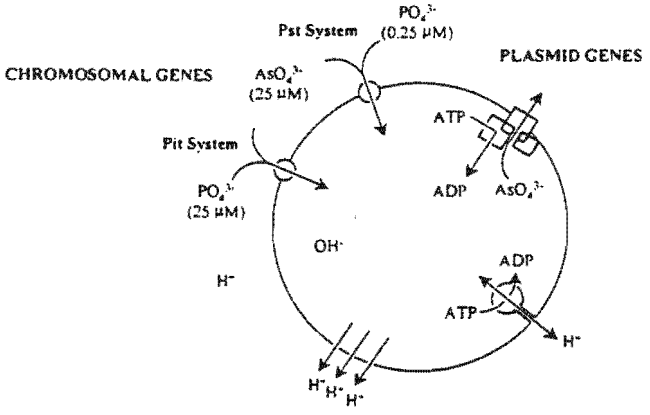

Figure 2. Model for phosphate (arsenate) transport systems and the arsenate efflux system of *Escherichia coli*. 0.25 and 25 μM, are the K_m for PO_4^{3-} and AsO_4^{3-} as a competitor for the Pit and Pst chromosomal transport systems. The three boxes for the plasmid arsenic ATPase represent the ArsA, ArsB and ArsC polypeptides (modified from Silver and Nakahara[35], Silver and Misra[41]) (after Breed[24])

and the arsenate efflux system of Escherichia coli is shown in Figure 2.

Most researchers have reported that elevated arsenite concentrations result in an extended lag phase after which normal growth occurs[21,23,30,31], whereas elevated arsenate levels cause a reduction in the maximum growth capacity[28]. However, during the batch bioleaching of an arsenopyrite/pyrite concentrate, exposure to elevated arsenite concentrations did not result in an increase in the lag phase, whereas exposure to elevated arsenate concentrations resulted in a significant increase in the lag phase[44]. The results obtained by Breed *et al.*[44] are shown in Figure 3.

From Figure 3 it is apparent that exposure to an initial concentration of 20 mmol $As^{3+}.\ell^{-1}$ retarded the initial rate of bacterial metabolism. This effect was more pronounced when 40 mmol $As^{3+}.\ell^{-1}$ was added. The culture exposed to an initial concentration of 20 mmol $As^{3+}.\ell^{-1}$ appeared to recover from the effect of the added arsenic whereas the culture exposed to an initial concentration of 40 mmol $As^{3+}.\ell^{-1}$ did not achieve an equivalent maximum oxygen utilization rate (data not snown) and showed a lower cumulative oxygen usage.

Exposure to an initial concentration of 107 mmol $As^{5+}.\ell^{-1}$ to the increased the lag phase by 15 days and retarded the initial rate of bacterial metabolism. Furthermore, the culture did not appear to recover from the effect of the added arsenate over the 31-day period studied. The addition of 220 mmol $As^{5+}.\ell^{-1}$ to the nutrient solution prior to inoculation resulted in a lag phase which lasted in excess of 31 days; the bacteria exposed to an initial concentration of 220 mmol $As^{5+}.\ell^{-1}$ did not consume any oxygen for the duration of the experiment.

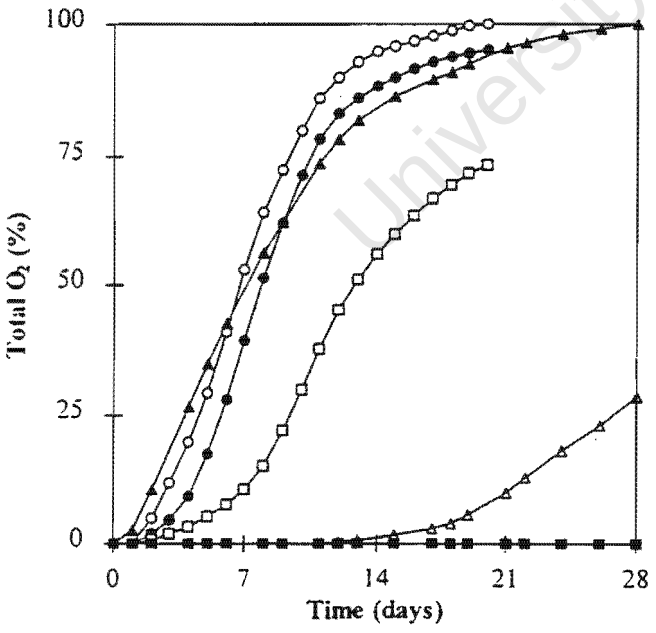

Figure 3. Variation in the cumulative amount of oxygen consumed by the bacterial culture with time at different initial arsenite and arsenate concentrations. [o] 0 mmol $As^{3+}.\ell^{-1}$; [●] 20 mmol $As^{3+}.\ell^{-1}$; [□] 40 mmol $As^{3+}.\ell^{-1}$; (▲) 0 0 mmol $As^{5+}.\ell^{-1}$; (△) 107 mmol $As^{5+}.\ell^{-1}$; (■) 0.220 mmol $As^{5+}.\ell^{-1}$ (after Breed *et al.*[44])

The rate at which oxygen is utilized by the bacteria is a function of both the bacterial concentration and their activity, i.e.

$$r_{O_2} = q_{O_2} c_x \qquad [6]$$

The specific oxygen utilization rate, q_{O_2}, can be described using an equation of the form[10]:

$$q_{O_2} = \frac{q_{O_2}^{max}}{1 + K_{O_2}\frac{[Fe^{3+}]}{[Fe^{2+}]}} \; 10 \qquad [7]$$

Hence, it was not possible to ascertain whether the arsenic species inhibit bacterial oxidation (i.e. they affect $q_{O_2}^{max}$ or are toxic to the bacteria (i.e. they affect c_X).

Although concentrations of up to 145 mmol $As^{3+}.\ell^{-1}$ have been reported in actively growing cultures accustomed to high arsenite concentrations[45], several researchers have found arsenite to be toxic at concentrations similar to those shown in Figure 3[21,23]. Furthermore, although some researchers have suggested that arsenite is in the region of 2 to 3 times more toxic than arsenate[21,23], Figure 3 shows that exposure to 107 mmol $As^{5+}.\ell^{-1}$ had a far more pronounced effect than 40 mmol $As^{3+}.\ell^{-1}$. It should, however, be noted that most researchers have performed toxicity experiments in ferrous-iron media, or in slurries supplemented with ferrous-iron. Because ferrous-iron is the most easily used source of energy for iron-oxidizing bacteria, and because the extent of arsenic inhibition is less pronounced if the substrate is a sulphide mineral[46,47], the conditions used may have influenced their results.

It is also important to note that the levels of arsenite shown in Figure 3 were in the region of 10 times those observed in the mini-plant from which the inoculii were obtained[25]*, yet where an inhibitory effect was observed the bacterial culture exhibited the ability to recover. However, the levels of arsenate added to the bioreactors were similar to those observed in the mini-plant, yet the effect of the added arsenate was severe. This result, together with the hypothesis that the ferric leaching of arsenopyrite, the ferric oxidation of arsenite and the precipitation of ferric arsenate are competing reactions, suggest that the inhibitory effect of arsenate may be linked to the availability of an energy source. At elevated arsenate concentrations the precipitation of ferric arsenate results in no ferric-iron being available for the leaching of the mineral. This results in a reduced availability of ferrous-iron, which in turn results in the inhibitory effect of arsenate becoming apparent at arsenate concentrations to which the culture has been adapted.

The above suggestion is consistent with the results of perturbation studies performed using the continuous bioleaching mini-plant from which the cultures used in the experiments shown in Figure 3, were obtained. Two disruption tests were carried out. The first discription test consisted of a 15 minute interruption in the agitation and aeration of the bacterial culture in the secondary bioreactor. This did not have an effect on either the short-term (or long-term) activity and viability of the culture (data not shown).

*The same concentrate as used in the mini-plant was used in the batch bioleaching experiments shown in Figure 3.

However, a 17-hour interruption in the agitation and aeration of the culture in the primary bioreactor resulted in a reduced level of bacterial activity that persisted once aeration and agitation had been restored. The variation in the measured oxygen utilization rate, $-r_{O_2}$, for the duration of the perturbation study performed using the primary bioreactor is shown in Figure 4. It is apparent from Figure 4 that the $-r_{O_2}$ decreased during the period in which aeration and agitation of the culture was stopped and increased on resumption of aeration and agitation. However, the $-r_{O_2}$ of the culture did not reach the same level of bacterial activity after the restoration of aeration and agitation.

During both the short and long interruptions in the aeration and agitation of the bioreactor, the ferrous-iron and arsenite concentrations increased in the absence of bacterial activity, and decreased once aeration and agitation had been restored. However, the concentrations of these species did not reach greater concentrations than observed during the lag phase of the batch culture to which no arsenic was added (data not shown). Furthermore, the arsenate and ferric-iron concentrations did not increase, relative to their steady-state concentrations, during the course of the experiment[25]. Therefore, the reduced level of bacterial activity after the restoration of aeration and agitation could not be attributed to 'elevated' arsenic concentrations. This in turn suggests that the inhibitory effect must be attributable to the arsenic concentration and speciation present during steady-state operation†.

Therefore, the results shown in Figures 3 and 4, together with those of previous research suggest that the mechanism of arsenic resistance in the (mesophilic) bacteria used in the bioleaching of sulphide minerals may be attributed to Pst^+ Pit^- mutations and an energy dependent efflux pump. The Pst^+Pit^- mutations result in a reduced uptake of arsenate which enables the bacteria to survive in solutions in which the dissolved arsenate concentration is significantly higher than the dissolved arsenite concentration. However, the excretion of arsenate which enters the cell, presumably via the phosphate uptake system, requires energy. Therefore, in the absence of an energy source, e.g. ferrous-iron and/or O_2, or during periods of reduced bacterial activity, the inhibitory effect of arsenate may manifest at arsenate concentrations to which the culture has been adapted.

The above results are important if one considers that during commercial bioleaching operations disruptions in the aeration and agitation of the bioreactors may occur as a result of power failures or breakdowns. These perturbations will result in a reduced level of bacterial activity during the interruption, and may have a long-term effect on the viability of the bacterial culture, which in turn may result in a significant loss in production.

The ferric leaching of arsenopyrite

To date a number of models have been used to describe the ferric leaching kinetics of sulphide minerals[48-51]. The simplest model assumes a linear relationship between the redox potential of the solution and the mineral rest potential[49]. Other postulated models include those based on electrochemical theory[48,51] and on the Monod Equation[50].

Although considerable work on the leaching of pyrite using ferric-iron has been reported in the literature[13,51-53], to date very little work on the leaching of arsenopyrite, using ferric-iron at concentrations and conditions similar to those used in bioleaching, has been reported. However, recent research has shown that the ferric leaching kinetics of pyrite[50,51] and arsenopyrite (Breed *et al.* 1997) may be dependent on the ferric/ferrous-iron ratio (i.e. redox potential), and not a function of the total or ferric iron concentrations.

Boon[50] suggested that the ferric leaching of pyrite could be described by means of Monod-type Equation, viz.:

$$\upsilon_{Fe^{2+}} = \frac{\upsilon_{Fe^{2+}}^{max}}{1 + B\dfrac{[Fe^{2+}]}{[Fe^{3+}]}} \qquad [8]$$

However, May *et al.*[51] suggested that the ferric leaching of pyrite was an electrochemical (corrosion) phenomenon, and hence chose to use an equation similar in form to the Butler-Volmer equation to describe the leaching rate, viz.:

$$-r_{Fe^{2+}}^{chem} = r_o\left(e^{\alpha\beta(E-E^*)} - e^{(1-\alpha)\beta(E-E^*)}\right) \qquad [9]$$

The leach rates of the pyrite were calculated using the measured variation in the redox potential and the initial total iron concentration. According to the Butler-Volmer equation the dependence of the ferric leaching kinetics on the overpotential is linear at low overpotentials (0-20 mV). However, most bioleaching plants operate at higher overpotentials, which result in non-linear kinetics. In

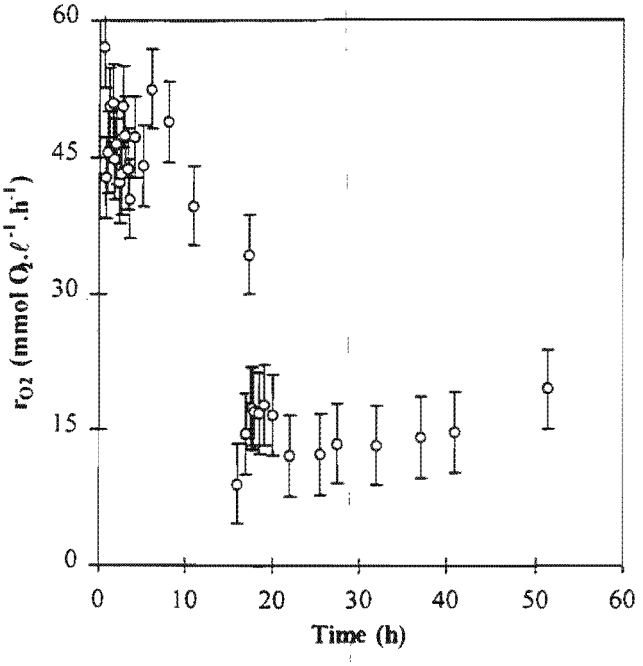

Figure 4. Variation in the oxygen utilization rate during the disruption test carried out using the primary bioreactor. The error bars represent the measured $-r_{O_2}$ ± the average variation in $-r_{O_2}$ measured during steady-state operation, at τ = 4 days (after Breed *et al.*[25])

†As the feed to the bioreactor was diverted during, and immediately after, the perturbation, the reduced level of bacterial activity could not be attributed to washout. In addition, the residence time chosen once continuous operation was begun, i.e. after the perturbation, was varied to ensure that the bacteria were neither substrate limited, nor 'washed out' of the bioreactor.

addition, May *et al.*[51] showed it was possible to achieve leaching rates in sterile media which were comparable with those achieved in bioleaching, provided that the redox potential was comparable with those observed in bioleaching.

The variation in the ferric leaching rate of arsenopyrite with changes in the solution redox potential displays the same trend, irrespective of the experimental conditions employed[54].

In the experiments performed by Ruitenberg *et al.*[54] the ferric leaching rate of arsenopyrite initially increased with a decrease in the redox potential, reached a maximum, and then decreased with a further decrease in the redox potential. An increase in the initial ferric leaching rate with decreasing redox potential was also observed during the ferric leaching of pyrite[51]. It is therefore suggested that this is a transient phenomenon, and can be attributed to the rearrangement of the ions on the surface of the mineral and in the electrical double layer surrounding the mineral. It is not a result of the leaching of the mineral itself. This postulate is supported by the fact that the process was very rapid‡ and by observations made during studies on the effect of the ferric-iron concentration on the electrophoretic mobility of arsenopyrite[55]. Furthermore, no surface products responsible for passivation of the mineral surface were observed, nor was a decrease in reactivity observed when mineral that had been leached previously was leached for a second time. Although previous workers have detected a sulphur layer on the mineral surface after both the acid, and the ferric leaching of arsenopyrite, it has not been found to hinder the dissolution reaction[14,56–58]. The absence of a surface layer in this investigation may be a result of the high redox potentials used.

The decrease in the rate of leaching with a decrease in the redox potential of the solution observed for most of the experiment is in agreement with previously reported trends for the ferric leaching of sulphide minerals[51,59–61]. This suggests a dependency of the ferric leaching rate on the redox potential of the leaching solution, which in turn suggests that an electrochemical model be used to describe the ferric leaching kinetics of arsenopyrite.

An electrochemically driven reaction should exhibit a half order dependence on the ferric-iron concentration[62]. However, the ferric leaching rate of pyrite was found independent of the total iron concentration, for iron concentrations ranging from 50 to 500 mmol $Fe.\ell^{-1}$ [51]. Although the leaching rate of arsenopyrite did not exhibit a half order dependence on the ferric-iron concentration, it was not found to be independent of the total iron concentration. In addition, it was not possible to fit the electrochemically-based model proposed by Verbaan and Crundwell[48], or the Monod-type model proposed by Boon[50]. However, it was possible to model the ferric leach kinetics using the Butler-Volmer based model suggested by May *et al.*[51] (Equation [7]). Comparison of the Butler-Volmer based model prediction with a typical set of experimental results is shown in Figure 5. From Figure 5 it is apparent that the agreement between the Butler-Volmer based model and the experimental results is good.

Although it was possible to model the ferric leach kinetics of arsenopyrite across a wide range of conditions using this model, a limitation of the model appears to be its dependence on the rest potential of the mineral, E'^*. The rest potential of arsenopyrite was found to increase when the initial (starting) redox potential or total iron concentration was increased, and decreased when the solids concentration or pH was increased. The results therefore suggest that an increase in the concentration of either ferric-iron or protons (based on the arsenopyrite surface area) result in a reduction in the reactivity of the mineral. This is regarded as highly unusual as most reaction mechanisms are favoured by an increase in reactant concentration.

Although the underlying mechanism responsible for the observed influence of the different parameters on the leaching rate is not clear at present, it is suspected that they affect the speciation of the iron, sulphur and arsenic complexes in the solution. It is therefore necessary to modify the model to include the effect of parameters such as the pH and the ferric-iron concentration on the ferric leaching rate of arsenopyrite. However, the results obtained thus far suggest that the Butler-Volmer based model has potential for predicting the ferric leaching rate of sulphide minerals over a wide range of solution conditions.

Ferrous-iron oxidation kinetics

To date a number of kinetic models for bacterial ferrous-iron oxidation have been proposed[63]. These models can be broadly classified as either empirical or Michaelis-Menten/Monod based. Empirical models use tools such as the logistic equation to model the kinetics whereas Michaelis-Menten based models assume that the rate limiting reactions can be described using traditional enzyme kinetics. A number of workers have Michaelis-Menten/Monod based models modified to account for

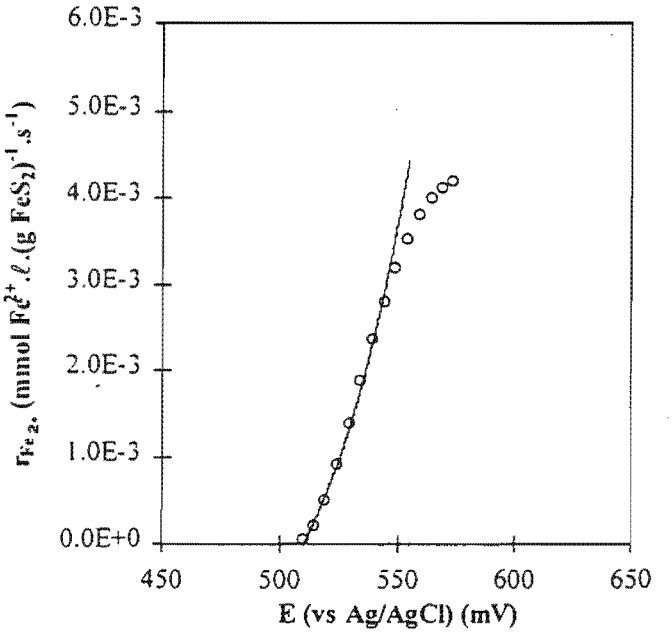

Figure 5. Comparison between the [—] Butler-Volmer based model prediction ($r_0 = 5x10^{-4}$, $\alpha = 0.498$, $\beta = 0.0272$, $E' = 510$) and the [o] experimental leaching rate data (after Ruitenberg *et al.*[1999])

‡The maximum calculated leaching rate was attained within ±20s; the overall duration of the experiments was in the region of 2 hours

ferric-iron inhibition[64,65] and a threshold ferrous-iron concentration[66]. Boon[50] showed that the threshold ferrous iron concentration and ferrous-iron saturation terms could be ignored. Instead, the ferrous iron oxidation kinetics are assumed to be proportional to the ferric/ferrous-iron ratio (i.e. the redox potential) viz.

$$q_{Fe^{2+}} = \frac{-r_{Fe^{2+}}}{c_X} = \frac{q^{max}_{Fe^{2+}}}{1 + K_{Fe^{2+}} \frac{[Fe^{3+}]}{[Fe^{2+}]}} \quad 50 \qquad [10]$$

Equation [10] is consistent with the chemiosmotic theory proposed by Ingledew[67] and has been used to describe the kinetics of *T. ferrooxidans* and *L. ferrooxidans* over the range of ferric/ferrous-iron ratios found in bioleaching systems[10,11,68,69].

Most commercial bioleaching operations using mesophilic bacteria are continuous processes and are carried out using mixed cultures. They usually operate at temperatures in the region of 40°C and pH values ranging from pH 1.2–2.0. However, most research performed to date has been carried out using pure cultures in batch reactors, at temperatures in the region of 30°C and pH values in the region of pH 1.8–2.0. These conditions are similar to those that have been reported to be the optimum conditions for *T. ferrooxidans*. This has resulted in most workers having reported *T. ferrooxidans* to be the organizm responsible for the bioleaching of sulphide minerals. However, recent work has suggested that *T. ferrooxidans* is unlikely to predominate in many systems[10–12, 70–74]. an explanation for this has been offered by Rawlings *et al.*[75]. Furthermore, apart from the work of Nemati and Webb[76], the effect of temperature on bioleaching micro-organizms has not been studied extensively.

During a recent investigation, the ferrous-iron oxidation kinetics of a predominantly *L. ferrooxidans* culture were studied in continuous-flow bioreactors at dilution rates ranging from 0.01 to 0.10 h^{-1}, temperatures ranging from 30 to 40°C and pH values ranging from pH 1.10 to pH 1.70. Although the bacterial culture maintained at 40°C and pH 1.30 'washed out' at the highest dilution rate, the highest calculated maximum specific growth rate, $\mu^{max} = 0.1238$ h^{-1}, occurred at 40°C and pH 1.50[69].

The maximum bacterial specific ferrous-iron and oxygen utilization rates, $q^{max}_{Fe^{2+}}$ and $q^{max}_{O_2}$, respectively, and their respective kinetic constants, $K_{Fe^{2+}}$ and K_{O_2}, increased with increasing temperature, across the range from 30 to 40°C. The temperature dependence of the maximum bacterial specific ferrous-iron and oxygen utilization rates could be accurately described using the Arrhenius Equation. However, the relationship between temperature and the kinetic constants appeared to be linear.

The kinetic constants, $K_{Fe^{2+}}$ and K_{O_2}, also appeared to increase linearly with increasing pH. Although the maximum bacterial specific ferrous-iron and oxygen utilization rates appeared to achieve maximum values at pH 1.50, no simple relationship between these parameters and

*The rest potential of the mineral is defined as redox potential of the solution at which the mineral dissolution stops.

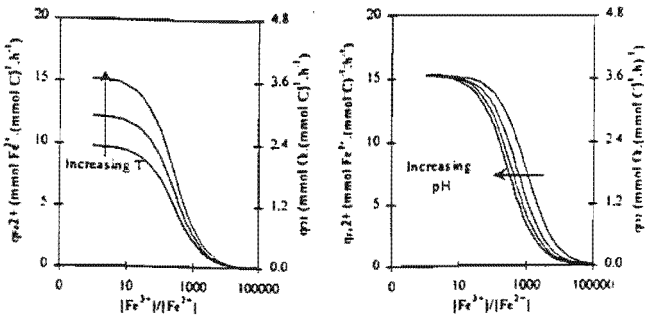

Figure 6. Effect of temperature and pH on the bacterial specific ferrous-iron and oxygen utilization rates (after Breed *et al.*[24])

the solution pH was apparent. Furthermore, the variation in the maximum specific ferrous-iron and oxygen utilization with changes in pH was considerably less pronounced than the variation observed with changes in temperature. It is therefore possible to depict the primary differences in the effect of temperature and pH on the ferrous-iron oxidation kinetics of *L. ferrooxidans* as indicated in Figure 6.

The above trends and assumptions led to a model that predicts the bacterial specific ferrous-iron and oxygen utilization rates as a function of the ferric/ferrous-iron ratio, for temperatures ranging from 30 to 40°C and pH values ranging from pH 1.10 to pH 1.70[24], viz:

$$q_{Fe^{2+}} = \frac{1.204 \times 10^{7} e^{-\frac{25.33}{RT}}}{1 + (1.006 \times 10^{-4} T + 0.0043 \mathrm{pH} - 0.0040) \frac{[Fe^{3+}]}{[Fe^{2+}]}} \qquad [11]$$

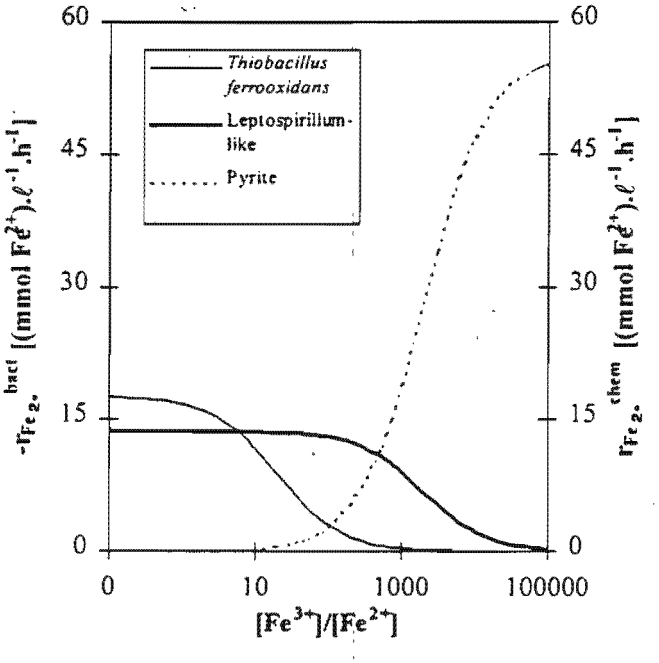

Figure 7. Variation in the ferrous-iron production rate during the ferric leaching of pyrite and the bacterial ferrous-iron consumption rate during the biooxidation of ferrous-iron by *T. ferrooxidans* and a *Leptospirillum*-like bacterium as a function of the ferric/ferrous-iron ratio (redox potential). Data were calculated from the results of Boon[50] and Van Scherpenzeel *et al.*[68] (after Breed *et al.*[24])

$$q_{O_2} = \frac{0.301\times10^{7} e^{-\frac{35.33}{RT}}}{1+\left(1.006\times10^{-6}T + 0.0043\text{pH} - 0.0042\right)\frac{\left[Fe^{3+}\right]}{\left[Fe^{2+}\right]}} \quad [12]$$

Comparison between the experimentally measured variation in the specific ferrous-iron and oxygen utilization rates with changes in the ferric/ferrous-iron ratio and the predictions of Equations [10] and [11] showed good agreement (data not shown)[24].

Modelling continuous bioleach reactors

Figure 7 shows the chemical ferrous-iron production rate from the chemical ferric leaching of pyrite and the bacterial ferrous-iron consumption rate by *T. ferrooxidans* and a *Leptospirillum*–like bacterium as a function of the ferric/ferrous-iron ratio (redox potential). The point of intersection of the curves represents the steady-state mineral leaching rate and ferric/ferrous-iron ratio, or redox potential of the system; hence, it is the point that a model of the system must be able to predict.

If it is assumed that the bioleaching of sulphide minerals occurs via a multiple sub-process mechanism, then for a CSTR operating at steady-state, a ferrous-iron material balance yields;

$$Q_{in}\left[Fe^{2+}\right]_{in} - Q_{out}\left[Fe^{2+}\right]_{out} = V\left(r^{bact}_{Fe^{2+}} + r^{chem}_{Fe^{2+}}\right) \quad [13]$$

From Figure 7 it is also apparent that for the case of pyrite bioleaching, the rate of chemical ferrous-iron production intersects the *T. ferrooxidans* and *Leptospirillum-like* curves at ferric/ferrous-iron ratios in the region of 200 and 700, respectively*. In continuous bioleaching reactors the ferric-iron concentration is in the region of 300–600 mmol $Fe^{3+}\ell^{-1}$ [25], hence it can be assumed that the outlet ferrous-iron concentration is zero. Furthermore, for the case of a single bioreactor $[Fe^{2+}]_{in}$ = 0, hence Equation [12] can be simplified to give;

$$-r^{bact}_{Fe^{2+}} = r^{chem}_{Fe^{2+}} \quad [14]$$

In other words, during the steady-state bioleaching of pyrite the bacterial and chemical sub-processes are linked by the rate at which the iron is turned over in the system.

Steady-state ferrous-iron oxidation

If it is assumed that the maximum growth yield and the maintenance coefficient are constant for a particular bacterial species/substrate combination, and can be related via the Pirt Equation[77], then, for the case where the substrate is ferrous-iron,

$$-r^{bact}_{Fe^{2+}} = \frac{r_X}{Y^{max}_{Fe^{2+}X}} + m_{Fe^{2+}}c_X \quad [15]$$

Division of Equation [14] by c_X, and substitution assuming chemostat operation with sterile feed, yields;

$$q_{Fe^{2+}} = \frac{1}{Y^{max}_{Fe^{2+}X}\tau} + m_{Fe^{2+}} \quad [16]$$

If $q_{Fe^{2+}}$ can be related to the ferric/ferrous-iron ratio using an equation of the form of Equation [9], then substituting Equation [9] into Equation [16] and rearranging yields;

$$\frac{\left[Fe^{3+}\right]}{\left[Fe^{2+}\right]} = \frac{\left(\frac{\tau q^{max}_{Fe^{2+}} Y^{max}_{Fe^{2+}X}}{1+m_{Fe^{2+}}\tau Y^{max}_{Fe^{2+}X}}\right) - 1}{K} \quad [17]$$

Equation [17] shows that the ferric/ferrous-iron ratio is a function only of the residence time and the characteristics of the bacterial species used; i.e. it is not dependent on the mineral concentration, nor the total or ferrous-iron concentrations, i.e.;

$$\frac{\left[Fe^{3+}\right]}{\left[Fe^{2+}\right]} = f(\tau) \neq g\left(\left[FeS_2\right]_{in}, \left[Fe_T\right], \left[Fe^{2+}\right]\right) \quad [18]$$

Although this is not an intuitive result, it is expected from the assumption of Monod or Michaelis-Menten type kinetics.

Steady-state chemical (ferric) pyrite leaching

During the steady-state chemical ferric leaching of pyrite in a continuous reactor performing a pyrite mass balance yields;

$$Q_{in}\left[FeS_2\right]_{in} + Vr_{FeS_2} = Q_{out}\left[FeS_2\right]_{out} \quad [19]$$

which can be simplified to give;

$$\left[FeS_2\right]_{in} - \left[FeS_2\right]_{out} = -\tau r_{FeS_2} \quad [20]$$

The rate of ferrous-iron production during the ferric leaching of pyrite is related to the rate of pyrite leaching via Equation [1], i.e.;

$$r_{FeS_2} = -\frac{r^{chem}_{Fe^{2+}}}{15} \quad [21]$$

Substituting Equation [21] into Equation [20] yields;

$$\left[FeS_2\right]_{in} - \left[FeS_2\right]_{out} = \frac{\tau r^{chem}_{Fe^{2+}}}{15} \quad [22]$$

By definition;

$$r^{chem}_{Fe^{2+}} = \upsilon_{Fe^{2+}}\left[FeS_2\right]_{out} \quad [23]$$

If it is assumed that the ferric leaching of pyrite can be described by an Equation of the form suggested by Boon[50], substitution of this equation into Equation [23] yields;

$$r^{chem}_{Fe^{2+}} = \frac{\upsilon^{max}_{Fe^{2+}}\left[FeS_2\right]_{out}}{1+B\frac{\left[Fe^{2+}\right]}{Fe^{3+}}} \quad [24]$$

Substituting Equation [24] into Equation [22] and rearranging yields;

$$\frac{\left[FeS_2\right]_{in}}{\left[FeS_2\right]_{out}} = 1 + \frac{\frac{\tau}{15}\upsilon^{max}_{Fe^{2+}}}{1+B\frac{\left[Fe^{2+}\right]}{\left[Fe^{3+}\right]}} \quad [25]$$

The fraction of mineral leached, X, is defined as;

*The pyrite curve intersects the *Leptospirillum*-like curve at a higher rate of iron turnover than that of *T. ferrooxidans* therefore Figure 7 predicts that *Leptospirillum*-like bacteria will dominate during the bioleaching of pyrite,which is consistent with previous research[10–12, 70–74].

$$X = \frac{[FeS_2]_{in} - [FeS_2]_{out}}{[FeS_2]_{in}} = 1 - \frac{[FeS_2]_{out}}{[FeS_2]_{in}} \quad [26]$$

Hence combining Equations [25] and [26] yields:

$$X = \frac{\frac{\tau}{15} \upsilon^{max}_{Fe^{2+}}}{1 + B\frac{[Fe^{2+}]}{[Fe^{3+}]} + \frac{\tau}{15}\upsilon^{max}_{Fe^{2+}}} \quad [27]$$

From Equation [27] it is clear that the mineral conversion is a function of the ferric/ferrous-iron ratio, the residence time and the characteristics of the pyrite itself, not of the inlet mineral concentration,

$$X = h\left(\frac{[Fe^{3+}]}{[Fe^{2+}]}\right) = j(\tau) \neq k\left([FeS_2]_{in}\right) \quad [28]$$

However, the ferric/ferrous-iron ratio is determined by the characteristics of the bacterial species used and the prevailing residence time, hence substitution of Equation [17] into Equation [27] and rearranging yields;

$$X = \frac{\frac{\tau}{15}\upsilon^{max}_{Fe^{2+}}}{1 + B\left(\frac{K}{\left(\frac{\tau q^{max}_{Fe^{2+}} Y^{max}_{Fe^{2+}X}}{1 + m_{Fe^{2+}}\tau Y^{max}_{Fe^{2+}X}}\right) - 1}\right) + \frac{\tau}{15}\upsilon^{max}_{Fe^{2+}}} \quad [29]$$

From Equation [29], it is clear that

$$X = l(\tau) \quad [30]$$

Figure 8 shows the predicted variation in the pyrite conversion, using *T. ferrooxidans* and a *Leptospirillum*–like bacterium in a continuous-flow bioreactor, at residence times ranging from 0 to 20 days. These predictions are compared with the results of Hansford and Chapman[6] for the continuous bioleaching of a similar sized euhedral pyrite by an unidentified microbial species.

From Figure 8 it is apparent that the data of Hansford and Chapman[6] follows the trend predicted by the model if the kinetic parameters for the *Leptospirillum*–like bacterium are assumed. Furthermore, the values of the predicted and experimental values are similar. Although the microbial species used by Hansford and Chapman[6] was not identified, their results and those of other research[10–12,70–74] suggest that the micro-organizm would have been *L. ferrooxidans*.

At this stage, it is important to note that the kinetic parameters of the bacteria were determined at residence times of between 10 and 100 hours, while the kinetic parameters of the pyrite were determined in batch culture. Furthermore, neither the bacterial species, nor the pyrite used to determine the kinetic parameters were the same as those used by Hansford and Chapman[1992]. In spite of this it appears as though the model developed is able to predict the performance of a continuous bioleach reactor.

To date a number of researchers have reported that both the chemical ferric leaching[5,1] and the bioleaching[4,6] of sulphide minerals is dependent on the surface area of the mineral present. Although the results presented above are described in terms of the pyrite concentration in mmol $FeS_2.l^{-1}$ it is possible to relate the pyrite specific ferrous-iron production rate based on the pyrite concentration to the pyrite specific ferrous-iron production rate based on the pyrite surface area using:

$$r^{chem}_{Fe^{2+}} = \xi_{Fe^{2+}}.\alpha[FeS_2] \quad [31]$$

where the pyrite specific ferrous-iron production rate based on the pyrite surface area can be described using equations analogous to Equations [8] or [9].

Summary

The multiple sub-process mechanism suggests that the kinetics of the chemical and bacterial sub-processes may be studied independently, and then combined in order to predict the steady-state and dynamic performance of bioleach reactors.

The chemical ferric leaching rate of arsenopyrite decreases with a decrease in the solution redox and may be described using a modified Butler-Volmer Equation. The bacterial ferrous-iron oxidation kinetics of *L. ferrooxidans* also depends on the redox potential, and can be described using a Michaelis-Menten type model modified to account for both temperature and pH.

Although the effect of arsenic on the kinetics has yet to be determined, it is suggested that the mechanism of arsenic resistance may be attributed to the Pst+Pit- mutation and an energy dependent efflux pump. The Pst+Pit- mutation enables the bacteria to survive in solutions in which the arsenate concentration is significantly higher than the arsenite concentration. However, because the excretion of arsenate requires energy, in the absence of an energy source or during periods of reduced bacterial activity, the inhibitory effect of arsenate may manifest at concentrations

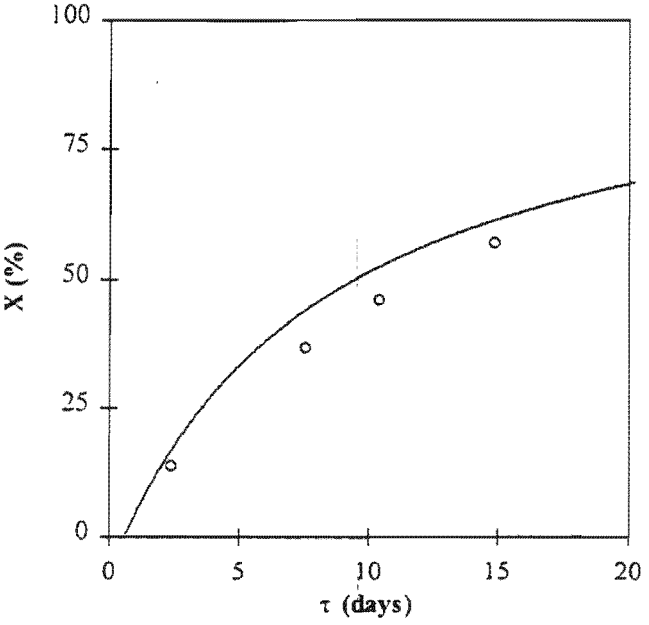

Figure 8. Comparison between the [—] predicted variation in the pyrite conversion with changing residence time for *T. ferrooxidans* and a *Leptospirillum*-like bacterium and the [o] experimental results obtained by Hansford and Chapman[6]. Data were calculated from the results of Boon[50] and Van Scherpenzeel *et al.*[68] (after Breed *et al.*[19])

to which the culture has previously been adapted.

The point of intersection of the chemical and bacterial oxidation curves defines the redox potential within the bioreactor and can be related to the rate of leaching of the mineral. It depends on the characteristics of the bacterial species used, the residence time employed, the characteristics of the mineral being used and its active surface area.

The proposed model suggests that the residence time and microbial species present determine the bacterial growth rate, which in turn determines the redox potential of the bioleaching solution. The residence time and redox potential in turn determine the mineral conversion. Refinement of the model is necessary to include the effect of changes in the surface area, the formation of precipitates and the fate of the sulphur moiety. However, it appears to have potential for predicting the performance of continuous bioleach reactors.

Acknowledgements

The authors would like to acknowledge the financial support received from The Foundation for Research Development (South Africa), Billiton Process Research and the Gold Fields Foundation.

Nomenclature

B	kinetic constant in chemical ferric leaching	dimensionless
c_x	concentration of bacteria	mmol C.ℓ$^{-1}$
E	solution redox potential	mV
E′	mineral rest potential	mV
F	Faraday constant	C.mol^{-1}
$[Fe^{2+}]$	concentration of ferrous-iron	mmol Fe^{2+}.ℓ$^{-1}$
$[Fe^{3+}]$	concentration of ferric-iron	mmol Fe^{3+}.ℓ$^{-1}$
$[Fe^{2+}]_{in}$	inlet ferrous-iron concentration	mmol Fe^{2+}.ℓ$^{-1}$
$[FeS_2]$	FeS_2 concentration	mmol FeS_2.ℓ$^{-1}$
$[FeS_2]_{in}$	concentration of FeS_2 in the feed	mmol FeS_2.ℓ$^{-1}$
$[FeS_2]_{out}$	concentration of FeS_2 in the outlet	mmol FeS_2.ℓ$^{-1}$
$[Fe_T]$	concentration of total iron	mmol Fe.ℓ$^{-1}$
$K_{Fe^{2+}}$	kinetic constant in bacterial ferrous-iron oxidation	dimensionless
K_{O_2}	kinetic constant in bacterial ferrous-iron oxidation	dimensionless
$m_{Fe^{2+}}$	maintenance coefficient on ferrous-iron	mmol Fe^{2+}.(mmolC)$^{-1}$.h^{-1}
Q_{in}	volumetric flow rate into the bioreactor	ℓ.h^{-1}
Q_{out}	volumetric flow rate out of the bioreactor	ℓ.h^{-1}
$q_{Fe^{2+}}$	bacterial specific ferrous-iron oxidation rate	mmol Fe^{2+}.(mmolC)$^{-1}$.h^{-1}
$q^{max}_{Fe^{2+}}$	maximum bacterial specific ferrous iron oxidation rate	mmol Fe^{2+}(mmol C)$^{-1}$.h^{-1}
q_{O_2}	bacterial specific oxygen utilization rate	mmol O_2.(mmolC)$^{-1}$.h^{-1}
$q^{max}_{O_2}$	maximum bacterial specific oxygen utilization rate	mmol O_2.(mmolC)$^{-1}$.h^{-1}
R	universal gas constant	kJ.mol^{-1}.K^{-1}
r_0	kinetic constant in chemical ferric leaching	mmol Fe^{2+}.ℓ.(g FeS_2)$^{-1}$.s^{-1}
$r^{bact}_{Fe^{2+}}$	bacterial ferrous-iron production rate	mmol Fe^{2+}.ℓ$^{-1}$.h^{-1}
$r^{chem}_{Fe^{2+}}$	chemical ferrous-iron production rate	mmol Fe^{2+}.ℓ$^{-1}$.h^{-1}
r_{FeS2}	pyrite production rate	mmol FeS_2.ℓ$^{-1}$.h^{-1}
r_{O2}	oxygen production rate	mmol C.ℓ$^{-1}$.h^{-1}
T	absolute temperature	K
$Y^{max}_{Fe^{2+}X}$	maximum bacterial yield on ferrous-iron	mmol C.(mmol Fe^{2+})$^{-1}$
V	bioreactor volume	ℓ
X	fraction of mineral leached	dimensionless
z	number of electrons involved in the reaction	dimensionless
α	specific surface area	m^2 FeS_2(mmol FeS_2)$^{-1}$
β	$\frac{RT}{}$	mV^{-1}
μ^{max}	maximum bacterial specific growth rate	h^{-1}
τ	residence time	h
$\upsilon_{Fe^{2+}}$	pyrite specific ferrous-iron production rate	mmol Fe^{2+}.(mmol FeS_2.)$^{-1}$.h^{-1}
$\upsilon^{max}_{Fe^{2+}}$	maximum pyrite specific ferrous-iron production rate	mmol Fe^{2+}.(mmol FeS_2)$^{-1}$.h^{-1}
$\xi_{Fe^{2+}}$	surface area specific ferrous-iron production rate	mmol Fe^{2+}.(m^2 FeS_2.)$^{-1}$.h^{-1}

References

1. VAN ASWEGEN, P.C. Commissioning and operation of bio-oxidation plants for the treatment of refractory gold ores. Hydrometallurgy; Fundamentals, Technology and Innovations. Hiskey, J.B., and Warren, G.W. (eds.). Littleton, *Soc. Min. Metall. Explor. AIME*. 1993. pp. 709–725.
2. POULIN, R., and LAWRENCE, R.W. Economic and environmental niches of biohydrometallurgy. *Miner. Eng.*, vol. 9, no. 8, 1996. pp. 799–810.
3. PINCHES, A., CHAPMAN, J.T., TE RIELE, W.A.M., and VAN STADEN, M. The performance of bacterial leach reactors for the pre-oxidation of refractory gold-bearing sulphide concentrates. *Proceedings of International Symposium on Biohydrometallurgy*, Warwick. Norris, P.R., and Kelly, D.P. (eds.). Kew, Science and Technology Letters, 1988. pp. 329–344.
4. MILLER, D.M., and HANSFORD, G.S. Batch bio-oxidation of a gold-bearing pyrite/arsenopyrite concentrate. *Miner. Eng.*, vol. 5, no. 6, 1992. pp. 613–629.
5. MILLER, D.M., and HANSFORD, G.S. The use of the logistic equation for modelling the performance of a bio-oxidation plant treating a gold-bearing pyrite/arsenopyrite concentrate. *Miner. Eng.*, vol. 5, no. 7, 1992. pp. 737–749.
6. HANSFORD, G.S., and CHAPMAN, J.T. Batch and continuous bio-oxidation kinetics of a refractory gold-bearing pyrite/arsenopyrite concentrate. *Miner. Eng.*, vol. 5, no. 6, 1992. pp. 597–612.

7. HANSFORD, G.S., and BAILEY, A.D. The logistic equation for modelling bacterial oxidation kinetics. *Miner. Eng.*, vol. 5, no. 10–12, 1992. pp. 1355–1364.

8. HANSFORD, G.S., and MILLER, D.M. Biooxidation of a gold-bearing pyrite-arsenopyrite concentrate. *FEMS Microbiology Reviews*, vol. 11, 1993. pp. 175–182.

9. DEW, D.W., LAWSON, E.N., and BROADHURST, J.L. The BIOX process for biooxidation of gold-bearing ores and concentrates. *Biomining: theory, microbes and industrial processes*. Rawlings, D.E. (ed.), Berlin, Springer-Verlag, 1997. pp. 45–80.

10. BOON, M., HANSFORD, G.S., and HEIJNEN, J.J. The role of bacterial ferrous-iron oxidation in the bio-oxidation of pyrite. Biohydrometallurgical processing. *Proceedings of International Biohydrometallurgy Symposium* IBS-95, Vina del Mar. Vargas, T., Jerez, C.A., Wiertz, J.V., and Toledo, H. (eds.). Santiago, University of Chile, vol. I, 1995. pp. 153–163.

11. BREED, A.W., DEMPERS, C.J.N., SEARBY, G.E., RAWLINGS, D.E., and HANSFORD, G.S. The effect of temperature on the continuous ferrous-iron oxidation kinetics of a predominantly *Leptospirillum ferrooxidans* culture. *Biotechnology and Bioengineering*, vol. 65, no. 1, 1999. pp. 44–53.

12. RAWLINGS, D.E., CORAM, N.J., GARDNER, M.N., and DEANE, S.M. *Thiobacillus caldus* and *Leptospirillum ferrooxidans* are widely distributed in continuous flow biooxidation tanks used to treat a variety of metal containing ores and concentrates. Biohydrometallurgy and the Environment Toward the Mining of the 21st Century, *Proceedings International Biohydrometallurgy Symposium IBS '99*, Madrid. Amils, R., and Ballester, A. (eds.). Amsterdam, Elsevier, 1999. Part A, pp. 777–786.

13. GARRELS, R.M., and THOMPSON, M.E. Oxidation of pyrite by iron sulphate solutions. *American Journal of Science*, vol. 258A. 1960. pp. 57–67.

14. IGLESIAS, N., PALENCIA, I., and CARRANZA, F. Removal of the refractoriness of a gold bearing pyrite-arsenopyrite ore by ferric sulphate leaching at low concentration. *Proceedings of EPD Congress 1993*. Hager, J.P. (ed.). Warrendale, The Minerals, Metals and Materials Society, 1993. pp. 99–115.

15. ZEMAN, J., MANDL, M., and MRNUSTIKOVA. Oxidation of arsenopyrite by *Thiobacillus ferrooxidans* detected by a mineral electrode. *Biotechnology Techniques*, vol. 9, no. 2, 1995. pp. 111–116.

16. BREED, A.W., HARRISON, S.T.L., and HANSFORD, G.S. A preliminary investigation of the ferric leaching of a pyrite/arsenopyrite concentrate. *Minerals Engineering*, vol. 10, no. 9, 1997. pp. 1023–1030.

17. SILVERMAN, M.P., and EHRLICH, H.L. Microbial formation and degradation of minerals. *Adv. Appl. Microbiol.*, vol. 6, 1964. pp. 181–183.

18. SAND, W., GEHRKE, T., JOZSA, P.-G., and SCHIPPERS, A. Direct versus indirect bioleaching. Biohydrometallurgy and the Environment Toward the Mining of the 21st Century, *Proceedings International Biohydrometallurgy Symposium IBS '99*, Madrid. Amils, R., and Ballester, A. (eds.). Amsterdam, Elsevier, 1999. Part A, pp. 27–49.

19. BREED, A.W. and HANSFORD, G.S. Modelling continuous bioleach reactors. *Biotechnology and Bioengineering*, in press.

20. SHRESTHA, G.N. Microbial leaching of refractory gold ores. *Australian Mining*, October, 1988. pp. 48–51.

21. POL'KIN, S.I., PANIN, V.V., ADAMOV, E.V., KARAVAIKO, G.I., and CHERNYAK, A.S. Theory and Practice of Utilizing Microorganizms in Difficult-to-dress Ores and Concentrates. *Proceedings 11th International Mineral Processing Congress*, Cagliari. University of Cagliari, 1975. pp. 901–923.

22. TREVORS, J.T., ODDIE, K.M., and BELLIVEAU, B.H. Metal resistance in bacteria. *FEMS Microbiology Reviews*, vol. 32, 1985. pp. 39–54.

23. BARRETT, J., EWART, D.K., HUGHES, M.N., NOBAR, A.M., and POOLE, R.K. The oxidation of arsenic in arsenopyrite: the toxicity of As(III) to a moderately thermophilic mixed culture. *Proceedings Biohydrometallurgy-89, Jackson Hole*. Salley, J., McCready, R.G.L., and Wichlacz, P.L. (eds.). Warrendale, *The Minerals, Metals and Materials Society*, vol. I, 1989. pp. 49–57.

24. BREED, A.W. Studies on the mechanism and kinetics of bioleaching with special reference to the bioleaching of refractory gold-bearing arsenopyrite-pyrite concentrates, Ph.D. thesis. Cape Town, University of Cape Town, 1999.

25. BREED, A.W., HARRISON, S.T.L., and HANSFORD, G.S. The bioleaching of a pyrite-arsenopyrite concentrate in a continuous bioleaching mini-plant. Steady-state operation and behaviour during periods without aeration and agitation. *Proceedings IBS-BIOMINE 97*, Sydney. Glenside, Australian Mineral Foundation, 1997. pp. M.8.3.1–M.8.3.10.

26. SILVER, S., BUDD, K., LEAHY, K.M., SHAW, W.V., HAMMOND, D., NOVICK, R.P., WILLSKY, G.R., MALAMY, M.H., and ROSENBERG, H. Inducible plasmid-determined resistance to arsenate, arsenite and antimony(III) in *Escherichia coli* and *Staphylococcus aureus*. *Journal of Bacteriology*, vol. 146, no. 3, 1981. pp. 983–996.

27. DABBS, E.R., and SOLE, G.J. Plasmid-borne resistance to arsenate, cadmium, and chloramphenicol in a *Rhodococcus* species. *Mol. Gen. Genet.*, vol. 211, 1988. pp. 148–154.

28. LINDSTRÖM, E.B. and SEHLIN, H.M. Toxicity of arsenic compounds to the sulphur-dependent archaebacterium *Sulfolobus*. *Proceedings Biohydrometallurgy–89, Jackson Hole*. Salley, J., McCready, R.G.L., and Wichlacz, P.L. (eds.). Warrendale, *The Minerals, Metals and Materials Society*, 1989. vol. I. pp. 59–70.

29. HUYSMANS, K.D., and FRANKENBERGER, W.T. Microbial resistance to arsenic. Engineering aspects

of metal-waste management. Iskander, I.K., and Selim, H.M. (eds.). London, *Lewis Publishers*, 1992. pp. 93–116.

30. COLLINET, M.-N., and MORIN, D. Characterization of arsenopyrite oxidising *Thiobacillus*. tolerance to arsenite, arsenate, ferrous and ferric iron. *Antonie van Leeuwenhoek*, vol. 57, 1990. pp. 237–244.
31. CASSITY, W.D., and PESIC, B. Interaction of *Thiobacillus ferrooxidans* with arsenite, arsenate and arsenopyrite, New remediation technology in the changing environmental arena. Scheiner, B.J., Chatwin, T.D., El-Shall, H., Kawatra, S.K., and Torma, A.E. (eds.), Littleon, Society for Mining, *Metallurgy, and Exploration, Inc.*, 1995. pp. 223–228.
32. LAWSON, E.N. Arsenic toxicity, bacterial resistance and bacterial oxidation/reductions. phase 1: literature review. Report No. PR 93/109C of Project No. PR 93/132. Johannesburg, *GENMIN Process Research*, 1993.
33. CODDINGTON, K. A review of arsenicals in biology. *Toxicological and Environmental Chemistry*, vol. 11, 1986. pp. 281–290.
34. NOVICK, R.P., and ROTH, C. Plasmid-linked resistance to inorganic salts in *Staphylococcus aureus*. *J. Bacteriol.*, vol. 95, no. 4, 1968. pp. 1335–1342.
35. SILVER, S., and NAKAHARA, H. Bacterial resistance to arsenic compounds. *Arsenic: industrial, biomedical, environmental perspectives*. Lederer, W.H., and Fensterheim, R.J. (eds.). New York, Van Nostrand Reinhold, 1983. pp. 190–199.
36. CULLEN, W.R., and REIMER, K.J. Arsenic speciation in the environment. *Chem. Rev.*, vol. 89, no. 4, 1989. pp. 713–764.
37. SILVER, S. Transport of Cations and Anions, *Bacterial Transport*. Rosen, B.P. (ed.). New York, Marcel Dekker Inc., 1978. pp. 221–324.
38. WILLSKY, G.R., and MALAMY, M.H. Effect of arsenate on inorganic phosphate transport in *Escherichia coli*. *J. Bacteriol.*, vol. 144, no. 1, 1980. pp. 366–374.
39. MOBLEY, H.T., and ROSEN, B.P. Energetics of plasmid-mediated arsenate resistance in *Escherichia coli*. *Proc. Natl. Acad. Sci. U.S.A*, vol. 79, 1982. pp. 6119–6122.
40. SILVER, S., and KEACH, D. Energy-dependent arsenate efflux: the mechanism of plasmid-mediated resistance. *Proc. Natl. Acad. Sci. USA.*, vol. 79, 1982. pp. 6114–6118.
41. SILVER, S., and MISRA, T.K. Plasmid-mediated heavy metal resistances. *Ann. Rev. Microbiol.*, vol. 42, 1988. pp. 717–743.
42. ROSEN, B.P., HSU, C.M., KARKARIA, C.E., OWOLABI, J.B., and TISA, L.S. Molecular analysis of an ATP-dependent anion pump. *Phil. Trans. R. Soc. Lond.*, vol. B 326. 1990. pp. 455–463.
43. ROSENSTEIN., R, PASCHEL, A., WIELAND, B., and GÖTZ, F. Expression and regulation of the antimonite, arsenite and arsenate resistance operation of *Staphylococcus xylosus* plasmid pSX267. J. Bact., vol. 174, no. 11, 1992. pp. 3676–3683.
44. BREED, A.W., GLATZ, A., HARRISON, S.T.L., and HANSFORD, G.S. The Effect of As(III) and As(V) on the batch bioleaching of a pyrite-arsenopyrite concentrate. *Minerals Engineering*, vol. 9, no. 12, 1996. pp. 1235–1252.
45. MORIN, D., OLLIVIER, P., TOROMANOFF, I., and LETESTU, A. Bioleaching of gold refractory arsenopyrite rich sulphide concentrate laboratory and pilot case studies. *Proceedings EPD Congress '91*. Gaskell, D.R. (ed.). Warrendale, *The Minerals, Metals, and Materials Society*, 1991. pp. 577–589.
46. TUOVINEN, O.H., NIEMELÄ, S.I., and GYLLENBERG, H.G. Tolerance of *Thiobacillus ferrooxidans* to some metals. *Antonie van Leeuwenhoek*, vol. 37, 1971. pp. 489–496.
47. NORRIS, P.R., BARR, D.W., and HINSON, D. Iron and mineral oxidation by acidophilic bacteria: affinities for iron and attachment to pyrite. *Proceedings International Symposium on Biohydrometallurgy*, Warwick. Norris, P.R., and Kelly, D.P. (eds.). Kew, Science and Technology Letters, 1987. pp. 43–59.
48. VERBAAN, B., and HUBERTS, R. An electrochemical study of the bacterial leaching of synthetic nickel sulfide (Ni_3S_2). *International Journal of Mineral Processing*, vol. 24, no. 3-4, 1988. pp. 185–202.
49. NAGPAL, S., DAHLSTROM, D., and OOLMAN, T. A mathematical model for the bacterial oxidation of a sulphide ore concentrate. *Biotechnology and Bioengineering*, vol. 43, no. 5, 1994. pp. 357–364.
50. BOON, M. Theoretical and experimental methods in the modelling of the bio-oxidation kinetics of sulphide minerals, Ph.D. thesis. Delft, Delft University of Technology, 1996.
51. MAY, N., RALPH, D.E., and HANSFORD, G.S. Dynamic redox potential measurement for determining the ferric leach kinetics of pyrite. *Miner. Eng.*, vol. 10, no. 11, 1997. pp. 1279–1290.
52. MATHEWS, C.T., and ROBINS, R.G. The oxidation of iron disulphide by ferric sulphate. *Australian Chemical Engineering*, August, 1972. pp. 21–25.
53. McKIBBEN, M.A., and BARNES, H.B. Oxidation of pyrite in temperature acidic solutions: rate laws and surface tectures. *Geochimica et Cosmochimica Acta*, vol. 50, 1986. pp. 1509–1520.
54. RUITENBERG, R., HANSFORD, G.S., REUTER, M.A., and BREED, A.W. The ferric leaching kinetics of arsenopyrite. *Hydrometallurgy*, vol. 52, no. 1, 1999. pp. 37–53.
55. MACDONALD, A., and HANSFORD, G.S. Zeta potential measurement of *Thiobacillus ferrooxidans* and *Leptospirillum ferrooxidans* in the presence of pyrite. *Proceedings Biotech SA '97*, Grahamstown. 1997. p. 57.
56. KOSTINA, G.M., and CHERNYAK, A.S. Electrochemical conditions for the oxidation of pyrite and arsenopyrite in alkaline and acid solutions. *Zhurnal Prikladnoi Khimii*, vol. 49, no. 7, 1976. pp. 1534–1570.

57. DUNN, J.G., FERNANDEZ, P.G., HUGHES, H.C., and LINGE, H.G. Aqueous oxidation of arsenopyrite in acid. *Proceedings Annual Australasian Institute Mining and Metallurgy Conference*, Perth. Australasian Institute of Mining and Metallurgy, Melbourne, 1989. pp. 217–220.

58. LÁZARO, I., CRUZ, R., GONZÁLEZ, I., and MONROY, M. Electrochemical oxidation of arsenopyrite in acidic media. *International Journal of Minerals Processing*, vol. 50, nos. 1–2, 1997. pp. 63–75.

59. JORGE, P.F., AND MARTINS, G.P. Electrochemical and other aspects of indirect electrooxidation process for the leaching of molybdenite by hyperchloride. Hydrometallurgical reactor design and kinetics. Bautista, R.G., Wesely, R.J., Warren, G.W. (eds.). Warrendale, *The Metallurgical Society*, 1986. pp. 263–292.

60. CRUNDWELL, F.K. Kinetics and mechanism of the oxidative dissolution of a zinc sulphide concentrate in ferric sulphate solutions. *Hydrometallurgy*, vol. 19, no. 2, 1987. pp. 227–242.

61. VERBAAN, B., and CRUNDWELL, F.K. An electrochemical model for the leaching of a sphalerite concentrate. *Hydrometallurgy*, vol. 16, no. 3, 1986. pp. 345–359.

62. PLETCHER, D. Industrial Electrochemistry. New York, *Chapman and Hall*, 1984.

63. NEMATI, M., HARRISON, S.T.L., WEBB, C., and HANSFORD, G.S. Biological oxidation of ferrous sulphate by *Thiobacillus ferrooxidans:* a review on the kinetic aspects. *Biochemical Engineering Journal*, vol. 1, 1998. pp. 171–190.

64. LACEY, D.T., and LAWSON, F. Kinetics of the liquid phase oxidation of acid ferrous-sulphate by the bacterium *Thiobacillus ferrooxidans. Biotechnology and Bioengineering*, vol. 12, no. 1, 1970. pp. 29–50.

65. JONES, C.A., and KELLY, D.P. Growth of *Thiobacillus ferrooxidans* on ferrous-iron in chemostat culture: influence of product and substrate inhibition. *J. Chem. Tech. Biotechnol.*, vol. 33B, no. 4, 1983. pp. 241–261.

66. BRADDOCK, J.F., LUONG, H.V., and BROWN, E.J. Growth kinetics of *Thiobacillus ferrooxidans* isolated from arsenic mine drainage. *Appl. Environ. Microbiol.*, vol. 48, no. 1, 1984. pp. 48–55.

67. INGLEDEW, W.J. Ferrous-iron oxidation by *Thiobacillus ferrooxidans. Biotechnology Bioengineering Symposium Series*, vol. 16, 1986. pp. 23–33.

68. VAN SCHERPENZEEL, D.A., BOON, M., RAS, C., HANSFORD, G.S., and HEIJNEN, J.J. The kinetics of ferrous-iron oxidation by *Leptospirillum* bacteria in continuous cultures. *Biotechnol. Prog.*, vol. 14, 1998. pp. 425–433.

69. BREED, A.W., and HANSFORD, G.S. Effect of pH on ferrous-iron oxidation kinetics of Leptospirillum ferrooxidans in continuous culture. *The Biochemical Engineering Journal*, vol. 3, no. 1, 1999. pp. 193–201.

70. HALLMAN, R., FRIEDRICH, A., KOOPS, H.P., POMMERING-RÖSER, A., and SAND, W. Physiological characteristics of Thiobacillus *ferrooxidans* and *Leptospirillum ferrooxidans* and physiochemical factors influence on microbial metal leaching. *Geomicrobiology Journal*, vol. 10, 1987. pp. 193–205.

71. HELLE, U., and ONKEN, U. Continuous bacterial leaching of pyritic flotation concentrate by mixed cultures. *Proceedings International Symposium on Biohydrometallurgy*, Warwick. Norris, P.R., and Kelly, D.P. (eds.). Kew, Science and Technology Letters, 1987. pp. 61–75.

72. NORRIS, P.R., and KELLY, D.P. Toxic Metals in Leaching Systems. Metallurgical Applications of Bacterial Leaching and Related Microbiological Phenomena. Murr, L.E., Torma, A.E., and Brierley, J.A. (eds.). New York, *Academic Press*, 1978. pp. 83–102.

73. SAND, W., ROHDE, K., SOBOTKE, B., and ZENNECK, C. Evaluation of *Leptospirrillum ferrooxidans* for leaching. *Appl. Environ. Microbiol.*, vol. 58, no. 1, 1992. pp. 85–92.

74. RAWLINGS, D.E. Restriction enzyme analysis of 16S rDNA genes for the rapid identification of *Thiobacillus ferrooxidans, Thiobacillus thiooxidans* and *Leptospirillum ferrooxidans* strains in leaching environments. Biohydrometallurgical processing. *Proceedings of International Biohydrometallurgy Symposium IBS-95*. Vina del Mar. Vargas, T., Jerez, C.A., Wiertz, J.V., and Toledo, H. (eds.). Santiago, University of Chile, 1995. vol. I. pp. 9–17.

75. RAWLINGS, D.E., TRIBUTSCH, H., and HANSFORD, G.S. Reasons why '*Leptospirillum*'-like species rather than *Thiobacillus ferrooxidans* are the dominant iron-oxidizing bacteria in many commercial processes for the biooxidation of pyrite and related ores. *Microbiology*, vol. 145, 1999. pp. 5–13.

76. NEMATI, M., and WEBB, C. A kinetic model for biological oxidation of ferrous-iron by *Thiobacillus ferrooxidans*. Biotechnology and Bioeningeering, vol. 53, no.5, 1987. pp. 478–486.

77. PIRT, S.J. Maintenance energy: a general model for energy limited and energy sufficient growth. *Arch. Microbiol.*, vol. 133, 1982. pp. 300–302.

Everything
in this book
may be
wrong.

ILLUSIONS – Richard Bach